

Chemosensation in the marine annelid Platynereis dumerilii: anatomy, physiology, behaviour

Thomas F. Chartier

▶ **To cite this version:**

Thomas F. Chartier. Chemosensation in the marine annelid Platynereis dumerilii: anatomy, physiology, behaviour. Neurobiology. Ruperto-Carola University of Heidelberg, 2017. English. ⟨NNT : ⟩. ⟨tel-04865112⟩

HAL Id: tel-04865112

https://hal.science/tel-04865112v1

Submitted on 5 Jan 2025

HAL is a multi-disciplinary open access archive for the deposit and dissemination of scientific research documents, whether they are published or not. The documents may come from teaching and research institutions in France or abroad, or from public or private research centers.

L'archive ouverte pluridisciplinaire **HAL**, est destinée au dépôt et à la diffusion de documents scientifiques de niveau recherche, publiés ou non, émanant des établissements d'enseignement et de recherche français ou étrangers, des laboratoires publics ou privés.



HAL Authorization

Dissertation
submitted to the
Combined Faculties for the Natural Sciences and for Mathematics
of the Ruperto-Carola University of Heidelberg, Germany
for the degree of
Doctor of Natural Sciences

presented by

Dipl.-Ing. Thomas Chartier
born in Rodez, Aveyron, France
Oral-examination : Tuesday, November 28th 2017

Chemosensation in the marine annelid *Platynereis dumerilii* : anatomy, physiology, behaviour

Referees : Prof. Dr. Francesca Peri
Prof. Dr. Christoph Schuster

« […]
Le voilà qui déteste et jure de son mieux,
Pestant, en sa fureur extrême,
Tantôt contre les trous, puis contre ses chevaux,
Contre son char, contre lui-même.
Il invoque à la fin le dieu dont les travaux
Sont si célèbres dans le monde :
Hercule, lui dit-il, aide-moi, si ton dos
A porté la machine ronde,
Ton bras peut me tirer d'ici.
Sa prière étant faite, il entend dans la nue
Une voix qui lui parle ainsi :
Hercule veut qu'on se remue ;
Puis il aide les gens. Regarde d'où provient
L'achoppement qui te retient,
Ote d'autour de chaque roue
Ce malheureux mortier, cette maudite boue
Qui jusqu'à l'essieu les enduit,
Prends ton pic et me romps ce caillou qui te nuit ;
Comble-moi cette ornière. As-tu fait ? - Oui, dit l'homme.
- Or bien je vais t'aider, dit la voix ; prends ton fouet.
- Je l'ai pris... Qu'est ceci ! mon char marche à souhait !
Hercule en soit loué ! Lors la voix : Tu vois comme
Tes chevaux aisément se sont tirés de là.
Aide-toi, le ciel t'aidera. »

Jean de La Fontaine (1621-1695)
Book VI, Fable XVIII

Acknowledgements

This PhD time has been a true commitment, a time I will remember for sure. I am grateful to people who have helped me and accompanied me along this way and before.

First, thanks to Detlev for giving a chance in his lab to the motivated and ignorant engineer that I was, thanks for giving me lots of freedom and for providing the fantastic opportunity to be part of the NEPTUNE network. Thanks to Arendt Lab members for accompanying me through the years, notably those who have taught me a lot in the first months, Kaia, Heather, Elia… Thanks to Nirupama for teaching me soft lithography. Thanks to Maria Tosches who had first observed calcium responses in the nuchal organs, which prompted one and a half year of PhD and a major thesis chapter.

Thanks to Gáspár Jékely for sharing a lot of often unpublished knowledge, and for being so flexible on hosting me in his lab, notably for my 6-weeks stay improvised overnight in summer 2016, during which the first calcium imaging results have been obtained. Thanks to his whole lab for being welcoming and patient with me. Thanks to Csaba for technical advice and encouragements, thanks to Luis and Cristina for teaching me some molecular biology (and for passionate ping pong games on the Max-Planck terrace). Thanks to Milos the Bosniac, whose silhouette in the corridors made my imaging nights at the Max Planck less lonely.

Thanks to all members of the NEPTUNE network for unforgettable moments spent together all over Europe and for transmitting me their passion for marine biology. I have felt very lucky to spend entire weeks with friendly, enthusiastic and generous people, my PhD would have been quite different without them.

A special thanks to my friend Joran, for his comforting presence during this four years, for continuous support on many aspect of my project, for doing music and painting together, for singing Brassens, playing 10.000 with kleines Altbier, making tape roll drops, and above all for countless corridor chats. Without him I would still be operating my syringe pumps by hand, making my plots in Excel, and my figures in Paint : MERCI. Thanks to Laura for always welcoming me at their home and teaching me Lithuanian in the corridors. Thanks to Pierre-Luc for making my life so much better by moving to Heidelberg for his PhD. Thanks to Mathylde, Serge, Vlada, Kathi, Johannes, Claudia, Sara, Matthias, Yohann, Nelly, Veronika…

Thanks to my grandfather for telling me *Australopithecus* stories before I could even speak.

Thanks to my father for transmitting me his passion about neurology, and for always pushing me to give my best. Thanks to my mother who has supported me and my brothers in everything we did. And thank you Mum for permanent and invaluable supply of French food and home-made specialties, which helped me survive four years in a hostile culinary environment.

Thanks to my brothers for providing endless possibilities of physical exercise in our new house during holidays, and for keeping me connected with home.

Thanks to Marius for sparkling my interest in biology in long evening discussions, at a time when we were both lost.

Thanks to Alexandra Elbakyan for her courage and energy, her resource has been useful even at EMBL.

Finally, a special thanks goes to the 2017 Tour de France organisers, for giving Joran and myself an additional reason to stand up from bed every day while writing our thesis last July, and to the French “pâtés“ from Dordogne and Aveyron, for keeping us smily at any meal, any time, any place.

Three years of this work have been funded by the NEPTUNE Marie Curie grant, which has been a fantastic motor for scientific training and for travels.

Table of Contents

Abstract 1

Zusammenfassung 2

I – Introduction 3

I – 1 Comparative and evolutionary aspects of chemosensation 4

1.1 What is chemosensation ? 4

1.2 Chemical stimuli 4

1.3 Chemosensory behaviours 5

1.4 Mechanisms of chemosensation 5

1.5 Chemoreceptor proteins 7

1.6 Glomerular neuropils 10

1.7 Evolutionary scenarios of chemosensation 10

I – 2 *Platynereis* as a model for nervous system evolution 12

2.1 Lifestyle and characteristics 12

2.2 Available experimental techniques and resources 13

2.3 *Platynereis* for physiological studies of chemosensation 13

I – 3 Specific aims of the thesis 15

II – A comparative review of chemosensation in annelids. 16

II – 1 Introduction 17

II – 2 Anatomy 19

2.1 General body and nervous system architecture 19

2.2 Sensory structures and appendages in polychaetes 22

2.3 Sensory cell types in polychaetes 31

II – 3 Physiology 38

3.1 Physiological evidence for chemosensation in polychaete organs 38

3.2 Molecular physiology 43

II – 4 Chemosensory ecology : cues and behaviours 44

4.1 General chemical cues 45

4.2 Reproduction 45

4.3 Feeding 45

4.4 Larval settlement and metamorphosis 46

4.5 Aggression and avoidance 47

4.6 Environment probing 47

II – 5 Review summary 48
II – 6 Chemosensation in *Platynereis dumerilii* 49
6.1 Available literature on *Platynereis* 49
6.2 Putative chemosensory organs and their function 50
6.3 Relevant chemical cues 52
6.4 Chemoreceptor proteins 53
6.5 Summary for *Platynereis* 53
III – Neuroanatomy and development of presumed chemosensory organs 54
III – 1 Introduction 55
1.1 Candidate chemosensory organs are poorly characterised in *Platynereis* 55
1.2 A precise neuroanatomy is needed at 6 dpf 56
1.3 Experimental approach 56
III – 2 Materials and Methods 57
2.1 *Platynereis* culture 57
2.2 Anatomical stainings 57
2.3 Confocal imaging settings 58
2.4 Image processing 58
III – 3 Results 59
3.1 Most sensory appendages in *Platynereis* juveniles have at least two sensory cell types. 59
3.2 Development of head sensory organs 64
3.3 The main adult putative chemosensory organs are differentiated at 6 dpf and their nerves are formed 76
3.4 Mushroom Bodies are probably differentiated at 6 dpf 85
III – 4 Discussion 87
4.1 Candidate chemosensory organs : sensory cells and possible function 87
4.2 Development of the candidate chemosensory organs 89
4.3 Candidate chemosensory organs at 6 dpf 91
4.4 Conclusion 91
IV – Functional imaging of chemically-evoked neuronal responses 92
IV – 1 Introduction 93
1.1 Choice of a method for functional imaging of chemosensation 93
1.2 Principle of calcium imaging experiments 93
1.3 *In vivo* calcium imaging in a microfluidic device 96
1.4 Choice of stimuli 97
IV – 2 Materials and Methods 99
2.1 *Platynereis* culture 99
2.2 Microinjections of GCaMP mRNA 99

2.3 Chip design 99
2.4 Stimulus delivery 100
2.5 Stimulus protocol 101
2.6 Measurements of stimulus timing 102
2.7 Stimulus preparation 102
2.8 Experimental setup 102
2.9 Imaging settings 104
2.10 Image analysis 105
2.11 Mastermould and PDMS chips fabrication 105
IV – 3 Results 107
3.1 The setup allows a precise stimulus delivery 107
3.2 Calcium imaging with late nectochaete larvae is possible in this microfluidic setup 110
3.3 Anatomical identification is possible from the calcium signal alone 111
3.4 Calcium activity in the candidate chemosensory organs upon chemical stimulation 113
3.5 Calcium activity outside of the candidate chemosensory organs, related to the chemical stimulations 129
3.6 Calcium activity outside of the candidate chemosensory organs, with no direct link to the chemical stimulations 134
3.7 Calcium activity at the head surface 140
IV – 4 Discussion 141
4.1 Chemosensory systems in the head of 6dpf *Platynereis* larvae 141
4.2 Technical comments on calcium imaging 150
4.3 Conclusion 155
V – Chemosensory behaviour and associative learning assay 156
V – 1 Introduction 157
1.1 Microfluidic devices for behavioural experiments on marine larvae 157
1.2 Principle of a classical conditioning protocol 158
1.3 Learning in annelids 162
1.4 Strategy for establishing a chemosensory associative learning protocol 164
V – 2 Materials and Methods 165
2.1 *Platynereis* culture 165
2.2 Chip designs 165
2.3 Stimulus delivery 166
2.4 Conditioning protocol 167
2.5 Stimulus preparation 168
2.6 Experimental setup 168
2.7 Imaging 168

2.8 Preference index 169
2.9 Behavioural analysis 169
2.10 Master mould and PDMS chips fabrication 169
V – 3 Results 170
3.1 A constant flow in a microfluidic chamber influences larval behaviour 170
3.2 Larvae can interact with the chemical patterns 172
3.3 Towards a pavlovian assay for learning 174
V – 4 Discussion 181
4.1 Experimental setup 181
4.2 Stimuli 181
4.3 Response and quantification 183
4.4 Protocol parameters 185
4.5 Perspectives 185
VI – Other behavioural and physiological results 186
VI – 1 Behavioural experiments 187
1.1 A one-chamber design cannot provide a fast stimulus switching 187
1.2 Identifying an optimal animal density in a microfluidic chamber 187
VI – 2 Functional imaging 188
2.1 Identifying relevant dimensions for a microfluidic trap 188
2.2 Adding a 5'UTR sequence to the GCaMP mRNA improves expression of the calcium sensor 189
2.3 Looking for an inert dye to visualise stimulus changes 190
2.4 Calcium imaging with non-genetic dyes 191
VII – General discussion 194
VII – 1 Polychaete chemical senses and the evolution of chemosensation 195
1.1 The function of polychaete sensory appendages 195
1.2 Chemosensory systems in *Platynereis* compared to other phyla 197
1.3 Towards a study of chemical senses in other marine invertebrates ? 200
1.4 Evolution of chemical senses and the adaptation to terrestrial life 201
VII – 2 *Platynereis* as a model for neurobiology 203
2.1 Is an annelid model relevant in neurobiology ? 203
2.2 Functional imaging in *Platynereis* 204
2.3 Connectomic data and behaviour 204
2.4 Single-cell gene expression data 206
2.5 Molecular and functional tools 206
2.6 Conclusions 207

Appendix ……210

A. Species and synonyms in the comparative review……209
B. Microinjections in fertilised *Platynereis* eggs……215
C. Plasmids used for GCaMP mRNA synthesis……219
D. Aladdin pumps hardware-software configuration……224
E. Operational protocol for master mould fabrication……227
F. Additional calcium activity traces……229

References ……233

Abstract

Chemical stimuli are omnipresent in driving all kinds of animal behaviours. The comparative study of chemosensory systems has revealed a wide variety of organs, neuronal circuits, and above all of receptor proteins. Despite some conserved features, no clear picture has emerged yet about the origins of chemoreception, and new animal models are needed to understand its evolutionary history.

The marine worm *Platynereis dumerilii* (Nereididae, Polychaeta, Annelida, Lophotrochozoa) is a model system for evolutionary developmental biology, and recent achievements have revealed its potential for neurobiology. The head of marine annelids is generally equipped with abundant sensory appendages, chemosensory based on numerous morphological descriptions. Surprising as it may seem for this ecologically important phylum, there exists still no direct physiological proof of chemosensitivity in these prominent organs. Moreover, in the absence of appropriate assay systems, physiological experiments in *Platynereis* have so far concentrated on photic and mechanical stimuli.

The aim of this thesis was the description and physiological study of chemosensory systems in *Platynereis*, as well as the establishment of microfluidics-based methods to enable functional imaging and behavioural assays upon chemical stimulations. The 6-days-post-fertilisation larval stage (6dpf), at which most adult anatomical structures are already present, has emerged as a powerful stage for cross-species comparisons of cell types, thanks notably to a unique whole-body atlas of gene expression. It was thus chosen as a target stage for the study of chemosensation.

An anatomical investigation of *Platynereis* head appendages at various stages has allowed to better understand how the hemispheric head of larvae transforms into the complex, appendage-rich head of juveniles and adults. Neuroanatomical stainings have confirmed the presence already at 6dpf of different architectures, innervation patterns, and sensory cell types across appendages. A reference anatomical description has been established at 6dpf to characterise the position of nerves and sensory ganglia, which constitutes a useful basis for *in vivo* studies.

After having developed a microfluidic setup for confocal calcium imaging of the whole head upon chemical stimulations, I have tested the physiology of candidate chemosensory organs in 6dpf animals. These experiments have revealed that antennae, not nuchal organs as thought previously, are probably the main chemosensory organ in *Platynereis*, that nuchal organs and palps are endowed with chemosensitivity, and that so are tentacular cirri though to a lesser extent. Prominent fluctuating apical organ activity was seen, though not obviously related to chemosensation. Finally, new components of the chemosensory systems have been described based on their activity patterns, including sensory cells and probably interneurons. Based on these results, a first understanding of chemical stimulus detection has emerged. Partial evidence was given that Mushroom Bodies may play a role in these systems at 6dpf, which motivates the study of associative learning in relation with chemical cues.

To link chemical stimuli to larval behaviours, additional microfluidic devices have been developed in which freely-moving larvae can be exposed to controlled spatial and temporal patterns of chemical stimuli and their behaviour monitored. In the perspective of establishing an assay for chemosensory associative learning, aversive compounds such as quinine have been tested and found to produce stereotypical avoidance behavioural responses, thus they could be used as unconditioned stimuli in pavlovian assays. A neutral cue identified in functional imaging, 1-butanol, was shown to be a valid candidate as a conditioned stimulus. Thanks to these preliminary results, an experimental setup for quantitative studies of behavioural modifications is now available.

Overall, this work has laid a basis for the study of chemosensation in *Platynereis*, informed about sensory organ physiology in polychaetes, and shown the suitability of microfluidic setups for physiological and behavioural assays at larval stages. It suggests a possibly broad chemosensory repertoire in marine invertebrate larvae. Chemical stimuli in annelids are worth new attention for comparative studies of sensory systems, and in the search for associative learning abilities.

Zusammenfassung

Die Perzeption von chemischen Stimuli ist die Grundlage für eine Vielzahl an tierischen Verhaltensweisen. Durch den Vergleich von chemosensorischen Systemen wurde eine große Vielfalt von Organen, neuronalen Schaltkreisen und vor allem von Rezeptoren entdeckt. Obwohl eine Vielfalt an Mechanismen konserviert ist, ist es bis jetzt unklar wie sich die Chemorezeption im Laufe der Evolution entwickelt hat. Neue Modellorganismen sind nötigt, um diese Entwicklung besser nachvollzuziehen zu können.

Der Borstenwurm *Platynereis dumerilii* (Nereididae, Polychaeta, Annelida, Lophotrochozoa) ist ein Modellorganismus in der evolutionären Entwicklungsbiologie und Neurobiologie. Im Allgemeinen ist der Kopf von Seeanneliden mit vielen Sinnesorganen augestattet, die laut anatomischen Studien als chemosensorisch betrachtet werden. So überraschend es klingen mag, für diesen aus ökologischen Sicht wichtigen Stamm ist die Chemosensitivität von diesen prominenten Organen noch durch keine physiologische Befunden gestützt. Da bisher keine geeignete Versuchsmethode vorhanden war, wurde durch physiologische Experimente vor allem die Reaktion auf Lichtreize und mechanische Stimuli untersucht.

Das Ziel dieser Doktorarbeit ist die anatomische Beschreibung und physiologische Charakterisierung von chemosensorischen Systemen in *Platynereis*, sowie die Etablierung von Mikrofluidik basierenden Methoden zur funktionellen Bildgebung von chemischen Stimulierungen bei Verhaltensexperimente. Die 6 Tage alten Larve (6dpf, days-post-fertilization) wurde hierfür gewählt, da die meisten anatomischen Strukturen der adulten Tiere schon ausgebildet sind und für dieses Stadium zudem ein Genexpressionsatlas erstellt wurde, der den Vergleich von Zelltypendentitäten zwischen Spezies auf der molekularen Ebene ermöglicht.

Die schrittweise Umwandlung des runden larvalen Kopfes in den komplexen Kopf der adulten Tiere wurde durch anatomische Studien der Sinnesorganen von *Platynereis* in verschiedenen Entwicklungsstufen dokumentiert. Neuroanatomische Färbungen der Sinnesorgane der 6 Tage alten Larve haben die Präsenz von verschiedenen Organarchitekturen, Innervationsweise und Sinneszelltypen aufgedeckt. Außerdem wurde für die 6 Tage alte Larve eine anatomische Beschreibung der Lage von Nerven und sensorischen Ganglien gegeben, die Grundlage für folgende *in vivo* Studien darstellt.

Nachdem ich eine neue Mikrofluidik-basierte Methode für kopfweite Calcium-Bildgebung durch Konfokalmikroskopie aufgestellt hatte, habe ich die Physiologie der mutmaßlich chemosensorischen Organe in der 6 Tage alten Larve getestet. Die Ergebnisse zeigten, dass die Antennen, und nicht die Nuchalorgane, wahrscheinlich das zentrale chemosensorische Organ von *Platynereis* sind. Zudem konnte gezeigt werden, dass die Nuchalorgane und die Palpen tatsächlich chemosensorische Eigenschaften haben, sowie die tentakulären Cirren, wenn auch in geringerem Ausmaß. Eine prominente, fluktuierende Calcium-Aktivität wurde im Apikalorgan beobachtet, jedoch ohne deutliche Verbindung mit den chemischen Stimuli. Des Weiteren wurden neue Elemente des chemosensorischen Systems beschrieben, einschließlich Sinneszellen und Interneurone. Diese Ergebnisse legen die Grundlage für das Verständnis der chemischen Wahrnehmung. Es wurde teilweise nachgewiesen, dass die Pilzkörper (Mushroom Bodies) in diesem chemosensorischen System in der 6 Tage alten Larve involviert sind. Dieses Beobachtung fördert die weitere Untersuchung von assoziativen Lernfähigkeiten im Zusammenhang mit chemischen Stimuli.

Um die Auswirkung von spezifischen chemischen Reizen auf dem larvalen Verhalten zu untersuchen, wurden zusätzliche Mikrofluidik-Plattformen entwickelt, in denen sich die Larven in raum-zeitlich kontrollierten chemiksche Reizen frei bewegen. Bei dem test von Substanzen wie Chinin has sich ergeben, daß diese einen aversiven Reiz auslösen, undzwar sogar mit stereotypischen Vermeidungsverhalten, und daher passende unbedingte Stimuli darstellen in der Perspektive eines Versuchs für assoziatives Lernen. 1-butanol hingegen konnte als neutraler Stimulus identifiziert werden. Dank dieser Ergebnisse ist jetzt ein geeigneter Versuchsaufbau für die quantitative Untersuchung von Verhaltensmodifizierungen von *Platynereis* etabliert.

Diese Arbeit legt eine Basis für die weitere Studien zur chemosensorischen Perzeption in *Platynereis*. Sie liefert Informationen über die Physiologie der Sinnesorganen in Polychäten und hat gezeigt, das Mikrofluidik für physiologische und Verhaltensversuche in larvalen Stadien geeignet ist. Zudem deuten die Ergebnisse auf ein breites Verhaltensrepertoire von marinen Invertebratenlarven hin. Die Verarbeitung von chemischen Stimuli in Anneliden sist neuer Aufmerksamkeit würdig, sowohl für die vergleichende Studie von Sinnesystemen als auch für das Verständnis von assoziativen Lernfähigkeiten.

I – Introduction

I – 1 Comparative and evolutionary aspects of chemosensation

1.1 What is chemosensation ?

Chemosensation is the ability to detect chemical compounds. It is found in all living forms, from unicellular organisms like bacteria [1] and slime molds [2], to complex multicellular organisms such as plants [3] or animals (molluscs [4], insects [5] or vertebrates). All other sensory abilities in contrast, photosensation, mechanosensation, electrosensation, magnetosensation, thermosensation, deal with the detection of physical and not chemical signals.

In humans, the most obvious forms of chemosensation are the senses of smell and taste, which are respectively the detection of volatile cues acting at a distance and the detection of soluble cues acting at contact. However this traditional distinction can become troublesome when taking a broader look, for example when comparing aquatic and non-aquatic species – this point will be dealt with later on. For the moment, it is preferable to keep a more general definition and simply speak about chemosensation, or its synonym chemoreception, as being any chemical sense.

Words like 'odour', 'smell', 'scent', 'fragrance', 'aroma', 'flavour', 'odorant' will be avoided since they convey meanings that vary according to the context and the authors, and carry with them human biases due to our own perceptions of chemicals and subjective experiences. Instead, the word 'chemical compound' will be used for a molecule (or ion) in general, and 'chemical cue' or 'chemical stimulus' will be used if this molecule (or mixture of molecules/ions) can be detected by the species considered.

1.2 Chemical stimuli

Chemosensation is the only sensory modality for which a stimulus consists of actual material elements – a molecule or an ion that binds to a receptor. For all other modalities, the stimuli reside in physical phenomena : electromagnetic radiations (photic, electric or magnetic stimuli), mechanical waves and contact forces (mechanical stimuli, including acoustic ones), molecular kinetic energy (temperature), gravitational forces (gravity).

A compound is not *per se* a stimulus or not. A compound is a stimulus only in the context of an animal detecting it, in the same way that we humans do not detect radio waves though they have exactly the same nature as visible light : they are electromagnetic waves. Dinitrogen as a gas is not a cue for humans because we cannot smell it although we breathe it constantly.

A wide variety of compounds can act as chemical stimuli for living organisms, depending on a species' evolutionary history, genome and ecology [6]. In fish for example, it was shown that amino acids, peptides, steroids, prostaglandins, nucleotides or aliphatic acids are major chemosensory cues [7]. In insects, different classes of compounds act as cues, typically small volatile molecules alcohols, esters, terpenes or arenes [8]. It should be noted that both aquatic and non-aquatic animals can have at the same time contact and distance chemoreception, as is true for the fly *Drosophila* [9], and for the marine gastropod *Aplysia* [10].

There are two principal parameters in a chemical stimulus : nature (identity of the molecule) and intensity (molecular concentration in immediate proximity of the organism). Moreover, chemical cues rather occur as pure compounds in nature, but rather as mixtures of compounds [11], and chemosensory systems can also encode for mixtures as being different from the sum of their compounds, as was demonstrated in rats [12] or honeybees [13]. Chemical cues by essence are non-directional, nevertheless spatial information can be extracted regarding their distribution and

provenance, which requires either detection from parts of the body that are distant enough to capture relevant differences, or integration over time as the organism or the source is moving. This has been described both for volatile compounds in aquatic environments, and for soluble compounds in aerial environments. Diffusion is a very slow process over the millimetric scale, thus mobile cues are mostly transported by turbulent flows of the medium, with the consequence that stimulus intensity can be comparable at the source and far from it, and is not always informative about distance. However, integration of temporal patches of stimulus in a regular flume can be enough to locate the source, as was demonstrated for seabirds with dimethylsulfide [14], moths with pheromones [15], and prey metabolites in crustaceans [16],[17]. In accordance with such abilities, it was shown that in species with complex brains neuronal networks are capable of temporal odour coding [18], depending on frequencies relevant for their ecology (for example, up to 4 Hz for a lobster, up to 10 Hz in the moth *Manduca*).

1.3 Chemosensory behaviours

Chemical cues provide useful information on the nature, location, quantity of matter and organisms around an individual. Not surprisingly, chemosensation has been shown to be involved in most animal activities. On a short time scale, in order to survive an animal needs to avoid being killed or injured, for example by rapid environmental changes or by predation. Chemical cues can inform about changes in physiological parameters such as oxygen levels [19] or acidification, or presence of a predator [20]. On a longer time scale, in order to survive an animal needs to feed. It is obvious that chemosensation is used to identify food and decide whether or not to consume it [21], but it also used to locate and reach sources of food [8],[22], as well as assess [23] and remember their value [24]. On a yet longer time scale, in order to survive a species need its individuals to reproduce, and here again chemical stimuli are used for behaviours such as egg-laying in insects [8], or parental care in mammals [25] or crustaceans [26].

Importantly, chemical cues are also used in inter-individual communication, notably in aggression, aggregation, territory marking, mating, kin recognition. Chemical cues used for communication between conspecifics are called pheromones. For example, the lobster *Panulirus argus* uses urine-borne chemical compounds to support social status in fights with conspecifics, and it was showed that aggressive behaviours lasted longer if this urine release was prevented [27] ; sulcatol was shown to be an aggregation pheromone in the beetle *Gnathotrichus sulcatus* [28] ; many species mark their territory with urine and other chemical signals, as is well known is dogs, but also ants [29], beavers [30], and mice [31] ; sexual pheromones are used by moth to attract mates and favour reproduction, which has been exploited for the control of pest species in agriculture [32], and used by marine polychaete worms to triggers egg and sperm release [33] ; kin recognition is mediated by chemical cues in species like social wasps [34] and salmon [35].

As this variety of examples illustrates, chemoreception in the animal world is a much more important sense than one would maybe expect based on our human perspective, since as primates we are an eminently visual species, and cultural as well as social aspects notably in occidental civilisations have often made olfaction a disregarded or even despised sense.

1.4 Mechanisms of chemosensation

Chemosensation starts with the detection of a molecule by a cell. Except for non-specific detections such as effect of osmotic stresses on cells, as far as is known such detection is performed by a receptor protein, situated across the membrane of the cell. Upon binding, a series of signalling reactions is initiated inside the cell which transmit the information. In an animal with a nervous system – that is, all animals except sponges and placozoans – this information is passed on to the next cells of the neuronal circuit, and can ultimately result in a behaviour or a change in physiological state.

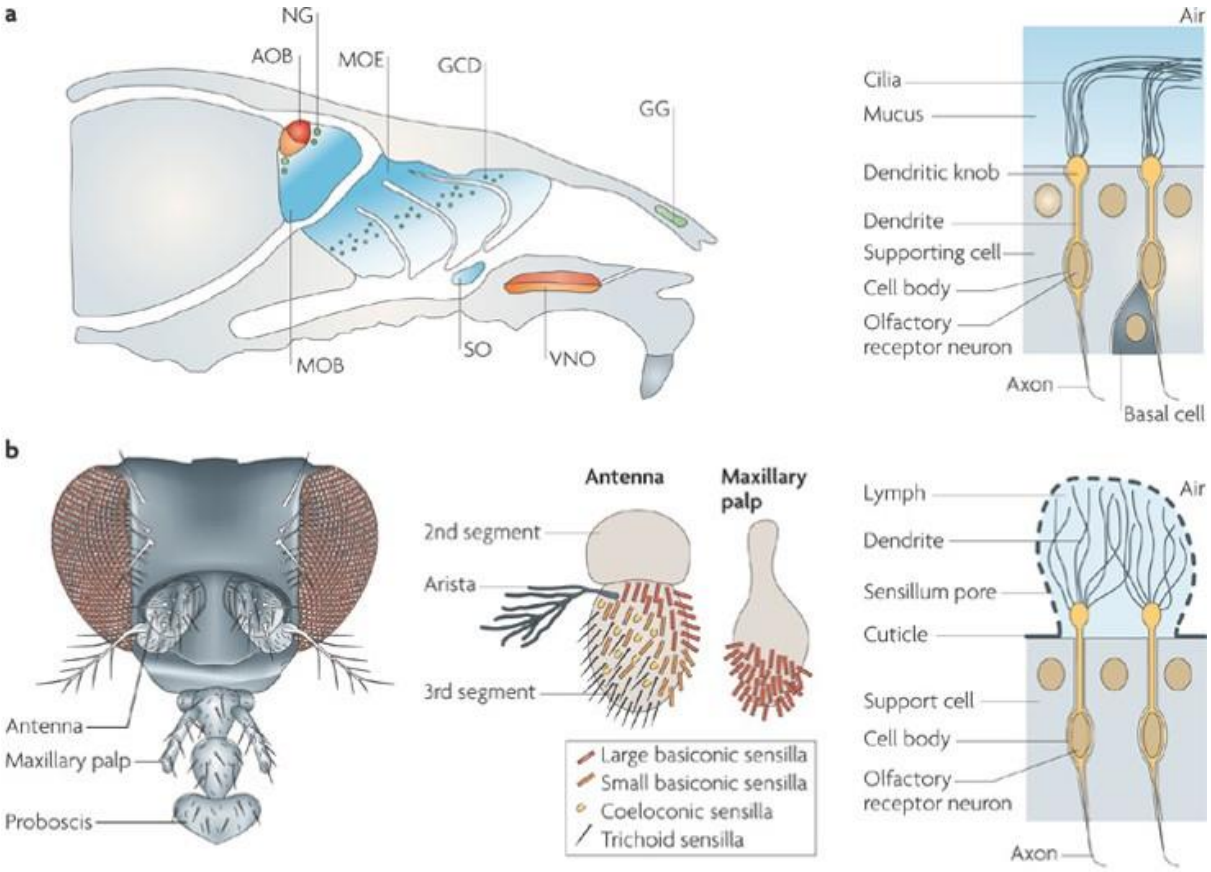


Figure I-1 Localisation and morphology of chemosensory cells. Example of the olfactory systems in (a) the mouse (Mus musculus), and (b) the fruit fly (Drosophila melanogaster). Reproduced from Knaupp, 2010 [36].

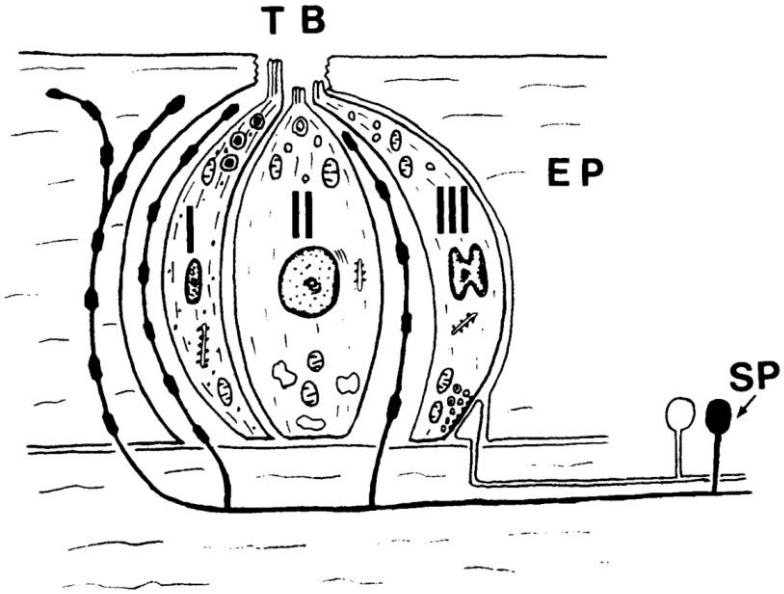


Figure I-2 Taste bud in the rat. Drawing based on an electron microscopic study. TB indicates the opening in the epithelial surface (EP), taste cells of type I to III are represented. Note synaptic contact of cell III with a dendrite, which is the site where gustatory information is transferred. Reproduced from Yamasaki, 1984 [37].

The detection of a molecule by a cellular organism surely does not require neurons, like the reports of chemotaxis in unicellular organisms such as bacteria [38],[1] and slime molds [2] or multicellular organisms such as sponge larvae [39] have clearly demonstrated. Nevertheless, it has been best studied in the context of neurons.

Chemosensory neurons in the olfactory system of mammals and insects are typically bipolar cells with one or several dendritic processes protruding from a protective epithelium, and in communication with the outside medium via a mucus that either covers the epithelial surface (mammals), or fills the inside of a porous sensillum (insects). Figure I-1 illustrates this receptor morphology in a mouse and in a fruit fly ; note that in the fly the mucus is inside the porous cuticle are communicates with the air only through minute openings, whereas in the mouse it is directly exposed to the air. Not all chemoreceptor cells are neurons, indeed in the gustatory system of vertebrates reception takes place in modified epithelial cells located in small cavities called taste buds [37], as depicted on Figure I-2. These sensory cells possess apical microvilli, and communicate with neurons via neurotransmitter release [40].

1.5 Chemoreceptor proteins

The first chemoreceptor proteins have been discovered in 1991 by Richard Axel and Linda Buck [41], who have been awarded the Nobel Prize in 2004 for their discovery, and since then our understanding of the molecular mechanisms of chemosensation have made tremendous progress. These proteins are part of the large family of G-protein-coupled receptors (GPCRs), which constitute up to 10% of an animal's genes as in the case of the elephant, and possess seven transmembrane domains. Other types of chemoreceptors have been identified, notably in insects the so-called inverted receptors, that have also seven transmembrane domains but have their N- and C-terminus on opposite side of the membrane as compared to GPCRs [42], and variant of the glutamate ionotropic receptors, called IRs for Ionotropic Receptors, which are proteinic receptors with yet another structure [43].

To date, at least sixteen types of chemoreceptors are described, whose variety of structure is represented in Figure I-3. It appears that the use of GPCRs as chemoreceptors is far from being the rule, contrary to what could have been hypothesised after the initial discovery of GPRC-ORs in mammals.
Receptors overall can be sorted in two categories : (1) metabotropic receptors like the GPCRs or the guanylyl cyclase receptors, which use a signalling cascade to indirectly induce ion entry in the cell upon binding of their ligand, and which are predominant in mammals, and (2) ionotropic receptors like the insect ORs and GRs or the widespread protostomian IRs, which directly permit ion entry in the cell upon binding of their ligand. These two operating modes are depicted in Figure I-4. Ionotropic receptors are more direct hence faster, metabotropic receptors are less direct thus open to more modulation. For more details on the two modes of signalling, see [44]. It should be noted also that insect inverted ORs function as a heterodimer with the co-receptor OR83b [42],[45]. Similarly, it has been suggested that mammalian ORs would function as dimers, in this case homodimers since only one receptor gene is expressed per cell [46].

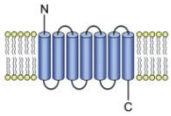
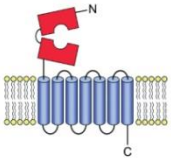
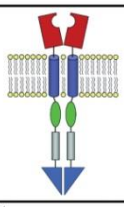
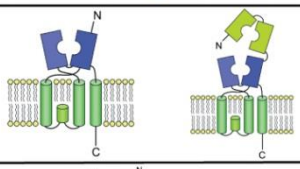
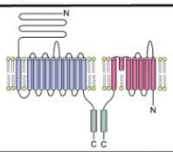
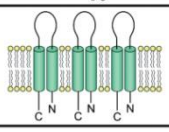
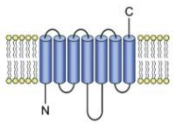
Type	Molecular Structure	Name	Taxa
Metabotropic 7TM GPCR		OR-like	Cnidaria, Cephalopoda, Echinodermata
		OR	Nematoda, Mollusca
		OR	Chordata
		TAAR	Chordata
		V1R	Chordata
		T2R	Chordata
		FPR	Chordata
		V2R	Chordata
		T1R	Chordata
Metabotropic 1TM		rGC	Nematoda, Vertebrata
Ionotropic		IR	Protostomia (including Crustacea)
		TRP	Insecta, Vertebrata
		ENaC	Vertebrata
Ionotropic 7TM		Grl	Cnidaria, Placozoa, Lophotrochozoa, Ecdysozoa, Echinodermata, Hemichordata
		GR	Chelicerata, Myriapoda, Crustacea (Branchiopoda), Insecta
		OR	Insecta

Figure I-3 Summary of the receptor molecules, with distribution, characteristics, and schematized molecular structure. OR, odorant receptor ; OR-like, OR-like receptor ; TAAR, trace amine-associated receptor ; V1R and V2R, vomeronasal receptor type 1 and 2 ; FPR, formyl-peptide receptors ; T1R and T2R, taste receptor type 1 and 2 ; rGC, receptor guanylyl cyclase ; ENaC, epithelial sodium channel ; TRP, transient receptor potential channel ; Grl, gustatory receptor like receptor ; IR, ionotropic receptor ; GR, gustatory receptor ; TM, transmembrane. Reproduced from Derby et al., 2016 [47].

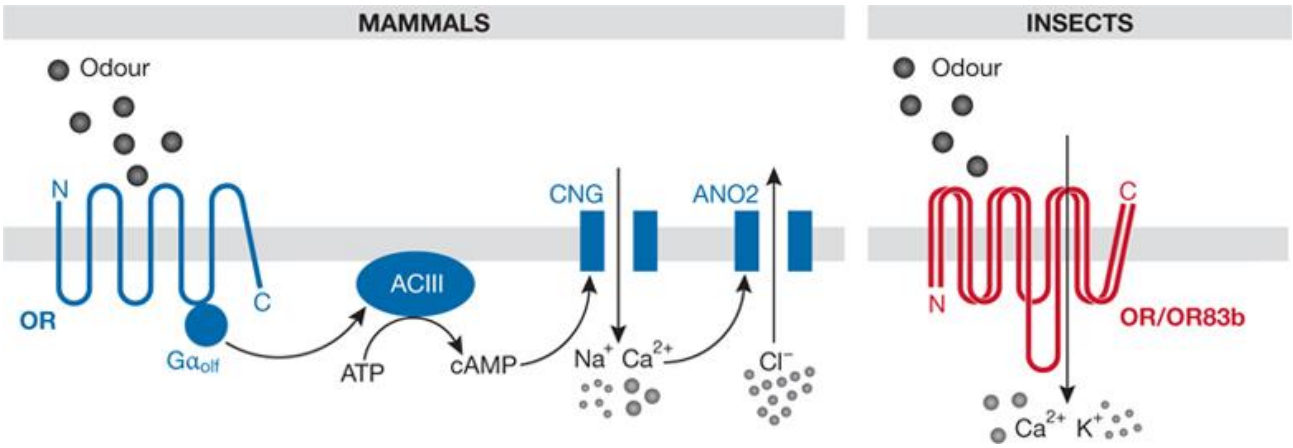


Figure I-4 Comparison between metabotropic (blue, left, GPCR) and ionotropic (red, right, inverted GPCR) chemoreceptors. Reproduced from Silbering and Benton, 2010 [44].

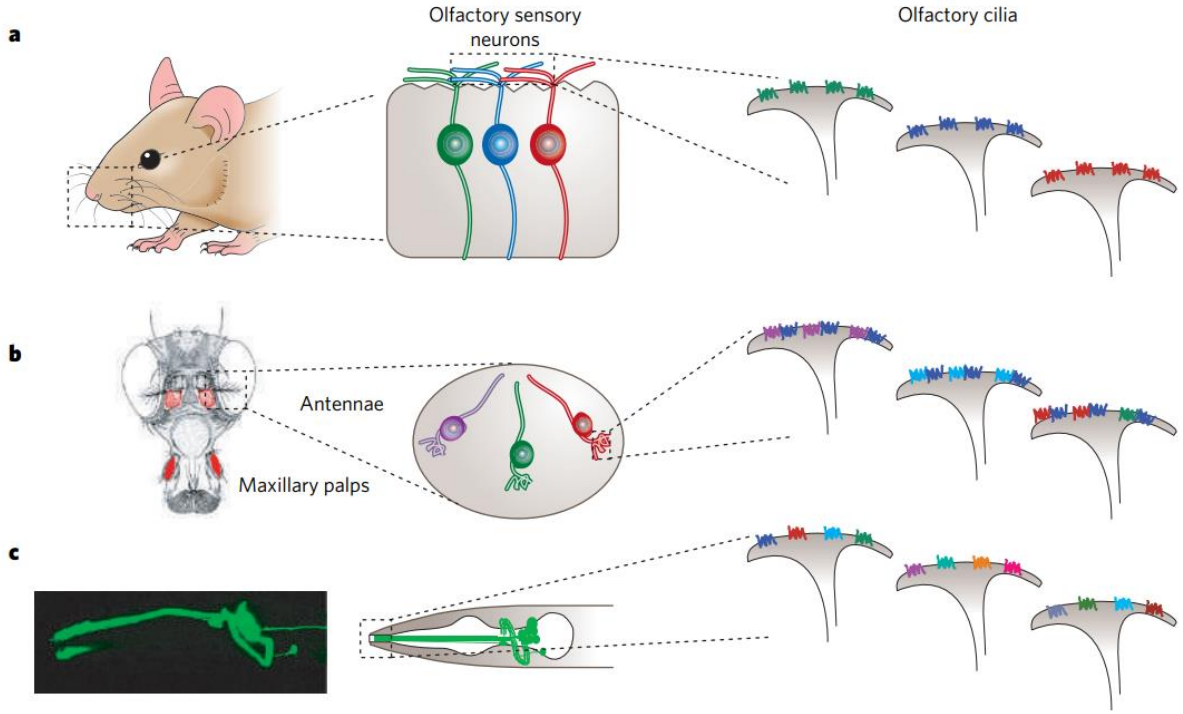


Figure I-5 Localisation and expression of chemoreceptors in (a) the mouse (Mus musculus), (b) the fruit fly (Drosophila melanogaster) and (c) the nematode (Caenorhabditis elegans). In the dendritic endings represented on the right part of the figure, each colour stands for a particular receptor protein. One (a,b) or several (c) specific receptors can be expressed per sensory neuron. In the fruit fly, a specific receptor always occurs together with a general co-receptor (dark blue). Reproduced from Bargmann, 2006 [48].

For receptors detecting air-borne cues in terrestrial animals, additional proteins called Odorant-Binding Proteins (OBPs) can be found in immediate proximity, that help solubilise the hydrophobic volatile compounds and promote their binding to the receptor. Such proteins have been only described in vertebrates, and in insects but not in crustaceans and not even in non-insect terrestrial Arthropods [47]. They thus may represent two independent innovations linked with adaptation to life on land.

Chemoreceptor proteins are located in the membrane of these dendritic endings, where they can bind chemical signals. Different expression strategies have been implemented in different phyla : one specific receptor only per chemosensory neuron (mammals, Figure I-5A), one specific receptor and one general co-receptor per chemosensory neuron (insects, Figure I-5B), several specifics receptors per chemosensory neuron (nematodes, Figure I-5C). These different strategies can also be understood if one compares the number of sensory neurons (10 million in the mouse, a few tens in the nematode) and the number of receptor genes (around 1.000 both for the mouse [41] and for the nematode [48]) : even though expressing one receptor per cell probably enhances the olfactory signal accuracy, this would not allow the nematode to make full use of its genetic olfactory potential.

1.6 Glomerular neuropils

In the olfactory system of vertebrates, arthropods, crustaceans and some molluscs, a neuropil architecture called 'glomeruli' is commonly found. Is consists of discrete entanglements of nervous fibres located in the central nervous system, at the level of the axonal projections of primary sensory neurons. These glomeruli are a place of synaptic contacts, and involve projection neurons as well as local interneurons. They can be of round shape as in vertebrates, insects and isopod crustaceans, or of conical shape as in decapod crustaceans [49]. No obvious correspondence exists between the location of a glomerulus and the stimulus that activates it, but there is only a given set of stimuli that will activate a given glomerulus [50]. In vertebrates as well as in insects, it seems that all sensory neurons that express the same receptor project on the same glomerulus [51][52]. There is a consensus that the glomerular organisation is crucial for olfactory coding, though it remains unclear how [50]. Despite striking morphological similarities in this neuronal organisation across distant species, the fact that they are absent in cephalochordates and urochordates [53][54] which are close outgroups to vertebrates, as well as in the taxa of damselflies, dragonflies and mayflies [55] which are close outgroups to neopteran insects, strongly suggest that they have evolved several times independently, and are thus good examples of convergent evolution.

1.7 Evolutionary scenarios of chemosensation

No clear picture has emerged yet concerning how the different animal chemosensory organs and receptor proteins would have evolved and diversified. In contrast with photoreception, for which a clear scenario involving an early split between ciliary and rhabdomeric opsins is now well supported [56], there does not seem to be such a unified evolutionary history for chemoreception, as the enormous variety of receptor proteins suggests. Gene duplication and genetic drift have played important roles in the evolution of these receptors [57], and as a consequence chemoreceptor families are often rich in pseudogenes – for example about 20% in the case of the mouse [58].

A major question concerns the evolution of the chemosensory nervous systems, in which striking organisational similarities have been uncovered. These systems in insects and vertebrates have the following common characteristics : 1) bipolar primary sensory neurons expressing one specific receptor each, 2) projection of the primary sensory neurons to a glomerulus structure that contains inhibitory interneurons, 3) all primary neurons projecting to a glomerulus express the same receptor. Since the organisation of the first layer of neurons is so similar, is that a necessary architecture for a chemosensory system ? Does this represent rather an ancestral state in bilaterian animals or rather an

evolutionary convergence ? Moreover, secondary neurons project to the Mushroom Bodies in insects, and to the olfactory cortex in vertebrates, two brain regions that have similarities in developmental gene expression and in anatomy [59]. For example, it was shown that in insects the size and partitioning of Mushroom Bodies correlates with feeding ecology, even within taxa that are distantly related, with generalist plant feeders having more surface area and volume of their Mushroom Bodies than specialist feeders [60]. The authors have hypothesised that this increase would be due to a demand for more complex and more rapid sensory information processing, and have related this observation with the evolution of enlarged cortical areas in mammals and notably primates. What is thus the degree of homology of Mushroom Bodies and olfactory cortex, and has the chemical sense played an important role in their evolution ?

To date, most of our knowledge on chemosensation in the animal kingdom concerns the phyla of chordates (fish, amphibians, mammals), and arthropods (insects, crustaceans) as well as – though to a lesser extent – nematodes (with one species, *Caenorhabditis elegans*) and molluscs (only gastropods), as reviewed in [50]. Non-deuterostomes, and specially the superphylum of Lophotrochozoa, are underrepresented, and our current lack of understanding calls for a better taxon sampling in comparative studies of chemosensation, including other important lophotrochozoan groups such platyhelminthes (flatworms, 25.000 species [61], compare with mammals 5.500 species) or annelids (16.500 species [61]).

With the recent surge of genomes available, it has become possible to compare families of chemoreceptors across numerous species. One of the surprises has been the unexpected diversity of receptors, even in closely-related taxa. As mentioned already, mammals and insects use completely different sets of receptors. More striking examples are dipterans such as the fruit fly *Drosophila melanogaster* or the mosquito *Anopheles gambiae*, that have quite different chemoreceptors than the hymenopteran honey bee *Apis mellifera* [62] which shows a strong expansion of its olfactory receptor family, and the crustacean *Daphnia pulex*, which despite being an arthropod as are insects, has none of the insect olfactory receptors in its genome [63].

In the present work, chemosensation is studied in the annelid *Platynereis dumerilii*, a marine worm representative of Lophotrochozoa and already established as a laboratory model organism.

Further documentation on chemosensation can be found in the following reviews :
on chemosensory receptor genes, Nei, Niimura & Nozawa 2008 [57] ;
on olfactory receptor types, Spehr & Munger 2009 [64] ;
on olfactory signalling in vertebrates and insects, Kaupp 2010 [36] ;
on ionotropic and metabotropic receptors, Benton 2010 [44] ;
on the evolution of chemosensory nervous circuits, Eishten 2002 [50] and Bargmann 2006 [48] ;
on the evolution of insect olfaction, Hansson & Stensmyr, 2011 [8].

I – 2 *Platynereis* as a model for nervous system evolution

2.1 Lifestyle and characteristics

Platynereis dumerilii is a model organism for evolutionary developmental biology (evo-devo). It is a marine segmented worm, from the phylum of Annelida, which includes also earthworms and leeches. *Platynereis* belongs to the class of Polychaeta, which comprises around 10.000 species.

Its lifestyle is typical of marine invertebrates, since it includes a pelagic, larval period, and a benthic, adult period (Figure I-6). Adults become sexually mature at the end of their lifetime only (3 to 6 months in the laboratory) and become pelagic again for a few days until they reproduce by releasing gametes in the open water. Reproduction is synchronised by the moon cycles [65].

Genomic analyses have revealed that *Platynereis* has been evolving at a slower pace than standard invertebrate models such *Drosophila* and *Caenorhabditis*, and that its genome shares more features with vertebrates than with Protostomes [66].

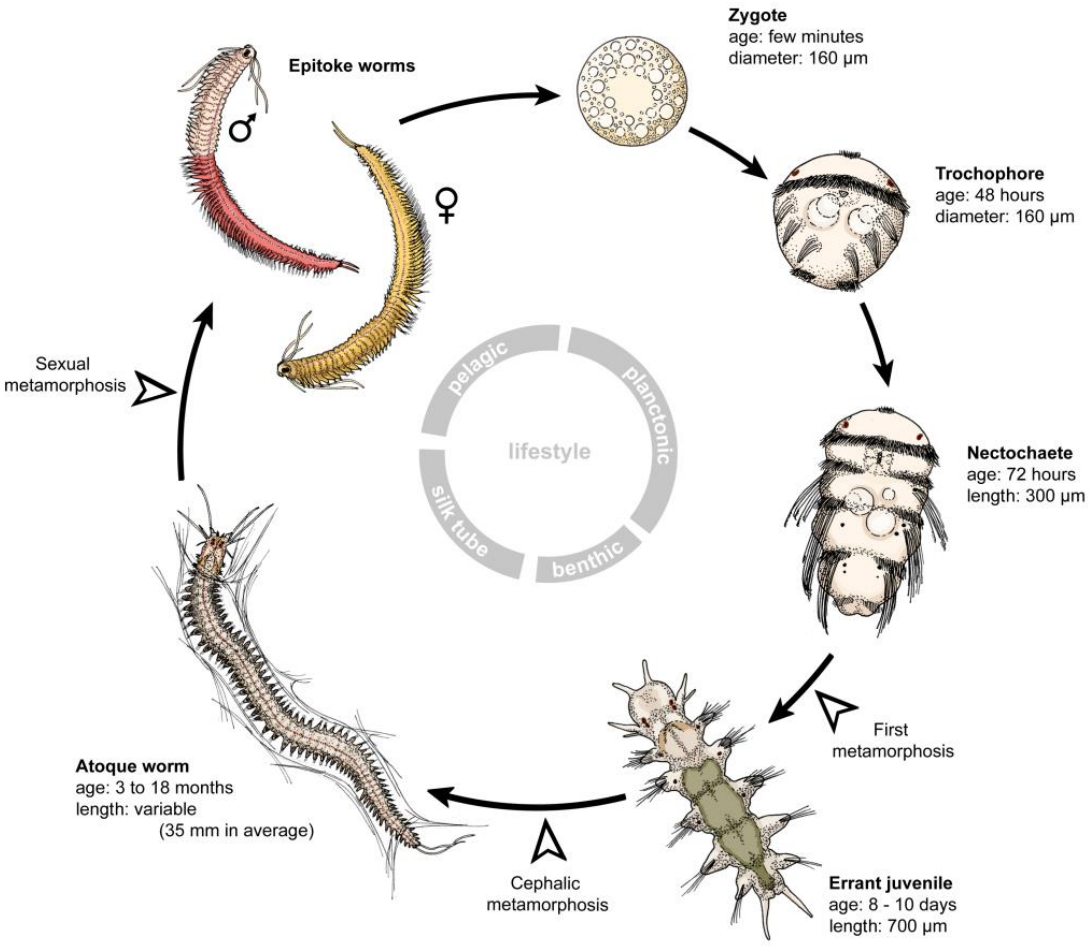


Figure I-6 Platynereis life cycle. Artwork copyright : Adrien Demilly (modified from Hauenschild, 1974 ; Fischer et al., 2010).

Platynereis larvae notably have been studied, thanks to their transparency, to their stereotypical and synchronised development. *Platynereis* has proved to be a valuable model in the study of nervous system evolution in Bilateria. Some of the main findings relate to eyes and photoreception [67], [68], nervous system centralization, circadian rhythms, segmentation [69]–[71], and evolutionary

connections have been established for some anatomical structures of annelid with the insect Mushroom Bodies and vertebrate cortex [59], as well as with the vertebrate notochord [72].

2.2 Available experimental techniques and resources

Platynereis is amenable to a wide variety of techniques, which include all kinds of light and electron microscopy [73][74], mRNA *in situ* hybridization, zygote microinjection, functional studies with morpholinos [75] and knock-outs [76]. Stable transgenesis has been achieved thanks to transposons [77].

Its genome and transcriptome have been sequenced, and whole-body single-cell transcriptomic data has been obtained [78].

Two major resources are being developed, notably a whole-body atlas of gene expression that allows cross-species comparisons of cellular types [73], and a whole-body neuronal connectome as part of which entire functional neuronal circuits could already be reconstructed.

Despite all these techniques, most of the knowledge currently available for *Platynereis* concerns anatomy, development and gene expression ; limited knowledge has been gathered regarding the physiology of its different body systems or cell types. Nevertheless, several studies have been conducted concerning the function of neuronal circuits, notably for visual phototaxis, ciliary locomotion and the startle response, but behavioural experiments have been mostly restricted to light and mechanical stimuli.

In order to investigate the physiology of chemosensory systems, new assays and approaches are needed, as will be explained in further detail in Section IV.

2.3 *Platynereis* for physiological studies of chemosensation

Physiological studies on sensory systems are best conducted *in vivo*, meaning that sensory organs or cells of interest need to be recognised in living specimens. If the straightforward observation of transmitted light under a microscope is not sufficient to distinguish a structure, some help can be found in specimen preparation, to artificially render this structure easier to localise and identify. This is typically achieved by the use of stains.

In a fixed *Platynereis* specimen, in addition to classical neuroanatomical staining techniques for transmitted light, such as Golgi staining, iron haematoxylin staining or Cason's trichrome staining, a variety of fluorescent staining techniques are available from general histochemistry (e.g. DAPI, Rhodamine-phalloidin, FM 4-46 FX) and immunohistochemistry (e.g. antibody against α-acetylated tubulin for nervous fibres, or against the neuropeptide FMRF-amide, see [68]). Besides, primary antibodies specific for *Platynereis* proteins have been successfully developed, notably for neuropeptides (see [79]). It is thus possible to visualise cell nuclei, membranes, muscle fibres, cytoskeleton elements, nervous fibres, as well as the presence of various neurotransmitters and neuromodulators. Rich anatomical knowledge can therefore be obtained in fixed animals, notably about the nervous system.

In a living *Platynereis* specimen however, anatomical visualisation is mostly limited to general features such as cell nuclei, muscle fibres, membranes. These features can be stained respectively with DAPI or Hoechst, Rhodamine-phalloidin, FM 1-43 FX. However, it can be feared that the use of such dyes would interfere with cellular physiology – hence with physiological measurements – and it would be preferable to use genetic markers. Unfortunately, even though a few promoter constructs exist for example for some anterior mechanosensory cells (Luis-Alberto Bezares-Calderón, personal

communication), no specific genetic marker is available to this day that would reveal *in vivo* a cell population such as palpal or antennal neurons. At best, nuclei or membranes can be marked via mRNA zygotic microinjection of H2A-mCherry or membrane-YFP.

While sensory organs can easily be identified in adults, the advantage of *Platynereis* compared to *Nereis* as a polychaete model lies in the substantial knowledge established for larval stages on molecular signatures of cells [80] and in the vast experimental possibilities offered by these transparent larvae, notably in link with the developing connectomic resource at 3 dpf that has already enabled the characterisation of several physiological neuronal circuits [81],[82]. To gain physiological understanding about polychaete chemosensation, *Platynereis* is therefore particularly interesting at its larval or early juvenile stages, not in adult stages where techniques such as electrophysiology would be harder to employ than in *Nereis*. Consequently, physiological studies in *Platynereis* will be conducted at stages at which the identification of chemosensory organs is not straightforward.

More precisely this means that while performing, say, functional imaging based on a fluorescent calcium reporter in a *Platynereis* larva, the experimenter has to rely before all on the medium-quality calcium signal to recognize anatomical regions and assign cells to an organ, and in larvae sensory organs are not as compartmentalised as in adults. At best, the calcium signal can be complemented by a general nuclear marker such as H2A-mCherry in mRNA microinjections.

Consequently, before conducting any physiological study in *Platynereis* larvae, their anatomy needs to be described and learned in detail, and it takes a trained experimenter to recognize regions of interest while conducting the experiments. Only through accurate observation based on a precise anatomical knowledge will it be possible to adequately attribute a physiological role to a certain organ.

Both a description of the sensory cell types found in these organs and an account of how these organs develop into massive sensory appendages in adults would be useful for a general comprehension of sensory inputs, especially in combination with a description of sensory innervation.

I – 3 Specific aims of the thesis

The aim of this PhD thesis was the description and physiological study of chemosensory systems in *Platynereis*, and the establishment of microfluidics-based methods to enable functional imaging and behavioural assays upon chemical stimulations. The 6-days-post-fertilisation stage (6dpf), at which most adult anatomical structures are already present, has emerged as a powerful stage for cross-species comparisons of molecular cell identity thanks to a yet unmatched whole-body atlas of gene expression. It was thus chosen as a target stage for all experiments.

In the first place, I have investigated the polychaete literature of the past 130 years, to review and synthesise the currently available knowledge on sensory organ anatomy and physiology in annelids, with an emphasis on presumed chemosensory organs in polychaetes. This review constitutes Section II of the thesis. Surprising as it may seem, there exists still no physiological proof of chemosensitivity in the polychaete head, despite them carrying prominent and presumably chemosensory appendages.

To establish a solid basis for physiological studies, I have investigated the neuroanatomy and development of head appendages, by the means of immunostainings and confocal imaging. This has allowed to better understand how the hemispheric head of larvae transforms into the complex, appendage-rich head of juveniles, and to recognise unambiguously candidate chemosensory organs in larvae. These descriptions, reported in Section III, also include a neuroanatomical staining at 6dpf in dorsal and lateral view, intended to be used as a reference for further *in vivo* studies.

Next, I have tested the function of candidate chemosensory organs in 6dpf animals by performing confocal calcium imaging of the whole head upon chemical stimulations. The method I have developed uses transient expression of the genetic calcium reporter GCaMP6s, and relies on a new, customised microfluidic setup for animal immobilisation and controlled stimulus delivery. These experiments, exposed in Section IV, have shown that nuchal organs are indeed chemosensory as had long been hypothesised, and so are palps, antennae and tentacular cirri. Antennae appear to be the main chemosensory organ in *Platynereis* larvae, which was unexpected. Other components of the chemosensory systems have been described, and a first understanding of chemical stimulus detection has emerged.

In parallel, the behaviour of larvae has been studied, in the perspective of establishing a behavioural protocol for chemosensory associative learning. To that aim, I have designed new microfluidic devices to generate spatial and temporal patterns of chemical stimulations. Chemical compounds were identified to which larvae show clear and reproducible aversive responses. No associative effects have been observed so far, but the preliminary results inform about the relevant stimulus intensities and temporal scales to be further investigated. These experiments presented in Section V are especially motivated by the presence in *Platynereis*' brain of Mushroom Bodies, a neuronal structure that shows chemically-evoked calcium activity already at 6dpf and, based on published molecular data, may potentially be homologous to the Mushroom Bodies that in insects are responsible for odour associative learning.

Eventually, Section VI gathers various practical observations and some comments on technical developments, that may be useful for someone wanting to establish physiological and behavioural microfluidic setups for small aquatic animals.

II –A comparative review of chemosensation in annelids.

II – 1 Introduction

Annelids have been the object of numerous anatomical studies since the 19th century, comprising the classical works by Quatrefages (1850 [83]), Ehlers (1864 [84]), Langerhans[1] (1880 [85]), Friedländer (1888 [86]), Lenhossék (1892 [87]), Cerfontaine (1892 [88]), Retzius (1892-1902 [89][90][91][92], see Figure II-1), Racowitza (1896 [93]), Hamaker (1898 [94]), Langdon (1900 [95]), Hempelmann (1911 [96]), Holmgren (1916 [97]) and Hanström (1928 [98]). Anatomists in these times gave precise, thorough descriptions of general and nervous anatomy (Figure II-1), and it is remarkable that, as in the field of embryology, these patient and meticulous studies are sometimes the most up-to-date knowledge in 2017, one century later. Starting from hand dissections and microscopical observations combined with traditional staining techniques such as methylene blue staining or Golgi staining, anatomical studies have been progressively enriched by the use of new histochemical [99] and immunochemical [100],[101],[102] techniques, of electron microscopy [103], and of confocal scanning light microscopy [101],[102].

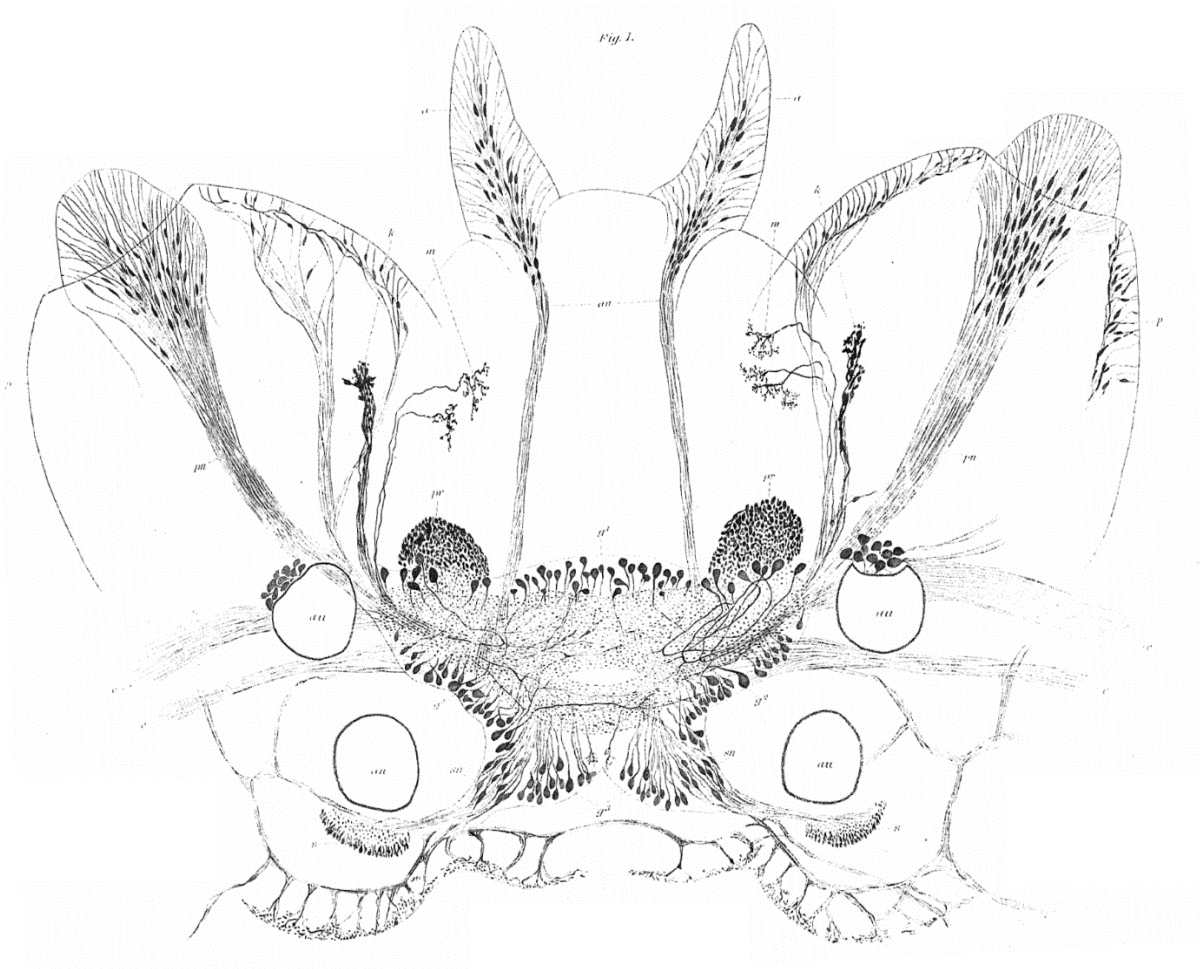


Figure II-1 Head and nervous system anatomy in the polychaete annelid Nereis diversicolor (Retzius 1895 [90]*). Drawing based on methylene blue stainings. Various neurons and their dendritic and axonal processes are depicted ; the black spots are the neuronal cell bodies, the four empty circles are the eyes.*

[1] Better known for his work as a medical doctor and pathologist, Langerhans started working on marine invertebrates after tuberculosis had caused him to settle on the Island Madeira, where he died at the age of 40.

Several morphological reductions or absences can be seen in non-polychaete annelids when compared with polychaetes (Figure II-4). It is obvious for external features such as locomotory and sensory appendages, but holds true for some internal features, for example the apparent lower complexity of oligochaete brains as noted early on by Hanström (1928*) : "The brain in Oligochaetes is much simpler than in most Polychaetes ; even though it possesses a fairly dense neuropil, its ganglion cells have a uniform constitution*[2]*."(*[98], p.293) This paucity of features should be put in relation with evolution, during which annelids originated as a marine group before colonising terrestrial habitats. Nowadays, most oligochaetes and leeches are either terrestrial or freshwater species, whereas most polychaetes are marine species [104] ; moreover, annelid fossils from the Cambrian period are polychaete-like [105]. This speaks in favour of oligochaetes and leeches being derived polychaetes, and these morphological differences being evolutionary reductions or losses.

The study of the polychaete nervous system by Hamaker in 1898 was part of a comparative effort from zoologists and anatomists, in which nervous systems of "*representatives of all the chief groups of the metazoa*" should be described, to gain a more general understanding on animal neural circuits, which he calls "*myo-neural systems*". He argues that animals with simple nervous systems, in particular polychaete annelids, are best suited to that aim : "*In the higher animals the complexity of this system makes such a task almost impossible. At any rate, the most promising method of approaching the subject would seem to be through the simpler forms. Some of the homodynamously segmented animals offer advantages in this respect which no other forms do*."

Here are some advantages he lists about polychaetes as a choice in the study of nervous systems : "*(1) […] a sharply centralized nervous system […], (3) A typical body segment of the animal is simple in structure […], (4) There is almost no serial differentiation of the body segments […] hence it is necessary to determine the structure of one segment only in order to know the structure of nearly the whole animal, (5) Since there are only a few muscles, the movements of the animal are limited in number, and may readily be analysed and classified. (6) Physiological experiments may be performed with more than usual facility, because the worms are hardy and live well in the aquarium.*" Hamaker describes these considerations as "*applying particularly to the polychaete annelid, Nereis*" and thus qualifies this genus as "*a favourable subject for this kind of study*", to which he adds the strong pragmatic argument that "*Nereis may be easily obtained in unlimited quantities*" (all citations from [94], p.89-90).

Species of choice for annelid anatomy have been the medicinal leech *Hirudo medicinalis* for leeches, common earthworms from the genera *Lumbricus* and *Eisenia* for oligochaetes, and coastal ragworms from the family Nereididae for polychaetes, which are popular fishing baits (see http://britishseafishing.co.uk/ragworm/, as of June, 23rd 2017). This family includes[3] the genera *Platynereis, Perinereis, Nereis, Hediste, Eunereis, Alitta*, *Neanthes*, and indeed investigations in polychaete anatomy, maybe following Hamaker's recommendation, have had a large preference for nereidids in general and the genus *Nereis* in particular, well suited for dissection and observation due to its size – over 10cm, and endowed with the major annelid features (see Table 1 in Appendix A, summarizing the species studied in all article cited in this Chapter). Bullock and Horridge, in their textbook on invertebrate nervous systems dated from 1965, also stress the relevance of this choice : "*From the standpoint of comparative neurology, there could hardly be a better choice of a polychaete as the common classroom type than Nereis. Well provided with sense organs, its brain and hence the rest of the nervous system is well differentiated and exhibits virtually all features of advanced polychaetes*". ([106], p.735).

[2] Translated from the German : „*Das Gehirn ist bei den Oligochäten sehr viel einfacher als bei den meisten Polychäten ; es besitzt zwar ein ziemlich dichtes Neuropilem, aber die Ganglienzellen haben einförmigen Bau.*"

[3] *Nereis, Hediste, Eunereis, Alitta*, *Neanthes* are currently considered as synonymous, according to the Marine Species Identification Portal, consulted on June, 23rd 2017 : http://species-identification.org/index.php

II – 2 Anatomy

2.1 General body and nervous system architecture

The basic shape of an annelid body is that of a tube, with mouth and anus representing both ends of the central hole. To a mathematician concerned primarily with topology – the study of shapes and their preservation through continuous transformations – the annelid body would fall in the same category as a doughnut or a coffee mug. That is, if they were made of plasticine, one shape could be stretched and twisted into the other without affecting its essence. This body has a strong left-right (i.e. bilateral) symmetry.

Annelids are segmented worms : the tube-like body is divided in a series of very similar compartments, or segments, which share developmental and structural patterns and are thus qualified as homonomous. Each end of the body is an exception to this repetitive or metameric architecture, and made of a non-segmental region : they are called the prostomium (anterior end) and the pygidium (posterior end). The mouth opening is located in the first segment called peristomium, the anus in the pygidium. Body growth takes place by the successive addition of new segments in the prepygidial zone, as well as by radial and axial growth of the existing segments. The whole body epidermis is covered by a collagenous cuticle, which shows substantial variation across the phylum, especially in interstitial species [104]. Most annelid species possess chaetae, chitinous bristles that extend outside of the body and are used notably for locomotion ; chaetae are "*generally regarded as the most characteristic feature of Annelida*" (Purschke, [104]). Widespread is also the occurrence of locomotory cilia on the body surface, they are however lacking in Clitellata [104].

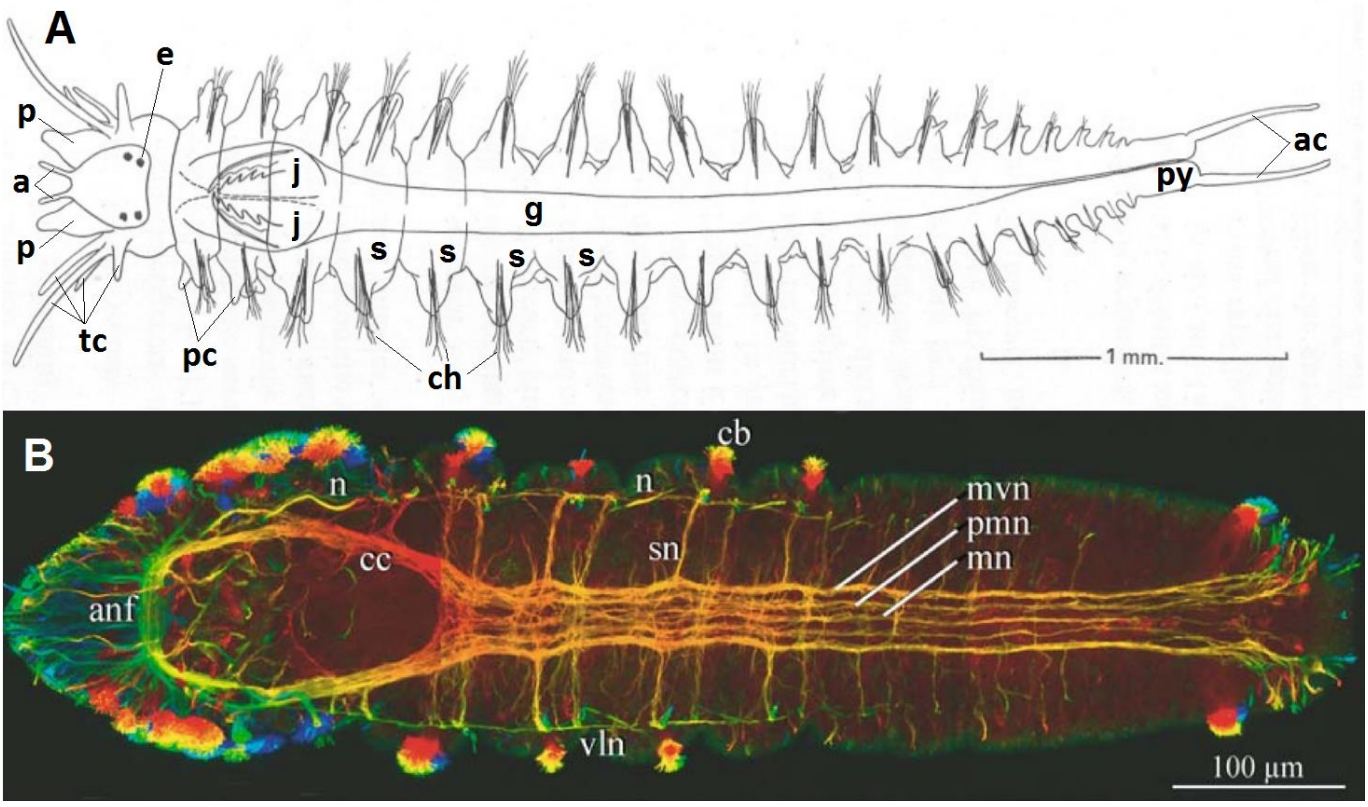


Figure II-2 (previous page) The segmented body plan of annelids, examples of external and internal morphology. (A) Drawing of a 10-weeks old polychaete (Nereis diversicolor) possessing 19 segments endowed with parapodia and chaetae (ch). Dorsal view, anterior left. The head, bearing two pairs of eyes (e), and the pygidium (py) are clearly differentiated. Note the metameric nature of the body with its repetitive segments (s), which are formed in a terminal growth zone next to the pygidium. Several sensory appendages are present : antennae (a), palps (p), tentacular cirri (tc), parapodial cirri (pc) and anal cirri (ac). The gut (g) runs along the whole body in its centre, and the jaws (j) are located inside the first segments. Adapted from Dales, 1950 [107] *p. 342. (B) Nervous system architecture in a polychaete (Scoloplos armiger). A fluorescent staining based on α-acetylated tubulin immunoreactivity reveals nervous fibres and ciliated elements of the whole body, which are displayed in a 3D color-coding from periphery (blue) to centre (red). Ventral view, anterior left. The ventral nerve cord and the circum-oesophageal connectives appear clearly in orange along the central axis of the image ; note the metameric structure of the segments and their nerves. Anterior neurites (anf), circum-oesophageal connective (cc), main (mvn), median (mv) and paramedian (pmn) nerves of the ventral cord, segmental nerve (sn). Reproduced from Orrhage & Müller, 2005* [108].

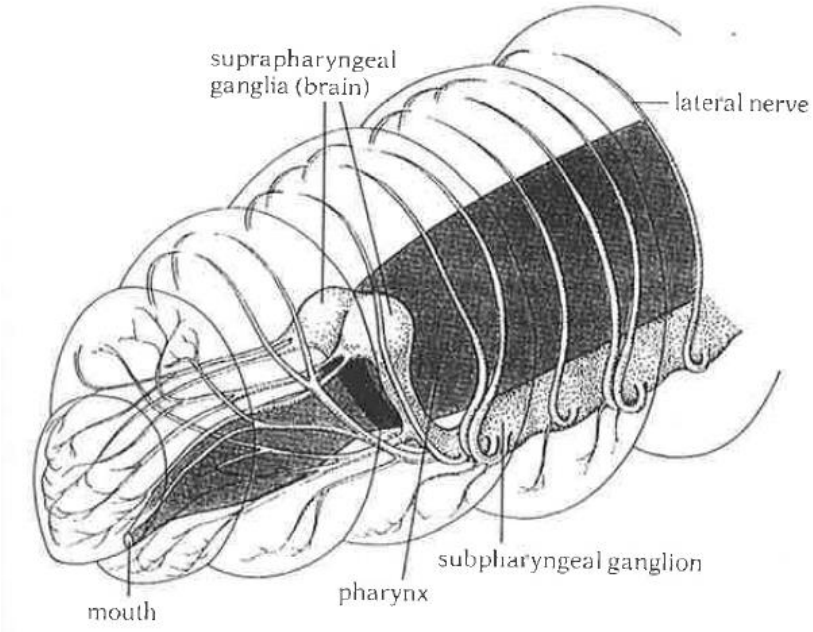


Figure II-3 Basic nervous system architecture in the annelid head, example of the earthworm. Brain and ventral nerve cord are located on either side of the gut (black) and joined by the circum-oesophageal connectives. Note the more complex innervation of the prostomium above the mouth. Reproduced from

The two main parts of the central nervous system are the brain, also called supra-oesophageal ganglion, positioned dorsally at a location ranging from the prostomium (in polychaetes) to the third segment (in earthworm), and a nerve cord that resembles a rope ladder, running ventrally along the entire body. Both parts, located on either side of the gut, are connected by two large, symmetric bundles of nervous fibres running around the oesophagus (Figure II-3), which constitute the circum-oesophageal connectives. In polychaetes these connectives enter the brain typically in two roots, one dorsal and one ventral [108] (see Figure II-6C), whereas in clitellates there are always unbranched (see chapter “Annelida” in [106]). Other features of the nervous system can be used as criteria to distinguish between clitellates and polychaetes, notably the position of the brain within the first segments as opposed to within the prostomium. For an example of such discussion on the genus *Potamodrilus* see [109]. At the most anterior part of the ventral nerve cord lies an accumulation of neurons called sub-oesophageal ganglion. The nerve cord, in the same way as the body, has a metameric structure (Figure II-2). A symmetric pair of neuronal ganglia is present in each segment, which is connected intra- and inter-segmentally by longitudinal connectives and transverse commissures [110],[106].

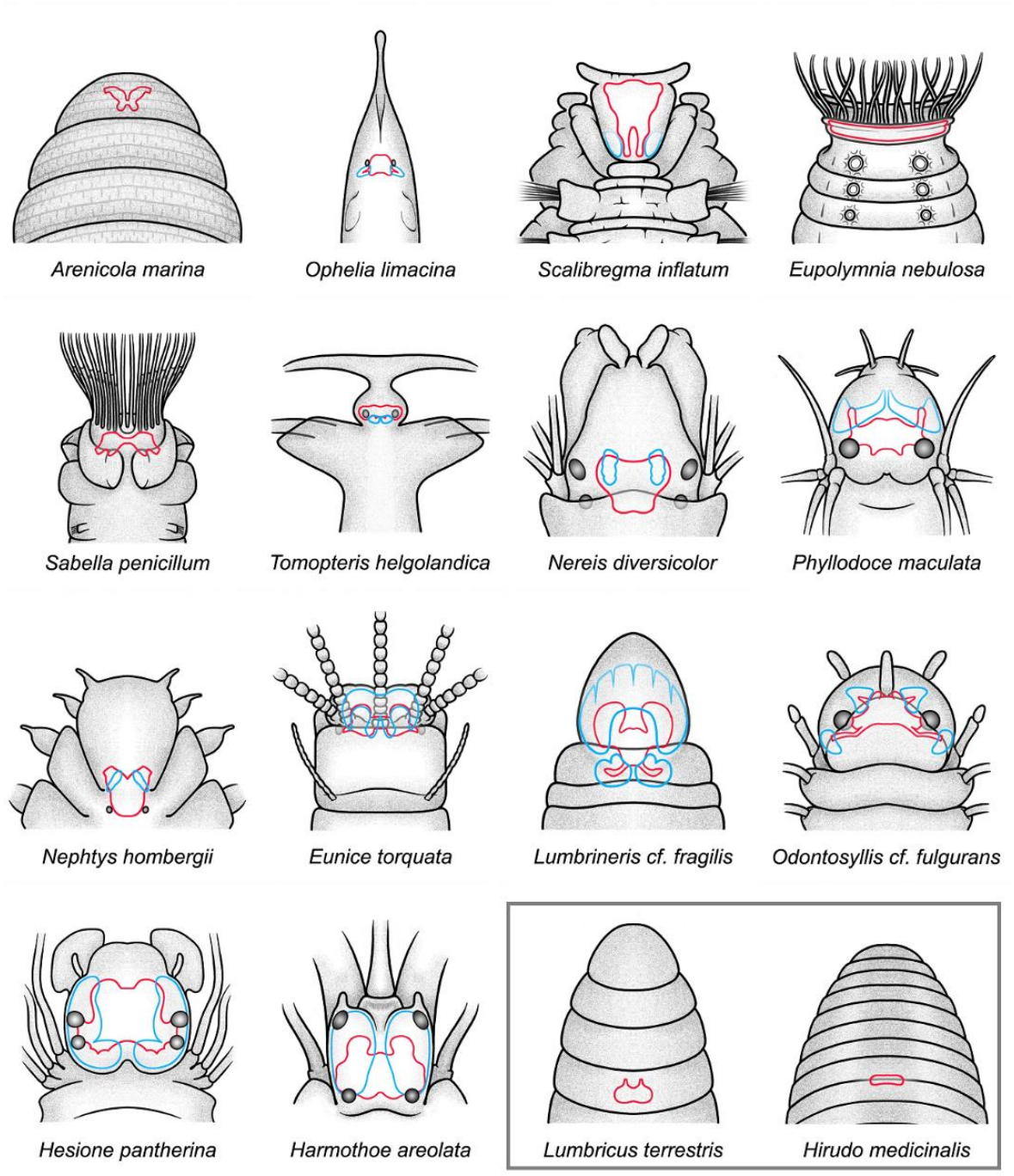


Figure II-4 Schematic head anatomy of worms representative of 16 annelid families, illustrating morphological diversity of the head within the phylum. Brain neuropile is outlined in red, Mushroom-Bodies-like structure are outlined in blue when identified. The two species inside the grey rectangular box illustrate the more simple head morphology in non-polychaetes : Lumbricus terrestris (earthworm, left) and Hirudo medicinalis (medicinal leech, right). Adapted from Heuer et al., 2010 [111].

2.2 Sensory structures and appendages in polychaetes

While polychaetes have elaborate body and head appendages and organs, other major annelid groups such as clitellates lack body appendages as well as the main head appendages altogether [104]. The head of polychaetes shows far more morphological complexity and variation than that of non-polychaete annelids (Figure II-4, see also [112],[113]). This correlates with less developed sensory structures, and may explain why studies on earthworms and leeches have focused on locomotory systems rather than on sensory systems [114][115].

The following description concentrates on polychaetes and their sensory structures, particularly those potentially involved in chemoreception. Photoreception is outside the scope of the present chapter ; eyes in polychaetes are present in the form of pigmented and non-pigmented ocelli with varying degrees of complexity, can be found on the head as well as the whole body, and their sensory pathways can use either rhabdomeric or ciliary opsins (see [116], [117], [118] for generalities on annelid photoreception, see [119], [67], [120], [77], [81] for visual system studies in *Platynereis dumerilii*).

All body parts of polychaete worms can carry prominent appendages, with considerable variation in size, shape and number (Figure II-4, also Figure II-10 with highlight on palps), depending on the families and their ecology. The appendages called antennae, palps and tentacular cirri, as well as the structures called nuchal organs, can be found on the head, and are all sensory structures. A pair of lateral parapodia is often present on each segment, which are locomotory structures used for crawling and swimming. Parapodia show sensitivity notably, but not only, through sensory structures called parapodial cirri. When present, parapodia carry the chaetae. Further appendages called anal cirri can be found on the pygidium, that closely resemble the cirri found on parapodia and on the peristomium, and are sensory as well. Additionnaly, dorsal organs and lateral organs are present in some polychaete families [116], however they are absent in nereidids and will not be detailed hereafter.

Figure II-5 gives an example of these appendages for the genus *Brania*, Syllidae, Figure II-6 gives an example of these appendages and their innervation for the genus *Nereis*, Nereididae (see also Figure II-1, Figure II-4, and Figure II-10U) ; note that none of these exist in clitellates (Figure II-4). Whereas antennae, palps, and nuchal organs are innervated directly from the brain, the tentacular cirri are innervated indirectly and project their nerve to the circum-oesophageal connectives first. All appendage nerves form a complex system of commissures (Figure II-6C), which in *Nereis* is established early on in development as demonstrated by Gilpin-Brown ([121] p. 330).

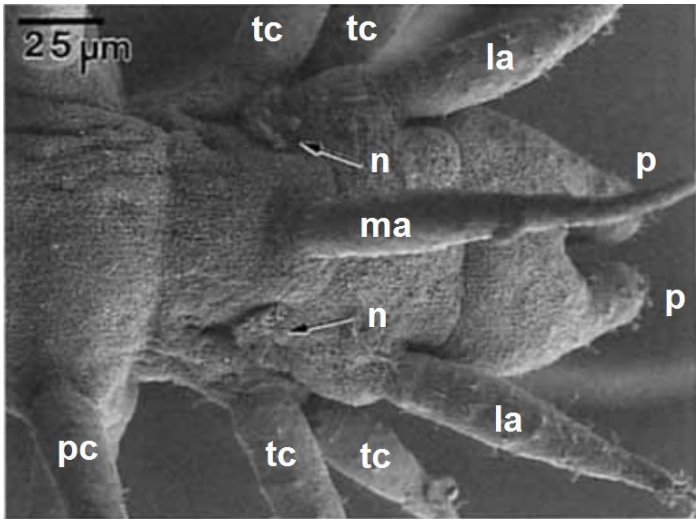


Figure II-5 Example of typical appendages around the polychaete head, in a Scanning Electron Microscopy image. Brania subterranea (Syllidae), dorsal view, anterior right. Lateral antennae (la), median antenna (ma), nuchal organs (n) indicated by black arrows, palps (p), dorsal parapodial cirrus (pc), tentacular cirri (tc). Note the abundance of groups of cilia at the surface of antennae, palps and cirri, and the densely ciliated area of the nuchal organs. Eyes are not clearly visible on the image. Adapted from Purschke, 1997 [122].

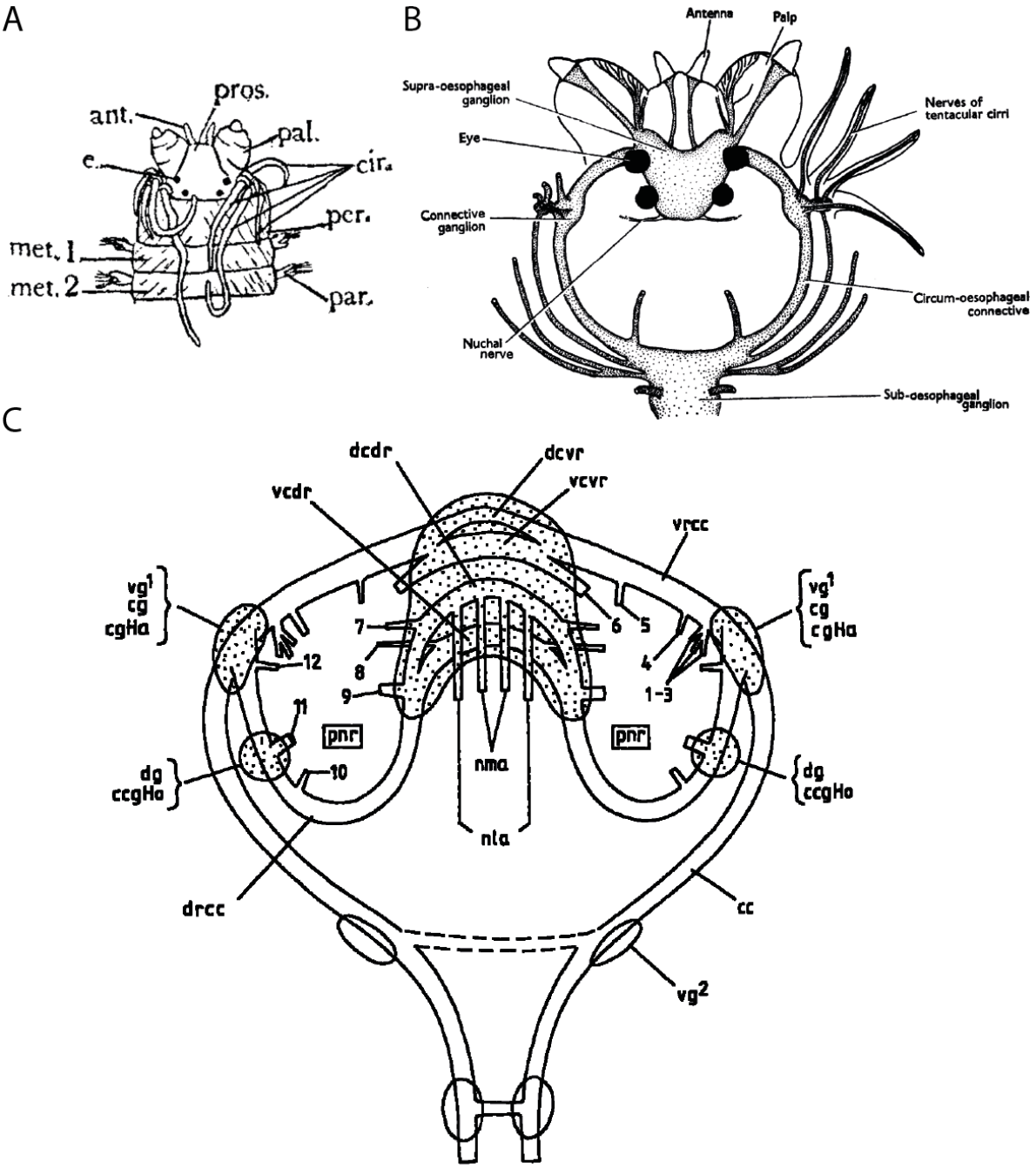


Figure II-6 Polychaete head, appendages and innervation, schematic representation for the genus Nereis (Nereididae). All in dorsal view with anterior up. (A) Nereis virens, sensory appendages around the head : antenna (ant.), palp (pal.), tentacular cirri (cir.), parapodium (par.). Also depicted are the prostomium (pros.), one eye (e.), the peristomium (per.), and the first two segments or metameres (met. 1 and met. 2). Nuchal organs are not represented. Adapted from Langdon, 1900 [95] *(B) Nereis diversicolor, major innervations around the head. The brain or supra-oesophageal ganglion is clearly visible, as well as the sub-oesophageal ganglion at the beginning of the ventral nerve cord, and the circum-oesophageal connectives. Antennae, palps, and nuchal organs are innervated directly from the brain, the tentacular cirri indirectly via the circum-oesophageal connectives. Reproduced from Flint, 1965* [123]. *(C) Tentative general diagram of the cephalic nervous system of polychaetes, with emphasis on the innervation of the cephalic appendages. The roots of the stomatogastric nerves are omitted. Dorsal (drcc) and ventral (vrcc) root of the circum-oesophageal connectives (cc), dorsal (dcdr) and ventral (vcdr) commissure of drcc, dorsal (dcvr) and ventral (vcvr) commissure of vrcc, dorsal ganglion (dg), ventral ganglion 1 (vg^1) and 2 (vg^2), nerve of lateral antenna (nla), nerve of median antenna (nma). Palp nerve roots (pnr) 1 to 12 are indicated. Reproduced from Orrhage, 1995* [124].

2.2.1 Nuchal organs

Nuchal organs are the most characteristic sensory structures found in polychaetes and have been the object of the majority of studies on sensory organs ; they are absent in clitellates. According to Racovitza ([93] p.246), the widespread occurrence of nuchal organs in polychaetes was already pointed at in 1881 by Spengel [125], who recognised them in eleven families. Retzius, who gives in 1895 a description of a supposedly new organ in *Nereis* ([90] p.9) which is nothing else than the nuchal organ, seems not to have known the existing literature on the topic. Even though nuchal organs show wide morphological variation between taxa [122],[126], and are possibly absent in some of them, they have become "*the most important sensory structure of Annelida in terms of their phylogenetic value*" (Purschke, [116]). Indeed today, their homology across annelids is almost certain, and they may even represent an autapomorphy of polychaetes [104],[122], thus confirming the evolutionary hypothesis brought forward by Racovitza as early as in 1896 : "*One can thus assert that the nuchal organ is an organ typical for the encephalic lobe of Polychaetes, meaning that it is inherited from the stem and not a new acquisition, or put differently, that all Polychaetes have it or must have had it at a certain stage of their embryonic or phylogenetic development*[4]."([93], p. 248)

Nuchal organs are generally a paired structure, located at the posterior end of the peristomium (Figure II-5), but can extend over the first segments. They appear as a densely ciliated epidermal area, typically located in a pit or groove of variable depth (Figure II-7), and are often retractile, as noted by Racovitza : "*If one observes Polychaetes with evaginable nuchal organs, it can be seen that they evaginate them only when they are completely quiet, after water movements have ceased. As soon as one stirs the water of the tank that contains them, they retract them rapidly*[5]." ([93] p.257). In some species however, they are also eversible, as reported for example in *Nephtys* by Clark, who adds that they are "*generally found everted in preserved specimens*" ([127] p. 213).

Despite a highly variable position, size and external morphology, nuchal organs have overall a similar internal structure (see Figure II-21 and text below). They are composed of ciliated supporting cells, bipolar primary sensory cells [122], and often possess a retractor muscle. The cilia visible from the outside, which are mobile, belong to the supporting cells and generate water currents which are believed to enable a rapid water exchange. Specialised cuticular or microvillar layers cover an internal cavity, called sensory or olfactory chamber [122],[128],[129]. There can be between two and several

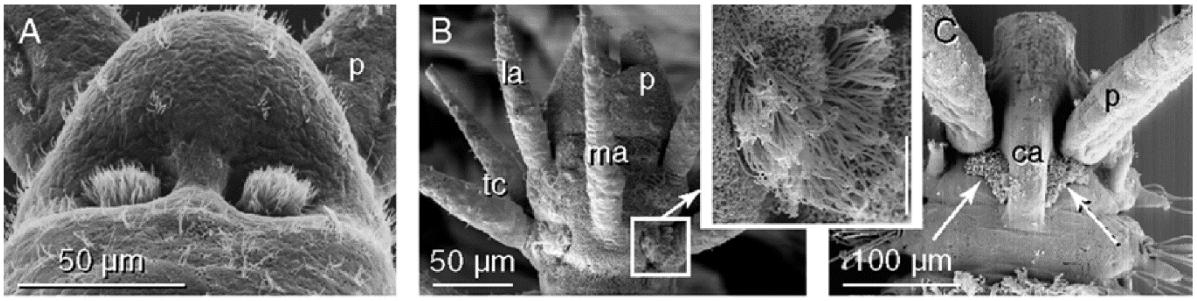


Figure II-7 Nuchal organs external morphology. Examples showing the typical appearance of nuchal organs as ciliated pits or grooves. Scanning Electron Microscopy images. Head shown in dorsal view with anterior up, for representatives of the following polychaete families : (A) Saccocirridae (B) Syllidae (C) Spionidae. Reproduced from Purschke, 2005 [116].

[4] Translated from the French : « On *peut donc dire que l'organe nucal est un organe typique du lobe encéphalique des Polychètes, ce qui veut dire qu'il est hérité de la souche et non une nouvelle acquisition, ou encore que tous les Polychètes l'ont ou ont dû l'avoir à un certain stade de leur développement embryonnaire ou phylogénétique*. »
[5] Translated from the French : « *Si l'on observe les Polychètes à organes nuchaux dévaginables, on voit qu'ils ne les évaginent que lorsqu'ils sont tout à fait tranquilles, après que les mouvements de l'eau ont cessé. Dès qu'on remue l'eau du récipient qui les contient, ils les rétractent avec rapidité.* »

hundreds of sensory cells. Their axons gather as a bundle, the nuchal nerve (see Figure II-6B), which forms a commissure of variable position in the brain ([108] p. 85, see also Figure II-6C). Supporting cells have an efferent innervation [128], which is distinct from the nuchal nerve [122]. The nuchal nerve is thus afferent only. Nuchal organs develop early on, with no major difference between juvenile and adult organs, as was shown in Opheliidae [126] and in Spionidae [130],[131].

2.2.2 Palps

Palps are the second most widespread sensory structure of polychaetes. They are prominent, paired anterior appendages located on the prostomium (Figure II-2A, Figure II-5, Figure II-6A,B), and are present in a majority of taxa [108]. Palps, as nuchal organs, and as polychaete appendages in general, show a wide range of variation across taxa, as illustrated by Figure II-10. They can be massive, and equipped with a complex musculature, blood vessels, and even coelomic cavities in some taxa (clade Canalipalpata described in [132], see the example of Protodrilidae Figure II-10K), or be rather thread-like and devoid of these features as in Hesionidae (Figure II-10T). They can have different orientations and functions, for example antero-ventral and sensory in errant polychaetes such as nereidids (Figure II-6A, Figure II-10U), or postero-dorsal and used for feeding in Spionidae (Figure II-10G).

The palp innervation is complex, as described early on by Retzius (Figure II-1) or Holmgren (Figure II-8). Up to twelve palp nerves can be found that emanate from dorsal and ventral root of the circum-oesophageal connectives (for a generalised diagram of polychaete head innervation see Figure II-6C). Nevertheless, Orrhage has demonstrated that they can be homologised on the basis of nerve structure [133],[108],[124].

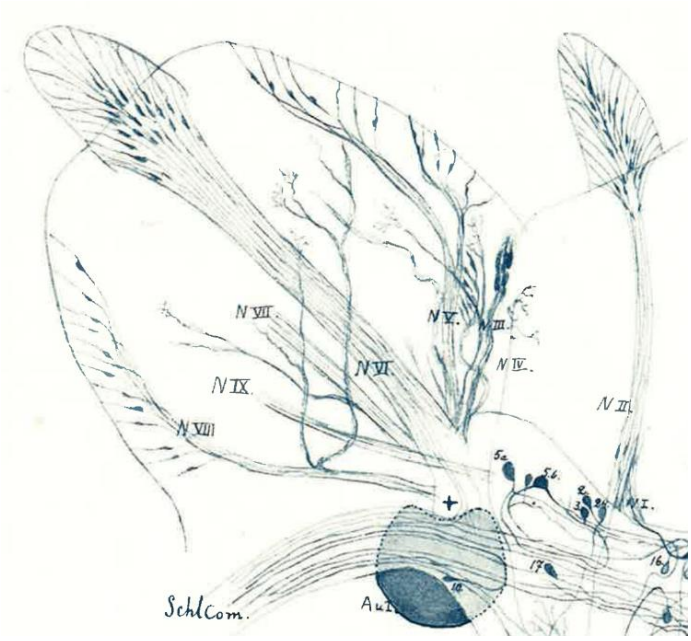
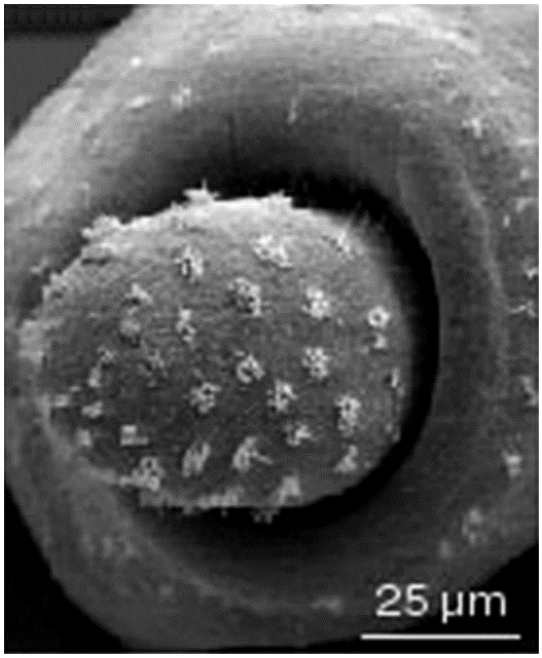


Figure II-8 Palp innervation in Nereis diversicolor. Seven different nerves are described (N III to N IX). Note the sensory neurons concentrated in the tip of the palp. Reconstruction based on 400 methylene blue preparations. Detail from plate IV, reproduced from Holmgren, 1916 [14].

The absence of palps not only in clitellates but also in some taxa of polychaetes raises the question of their ancestrality within annelids. It seems that this absence would represent rather a loss than a primary character [104][133], but the question in still debated.

Palps in nereidids are composed of a large proximal mass with musculature and coelomic cavities, and a small, mobile distal tip where numerous sensory cells (Figure II-1, Figure II-8) and sensory endings (Figure II-9) are concentrated, which ascertains that they are sensory structures. The surface of the proximal mass also contains clusters of cilia, though to a lesser extent.

Figure II-9 Detail of a palp tip in Nereis, Scanning Electron Microscopy image. Note the numerous clusters of cilia covering the whole tip surface, which are the endings of sensory neurons. Reproduced from Purschke, 2005 [39].



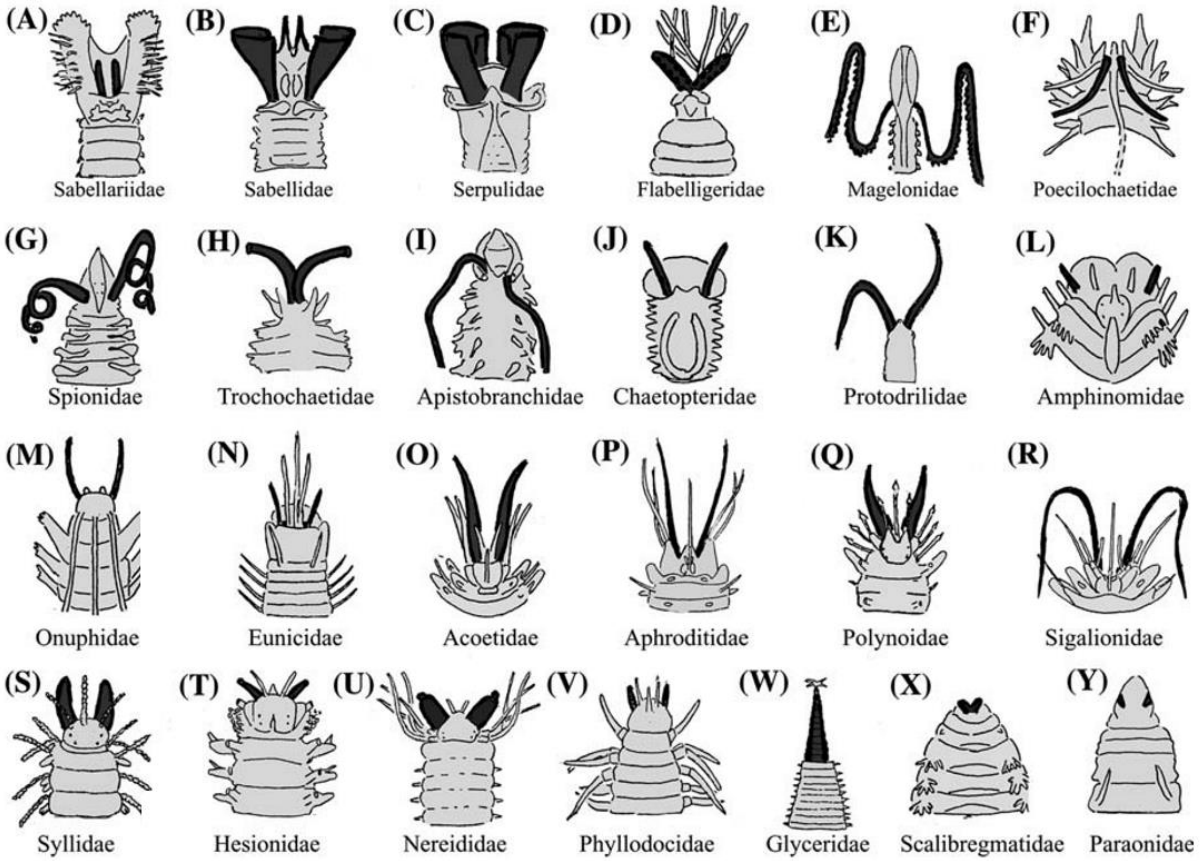


Figure II-10 Schematic head anatomy of worms representative of 24 polychaete families, illustrating morphological diversity of head and body appendages (antennae, palps, cirri, parapodia) within polychaetes. The palps of the nereidids and their homologues are coloured in black. Reproduced from Orrhage & Müller, 2005 [108].

2.2.3 Antennae

The prostomium often bears another type of sensory appendages, quite different from the palps : the antennae (Figure II-2A, Figure II-5, Figure II-6A,B). When present, there can be either two, three or five of them, namely one or two pairs of lateral antennae supplied with one nerve each, with or without one median antenna supplied with two nerves [104]. As a general rule, these nerves connect to the dorsal commissure of the dorsal root of the circum-oesophageal connectives (see Figure II-6C).

Antennae are overall thinner than palps, can be annulated (e.g. in *Eunice torquata* in Figure II-4) or more generally smooth, and show substantial variation in shape and size between taxa, though they can also be homologised based on their innervation [108]. A median antenna is found in most species of the following families : Amphinomidae, Onuphidae, Eunicidae, Acoetidae, Aphroditidae, Polynoidae, Sigalionidae, Syllidae, Hesionidae and Phyllodocidae ([108], see Figure II-10L, M, N, O, P, Q, R, S, T, V for illustration). Orrhage and Müller indicate that "*in all probability [median antennae] are also equivalent to the occipital tentacle found in many Spionidae*" ([108] p. 87). Presence of the median antenna thus seems to be rather the rule than the exception. Regarding evolution and phylogenetic systematisation of polychaetes, a similar statement can be made for antennae as for palps regarding their origin and their absence in some polychaete taxa ([104], see also paragraph above). Purschke specifies that antennae in polychaetes are not homologous with antennae in Arthropods, despite a common name and a similar position [104]. In nereidids, they are the most frontal appendages. In their fine structure, antennae show, as in the palp tip, numerous sensory neurons with free nerve endings reaching the surface of the cuticle (Figure II-11). Axons gather in the centre of the antenna to form the antennal nerve, that projects into the brain. Multiple clusters of cilia are present at the antennal surface (Figure II-5). There is no doubt about the sensory nature of the antennae.

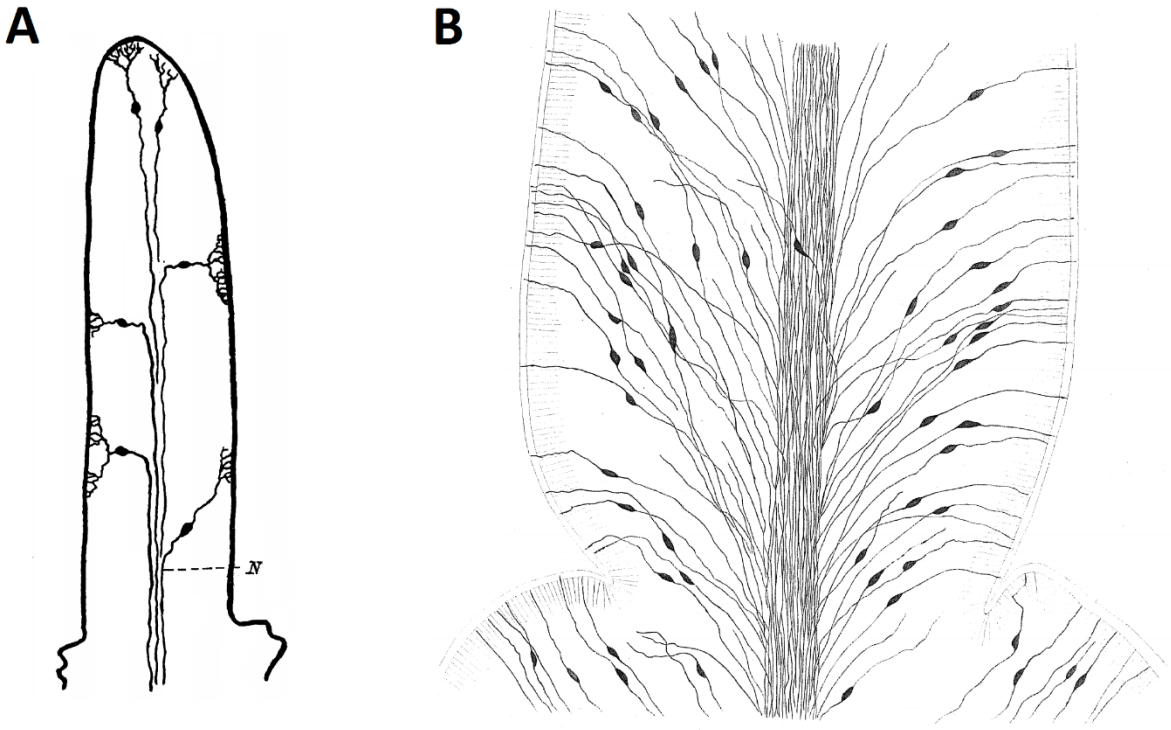


Figure II-11 Polychaete antennae and their sensory neurons. (A) Sthenelais picta (Aphroditidae), a few antennal sensory neurons and their axon joining the antennal nerve (N) in the centre. Drawing based on Golgi stainings. Reproduced from Hanström 1927 [134] *p.261 (B) Nereis diversicolor (Nereididae), base of the antenna showing antennal sensory neurons and in the centre the antennal nerve. Drawing based on methylene blue stainings. Reproduced from Retzius 1895* [90] *plate III.*

2.2.4 Tentacular, parapodial and anal cirri

Just posterior to the prostomium, the peristomium (or sometimes the first segments) often carries another type of appendages called **tentacular cirri** (Figure II-2A, Figure II-5, Figure II-6A,B). They are less common than palps and antennae, nevertheless they can be found in the following polychaete families : Acoetidae, Aphroditidae, Polynoidae, Sigalionidae, Syllidae, Pilargidae, Hesionidae, Nereididae, Phyllodocidae (for examples see Figure II-10 O, P, Q, R, S, T, U, V). Tentacular cirri occur in a variable number of bilaterally symmetric pairs, between one and eight. They are variable in size and shape, and are typically longer than antennae though not always. They are equipped with muscles that allow the animal to move them around.

As for palp tips and antennae, the surface of these cirri is covered by numerous clusters of cilia [95] that indicate the presence of individual sensory formations (Figure II-12). And in the same way as for the antennae, the axons of the corresponding cells gather as a nerve in the centre of the appendage (not shown here).

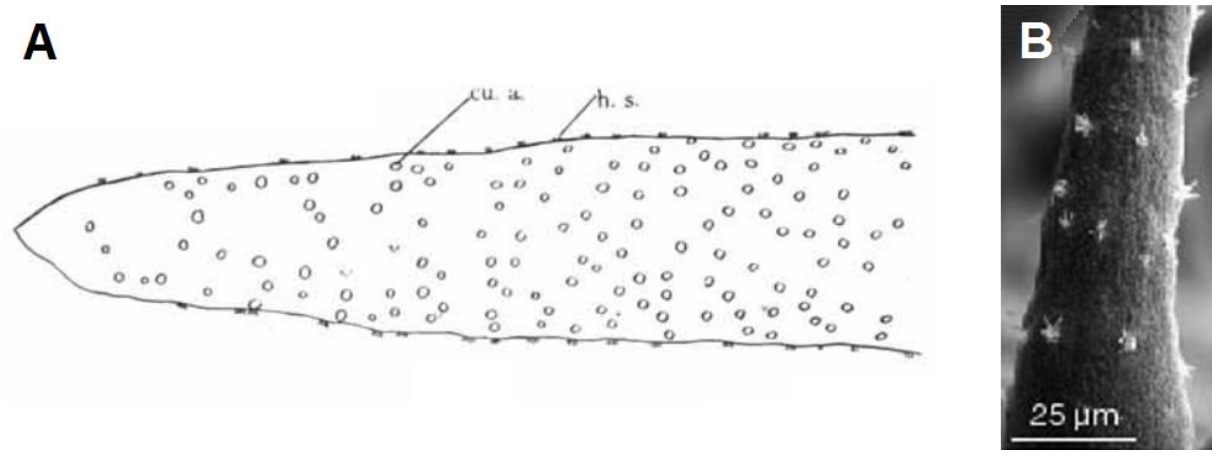


Figure II-12 Tentacular cirrus, genus Nereis. (A) Distal part of a tentacular cirrus, Nereis virens. Surface view, proximal right, drawing from living, stained material. Over the surface, circles indicate the location of modified cuticular areas (cu. a.) around individual sensory organs ; around the margin, the same areas are indicated by groups of sensory hair (h. s.). Reproduced from Langdon, 1900 [95]*. (B) Enlargement of the first ventral tentacular cirrus in a Nereis species, Scanning Electron Microscopy image. The clusters of sensory cilia appear in light grey. Reproduced from Purschke, 2005* [135].

To fully understand the tentacular cirri, it makes sense to consider the constitution and position of the main sensory appendages present on the body segments, the **parapodial cirri**, which are carried by the parapodia (Figure II-2A). The parapodium is a complex locomotory appendage widespread in polychaetes, present symmetrically on the side of each body segment, and qualified as biramous, i.e. consisting of two main branches. These are the notopodium (dorsal) and the neuropodium (ventral) ; they are differentiated in shape and somewhat in function, but both carry a set of chaetae, as well as a sensory structure called parapodial cirrus, located on the dorsal side for the notopodium, on the ventral side for the neuropodium. Figure II-13 shows examples of parapodial cirri in nereidids. Cirri vary in length and shape within an individual depending on the position of its segment [136].

Parapodial cirri are slender appendages. They contain numerous bipolar sensory neurons [110] as described already by Retzius in 1892 [89], and bear regularly spaced groups of cilia at their surface, in the same way as palp, antennae and tentacular cirri do, and as described by Langdon in 1900 [95]. Dorsett observed that, in *Nereis*, "*The dorsal and ventral cirri have the highest concentration of sensory cells to be found in the integument, with the exception of the appendages of the head*"([137] p. 655). The rest of the parapodium is also endowed with sensitivity, albeit to a much smaller extent than the cirri ([110] fig. 26, [137]). Cirri therefore appear as a sensory specialisation within the parapodium.

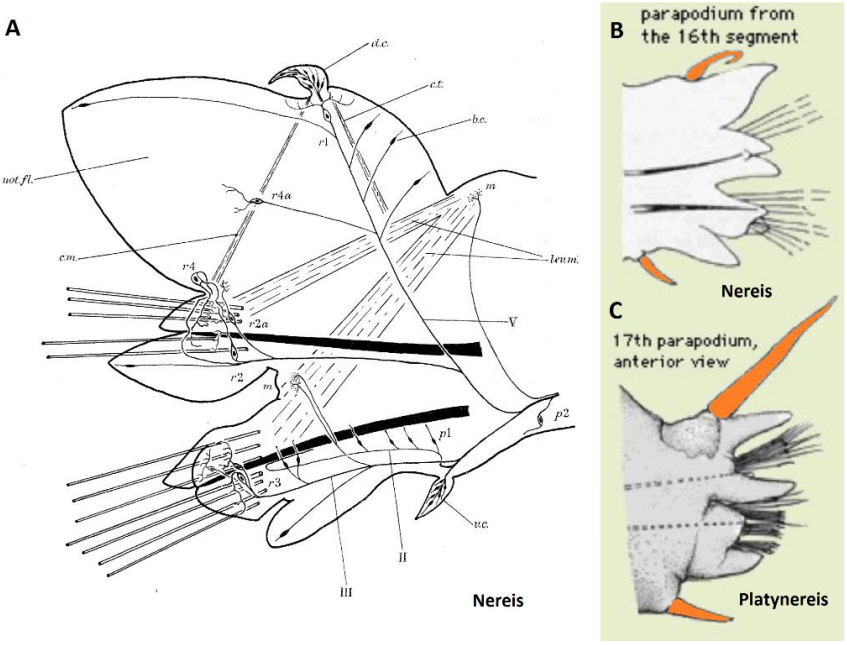


Figure II-13 Parapodium morphology and parapodial cirri, example for nereidids. (A) Schematic diagram showing partial innervation and musculature of a parapodium in Nereis. Dorsal cirrus (d.c.), ventral (v.c.) cirrus, cirrus muscle (c.m.), notopodial flap (not.fl.). Reproduced from Dorsett, 1964 [137] *p. 656. (B-C) Example of a parapodium and its cirri in Nereis (B) and Platynereis (C). Cirri are highlighted in orange. Adapted from Imajima, 1972* [136].

Figure II-14 shows the fine structure of parapodial cirri in nereidids, with details of sensory neurons, sensory hairs, and the cirrus nerve.

Even if tentacular cirri are generally longer than parapodial ones, it is obvious that the anatomy of parapodial and tentacular cirri is similar in many aspects : similar type and distribution of sensory cells and hairs, presence of a central nerve, presence of clusters of sensory cilia at the surface of the cuticle, presence of muscles to orient the appendage. This is no coincidence, and it is indeed believed that the adult peristomium in polychaetes has evolved from body segments.

A good evidence for that comes from nereidids, in which an actual metamorphosis of the first parapodium into the posterior part of the peristomium is observed during development. The future adult dorsal posterior cirri that arise during this transition are a modification of the first parapodium's dorsal cirri. In *Platynereis dumerilii*, this metamorphosis occurs when juvenile worms have reached the 5-segmented stage : the first segment transforms into the posterior peristomium through anteriorisation and progressive loss of chaetae, then a new fifth segment is added in the pygidial zone and development carries on (for a description with images, see [138]). The ventral posterior peristomial cirri form later on. Although this episode is called a 'cephalic metamorphosis', no major rearrangement of the nervous system takes place except a migration of the parapodial ganglia anteriorly, hence it would be less misleading to use a term such as 'cephalisation'.

This developmental transformation was observed long ago (Langerhans 1880 [85], Racovitza 1896 [93], Hempelmann 1911 [96]). Gilpin-Brown, who studied in 1958 the development of cephalic nerves in *Nereis diversicolor*, made the following statement : "*there can be little doubt that the posterior part of the peristomium is derived from a chaetigerous segment and that the posterior cirral ganglion and the sub-oesophageal ganglion represent its pedal and ventral ganglia respectively."* He goes even further : *"Since the anterior and posterior pairs of tentacular cirri are anatomically so similar […] it is very probable that the anterior part of the peristomium is also derived from a segment and that the anterior cirral ganglion represents a pedal ganglion*." And then, as a conclusion : "*The peristomium is therefore probably derived from two segments each of which originally carried parapodia and chaetae*." (all citations from [121], p. 343-4).

According to all these observations, it seems reasonable to assume that in polychaetes, as examplified with *Nereis* and *Platynereis*, the peristomium derives from the first body segments. The developmental cephalic metamorphosis observed in some species would therefore represent an example of

recapitulation in the sense of Haeckel. Fundamentally, both cirral ganglia and SOG are modifications of ganglia previously belonging to the ventral nerve cord, the former having split and 'slided' anteriorly along the COR, around the pharynx. **Tentacular cirri are thus nothing but transformed parapodial cirri** that have been cephalised during evolution.

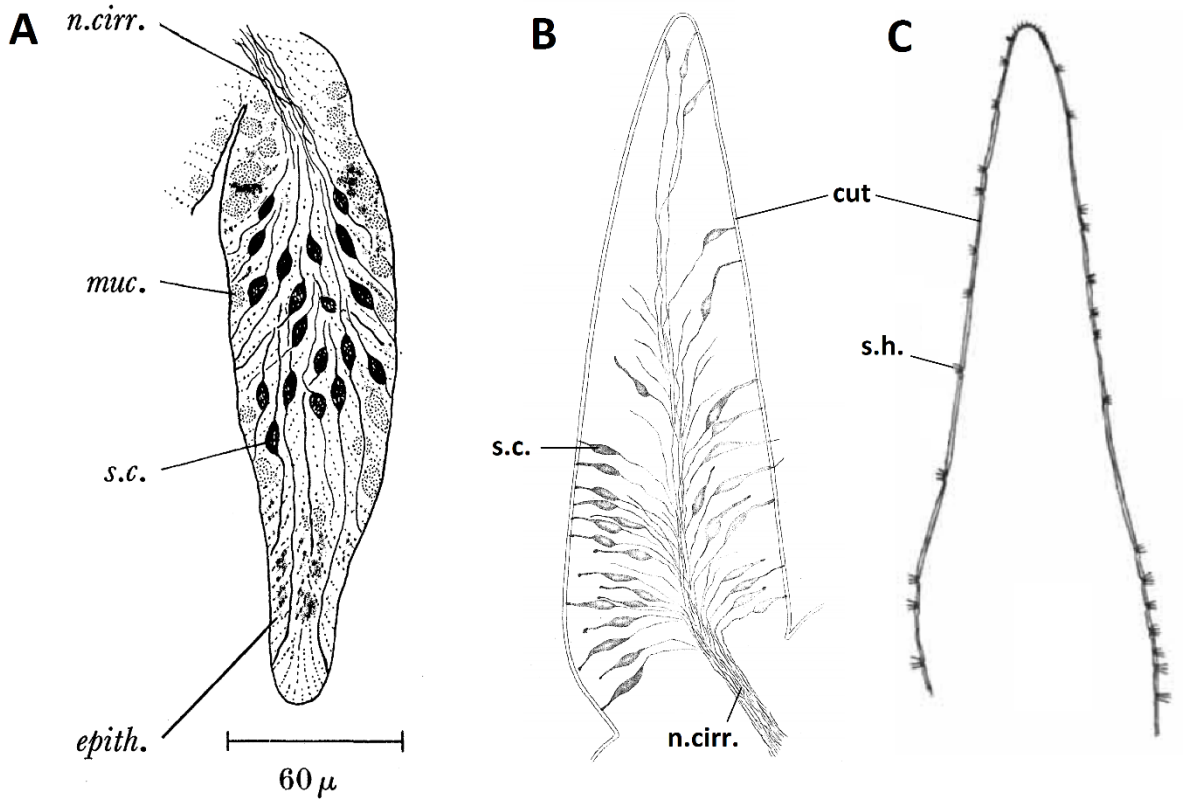
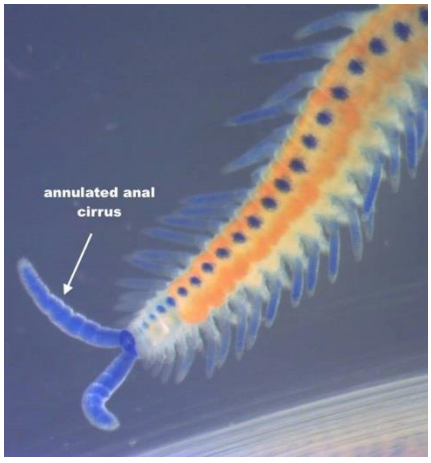


Figure II-14 Fine structure of parapodial cirri in nereidids, showing sensory cells (s.c.), sensory hairs (s.h.), cirrus nerve (n.cirr.), epithelial cells (epith.), mucus glands (muc.) and cuticle (cut.). (A) Platynereis dumerilii. Drawing based on methylene blue stainings. Reproduced from Smith, 1957 [110] *p.177. (B) Nereis diversicolor. Drawing based on methylene blue stainings. Adapted from Retzius, 1892* [89] *plate I. (C) Nereis virens, surface of the cirrus with clusters of sensory hairs. Drawing from living, unstained material. Adapted from Langdon 1900* [95] *plate I.*



The last sensory appendages found in polychaetes are the **anal cirri**, a paired structure located on the pygidium and pointing posteriorly (Figure II-2A, Figure II-15). Even though they are less often described in the literature, anal cirri are also highly similar in shape and fine structure to tentacular and parapodial cirri. One can venture to say without too much risk that, in the same way that tentacular cirri are modified parapodial cirri that have been specialised for the non-segmental, head region, anal cirri are probably modified parapodial cirri as well, that have been specialised for the non-segmental, pygidial region.

Figure II-15 Example of anal cirri in Myrianida pachycera (Syllidae). In this species anal cirri are annulated. Copyright Alexandra Nance

2.3 Sensory cell types in polychaetes

In all the above-mentioned appendages and structures, several sensory cell types have been characterized, and there exists several ultrastructural studies of these cells, notably by Günther Purschke ([103], [104], [122], [116], [135], [139], [140], [141] and references therein). Purschke indicates that polychaete sensory cells are generally bipolar, with ciliated dendritic processes possibly supplemented by microvilli, and their cell body lies either within the nervous system or within the epidermis. Despite structural variation within individuals and between species, he indicates that these cells can be classified in five categories [116] :
(1) Multiciliated penetrative
(2) Monociliated non-penetrative
(3) Multiciliated non-penetrative
(4) Monociliated penetrative
(5) Basal ciliated

Only types (1) and (2) are externally visible since their cilia stick out of the cuticle. Sensory cells of type (1) are the most abundant in annelids, and Purschke stresses that they are variable in many aspects : "*number and length of cilia, […] number and length of additional microvilli, presence or absence of ciliary rootlets, structure of these rootlets, additional cytoskeletal elements and other fine-structural features. The number of cilia per cell ranges from 2 to more than 20*" ([116] p. 55). Their cilia are not always mobile. Type (2) cells are also present in most if not all polychaete families, and can be subdivided in two subtypes, depending on whether or not microvilli surround the cilium and create a pore in the cuticle ; in the latter case, a circular protrusion is visible around the base of the cilium, and hence the cells are called collar receptors, which is a cell type widespread in invertebrates [116]. Cells of type (3) and (4) are widespread in polychaetes, their cilia run in the basal layer of the cuticle and are thus invisible in Scanning Electron Microscopy for example. These cells are thought to be either mechano- or chemoreceptive, though no clear function has yet been attributed [116]. Cells of type (5) are rare and reported so far in the polychaete family Protodriloidae only [142]. They possess a bundle of cilia wrapped around the cell body that then reaches the cuticular layers ; nothing is known concerning their function [116].

Which cell types then are present in the variety of organs described previously ? Actually, these cells can be found all over the trunk and the appendages (palps, antennae and all types of cirri) where they may occur in isolation, in clusters, or in sense organs [116]. They can appear on the pharyngeal surface as well.

2.3.1 Sensory cells with penetrative cilia

Hanström (1927) has described in the antennae of *Sthenelais picta* (Sigalionidae, at that time regarded as belonging to Aphroditidae) bipolar sensory cells whose endings seem to go through the cuticle, judging from the cuticular deformations that seem to accompany them (Figure II-16). Though he did not report on their cilia, it is likely that such cells are of the type (1) or (2), i.e. penetrative. Ciliated sensory cells of type (1) have been observed at the surface of the feathered antennae of the sedentary polychaete *Sabella pavonina* (Sabellidae). These cells are rich in cilia, carrying at least twenty of them, and their nucleus lies close to the cuticular surface [143]. In another sedentary polychaete, *Lanice conchilega* (Terebellidae), whose antennae are not feathered but smooth, three types of sensory cells have been described by Schulte & Riehl. Cells of the first type are fusiform, and their apical part is directly exposed to the outside

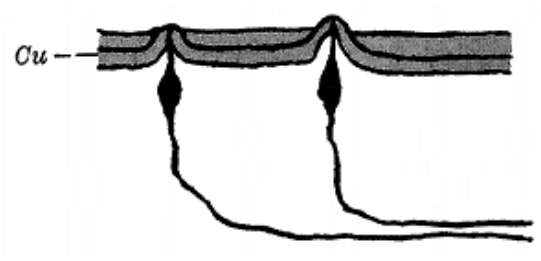


Figure II-16 Potential penetrative sensory cells described by Hanström in the antennae of Sthenelais. Cuticle (Cu). Reproduced from Hanström, 1927 [26].

medium. Below this apical surface, numerous centrioles can be found though no cilia are observed. The second cell type likewise is situated directly under the cuticle, and has multiple cilia as well as microvilli that penetrate it. This type is thus similar to the antennal cells described in *Sabella*. A third type is found which is equipped with an elongated cytoplasmic protrusion, devoid of cilia, and difficult to liken to other polychaete sensory cell types [144].

Langdon had described already in 1900 what she called "diffuse sense organs" in *Nereis virens* [95], which are groups of bipolar neurons situated in the epidermis that send a sensory hair exposed to the outside of the animal (Figure II-17B-D). She found them all over the body of *Nereis* with a particularly high concentration on tentacular cirri, antennae and palp tip (Figure II-17A), consistent with their sensory nature. Even though she gave precise descriptions of such grouped sensory cells, Dorsett and Hyde state in 1969 that "*their presence in polychaetes has not been generally accepted*" ([145] p.512), meaning that her work had been unnoticed or neglected – because she was a woman ? Whatever the reason has been for this ignorance, they have decided to re-investigate these organs in tentacular cirri and palps with electron microscopy, which allowed them to confirm and complement her conclusions : these compound sense organs are composed of 7 to 15 fusiform, monociliated, bipolar sensory cells, occurring together with secretory cells which they term "granular cells" and which possess microvilli (Figure II-18A). The sensory cilia have a sheath formed by the epicuticle, and are easy to distinguish from epidermal and epicuticular microvilii (Figure II-18B,C). The clusters of cilia seen on a tentacular cirrus in Figure II-18B are equivalent to those seen in Figure II-12B, and on the palp in Figure II-9.

Interestingly, Langdon had given light microscopy descriptions of these ciliated areas on tentacular cirri and at the tip of the palps ([95] Fig. 6 and 8), though the technique did not allow her to distinguish between cilia and microvilli, or to attribute a number of cilia to a cell. The sensory cells of the diffuse sense organs clearly are monociliated penetrative cells, thus sensory cells of the type (2) are found at

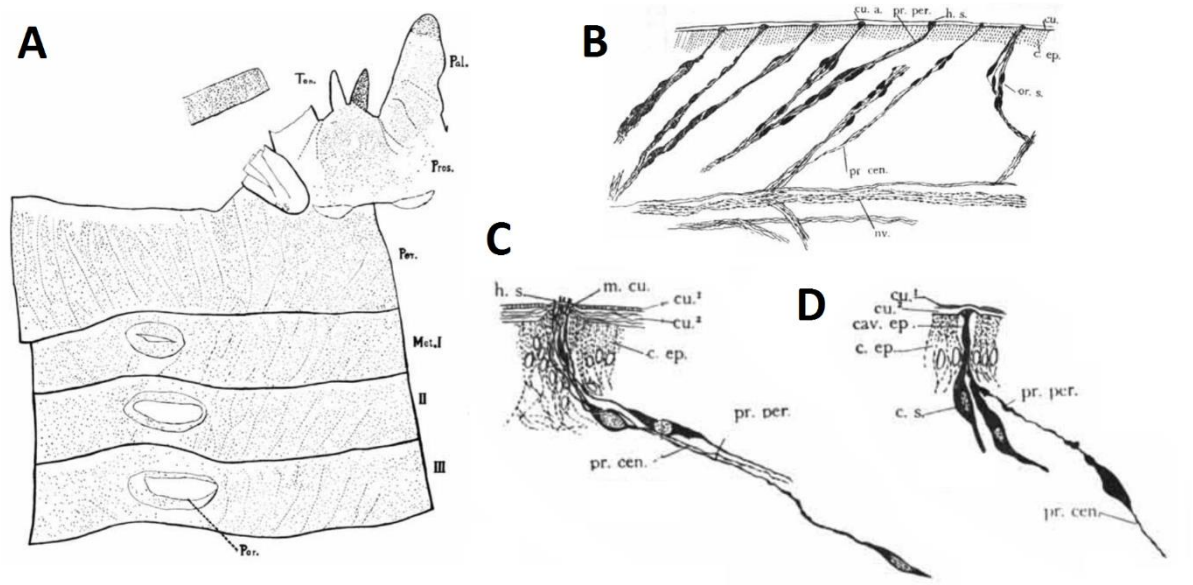


Figure II-17 (previous page) Diffuse sense organs in Nereis virens. Distribution of the organs (A), and examples of individual organs stained in (B) a tentacular cirrus, (C) an antenna, (D) a palp. (A) Organs indicated by black dots on the head (Pros. + Per.) and the first three segments (Met I-III). Note their abundance all over the body surface, with even higher concentration on antennae (Ten.), palp (Pal.) tips and tentacular cirri. Parapodia (Par.) have been excised. Drawing based on a projection of the removed cuticula. (B-D) The modified cuticular areas (cu.a.) with their sensory hairs (h.s.) correspond to the black dots in (A). Epithelial cells (c.ep.) and cuticle (cu.). Drawings based on methylene blue preparations restained by alum cochineal. Adapted from Langdon, 1900 [95] *plate I and III.*

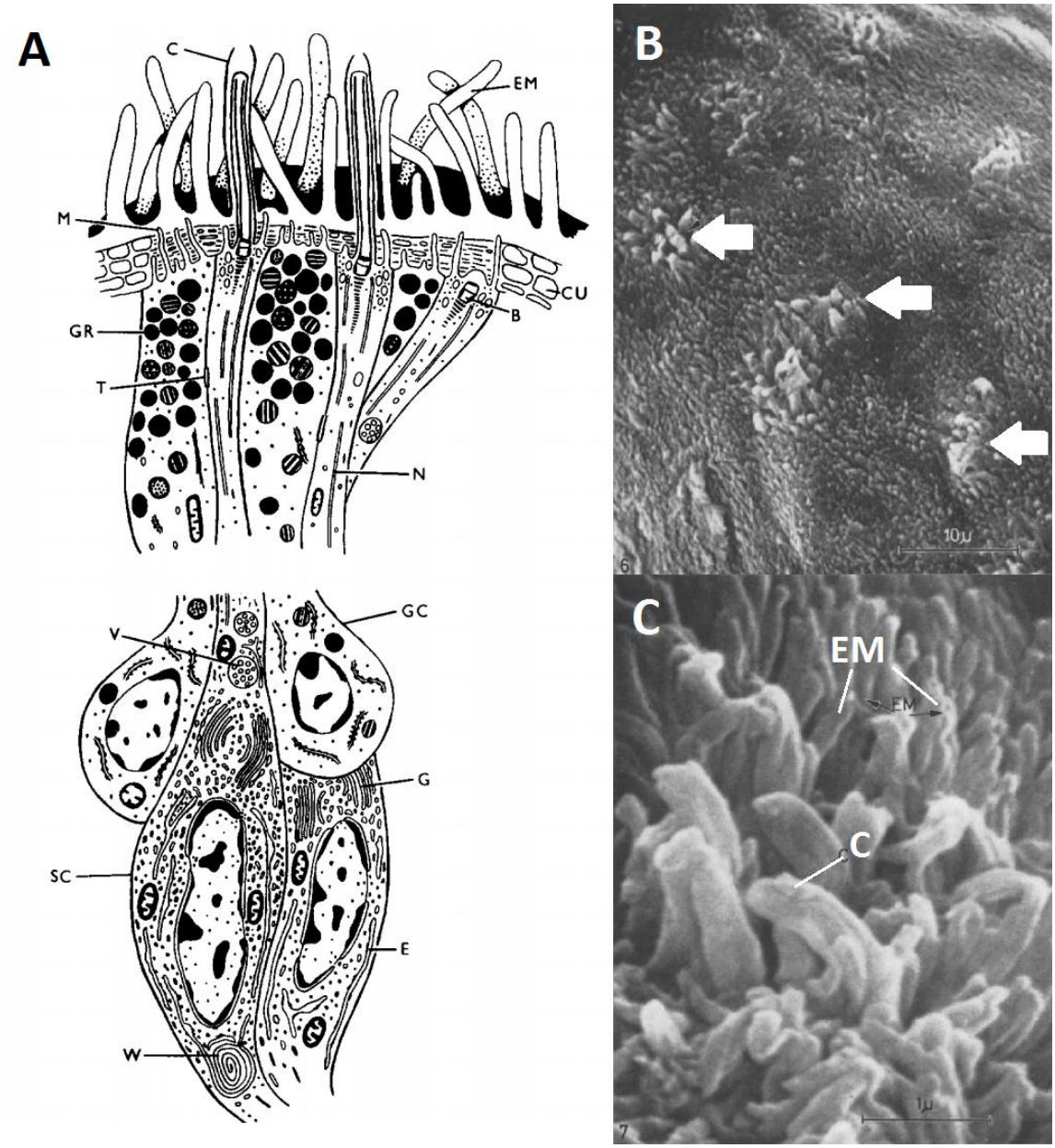


Figure II-18 Ultrastructure of the diffuse sense organ, with the sensory cilia (C) surrounded by epicuticular microvilli (EM). (A) Two fusiform, monociliated sensory cells (SC) penetrating the cuticle (CU), next to two supporting granular cells (GC) possessing epithelial microvilli (M). (B) and (C) Low-magnification Scanning Electron Microscopy images of the cuticular surface, showing the clusters (white arrows) of sensory cilia and epicuticular microvilli. Adapted from Dorsett and Hyde, 1969 [145].

least on tentacular cirri and palps. Dorsett & Hyde describe an additional type of cells which they believe are sensory. These are not ciliated but instead carry about 50 microvilli at their tip, and occur in isolation between epidermal cells. They would represent yet another category of sensory cells than those described by Purschke.

It is surprising to notice that groups of sensory cells have not been reported by Retzius in the closely-related species *Nereis diversicolor* ([89], see also Figure II-11B and Figure II-14B), even though he saw numerous isolated fusiform sensory cells and gave relatively precise descriptions of the head appendages. He might have overlooked their occurrence in groups, or not managed to stain them as such ; in any case, it is doubtful that *Nereis virens* would be equipped with diffuse sense organs but not *Nereis diversicolor*, since in *N. virens* they clearly are the organs that contain the epicuticular clusters of cilia observed at the body surface of so many polychaete species ([116], see also Figure II-5, Figure II-7, Figure II-21, Figure II-9, Figure II-12).

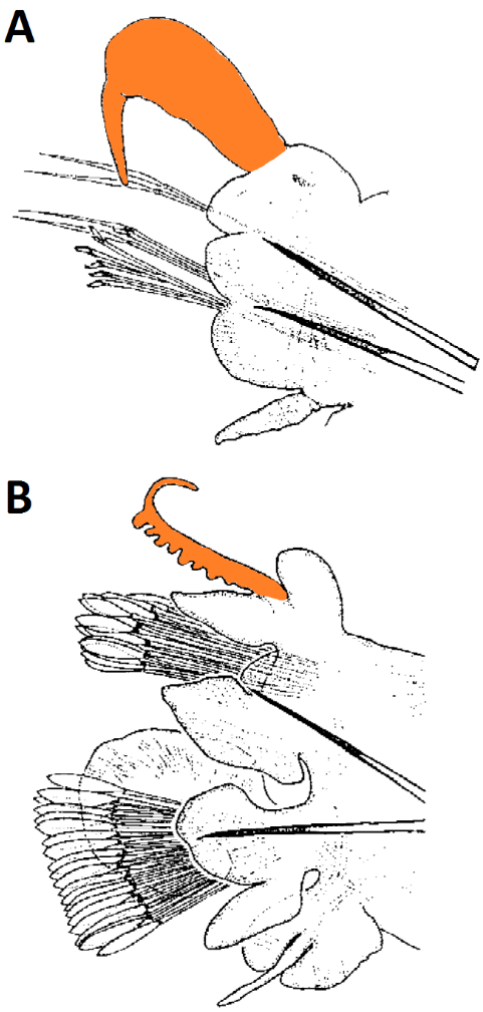


Figure II-19 Modified parapodial cirri after sexual metamorphosis, schematic drawings for Platynereis dumerilii. Examples of (A) an anterior parapodium with a massively enlarged cirrus, and (B) a posterior parapodium, with a serrated cirrus. Modified dorsal cirri are coloured in orange. Adapted from Hardege, 1999 [60]

Another account of sensory cell types in relation with a certain sensory appendage is given by Boilly-Marer, who has complemented the histological descriptions of bipolar sensory cells in nereidid parapodial cirri given by Retzius [89], Langdon [95], Smith [110] and Dorsett [137]. She has investigated the histology and ultrastructure of parapodial cirri in *Nereis pelagica* and *Platynereis dumerilii* after their transformation during sexual metamorphosis. In these species, sexual maturation results in cirrus hypertrophy (4-fold diameter increase) on the first seven segments and a notched appearance of dorsal parapodial cirri after the seventeenth segment in males, and cirrus hypertrophy on the first five or six segments in females (see [146] for the example of *Platynereis,* and compare Figure II-19 with Figure II-13C). In *Nereis pelagica*, she reports an increased number of sensory cells in male parapodial cirri and the abundance of protein-rich vacuoles under the cuticle [147]. These vacuoles are present in the epithelial cells where they originate from the Golgi, and more ribosomes and more glycogen are found in the bipolar sensory cells [148].

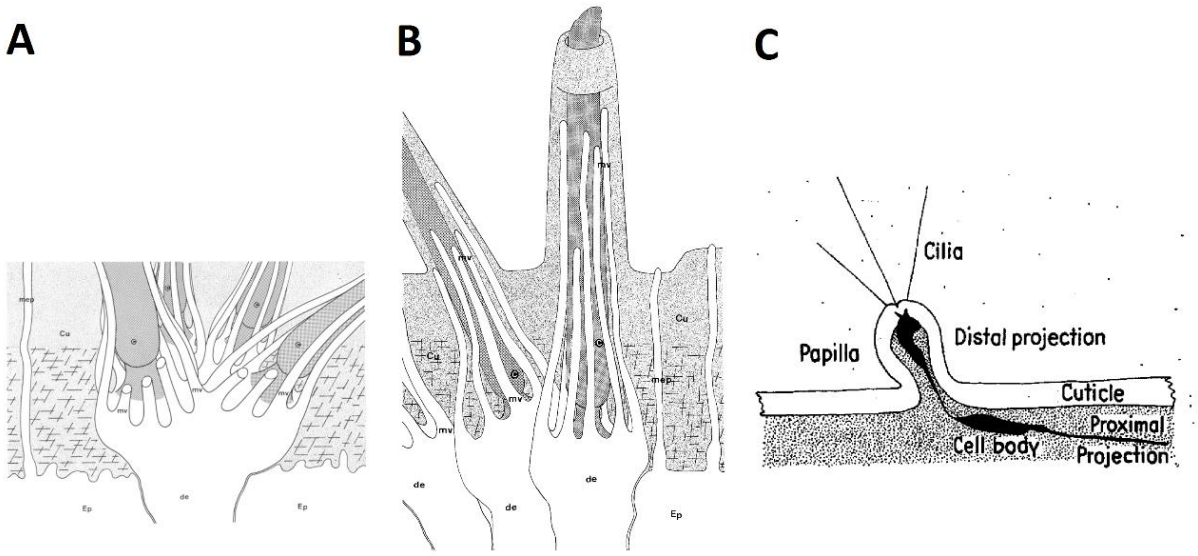


Figure II-20 Cilia of sensory cells in parapodial cirri. (A-B) Nereidids. Cilia (dark grey) and microvilli (white filaments) in dendritic processes of (A) isolated multiciliated cells and (B) grouped monociliated cells. Reproduced from Boilly-Marer, 1972 [149]*. (C) Harmothoë imbricata (Polynoidae). The sensory cell was stained with methylene blue. It sends its dendritic process into a papilla, and bears one or several cilia. Reproduced from Lawry, 1967* [150].

In an ultrastructural study of parapodial cirri in the non-sexually mature adults of *Nereis pelagica*, *Perinereis cultrifera* and *Platynereis dumerilii* [149], she distinguishes between two types of bipolar sensory cells which are both penetrative and whose cilia are always surrounded by eight to ten microvilli : some carry two to four cilia and occur in isolation (Figure II-20A), others are monociliated and occur in groups (Figure II-20B). Langdon in 1900 had described indeed in *Nereis virens* both isolated ([95] Fig. 7 and 23) and grouped sensory cells and cilia ([95] Fig. 5B and 23). The grouped monociliated cells described by Boilly-Marer in the parapodial cirri of *Nereis*, *Perinereis* and *Platynereis* are most likely the same cell type as those described by Dorsett & Hyde in tentacular cirri and palps in *Nereis*.

In the species *Harmothoë imbricata* (Polynoidae), penetrative ciliated cells have been described likewise in parapodial cirri, where their dendritic endings are located in cuticular papillae (Figure II-20C). The author does not mention whether these cells possess one or several cilia [150], they thus could belong either to type (1) or (2).

Mono- and multiciliated sensory cells have been found by Schlawny et al. all over the body surface in *Ophryotrocha puerilis* (Dorvilleidae), but particularly in antennae, palps, parapodial cirri and anal cirri, as well as the prostomium (*Ophryotrocha* does not possess tentacular cirri). They often occur in groups, have a similar ultrastructure [151] to those described in parapodial cirri in nereidids, and it could be shown that they are catecholaminergic, most likely dopaminergic [152]. This is another example of cells of type (1) and (2) in various areas of the polychaete body. The authors again report exosecretory cells, in close association with multiciliated sensory cells.

Purschke has reported in the prominent palps of protodrilids at least six types of sensory cells, comprising two types of multiciliated cells (one with numerous cilia and microvilli, the other with on average five cilia and numerous microvilli as well), two types of monociliated cells (with and without ciliary rootlet), one type of cells with non-penetrative cilia (isolated or grouped, with one or two cilia and microvilli), and cells of type (5) [142].

Ciliated sensory cells in other places than appendages or head have been described in the caudal epidermis of the lugworm *Arenicola marina*. They occur inside papillae in combination with supporting cells, and possess multiple cilia as well as microvilli [153], they are of type (1). Similar cells are actually found in the palps of Spionidae (e.g. in *Dipolydora quadrilobata* [154]).

2.3.2 Sensory cells with non-penetrative cilia

Non-penetrative sensory cells, i.e. cells of type (3) and (4), are most commonly found in nuchal organs, as evidenced by Purschke in a thorough comparative study of nuchal organ ultrastructure [122]. Their distal dendrite runs between the supporting cells and ends as a sensory bulb in the olfactory chamber, which is the subcuticular space covered by microvilli of the supporting cells and by extracellular layers. In this cavity, whose fluid is in contact with the outside medium, a few sensory cilia extend from each sensory bulb and run below the cuticle [122],[128]. Therefore, despite the appearance, only cilia of the supporting cells extend out of the cuticle, and the sensory cells are of the non-penetrative type. Purschke states that nuchal organ sensory cells are "*usually monociliated and bear several microvilli*" ([122] p. 139), thus are rather of type (4) than (3).

Non-penetrative sensory cells outside of nuchal organs have been reported in several species, notably in the dwarf male of *Dinophilus gyrociliatus* (another member of Dorvilleidae), whose complete nervous system[6] has been described in electron microscopy on serial ultrathin sections [155]. They are also described in Protodrilidae (*Parenterodrilus*, example in Figure II-1*,* Figure II-22A) and Parergodrilidae (*Stygocapitella*, example in Figure II-22B) [116]. From the literature, it is unclear however in which part of the body such cells are found.

[6] It is interesting to note that in this tiny animal, out of a total of 68 neurons, 40 are of sensory nature.

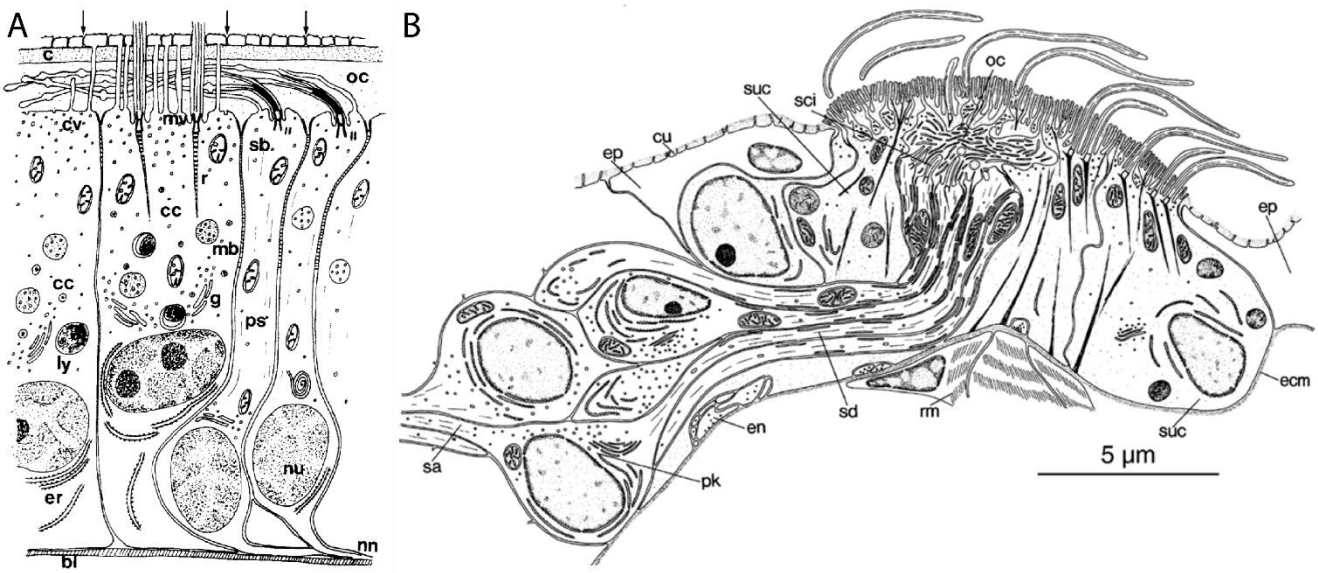


Figure II-21 Schematic representation of nuchal organs. (A) In Pygospio elegans (Spionidae), longitudinal section, exemplifying the non-penetrative character of the sensory cilia which appear here horizontal under the cuticle. Ciliated cell (cc), cuticle (c), olfactory chamber (oc), primary sensory cell (ps), rootlet (s), sensory bulb (sb). Reproduced from Schlötzer-Schrehardt, 1986 [130]. *(B) In Nerillidium troglochaetoides (Nerillidae). Reconstruction from cross sections, dorsal at left, exemplifying the typical internal morphology of nuchal organs : Ciliated supporting cells (suc) with modified cuticle and microvilli, monociliary sensory dendrites (sd), olfactory chamber (oc), perikarya (pk) of sensory cells from nuchal ganglion that give rise to axons (sa) running towards the brain, basiepithelial efferent innervation (en) and retractor muscle (rm). cu cuticle, ep epidermal cell, ecm extracellular matrix, sci sensory cell cilium. Reproduced from Purschke, 1997* [122].

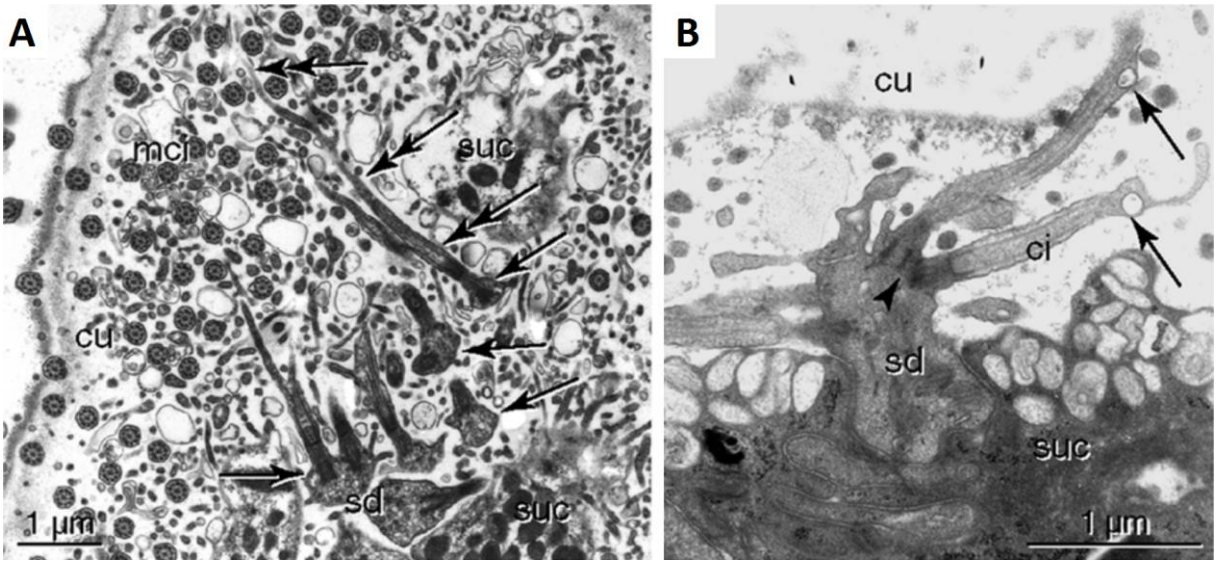


Figure II-22 Ultrastructure of non-penetrative sensory cells, sections of the cuticular region next to the dendrite, Transmission Electron Microscopy. Cilia (ci), cuticle (cu), sensory dendrite (sd), supporting cells (suc). (A) Parenterodrilus taenioides. Mono- and biciliated cells (arrows) with long cilia running parallel to epithelial surface (double arrows) (B) Stygocapitella subterranea . Reproduced from Purschke, 2005 [116].

2.3.3 Basal ciliated sensory cells

Basal ciliated cells of type (5) have been reported by Purschke and are known only in one genus so far, *Protodriloides*, in which they occur in palps and in the prostomium itself [141]. They are shown in Figure II-23.

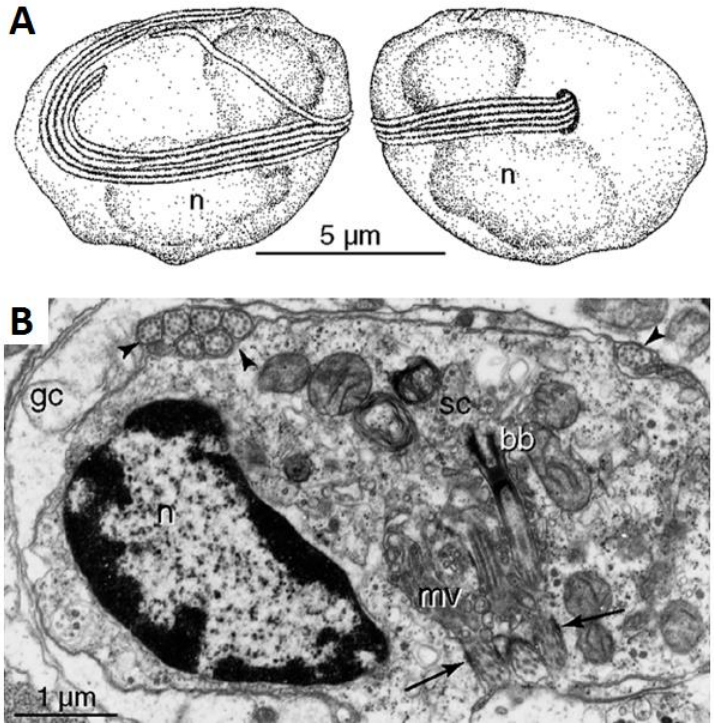


Figure II-23 Basal ciliated cells in the polychaete Protodriloides chaetifer. (A) Reconstruction of the cell with its bundle of cilia wrapped around. (B) Section of the sensory cell (sc) observed in Transmission Electron Microscopy, showing basal bodies (bb), glial cell (gc), microvilii (mv), and nucleus (n). Reproduced from Purschke, 2005 [43].

2.3.4 Location of sensory cells on the body

To summarize the preceding account of sensory cells in relation with body structures, sensory cells of type (1) and (2), penetrative multi- and monociliated respectively, are the sensory cell types that have been reported most often in polychaetes, they can be located anywhere on the body surface, and examples have been given for the following sensory structures : antennae, palps, nuchal organs, tentacular and parapodial cirri. It should be noted that cells of type (2) can co-occur with secretory epithelial cells ([145],[147],[148],[151]), which may indicate a physiological role of exosecretion in the sensory process. Cells of type (3) and (4), ciliated but non-penetrative, are seldom described ; only one study has described cells of type (5). It is reminded that photoreceptor cells, though abundant in polychaetes, have explicitly been excluded from this account.

II – 3 Physiology

In contrast to the substantial literature available on the anatomy of sensory systems in polychaetes, remarkably little is known regarding the function of the different structures and organs reviewed in the previous part, and of their sensory cells. This is all the more surprising given that appendages and sensory structures have proved to be useful characters for reconstructing phylogenetic relationships between polychaetes [104], [124], [133], and physiological data could potentially add strength to such statements.

A few electrophysiological studies have been conducted, for example in *Harmothoë* [156] and *Nereis* [137], that have allowed to attribute a sensory function to certain organs. However, the recordings have been obtained from nerves and not directly from sensory cells. Consequently, in most cases where a sensory modality has been attributed to some cells, this is based only on cellular morphology and on the resemblance with sensory cells whose function is known in other animal phyla [151]. Additionally, a few histological as well as behavioural experiments have been conducted, that provided elements of understanding about the function of polychaete chemosensory systems.

Overall, Purschke's assertion from 2005, "*To date the function of many sensory structures found in polychaetes is still uncertain or completely unknown*" ([116] p. 55), still holds today in 2017 as confirmed by Kamio and Derby in their recent review on chemical cues and food-searching behaviours in marine invertebrates : "*Polychaete worms possess a diversity of ciliated cells […] [which] have anatomical features of chemoreceptor cells, […] but rarely has the behavioral function of specific types of chemoreceptor cells been demonstrated.*" ([157] p. 516)

3.1 Physiological evidence for chemosensation in polychaete organs

3.1.1 Deductions based on cell morphology

Regarding the most conserved sensory structure in polychaetes, the nuchal organs, a chemosensory function was indicated by Racovitza in 1896, who reviewed the knowledge available at that time and complemented it with personal observations in different taxa [93]. His conclusion was based on position, histological and overall structure, that made this function the most likely, as well as some behavioural observations that spoke against a mechanosensory function. ([93], p. 257) Since then, more studies have been conducted, notably on the ultrastructure of the nuchal organs [103],[126],[122]. A possible role in osmoregulation has been suggested [158] but overall a chemosensory function for nuchal organs is accepted by the majority of authors. Yet it should not be forgotten, as reminded by Purschke, that all statements are no more than hypotheses and that "*clear physiological evidence is still lacking*" ([122] p. 123).

For the diffuse sense organs that Langdon described in *Nereis virens*, she suggested they were involved in the perception of the following stimuli : mechanical for those concentrated on antennae, palp tips and cirri, mechanical and chemical for those present at the whole body surface, and chemical for those present buccal cavity (she proposed to call them gustatory organs) ([95] p. 35-36). Even though she discusses the possible transduction mechanisms at the level of sensory hairs, her suggestions on modality were based primarily on the distribution of these organs and grounded by no physiological of behavioural experiment. Dorsett & Hyde, in their reinvestigation of her work, find that the diffuse sense organs found on palps and tentacular cirri in *Nereis* are composed of monociliated neurons, and regard a chemosensory function as the most likely, "*partly because of their position on the head and because the number of organs and neurons present is inconsistent with a purely mechanoreceptive function*" ([145] p. 526), but without physiological evidence. The rarer microvillous cells they describe are also hypothesised to be chemosensory.

Lawry, in his ultrastructural investigation of papillae on parapodial cirri in *Harmothoë*, confirms Horridge's conclusion regarding their chemosensory nature, but has tested physiologically only the secretory cells that accompany the sensory neurons, not the sensory neurons themselves [150].

Concerning the highly ciliated antennal cells of *Sabella pavonina*, Santer & Laverack do not indicate a chemosensory function, since "*preliminary physiological investigations suggest that these sense cells are mechanoreceptive, monitoring stimuli of a vibrational and tactile nature*" ([143] p. 169). They describe their ultrastructure and their groups of stiff yet motile cilia, which have spontaneous, coordinated beating, but they do not give any detail about these preliminary physiological experiments. They simply compare such cilia to those of mechanoreceptive cells found in Chaetognaths, Ctenophores and Echinoderms. Schulte & Riehl, who have observed similar sensory cells equipped with abundant penetrative cilia in *Lanice conchilega*, do not share this view, and argue for a chemosensory function, though they do not provide precise arguments and simply indicate that they agree with Boilly-Marer : "*By contrast [with Santer & Laverack], Boilly-Marer indicates chemoreception for this type of receptors of the parapodial cirri in nereids. In our opinion, in Lanice conchilega they seem to be chemoreceptors as well*[7]." ([144] p. 204) Indeed, Boilly-Marer has concluded to a chemosensory function for the two types of ciliated sensory cells she has described in parapodial cirri in nereidids. She remarks that these cells have the general structure of chemoreceptor cells, as they closely resemble the putative chemosensory cells found in molluscs and vertebrates – birds, reptiles, fish [148]. According to her, the epithelium of parapodial cirri itself can be likened to the non-secretive olfactory epithelium found in ducks and moles [149]. It should be noted that the multiciliated cells found in the antennae of the sedentary worms *Sabella* and *Lanice* carry many more cilia than those found in the tentacular cirri of *Nereis* and may thus be different. Such highly ciliated sensory cells are rare in polychaetes, as mentioned by Purschke : "*Receptors with a greater number of long cilia […] have seldom been described*." ([142] p. 17) Regarding the two other sensory cell types found in the antennae of *Lanice*, Schulte & Riehl attribute to the first one a mechanosensory function in agreement with sensory cells found in the oligochaete *Rhynchelmis limosella* [159], and to the last one, though different from known polychaete sensory cell types, a chemosensory function based on its resemblance with chemosensory cells described in fish taste buds.

Jouin et al. [153] give a thorough ultrastructural description of the multiciliated cells present in the caudal epidermis of *Arenicola* and termed by them R1 cells, which possess several features found in vertebrate [160] chemoreceptors : several apical cilia, one basal foot on each basal body, many mitochondria in the apical part of the cell, microtubules, a clear cytoplasm and short microvilii in association with cilia, as well as features found in the nuchal organs of polychaetes : thin and short striated rootlets [128]. They further indicate that the presence of mucous cells in association with the sensory cells, as described in their study, is very typical of invertebrate and vertebrate olfactory organs. The multiciliated R2 cells, which they describe as radically different, are believed to be mechanoreceptors, based on their large ciliary rootlets and their dense sheath of fibres located around the ciliary rootlets and the apical filaments [153], reminiscent of crustaceans mechanosensory organs. Their observations on the sensory nature of the R1 cells found on the caudal epidermis are to be put in relation with the strong chemical sensitivity observed in the caudal end of *Arenicola* by Schmidt in 1922 [161].

Multiciliated sensory cells similar to the ones present in *Arenicola* can be found in *Ophryotrocha*, also in association with secretory cells, and Schlawny et al. argue that they have a chemosensory function [151], a statement which again relies only on structure, not on physiological evidence. The two types of monociliated collar receptors they observe are regarded as mechanosensory, since they resemble mechanoreceptors known outside of annelids.

[7] Translated from the German : „*Dagegen gibt Boilly-Marer für diesen Rezeptor-Typ der Parapodialcirren von Nereiden Chemorezeption an. Bei Lanice conchilega scheint es sich unserer Auffassung nach ebenfalls um Chemorezeptoren zu handeln.*"

In the case of spionid palps, descriptions of sensory cells in several studies involving Scanning and Transmission Electron Microscopy suggest a chemosensory function based on their structure and position (Dauer [162][163][164][165], Worsaae [166], Lindsay et al. [154]), a statement which is reinforced by the feeding role of these appendages in Spionidae.

3.1.2 Evidence from electrophysiological experiments

Few studies are reported in the literature.

Horridge in 1963 has recorded responses from the parapodial nerve in *Harmothoë*, upon application of an acid solution of betaine on the isolated cirrus. He could observe slight electrical signals, that were nevertheless difficult to record [156]. Based on these results, together with the appearance of the cirri, and the size and number of axons, Horridge has attributed a chemosensory function to the parapodial cirri. Dorsett in 1964 also conducted electrophysiological experiments on parapodia, in *Nereis virens*, but obtained nerve recordings for mechanical stimulations only, and thus describes several cells involved in mechanoreception in the parapodium.

Boilly-Marer and Lassalle in 1980, interested in the chemical signals involved in sexual behaviours in nereidids, record signals from the brain and ventral nerve cord in six species : *Platynereis dumerilii, Nereis irrorata, Perinereis cultrifera, Nereis longissima, Nereis pelagica*, *Nereis succinea*. They demonstrate intense electrical activity upon exposure to the coelomic fluid of the other sex (which contains sex pheromones) [167]. In *Nereis succinea*, they could also show that the transformed anterior parapodial cirri were necessary to trigger this electrical activity characteristic of stimulus detection [168]. This shows that the nervous system of nereidid worms is involved in the detection of sexual signals, and brings further evidence supporting the role of the sensory cells found in the modified anterior parapodial cirri [147]. Building on these results, and on the previous identification of a glutathione derivative as the sperm-release pheromone in *Nereis succinea* [33], Ram et al. have recorded electrical activity from suction electrodes placed on parapodial cirri while the pheromone was pipetted next to the animal's head. They obtained "*rapid, reversible and repeatable responses*" ([169] p. 951) that correlated in sensitivity and duration with the behavioural responses observed in other individuals [169]. The study provides strong support for the pheromone being detected by the parapodial cirri's sensory cells, though the electrical response is still obtained from the whole appendage and not from single cells.

Direct electrophysiological evidence for the modality of individual sensory cell in polychaetes thus exists only for a few cases of mechanosensory [137] but not chemosensory modality.

3.1.3 Evidence from behavioural experiments

Some studies exist, that try to link a certain part of a polychaete's body with the detection of a chemical stimulus, and again these studies have mostly concerned nereidids.

In 1921, Gross tested the reaction of *Nereis virens* to several ionic solutions : HCl (3.33 mM), KOH (100 mM), NaOH (100 mM), KCl (100 mM), NH_4Cl (333 mM), NaCl (3 M). The animals were "*negatively chemotropic*" ([170] p. 431), exhibiting "*marked reactions*" (p. 432) while put in presence of these highly concentrated solutions. The author could measure the reaction times in a series of experiment [170]. First, he tested the reaction to solutions of KOH and HCl. Animals whose palps, antennae and tentacular cirri altogether had been removed showed a much longer reaction time, compared to before operation, and compared to non-operated animals. However, sensitivity was regained after appendage regeneration, as indicated by reaction times again similar to before operation. This showed that head appendages play an important role in the detection of these solution, though they are not strictly necessary and animals can still react when amputated, which suggests that the rest of the body has some sensitivity as well. Then, Gross quantified reaction times to KOH, HCl and NH_4Cl solutions,

after removal of one pair of appendages only : antennae, palps or tentacular cirri. Reaction times were significantly lengthened following the ablation of antennae or palps. Ablation of tentacular cirri did not affect the reaction time except in the case of reactions to the HCl solution, where it was only slightly lengthened. No effect on reaction time was seen for the ablation of anal cirri, though Gross indicates that they are sensitive to chemical stimulation. He concludes that palps and antennae in *Nereis* are endowed with a particular sensitivity to chemicals, more so than tentacular cirri despite their having a much greater surface exposed to the medium. Anal cirri are concluded not to be involved in the avoidance reaction to these solutions. The body integument has some sensitivity to chemicals, though less than head appendages. The author considers such results in line with the different innervation patterns of head appendages – directly to the brain for palps and antennae and indirectly for tentacular cirri. It should be noted that in the article no mention is made of nuchal organs. It is doubtful that the author would not have known about their existence, since they were described in many species for decades already [93]. Maybe he did not consider them because they are not protruding appendages in *Nereis* and cannot be ablated. However, it is possible that the sensitivity he observes in the absence of head appendages is the fact of nuchal organs and not of the general integument. Gross then comments on the evolutionary state of semi-centralisation of the nervous system represented by polychaete worms : "*In the higher animals, the nerves of special sense, such as sight, taste, etc., are directly connected with the brain. It is reasonable to infer that in a highly organized worm like Nereis, we have the beginnings of a concentration of sense receptors into more or less limited regions which have become secondarily but directly related to a centralized brain. This localization of the chemical sense has not progressed to any great degree, for the whole general integument of Nereis, though less sensitive than the palps and tentacles [i.e. antennae], is open to chemical stimulation. The same is true with the light sense. […] The conditions of these sense organs in Nereis are intermediate between those forms in which there is only the general integumentary sense and the higher forms in which the chemical sense is vested solely in special sense organs innervated by cranial nerves*." ([170] p. 439) It is interesting to witness, already in 1921, the opinion that the polychaete body plan is relevant for the understanding of nervous system evolution and in particular centralisation.

A second early account of chemical sensitivity in polychaetes is given by Schmidt in 1922[8], who has probed different parts of the body of *Arenicola piscatorum*, *Nereis pelagica* and *Nephtys hombergi* with droplets of sugar (most likely sucrose), saccharin and quinine : "*The chemicals were delivered with a thin pipette on certain well-delimited body parts, and these parts were thus so to speak palpated*[9]." ([161] p. 194) He also tested extracts obtained from different animals that he thought feed on polychaetes : fish, starfish and mussels. Contrary to Nagel's previous observations (1894, [171][10]), he finds that *Arenicola* is more, and not less, sensitive to chemicals than *Lumbricus* is (p. 195), and stresses the importance of performing such experiments on freshly fished animals. Schmidt reports that overall the three species react to all stimuli tested – probably avoidance reactions given the high concentrations : around 5 mM for quinine bisulphate, around 100 mM for sugar, and saccharin solutions of equivalent sweet taste. He also comments on the relevance for the worms' behaviour of chemical signals originating from other animals. Having tested front and rear end, as well as the trunk, he concludes the following : "*It is therefore apparent, that Arenicola, Nereis and Nephtys possess a sensitivity to chemical stimulations, which however is not tied to a particular part of the body but spread over the whole skin. Yet the front end is by far the most sensitive, the trunk the least sensitive,*

[8] As an interesting historical testimony, Schmidt relates with somewhat patriotic melancholy the post-First World War consequences on the island Helgoland and its ecology: "*Unfortunately, Nereis virens has almost completely disappeared from the island where it was frequently found near the port, probably due to the massive blastings through which the superb edifices of the military harbour are being destroyed, in accordance with the peace treaty*." (Translated from the German : „*Nereis virens ist leider bei der Insel, wo sie in der Nähe des Hafen häufig vorkam, wohl infolge der gewaltigen Sprengungen, durch die nach dem Friedensvertrage das großartige Werk des dortigen Kriegshafens zerstört wird, fast vollständig verschwunden*." ([73] p.194)

[9] Translated from the German : „*Mit einer feiner Pipette wurden die Chemikalien auf bestimmte, eng begrenzte Körperstellen gebracht und diese gewissermaßen damit abgetastet.*"

[10] I could not access this publication.

while the rear end invariably shows an intermediate sensitivity[11]." ([161] p. 200) Though his observations are less quantitative than those of Gross, these findings also indicate an increased chemical sensitivity in the head and in the pygidium. His conclusions on a general chemical sensitivity all over the body can be trusted more than those of Gross, since even though again nuchal organs are not mentioned, Schmidt has delivered chemicals locally on the body, and not globally in the medium as did Gross.

According to Lindsay ([172] p.348), Rullier in 1950 has demonstrated that nereidid polychaetes without nuchal organs failed to feed [173], though I could not access the publication and verify how the experiments have been conducted. Such a result could indicate that nuchal organs have a chemoreceptive function and can be used for food searching, however it cannot be excluded that experimental manipulation on nuchal organs, which do not protrude, are close to the brain in nereidids and are thus difficult to ablate, could have affected the general nervous physiology.

Another set of experiments conducted by Boilly-Marer in 1967 enabled her to conclude that modified anterior parapodial cirri play a strong role in the reception of sexual signals in *Platynereis dumerilii* [174]. Having ablated these cirri in sexually mature adults (epitokes), she observes that these animals fail to emit their genital products in presence of a normal partner, whereas this behaviour remains normal if only all other parapodial cirri are ablated, or only all head appendages (tentacular cirri, antennae and palps). This, together with her previous findings that anterior parapodial cirri acquire an increased number of bipolar sensory neurons during sexual metamorphosis [147],[148], provides almost direct evidence that these sensory neurons are responsible for the detection of sexual pheromones in nereidid polychaetes.

3.1.4 Evidence from activity-dependent cell labelling

Lindsay et al. have performed activity-dependent cell labelling in response to chemical cues, to determine whether chemosensory cells could be identified in the feeding palps of *Dipolydora quadrilobata* [154]. The method relies on the ability of agmatine, a cationic guanidinium analogue, to enter into stimulated neurons through non-specific cation channels upon their activation by ligand binding, and was initially developed to label activated olfactory neurons in zebrafish and spiny lobsters [175]. They observed that upon stimulation with a mixture of amino acids, agmatine accumulated in lateral and abfrontal cells of the palps, indicating that these cells could function as chemoreceptors, in line with their occurrence on a feeding appendage. The authors comment that such a method represents a promising approach for physiological studies in polychaete sense organs.

3.1.5 Summary of physiological evidence

Overall, a chemosensory function has been hypothesised for :
- the head (*Nereis, Arenicola, Nephtys*),
- the pygidium (*Nereis, Arenicola, Nephtys, Ophryotrocha*),
- the general body integument (*Nereis, Arenicola, Nephtys, Ophryotrocha*),
- the nuchal organs (most polychaetes species),
- the antennae (*Nereis, Ophryotrocha*),
- the palps (*Nereis, Ophryotrocha,* Spionidae),
- the tentacular cirri (*Nereis*),
- the parapodial cirri (*Nereis, Platynereis, Perinereis, Ophryotrocha, Harmothoë*).

[11] Translated from the German : *„so hat sich [...] gezeigt, daß Arenicola, Nereis und Nephtys ein Empfindungsvermögen für chemische Reize besitzen, daß dieses aber nicht an eine bestimmte Stelle des Körpers gebunden ist, sondern daß es über die ganze Haut verbreitet ist. Aber das Vorderende ist bei allen weitaus am stärksten empfindlich, am wenigsten der Rumpf, während das Hinterende stets eine mittlere Reizbarkeit zeigt."*

Partial evidence for a chemosensory function, though most often meagre, has been provided thanks to electrophysiological, behavioural or histochemical experiments for :

- the head (*Nereis, Arenicola, Nephtys*),
- the pygidium (*Nereis, Arenicola, Nephtys*),
- the general body integument (*Nereis, Arenicola, Nephtys*),
- the nuchal organs ? (Nereididae ?),
- the antennae (*Nereis*),
- the palps (*Nereis,* Spionidae),
- the tentacular cirri (*Nereis*),
- the parapodial cirri (*Nereis, Platynereis, Perinereis, Harmothoë*).

Even though a chemosensitive ability is indeed very likely for all these regions, the only convincing set of physiological evidence to date comes from the experiments conducted on the anterior parapodial cirri in nereidid polychaetes.

3.2 Molecular physiology

Almost nothing is known about chemosensory transduction in annelids. A few studies have looked for evidence for GPCRs being chemosensory receptors in polychaetes, by interfering with elements of GPCR signalling pathways : cAMP, protein kinase C

Biggers & Laufer, studying the induction by juvenile hormones of larval settlement in *Capitella* sp. I, found no induction of metamorphosis by increased intracellular cAMP [176] and concluded that cAMP is not part of the hormone transduction pathway, but however found that protein kinase C and ion channels activation mediated the settlement and the metamorphosis induced by the juvenile hormones [177]. The results of Holm et al., who also studied the chemical induction of larval metamorphosis but in *Hydroides elegans*, suggest that neither the phosphatidylinositol-protein kinase C pathway nor the adenylate cyclase-cAMP pathway play a role in the signal transduction [178]. Other investigations have targeted a more upstream molecular component of the pathway, the α subunit of the G protein itself. Among the different classes of this subunit, class q is known to be part of the chemosensory pathway in other invertebrates including insects [179], and one such protein was identified in the spionid *Dipolydora quadrilobata*, where expression was demonstrated in several sensory structures including the worm's feeding organs, the palps, which suggest a possible role of GPCR receptors in food chemoreception.

Altogether, although GPCRs are abundant in polychaetes and some of them have been deorphanised [180], no direct evidence exists about GPCRs being involved in chemoreception, and nothing is known about other chemoreceptor genes.

II – 4 Chemosensory ecology : cues and behaviours

Chemosensation in non-marine environments involves different sets of chemical cues and sensory mechanisms than in marine ones ; this is all the more true for non-aquatic environments [181]. Clitellate annelids such as earthworms and leeches are not marine animals, thus they will not be treated here. Focus will be kept on polychaetes and their chemoreception in marine environments. Chemoreception in earthworms has been a topic of abundant research, due to their relevance for agriculture and ecology, as well as their use for studies on soil toxicity. For references, the reader is referred to Edwards & Bohlen, 1996 [182], or to MacManus & Wyers, 1979 [183]. Fewer studies have been reported for the leech, for which emphasis was put on chemosensation as affecting feeding behaviours. For references, the reader is referred to Elliott, 1986 [184], or to Kornreich & Kleinhaus, 1999 [23].

In the aqueous environment, a large variety of animal behaviours are known to be influenced or caused by chemicals. These include basic behaviours of living organisms such as feeding, reproduction, defence, but also recruitment and orientation [22]. For polychaete worms, a significant body of evidence exists that demonstrates the importance of chemical signals in various behaviours [146], though "*many of the observations made by researchers in the late 1960s and the 1970s still represent our best knowledge concerning chemoreception in some polychaete taxa*" (Lindsay [172] p. 341). The following part exposes ecological and behavioural aspects of chemosensation in polychaetes, and is based partly on the review written by Lindsay in 2009 [172].

Compound or solution	Concentration used	Solvant	Reference and species studied
HCl KOH NaOH KCl NH_4Cl NaCl	3.33 mM* 100 mM* 100 mM* 100 mM* 333 mM* 3 M*	Sea water	Gross 1921 [170] *Nereis virens*
quinine (bisulphate) sucrose extract from fish, starfish or mussel	5 mM 100 mM -	Sea water	Schmidt 1922 [161] *Arenicola piscatorum*, *Nereis pelagica,* *Nephtys hombergi*
various small alcohols glutamate various amino acids mussel extracts (*Mytilus*) organic acids	≈0.5 to ≈150 mM ≈0.05 to ≈1 mM - - -	Sea water	Case 1962 [185] *Nereis virens*
amino acids sugars	5 mM 0.5 mM	Sea water	Riordan & Lindsay 2002 [186], Lindsay et al. 2004 [154] *Dipolydora quadrilobata*
NaCl H^+ (pH)	14 mM 1 µM	Sea water	Ramanathan et al. 2015 [187] *Platynereis dumerilii* (larvae)

*Table II-1 List of compounds used as cues in the polychaete literature. * effective concentration reaching the animals was lower in the experiments, due to dilution in the medium.*

4.1 General chemical cues

Regarding general chemical cues that polychaetes could detect with their elaborate sense organs, I found in the literature only a handful of studies giving useful hints. These compounds or solutions are listed in Table II-1. All these cues have been reported on the basis that they elicited behavioural responses (except for *Polydora*), hence the thresholds for detection are most likely inferior to those indicated.

4.2 Reproduction

In addition to these general stimuli, several specific active molecules have been identified which are involved in the coordination of spawning and mating in polychaetes. This has been notably the work of Zeeck, Hardege, Beckmann among others (see the review by Hardege 1999 [146]).

In nereidid polychaetes, several sexual pheromones have been described. Boilly-Marer in 1968 had established that spawning in sexually mature specimens of *Platynereis dumerilii* can be triggered by exposure to coelomic content from the other sex [188], thus clearly pointing at the existence of chemical signals involved in such communication between individuals. Zeeck et al. could identify in 1988 the first polychaete pheromone, 5-methyl-3-heptanone, which is active in *Platynereis dumerilii* [189]. Later works identified other pheromones in this species, as well as in *Nereis succinea*, *Nereis virens* and *Neanthes japonica* [190],[191]. Moreover, a specific behavioural effect could be attributed to certain molecules, for example sperm release by uric acid in *Platynereis dumerilii* [192], or induction of the nuptial dance by 5-methyl-3-heptanone for *Nereis succinea* [193].

Other studies have involved the lugworm *Arenicola marina*, in which it was shown that pheromones and hormones play a role in spawning [194], sperm release [195], water pumping [196], as well as gamete maturation [197],[198].

A few studies show the importance of chemical signals in reproduction for yet other polychaetes families, such as regarding spermatophore recognition in species of Spionidae [199], and in spawning, oogenesis, male attraction and pairing behaviour in the polynoid Harmothoe [200],[201].

4.3 Feeding

Early investigations on the species *Nereis virens* had come to opposite conclusions as to whether this polychaete uses its chemical sense for feeding. Copeland and Wieman in 1924 have investigated this sense in relation with food searching and feeding behaviour [202], though they did not attempt to relate it to a particular sensory structure. Following a series of experiments in which food items were presented next to the worms' burrow opening, and worms consequently came out of the burrows to try to seize the food, they concluded that "*there is positive evidence that Nereis depends upon a chemical sense in finding animal food*" (p. 238). Besides, they observed that vision or photoreception, despite *Nereis* having large lens-equipped eyes, is not relevant in such behaviours : it "*plays an insignificant if any part in these [food-searching] reactions, for if a pipetteful of filtered clam extract is substituted for the clam […], the worms show the same responses, extending their bodies towards the center of the dish where the extract was placed*" ([202] p. 236). These observations that *Nereis* uses chemoreception to locate food is in disagreement with Gross's statement in 1921 : "*A number of experiments were made with the natural food in an effort to localize the sense of taste, but the worms showed no consistent responses to food of any kind. They fed freely upon sea lettuce and other plants placed in the aquaria, but the finding of it was more or less accidental. Food hidden in sand, placed in cheese-cloth bags, or otherwise concealed was, as far as could be determined, never detected by the worms. Animals from which one or all of the pairs of cephalic appendages, such as the tentacular cirri,*

palps, and tentacles, were removed, fed and thrived as well as normal animals. It is evident that the sense of taste, or chemical sense, of Nereis virens does not play an important role in locating and selecting food." ([170] p. 430-431) Gross may have misdesigned his experiments, or may have used food items that released little chemicals and were thus irrelevant. Moreover, he did not consider the role of nuchal organs in his ablation experiments. It can thus fairly be said that Gross made an erroneous conclusion on that question, and that *Nereis* does use chemoreception to locate food, as demonstrated by Copeland and Wieman.

More recently, Watson et al. could show that foraging and feeding in *Nereis virens* is modulated by exposure to whole-body extracts of conspecifics [203]. Indeed worms display a reduced foraging activity upon detection of such signals, and the authors interpret these chemical cues as being alarm signals which would occur when conspecifics have been preyed upon.

The choice of feeding or not feeding is obviously important for deposit feeders, depending on what quality of organic material is available. It has been shown that some polychaete species use chemoreception to adapt their feeding behaviour in that way. For example, some spionid worms would feed less if fresh faeces are present on the bottom [204]. Conversely, the presence of fresh plant debris can rapidly increase feeding rates [205],[206]. Another species of spionid polychaetes, *Streblospio benedicti*, prefers to feed on sediments that are enriched in organic matter [207].

Regarding actual chemical cues involved, Mangum and Cox have shown that *Diopatra cuprea* (Onuphidae) reacts to extracts of many (32) marine organisms and to numerous other chemical substances including amino acids extracted from bivalve molluscs [208]. Irrigation currents or opening of the mouth were triggered by several sugars, by hemoglobin and by fresh blood of other polychaetes. Solutions of single amino acids (cysteine, hydroxyproline, methionine, phenylaline, proline, valine) also elicited these feeding currents, with threshold concentrations between 10 µM and 10 mM. A specific role could even be attributed to a few amino acids for the feeding behaviour.

Ferner and Jumars have identified both some phagostimulants and some phagodepressants for the species *Boccardia proboscidea* and *Pseudopolydora kempi* (Spionidae). These were respectively ADP, algal and crustacean extracts, commercial fish food on the one hand, and taurine, threonine, valine, and glycine on the other hand [209]. Other phagostimulants for the spionid worms *Dipolydora quadrilobata* [186] and *Streblospio benedicti* [210] are particle-bound amino acids and sugars.

Spionids are particularly interesting from the point of view of feeding and chemoreception due to their large palps that are used as feeding appendages.

4.4 Larval settlement and metamorphosis

Less obvious than feeding or reproduction, but no less of a challenge for marine invertebrate animals, is the critical phase of larval settlement [211][212][213]. Many of these marine larvae are indeed planktonic, living in the water column, while their adults are benthic, living on the sea floor. Settlement of the larvae to the bottom substrate constitutes an essential life-cycle transition, since larval survival and development, and thus species survival, will highly depend on what substrate they land on. This settlement is known to be induced by chemical cues from the environment [213][22], and to often implicate the apical organ [214], an anterior group of sensory neurons found in diverse ciliated larvae. The majority of polychaete species have larval settlement, and numerous experiments have demonstrated the role of chemical cues in this process.

Overall, it has been showed that larval is settlement influenced by amino acids [215], inorganic ions such as potassium [216], juvenile hormones [176], free fatty acids [213], polysaccharides [217], and several neurotransmitters [75]. Moreover, larvae are reported to respond to bacterial metabolites, probably some that are concentrated in the extracellular polymer matrix of the cells [218].

Multispecies bacterial biofilms are known to attract larvae [217],[219]. More precisely, Harder et al. showed that larval settlement in *Hydroides elegans* (Serpulidae), otherwise occurring on some monospecies bacterial films, can be recapitulated to the same degree by the lipophilic fractions of metabolites isolated from two bacterial species [220]. The bacterial biofilms commonly found at the sea bottom are likely to play a strong role in larval settlement, though it should be noted that most studies on biofilm attraction have concerned *H. elegans* only and were performed in the laboratory.

With regard to deterrence, Woodin et al. have showed that nereidid larvae avoid sediments inhabited by adult worms of *Thelepus crispus* (Terebellidae), and could identify a bromobenzyl alcohol produced by these worms as the rejection cue [221]. Burrowing times in newly settled *Arenicola cristata* juveniles are longer when they are placed on sediments enriched with brominated phenol derivatives such as 2,4-dibromophenol naturally produced by the other polychaetes *Notomastus lobatus* (Capitellidae) [222]. In *Streblospio benedicti* (Spionidae), larval settlement is inhibited by 1-chlorononane, which mimics a metabolite produced by adults. This indicates that larvae will avoid areas that are already densely inhabited by conspecifics [223]. More generally, higher ammonium concentrations and lower oxygen concentrations in surface sediments will lead newly settled polychaetes to avoid them [224]. Similarly, larvae of *Capitella teleta* tend to avoid sediments that had been disturbed by adults and had high content of faeces [225]. In *Arenicola cristata*, low ammonium concentrations, indicative of absence of adult worms, promote larval settlement [226].

Besides, it was known that for example some crustacean larvae were sensitive to cues emitted by their adults and directed at them [26]. Such an adult-larva chemical communication has been described as well in polychaete larvae, namely in *Platynereis* in which food-deprived adults produce a chemical signal that retard larval development [227].

These studies together clearly show that polychaete larvae will settle preferentially in areas that are rich in food and not occupied by too many competitors – typically, adults of the same or of other species.

4.5 Aggression and avoidance

Chemical cues can carry information about the presence, number and sex of conspecifics, which can be used for example to assess the number of reproductive competitors or partners present in close surroundings, as was demonstrated for *Ophryotrocha diadema* [228]. This enables this hermaphroditic species to regulate sex decision.

Detecting conspecifics from different populations can also trigger aggressive behaviours, as was observed in populations of *Nereis acuminata* by Weinberg et al [229]. They could show that exposing animals from a population of *N. acuminata* to sea water collected next to other populations of the same species specifically induced fighting behaviours, which they linked with population recognition and premating reproductive isolation. A later study by Sutton et al. 2005 confirmed that a chemical signal was likely to be involved in this behaviour [230].

4.6 Environment probing

Finally, it should be noted that polychaete worms can also actively probe their chemical environment. This is known in nereidids, and was observed early by Copeland and Wieman in *Nereis virens*. Surprised by the rapidity with which worms can detect the presence of food from inside their burrow, they could then link these reactions with the undulatory movements produced by the worms while resting inside their tubes [202]. Indeed, nereidid worms show intermittent undulations of their body [231] that create a water current to circulate inside their tube and can be visualised by addition of particles : "*Carmine grains dropped in the water a few centimeters above an opening of the burrow were*

immediately drawn inside. […] From this it is clear how Nereis, concealed in its passageway within the sand, receives not only a constant supply of fresh water but also may be stimulated by any chemical change in the water above. " ([202] p.237) In this way, worms protected inside their tube still have access to the chemical content of the water surrounding them, which potentially allows them to detect conspecifics, food or predators. Water irrigation currents are also well known in *Arenicola* where their role for respiration has been characterized [232], and the presence at the epidermal surface of sensory cells that are likely chemosensory [153] suggests that *Arenicola* as well as *Nereis* would indeed regularly sample the chemical environment present around its tube. Since many polychaete species live in tubes, such a behaviour is likely to be of general significance for polychaete chemical ecology.
James Case in 1962 has reported experiments showing that *Nereis virens* can detect several chemical cues (see Table II-1) while resting inside its tube, and he observed and quantified their approach or avoidance behaviours as a function of the stimulus concentration [185]. These findings confirm that tubicolous polychaetes can effectively sense their chemical environment while being protected inside their tube.

II – 5 Review summary

A rich literature is available on annelid anatomy and specially polychaetes, including old yet valuable descriptions from the 1880s to 1920s. In fact, some early and correct descriptions of cellular structures reported from studies based on light microscopy were sometimes not confirmed until electron microscopy was used in the 1960s and 1970s, as illustrated by ciliated sensory cells described by Fanny Langdon in *Nereis* in 1900. Even though many families have been investigated, a majority of studies have focused on the errant polychaete worms of the family Nereididae, notably the genus *Nereis* due to its experimental amenability.

Polychaete worms are endowed with elaborate sensory organs and appendages which their terrestrial relatives oligochaetes and leeches overall do not have. The main head sensory organs are, from most common to least common : nuchal organs, palps, antennae, tentacular cirri. On the segmented region of the body as well as on the other unsegmented extremity, the pygidium, sensory organs similar to tentacular cirri are found : the parapodial and anal cirri respectively. Actually, it is probable that anal and tentacular cirri are nothing but evolutionarily modified parapodial cirri.

All these organs are thought to be chemosensory, nevertheless no convincing proof was ever given except for the parapodial cirri in sexually mature adult nereidids. This paucity of evidence for function is in striking opposition with the abundant anatomical literature. The molecular mechanisms of chemosensation and the chemoreceptor proteins are to this day unknown in polychaetes.

Five main categories of sensory cells are known in polychaetes. The two most common types are multi- and monociliated cells that penetrate the body cuticle, they can be found all over the body surface with a particular concentration on sensory appendages. Both have been hypothesised to be chemosensory by several authors, but no experimental demonstration was reported.

It was shown that chemical cues play a crucial role in all basic types of behaviours in polychaetes, including feeding, defence, reproduction, navigation, and larval settlement, though only a few molecules have been identified with certainty as cues.

Polychaetes offer a fertile ground for the comparative and evolutionary study of chemosensation in the animal kingdom, especially in the context of marine habitats, and significant results can be expected if research is undertaken in that direction.

II – 6 Chemosensation in *Platynereis dumerilii*

6.1 Available literature on *Platynereis*

After this review of the available knowledge on chemosensation in annelids, let us summarise what is known for our species of interest, *Platynereis dumerilii*. Only a few articles in the vast literature cited above have dealt with sensory organs in this particular species ; they are listed in Table II-2. A similar table can be found in Appendix A, that details the species investigated in all articles cited in this chapter. As a matter of fact, the actual knowledge on *Platynereis* chemosensation is rather scarce.

Reference / Families	Species investigated	Type of study
Racowitza 1896 [93]	*Platynereis dumerilii*, Amphinomidae, Euphrosinidae, Spintheridae, Maldanidae, Chrysopetalidae	Anatomy
Hempelmann 1911 [96]	*Platynereis dumerilii*	Anatomy and life history
Smith 1957 [110]	*Nereis diversicolor, Nereis virens, Platynereis dumerilii*	Anatomy, electrophysiology
Boilly-Marer 1967 [174] 1968 [188] 1972 [149] 1980 [167]	*Nereis pelagica, Nereis irrorata, Nereis longissima, Nereis succinea, Perinereis cultrifera, Platynereis dumerilii*	Anatomy, behaviour, electrophysiology
Fischer et al. 2010 [138]	*Platynereis dumerilii*	Anatomy
Schmidtberg & Dorresteijn 2010 [233]	*Platynereis dumerilii*	Anatomy
Starunov et al. 2017 [102]	*Platynereis dumerilii*	Anatomy

Table II-2 Summary of articles related to sensory organs and chemosensation in Platynereis

The study by Smith in 1957 is the earliest I could find that concentrates on *Platynereis*' nervous system, but the author was interested in the body segments and has given only a superficial description of the head. Boilly-Marer in her extensive anatomical, physiological and behavioural experiments on *Platynereis* has focused mainly on one type of sensory organ, the parapodial cirri, which also belong to the trunk. A precise description of the nuchal organs is given by Schmidtberg & Dorresteijn in adult *Platynereis*. Valuable descriptions of *Platynereis*' early development have been given notably by Fischer and Dorresteijn [234],[65],[235], yet head sensory organs are hardly formed at the stages described.

The most detailed anatomical description available for *Platynereis* is probably that of Fischer et al., which comprises systematic brightfield images and anatomical stainings of tubulin, phalloidin, cell nuclei and serotoninergic cells until the 5 days stage, and brightfield images for stages older than 5 days. Anatomical stainings at later stages can be found in the recent article by Starunov et al., which have used antibody stainings to reveal RFamidergic, serotoninergic and catecholaminergic cells at different developmental stages in *Platynereis*, though the study concentrates on stages until 5dpf, and no specific description of the head region is given.

As can be observed, no detailed description of neuroanatomy is available in *Platynereis* for the head and its sensory organs at stages older than 5dpf. Yet these missing stages are exactly the ones that are crucial for the study of chemosensation, since head appendages and hardly formed in early larval stages.

6.2 Putative chemosensory organs and their function

As shown in Figure II-24*, Platynereis dumerilii* has two pairs of adult eyes located dorsally on the prostomium, one pair of frontal antennae, one pair of fronto-lateral, ventral palps, four pairs of lateral tentacular cirri (two long dorsal ones and two shorter ventral ones) located on the peristomium, one pair of nuchal organs (not visible), one dorsal and one ventral cirrus for each parapodium, and a pair of anal cirri located at the posterior body end or pygidium. The totality of these organs (except the eyes) have been suggested to be chemosensory, based on their morphology and on the expression of molecular markers. However, there exists currently no proof of chemosensitivity for any of them, except for the modified dorsal parapodial cirri which detect pheromones (Boilly-Marer [167],[174]). These physiological statements are summarised in Table II-3. In *Platynereis* only general descriptions in light microscopy exist for antennae, palps and tentacular and anal cirri [138],[235], with no details concerning internal architecture or cellular morphology. Parapodial cirri have been investigated in more details (Smith 1957, [110]), notably in electron microscopy (Boilly-Marer 1972, [149]). An ultrastructural study is available for the nuchal organs (Schmidtberg & Dorresteijn 2010, [233]), which had also been investigated in detail by Racovitza in light microscopy [93].

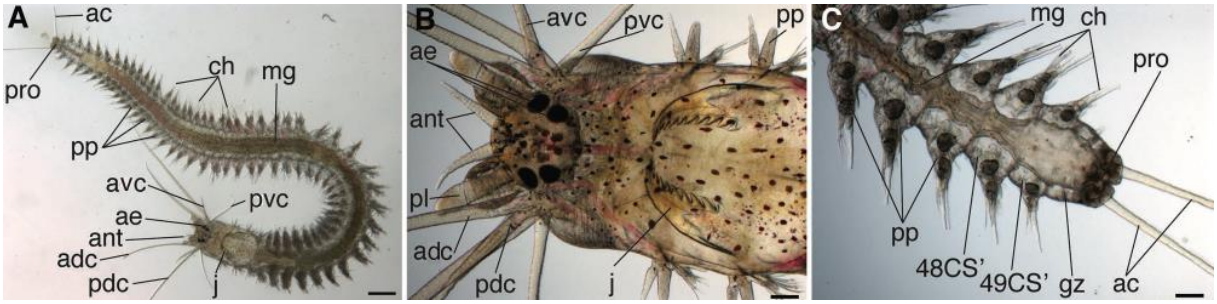


Figure II-24 Overview of body appendages and head anatomy in Platynereis dumerilii. 48-segmented juvenile in dorsal view (A), with detail of the head (B) and the pygidium (C). Anal cirri (ac), adult eyes (ae), antennae (ant), anterior (adc) and posterior (pdc) dorsal cirrus, anterior (avc) and posterior (pvc) ventral cirrus, palps (pl), parapodiae (pp). Note in (B) the cirri present on the parapodiae, they are shorter than antennae. Scale bar : 500 µm in (A), 100 µm in (B) and (C). Reproduced from Fischer et al., 2010 [138].

An important larval structure has been the focus of several studies : the **apical organ** (Figure II-25). Widespread in marine larvae, these surface ciliated organs are sensory and play a role in the control of settlement and metamorphosis [236]. This has been confirmed in *Platynereis* where a conserved myo-inhibitory peptide (MIP) is part of the signalling [75], and the apical organ contains several cell types [236] including so-called flask cells that are sensory-neurosecretory [68]. These flask cells express *otp*, *miR-7*, prohormone convertase 2 (*phc2*), carboxypeptidase-E (*cpe*) [236],[237], as well as the neuropeptide FMRFamide found in some vertebrate hypothalamic neurons [68] in the amphid chemosensory neurons of *Caenorhabditis elegans* [238]. The investigation of their ultrastructure in electron microscopy confirms a probable chemosensory function, since their dendrite ends with one or two cilia located in the subcuticular space in contact with the sea water medium [75],[68]. Two of them express MIP, and can be revealed by passive dye filling with MitoTracker at around 2dpf, which is often a property of chemosensory neurons [75]. Even though no direct proof exists yet, this together with the expression of several other neuropeptides [239] makes the apical organ a clear candidate sensory organ in *Platynereis* larvae.

Organ	Proof of chemosensory function coming from	Indication of chemosensory function coming from
Nuchal organs	-	cellular and general morphology (light [93] & electron [233] microscopy), molecular markers
Antennae	-	general morphology
Palps	-	general morphology
Tentacular cirri	-	general morphology
Parapodial cirri	ablations & behavioural experiments [174], electrophysiology [167].	cellular and general morphology (light [110] & electron [149] microscopy),
Anal cirri	-	general morphology
Foregut	-	cellular and general morphology (light & electron microscopy [240]), ablation & behavioural experiments [240], molecular markers [240].
Apical organ (larval)	-	cellular and general morphology (light & electron microscopy [75],[68]), molecular markers [75], [236], [68], [237]

Table II-3 Summary of physiological evidence for Platynereis candidate chemosensory organs.

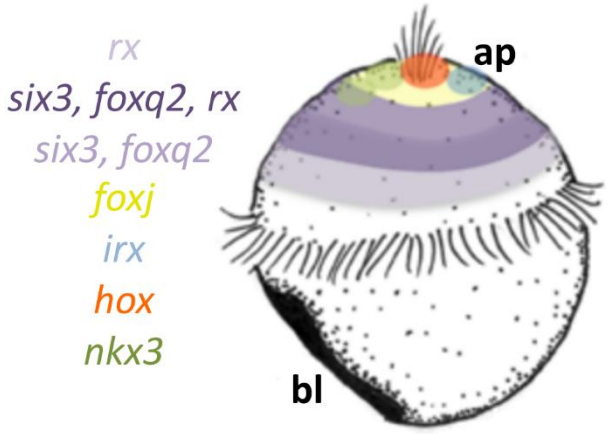


Figure II-25 Molecular territories in an annelid trochophore larva. Schematic drawing showing gene expression data around the ciliated apical organ (ap). Blastopore (bl). Adapted from Marlow et al., 2014 [236].

The amenability of *Platynereis* larvae to the molecular characterization of cell types has motivated gene expression studies in other organ systems. Sensory cell types in the larval foregut have been investigated in light and electron microscopy by Simakov (PhD thesis, 2013), who also conducted ablation experiments combined with feeding assays which showed a delayed feeding response upon ablation [240]. This constitutes only indirect evidence that the foregut is equipped with chemosensory cells, and behaviour experiments with the ablation of control cells would be needed.

Peripheral sensory neurons have been described in the parapodia by Lauri (PhD thesis, 2013), and are characterised by the expression of the transcription factors *prdm1*, *msx*, *phox2*, *brn3*, and *islet* (for a graphic summary see figure 72 p. 117, [241]). They are thought to detect physiological and/or environmental chemical signals.

A study of microRNAs by Christodoulou (PhD thesis, 2009) revealed some specificity of expression in sensory organs [242],[243]. miR-8 marks antennae, palps, parapodial sensory neurons, nuchal organs and foregut ; miR-9 and miR-9* mark the base of the antennae ; miR-71 marks the nuchal organ and the palps ; miR-252 and miR-2001 mark antennae, palps and parapodial sensory neurons ; miR-315

marks antennae, head, palps, nuchal organs as well as the head dorsal sensory organ or dorsal pit. Table II-4 shows a summary of these molecular characterisations, as well as the developmental timing of all candidate sensory organs.

Sensory organ	External morphology recognisable from stage	Molecular markers
Apical organ	1 dpf [138]	*otp*, *miR-7*, *phc2*, *cpe* [236],[237]
Nuchal organ	2 dpf [237]	*cry1* [237], *miR-8, miR-71, miR-315* [243]
Antennae	3 dpf [235]	*dlx, miR-8, miR-9, miR-9*, miR-252, miR-315, miR-2001* [243]
Palps	5-6 dpf [138]	*dlx, miR-8, miR-71, miR-252, miR-315, miR-2001* [243]
Tentacular cirrus – anterior dorsal	4 dpf [138]	*dlx* [243]
– anterior ventral	4-5 segments [138]	-
– posterior ventral	5 segments, post cephalic metamorphosis [138]	-
– posterior ventral	?	-
Parapodial sensory neurons	4 dpf [138]	*prdm1*, *msx*, *phox2*, *brn3*, *islet* [241], *trpv* [69], *miR-8, miR-252, miR-2001* [243]
Anal cirri	3 dpf [138]	-
Foregut		*nk2.1, nedx* [240], *miR-8* [243]

Table II-4 Developmental timing and molecular markers for Platynereis putative chemosensory organs.

6.3 Relevant chemical cues

In *Platynereis* sexual pheromones are the only chemical cues that have been identified with certainty : the two optical isomers of 5-methyl-3-heptanone released by one sex each, which trigger the nuptial dance [189], uric acid released by females, which triggers sperm release in males [192], and L-ovothiol A, which triggers egg release in females [244].

It was shown with behavioural experiments that *Platynereis* larvae detect variations of acidity and salinity [187], and some knowledge exists concerning the molecular aspects of pH detection [245], but pH and salinity constitute rather environmental parameters than specific chemical cues.

There is also evidence that parapodial sensory neurons detect the levels of CO_2 dissolved in sea water (Paola Bertucci, unpublished).

6.4 Chemoreceptor proteins

Nothing is known regarding which receptor proteins would be involved in chemosensation in *Platynereis*. GPCRs are present and abundant in the genome, but have so far been shown to bind only neuropeptides [180], not external chemical signals. The sensory flask cells of the apical organ are thought to mediate larval settlement via the secretion of MIP, but neither the environmental cue(s) by which they would be activated nor the potential receptors involved could be identified so far [75].

6.5 Summary for *Platynereis*

Sensory organs have been well described in *Nereis* but unfortunately not in *Platynereis*. The paucity of anatomical descriptions available for *Platynereis*' head sensory organs and their neuroanatomy at stages older than 5dpf makes it necessary to conduct an anatomical study at these stages before any physiological study can be undertaken.

Regarding physiological aspects of chemosensation in *Platynereis*, nothing has been demonstrated as to which head organs would be chemosensory, despite substantial molecular and anatomical data suggesting that antennae, palps, tentacular cirri, nuchal organs and the larval apical organ could all serve this sensory modality (in addition to anal cirri and ciliary folds of the foregut, in the rest of the body). Even if partial physiological evidence exists in the closely-related genus *Nereis*, which makes it reasonable to assume that at least the head appendages and the anal cirri are indeed chemosensory in *Platynereis*, direct physiological evidence for chemosensation was never given in except for modified parapodial cirri in sexually mature adults. Besides, nothing is known regarding chemoreceptor proteins or the molecular mechanisms of chemosensory transduction.

Three molecules only have been identified as relevant chemical cues, and behaviour in relation with chemical signals has been described mostly in the context of reproduction in sexually mature adults [174],[192], not in larvae.

Consequently, most anatomical aspects and almost all physiological aspects of chemosensation remain to be described in *Platynereis dumerilii*, despite the likelihood of chemical cues playing a major role in *Platynereis*' ecology and behaviours, as they do in other polychaete species and in marine species in general.

III – Neuroanatomy and development of presumed chemosensory organs

III – 1 Introduction

1.1 Candidate chemosensory organs are poorly characterised in *Platynereis*

Several polychaete organs present in *Platynereis* are presumed to be chemosensory, mostly based on their anatomy : nuchal organs, palps, antennae, tentacular cirri, parapodial cirri and anal cirri – that is to say, all body appendages as well as the nuchal organs are thought to be chemosensory.

As exposed in Chapter II, anatomical descriptions are rich within Nereididae and notably for the genus *Nereis*, but with a few exceptions [246] are restricted to adults : see [93], [94], [97], [134] for classical anatomical studies, [99] for a cytological and histochemical study, [110] for the nervous anatomy of body segments, [247] for comparisons of head innervation patterns, [135] for an electron microscopic study, [248] for an immunofluorescence study of the head. The detailed descriptions which exist in *Platynereis* are mostly restricted to embryonic stages, and to larval stages until 5 days of development : see [235], [138], [102] for developmental studies and nervous system anatomy, [80], [59] for studies of gene expression, [120], [81] for reconstructions of neuronal circuits. Unfortunately, at these stages the candidate chemosensory organs have hardly started to develop, hence such anatomical knowledge provides only a partial basis for the study of chemosensory organs. Fischer et al. have provided an overview in widefield light microscopy of head appendages development from late nectochaete stages on, but no description of their relative sizes and position, nor of their internal structure [138].

The innervation and internal anatomy of palps and antennae is not described in *Platynereis* ; for tentacular cirri they are sometimes partly apparent on images but are not the focus of interest (e.g. Figure 4 in [71]). Anal cirri and notably their innervation have been described in studies of the pygidium and its regeneration [249], [250], [251], [252] but their complement of sensory cells has not been investigated. The nuchal organs are probably the candidate chemosensory organs that have been described in most detail in *Platynereis*, with one ultrastructural study in sexually-mature adults [233] and one connectomic reconstruction after serial-section based electron microscopy at 3dpf [253].

Nuchal organs and the larval apical organ possess ciliated sensory cells with non-penetrative cilia [68], [233], modified parapodial cirri possess ciliated cells with penetrative cilia [149]. For the other candidate chemosensory organs, it is presently unknown in *Platynereis* which of the polychaete sensory cell type categories identified by Purschke [116] are present, even more so regarding which types are found in relation with which organ. Nothing physiological evidence exists regarding the function of the head sensory appendages and of the nuchal organs, beyond the obvious mechanosensitivity of tentacular cirri. Despite all candidate head appendages being prominent structures in adults, they have been the focus of no anatomical study to this day. It is apparent thus that more detailed anatomical descriptions are required if one wishes to investigate chemosensation in *Platynereis*.

Besides, neuroanatomy of the adult brain in errant polychaetes such as *Platynereis* reveals highly obvious organs : the Mushroom Bodies (MB). The MB are a paired neuronal structure consisting of densely packed cell bodies, located anteriorly and separated in two masses : a dorsal and a ventral lobe. Both lobes possess a so-called peduncle, which is a bundle of nervous fibres containing all axons projecting from the lobes. Although polychaete MB are easily stained and have been known to anatomists for more than a century [90],[97], still nothing is known about their function. Importantly, it has been speculated that they would play a role in learning phenomena, and their resemblance with the homonymous structure found in insect brains makes them of particular interest for evolutionary studies, since insect MB are known to mediate notably associative learning [254]. While the position and boundaries of MB are obvious in the brain of adult *Platynereis*, at early developmental stages they are not, and a description of their development in larval and early juvenile stages allowing their reliable identification would provide a useful basis for physiological studies. A first description of MB development was given in *Platynereis* [255], nevertheless the images provided do not allow a global

representation of how the MB are positioned compared to all other brain regions throughout development. Notably, it is important to know from what stage on the dense packing of neuronal somata observed in adults is established and can be used as a criterion to recognise the MB. For these reasons, a more precise description of MB anatomy will be useful.

1.2 A precise neuroanatomy is needed at 6 dpf

The 6-days-old stage in *Platynereis* has emerged as a reference stage for the description of gene expression patterns. While the current connectomic information is available at 3 days of development, at this stage the animal is still lacking well-differentiated sensory organs as well as other adult features. The 6 dpf stage on the contrary represents a sort of miniature adult, with antennae, palps, nuchal organs as well as a freshly developed pair of tentacular cirri, and corresponds to the stage when animals start settling on the sea ground and exploring the environment. It is thus more interesting in the perspective of studying behaviours and locomotion, in link with neuronal circuits and gene molecular identity of cells. Moreover, building on the suitability of *Platynereis* larvae for evo-devo studies, this stage may be of particular interest for comparative and evolutionary studies of chemosensation.

Unfortunately detailed neuroanatomical descriptions in *Platynereis* are available only until the 5 dpf stage, and larvae at such early stages show significant differences across days, hence research on *Platynereis* would benefit from a precise knowledge of head and nervous system anatomy at 6 dpf.

1.3 Experimental approach

To better resolve the formation and complexification of candidate chemosensory organs, as well as the progressive establishment of their innervation patterns, my approach has been to start from late juvenile animals, in which these organs have obvious external structures (typically, they are prominent appendages) and internal compartmentalisation (typically, they are enclosed in extracellular layers), and to trace them back step-by-step in developmental time, as they become increasingly harder to recognise. At the 6 dpf stage indeed, no obvious cell group stands out in the larval brain of *Platynereis* at first sight, and it mostly appears as an unordered mass of cell bodies packed in the head periphery. I have investigated the head anatomy in stages that are distant enough to avoid redundant experiments, and yet close enough to establish region correspondences across stages. Whenever possible, descriptions were given of sensory cells and their sensory processes.

After a description of sensory organ development, a precise description of neuroanatomy at the 6-days-old stage is provided, which comprises 10 representative planes in dorsal view and 10 representative planes in lateral view, to help visualise the spatial relationships between organs, nerves and neuronal ganglia in the whole volume of the head.

I had the pleasure during my PhD to supervise a motivated Master student, Wiebke Dürichen. Part of the anatomical work presented in this section was carried out with her. Taking advantage of the transparency of *Platynereis* specimens, we have performed and imaged fluorescent stainings in juveniles and larvae, using as a main marker a primary antibody against α-acetylated tubulin which reveals microtubules and hence mostly nervous fibres and cilia, in combination with membranes markers (FM 4-64 FX, mCLING-ATTO 647N), a muscle markers (Rhodamine-phalloidin) and a nuclear marker (DAPI) to reveal global cellular features. The idea of using mCLING, which proved to be the most reliable membrane marker, was given by Wiebke.

III – 2 Materials and Methods

2.1 *Platynereis* culture

Platynereis dumerilii larvae were obtained from a permanent breeding culture at EMBL, Heidelberg, following the protocol described in 1969 by Hauenschild & Fischer [65]. Adult *Platynereis* worms are maintained with an artificial moon cycle (1 week moonlight and 3 weeks darkness) to synchronize sexual maturation. After fertilization, *Platynereis* embryos were raised in Zentis cups, in natural sea water (NSW), in an incubator at the temperature of 18 ◦C, with a 16L:8D light cycle (Type KB53, Binder, Tuttlingen, Germany).

2.2 Anatomical stainings

(all dilutions refer to the stock solution concentrations indicated by the suppliers)

Fixation : Animals were collected at the desired stages from the laboratory culture. They were treated a first time with Proteinase K (50 µg/mL) for different amounts of time depending on the developmental stage (see Table III-1) to make their tissue permeable for later treatment. After three quick washing steps in FNSW, the animals were anaesthetized using 0.33 M Magnesium 18 chloride ($MgCl_2$) for 3 minutes, following fixation in 4 % Paraformaldehyde or PFA (Electron Microscopy Sciences, 15710, USA) in Phosphate Buffered saline with 0.1 % Triton X-100 or PTX (Sigma–Aldrich GmbH, Germany). This fixation step crosslinks proteins, thus stabilizing the morphology and disabling proteolytic enzymatic reactions. The fixation time was adjusted depending on the developmental stage (see Table III-1).

Digestion : Following fixation, five washing steps for 10 minutes in PTX were performed and the animals were digested a second time in Proteinase K (Merck KGaA, Germany) at 100 µg/mL for different time durations depending on the developmental stage (see Table III-1). The reaction was stopped using a 2 mg/mL freshly made glycine (Merck KGaA, Germany) solution in PTX, applied two times for 2 minutes. For post–fixation, animals were incubated in 4 % PFA/PTX for different durations depending on the developmental stage (see Table III-1) and afterwards washed in PTX five times for 10 minutes.

Duration of	1-2 dpf	3-4 dpf	5-6 dpf	4 seg	5 seg	15 seg	20+ seg	30+ seg
First ProK digestion	1 min	2 min	3 min	4 min	4 min	5 min	6 min	8 min
First PFA fixation	2 h	2 h	2 h	2 h 30	2 h 30	3 h	3 h 30	4 h
Second ProK digestion	1 min	2 min	3 min	4 min	4 min	5 min	6 min	8 min
Second PFA fixation	20 min	20 min	20 min	20 min	20 min	25 min	25 min	30 min

Table III-1 Fixation and digestion times depending on developmental stages

Primary antibody staining : After fixation, the animals were transferred to 1.5 mL Eppendorf tubes and were blocked with 5 % goat serum or GS (Abcam, Cambridge, USA) in PTX for 1 hour at room temperature (RT) to ensure that all epitopes and non–specific antibody (AB) binding sites are subsequently no longer accessible for the primary AB. For the primary AB binding, the animals were incubated overnight at 4 ℃ within 200 µL 5 % GS/PTX containing a commercial monoclonal mouse against alpha-acetylated tubulin (T6793, Sigma–Aldrich GmbH, Germany) at a final dilution of 1:250. Animals were washed again with PTX five times for 10 minutes.

Secondary antibody staining : After the first AB staining, the animals were incubated overnight at 4 °C in 200 µL of a 5 % GS/PTX solution containing DAPI (Sigma–Aldrich GmbH, Germany) in a 1:1000 dilution and a goat anti-mouse Alexa 488 secondary AB (Jackson Laboratories, USA) at a final dilution of 1:500. For the muscle fibre stainings, rhodamine phalloidin at a 1:100 dilution was added to this solution, whereas for a membrane staining, the fixable membrane dye FM 4–64 FX (Life Technologies, USA) was added at a 1:20 dilution. On the following day the animals were washed in PTX five times for 10 minutes. When the membrane staining was performed not with FM but with mCLING–ATTO 647N (Synaptic Systems GmbH, Germany), animals were incubated at this moment in a solution of mCLING in PTX at a dilution of 1:50 for 17 minutes (for 6 dpf) or 30 minutes (for 12 dpf) at 4 °C in darkness, and then washed five times for 10 minutes in PTX.

Mounting : After staining, the animals were incubated in 2.5 mg/mL DABCO (Sigma–Aldrich GmbH, Germany) in 85 % Glycerol for 1 hour at RT while shaking constantly in darkness. Fixed animals were stored at 4 °C or directly mounted between a slide and a coverslip. To avoid squeezing the animals, two layers of adhesive tape were stuck between the slide and the coverslip.

2.3 Confocal imaging settings

For animals under 15 segments, imaging of the head regions was performed with a Leica TCS-SP8 confocal laser scanning microscope (cLSM). Unless indicated, the nervous system was imaged using a 63X Glycerol immersion objective, with a 1.3 Numerical Aperture (NA) with an optical/digital zoom between 0.75 – 1.25. Image size was set to 1024 x 1024 pixels. Scan frequency was either 400 Hz or 600 Hz with bidirectional scanning in X. Noise filtering was achieved by using line average between 2 – 3. Pixel size was adjusted between 110 – 240 nm in x/y with a z resolution of 0.55 µm (except for 12 dpf where the z resolution was 1.1 µm). Detection of the secondary AB coupled with Alexa 488 was done using an Argon 488 nm laser at intensities between 8 – 80 % with a photomultiplier tube (PMT) or Hybrid Detector (HyD). Nuclear staining was detected using an infrared Diode laser 405 nm at intensities between 2 – 10 % with a PMT. The membrane dye FM 4–64 FX or mCLING–ATTO 647N were detected using a HeNe 633 nm laser at intensities between 0.5 – 2.5 % with a HyD. As the mCLING–ATTO 647N staining was weaker on the ventral side of the animal, laser intensity was increased with progressing imaging depth (z–compensation).
For older stages, imaging was performed at a Leica TCS-SPE cLSM. A 40X oil immersion objective with NA 1.15 was used with an optical/digital zoom of 1. Frame size was adjusted to 1024 x 1024 pixels. Pixel size was adjusted between 270 nm (15-segmented animal) and 430 nm (32-segmented animal) in x/y, and z resolution to 1 µm. Frame averaging of 2 or 3 was used to filter noise. Scanning frequency was 400 Hz. Acetylated tubulin signal was detected by a 488 nm laser at intensities between 50 – 90 % with a PMT detector. Nuclear staining was detected using an infrared laser 405 nm at intensities between 13 – 23 % with an PMT and the membrane dye FM 4–64 FX or the phalloidin staining were detected using a 532 nm laser at intensities between 26 – 74 % with a PMT.

2.4 Image processing

All processing was done using Fiji, a distribution of the popular free and open-source biomedical image analysis software ImageJ [256]. Standard procedures such as z-stack average or maximal projections were used to generate the plane images shown, and the built-in plugin “3D viewer” was used to generate 3D reconstructions of the heads.

III – 3 Results

3.1 Most sensory appendages in *Platynereis* juveniles have at least two sensory cell types

An overview of head appendages in a 32-segmented juvenile is shown in Figure III-1, which is a 3D-reconstruction obtained from a fluorescent staining, showing cell nuclei in blue, membranes in red, and cilia and nervous fibres in green (note that additional, autofluorescent structures can be seen in the green channel). This image is provided to give an impression on how the different organs are arranged in space in the adult head, and what their relative sizes are. It illustrates how large these sensory appendages are in comparison with the head itself, already in an animal that measures only one tenth of the typical adult length (2-3 cm).

The antennae have a slender tip devoid of cell nuclei. The densely ciliated area behind the head is one of the two nuchal organs, the only head sensory organ that does not protrude but instead is organised around a cavity. Each palp is almost as large as the head itself, and comprises a well-differentiated tip. On this tip, as well as all over the body surface, the green tubulin staining reveals numerous clusters of cilia (green spots in Figure III-1). They appear regularly spaced on the four tentacular cirri. Tentacular cirri are here not visible in full length, and are typically 5-10 times longer than the head. The four cirri have slightly different diameters, with the two dorsal ones being the largest. A particular anatomy of the sensory structures will be presented now.

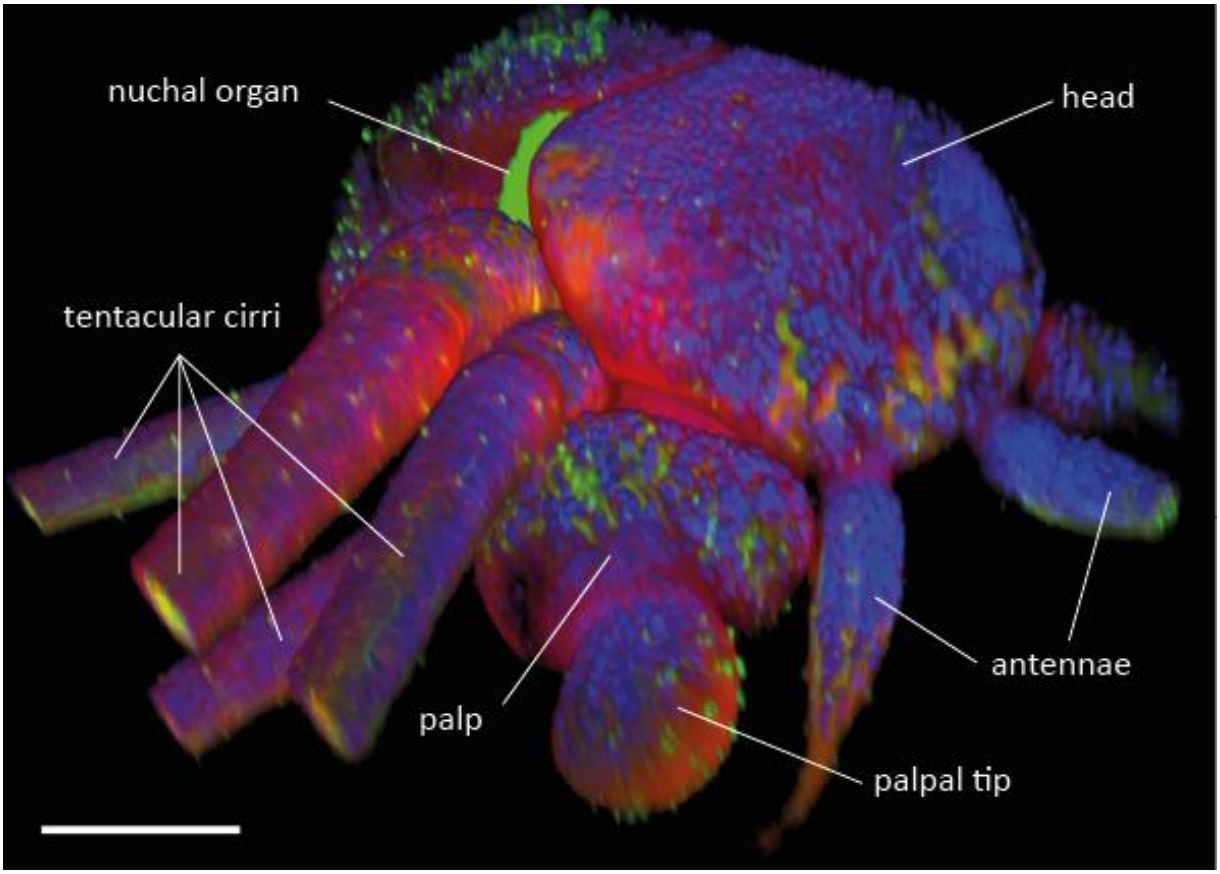


Figure III-1 Head of 32-segmented juvenile, showing the prominent head appendages present at that stage. 3D reconstruction based on fluorescent stainings. Note that some appendages are cut at the limits of the imaging volume. Red : FM 4-64 FX staining. Green : anti α-acetylated tubulin immunostaining. Blue : DAPI staining. Scale bar 100 µm.

3.1.1 Tentacular cirri

The most obvious feature observed in tentacular cirri is the large nerve occupying their centre, as revealed by a tubulin immunostaining at the 34-segmented stage (Figure III-2B). Nervous fibres with sensory endings reaching the surface of the appendage gather in its centre, and the diameter of the nerve increases from distal to proximal. A close look reveals two types of sensory endings at the surface of the cirri : some endings with groups of cilia protruding out of the cuticle (Figure III-2C) and some endings that do not protrude out of the cuticle (Figure III-2D). For the latter type, it is unclear whether cilia are present or not, and though it seems that the ending is in direct contact with the water medium it cannot be asserted from such a staining whether it actually penetrates the cuticle. The first type clearly belongs to type the (1) or (2) described by Purschke, for the second ones it is unclear. Both types of endings seem to belong to several cells, though it was not possible from the present staining to attribute particular cells to them. They can be found at regular interval all over the surface of the four cirri. The nuclear staining reveals that cell bodies are absent at the very tip of the cirri (not shown here). The base of the four tentacular cirri is wider than the rest of the appendage, and comprises numerous muscle fibres in its periphery that are parallel to each other and positioned longitudinally, as revealed by a phalloidin staining (Figure III-2B). Muscles are totally absent in the rest of the appendage (see also Figure III-4B). It can be noted that the tubulin antibody did not penetrate the cirrus base, which may indicate a different cuticular composition between the base and the remaining distal part of the cirrus. The cirral nerve, although not stained in green here, is evidently present in the centre of the cirral base (see also Figure III-10A, Figure III-11D). All four cirri are similar in anatomy and the same sensory endings can be found, hence only one has been described here.

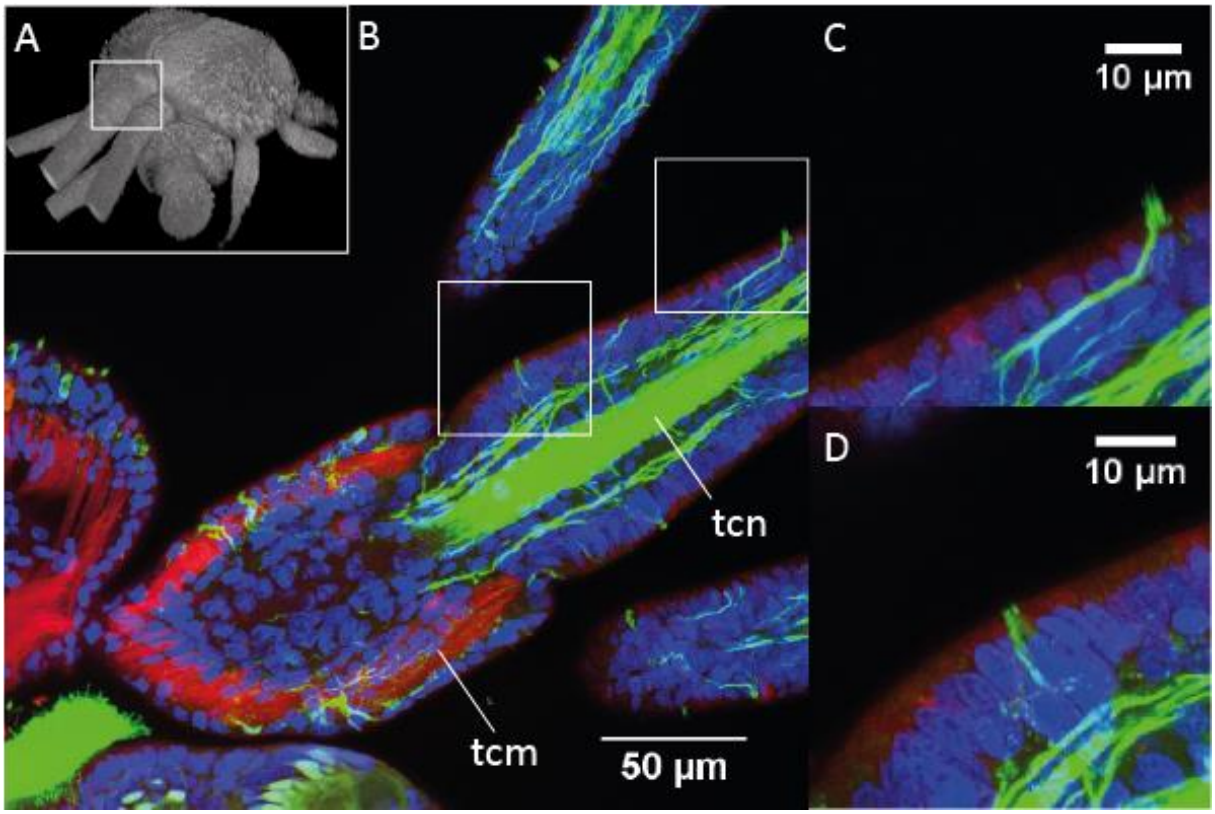


Figure III-2 Tentacular cirrus anatomy, 34-segmented juvenile. Red : Rhodamine-phalloidin staining. Green : anti α-acetylated tubulin immunostaining. Blue : DAPI staining. (A) 3D head overview, the rectangle indicates the region imaged. (B) Longitudinal section of the anterior dorsal cirrus, revealing the nerve (tcn) in the centre of the cirrus, and numerous muscular fibres (tcm) that surround its base. (C) and (D) detail of two different sensory endings indicated by the white squares in (B) : protruding (C) and non-protruding (D) endings.

3.1.2 Palps

These massive appendages are fronto-lateral and ventral, pointing towards the bottom, i.e. towards the substrate. Membrane and nuclear stainings reveal internal coelomic cavities at their periphery, as well as autofluorescent, abundant granular structures located inside the cavity, probably glands (Figure III-3B). The coelomic cavities seem to all communicate with each other, thus forming a single, peripheral cavity inside the palp. The tip of the palps possesses a dense innervation and numerous sensory endings at its surface, as revealed by a tubulin staining (Figure III-3B, Figure III-4C), and no cavity is present. Note in Figure III-3B that the tubulin antibody did not penetrate the inner mass of the palp, which may indicate a different cuticular composition between this base and the remaining distal part of the cirrus. A closer look actually reveals two types of sensory endings, as for the tentacular cirri : protruding (Figure III-3C) and non-protruding (Figure III-3D), which can be found in similar abundance at the surface of the tip. Tufts of protruding cilia are also present at the surface of the palpal mass ; I did not look for non- protruding cilia there.

Palps have a complex musculature. A staining for muscle fibres with phalloidin reveals an intricate arrangement of muscles, comprising external oblique muscles (Figure III-4B), as well as internal longitudinal and circular muscles (Figure III-4A). Oblique muscles cross the midline and are attached to the palp on their medial side. Longitudinal muscles appear to be present on either side of the coelomic cavity and are clearly attached to the palp tip, while circular muscles seem to be on the exterior side of the cavity only, and not attached to the tip.

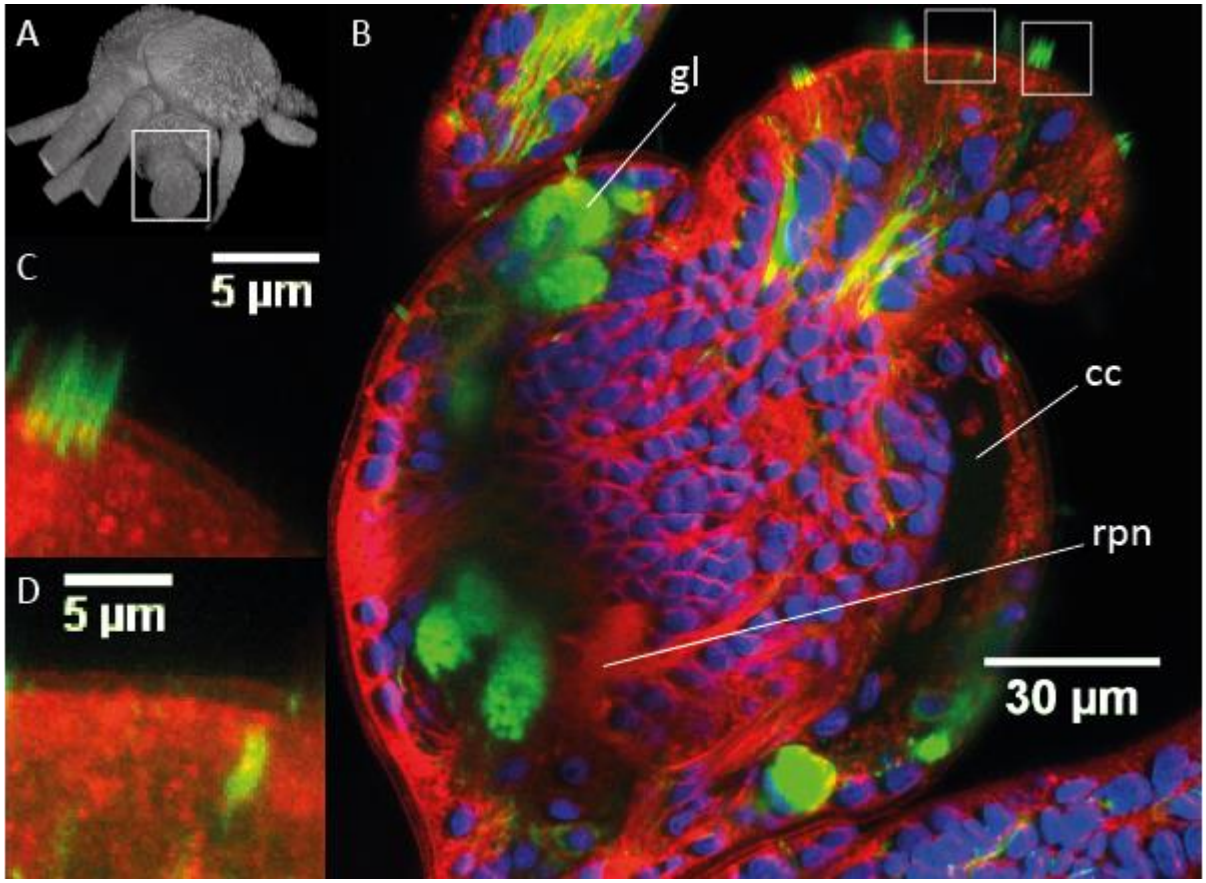


Figure III-3 Palp anatomy, 22-segmented juvenile. Red : FM 4-64 FX staining. Green : anti α-acetylated tubulin immunostaining. Blue : DAPI staining. (A) 3D head overview, the rectangle indicates the region imaged. (B) Longitudinal section of a palp, revealing numerous nervous fibres in the palp tip, coelomic cavities (cc) at the periphery of the appendage, as well as glandular structures (gl) which are autofluorescent in the green. Note that the root of the palpal nerve is stained by FM but not by the tubulin antibody. (C) and (D) detail of two different sensory endings at the palp tip surface indicated by the white squares in (B) : protruding (C) and non-protruding (D) endings.

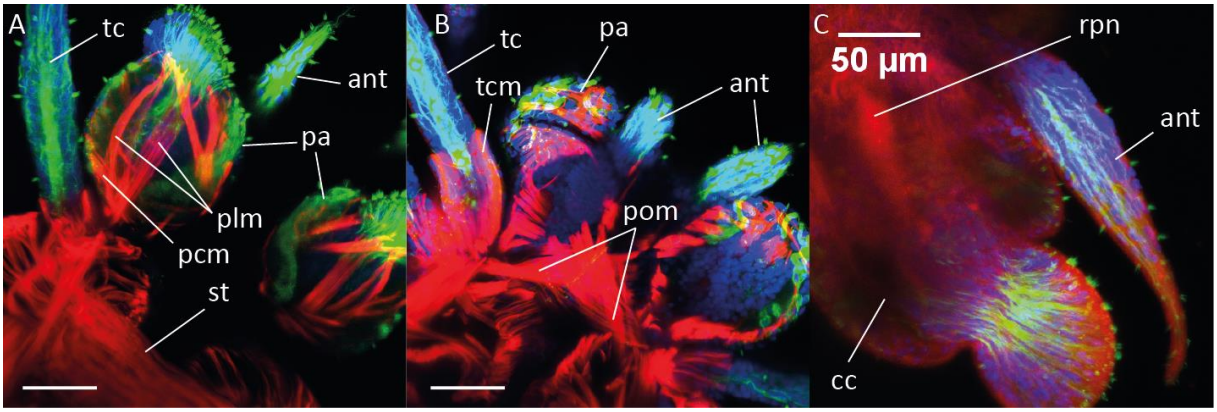


Figure III-4 Musculature and innervation of palps, antennae and tentacular cirri. Green : anti α-acetylated tubulin immunostaining. Blue : DAPI staining. (A) and (B) 23-segmented juvenile, red : rhodamine-phalloidin staining. Scale bar 50 µm. (C) 32-segmented juvenile, red : FM 4-64 FX staining. Antenna (ant), coelomic cavity (cc), palp (pa), palpal circular muscle (pcm), palpal longitudinal muscle (plm), palpal oblique muscle (pom), palpal nerve root (rpn), stomodeum (st), tentacular cirrus (tc), tentacular cirrus muscle (tcm).

3.1.3 Antennae

Antennae are the most frontal head appendages in *Platynereis*. They are superficially similar to tentacular cirri : regularly spaced clusters of protruding cilia at their surface, abundance of nervous fibres, absence of muscle fibres in the appendage (Figure III-4A-B). However, antennae do not have a condensed nerve in their centre (Figure III-4C), while in the tentacular cirri a nerve is present already in the 5-segmented stage (see Figure III-13). Instead it seems that in *Platynereis* the antennal nerve is confined to the inside of the head (see also Figure III-10). The antennal tip is devoid of cell nuclei, which was not reported so far. I could see only protruding endings at the antennal surface, but I did not look at sensory endings in close detail, so more observations would be needed to conclude about the absence of non-protruding ones.

3.1.4 Nuchal organs

The nuchal organs in adult epitoke *Platynereis* have been investigated in detail in electron microscopy by Schmidtberg & Dorresteijn ([233], see Chapter II). Figure III-5 does not provide further anatomical conclusion, but shows how they appear in a fluorescent staining. The tubulin staining reveals the abundant cilia belonging to the supporting cells ; cell nuclei are totally absent from the olfactory chamber or nuchal cavity. Nuchal organs are equipped with a retractor muscle [116], [233]. Several muscles could be seen indeed around the nuchal organs in phalloidin staining (not shown), but it was not possible to attribute them with certainty to the nuchal organs.

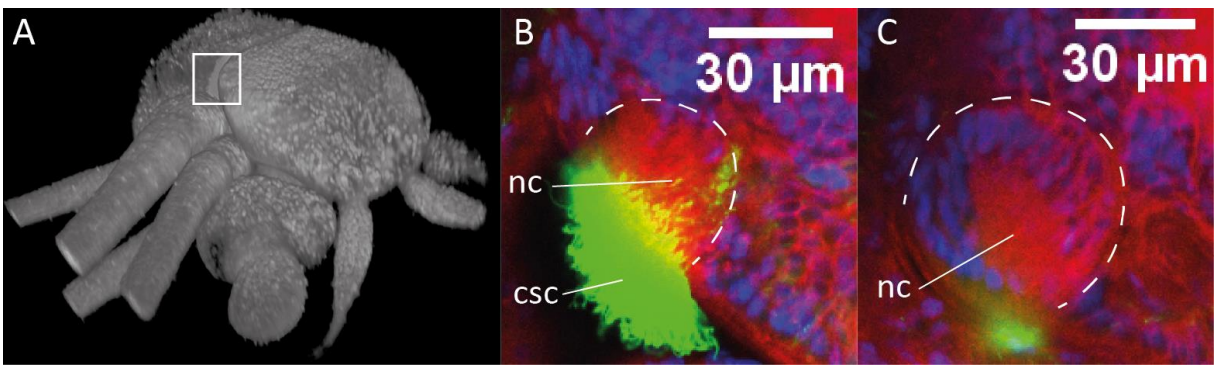


Figure III-5 Nuchal organ anatomy in a 32-segmented juvenile. (A) 3D head overview, the rectangle indicates the region imaged. (B) and (C) horizontal sections at two different depths, showing the nuchal cavity (nc) and cilia of the supporting cells (csc). Red : FM 4-64 FX staining. Green : anti α-acetylated tubulin immunostaining. Blue : DAPI staining. Dashed lines indicate the outlines of the organ.

3.1.5 Anal and parapodial cirri

The anal appendages called cirri are highly similar to the tentacular cirri (see Chapter II), except that no collar-like muscular structure is found at their base, hence it is unclear whether they can be actively moved by the animal. They have a central nerve (Figure III-6B), and cell nuclei are present all along the appendage except at their very tip. A combined tubulin and membrane staining reveals, as in tentacular cirri, the presence of two different types of sensory endings, constituted by clusters of either protruding or non-protruding sensory endings (inset in Figure III-6A). Each cluster is associated with a few nervous fibres (inset in Figure III-6B). As in the tentacular cirri, a different cuticular composition in the appendage compared to the body is probable, since the antibody almost did not penetrate the pygidium (Figure III-6B). The cirral nerve inside the pygidium is nevertheless slightly visible from the tubulin staining, as indicated by the red arrowheads in Figure III-6B. Note the presence of large glands at the tip of the pygidium, as in the parapodia. These glands are autofluorescent in the green channel.

These findings confirm the innervation pattern already reported [251], [252], but establish the existence of two sensory cell types, and their sensory endings, which had not been described in anal cirri so far.

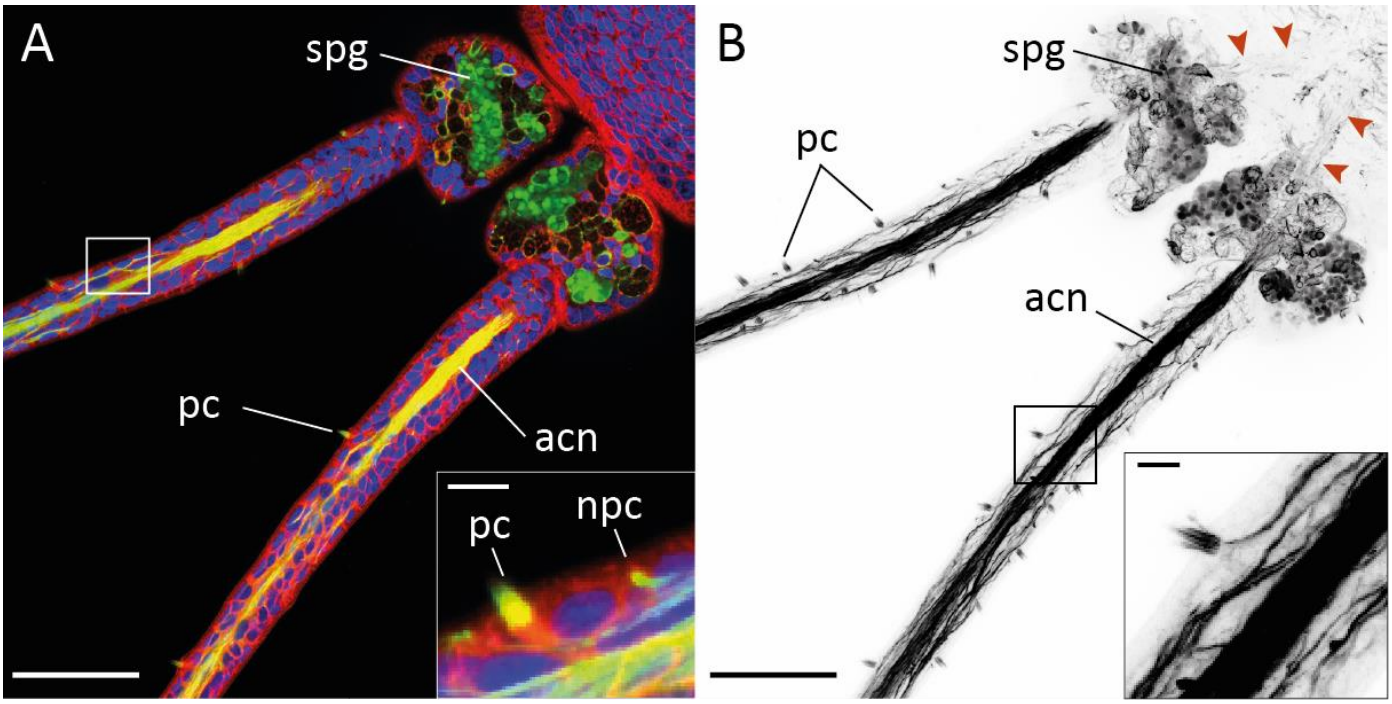


Figure III-6 Anal cirri anatomy, 22-segmented juvenile. Anal cirrus nerve (acn), clusters of protruding (pc). The spinning glands (spg) are autofluorescent in the green wavelengths. (A) Longitudinal section of the cirri, fluorescent staining. Red : FM 4-64 FX staining. Green : anti α-acetylated tubulin immunostaining. Blue : DAPI staining. Inset : z-projection close-up showing both protruding (pc) and non-protruding (npc) endings. (B) Maximal z-projection of the tubulin staining, revealing the full innervation of the cirri. Inset : close-up of a cluster of protruding endings. Red arrowheads indicate the cirral nerves inside the pygidium, which was not stained by the antibody. Scale bar 50 µm for (A) and (B), 5 µm for the insets.

The parapodial cirri are also similar to the anal ones, though much shorter. They possess clusters of protruding endings highly similar to the of antennae and tentacular cirri, as has been described in the closely-related genus *Nereis* [95]. A parapodial spinning gland is located at their base. At the 20-segmented stage, the nerve is visible at the base of the appendage only, as described by Smith in adults [110]. Their function would probably be the same as anal cirri, though I did not manage to see non-protruding endings.

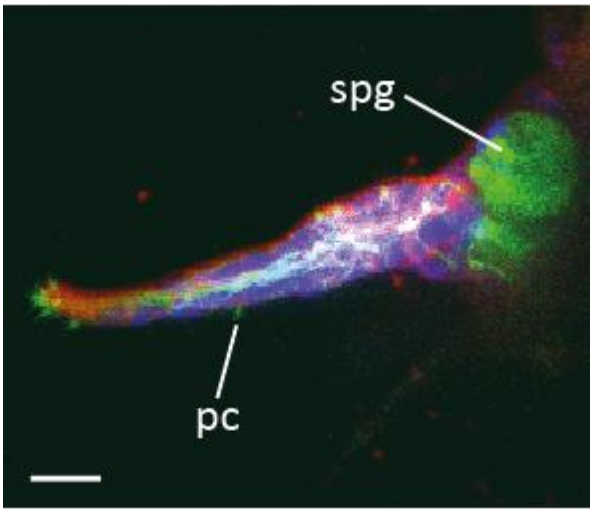


Figure III-7 Parapodial cirrus anatomy, 20-segmented juvenile. Red : FM 4-64 FX staining. Green : anti α-acetylated tubulin immunostaining. Blue : DAPI staining. Protruding cilia (pc), spinning gland (spg). Scale bar 20 µm.

3.2 Development of head sensory organs

Starting from a late juvenile stage, I describe hereafter the morphology and neuroanatomy of head sensory organs in *Platynereis*. Six different stages have been chosen, that are presented in backward developmental time, to help the reader relate anatomical structures from their most obvious to their least obvious states :

- 30/35 segments
- 20/25 segments
- 15 segments
- 5 segments, post-cephalic metamorphosis
- 4 segments
- 3 segments (12 dpf)

Developmental speed after the 3-segmented stage is highly variable, dependent on food availability and on an individual's history. In the laboratory culture, animals coming from the same batch of eggs can be observed with body sizes as different as 10 segments and 3 segments for example (personal observation). Hence, no precise statement can be made regarding the age of an animal based on the size of its body, and it is preferable to refer to developmental stages and body complexity in terms of number of body segments.

First, schematic drawings as well as 3D reconstructions based on fluorescent stainings are shown, to illustrate the transformations that are taking place in the external morphology : appearance of the organs, shape, number, relative size, position, orientation. Then, confocal images of fluorescent anatomical stainings are shown, to illustrate the changes in internal morphology and neuroanatomy that accompany this external development. A tubulin immunostaining, combined with a membrane and a nuclear marker as counterstaining, has been chosen to reveal the nervous system and the general anatomy at all these stages (except at 15 segments where a muscle marker has been used, which nevertheless also reveals membranes).

3.2.1 External morphology

All the following descriptions refer to Figure III-8 and Figure III-9.

The most striking feature of head development in *Platynereis* juveniles is probably the tremendous expansion of the **palps**. While a pair of antennae and a pair of tentacular cirri are already extending out of the head after 6 days of development, the palps are hardly protruding from the surface. At around 30 segments, they have become appendages that are each almost as large as the cephalic lobe itself, and include a large tip. The palpal tip starts to be distinguishable from the rest of the palpal mass around the 5-segmented stage and then continues its expansion. Palps are located on either side of the stomodeum opening from 6 dpf on, they constitute the most ventral part of the head are always oriented ventrally during development.

Another major difference between late nectochaete larvae and late juveniles is the number and size of **tentacular cirri**. The anterior dorsal cirrus is the first to appear during development. From about 50 µm at 6 dpf, which is comparable to the head width, it grows to about 1 mm at 32 segments, which is around five time the head width at this stage. Its ventral homologue starts to grow at the 4-segmented stage. The posterior tentacular cirri appear from the 5-segmented stage, first the dorsal one which is the metamorphosed cirrus of the first parapodium, then the ventral one which starts growing at the end of this metamorphosis (the protrusion is visible in Figure III-13E). The muscular collar at their base (see Figure III-2) is externally visible from 5 segments onwards. Tentacular cirri are slender appendages, which overall have diameters comparable with each other, albeit the ventral ones are slightly thinner. Their length however are different, with the dorsal ones, oriented upwards, being the longest, and the ventral ones, oriented downwards, being the shortest.

The **antennae** do undergo some morphological changes. A significant elongation compared to the head size can be observed between 3 and 5 segments. They are relatively thin until 5 segments, and their proximal part starts to widen afterwards. The antennae, from their formation at around 3 dpf, are frontal and forward-oriented. They start to point toward the substrate at 4-5 segments.

The **nuchal organs** are rather invariant in position from their formation at around 2 dpf. Externally, they are only visible as a densely ciliated area located on the latero-posterior, which simply extends during development. They are more dorsal than the tentacular cirri.

The **head** itself changes in general shape, from a half-globe at 6pd to a more flattened shape in late juveniles, with its antero-dorsal part somewhat flat and oblique in relation with the ground surface.

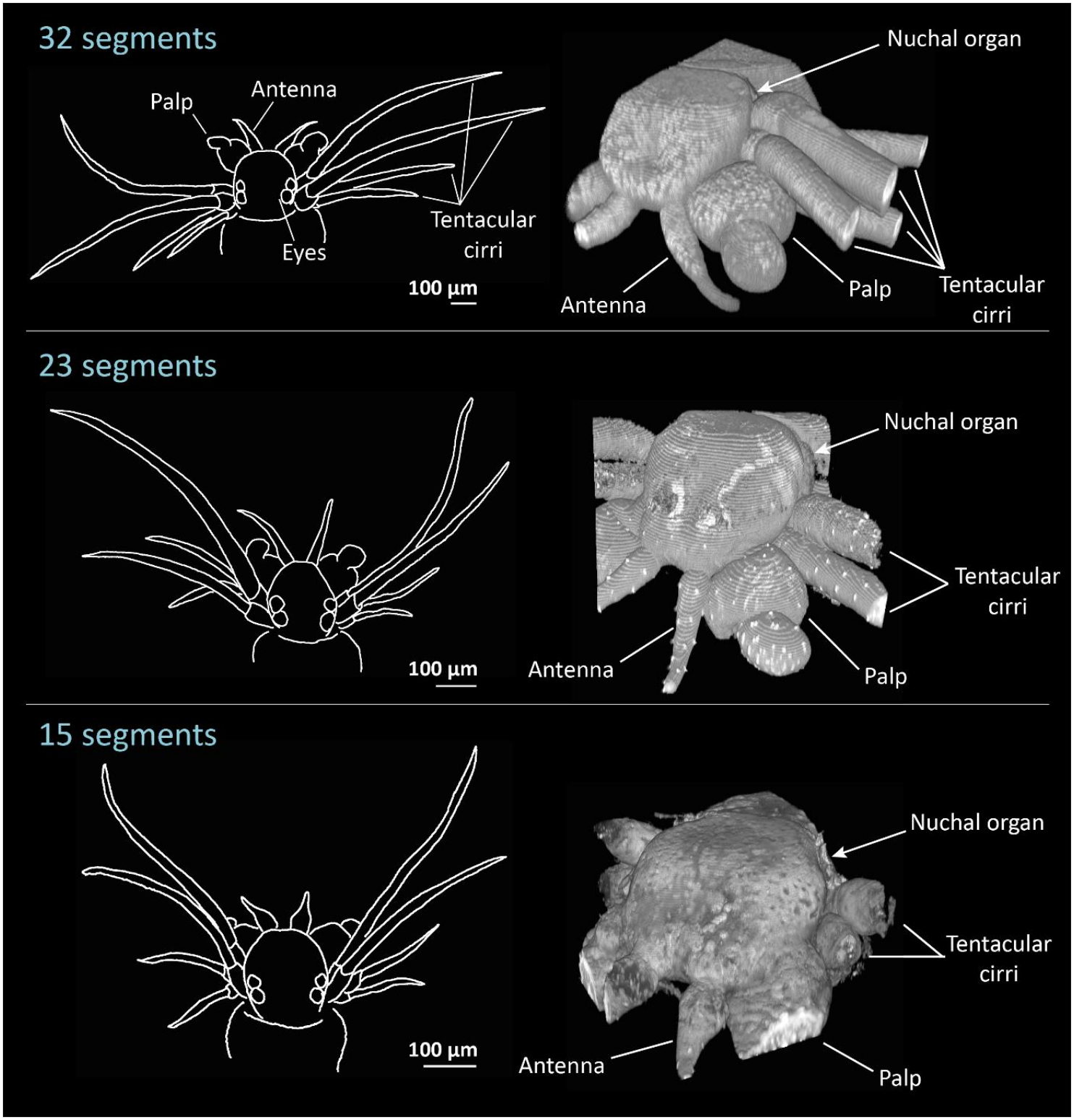


Figure III-8 External head morphology in late juveniles. Schematic drawings (left) are in dorsal view, with anterior up and posterior down. 3D volume reconstructions (right) are obtained from fluorescent anatomical stainings, and presented in a fronto-lateral, bird's eye view. Note that the heads were only

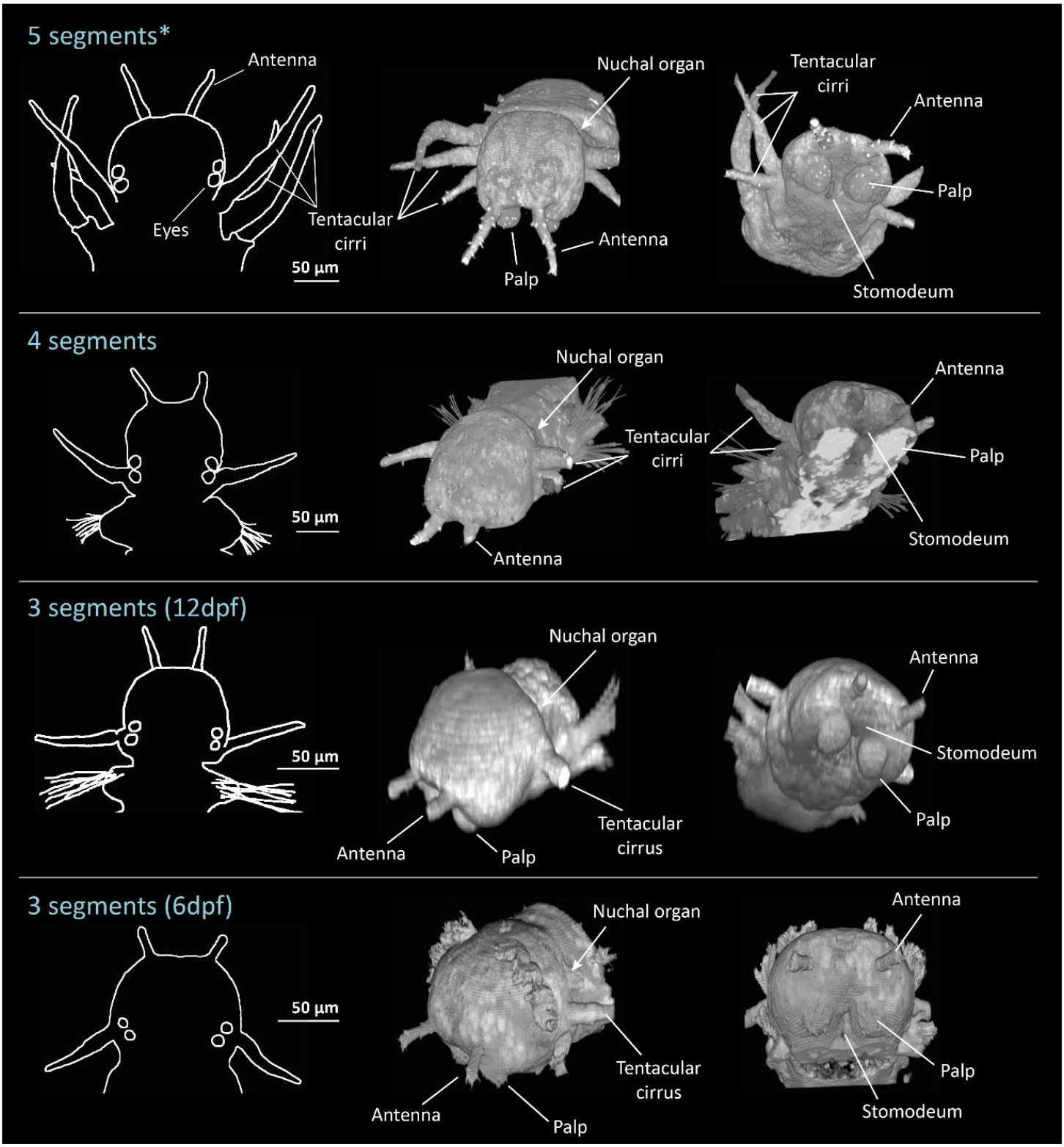


Figure III-9 External head morphology in early juveniles (= post-cephalic metamorphosis). Schematic drawings (left column) are presented in dorsal view, with anterior up and posterior down. 3D volume reconstructions (centre and right columns) are obtained from fluorescent anatomical stainings, and presented in a fronto-lateral, bird's eye view (centre column) and in a fronto-lateral, low-angle view.*

3.2.1 Internal morphology and neuroanatomy

All the following descriptions refer to Figure III-10 (32 segments),

Figure III-11 (23 segments), Figure III-12 (15 segments), Figure III-13 (5 segments post-cephalic metamorphosis), Figure III-14 (4 segments), Figure III-15 (3 segments - 12 dpf). For each stage optical sections are presented, which are taken in six different horizontal planes roughly equivalent across stages. The optical planes are not perfectly horizontal, due to the difficulty of an accurate mounting, and while this can be regarded as an imperfection – as indeed some left-right asymmetry will be apparent on the images – one can also appreciate that this degree of asymmetry provides more anatomical information, since virtually more depth of the animal is to be seen. These planes, from dorsal to ventral, show overall the following structures :

- plane 1 : nuchal organ
- plane 2 : antennal nerve and dorsal lobe of the Mushroom Bodies
- plane 3 : tentacular cirrus and ventral lobe of the Mushroom Bodies
- plane 4 : antennae, palpal nerve and roots of the circum-oesophageal ring
- plane 5 : palps and circum-oesophageal ring
- plane 6 : palp tips

In these figures, I have indicated what I presume to be the boundaries of the areas containing the cell bodies of the organs considered. The appendages themselves are sufficiently obvious and are not indicated. The reader is referred to the above description of external morphology. Note that at the 23- and 32-segmented stages, the tubulin antibody did not penetrate inside the head hence only the appendages are stained in the green channel, however the nervous system is still revealed by the membrane staining and appears in red. At the 15-segmented stage, a inadequacy in the staining protocol has somewhat affected the specimen quality and tissue morphology appears partly altered, nevertheless the main anatomical features are unchanged.

Common legend for all figures : tight dashed lines indicate the presumed boundaries of the areas containing the neurons of antenna (A), tentacular cirrus (C), nuchal organ (N), palp (P), and for the dorsal (dmb) and ventral (vmb) lobe of the Mushroom Bodies, loose dashed lines indicate the outline of the stomodeum (S). Anatomical landmarks : antennal nerve (an), cirral nerve (cn), nuchal nerve (nn), palpal nerve (pn), dorsal (dp) and ventral (vp) peduncle of the Mushroom Bodies, dorsal (dr) and ventral (vr) root of the circum-oesophageal ring (cor), mouth opening (m).

In the internal development of **palps**, a notable feature is the formation of a large peripheric coelomic spaces that seem to form one single cavity. These spaces are hardly visible at 3 segments, and already quite obvious at 5 segments. At 23 segments these cavities already contain large glands that appear in green autofluorescence. The neural part of the palps is located in their centre (Figure III-10E, Figure III-11E), comprising densely packed cell bodies and several nerves. A single nerve (the palpal nerve) at the base of the palp can be recognised early on, but is really individualised from 5 segments only (Figure III-13D). The nerve projects to the central neuropile in close proximity of the ventral root of the circum-oesophageal ring, which becomes obvious from 15 segments only. Most sensory endings of the palps are concentrated at the surface of the tip since the 3-segmented stage, though other sensory cilia can also be seen on the rest of the palpal mass later on (see Figure III-8). Note the large number of cells present in the palps in spite of them having large coelomic cavities, and note how large the distance between and the diameter of the mouth opening have become at 15 segments (Figure III-12F), and even more at 32 segments (Figure III-10F).

For **tentacular cirri**, cell bodies are present in the appendage itself at 3 segments already, however the nerve is not assembled inside the appendage until 5 segments (Figure III-13C), stage before which is it only visible at its base in the cirral ganglion (Figure III-14C). The anterior ventral cirrus can be seen to start developing at 4 segments (Figure III-14D, right side) and already contains cell bodies in its protrusion at 5 segments (Figure III-13E, right side). All cirral nerves, from their formation, connect to

the rest of the nervous system at the level of the circum-oesophageal ring, i.e. they project to this ring between the split of its two roots (anterior) and its emergence from the ventral nerve cord (see also general head innervation in Chapter II). At 23 segments the muscular collar structure present at the base of the tentacular cirri is well differentiated (Figure III-11C), it probably contains a majority of muscle cells and supporting cells and few neurons.

An important characteristic of the **antennae** is the total absence of cell bodies inside the appendage until the 5-segmented stage, where cell bodies only start to occupy the very base of the antennae (Figure III-13E). This had not been reported previously. Cell bodies are then abundant in the antennae, though their tip remains devoid of them even in late juveniles (Figure III-10F). The antennal ganglia are at first hardly distinguishable from their neighbouring cells in the brain. Later during development, these ganglia are progressively compartmentalised and isolated from the rest of the brain, as starts to be apparent at 5 segments (Figure III-13C-E). At the 32-segmented stage, antennal ganglia are easy to identify, and surrounded by coelomic spaces and glandular structures (Figure III-10C-E). From the 15-segmented stage, the antennal nerve truly constitutes a tract inside the brain, and projects to an intermediate antero-posterior position in the main neuropile (Figure III-11B).

No major changes are apparent in the development of the **nuchal organs**, which mostly acquire more abundant supporting ciliated cells. They can also be seen to expand, notably along the dorso-ventral axis, as a part of them is present in planes significantly more ventral than that of the antennal nerve at late stages (Figure III-10B, Figure III-11C) as opposed to early stages. It seems that the nuchal nerve is progressively taking a more posterior detour before projecting into the neuropile (Figure III-12A), though the was not obvious to identify in the stainings of the 23- and 32-segmented animals. This change probably has to be put in relation with the strong expansion of the posterior lobes, a dorsal pair of ganglia medial to the nuchal organs, which start occupying a significant portion of the brain at 15 segments and seem to be supplied with their own nerve (Figure III-12A-B). The nuchal cavity appears to be quite deep in the 32-segmented animal, about 30 µm (Figure III-10A).

Mushroom Bodies (MB) are easily recognisable in the 32-segmented animal, and the nuclear counterstaining is sufficient to localise their boundaries with precision, as the density of their cellular nuclei is much higher than in any part of the brain (Figure III-10). However, this criterion can already be used to identify them in late juveniles, since this packing takes place only around the 20-segmented stage (compare Figure III-12 and Figure III-11). Their peduncles on the contrary is formed early on, and constitutes the best criterion to localise them in early development. Both can be recognised in 3-segmented animals, though it is impossible to determine exactly which cells belong to them and which not ; it can only be guessed that the cells that are the closest to the peduncles do in fact belong to MB. The dorsal peduncle is located approximately at the same dorso-ventral level as the antennal nerve at 12 dpf (Figure III-15B), but becomes progressively more dorsal than this nerve at subsequent stages (Figure III-12A-B). The ventral peduncle is just dorsal to the palpal nerve, and can be seen to point in a fronto-lateral direction at 12 dpf (Figure III-15C), whereas it points in a fronto-medial direction at later stages (Figure III-13C). At later stages the ventral peduncle splits in two (visible in Figure III-10C and D) and authors have described MB in nereidid polychaetes as consisting either of two or three lobes. The dorsal MB lobe is overall located lateral to the antennal nerve, and in close proximity of the surface. The ventral lobe is immediately dorsal to the palp, more posterior and lateral than the antennal ganglion.

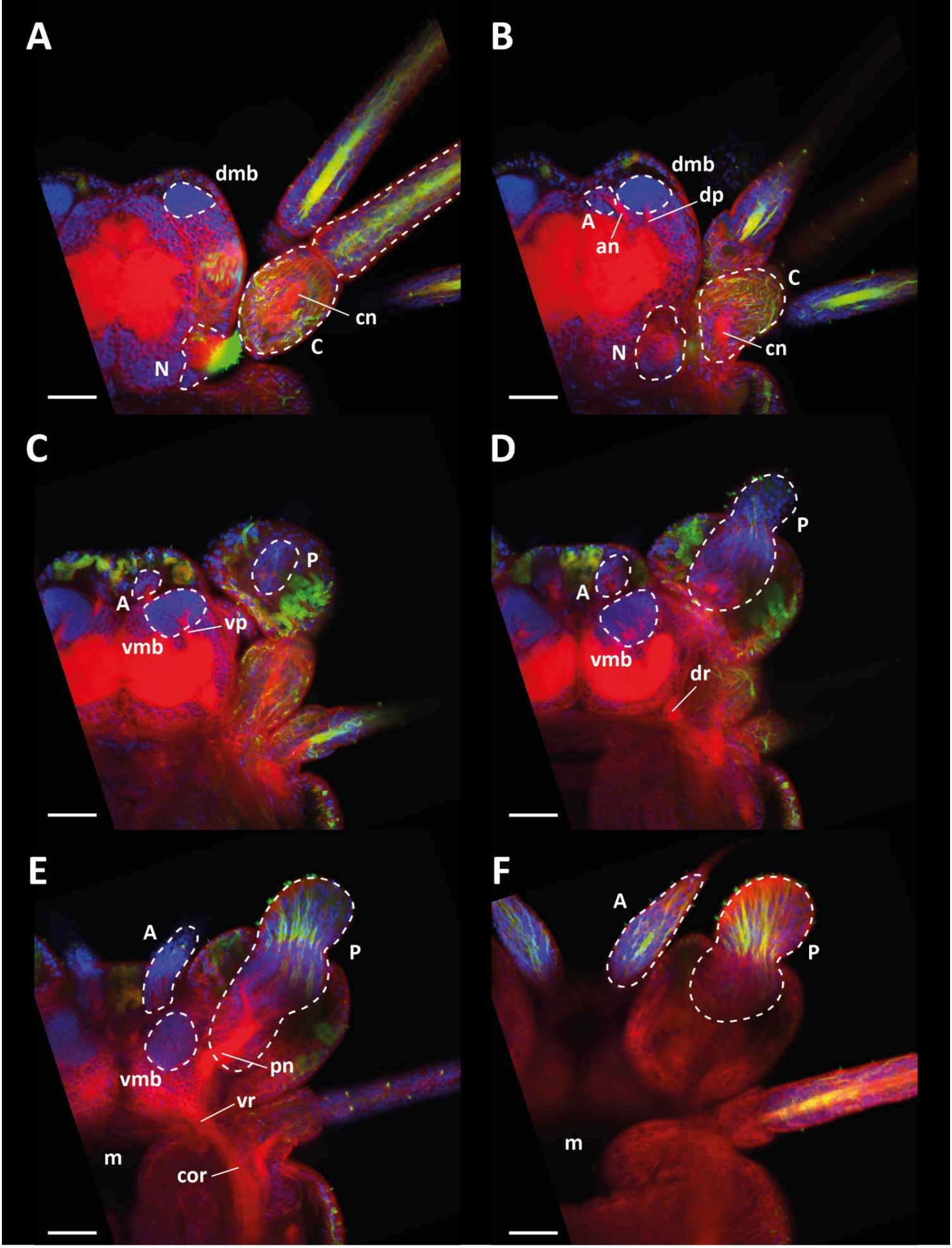


*Figure III-10 Internal head anatomy and nervous system anatomy – **stage 32 segments**. Six z-projections of 4-10 confocal planes each are shown in dorsal view, from dorsal (A) to ventral (F), with anterior up and posterior down. Only the posterior dorsal tentacular cirrus has been annotated here. Red : FM 4-64 FX. Green : Tubulin antibody. Blue : DAPI. Scale bar 50 µm.*

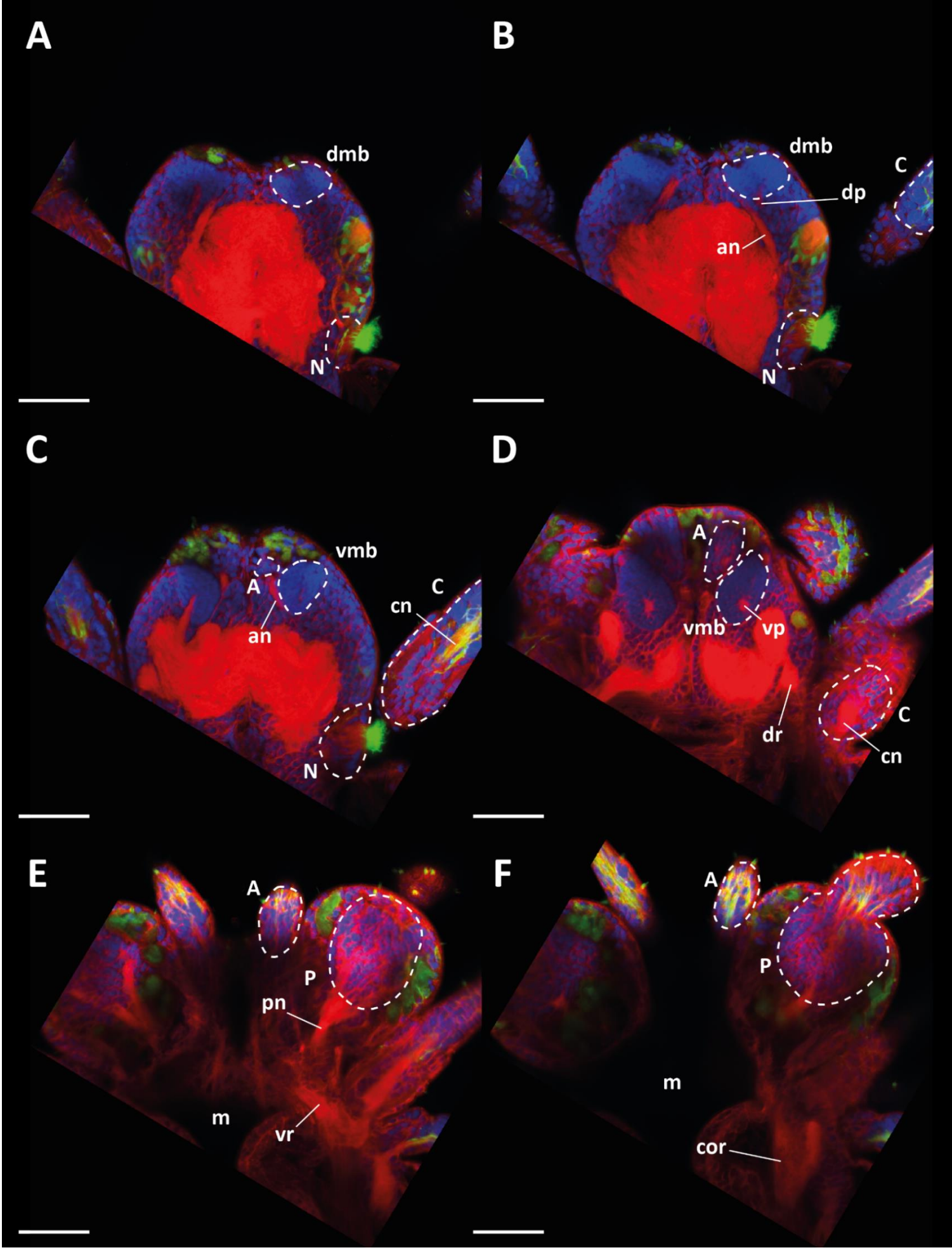


*Figure III-11 Internal head anatomy and nervous system anatomy – **stage 23 segments**. Six z-projections of 4-10 confocal planes each are shown in dorsal view, from dorsal (A) to ventral (F), with anterior up and posterior down. Only the anterior dorsal tentacular cirrus has been annotated here. Red : FM 4-64 FX. Green : Tubulin antibody. Blue : DAPI. Scale bar 50 µm.*

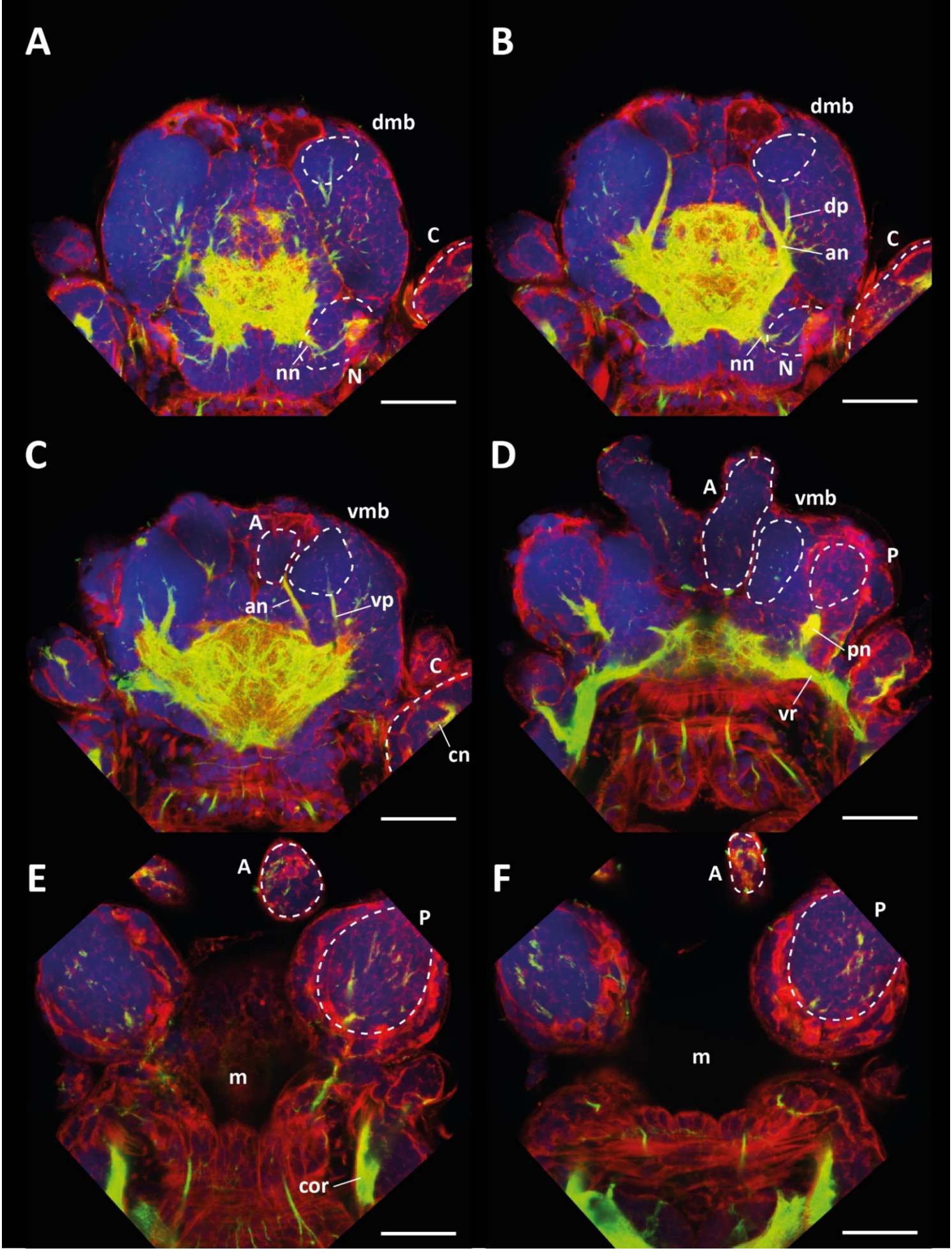


*Figure III-12 Internal head anatomy and nervous system anatomy – **stage 15 segments**. Six z-projections of 4-10 confocal planes each are shown in dorsal view, from dorsal (A) to ventral (F), with anterior up and posterior down. Only the anterior dorsal tentacular cirrus has been annotated here. Red : Rhodamine phalloidin. Green : Tubulin antibody. Blue : DAPI. Scale bar 50 µm.*

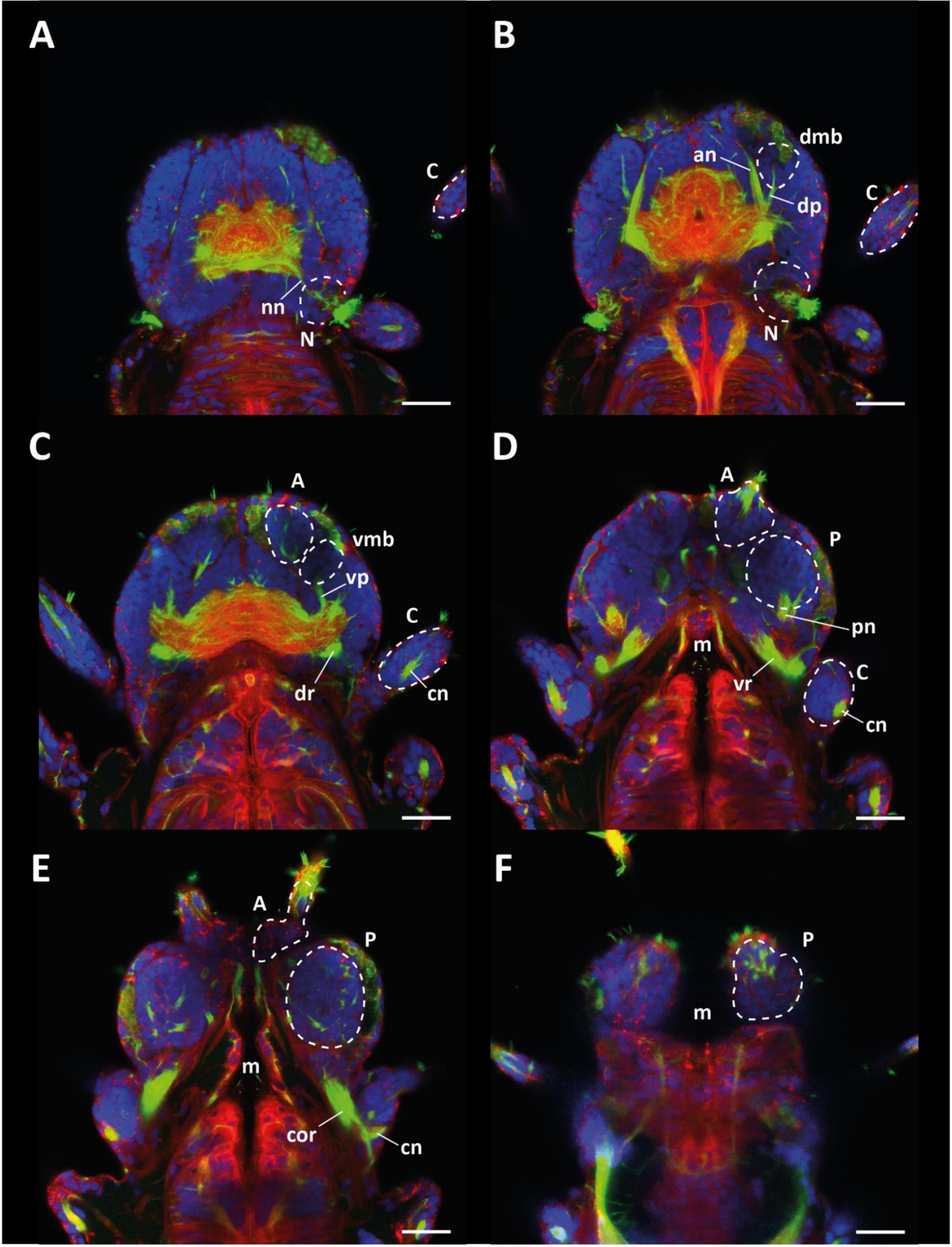


*Figure III-13 Internal head anatomy and nervous system anatomy – **stage 5 segments post-cephalic metamorphosis**. Six z-projections of 4-10 confocal planes each are shown in dorsal view, from dorsal (A) to ventral (F), with anterior up and posterior down. Only the anterior dorsal tentacular cirrus has been annotated here. Red : FM 4-64 FX. Green : Tubulin antibody. Blue : DAPI. Scale bar 50 µm.*

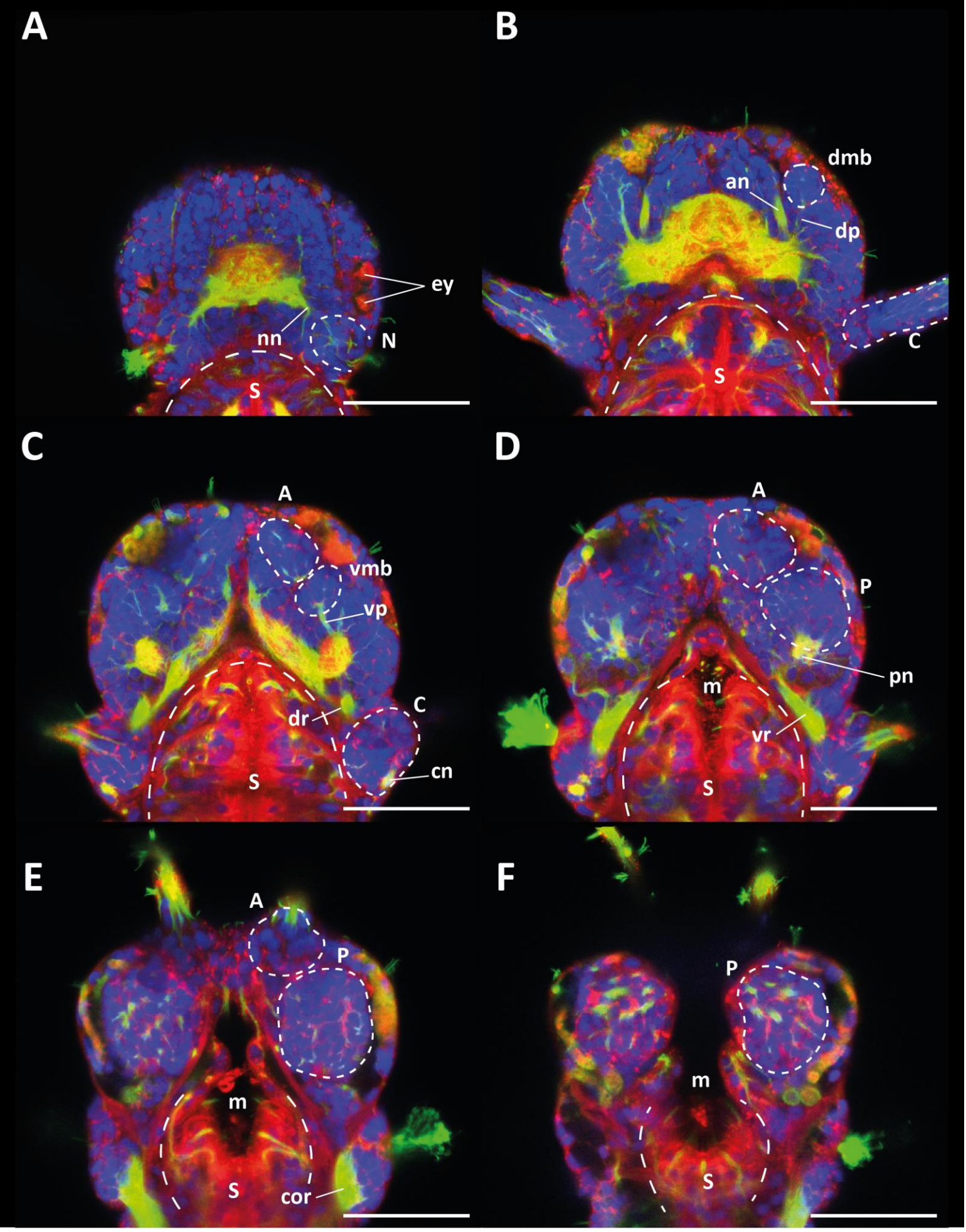


*Figure III-14 Internal head anatomy and nervous system anatomy – **stage 4 segments**. Six z-projections of 4-10 confocal planes each are shown in dorsal view, from dorsal (A) to ventral (F), with anterior up and posterior down. Red : FM 4-64 FX. Green : Tubulin antibody. Blue : DAPI. Scale bar 50 µm.*

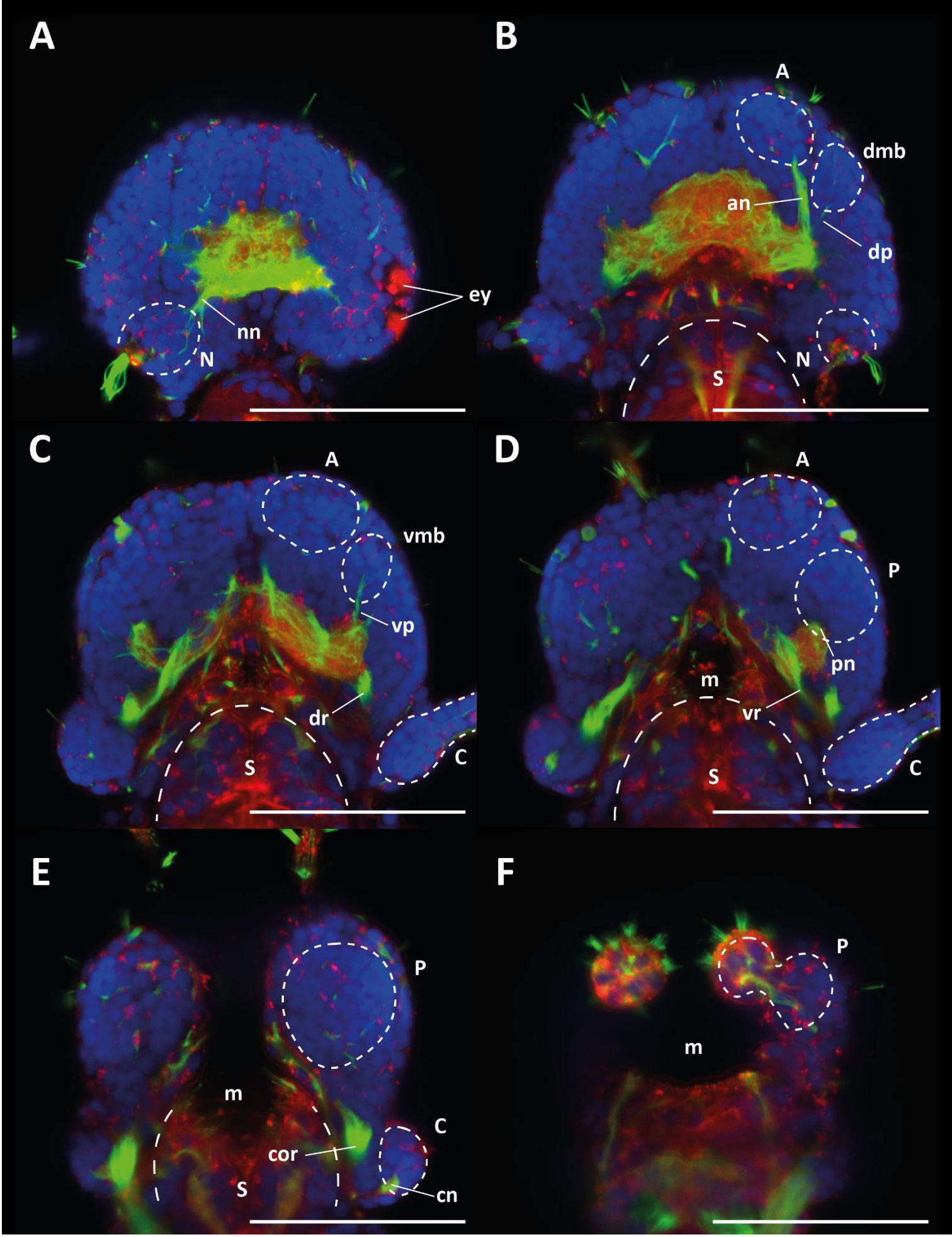


*Figure III-15 Internal head anatomy and nervous system anatomy – **stage 3 segments** (12 dpf). Six z-projections of 4-10 confocal planes each are shown in dorsal view, from dorsal (A) to ventral (F), with anterior up and posterior down. Red : FM 4-64 FX. Green : Tubulin antibody. Blue : DAPI. Scale bar 50 µm.*

3.3 The main adult putative chemosensory organs are differentiated at 6 dpf and their nerves are formed

After having described all adult putative chemosensory organs in juvenile stages, and having become familiar with their localisation and development, I was able to identify and describe them with precision in 6 dpf animals, stage at which little if any compartmentalisation between organs exists inside the brain, and the grouping of nervous fibres in nerves or tracts is not obvious yet.

Together with Wiebke Dürichen, we set out to establish a model anatomical staining at 6 dpf, that could subsequently be used as a reference for neuroanatomy and to facilitate the identification of cells observed in any other images taken in 6 dpf animals. Even though a confocal stack of images can be rotated in three dimensions with a computer programme and resliced from any angle, the signal is always best in the original direction of acquisition. Hence, our aim was to look for an animal that would be mounted as symmetrically as possible, so that the initial images would present the best quality and anatomical symmetry possible.

To reveal anatomical features, we decided to stain these animals with DAPI for nuclei, an antibody against α-acetylated tubulin for nervous fibres and cilia, and the membrane marker mCLING–ATTO 647N which had proved to be superior to FM at the 6 dpf stage. As was shown with the images obtained above, these three markers complement each other remarkably to provide a rich, though general, understanding of neuroanatomy. After staining and imaging many animals, we identified two of them that we chose as models : one imaged from the dorsal side (Figure III-16), and one imaged from the lateral side (Figure III-17). Both offer an excellent angle of view, which was especially challenging to obtain in terms of mounting for the lateral view. Small imperfections in the symmetry can be seen (for example in Figure III-16-7 where two slightly shifted planes have been assembled to for left and right half, or in Figure III-17-10 where the stomodeal nerve is not supposed to be seen in the same vertical plane as the dorsal pit), but they do not hinder precise understanding of the anatomy. For each animal, ten planes of interest have been chosen to show anatomical structures of interest, notably those of the nervous system. The original stacks evidently show even more information and are available on demand.

These structures are precisely annotated, and the presumed boundaries of cellular regions belonging to the sense organs are shown with dashed lines. Except for some parts of the palps and antennae, it is not possible to know with certainty where these boundaries actually are, since no clear extracellular compartments exist, hence these presumed boundaries are nothing more than the current best estimates based on the staining method used here and on available knowledge.

3.3.1 General observations

In *Platynereis*' head at 6 dpf, numerous isolated cilia can be seen all over the head surface, which are likely to be of sensory nature. Inside the head, all cell nuclei are densely and rather uniformly packed, more so than in other parts of the body (see in Figure III-16-9 or Figure III-17-8 for example). Most cells found in the head are supposedly neurons, and are organised around a central neuropile or plexus, which consists of a dense interweaving of nervous fibres (well visible is green in most planes). This neuropile occupies a significant volume inside the head (see Figure III-17-8 to 10). The ground pattern of annelid neuroanatomy (see Chapter II) is well visible at this stage, namely the ventral nerve cord connected to the brain by the circum-oesophageal ring of connectives that runs on each side of the stomodeum (Figure III-17-4 to 10). The two roots of these connectives are visible on Figure III-17-4 and 6 respectively. Note how close to the body surface the cells of the ventral nerve cord are located (Figure III-17-10).

At this stage the stomodeum is already large, and represents a volume comparable to that of the head (Figure III-16-7 and Figure III-17-10). It is densely innervated, and presents a number of ciliated cells at its frontal part, i.e. the mouth opening (top part in Figure III-16-9, right part in Figure III-17-9 and 10).

Note that the brain is so to say wrapped around the stomodeum, as it follows its ellipsoidal shape. A rather large coelomic cavity is present below the stomodeum (dark area in Figure III-16-10 and Figure III-17-5 to 10), its posterior border is in immediate proximity with the first commissure of the ventral nerve cord (Figure III-16-10).

The 6 dpf animal is perfectly capable of ciliary-beating mediated swimming, and accordingly two ciliary bands and found around its head : the prototroch (see for example Figure III-16-2 and Figure III-17-2), and the metatroch (see for example Figure III-16-9 and Figure III-17-2), the cilia of which appear as bright green tufts at the head surface in all planes.

The two pairs of adults eyes are located at the dorsal surface of the head, rather posteriorly (Figure III-17-3). The pigmented cups as well as the deeper photoreceptors cells (see [76]) can be seen. The cavity of the cups appears in red on these images, which probably corresponds to the abundant rhabdomes of the photoreceptors cells being revealed by the membrane stain.

3.3.2 Sensory organs

The **nuchal organs** are located dorsally, at the posterior side of the head. They are more posterior (Figure III-16-3) and more ventral (Figure III-17-3) than the pair of adult eyes. The cilia of their supporting cells are abundant and well visible (Figure III-16-4 to 6, Figure III-17-3). The nuchal cavity, also called olfactory chamber due to the supposed chemosensory function of that organ [116], is already formed as can be seen in Figure III-16-5 and Figure III-17-4, as well as in the inset of Figure III-16-5 that shows a close-up of that region in the DAPI channel only, revealing an absence of cell nuclei in the cavity. The nuchal nerve is formed already (Figure III-16-3 and 4, Figure III-17-7) and projects into the central plexus, its commissure can be recognised (Figure III-16-4).

The **antennae** as appendages are already protruding, they are as frontal as can be, and point rather downwards and laterally (Figure III-16-8, Figure III-17-3). They are situated at a central height compared to the head's height. No cell bodies are present in the appendages themselves yet, a characteristic that remains true until the 5-segmented stage as described above (see Figure III-13). The antennae therefore most likely consist only of cellular extensions and extracellular structures. Tufts of protruding cilia are clearly visible (Figure III-16-8), which most likely belong to sensory neurons. The antennal nerve is one of the most prominent structures visible in the brain at 6 dpf, it already consists of a thick, well-localised bundle of axons coming from antennal cells (Figure III-16-5, Figure III-17-5). It projects to an intermediate part of the plexus as in older stages. A sort of membrane groove or cleft can be seen dorsally to the antennal nerve (Figure III-16-3 and 4), which partly compartmentalises the dorsal brain. The cleft is visible in brightfield illumination in living, non-stained animals where it can easily be mistaken for the antennal nerve, which in reality has a more ventral position. This cleft can actually be used as a reliable landmark to localise the antennal nerve in brightfield observations, provided that such confusion is not made. The antennal cells can be localised with a higher degree of certainty than that of the nuchal organs, since faint compartments are present around them (see notably Figure III-16-6). Note that despite the antennal appendages being rather small, the cells attributed to the organ are numerous and occupy a rather large volume (see notably Figure III-17-5). From this staining however, in the absence of a neuronal marker, it cannot be asserted how many of these cells are actual sensory neurons. Antennae are mobile at this stage, as can be observed in living animals, and indeed at least three bundles of muscle fibres can be identified around them from the non-specific membrane staining (Figure III-17-3 and 4). A previous study, using a phalloidin staining, had shown that these muscles are differentiated at 4dpf but less so at 3dpf (see Figure 30 in[257]). The long and straight cilia visible between the antennal regions (Figure III-16-5 to 6, Figure III-17-8 to 10) belong to a small population of sensory cells, some of which are mechanosensory (Luis-Alberto Bezares-Calderón, personal communication).

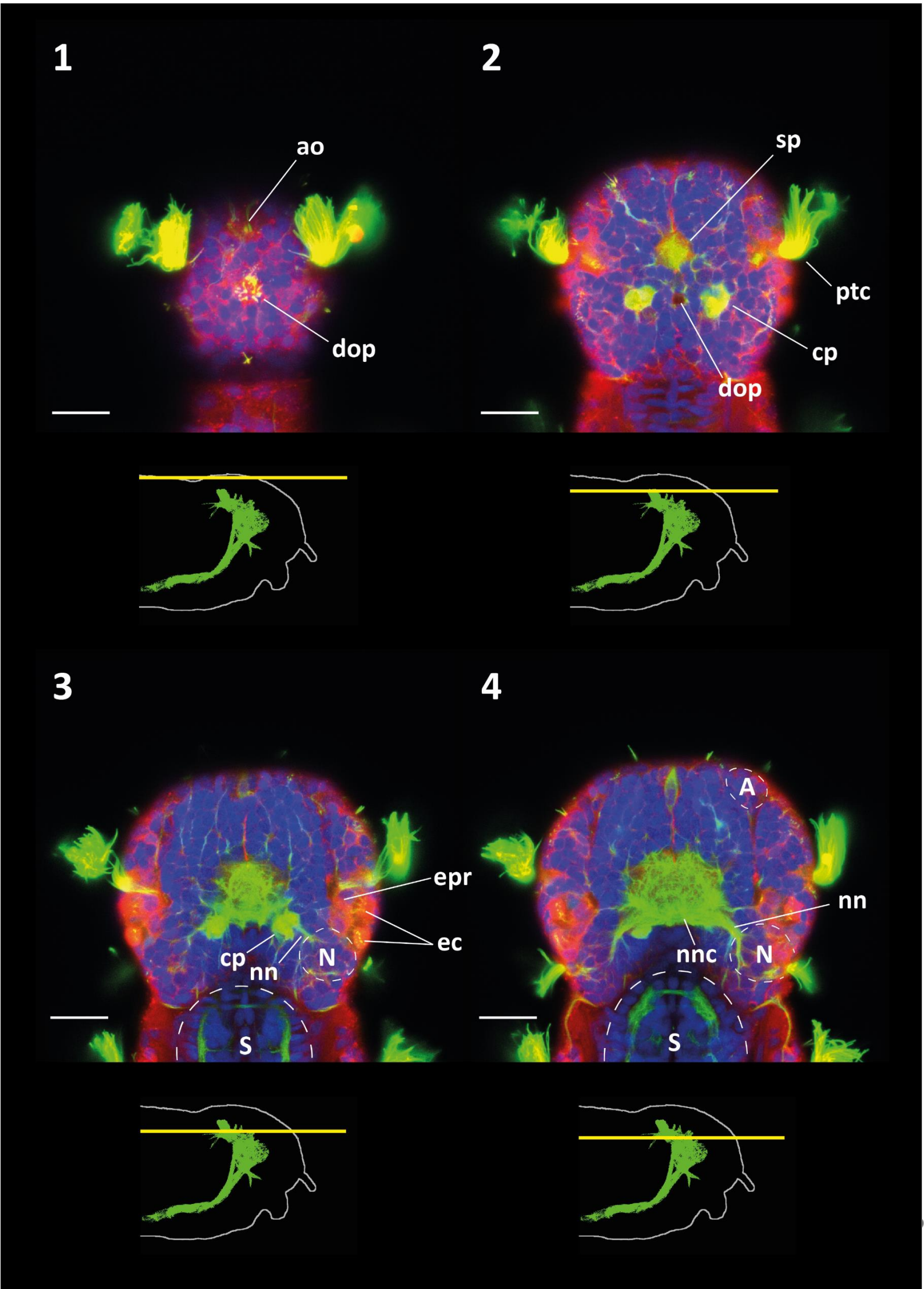
The two **tentacular cirri** are prominent appendages at this stage, with a length almost that of the head (Figure III-17-1, see also Figure III-9). They are situated approximately in the same horizontal plane as the antennae, ventrally to the nuchal organs (Figure III-17-3), and posteriorly to the roots of the

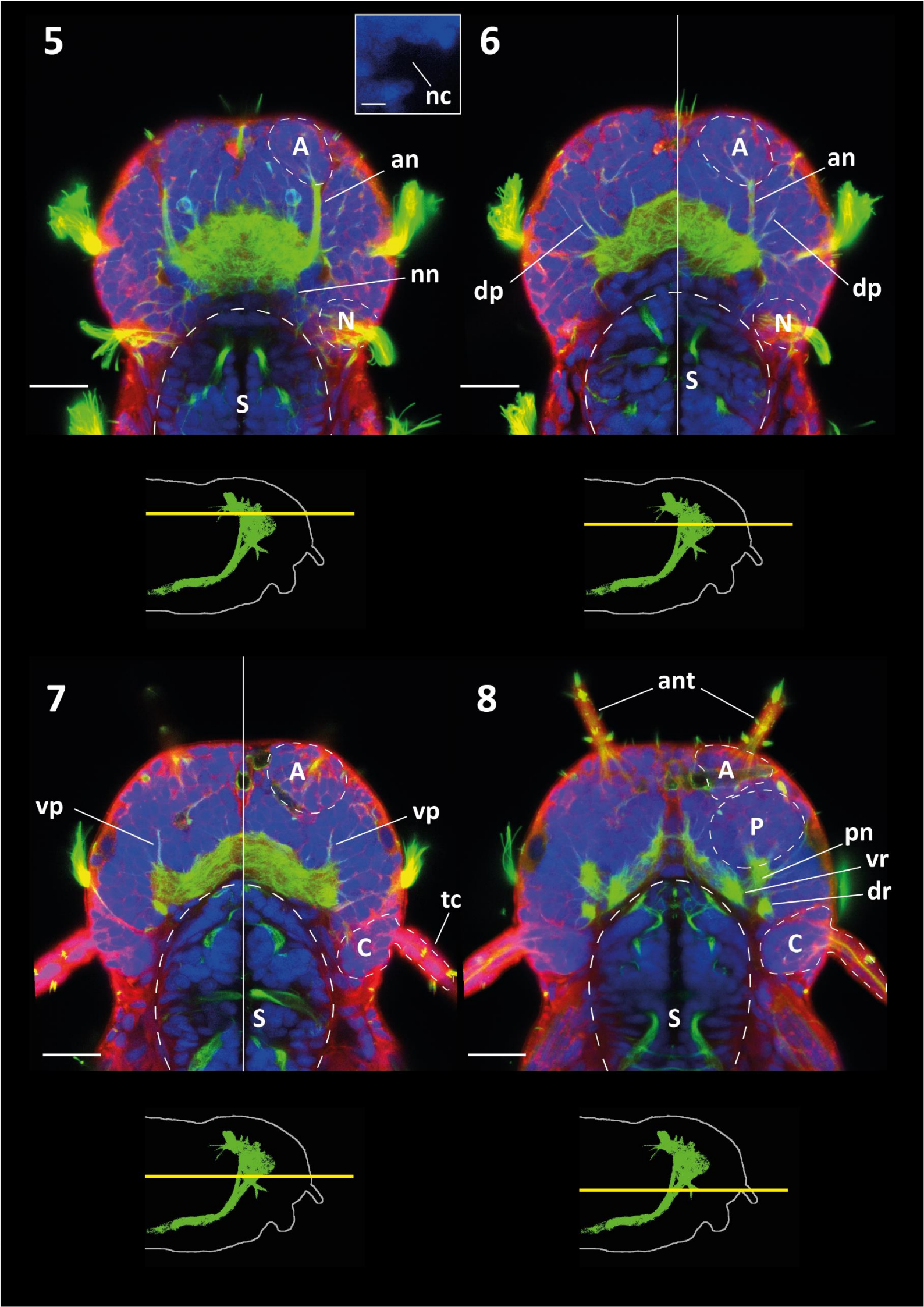
circum-oesophageal ring and the metatroch (Figure III-16-8 and 9, Figure III-17-2). They appear cut in the dorsal view (Figure III-16-7 and 8). Contrary to the antennae, cell bodies are present inside the appendages (Figure III-16-7 and 8). Tufts of penetrative cilia are also present (Figure III-16-7), and long nervous fibres can be seen to run through the appendage (Figure III-16-8). Inside the head, the area containing the cells bodies is rather well delimited (Figure III-16-7, Figure III-17-3), more so than for the antennae. This is probably accounted for by the presumed evolutionary origin of the cirral ganglia as parapodial ganglia (see Chapter II). Provided than one regards them as part of the brain, the cirral ganglia together with the nuchal ganglia are the most posterior part of it. The cirral nerve is clearly visible in the ventral part of the cirral ganglion (Figure III-16-9, Figure III-17-3), and projects directly to the circum-oesophageal ring (Figure III-17-3). As for the antennae, these cirri are orientable in space as can be observed in living animals, and indeed at least two dorsal cirral muscles can be seen next to them from the membrane staining (Figure III-17-2). The action of these muscles is particularly apparent when the animals adopt their swimming position, in which the cirri are moved and maintained posteriorly, parallel to the trunk.

The **palps** already occupy a large part of the head (Figure III-16-9, Figure III-17-5), and their tip starts to protrude (Figure III-16-10, Figure III-17-5), though they are still far from being the massive appendages seen at later stages (Figure III-1). The palps are ventral appendages, pointing ventrally i.e. towards the substrate on which the animal crawls. They are positioned on either side of the mouth opening (Figure III-16-9 and 10, Figure III-17-7 to 10). Tuft of penetrative cilia are visible as for antennae and cirri and concentrated at the tip surface (Figure III-16-10, Figure III-17-6), similar to what is observed at later stages. Their inner mass is located more posteriorly than the antennal mass, in direct contact with it, more anteriorly than the roots of the circum-oesophageal ring (Figure III-16-8), and are more ventrally than antennae and tentacular cirri (Figure III-17-4). Inside the head, it is partly possible to distinguish their boundaries, notably thanks to the future coelomic cavities (see Figure III-3) that start forming anteriorly and posteriorly (Figure III-16-9, Figure III-17-3 and 4). Palps in late juveniles have an abundant and complex musculature (Figure III-4A and B) which has started to develop already, and at least two muscles can be recognised from the membrane staining (Figure III-17-5 and 6). *In vivo* observations of freely-behaving animals reveal that palps can indeed be moved, and that the animals seem to somewhat probe the substrate surface with them (personal observations). The innervation shows at least three main nerve roots (Figure III-16-8 and 9, Figure III-17-4 and 5) that converge in the palpal nerve (Figure III-16-8, Figure III-17-4), however this nerve is short and its extremities hard to localise unambiguously.

3.3.3 Other remarkable anatomical structures

The position of **ciliary photoreceptor cells** can be clearly identified based on the tubulin staining, which reveals their abundant sensory cilia (Figure III-16-2 and 3, Figure III-17-7 to 9). These cells are dorsal and posterior to the prototroch (Figure III-16-2), their projection is more medial than the nuchal nerve (Figure III-16-3), and immediately posterior to the nuchal commissure (Figure III-17-8). For a more detailed description of these cells, see for adult *Nereis* fig. 4 in [258], for larval *Platynereis* fig. 1 in [67] and fig. 2 and 3 in [81]. Between the ciliary photoreceptor cells lies the **dorsal pit** (Figure III-16-1 and 2, Figure III-17-10), a ciliated structure of unknown function thought to be sensory, and which seems to contain a small cavity in contact with the surrounding water (Figure III-16-2). At the 6 dpf stage, the animal no longer has an obvious larval **apical organ**, though the remainings of it may still be seen around the midline at the head's surface, in a more anterior position than the ciliary photoreceptor cells and than the prototroch (Figure III-16-1, Figure III-17-10). The apical organ should not be mistaken for the dorsal pit, despite their morphological resemblance. However, the nervous projections of the apical organ, which form the **neurosecretory plexus** described at 48hpf [68],[236] and at 72hpf [259] can still be identified at 6 dpf. This plexus represents the most dorsal part of the head's neuropile, and in a lateral view appears as a sort of dorsal protrusion of this neuropile (Figure III-16-2, Figure III-17-10).


1
ao
dop
2
sp
ptc
cp
dop
3
epr
ec
cp
nn
N
S
4
A
nn
nnc
N
S


5
nc
A
an
nn
N
S
6
A
an
dp
dp
N
S
7
A
vp
vp
tc
C
S
8
ant
A
P
pn
vr
dr
C
S

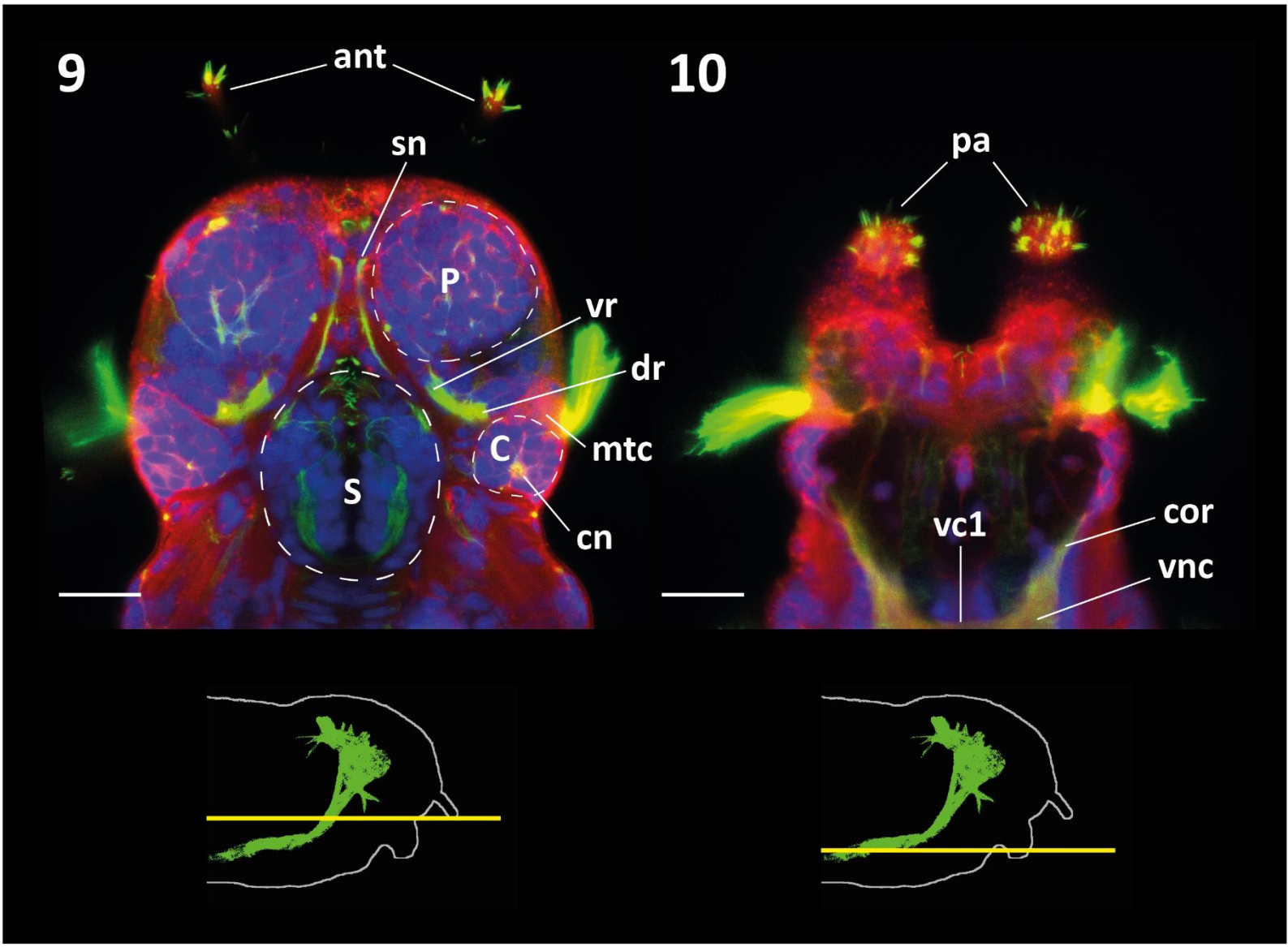
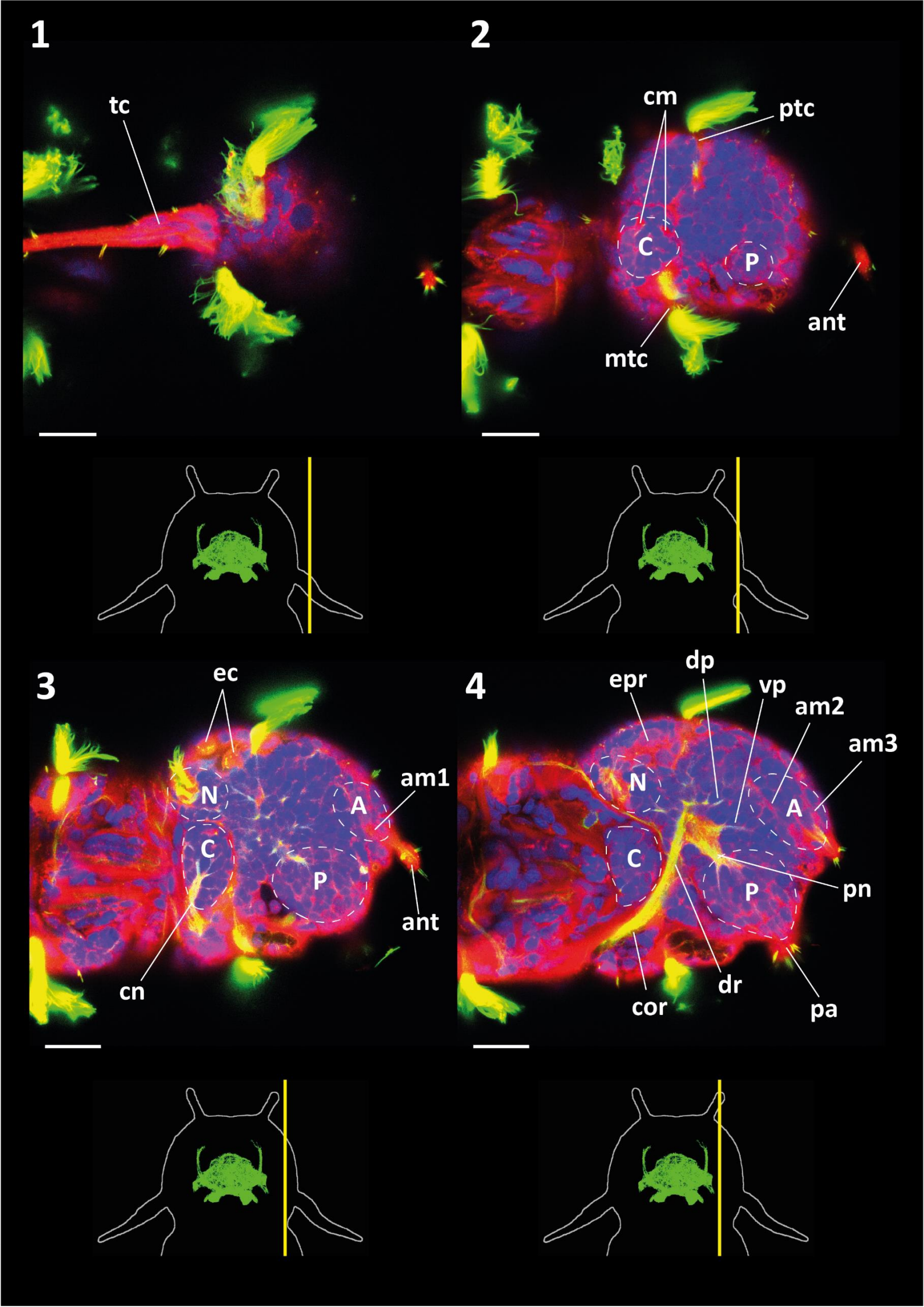
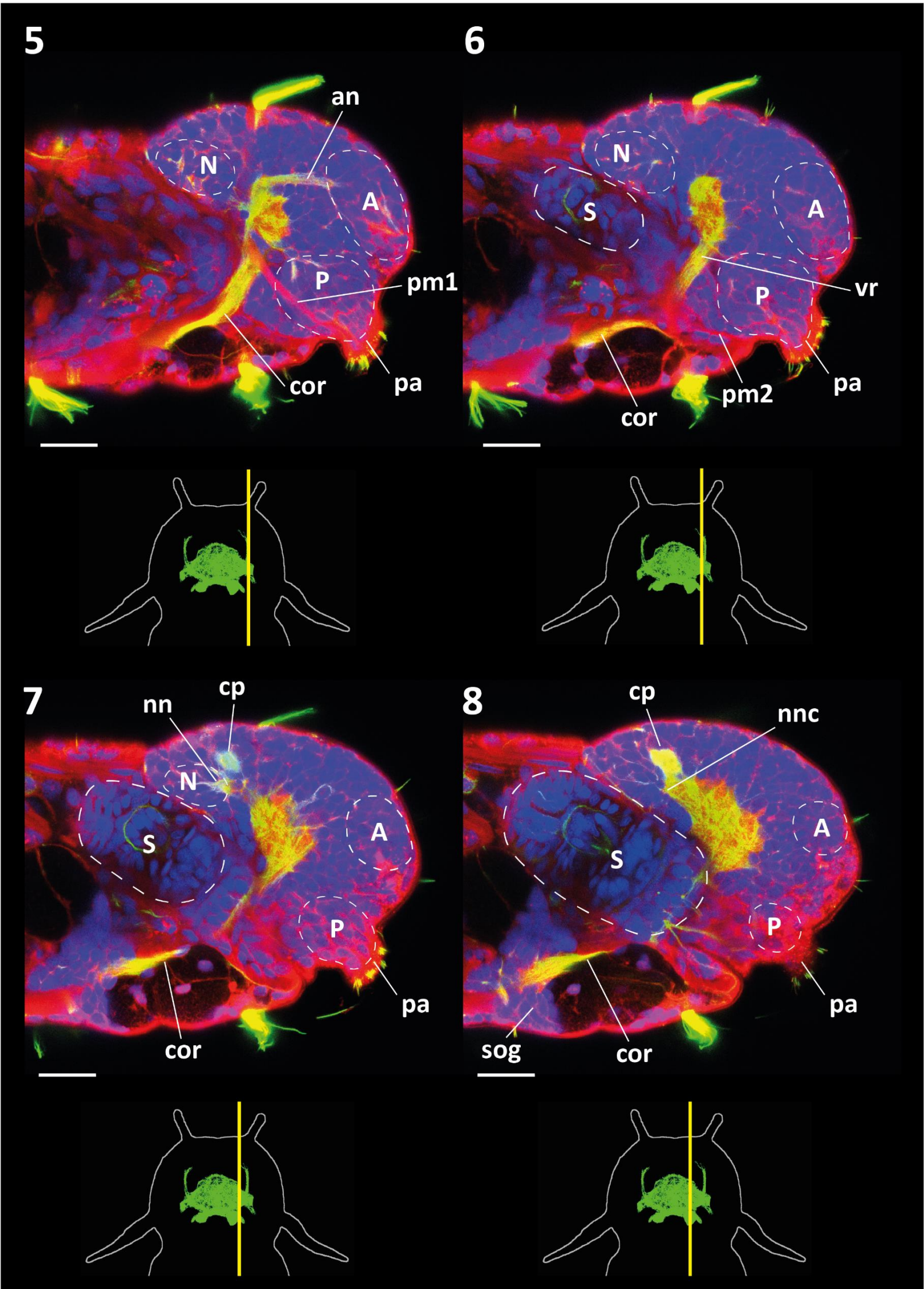


Figure III-16 Z-projections of the reference 6 dpf anatomical staining in 10 different planes, dorsal view. Anterior is up, posterior is down, left is left and right is right. Red : mCLING-ATTO 647N (membrane marker). Green : anti α-acetylated tubulin antibody (marker for nervous fibres and cilia). Blue : DAPI (nuclear marker). Planes are numeroted from dorsal (1) to ventral (10) ; (6) and (7) are reconstituted from two slightly different confocal planes to show both Mushroom Bodies peduncles. A schematic drawing of the head in lateral view is displayed below each plane, with the body outline in grey, a simplified nervous system in green and the corresponding plane in yellow. Inset in (5) : nuchal cavity in the Dapi channel only, scale bar 5 µm. Loose dashed lines indicate the outline of the stomodeum (S), tight dashed lines the presumed boundaries of the cell bodies areas for antenna (A), tentacular cirrus (C), nuchal organ (N), palp (P). Anatomical terms : antennal nerve (an), antenna (ant), circum-oesophageal ring (cor), ciliary photoreceptor cell (cp), dorsal pit (dop), dorsal (dr) and ventral (vr) root of the circum-oesophageal ring, eye cup (ec), eye photoreceptor cell (epr), dorsal (dp) and ventral (vp) peduncle of the Mushroom Bodies, metatroch cell (mtc), nuchal cavity (nc), nuchal nerve (nn), nuchal nerve commissure (nnc), nuchal organ (no), prototroch cell (ptc), palp (pa), palpal nerve (pn), one of the stomodeal nerves (sn), secretory plexus (sp), tentacular cirrus (tc), tentacular cirrus nerve (cn), first commissure of the ventral nerve cord (vc1), ventral nerve cord (vnc). Scale bar 20 µm. Staining and imaging : Wiebke Dürichen.


1
tc
2
cm
ptc
C
P
ant
mtc
3
ec
N
A
am1
C
P
ant
cn
4
epr
dp
vp
am2
am3
N
A
C
P
pn
dr
cor
pa


5
an
N
A
P
pm1
cor
pa
6
N
S
A
P
vr
cor
pm2
pa
7
nn
cp
N
S
A
P
cor
pa
8
cp
nnc
S
A
P
sog
cor
pa

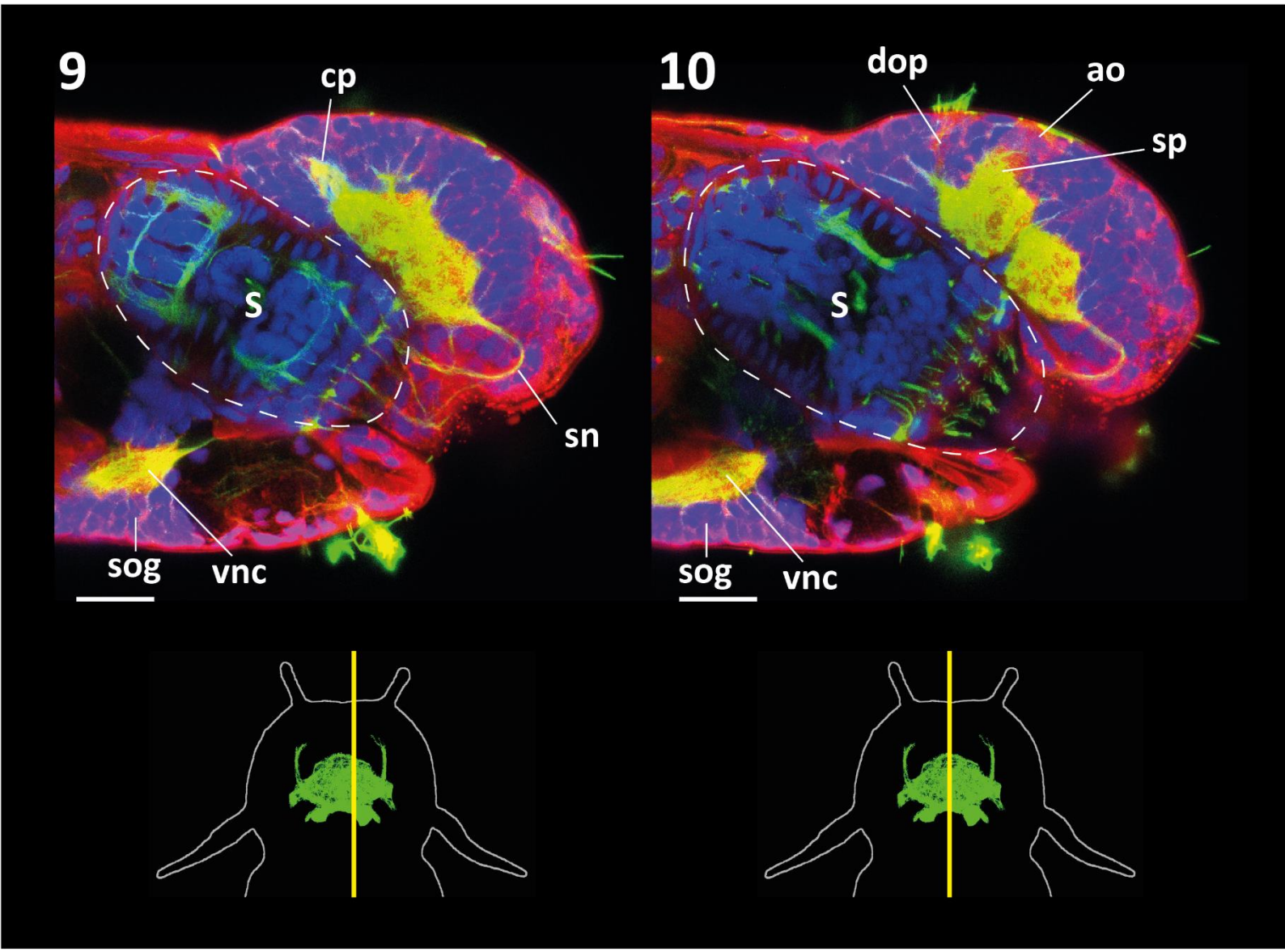


Figure III-17 Z-projections of the reference 6 dpf anatomical staining in 10 different planes, dorsal view. Anterior is right, posterior is left, dorsal is up and ventral is down. Red : mCLING-ATTO 647N (membrane marker). Green : anti α-acetylated tubulin antibody (marker for nervous fibres and cilia). Blue : DAPI (nuclear marker). Planes are numeroted from dorsal (1) to ventral (10). A schematic drawing of the head in dorsal view is displayed below each plane, with the body outline in grey, a simplified nervous system in green and the corresponding plane in yellow. Loose dashed lines indicate the outline of the stomodeum (S), tight dashed lines the presumed boundaries of the cell bodies areas for antenna (A), tentacular cirrus (C), nuchal organ (N), palp (P). Anatomical terms : antennal muscles (am1-am3), antennal nerve (an), antenna (ant), circum-oesophageal ring (cor), ciliary photoreceptor cell (cp), dorsal pit (dop), dorsal (dr) and ventral (vr) root of the circum-oesophageal ring, eye cup (ec), eye photoreceptor cell (epr), dorsal (dp) and ventral (vp) peduncle of the Mushroom Bodies, metatroch cell (mtc), nuchal cavity (nc), nuchal nerve (nn), nuchal nerve commissure (nnc), nuchal organ (no), prototroch cell (ptc), palp (pa), palpal muscles (pm1 and pm2), palpal nerve (pn), one of the stomodeal nerves (sn), sub-oesophageal ganglion (sog), secretory plexus (sp), tentacular cirrus (tc), tentacular cirrus muscle (cm), tentacular cirrus nerve (cn), first commissure of the ventral nerve cord (vc1), ventral nerve cord (vnc). Scale bar 20 µm. Staining and imaging : Wiebke Dürichen.

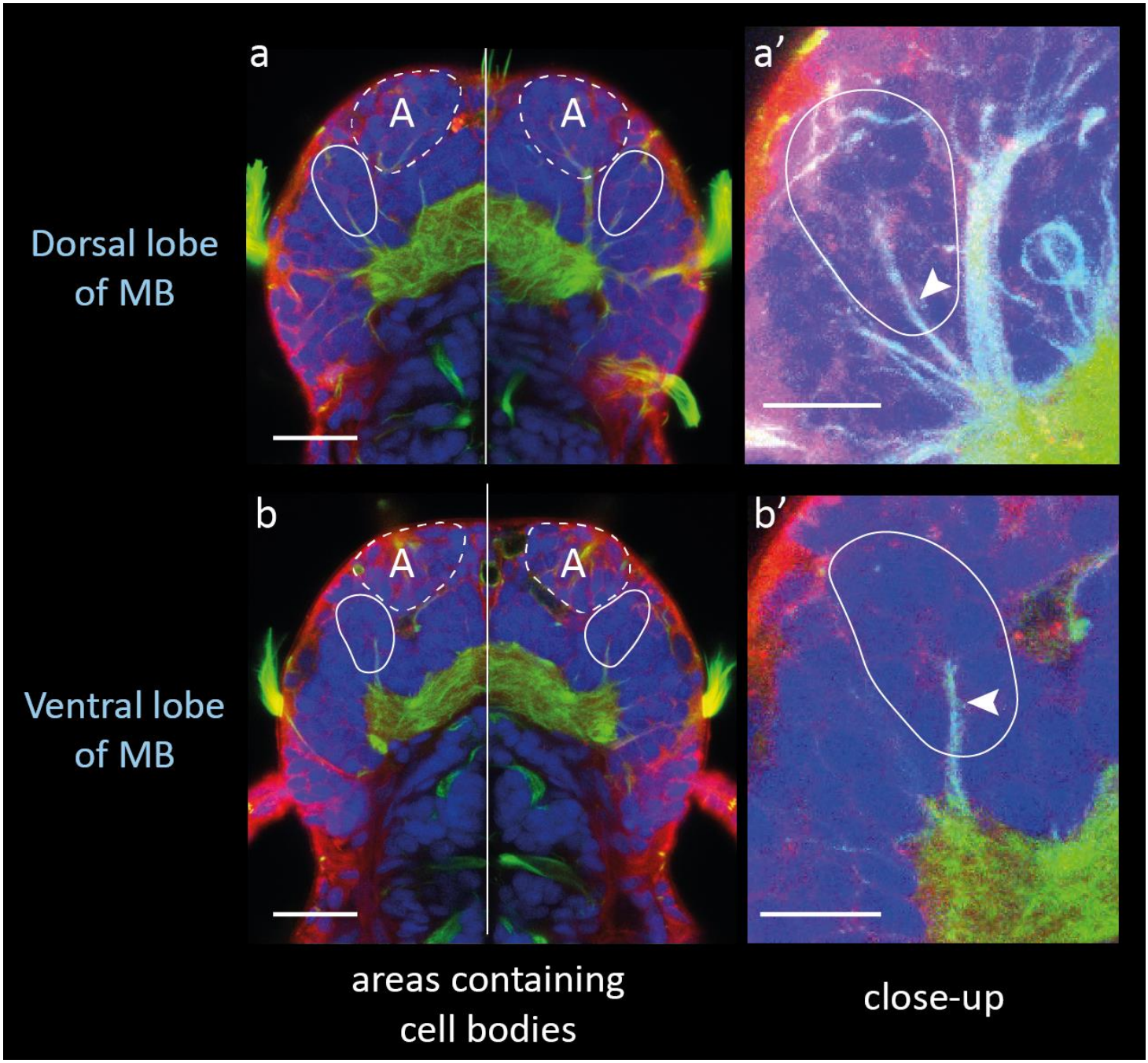


Figure III-18 Position and presumed boundaries of dorsal (a-a') and ventral (b-b') Mushroom Bodies lobes at 6 dpf. (a) and (b) correspond respectively to planes 6 and 7 of Figure III-16. (a') and (b') are close-ups of the left part of (a) and (b). Presumed boundaries of the areas containing the cell bodies are indicated in solid lines for the lobes and in dashed lines for the antennae (A). Red : mCLING-ATTO 647N. Green : anti α-acetylated tubulin antibody. Blue : DAPI. Scale bar 20 µm in (a) and (b), 5 µm in (a') and (b')

3.4 Mushroom Bodies are probably differentiated at 6 dpf

In addition to the future adult sensory organs, another neuronal structure of interest can be recognised and localised with some precision at 6 dpf : the Mushroom Bodies (MB), whose later development has been illustrated in Figure III-10 to Figure III-15. As explained above, no other morphological criterion

than the presence of the peduncles can be used to identify MB at stages younger than about 20 segments.

Both peduncles can be identified at 6 dpf with a tubulin immunostaining, as shown in details in Figure III-18. The following criteria can be used to identify these axon bundles. The dorsal peduncle is the first nervous fibre immediately lateral to the antennal nerve, than can be seen approximately in the same horizontal plane, and points fronto-laterally ; it projects slightly more laterally and ventrally than the antennal nerve. The ventral peduncle has a very similar position in dorsal view, and is simply located more ventrally. In its horizontal plane, the ventral peduncle is the most medial nervous fibre that projects to the lateral extremity of the main plexus, as shown in Figure III-18b'. Around the peduncles, and notably around the ventral one, cell nuclei sometimes have an appearance strikingly similar to a bunch of grapes, which suggests where the boundaries of the lobe would be, however this may not be a reliable criterion. For a more precise description of MB early development and MB peduncle in *Platynereis*, see the Master thesis of Wiebke Dürichen [260].

III – 4 Discussion

4.1 Candidate chemosensory organs : sensory cells and possible function

First, a description of the internal anatomy has been given for the candidate chemosensory organs in late *Platynereis* juveniles (25-35 segments). A precise description of the nuchal organs has already been given by Schmidtberg & Dorresteijn ([233], see Chapter II) using transmission electron microscopy. The present observations were made only to confirm some of their observations, the images presented to make the reader more familiar with their appearance in a fluorescent staining.

As is known from the polychaete literature, **tentacular cirri** typically comprise a nerve in their centre, which was confirmed by a tubulin immunostaining (Figure III-2B). I have described a wrapping musculature of longitudinal muscles at their base, which is consistent with the movements of cirri observed in living animals, as they can be seen pointed in many directions of the space while being flexible structures : muscular contractions at the base orient the soft appendage in the same way that bending only the base of an inflatable column would orient the whole object. At the surface of these cirri, both penetrative and non-penetrative types of sensory cilia have been observed. The penetrative ones most probably are the same sensory endings as described by Langdon and Dorsett & Hyde (see Chapter II) in the tentacular cirri of *Nereis virens.* These sensory endings must be neuronal processes of several cells for each cluster, though this point could not be determined with certainty from the stainings. Such a finding indicates that tentacular cirri may serve at least two different sensory modalities. It has been hypothesised in the literature that they are chemosensory, based on the structure of their ciliated cells. I could confirm the presence of these cells in *Platynereis*, but the anatomy brings no further conclusion regarding their function. From behaviour it is clear that these appendages are at least mechanosensory, since animals show clear retraction responses if one strokes their tentacular cirri (personal observations). Juveniles also use their cirri but not their eyes to detect conspecifics while crawling on the substrate, since they will react to each other only when they come in physical contact (personal observations). Regardless of the modalities – and maybe both are served – the four pairs of cirri probably provide the animal with a good spatial sampling of the water above the substrate, and indeed the two dorsal cirri which point upwards are by far the longest, whereas the two ventral cirri are much shorter and point towards the ground.

In **palps**, coelomic cavities have been described which seem to be unified. They contain gland-like structures whose function may be some mucus secretion. I have observed sets of external muscles, notably oblique ones, and internal ones, which comprise longitudinal and circular muscles. The palp musculature is powerful, as is apparent when the animals feed and actively use their palps to grasp food items (personal observations). Palps can be moved in many directions, and their tip can be retracted as known in the nereidid literature. Oblique muscles are probably used to bring the palp closer to each other to grasp food, or to cover the mouth opening which lies between the palps. The longitudinal muscles most likely serve the orientation or retraction of the tip, while the circular muscles could be used to contract the palp and in this way make the tip protrude thanks to the hydrostatic action of the coelomic cavity. As for the tentacular cirri, I have observed penetrative and non-penetrative types cilia at the palp surface, concentrated at their tip. Penetrative cilia have been described likewise in *Nereis* (see Chapter II), but not non-penetrative ones. The staining did not allow to conclude whether the cells were mono- or multiciliated, i.e. whether they would belong to the category (1) or (2) described by Purschke (see Chapter II). Palps are in contact with the substrate while the animal is crawling, and most likely come in contact with food since they are located on either side of the stomodeum opening. If they are mechanosensory, their role is probably rather in texture probing. If they are chemosensory, they probably serve a contact chemoreception. Nothing excludes that they could serve both sensory modalities.

Antennae do not have an obvious nerve in their centre, but rather a diffuse density of nervous fibres running from surface sensory endings towards the base of the appendage. From stainings at earlier

stages it is clear that the antennal nerve is only condensed inside the head. In this regard they differ from the antennae described in *Nereis* (Retzius 1895 [90], Heuer & Lösel 2008 [101]), at least up to the 30-35 segments stage, but the antennae are long differentiated at this stage and the animals so similar to adults that probably no nerve is ever formed in the appendage itself. Clusters of penetrative cilia are present at the antennal surface, and more investigations would be needed to determine whether or not non-penetrative ones are also present. It seems reasonable to hypothesise that antennae would be at least mechanosensory organ, involved in the frontal detection of objects – in this way tentacular cirri and antennae would adequately probe the whole semi-space to which the head is exposed while the animal is crawling on the sea floor. However their role in chemoreception cannot be excluded, as suggested by Gross's behavioural experiments in *Nereis* [170]. The most striking feature of early antennal development is the absence of cell nuclei in the appendage until the 5-segmented stage ; the antennal appendages must mostly consist of extracellular matrix and nervous fibres, which makes them a radically different sensory organ from cirri. Ultrastructural studies on *Platynereis* antennae at such early stages would provide more information regarding their composition and the arrangement of sensory processes inside them.

Anal cirri are highly similar to tentacular ones, except that no muscular collar is present at their base, making it unlikely that the animals could orient these appendages. They are probably used a passive sensors. Penetrative and non-penetrative cilia can be seen at their surface as for tentacular cirri. It is likely that the corresponding cell bodies are located in close proximity, as described in the tentacular cirri and palps of *Nereis* [95],[145] but it was not possible to determine this from this staining. Such a similarity in anatomy between anal and tentacular cirri suggests that they would serve the same sensory functions at opposite sides of the body. Straightforward behavioural tests reveal that the anal cirri are mechanosensory, as the animal react when these appendages are touched. Moreover, Gross [170] has indicated that in *Nereis* they are sensitive to chemical stimulation, though he did not provide data to support his claim. In the same way as for the tentacular cirri, they may be both mechano- and chemosensory. A large paired spinning gland is present at the base of the anal cirri. The use of this gland is apparent for example when the worms escape from a plastic pipette, as they are indeed able to weave a fine thread from their pygidium and secure their way out of the pipette down in the air, in the same way that a spider would do (personal observations).

Overall, I have observed both protruding and non-protruding types of sensory endings, present in similar abundance in tentacular cirri and palps. The protruding ones contain tufts of cilia that are clearly penetrative, and are similar to the "diffuse organs" described by Langdon in *Nereis* [95]. Dorsett & Hyde have shown that in palps and tentacular cirri of *Nereis* the corresponding neurons are monociliated [145], it is thus reasonable to assume that this would be true as well in *Platynereis* but awaits verification in electron microscopy. These cells would thus belong to the type (1) or (2) described by Purschke ([116] and see Chapter II), with (2) i.e. monociliated being more likely. For the non-protruding endings, it is unclear whether cilia are present or not though the tubulin staining would suggest that they are, and whether the cuticle is penetrated. They may be similar to the ones described by Hanström in the antennae of *Sthenelais* [134]. To my knowledge, non-protruding sensory endings are not described in nereidids, but likewise electron microscopy studies will be necessary to investigate their nature, verify the absence or presence of cilia, and exclude that the absence of protruding cellular endings could be an artefact of fixation. In any case, two types of sensory endings have been consistently observed in palps and tentacular cirri, which leaves no doubt regarding the existence.

4.2 Development of the candidate chemosensory organs

A description of sensory structures has been given at six different stages representative of juvenile development, with emphasis on the localisation of cells belonging to them.

Palps undergo a tremendous growth between the 3-segmented and the 20-segmented stage : they become large protruding structure, and their tip progressively differentiates. This morphological change is accompanied by the development of large, peripheral coelomic cavities inside the palps, that surround their inner mass. Most palpal sensory neurons are in all likelihood located in this inner cellular mass. While palps are initially relatively close to each other, they become further apart in late juveniles as the mouth opening massively grows, and start pointing laterally. Orrhage has pointed at the multiplicity of projection points possible for the palpal nerve in polychaetes (see Chapter II). Here, this nerve does not project to the roots of the circum-oesophageal ring but directly to the main plexus. It becomes only obvious from around the 20-segmented stage, as it is short and somewhat merged with the lateral part of the plexus at earlier stages. The high density of sensory endings observed at their tip is present in 3-segmented animals already.

Tentacular cirri appear successively and all four of them are well-formed at the 15-segmented stage. Their nerve project ventrally to the circum-oesophageal ring, which confirms the observations made by Gilpin-Brown in *Nereis* [121]. No major rearrangement other than the migration of the cirral ganglia closer to the prostomium and the growth of the cirral nerves is observed during the so-called cephalic metamorphosis. A clear nerve can be seen inside the first tentacular cirri (the anterior dorsal ones) at the 5-segmented stage already. Cell bodies, including most likely those of sensory neurons, are present inside the cirri early on, already at the 3-segmented stage.

Inside the antennae, no cell bodies are observed until the 5-segmented stage nevertheless sensory cilia are present at their surface before, and indeed long nervous fibres can be seen to run along the appendages from their base. The thickening of the antennae probably takes place around the 10-segmented stage.

Nuchal organs are present early on, and the major change that can be observed seems to be a progressive migration of their nerve posteriorly. Next to the nuchal organs, medially to them, the posterior ganglia undergo a significant growth, and their projection seem to have some relation with the nuchal nerve. It is unknown what the relationship between these two structures is, or even whether these ganglia actually belong to the nuchal organs.

Mushroom Bodies (MB) have also been described. The dense packing of their cell bodies, so characteristic of MB in adult brains, is established only around the 20-segmented stage, making it impossible to identify MB in early juveniles based on cellular density only. However, the presence of their peduncles, both dorsal and ventral, can be used reliably to localise MB at such early stages, and get some impression about what cell bodies belong to them

Overall, cell bodies belonging to all candidate chemosensory organs are easily distinguishable from the rest of the brain only after the 5-segmented stage, which corresponds to the cephalisation of the first pair of parapodia and their metamorphosis into a new pair of tentacular cirri. In a 5-segmented animal, cell bodies can be localised with certainty for tentacular cirri and antennae, with some confidence for the palps, but only imprecisely for the nuchal organs (see Figure III-13). At earlier stages, it is possible to attribute with certainty cell bodies to an organ only in close proximity of a landmark such as a nerve, or in the centre of the corresponding cellular region, whereas the boundaries are difficult to distinguish. Some partial compartmentalisation can be seen for tentacular cirri, palps and antennae in a 3-segmented animals, but for the nuchal organs no other criterion than proximity with the nuchal cavity can be used.

Some confusion can appear when looking at overall head shape and size at early stages : despite a clear brain complexification and the growth of appendages, the width of the head itself does not increase but actually decreases between the 3 dpf and the 5-segmented stage – that is, during several

weeks of development. This fact appears less paradoxical if one considers internal anatomy, as indeed the brain at 3 days is restricted to a short frontal portion of the animal and the whole head then develops frontally, meaning that the brain volume does increase over development. While the head is hardly formed at 3 dpf, massive and rapid morphological transformations take place after this stage and the head is well distinguishable at 4 dpf already (see brightfield images in [138]).

Comparing scale bars in images taken at different magnifications does not give a good mental representation of relative sizes. I thus though this point would be best clarified by a single brightfield picture showing, next to each other, living *Platynereis* from different developmental stages. Figure III-19 shows such a picture I took from living animals paralysed with a 300 µM magnesium chloride solution in natural sea water. The approximate posterior boundary of the brain is indicated in dashed lines. This picture makes it clear how the development of the head and of the stomodeum proceeds after 3 dpf.

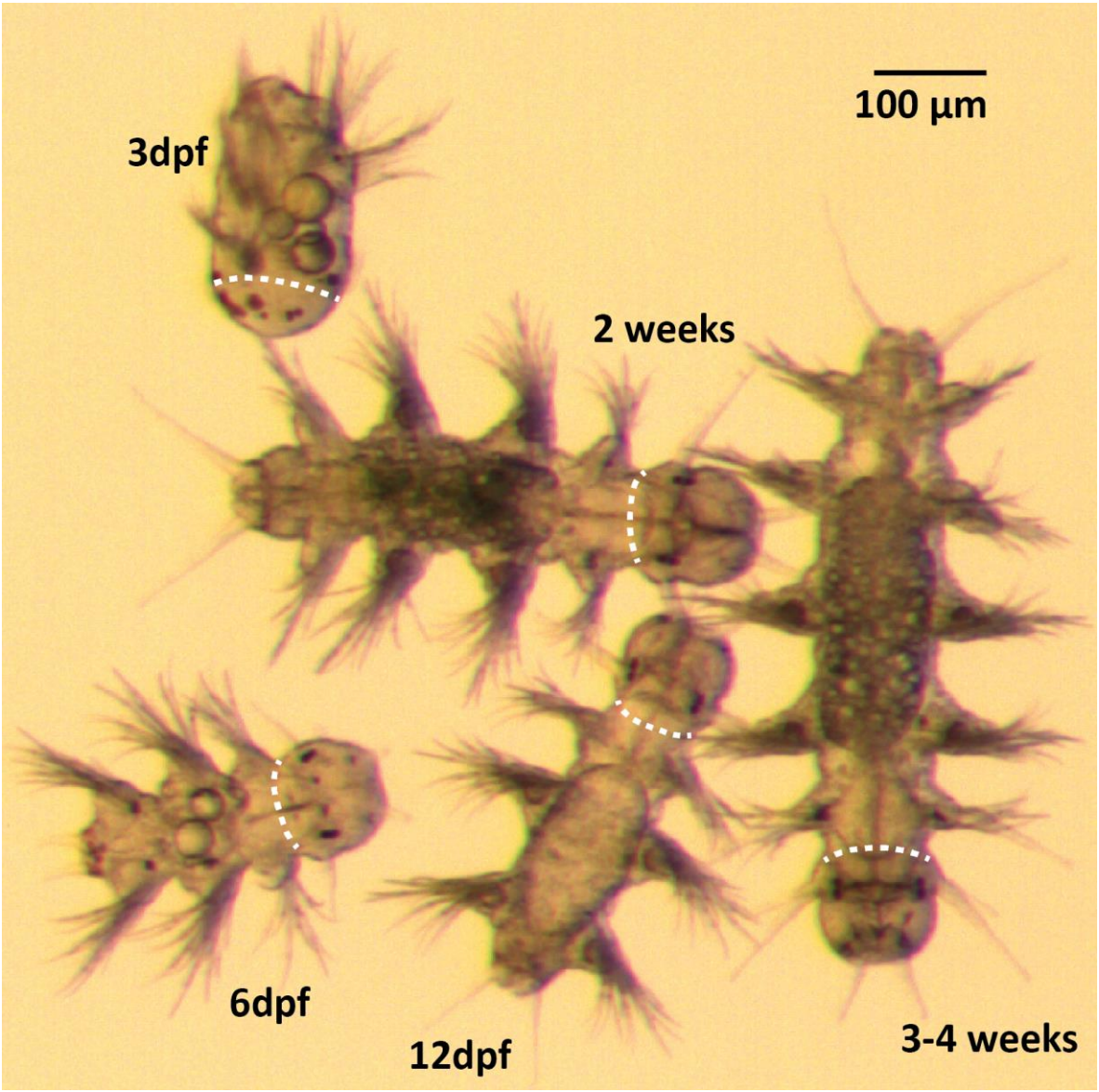


Figure III-19 Comparison of different larval and juvenile stages. Living animals paralysed with magnesium chloride. The 5-segmented animals (3-4 weeks old) is seen before cephalic metamorphosis. Note the relative sizes of heads. The white dashed line in all animals indicate approximately the posterior border of the brain.

4.3 Candidate chemosensory organs at 6 dpf

After candidate chemosensory organs have been reliably identified across development, a precise description of the head neuroanatomy has been given for the 6 dpf stage, notably to facilitate the localisation of the cell bodies belonging to these organs.

Antennae have a significant length at 6 dpf, and are equipped with regularly spaced tufts of penetrative cilia all over their length. No cell bodies are present in the appendage, which comprises mostly nervous fibres and probably supportive tissues. The antennal ganglia are large but restricted to the inside of the head contrary to older animals, and antennal muscles are already functional. Palps hardly protrude out of the head but their tip likewise bears the penetrative cilia observed at later stages. Some muscles are developed already, and the major innervation is established. The tentacular cirri have a clearly individuated ganglion and a nerve is well-formed at their base, whose projection pattern is identical to that in late juveniles. The ground morphological pattern of nuchal organs [122] is clearly established at 6 dpf, with a cavity, supporting ciliated cells, a nerve and a commissure visible in dorsal views.

It is thus apparent that the major anatomical characteristics found in these organs at older stages are already present. These observations altogether suggest that the four candidate chemosensory organs, whatever their true sensory modality, are functional at 6 dpf.

For each of these organs, the presumed limits of their cellular mass have been indicated on the anatomical plates, nevertheless such statement cannot be totally accurate based on the information available. The tentacular cirri are the only organs for which these boundaries are clear, since they are indeed separated by what seems to be extracellular structures (Figure III-17-7, Figure III-18-3 and 4). For antennae and palps, the cellular mass is somewhat compartmentalised. The least obvious boundaries are those of the nuchal organs.

Interestingly, Mushroom Bodies can be localised thanks to their peduncles, although it should be kept in mind that the identification is not unambiguous in some animals, due to anatomical variability and to the similarity of these small peduncles with other neighbouring nervous fibres.

At 6dpf the external morphology of the larval apical organ is not easily as recognisable as it is at earlier stages, but the neurosecretory plexus can be identified. It is thus possible that the sensory cells described at 48 hpf are still present and functional. The regions of the apical organs appears to have become more dorsal than at 2 or 3 dpf, and the shape of the main plexus has more depth along the antero-posterior axis. These changes may be linked to the significant growth of palps and stomodeum at these stages already, and to the overall frontal growth of the head mentioned before.

It should be noted that in the preceding description at 6 dpf, a significant part of the brain areas have not been described, and have to this day a still unknown function. This is notably true for the cells present between the antennal nerves (Figure III-17-3 to 7), for the cells present on each side between the palp and the cirral ganglion (Figure III-17-8), and for most of the dorsal brain (Figure III-18-5 to 10).

4.4 Conclusion

All adult candidate chemosensory organs can be recognised, and their boundaries identified with some degree of certainty. It appears possible and relevant to perform *in vivo* physiological studies of chemosensation at the 6 dpf stage, provided that the observation technique chosen allows major landmarks to be seen, such as main plexus, antennal and palpal nerve, nuchal organ cavity, circum-oesophageal ring or neuro-secretory plexus.

IV – Functional imaging of chemically-evoked neuronal responses

IV – 1 Introduction

1.1 Choice of a method for functional imaging of chemosensation

For the purpose of investigating chemosensory systems in *Platynereis*, given the small size of the larvae, a method enabling to test the physiology of all cells of the head at once would be preferable. Such a method would be even more useful if it can be equally be applied to any chemical stimulus and to any sensory cell regardless of its location, in that it would provide a global and unbiased understanding of chemosensation.

Lindsay et al. have used an interesting approach to perform activity-dependent labelling of chemosensory cells in polychaetes [154], based on the permeation of the cationic molecule agmatine through ion channels following chemical stimulation. This method can be applied to large tissues and allows to identify single cells, but it suffers from several limitations :
1) it relies on agmatine permeation through sodium-gated non-selective cation channels [175], thus receptor neurons could be missed if they have other transduction modes, and other cells than chemoreceptor neurons may as well by labelled,
2) successful labelling is conditional upon the medium used for stimulation [175],
3) agmatine itself can be a weak chemical stimulus, as shown in lobsters and in zebrafish [175],
4) the response dynamics are not captured, since labelling is observed after immunostaining.
Such a method is interesting for a gross mapping of chemoreceptors and is not limited by size, however it cannot reveal an objective and complete picture of chemosensory responses, thus it is not suitable for the present experimental purpose.

Taking advantage of the wide experimental potential offered by *Platynereis* larvae, and encouraged by the success of recent pioneering experiments using calcium reporters for physiological studies of motoneurons [70] and photoreceptors [76], a method based on *in vivo* calcium imaging of neurons was chosen for all subsequent physiological experiments.

1.2 Principle of calcium imaging experiments

In calcium imaging experiments, the intracellular levels of calcium are revealed by a fluorescent indicator, whose light intensity levels match the levels of calcium. Variations of fluorescence intensity are thus a direct readout of calcium fluctuations inside the cells, and indicate notably the activity of neuronal cells.

Calcium indicators can be synthetic chemical dyes like for example the commonly used OGB1-AM (Oregon Green Bapta-1-AM) and Fluo-4, or proteins like the different variants of the family called GCaMP (for GFP-CalModulin Probe) initially developed by Nakai et al., 2001 [261]. Synthetic dyes work best for cell cultures but can also be used in brain tissues, they are introduced into cells by microinjection, diffusion from patch clamp pipettes, electroporation, lipotransfer or simple immersion [262], and will be non-specifically located ; proteic dyes are genetically encoded and can be expressed permanently via transgenesis or transiently via plasmids or mRNAs. The use of promoter constructs allows to express them specifically in structures of interest, which is not possible with the chemical dyes. Until the sixth generation of GCaMP proteins appeared in 2013, chemical dyes were brighter than genetic ones.

GCaMP calcium sensors are composed of a circularly permuted green fluorescent protein (cpGFP), the calmodulin protein (CaM) which can bind calcium, and a peptide called M13 that interacts with calmodulin (see Figure IV-1a). Upon calcium binding, conformational changes of the CaM-M13 complex modulate the pKa of the chromophore located inside the GFP, as well as solvent access, which

increases the emitted fluorescence intensity [263] – note than some other proteic sensors used resonance energy transfer.

Several generations of GCaMP proteins have been developed since 2001, and targeted amino acid substitutions have allowed to modulate sensitivity, speed and brightness. Since 2013, three variants of GCaMP6 are available that are brighter than the best synthetic dyes (see Figure IV-1b) and have different kinetics : the s (**s**low) version is the most sensitive, the f (**f**ast) version is the fastest, the m (**m**edium) version has intermediate characteristics. Figure IV-1b shows the response kinetics of the three versions, compared to a 5th- and 3rd-generation GCaMP and to the synthetic dye OGB1. Figure IV-1c compares the kinetics of GCaMP6s and 6f correlated with action potentials. After one or several action potentials, it takes longer for 6s to reach its maximum level of fluorescence, and also to relax to its baseline level. For more technical details on the properties of GCaMP6 indicators, see the original publication, Chen et al. 2013 [263].

Voltage indicators already exist, that allow to capture neuronal events with a much better time resolution, yet they still require further development before they can be considered an established technique. Moreover, since my aim was in the first place to localise and identify chemosensory neurons, calcium sensors are largely sufficient, and more detailed studies of neuronal physiology are far from being the priority in *Platynereis*, hence I chose calcium imaging as a method.

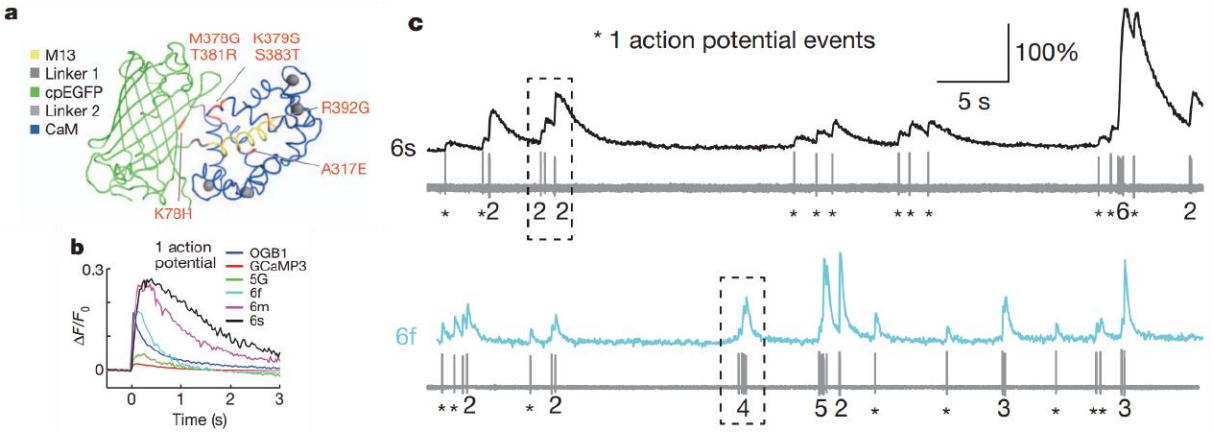


Figure IV-1 The fluorescent calcium sensor GCaMP and its temporal characteristics. (a) GCaMP structure indicating the different single amino acid substitution sites used for the engineering of generations 5 and 6 of GCaMP. (b) Comparison of fluorescence variations in response to a single action potential, measured on dissociated rat hippocampal neurons for different calcium sensors : GCaMP3, 5G, 6f, 6m, 6s, and OGB1-AM. (c) Comparison of temporal responses for variants 6s and 6f or GCaMP. The black and the blue graph represent fluorescence variation, the grey graphs represent electrophysiological recordings in the same neurons. Responses of mouse pyramidal neurons in the V1 visual cortex. Adapted from Chen et al., 2013 [263].

The genetically encoded calcium indicator GCaMP6s has been successfully used in *Platynereis* larvae (see Figure IV-2) to monitor the activity of muscles [81], as well as of single photoreceptor cells [76] and single motoneurons [70],[82]. Such experiments have allowed to investigate the specificity of photoreceptor cell response depending on wavelength [76], the modulation of motoneuron activity by melatonin [70], the role of motoneurons in the whole-body coordination of locomotion [82], and altogether have demonstrated the relevance of calcium imaging methods to study the physiology of single cells in *Platynereis* larvae.

Importantly, thanks to *Platynereis*' small size and transparency, the whole head width can be observed with a 63x microscope objective, and the entire ranges of depths in the head can be imaged from a single side of the animal without too a detrimental loss of signal quality. This means that it is optically possible to image the whole head of a *Platynereis* larva from a given position of the microscope's objective, and indeed he results presented below will show that the whole head can be imaged in 12 optical planes with a sufficient time resolution to traack neuronal activity. Serial-section electron microscopy based neurite reconstruction has shown that the head of *Platynereis* larvae already contains at 3dpf a large number of sensory neurons (Gáspár Jékely, personal communication), a significant part of which could be chemosensory. It was thus crucial to investigate chemosensory responses in the candidate organs while still being able to reveal other unknown sensory structures or cells related to the chemosensory systems.

GCaMP6s has been used for all the experiments reported in this section. This protein was ubiquitously expressed in *Platynereis* larvae by microinjection of its mRNA in fertilised zygotes ; for details on the injection procedure see the Material & Methods section. GCaMP6s is slower but more sensitive than GCaMP6f, therefore it was chosen as was done in the 48hpf experiments, since signal intensity is inevitably low six days after mRNA injection. It takes in the order of 0.2-0.3s for GCaMP6s to reach its maximum fluorescence intensity when a neuron is stimulated (Figure IV-1b).

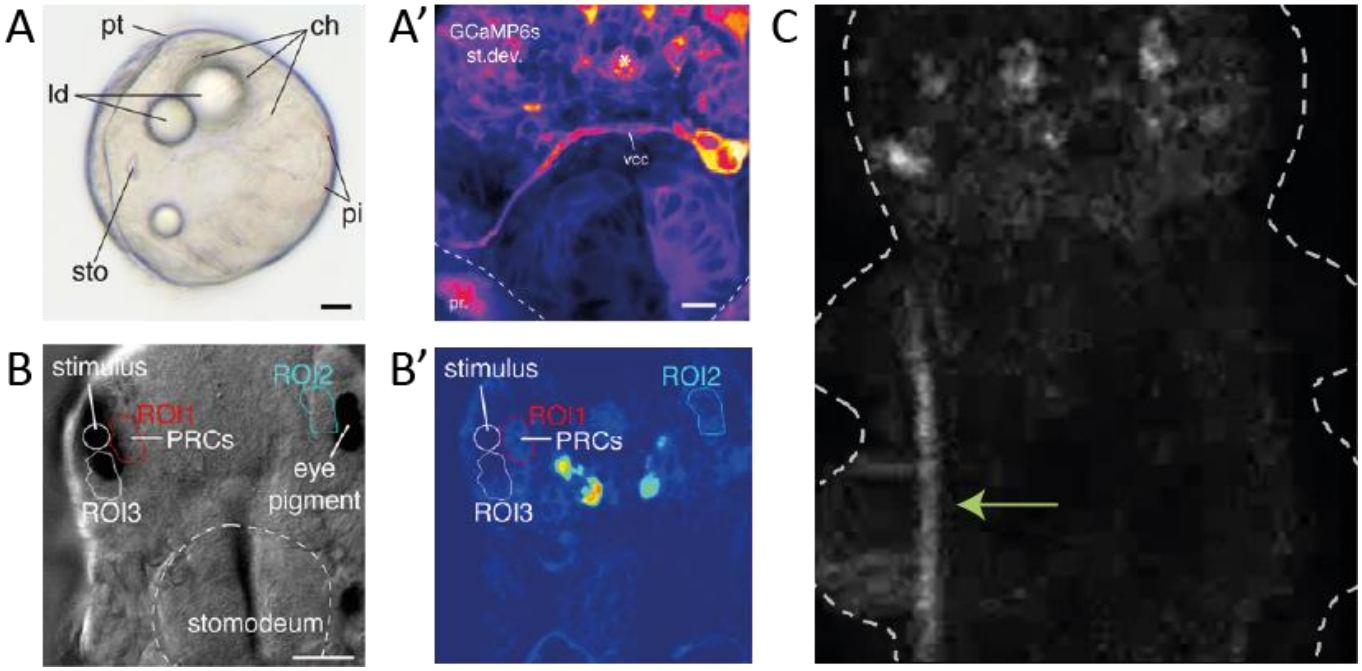


Figure IV-2 (previous page) Examples of calcium imaging in Platynereis. (A-A') 2dpf larva seen in transmitted light channel (A) and calcium channel (A') slightly zommed in. Axons (vcc) of ventral motoneurons are visible in the centre of the image, their cell bodies are the bright area on the right side. Reproduced from Fischer et al., 2010 [138] *and Tosches et al., 2014* [70]. *(B-B') 4dpf larva seen in transmitted light channel (B) and calcium channel (B'). Photoreceptor (PRCs) cells are outlined. Reproduced from Gühmann et al., 2015* [76]. *(C) 4dpf larva seen in calcium channel, showing contraction of the dorsal longitudinal muscle (green arrow). Reproduced from Randel et al., 2014* [81]. *Scale bar 20 µm in (A) and (B), 10 µm in (A').*

To make calcium imaging of chemosensation widely applicable in *Platynereis* larvae, two main difficulties need to be overcome : movement, and stimulus delivery. From 3dpf onwards, larvae are endowed with a substantial complement of muscles [138], and can have strong contractions. The immobilisation strategies used so far have been either to trap the larva between slide and coverslip [81],[76], or to embed them in low-melting agarose [70],[82]. Both techniques start to show their limits from 4dpf on, and cannot be used at 6dpf to monitor calcium levels in individual cells with reasonable movement artefact. Moreover, both techniques restrict the experimental possibilites in that chemical

stimuli cannot be used effectively – at best a stimulus can be delivered once to the animal but not be washed away. Yet, an experiment aimed at demonstrating that a cell responds specifically to a chemical stimulus will require delivery of the stimulus together with at least one control, and probably observation of the same cell upon repeated stimulus exposure. A more elaborate experimental approach was thus necessary in the perspective of investigating the physiology of individual cells via calcium imaging.

1.3 *In vivo* calcium imaging in a microfluidic device

In order to immobilise 6dpf *Platynereis* larvae, a purely mechanical method was preferred, to avoid any perturbation of the animal's physiology that could be introduced by a method involving chemicals : drugs like neurotransmitter antagonists or ionic solutions like $MgCl_2$ used to block muscle contraction could change osmotic levels or affect ion channels physiology as well as general physiology. The idea was thus to design a trap that would hold the animal not only dorso-ventrally as with a standard slide-coverslip method does, but also laterally, so as to reduce local constraints by distributing them.

In terms of chip fabrication, PDMS microfluidic devices were chosen in which animals could be introduced, immobilised and exposed to stimuli while imaged under a confocal microscope. Such an approach has been successfully used for functional imaging in the nematode *Caenorhabditis elegans* [264] as well as in larvae of the zebrafish *Danio rerio* [265], and has allowed numerous studies on their chemosensory neurons and circuits. When a PDMS chip is closed with a glass coverslip and an animal immobilised inside, the mounting is optically equivalent to the animal being held against a coverslip, and once trapped inside a channel the animal can be exposed to stimuli in a controlled fashion. The principle of trapping is illustrated in Figure IV-3. The channels' height is constant in the whole chamber. Preliminary chip designs allowed to identify the relevant trap dimensions (see Chapter VI).

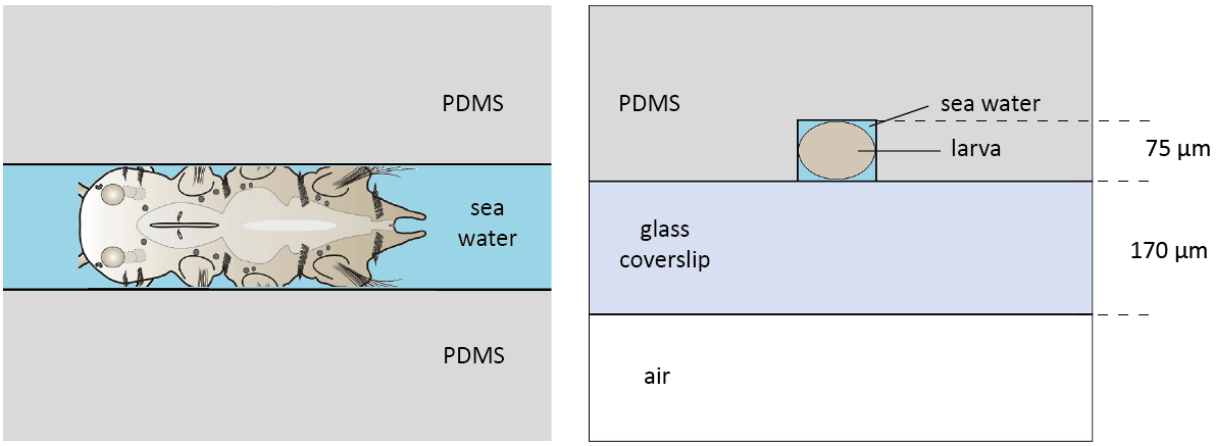


Figure IV-3 Principle of larva trapping inside a PDMS channel. The channel is filled with sea water and is sealed by a regular 0.17 mm glass coverslip. Left : top view. Right : front view. Note that both coverslip and PDMS are actually transparent. Platynereis drawing adapted from Antje Fischer.

The automation of the experimental setup has been key in obtaining all physiological results reported below. Such development was done in collaboration with Joran Deschamps, a PhD student in the Ries Lab at EMBL. Joran has created the Micro Manager device adapter specifically for these syringe pumps, implemented the RS-232 communication for loading the programmes into the pumps and the TTL communication to synchronise them, and helped to write the BeanShell scripts for stimulus protocols. He also provided continued technical assistance on the microscopy and the image processing throughout the project.

1.4 Choice of stimuli

A small set of chemical cues was chosen as being representative of different families of compounds. As explained in Chapter II, ionic solutions, sugars, alcohols, amino acids and animal extracts have been found to elicit behavioural responses in some polychaetes. Ionic solutions were excluded on the basis that they did not seem likely to represent specific chemosensory cues, but rather general environmental cues. Food-related solutions or filtrates were excluded on the basis that it would be hard to know or even reproduce their chemical composition, and that they could elicit strong movements notably for the proboscis, which in 6dpf is muscular and as big as the whole head.

The following stimuli were thus finally chosen : amyl acetate as an ester, 1-butanol as an alcohol, glutamate as an amino acid, sucrose as a sugar, uric acid as a polychaete pheromone, and quinine as an alkaloid. Table IV-1 shows their molecular structure and some of their physico-chemical properties. All these compounds are rather small molecules, with molecular weights inferior to 350 g/mol.

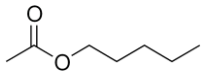
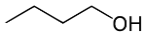
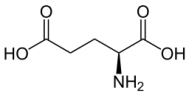
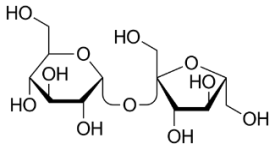
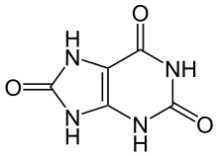
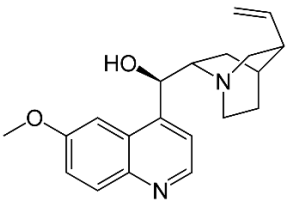
Compound	Molecular weight (g/mol)	Density	Solubility in water (g/L)	Vapour pressure (Pa)
 amyl acetate	130.19	0.876	10	530
 1-butanol	74.12	0.81	73	800
 glutamic acid	147.13	1.46	7.5	1.46×10^{-4}
 sucrose	342.3	1.587	2100	?
 uric acid	168.11	?	0.00006	1.05×10^{-7}
 quinine*	324.42	?	0.5	?

*Table IV-1 Chemical structure and physico-chemical properties of the stimuli used. *used as hydrochloride dihydrate to enhance water solubility and facilitate its use in solution. Data from Sigma's commercial website, from Wikipedia and from* [181].

Esters are often aerial olfactory molecules, typically responsible for odours like those of fruit. **Amyl acetate** is both volatile and soluble, has a strong banana smell to humans, and has been used as a chemosensory cue in experiments conducted on the freshwater snail *Lymnea* [266] or on rats [267], so both in the air and in water.

Alcohols have been showed by Case to be chemical cues in the polychaete *Nereis* [185], they are also volatile and soluble. The linear **1-butanol** is one of the shortest alcohols, it has a strong, slightly unpleasant smell to humans. It has been used as a stimulus for example in *Drosophila* [45].

Amino acids are relevant cues for many aquatic organisms [157], and were used for agmatine labelling in the polychaete *Dipolydora* [154]. **Glutamate** is the aqueous form of glutamic acid, one of the amino acids constituents of proteins.

Sugars are present in numerous plants and serve as nutrients for many species of mammals, birds, insects, bacteria. **Sucrose** or saccharose has been used as a cue for classical conditioning in honey bees [268] and in *Lymnea* [266], so both for terrestrial and aquatic species.

Uric acid is a common excretory product of terrestrial animals, and serves as the sperm-release pheromone in *Platynereis dumerilii* [192]. It should be noted that the effective threshold concentration in nature, which was measured as around 1 µM, is several orders of magnitude higher than the typical concentrations used for pheromones.

Quinine is a plant alkaloid, is known to have a bitter taste, and has been used as a chemosensory cue for example in experiments on insects like the fly *Phormia* [269] or on rats [270]. After preliminary tests, quinine was excluded from subsequent experiments since it provoked a strong reaction of the animals with movement that made the quantification of cell activity impossible, and caused the majority of cells in the head to become active. Instead quinine proved to be a relevant aversive stimulus for the learning experiments, and more about quinine will be found in Chapter V.

IV – 2 Materials and Methods

2.1 *Platynereis* culture

See Chapter III. Late nectochaete larvae between 6 and 7 dpf were used for all calcium imaging experiments.

2.2 Microinjections of GCaMP mRNA

To transiently express the calcium reporter, *Platynereis* eggs were injected with GCaMP6s mRNA between 1 hour post-fertilisation and the first cleavage, at a concentration of 1.000 ng/µL. These RNAs, capped and polyA-tailed, were synthesised with the mMESSAGE mMACHINE T7 Ultra Kit (Life Technologies) from a PCR product generated from a vector (pUC57-T7-RPP2-GCaMP6) containing the GCaMP6s ORF placed downstream of a 169-base-pairs 5' UTR from the *Platynereis* 60S acidic ribosomal protein P2, as described in [81]. In the days following micro-injections, larvae were kept in Filtered Natural Sea Water (FNSW) and regularly observed to remove possible misdevelopers. A detailed method for micro-injections, including an operational protocol, instructions for needle and agar stage preparation, and a detailed protocol for GCaMP mRNA synthesis, are given in Appendix B. Maps and full sequences of the different GCaMP6s plasmids used during or generated as part of this work can be found in Appendix C.

2.3 Chip design

Olfactory chip : A microfluidic chip organised around a central trapping channel was used in all experiments, which comprises one introduction channel for the animal, three inlet channels and one general outlet channel. The chip design is symmetric with a general height of 60 µm, it is shown in Figure IV-4A. The introduction channel starts with a width of 150 µm that linearly decreases to reach 75 µm at its end, which constitutes the trap. The chamber upstream of the animal has a width of 2 mm, and then splits into two lateral chambers with a width of 1 mm each.

Importantly, larvae can be chosen to be positioned either dorsal up or ventral up when manually introduced in the chip. Light scattering inevitably occurs in the tissues, which can result in inevitable loss of signal quality from a depth of around 50 µm. Orienting the animals thus allows to image the side of interest from the relevant side. This is especially crucial for a weak signal, as is the case here. Once trapped, the animal has its head freely exposed to water streams, as would be the case in a natural situation.

The inlet channels are numbered from 0 to 2. Channel 0 was filled with FNSW, channel 1 and 2 were filled with stimulus solutions. Each inlet channel was supplied by a dedicated 5 mL syringe (Luer Plastipak 302817, BD, USA, with an inner diameter of 11.99 mm). Polytetrafluotoethylene (PTFE) tubing (inner diameter 0.59 mm, outer diameter 1.06 mm, wall thickness 0.25 mm, TW24, Adtech Polymer Engineering Ltd, UK) was used to connect chip and syringes in all experiments. Since the outer diameter (1.06 mm) is slightly larger than the hole size (1 mm), tubings can be connected to the chip by simply forcing them into the PDMS holes, which ensures sufficient sealing at the ranges of pressure used here. Connection of the tubings to the syringes was done with metallic needles (Microlance #20, 302200, BD, USA). The outflow was collected in a disposal beaker.

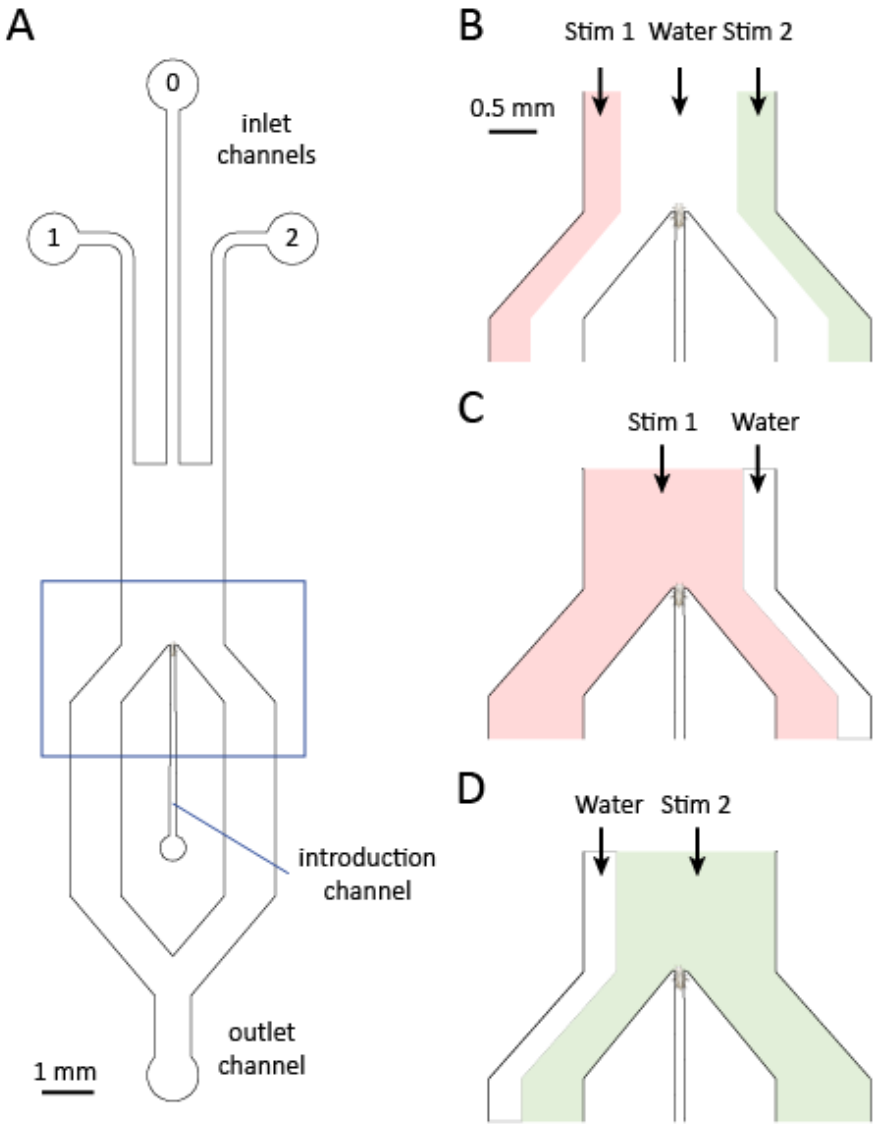


Figure IV-4 Chip design (A) and principle of stimulus delivery (B-D). Flow direction is from top to bottom. The animal is trapped in the centre of the microfluidic chamber, at the end of the introduction channel. (B) Resting situation, the animal is exposed to a continuous flow of natural sea water, the stimuli are flowing in the side streams. r0 = rWater, r1 = r2 = rSide. (C) Animal exposed to stimulus 1, channel 2 is off. r0 = rSide, r1 = rActive, r2 = 0. (D) Animal exposed to stimulus 2, channel 1 is off. r0 = rSide, r1 = 0, r2 = rActive.

2.4 Stimulus delivery

The chip is used in a regime of laminar flow, and three parallel streams of sea water flow continuously through the chamber. The sum of flow rates for channel 0, 1 and 2 is kept constant during the experiments, so that when one rate is decreased or increased the two others are adjusted accordingly. This allows to displace stream boundaries without changing the overall fluid velocity, and thus to expose the animal to whichever stream without major mechanical disturbance. A total flow rate in the chamber of 3000 µL/h = 50 µL/min was used in all experiments, which corresponds to a maximum flow speed of $\frac{50}{60} \times \frac{1}{0.060 \times 2.0} = \frac{0.833}{0.12} \approx 7\ mm/s$ experienced by the animal in the chamber. Three different flow rates are used for the inlet channels : rActive = 41.66 µL/min, rWater = 33.33 µL/min and rSide = 8.333 µL/min. Figure IV-4B-D shows how switching between these flow rates enables stimulus delivery. The flow rates for channels 0, 1 and 2 are called r0, r1 and r2 respectively. In the resting situation, the

animal is exposed to the central stream (Figure IV-4B), but on demand can be exposed to the left-hand side stream (Figure IV-4C) or the right-hand side stream (Figure IV-4D). In an experiment, these side streams are used as stimulus channels, and can contain any solution to be used as a stimulus. When a flow rate is strongly decreased, e.g. from rActive to 0, some pressure release takes place in the corresponding channel, since pressure is stored in the tubing and in the PDMS walls of the chip itself. Thanks to the chamber's width, the slow boundary adjustments between streams due to this pressure release take place on the side far away from the animal, which allows a fast stimulus switch even in the absence of valves to operate the channels. For both designs, the total flow speed corresponds to a Reynolds number of about 0.7, which satisfies the conditions for laminar flow explained in Chapter V, Introduction.

The syringes were operated each by a separate pump (Aladdin dual syringe pump 220V, AL4000-220Z, World Precision Intruments Germany, GmbH). The pumps are controlled by a Windows computer via Micro Manager (version 1.4.21), a popular free and open-source software for automated hardware control [271], which was designed as a plugin to ImageJ (https://imagej.nih.gov/ij/). For each kind of experiment, a script written in BeanShell language is loaded in the pumps' memory beforehand. A so-called *device adapter* is required for Micro Manager to be able to communicate with the pumps. Such a code did not exist for the Aladdin pumps and was developed for these experiments by Joran Deschamps. The code has been submitted to Micro Manager developers, it should be integrated in one of the next versions of the software, and thus automatically installed and ready for use for anyone downloading Micro Manager.

A detailed description of the hardware-software configuration is given in Appendix D, the scripts used in the present experiments are available at https://github.com/ThomasChartier/Experimental_scripts.

2.5 Stimulus protocol

The stimulus protocol, represented in Figure IV-5, consisted of an initial habituation period, stimulation periods of 15s and resting intervals of 20s. The chip was filled with FNSW, and each experiment was done with one chemical cue only. Several animals could be used in the same chip successively, after appropriate rinsing of the chamber with FNSW. To be certain that a neuronal activity would be due to a compound tested, only one compound was ever used for each chip, to make sure no stimulus contamination would happen. No dye was used in experiments with chemical stimuli.

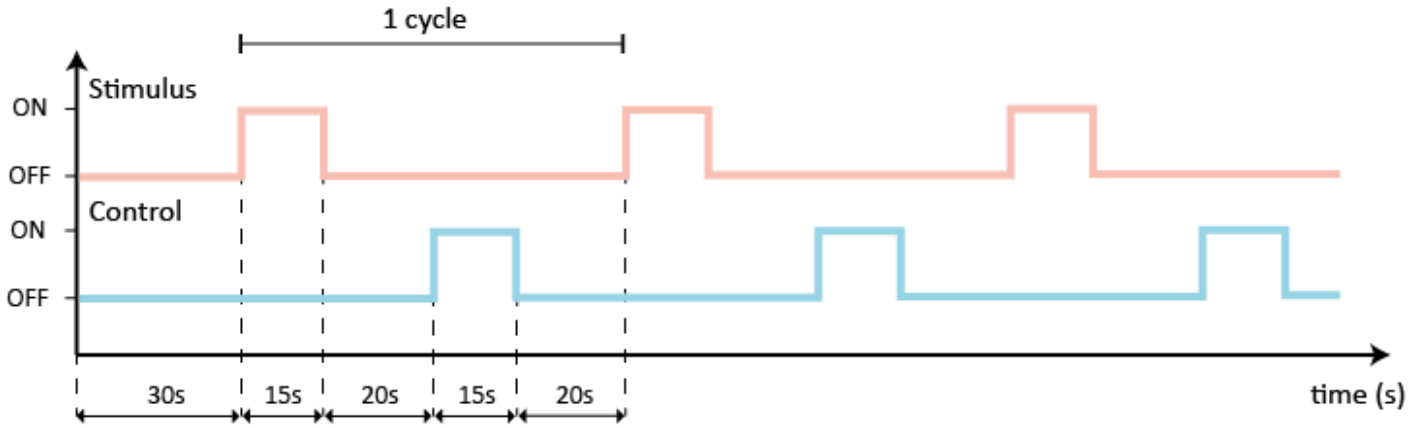


Figure IV-5 Stimulus protocol with chemical cue and water control, used for most experiments.

The central channel contains FNSW as the baseline medium. The side channel 2 is also filled with FNSW to serve as a control for flow detection : since it has the same chemical composition as the central channel, it will reveal any neuronal activity that is due to the flow switching itself but not to the

chemical stimulus. Indeed, even though theoretically the fluid velocity is constant, small variations occur in practice due to unloading of the pressure stored in the tubing walls and in the PDMS chip itself when a pump is turned off, therefore the animal will be exposed to small pressure variations and this needs to be controlled. The side channel 1 is filled with the stimulus solution. Exposure to the stimulus and to the control alternate three times per experiment, which allow to verify if a neuronal response observed is reproducible for a given animal. The durations indicated in Figure IV-5 are expressed as durations between pump switches. In the calibration experiments with the dyes, the same protocol was used, except that channel 1 and 2 were filled with dye solutions.

2.6 Measurements of stimulus timing

Since the stimulus solutions are transparent, nothing during the calcium imaging experiments can reveal the position of the stimulus flow inside the chip – except the animal's reactions or its neuronal activity. Calibration experiments were performed with dyes instead of stimuli, using the same flow protocol, to measure the temporal characteristics of stimulus onset and offset. Usual food dyes, the red Ponceau 4R = E124 and the green Tartrazine = E102, were introduced in the stimulus channels to allow visualisation of the stream boundaries, and changes in light intensity caused by the dyes allowed to make the required measurements. Light intensity was taken as a proxy for dye concentration – thus for stimulus concentration in the real experiments to be conducted later – with the highest light intensity representing absence of stimulus and the lowest intensity representing stimulus at maximum concentration. Light intensity was measured in a Region Of Interest (ROI) of constant size and position, corresponding to a small area located just upstream of the animal's head, and normalised between 0 = minimum stimulus concentration, and 1 = maximum stimulus concentration.

2.7 Stimulus preparation

All solution were prepared in Filtered Natural Sea Water (FNSW), obtained by sterile filtering of Natural Sea Water with 0.22 µm filters (Millipore). For all stimuli, a stock solution of at least 50 mL at 1 mM in FNSW was prepared that was never older than 5 days, and kept at 18°C. On the day of the experiment, a solution at working concentration (10 µM for all compounds) was prepared in FNSW from the stock solution. For uric acid, the powder could never be fully dissolved at 1 mM, hence a larger volume of 500 mL was prepared for the stock solution, which was heavily stirred before dilution to homogenise the saturated stock solution. Solutions were always handled and kept in glassware until they were loaded in syringes, since preliminary calcium imaging experiments had revealed that the animals could probably detect substances originating from plastic containers such as Falcon tubes. Importantly, the same bottle of FNSW was always used for all solutions and controls used in a set of experiments, to avoid differences in chemical composition. The room temperature for experiments was set at 18-20°C, and syringes loaded with the solutions were places in the room one hour before starting the experiments. All syringe and tubing manipulations were done while wearing latex gloves.

2.8 Experimental setup

An overview of the setup is shown in Figure IV-6. The syringe pumps were positioned next to the microscope stage, with a constant tubing length of 20cm used to connect syringes and chip. The pumps were connected to a computer, and operated one inlet syringe each. A customised metallic chip holder (see Figure IV-7) was built to maintain the fragile chip and allow its observation under an upright microscope. To introduce a new stimulus in the chip, the syringes were changed manually and a



Figure IV-6 Setup overview, showing the three syringe pumps (red) on the left side of a confocal microscope. Each pump operates a syringe connected to an inlet channel of the chip. The syringe visible on the right side is used for animal introduction, the beaker for collection of the outflow.

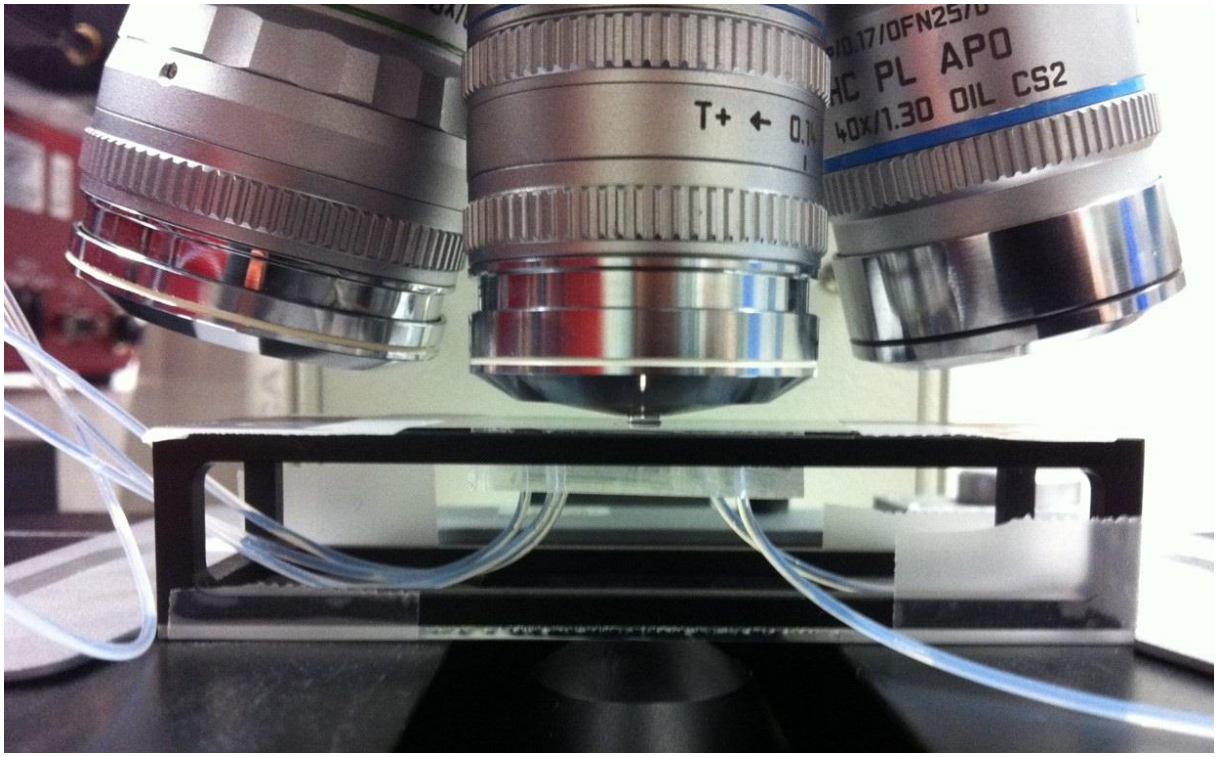


Figure IV-7 Imaging mounting, showing the customised chip holder (black) maintaining the chip under a water-immersion objective. The three inlet tubings are visible on the left side, the introduction tubing and the outlet tubing on the left side. The chip is taped to the holder.

washing programme run with the pumps. During the experiments, the pump programmes were started via Micro Manager. The required precise and reproducible synchronisation between image acquisition and stimulus programme was obtained thanks to a software for automated mouse actions, Auto Mouse Click (MurGee.com). This software was set to start simultaneously image acquisition in the microscope software and pump operation in Micro Manager. This little trick makes it unnecessary to set up a TTL communication between the commercial microscope and the computer, which would require to buy a dedicated and expensive electronic box.

To incorporate rapid feedback in the imaging experiments, it is crucial to be able to look on the spot at the raw images after each acquisition. For multi-plane recordings, looking at individual planes separately does not provide a good perception of the global activity, thus a simple macro script in ImageJ was used to recombine all planes (as can be seen in Figure IV-15), that allowed to look at the whole brain in a single image, and helped improve the data quality.

2.9 Imaging settings

While the immobilised animal was being chemically stimulated (see Figure IV-3, Figure IV-4 and Figure IV-9), confocal images of the calcium signal were taken through the chip's coverslip with a Leica TCS-SP8 confocal microscope, through either a 40x (NA 1.1) or a 63x (NA 1.2) objective. Water-immersion objectives were always used for the experiments, since oil would have rendered the necessary and repeated manipulations of the chip most inconvenient. GCaMP6s fluorescence was excited at 488nm with an argon laser, using its main power setting between 10 and 35% and its AOTF gain between 2 and 40 % depending on signal intensity, which corresponded to laser powers between 1,3 and 28 µW. Powers above 6 µW were used only for the 8-, 12- or 16-planes imaging settings in which the scanning speed (resonant mode) is much higher, and light damage thus reduced. The fluorescent signal was recorded with a hybrid detector (HyD) in photon-counting mode. Transmitted light images were recorded with a standard PMT detector, from the same excitation light as GCaMP.

Single-plane imaging settings :
- xy spatial resolution for each plane : 456 x 456 pixels
- pixel size : 0.32 µm
- time resolution for each plane : 3.02 frames per second (fps)
- laser scanning speed : 700 Hz (bidirectional mode)
- pinhole opening : 3 Airy Units (AU)

Multi-plane imaging settings :
- 8, 12 or 16 planes
- xy spatial resolution for each plane : 504 x 504 pixels for 8 and 12 planes, 256 x 256 pixels for 16 planes
- pixel size : 0.3 µm
- z spatial resolution : maximum 5 µm between two consecutive confocal planes
- optical plane thickness with pinhole wide open : 5 µm
- time resolution for each plane : 1 frame per second (fps)
- laser scanning speed : 8 000 Hz (resonant mode) with a phase X correction of 1.32
- pinhole opening : 6.4 Airy Units (AU)

Figure IV-8 illustrates the spatial sampling of a 6dpf larval head in the z direction for a 12-planes imaging ; note that the actual thickness of the optical planes (5 µm) is higher than that displayed on the figure, allowing effectively a full coverage of the head. All candidate sensory organs are being imaged with at least two planes each : nuchal organ, antennae, palps and tentacular cirri.

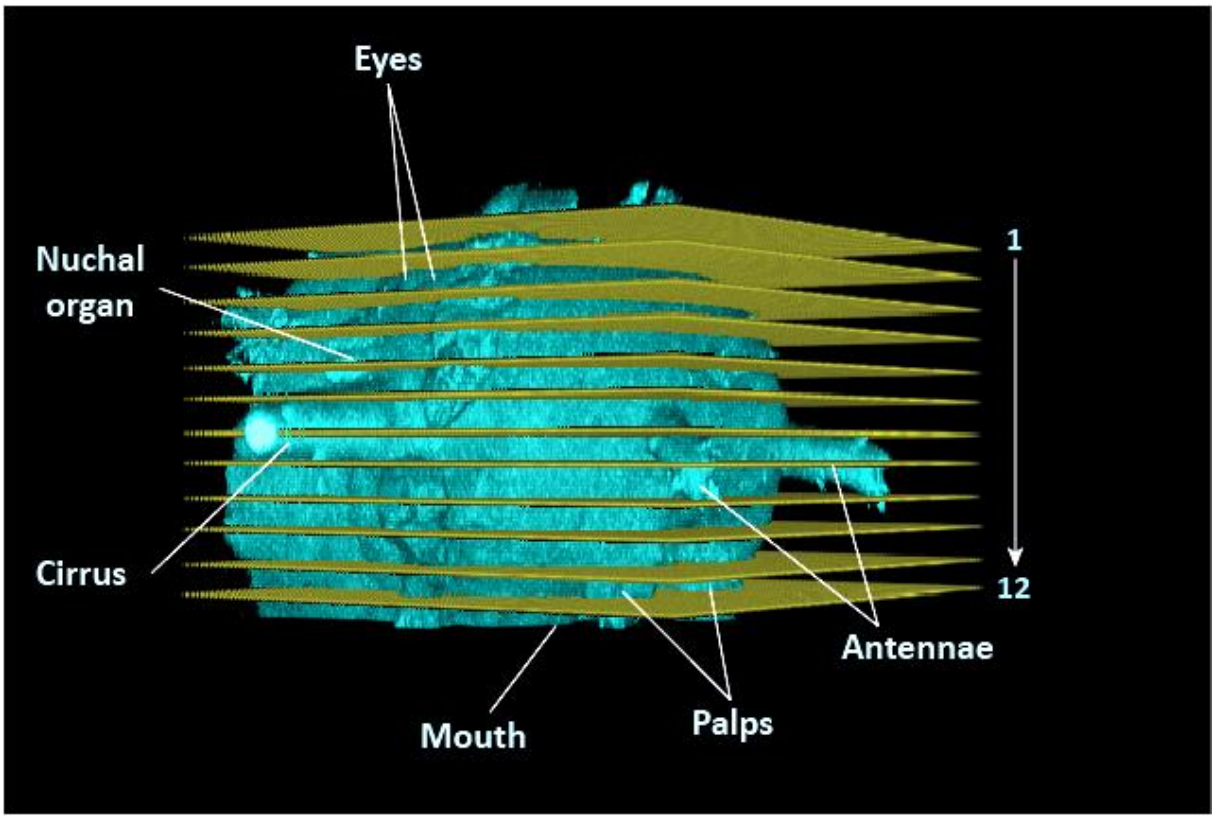


Figure IV-8 Confocal imaging planes for the volumic imaging at 1 fps, shown on a 3D reconstruction of a 6dpf Platynereis head. Fronto-lateral view

2.10 Image analysis

Images of the calcium signal were processed with ImageJ (version 1.50a, Fiji distribution), a popular free and open-source software for biomedical image analysis ([272], https://imagej.nih.gov/ij/) and with MATLAB (version student 2014a), a commercial software for numerical computing (https://uk.mathworks.com/). To obtain activity traces from single cells, movement artefacts were first corrected in Image J using the plugin StackReg [273] with rigid body transformations. Mean fluorescence intensity was then calculated from manually-drawn Regions Of Interest (ROI) in ImageJ, and the data exported as .xls files. Data were then sorted, normalized and plotted using in MATLAB. The same ROI was always used for a response to a stimulus and to its water control. The water control was always chosen to be temporally adjacent to the stimulus exposure. Traces are plotted as $\Delta F/F_0$, with F_0 calculated as the mean fluorescence value in the 5 seconds preceding the stimulus onset. Scripts used for data analysis are available at :
https://github.com/ThomasChartier/Experimental_scripts

2.11 Mastermould and PDMS chips fabrication

A standard technique of soft-lithography [274],[275] was used to make the microfluidic devices, that were made of polydimethylsiloxane (PDMS, Sylgard 184 silicone elastomer kit, Dow Corning Corp.). All fabrication work was done at EMBL in the clean room of the Genome Biology Unit ; an operational protocol is available in Appendix E. Mask design was made with the free student version of the AutoCAD 2014 software (Autodesk Inc.). Designs were sent to an external company (Selba S.A., Versoix Switzerland) for photomask printing at a resolution of 25400 dpi (dark background, clear design).

To produce moulds from a photomask, the SU-8 photoresist (MicroChem Corp., Newton MA) was used. About 5 mL of the photoresist is poured on a heat dried silicon wafer (3 or 4 inches; Siltronix, France

or Silicon Materials, Germany). The resist is then uniformly spread on the silicon wafer using a spin coater, then a soft baking is done. Following the soft bake, the photomask is placed on the coated wafer and exposed to ultra violet light [276] using a mask aligner (Karl Suss MA45) for 120 seconds. Photo-crosslinking occurs at regions exposed to the UV (for negative photoresist) thereby transferring the pattern on the photomask to the resist. The photomask was then removed and can be reused to make more moulds of the same pattern. The cross-linking of the resist was completed by another series of post-baking procedures in the suggested temperatures and times from the manual. Finally, the wafers were developed using mr-Dev 600 (micro resist technology GmbH, Berlin). This step removes all non-cross-linked photoresist leaving the structure of the channel behind. Lastly, a hard baking procedure was performed at around 150 ^{o}C. This step solidifies the structure on the mould. All bakes were performed first at 65°C then at 95°C. Silanization of the mould using trichloromethylsilane (TCMS) (abcr GmbH & Co. KG, Germany) prevented the structures on the mould from being destroyed while producing PDMS chips. This was done by simply placing a drop of the chemical next to the mould in a closed glass Petri dish for an hour, while keeping everything under a hood since silane is highly toxic. The height of the attained structures was measured using a Surface Profiler Profilometer (Faulhaber), compatible with structures lower than 110 µm.

The mould for the calcium imaging chip has a single layer, which was made using SU-8 2050, a spinning speed of 500 rpm for 10s then 1900 rpm for 40s, and baking times of 3+9 and 2+7 minutes for soft and post-bake at 65°C/95°C respectively. Information on temperatures and duration were adapted from the manufacturer's manual.

Finished moulds were placed on plastic Petri dishes and filled with freshly prepared and degassed PDMS mixture. For chips a 10:1 ratio of elastomer PDMS:curing agent was used. All air bubbles were degassed using a vacuum desiccator and the dishes with the mould and the PDMS mixtures were baked in a 65 ^{o}C oven overnight (or for a minimum 4 hours).

To assemble a chip for experiments, the cast PDMS was cut using a scalpel and peeled off from the mould. Thus the PDMS retains the channel structures on one side. Access holes are punched using biopsy punches (Harris Unicore) all the way through the structures to the other side making it possible to access the channels after they are sealed. Different sizes of biopsy punches exist depending on the size of the tubing used for experiments. Here, a diameter of 1 mm was used for all holes. Pressurized air from an air gun and sticky tape was used to remove any unwanted particles from the PDMS. The chip was then completed by covalent bonding of PDMS (on the structured side) to a 24 x 50 mm glass coverslip with a 0.17mm thickness (1871, Carl Roth GmBH, Germany). The bonding was achieved by exposing the surfaces that needed to be bonded to oxygen plasma generated using a plasma oven (Femto, Diener electronic GmbH & Co. KG, Germany), and then bringing them in contact with each other. The plasma treatment for producing chip was usually done for 1 minute at 2.5 V in the presence of oxygen. To facilitate bonding without any delamination, the chip was placed in the 65^{o}C oven or hotplate for at least 1 minute. The finished chip was protected by transparent adhesive tape on its PDMS side for storage in a dust-free environment. Due to the coverslip, these chips are fragile, and care should be taken to not break the coverslip, especially when removing the adhesive tape. Before usage, the chips were directly filled with natural sea water, since this design does not require the help of a desiccator to properly fill all channels with water.

IV – 3 Results

3.1 The setup allows a precise stimulus delivery

In order to correlate the neuronal responses with the chemical stimulations, it is crucial to be able to know precisely when the latter occur, and how the former are distributed in time with regard to them. Durations in the stimulus protocol (see Materials & Methods) are expressed as target values, i.e. as the durations during which the pumps that control the channels are switched to a certain state. So as to know the actual temporal changes of stimulus concentration experienced by the animal inside the chip, as well as the potential variation in the delay between pump switch and stimulus change, an experimental quantification of the stimulus timing was necessary.

Dyes were used to visualise the different water streams (see Materials & Methods). The images in Figure IV-9 show a switch from the central stream to a side stream called 'stimulus onset' (a to a''), and the switch back from the side stream to the central stream, called 'stimulus offset' (b to b''). Since the chip design has a left-right symmetry, onset and offset on the left side are identical and therefore not shown. Light intensity is plotted on the central graph, and represents variations of stimulus concentration during one calibration experiment, i.e. three cycles with exposure to the two stimuli successively in each cycle. The flow is vertical from top to bottom on the pictures, and flow boundaries are displaced horizontally. Note the sharp stream boundaries between dyed and non-dyed water, and the reproducibility of the stimulation (Figure IV-9, graph).

Temporal quantification of the stimulus delivery. A series of 24 experiments with a total of 6 animals (for each animal, 4 experiments = 4x3 cycles) was carried out to measure the following parameters :
- onset duration = average time needed to go from 0 to maximal concentration (a to a'' in Figure IV-9)
- onset duration variability = standard deviation of onset duration,
- onset delay = average time between when stimulus channel is switched on and when maximal concentration is reached,
- onset precision = standard deviation of absolute time when max concentration is reached,

and the corresponding parameters for the stimulus offset.
These measurements of these parameters, averaged across all experiments, are presented in Table IV-2. Both onset and offset take around one second to happen, with a precision of about 0.2 second. The delay is comparable for onset and offset, albeit with a greater variability of about 0.75 second.

Parameter	Duration (s)	Duration variability (s)	Delay (s)	Precision (s)
Onset	0,91	0,29	3,30	0,72
Offset	1,06	0,18	3,00	0,76

Table IV-2 Temporal characteristics of stimulus delivery, as measured from calibration experiments.

The variability is globally substantial, but minor within individual series of experiments. To illustrate the variability of the stimulus timing, stimulus intensities have been plotted and superimposed in Figure IV-10A for all 6 x 24 = 144 exposures, with left and right side pooled. As can be seen, during stimulus onset the full concentration may be reached between around 2.5 and 5 seconds after the pump switch. This appears to mean that no statement could be made regarding the reproducibility in the timing of a neuronal response in a given experiment. However, a closer look at a series of experiments concerning a single animal reveals that this uncertainty on the stimulus timing is much lower. For the example of animal #5, the superimposed traces of stimulus concentration for all 4 experiments are plotted in Figure IV-10B, and the traces are plotted separately for each side and cycle in Figure IV-10C. For this animal,

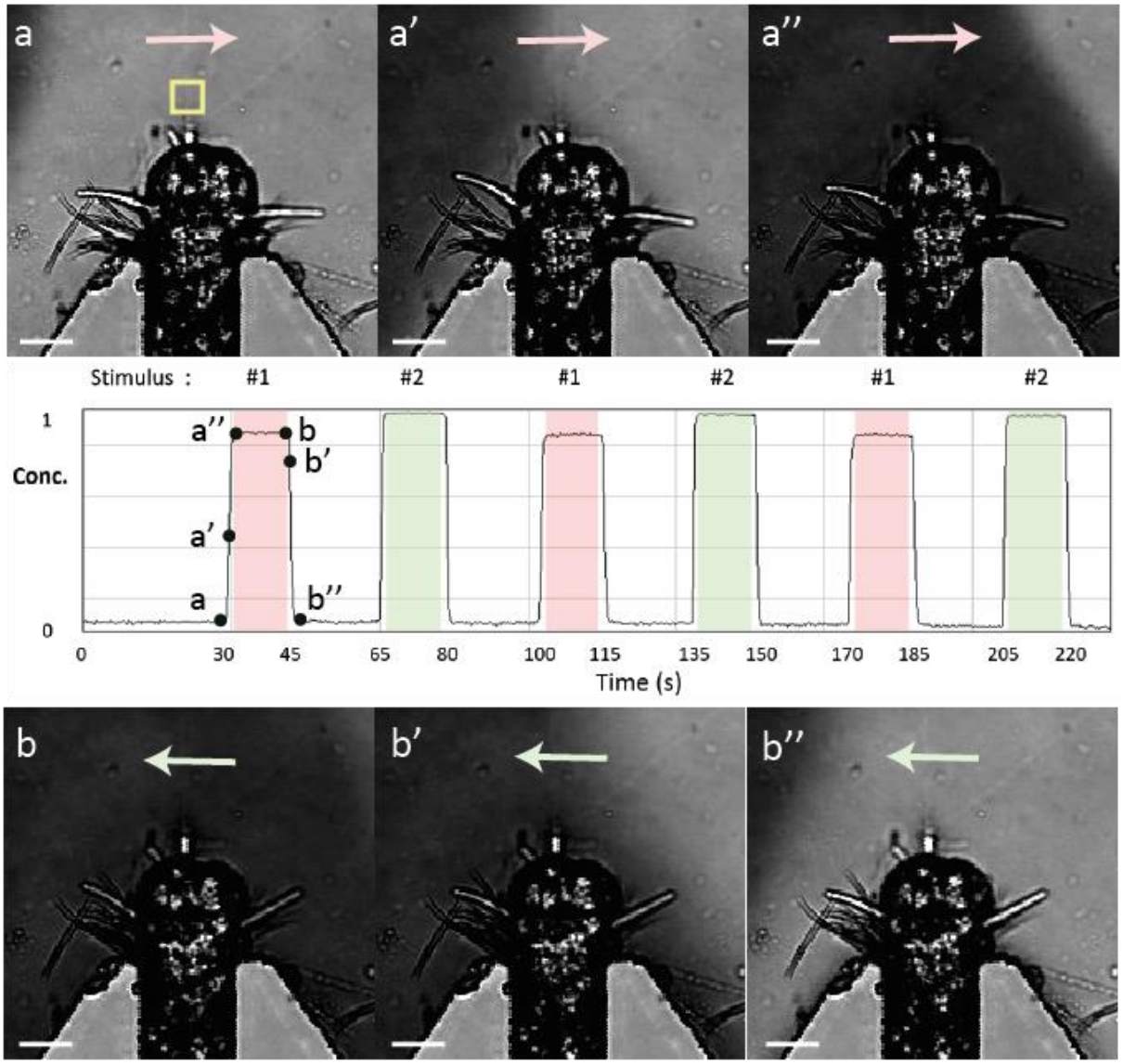


Figure IV-9 Temporal variations of stimulus concentration during a calibration experiment, with photos showing onset and offset of a stimulus from the channel located on the left side of the animal, visualised with a dye. Stimulus concentration, as estimated from light intensity and measured in the yellow square shown in (a), is plotted in the central graph. Colours on the graph indicate the periods during which the animal is exposed to stimulus 1 (red) or stimulus 2 (green). Photos taken in the confocal microscope's transmitted light channel correspond to the time points indicated on the graph, and illustrate consecutive steps during onset (a-a'') and offset (b-b'') of stimulus 1 from the left side. Flow is from top to bottom, arrows indicate the movement of the stream boundary. Trap width 80 µm and scale bar 40 µm.

the onset precision across the 4 experiments is better than that estimated from the pooled measurements : the maximum difference observed in stimulus onset is on the order of 1s instead of 2.5s, with a standard deviation of 0.13s instead of 0.72s. For the offset, the maximum difference is on the order of 1.5s, with a standard deviation of 0.14s instead of 0.76s. For a given cycle and side (Figure IV-10C), the precision is even better, with a maximum difference on the order of 0.5s. This indicates that a small temporal delay may be introduced progressively by the pumps, which artificially deteriorates the apparent onset or offset precision when measurements are pooled from several cycle numbers. Unfortunately, such a shift cannot be accounted for in the data analysis, since the interval between frames is 1 second, i.e. much higher. These results show that in a given experiment, the stimulus will indeed be delivered reproducibly, with a delay relative to the pump switch that does not

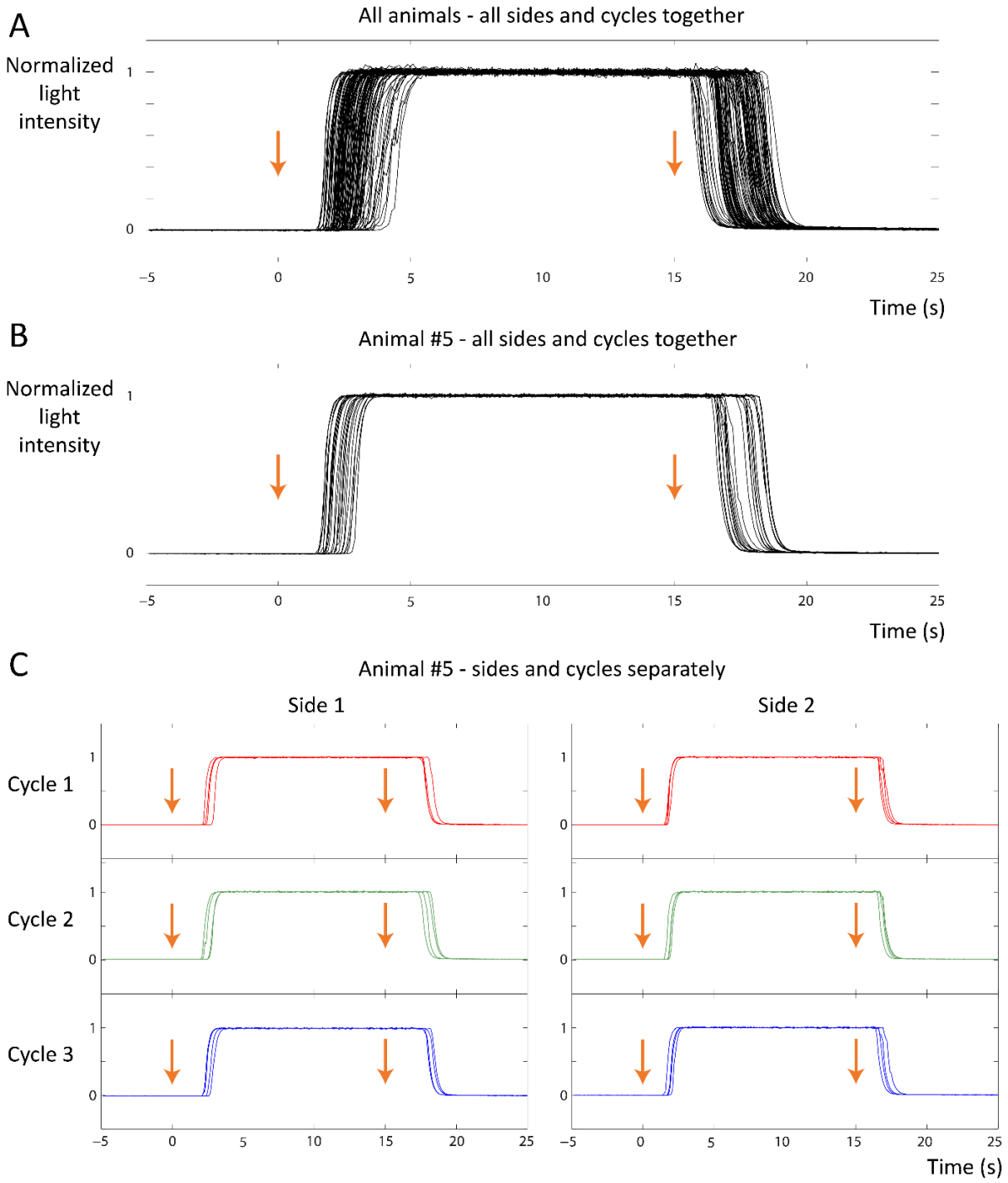


Figure IV-10 Temporal variation of dye concentration for four consecutive calibration experiments per animal : all animals together (A), animal #5 with all cycles and stimulus sides together (B) and with cycles and by stimulus sides separately (C). Orange arrows represent the time points when syringe pumps are switched. In (C), the first cycle of each experiment is plotted in red, the second in green, the third in blue.

vary by more than 0.5s. Given the 1Hz temporal resolution of the signal acquisition, the relative stimulus timing can thus be considered as constant for each cycle in a given experiment. This means that in a given experiment, even though one cannot know when the stimulus has occurred between +2s and +5s after the pump switch, one can be certain that this delay has been the same for each exposure, and thus any variability in the delay of neuronal responses can be attributed to biological, not technical variability. The much higher variability observed in overall pooled measurements is probably attributable to the manipulations of chip, tubing and syringes that take place while replacing

an animal by another, and shows that variability in the stimulus control comes from the materials used here, not from the setup design.

Left-right asymmetry in stimulus delivery. The measurements reveal that asymmetry can occur in the stimulus delivery between both sides. In Figure IV-10C, it is apparent that the offset takes place earlier for side 2 than for side 1, and, to a lesser extent, that the onset also takes places earlier for side 2 than for side 1. This bimodality for the stimulus offset distribution is even more apparent in Figure IV-10B. However this asymmetry remains consistent across experiments for a given animal, as can be seen for Figure IV-10C. Such asymmetry, cannot be due to the chip design which is symmetric, and is probably attributable to friction differences between the syringes or the pumps used for the left and the right side. Nevertheless, the timing remains reproducible for a given side, which means that in the real experiments this timing will be the same for a given stimulus.

3.2 Calcium imaging with late nectochaete larvae is possible in this microfluidic setup

A mRNA-injection-based approach is valid for GCaMP expression at 6 dpf. Stable transgenic expression of a calcium reporter has not yet been achieved in *Platynereis*. The validity of transient GCaMP expression via mRNA injection for calcium imaging experiments has been demonstrated at early larval stages, but so far no activity traces of single cells have been obtained in stages older than 4 days (rhabdomeric photoreceptor cells in [76]). The main difficulty comes from the animal's movement, which cannot be coped with in the mounting approaches used previously. It thus remained to be proved whether such calcium recordings could be obtained in late nectochaete larvae. It had been shown already that the expression of the calcium reporter GCaMP6s was sufficiently high up to one week after microinjection (Hernando Martinez, PhD thesis [277]), and allowed to monitor cellular activity in the ventral nerve cord. Figure IV-11 shows an example of calcium signal recorded in the head of a 6dpf animal, in a single confocal plane. The signal quality does not allow to see as many anatomical details as an immunostaining (see Chapter III), yet it is high enough to see individual cell contours as well as axonal elements in the central neuropile, which make it possible to localize individual neurons and measure their calcium activity.

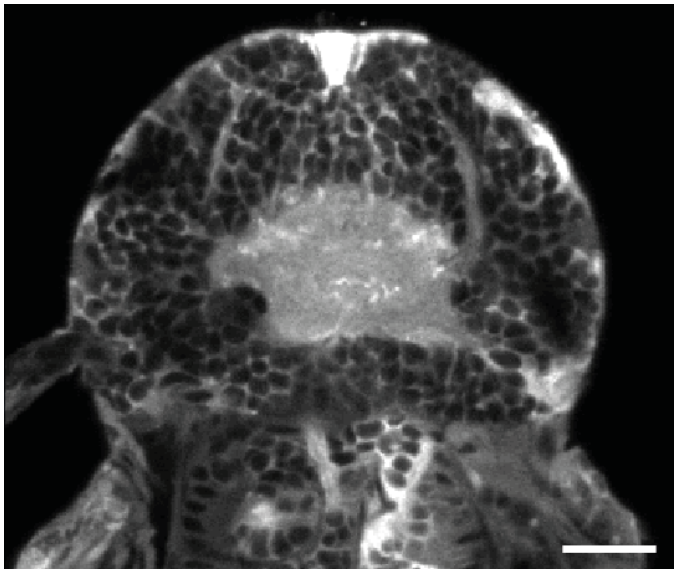


Figure IV-11 Example of baseline calcium signal in a 6dpf larva.
Single-plane imaging, plane of the antennal nerves. Scale bar 20 µm.

Immobilisation in the microfluidic trap is sufficient for single-cell recordings. To record cellular activity, not only should the signal intensity be high enough, but the animal also should not have too strong

movement. The calibration experiments reported above have revealed that the larvae and notably their head are overall immobile, while the animals remain free to move their appendages (compare for example antennae and tentacular cirri in Figure IV-9a' and b''). The head can move to some degree but is overall still (Figure IV-9). It became soon clear while performing the first experiments, not only that the animals stay in place and do not have permanent escape movements and muscle contractions, but also that the calcium activity in the head of an immobilised 5-7dpf larva is rather low and stable in the absence of stimulus, which makes the detection of neuronal responses more obvious. There exist periods of spontaneous movement during which most of the head and notably the main plexus light up in the calcium channel, and individual cell signals cannot be tracked anymore, but these moments are as rare as intense. Even if the animals do not move, they could be too constrained and show signs of discomfort that would result for example in constant activation of motoneurons, but this was not seen to be the case. Occasionally, the animal will spontaneously move its head, which can result in a change of focal plane, however these movements most often last only for a few frames and are reversible. If needed, the signal quantification will be interrupted for a few points. It is important that animals also stay immobile in the presence of a stimulus, otherwise responses of individual neurons could not be recorded. Figure IV-12 shows that this is indeed true. Detection of a stimulus by the animal coincides with a rather strong calcium activity in the main plexus, an example of which is shown in Figure IV-12. This plexus activity probably corresponds to a calcium increase both in the sensory cells involved and in their postsynaptic targets, and is always a good indicator of stimulus detection (it can be helpful to identify neuronal responses in recordings with a weak signal intensity). As can be seen by comparing both pictures in this figure, the same anatomical elements are present before and during stimulus detection, which illustrates that the focal plane generally has not changed even when the animal is sensing a chemical.

These observations together validate the immobilisation strategy with a microfluidic device, and show that calcium imaging experiments are feasible in late nectochaete larvae with such a setup.

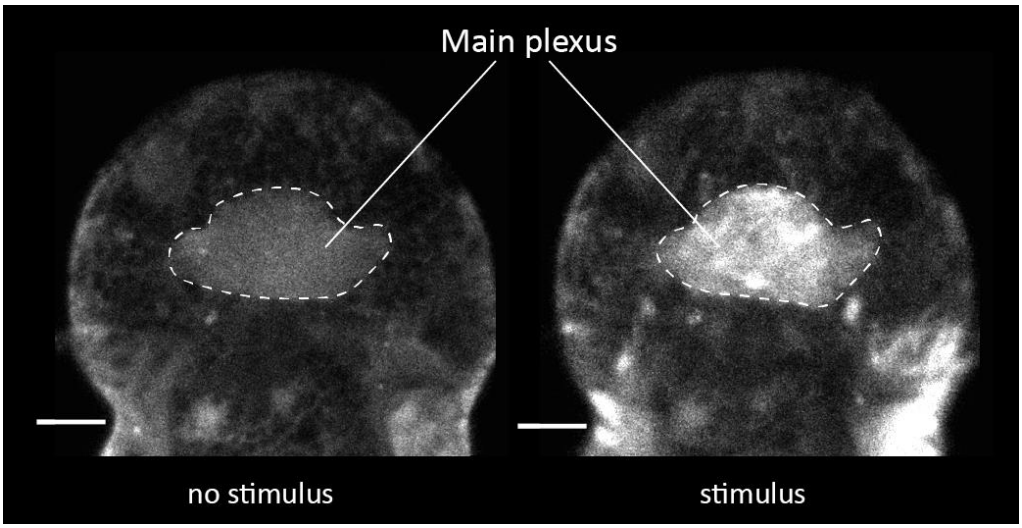


Figure IV-12 Example of main plexus activation in response to a chemical stimulus. 6 dpf, scale bar 20 µm.

3.3 Anatomical identification is possible from the calcium signal alone

Relevant anatomical landmarks cannot be marked in vivo. For *Platynereis*, the only anatomical structures which can be specifically labelled *in vivo* are currently the rhabdomeric photoreceptors of the adult eyes, thanks to a transgenic line developed by the Tessmar lab [77], that uses eGFP as a reporter for r-opsin expression. However, these cells are not highly informative about the head's general anatomy, and can anyway be recognised from the calcium signal (see Figure IV-13). Hence, no specific *in vivo* marker exists, and at best a general fluorescent reporter labelling nuclear proteins such as histone H2A or membrane proteins can be used in combination with the green fluorescence of

GCaMP. This has the important implication that during calcium imaging experiments, one has to rely primarily on the calcium signal itself to localize anatomical regions. After some practice, it is possible to do so, despite some variability of the labelling between individuals, as well as some variability in the exact orientation of the larvae in the trap.

Known neurons can be recognised at 6dpf in the calcium signal. Before investigating calcium activity in the animal's candidate chemosensory organs, I asked whether active neurons that had already been described in earlier developmental stages could be observed at 6dpf. Figure IV-13A-D shows the examples of the rhabdomeric photoreceptor cells whose projections at 3dpf were described in [81] and whose calcium activity at 4dpf was investigated in [76]. Figure IV-13E shows one of the two frontal mechanoreceptor cells called MS mechanoreceptors (belonging to the frontal population of cells mentioned in Chapter III). These cells have been described in a position slightly more ventral than the apical organ at 48hpf [236], and their ultrastructure and function is being studied at 72hpf (Luis-Alberto Bezares-Calderón, unpublished). Position and shape allow to unambiguously recognize these neurons, which serve as another positive control to assess the calcium signal quality.

Consequently, it will be possible to recognise individual neurons in the calcium recordings, and probably to assign them to certain regions. After this further validation of the experimental approach, it was possible to carry on with observations in the candidate chemosensory organs.

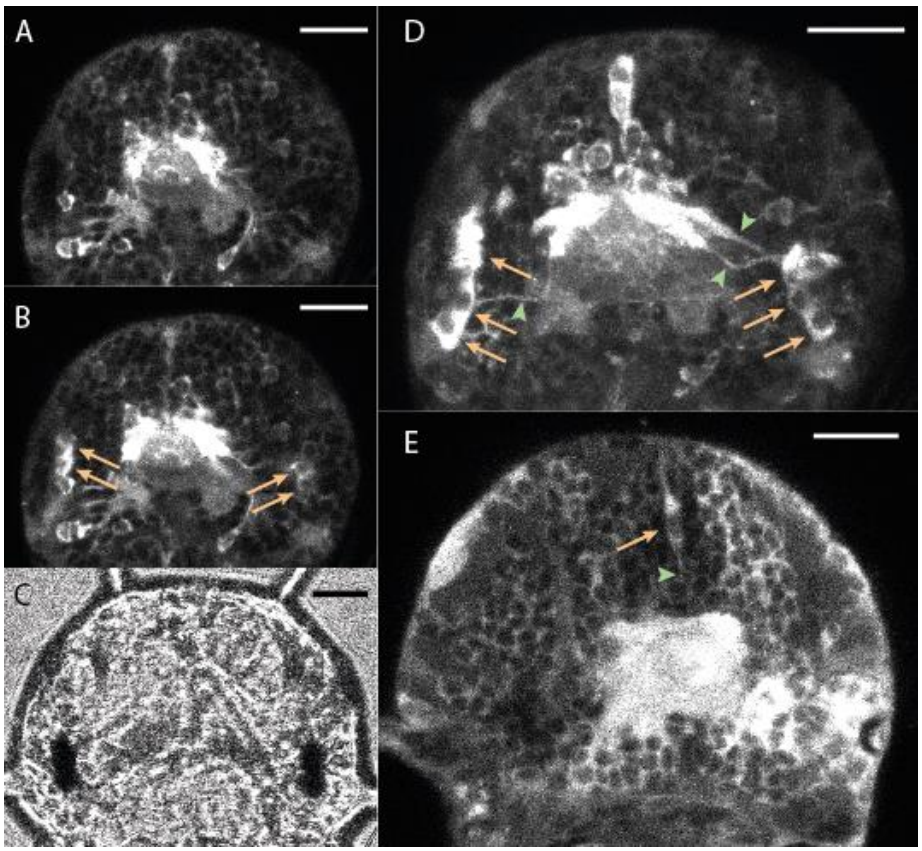


Figure IV-13 Eye rhabdomeric photoreceptor cells (A-D) and a frontal mechanoreceptor cell (E) in two different animals. Photoreceptors in inactive state immediately after (<0.3s) light has just been turned on (A), and in active state slightly later (>0.3s) (B), as well as with their projections into the main plexus (D). Only 3 out of 4 photoreceptor nerves are visible on this picture. (C) shows a transmitted light picture of the same animal, with eye pigmented cups appearing as thick black spots. Orange arrows indicate cell bodies, green arrowheads axonal projections. For more details on the photoreceptors and their projection see fig. 2 in [81]*. Both animals 6dpf, scale bar 20 µm.*

3.4 Calcium activity in the candidate chemosensory organs upon chemical stimulation

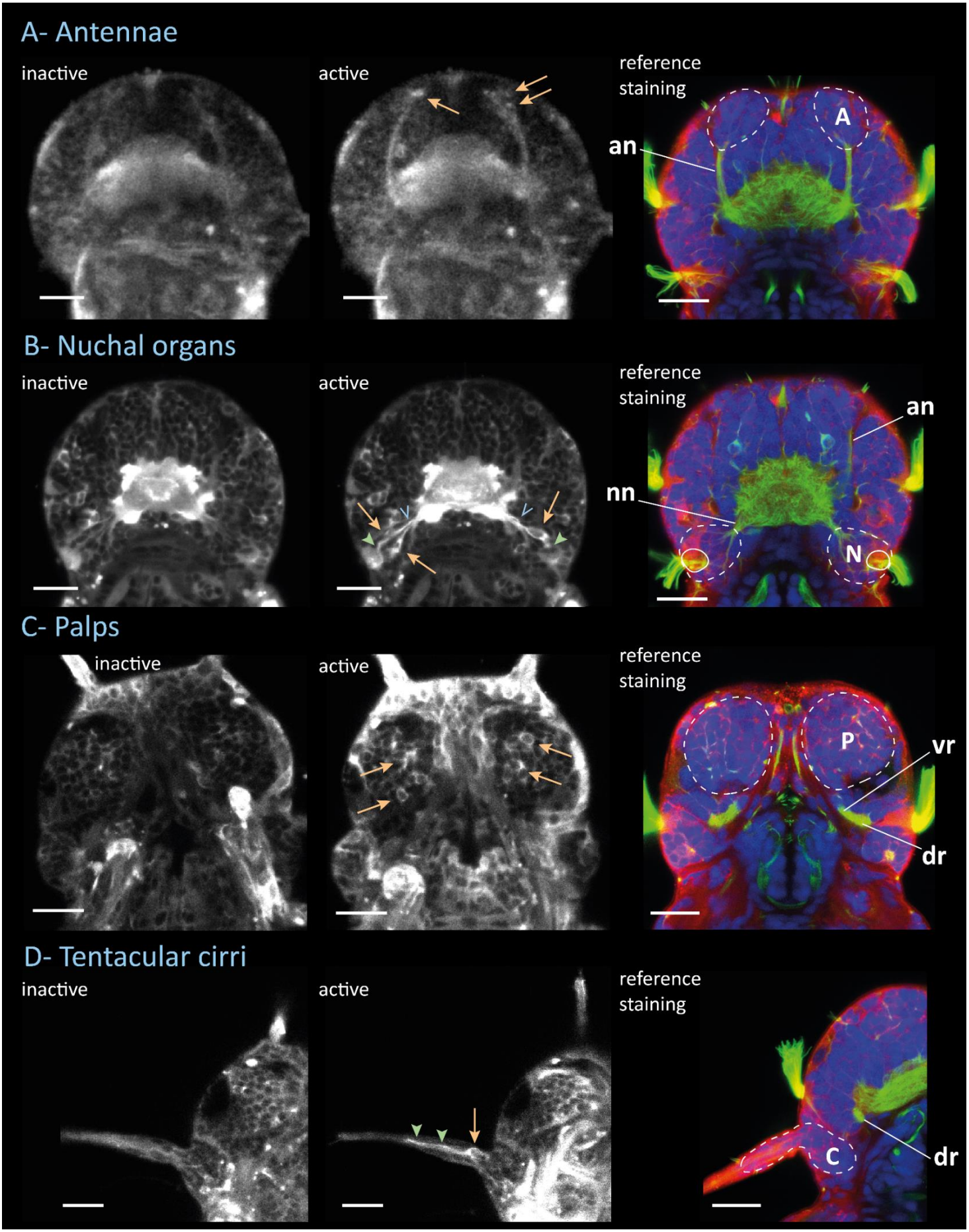
Experimental design. To test the hypotheses that nuchal organs, antennae, palps and tentacular cirri are chemosensory organs in *Platynereis*, late nectochaete larvae (at 6 or 7 dpf) were imaged in a series of experiments, in which calcium signal was acquired in whole-brain imaging settings (see 2.9) at 1 frame per second for each plane, while the animal was being intermittently exposed to a chemical stimulus (see protocol stimulus in 2.5). Each animal was thus exposed alternately to a chemical stimulus (a compound) and to a control stimulus (water), to control for potential flow detection responses that would be mechanosensory and not chemosensory. For each compound, recordings with sufficient quality were obtained for eight to ten animals (see Table IV-3) which came from at least two different batches. For each animal, between 2 and 5 experiments were conducted depending on signal quality and movement artefacts. This was done to ensure that enough events of stimulus exposure would be available from which activity traces could be plotted. Each experiment started with a 1 minute habituation time to the general flow, comprised a total of three exposures to the chemical stimulus and three exposures to the flow control, and lasted 4 minutes. Experiments in a given animals were conducted at intervals of 1 to 5 minutes.

Stimulus	uric acid	1-butanol	amyl acetate	glutamate	sucrose
Number of larvae observed	n = 9	n = 8	n = 10	n = 10	n = 9

Table IV-3 Number of late nectochaete larvae imaged in whole-brain settings upon intermittent chemical stimulation.

Individual, active cells have been identified from the calcium recordings. As was shown in Chapter III, the ganglia of these four pairs of organs can be localised from 6dpf with a neuroanatomical staining. In GCaMP6s-injected 6dpf larvae, the calcium signal alone is sufficiently bright to recognise these regions, and attribute to them with confidence some cellular bodies that become active upon chemical stimulation. Figure IV-14 shows for each of these regions some examples of cells in their inactive (left column) and active (central column) state, as imaged with single-plane settings. The corresponding plane of the reference immunostaining (right column) is shown next to them for comparison. The observed active cells resided inside the ganglia for the antennae and the palps, inside the ganglia and sometimes at the base of the appendages for the tentacular cirri, and around the nuchal cavities (appearing as light areas) for the nuchal organs. Together with these individual cell bodies, the antennal nerve (Figure IV-14A, centre) and the nuchal nerve (Figure IV-14B, centre) are easy to distinguish in the calcium signal. With whole-brain imaging settings, despite a decreased image quality, it is still possible to recognise cell bodies belonging to these organs. Figure IV-15 shows a representative example of how the baseline head calcium signal appears, in the absence of chemical stimulation. Major anatomical landmarks can be identified : main plexus and neurosecretory plexus, ciliary photoreceptors, antennal nerves, nuchal nerves and cavities, palpal nerves, cirral ganglia.

Figure IV-14 (next page) Examples of response of individual cells in the candidate chemosensory regions. Column 1 and 2 : calcium signal in a confocal plane before and during activity, animals imaged from dorsal side except for (C). Column 3 : corresponding plane from the reference immunostaining. Dashed lines indicate the presumed areas containing the corresponding cell bodies, orange arrows indicate cell bodies of active cells, green arrowheads their dendrites, blue Vs their axon, solid lines in (B)-right indicate the nuchal organ cavities. Antennal nerve (an), nuchal nerve (nn), palpal nerve (pn), dorsal (dr) and ventral (vr) root of the circum-oesophageal ring. All animals 6dpf, scale bar 20 µm.


A- Antennae
inactive
active
reference staining
A
an
B- Nuchal organs
inactive
active
reference staining
an
nn
N
C- Palps
inactive
active
reference staining
P
vr
dr
D- Tentacular cirri
inactive
active
reference staining
C
dr

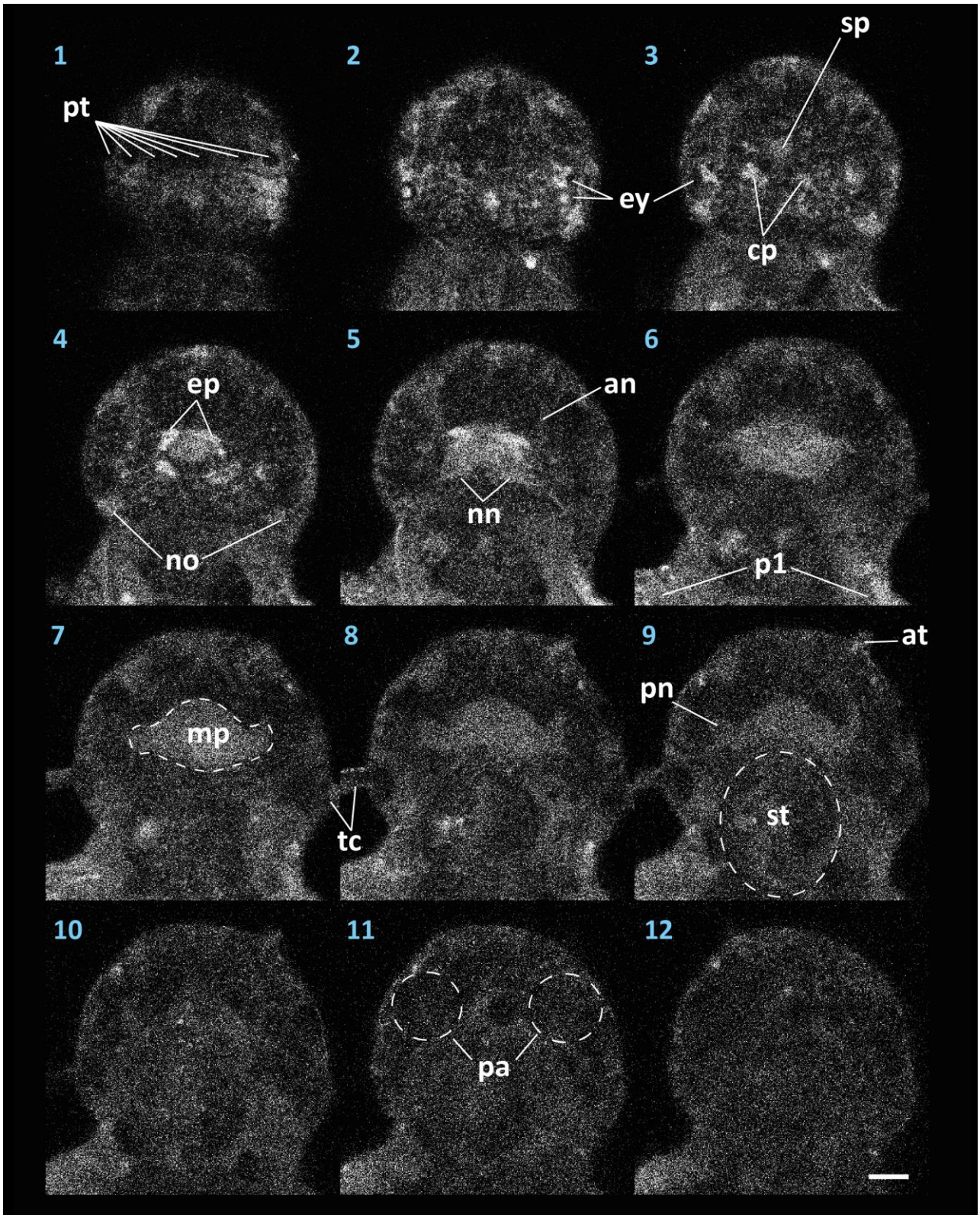


Figure IV-15 Example of baseline calcium signal in a 6 dpf Platynereis larva observed from the dorsal side, as seen with the whole-brain imaging settings ; raw images of the 12 planes indicated in Figure IV-8, from most dorsal (1) to most ventral (12). Antennal nerve (an), antenna (at), ciliary photoreceptors (cp), eye photoreceptor projection (ep), eyes (ey), main plexus or main neuropile (mp), nuchal nerve (nn), nuchal organ (no), first pair of parapodia (p1), palps (pa), root of the palpal nerve (pn), ciliary cells of the prototroch (pt), secretory plexus (sp), stomodeum (st), tentacular cirri (tc). Scale bar 20 µm.

Some individual cells could thus be localised in the whole-brain recordings, and their calcium activity traces plotted against time to reveal any temporal correlation with the chemical stimulation. All activity traces in the following figures are obtained from one the twelve confocal planes (or a merge of two planes in a few cases), after image registration and manual definition of a Region Of Interest (ROI).

Validity of the activity traces, quantification of the response prevalence. It should be noted that activity traces are plotted only for periods of time during which the cells could be tracked reliably, notably without change of focal plane. The absence or interruption of a trace indicates the impossibility to see the cell (typically due to movement artefact), **not an absence of response**. There were many instances of response for which no activity trace could be plotted, hence the amount of traces shown is only partially representative of how often a response was seen. To quantify the overall prevalence of responses to a stimulus onset or offset – either for the chemical stimulus or the flow control – numbers are provided for each organ : a cell was considered to respond only if a change in calcium level was observed within 10 seconds after the pump switch, which corresponds to 5 to 8s after the real stimulus onset or offset (*cf*. precision of stimulus delivery in 3.1). No obvious cellular response was ever observed after the offset of stimulations, hence only the stimulus onsets will be considered in these quantifications. All responses observed always consisted in a transient calcium increase compared to the baseline level.

3.4.1 Antennae

Prevalence of the responses observed. The cellular activity observed in the antennal ganglia upon chemical stimulation was the most obvious of all brain regions. Across all animals, a response in individual cells was seen in a vast majority of cases and almost always together with a transient calcium increase in the antennal nerves. In cases were no cell bodies were seen to be activated, the antennal nerves often did become activated. The details of response occurrences across all experiments are given in Table IV-4. For each compound, the total number of stimulus exposure sequences without movement artefact and across all animals is given, both for the chemical stimulus and the flow control, as well as among all these exposures the number of times when a response was observed at least on one side of the animal. For example, out of a total of 79 sequences which have been recorded with exposure to glutamate, a response was observed 61 times in the antennal nerves, and 69 times in the some cellular bodies. For the same stimulus, a response to the flow control has been observed in the nerves 7 times out of 67 exposures and in some cells 6 times. As different numbers of experiments were conducted for each animal (between 2 and 5), these quantifications could be biased by a few individuals. Hence, for each animal a percentage of often a response has been observed was calculated, and these percentages averaged across all animals. For example, across all experiments involving glutamate as a chemical stimulus, an antennal response from either some cells or the nerves was observed on average 85% of the times when glutamate was applied, and 10% of the times when the flow stimulus was applied.

Stimulus used		uric acid	1-butanol	amyl acetate	glutamate	sucrose
Number of antennal responses observed	**Nerves (stimulus)**	**57 / 69**	**44 / 55**	**61 / 86**	**61 / 79**	**50 / 63**
	Nerves (flow control)	4 / 35	5 / 48	9 / 66	7 / 67	4 / 56
	Cell bodies (stimulus)	**59 / 69**	**50 / 55**	**55 / 86**	**69 / 79**	**52 / 69**
	Cell bodies (flow control)	4 / 35	6 / 48	4 / 66	6 / 67	3 / 56
Average percentage of responses	**Stimulus**	**81 %**	**89 %**	**71 %**	**85 %**	**73 %**
	Flow control	9 %	14 %	11 %	10 %	7 %
	(number of animals)	*(n = 9)*	*(n = 8)*	*(n = 10)*	*(n = 10)*	*(n = 9)*

Table IV-4 Quantification of response prevalence for the antennae.

Some responses to the flow control were observed but in a number of cases much lower than to the chemical stimuli, which confirms that the responses are chemically-evoked. Hence, antennal responses appear to have almost systematically taken place in an animal whenever a chemical stimulus was delivered, showing that antennae are a general detector of chemical stimuli. The rates of responses are comparable for all compounds, which does not indicate an overall increased activity for certain compounds.

Position and morphology of individual active cells. Figure IV-16 shows, for each of the compounds tested, examples of activity traces for antennal cells, as well as the confocal plane in which they were observed (cells are shown in their active state). For a few additional animals, only the antennal ganglia were imaged instead of the whole brain, with 6 to 8 confocal planes ; an example is given in Figure IV-16H. Cell bodies were of rather small size (≈ 4-5 µm), with no particular shape. These antennal cells were observed in at least two distinct regions of the antennal ganglia :

- one located close to the tip of the antennal nerve, corresponding to plane #5 of the 6dpf reference immunostaining (see Chapter III) : Figure IV-16B (right 2), C, D (right), F, H
- one located close to the base of the antennal appendage, corresponding to plane #8 of the 6dpf reference immunostaining : Figure IV-16A, B (right 2), D (left), J, L. Sometimes a cellular extension that seemed to belong the cell, most likely a sensory dendrite, was seen to run into the appendage, as shown in Figure IV-16D (left).

Some were located in a rather intermediate position, as can be seen in Figure IV-16E, G, I, K.

Calcium activity. These antennal cells repeatedly responded to the chemical stimulus and not to the control stimulus, and were often seen to fire as synchronous bilateral pairs (Figure IV-16A, C, E, F). Among the significant number of cases in which an activity trace is given for one side only (Figure IV-16G-L), the cause was either the impossibility of performing a signal quantification for the symmetric cell body, or sometimes the impossibility of locating a symmetric cell body at all. Both antennal nerves were seen to fire together with the cell bodies in most cases, as well as when cell bodies were seen only on one side. The activity traces reveal that these cells are consistently activated upon stimulus onset, with an amplitude of calcium response in the order of 100 to 200%. Within a couple of seconds, the calcium level reaches a maximum, and then starts to more slowly decrease while the stimulus is still present. In most cases, the baseline level is reached again after the stimulus is gone, i.e. more than 15s after stimulus onset. The stimulus offset does not seem to trigger any reaction in these cells, nor does the control stimulus. This latter absence of response could result from a refractory period following a response, potentially preventing the cells to respond to a stimulation that would be too close in time (here 20s after stimulus offset). To control for this effect, antennal responses were recorded in a few animals for which the chemical stimulus was delivered at a period of 35s instead of 70s, and with no control stimulus, which corresponded to an interval of 20s between a stimulus offset and the next stimulus onset. Two examples of responses are shown here : one with uric acid at the usual concentration of 10 µM (Figure IV-16L), one with sucrose at the higher concentration of 1 mM (Figure IV-16K, a recording from another animal with sucrose at 10 µM is available in Appendix F). In both cases, some antennal cells fired to every stimulus presentation, ruling out the existence of such a refractory period. Some habituation is visible in the case of sucrose (Figure IV-16K), as the amplitude of response progressively decreases. The opposite effect, i.e. a sensitisation, would seem to take place in the case of uric acid (Figure IV-16L), however in this particular case the increase of response amplitude was due to a slow focus drift, and such an effect should be excluded. Outside of the stimulation period, no spontaneous firing of these cells was observed, nevertheless other antennal cells were sometimes seen to be active, most often together with some movement of the animal.

More examples of activity traces and their corresponding images are available in Appendix F. Yet more instances of responses have been seen in the recordings, for which however, due to movement artefacts, activity traces were too fragmented to be plotted.

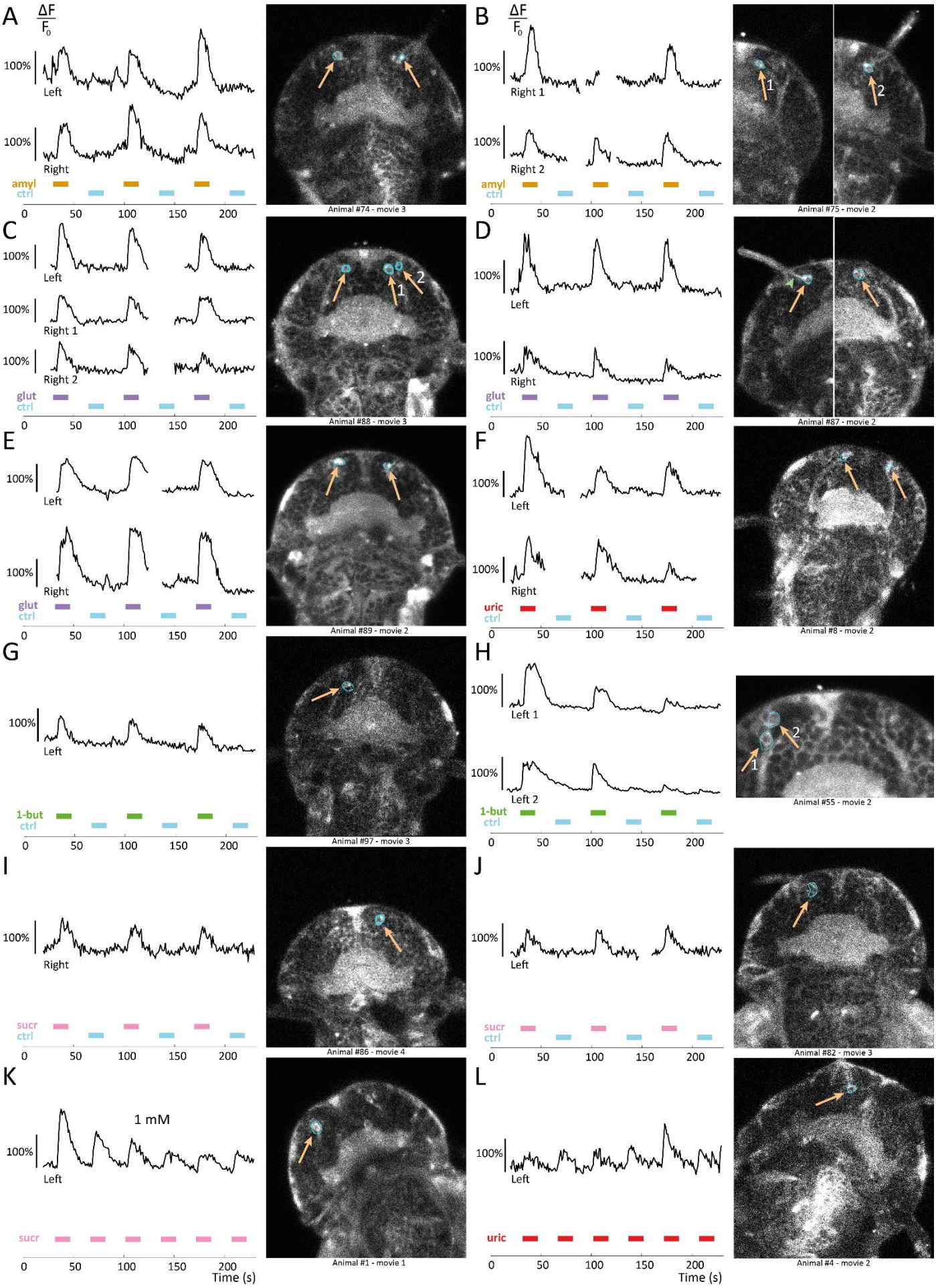

A
ΔF/F0
100%
Left
100%
Right
amyl
ctrl
0 50 100 150 200
Animal #74 - movie 3
B
Right 1
Right 2
Animal #75 - movie 2
C
Left
Right 1
Right 2
glut
ctrl
Animal #88 - movie 3
D
Animal #87 - movie 2
E
Animal #89 - movie 2
F
uric
Animal #8 - movie 2
G
1-but
Animal #97 - movie 3
H
Left 1
Left 2
Animal #55 - movie 2
I
sucr
Animal #86 - movie 4
J
Animal #82 - movie 3
K
1 mM
Animal #1 - movie 1
L
Animal #4 - movie 2
Time (s)

Figure IV-16 (previous page) Activity traces of individual cells in the antennal ganglia. Signal plotted as normalised variation of fluorescence $\Delta F/F_0$. Colour bars indicate the durations of chemical stimulations : amyl acetate (amyl), glutamate (glut), uric acid (uric), 1-butanol (1but), sucrose (sucr), all at 10 µM except (K) at 1 mM. Orange arrows on the images point at the cell bodies, green arrowheads at dendrites. The ROIs from which calcium activity was quantified are indicated in blue around the cell bodies. For all images, anterior is up, with animals imaged either from the dorsal or the ventral side. Images in (B) and (D) are combined from two different optical planes.

3.4.2 Nuchal organs

Prevalence of the responses observed. Significant cellular activity upon chemical stimulation was observed in nuchal organs, though this activity was lower compared to that in the antennae. Responses have been observed notably for uric acid, less frequently for amyl acetate, sucrose and 1-butanol, and rarely for glutamate. A cellular response almost always co-occurred with an activation of the nuchal nerves ; in a number of cases, the nuchal nerves were seen to fire but no cells, suggesting that the responses in the corresponding cell bodies were real but could not be imaged. The details of response occurrences across all experiments are given in Table IV-5.

Stimulus used		uric acid	1-butanol	amyl acetate	glutamate	sucrose
Number of nuchal responses observed	**Nerves (stimulus)**	**56 / 67**	**8 / 44**	**21 / 77**	**1 / 72**	**14 / 59**
	Nerves (flow control)	3 / 32	2 / 41	9 / 58	2 / 65	4 / 56
	Cell bodies (stimulus)	**44 / 67**	**11 / 44**	**26 / 77**	**4 / 72**	**14 / 59**
	Cell bodies (flow control)	3 / 32	1 / 41	4 / 58	1 / 65	3 / 56
Average percentage of responses	**Stimulus**	**79 %**	**23 %**	**32 %**	**5 %**	**17 %**
	Flow control	8 %	4 %	2 %	3 %	6 %
	(number of animals)	*(n = 9)*	*(n = 8)*	*(n = 10)*	*(n = 10)*	*(n = 9)*

Table IV-5 Quantification of response prevalence for the nuchal organs.

Some responses to the flow control were observed but in a number of cases much lower than to the chemical stimuli, which confirms that the responses are chemically-evoked. Hence, antennal responses appear to have almost systematically taken place in an animal whenever a chemical stimulus was delivered, showing that antennae are a general detector of chemical stimuli. The rates of responses are comparable for all compounds, which does not indicate an overall increased activity for certain compounds.

Position and morphology of individual active cells. Figure IV-17 shows, for each of the compounds tested, examples of activity traces for such cells, as well as the confocal plane in which they were observed (cells are shown in their active state). Activity was observed in at least two distinct positions around the nuchal cavity :

- in the majority of cases, in one pair of characteristic cells, whose cell body was larger (≈ 5 µm width and ≈ 10-12 µm length) than that of surrounding cells, and which were always located immediately posterior to the adult eyes (Figure IV-17A, B, C, D, E, F, H, approximately plane #4 of the 6dpf reference immunostaining, see Chapter III). Their proximal end reaches to the nuchal cavity with a large dendrite consistently curved towards the posterior side, which together with their oval cell body gives these cells a peculiar revolver shape, not seen elsewhere in this area. Due to this particular position, shape and activity, these cells are likely to be unique at the 6-7dpf stage, and are thus named hereafter **"revolver cells"**. Their morphology and activity is further illustrated in Figure IV-18.

- in other cases, in cells which were more posterior and more dorsal, and had a smaller and rather round cell body (Figure IV-17G, I, J, K, L, approximately plane #2 or 3 of the 6dpf reference immunostaining, see Chapter III).

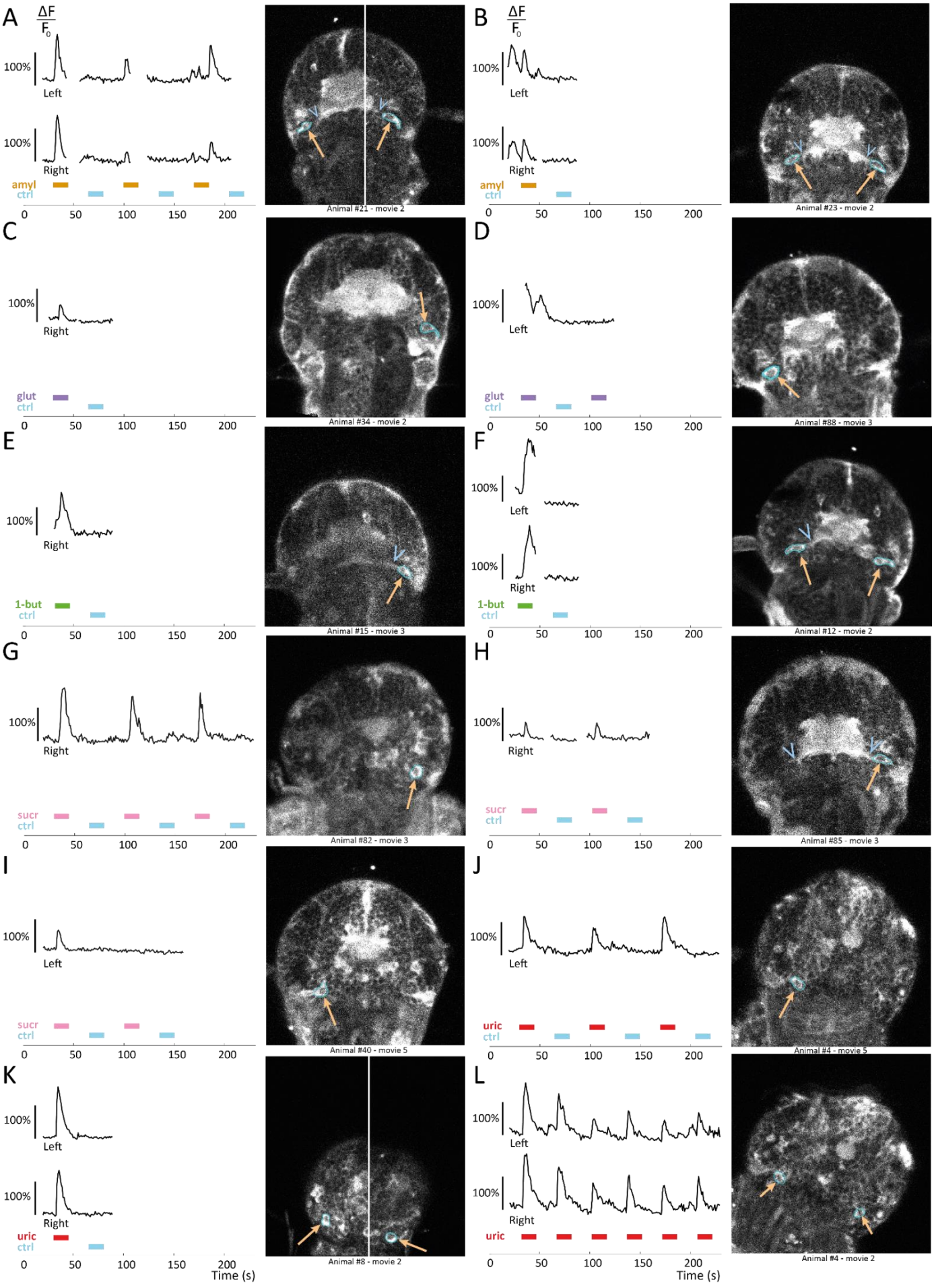
Consequently, there seems to be at least two types of cells that respond to chemical stimulations in the nuchal organ area.

Calcium activity. Whenever responses were observed, the cells responded to the chemical stimulus and not to the flow control, though the responses were by far less systematic than for the antennal cells. For some animals, it was possible to record cellular activity during several exposures to the chemical stimulus (Figure IV-17A, G, H, I, J, L) ; but for some others, the rarity of responses, combined with some movement artefacts, made it impossible to record activity during more than one exposure (Figure IV-17B, C, D, E, F, K). Cells were often seen to fire as synchronous bilateral pairs (Figure IV-17A, B, F, K, L), almost always together with the nuchal nerves. In a number of cases where active cell body(ies) could be seen on one side only, both nuchal nerves were seen to fire, suggesting that the cellular response was indeed bilateral. The activity traces reveal that these cells are typically activated upon stimulus onset, though not only. Indeed, even though most responses co-occur with an onset of the chemical stimulus (Figure IV-17A, C, E, F, G, H, J, K, L), these cells occasionally fired outside of the stimulus exposure, as can be seen in Figure IV-17A (third exposure), B and D. The cellular response that precedes the stimulus onset in Figure IV-17B and D casts some doubt concerning the causal link between the second response that co-occurs upon stimulus onset. Figure IV-17I shows an example of a cell that responds to the first, but not to the second stimulus exposure. For nuchal organ cells in general, the activity peak in response to a stimulus exposure appears to be shorter than for the antennal ones, since the calcium level is often back to its baseline level before the end of the 15s stimulus exposure. The stimulus offset was never seen to trigger a reaction in these cells, nor was the control stimulus. To test whether this latter absence of response could result from a refractory period that would unable the cells to react until 20s after a response, nuchal activity was quantified in one animal for which uric acid was delivered at a period of 35s instead of 70s, and with no control stimulus (Figure IV-17L), which corresponded to an interval of 20s between a stimulus offset and the next stimulus onset. A pair of cells in the nuchal organ region was seen to respond to each stimulus exposure, which speaks against the existence of a refractory period, at least for cells responding to uric acid.

More examples of activity traces and their corresponding images are available in Appendix F. Yet more instances of responses have been seen in the recordings, for which however, due to movement artefacts, activity traces were too fragmented to be plotted.

Overall, it is clear that nuchal organs respond to uric acid. Responses to sucrose are less frequent (Table IV-5) but activity traces confirm that they are real (Figure IV-17G, H) though not systematic for a given cell (Figure IV-17G, H). Habituation effects are unlikely to be responsible for the absence of response observed in such a case (see Figure IV-17L). Few traces could be obtained to support the reality of responses to amyl acetate, however they were observed more often than to sucrose (Table IV-5) and are probably of equal significance. Responses to 1-butanol are rarely seen, and only single responses could be plotted, which makes it uncertain that these responses are meaningful. Finally, the data do not support that glutamate would be detected by the nuchal organs. These organs thus have some clear chemosensitivity, but seem to be of less general a stimulus scope than the antennae.

Figure IV-17 (next page) Activity traces of individual cells around the nuchal cavities. Signal plotted as normalised variation of fluorescence $\Delta F/F_0$. Colour bars indicate the durations of chemical stimulations : amyl acetate (amyl), glutamate (glut), uric acid (uric), 1-butanol (1but), sucrose (sucr), all at 10 µM. Orange arrows point at the cell bodies, blue empty arrowheads at nuchal nerves. The ROIs from which calcium activity was quantified are indicated in blue around the cell bodies. For all images, anterior is up, with animals imaged either from the dorsal or the ventral side. Images in (A) and (K) are combined from two different optical planes.


A
ΔF/F0
100%
Left
100%
Right
amyl
ctrl
0 50 100 150 200
Animal #21 - movie 2
B
ΔF/F0
100%
Left
100%
Right
amyl
ctrl
0 50 100 150 200
Animal #23 - movie 2
C
100%
Right
glut
ctrl
0 50 100 150 200
Animal #34 - movie 2
D
100%
Left
glut
ctrl
0 50 100 150 200
Animal #88 - movie 3
E
100%
Right
1-but
ctrl
0 50 100 150 200
Animal #15 - movie 3
F
100%
Left
100%
Right
1-but
ctrl
0 50 100 150 200
Animal #12 - movie 2
G
100%
Right
sucr
ctrl
0 50 100 150 200
Animal #82 - movie 3
H
100%
Right
sucr
ctrl
0 50 100 150 200
Animal #85 - movie 3
I
100%
Left
sucr
ctrl
0 50 100 150 200
Animal #40 - movie 5
J
100%
Left
uric
ctrl
0 50 100 150 200
Animal #4 - movie 5
K
100%
Left
100%
Right
uric
ctrl
0 50 100 150 200
Time (s)
Animal #8 - movie 2
L
100%
Left
100%
Right
uric
0 50 100 150 200
Time (s)
Animal #4 - movie 2

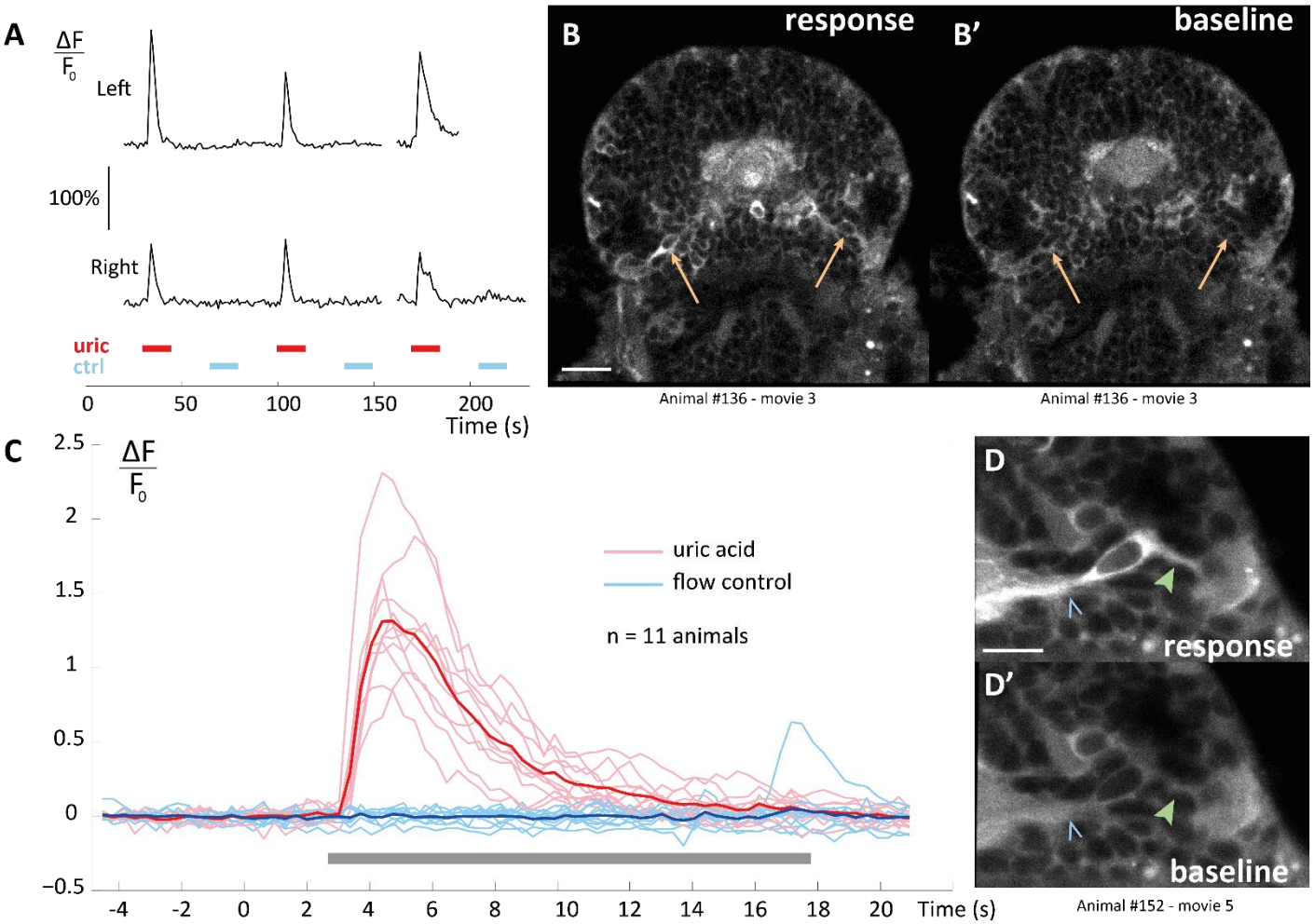


Figure IV-18 Systematic calcium responses of the nuchal organs' revolver cells to a 10 µM uric acid stimulation. (A-B') Repeated bilateral responses to uric acid (uric) and not to the flow control (ctrl) in the revolver cells of a single animal (A) ; signal downsampled to 1 fps. Calcium signal in a single confocal plane showing the nuchal organs of these animals in their active (B) and inactive state (B') state. Orange arrows indicate the revolver cells. (C) activity traces of one revolver cell in n = 11 animals at 5 to 6 dpf. The calcium activity recorded at 3 fps during one 10 µM uric acid exposure and one flow control is shown for each animal. Normalised traces are aligned on the beginning of response and superimposed. The grey bar indicates the duration of the stimulus, t=0s corresponds to the pump switch. (D-D') a revolver cell in local single-plane confocal imaging, shown in its active (D) and inactive (D') state. Blue arrowheads indicate the nuchal nerve, green arrowheads the sensory dendrite. The diffuse light grey area on the right of the image is the nuchal cavity. Scale bar 20 µm in (B-B') and 10 µm in (D-D').

The revolver cells are unique and consistently respond to uric acid. To further investigate the responses of the revolver cells, a series of additional experiments was conducted in which the nuchal organ region was specifically imaged, either in single-plane settings at 3fps for the whole head width or the nuchal region, or in local volume imaging of one nuchal region with 3 to 4 planes at 1fps each. The calcium imaging reveals that these cells systematically respond to uric acid at 10 µM, with no clear sign of habituation. The response is bilateral, symchronised for both cells and reproducible for each animal (see an example in Figure IV-18A-B'). Across animals, the cells have a consistent position and shape as described above, and no comparable cell is ever observed in the nuchal organ region. Figure IV-18D illustrates the typical revolver shape, and the position of the sensory dendrite reaching to the nuchal

cavity, which fits exactly the general morphology of nuchal organ cells described by Purschke (see Figure II-21 in the review). Moreover, the activity traces reveal comparable calcium kinetics (Figure IV-18C), which further supports that the same cells are indeed observed in all animals. These results clearly demonstrate that this pair of cells are chemosensory neurons belonging to the nuchal organs. Based on their shape and position, these particular cells are most likely the ones shown activated in Figure IV-17A, B, C, D, E, F and H. Hence, it appears that they can probably detect other chemical compounds, at least sucrose (Figure IV-17H) since the validity of the responses is doubtful for the other stimuli.

Besides, a preliminary experiment in a 3dpf animal (80hpf) has revealed in the nuchal organ a cell immediately posterior to the eyes, though slightly more medial, which has a very similar shape and also responds to uric acid at 10 µM (Figure IV-19). There is little doubt that this cell was a revolver cell. This finding indicates that the nuchal organ is most likely functional at 3dpf already. If the revolver cells are differentiated and functional so early in *Platynereis*, they certainly have an important role which should be further investigated. Moreover, they could be identified in the 72hpf connectomic data.

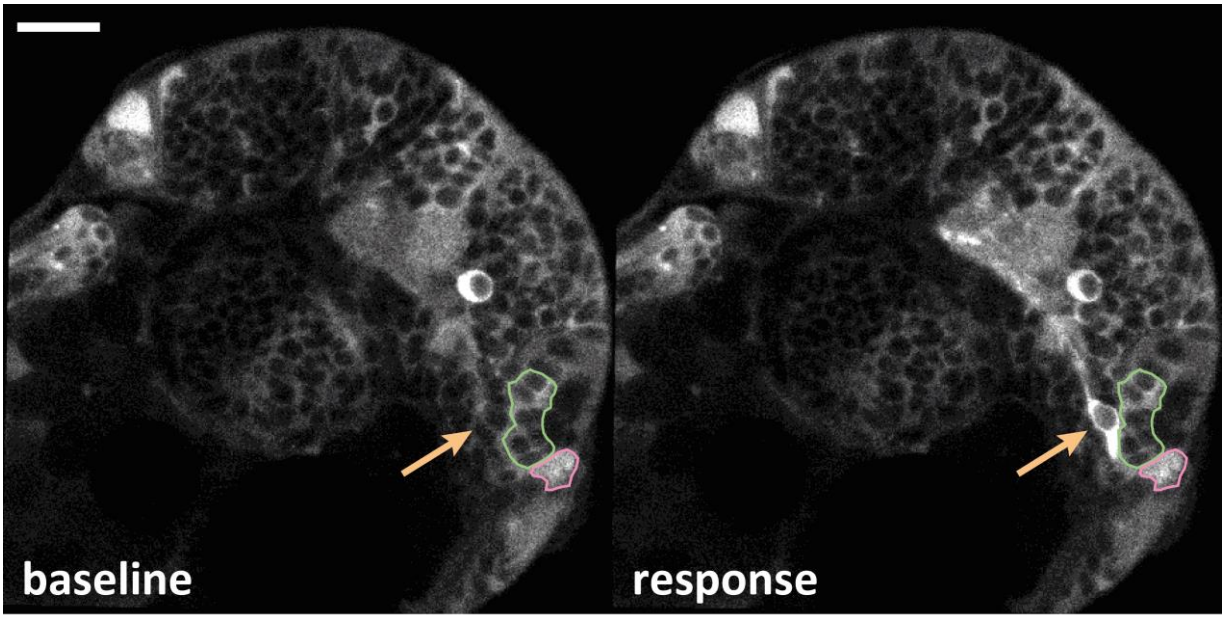


Figure IV-19 Response of a revolver cell to 10 µM observed in a 80hpf animal, shown in its inactive (left) and active state (right). The orange arrow indicates the cell's position, the rhabdomeric photoreceptors are outlined in green and the nuchal cavity in pink. Note that the animal is tilted and the nuchal organ is visible on one side only. Scale bar 20 µm.

3.4.3 Palps

Prevalence of the responses observed. Occasional cellular activity upon chemical stimulation was observed in the palps. This activity was low compared to that of the antennae. A higher total number of responses has been observed for glutamate and sucrose than for the other compounds (see Table IV-6), nevertheless the prevalence of response, when averaged across animals, reveals that amyl acetate and uric acid have a likelihood to produce an observable response comparable to that of sucrose (24, 23 and 28% respectively), and inferior to that of glutamate (38%). However, 1-butanol does not seem to reliably activate the palps, which indicates some specificity of the responses. Responses in the palpal nerve are not quantified in this table : due to the proximity of the palpal nerve with the most ventral parts of the lateral neuropile, it was not possible to attribute with confidence nervous fibre activations to the palpal nerve.

Stimulus used		uric acid	1-butanol	amyl acetate	glutamate	sucrose
Number of palpal responses observed	**Cell bodies (stimulus)** Cell bodies (flow control)	**8 / 55** 1 / 27	**4 / 48** 3 / 41	**15 / 64** 4 / 55	**27 / 76** 5 / 66	**24 / 59** 7 / 58
Average percentage of responses	**Stimulus** Flow control *(number of animals)*	**24 %** 2 % *(n = 9)*	**7 %** 8 % *(n = 8)*	**23 %** 5 % *(n = 10)*	**38 %** 8 % *(n = 10)*	**28 %** 10 % *(n = 9)*

Table IV-6 Quantification of response prevalence for the palps.

Position and morphology of individual active cells. Figure IV-20 shows, for each of the compounds tested, examples of activity traces for palpal cells that responded to chemical stimulations, as well as the confocal plane in which they were observed (cells are shown in their active state). Cell bodies were of rather small size (≈ 3 to 5 µm), with no particular shape. In a few cases a bilateral pair of cells was seen to fire in synchronously (Figure IV-20C, F, G), yet in most cases an active cell could be seen only on one side of the animal (Figure IV-20A, B, D, E, H, I, J). Cellular activity almost always coincided with activity infibres that are likely to belong to the palpal nerves, though these nerves are short and less unambiguously identified in the recordings than the antennal or nuchal nerves. This suggests than even when only one cell is seen to respond, the response is probably bilateral. These palpal cells were observed in planes corresponding approximately to planes #8 and #9 of the 6dpf reference immunostaining (see Chapter III).

Calcium activity. Whenever such palpal cells could be seen, they responded to the chemical stimulus and not to the control stimulus, in a manner that was reproducible for each animal (Figure IV-20A-J). Even though the prevalence of responses is comparable to that observed in the nuchal organs, the palpal responses differ from the nuchal responses in that cells show more consistent activities, that are in fully in agreement with a chemosensory nature. The activity traces reveal that these cells consistently respond to the onset of chemical stimulation, not to the offset. The calcium level reaches a maximum, typically in the order of than 100%, and is typically back to its baseline level after the stimulus offset, i.e. more than 15s after stimulus onset. To test whether the absence of response to the control stimulus could be due to a refractory period of the cells, unabling them to react 20s after the stimulus has disappeared, palpal activity was quantified in one animal for which 1 mM sucrose was delivered at a period of 35s instead of 70s, and with no control stimulus, which corresponded to an interval of 20s between a stimulus offset and the next stimulus onset (Figure IV-20J). One palpal cell was seen to respond consistently to every stimulus onset, which speaks against the existence of a refractory period, at least in palpal cells responding to sucrose. Outside of the stimulation period, no spontaneous firing of these cells was observed, nevertheless other palpal cells were frequently active and most often together with some movement of the animal.

All of the palpal responses for which signal quality was sufficient to plot the activity traces have been shown in Figure IV-20. More instances of responses have been seen in the recordings, for which however, due to movement artefacts, activity traces were too fragmented to be plotted.

Overall, reliable calcium responses of palpal cells have been observed. The palps do detect chemical stimulations, with some compound specificity, but their sensory activity is lower than that of antennae. Responses were the most frequent for the amino acid glutamate, which may indicate a link with food detection.

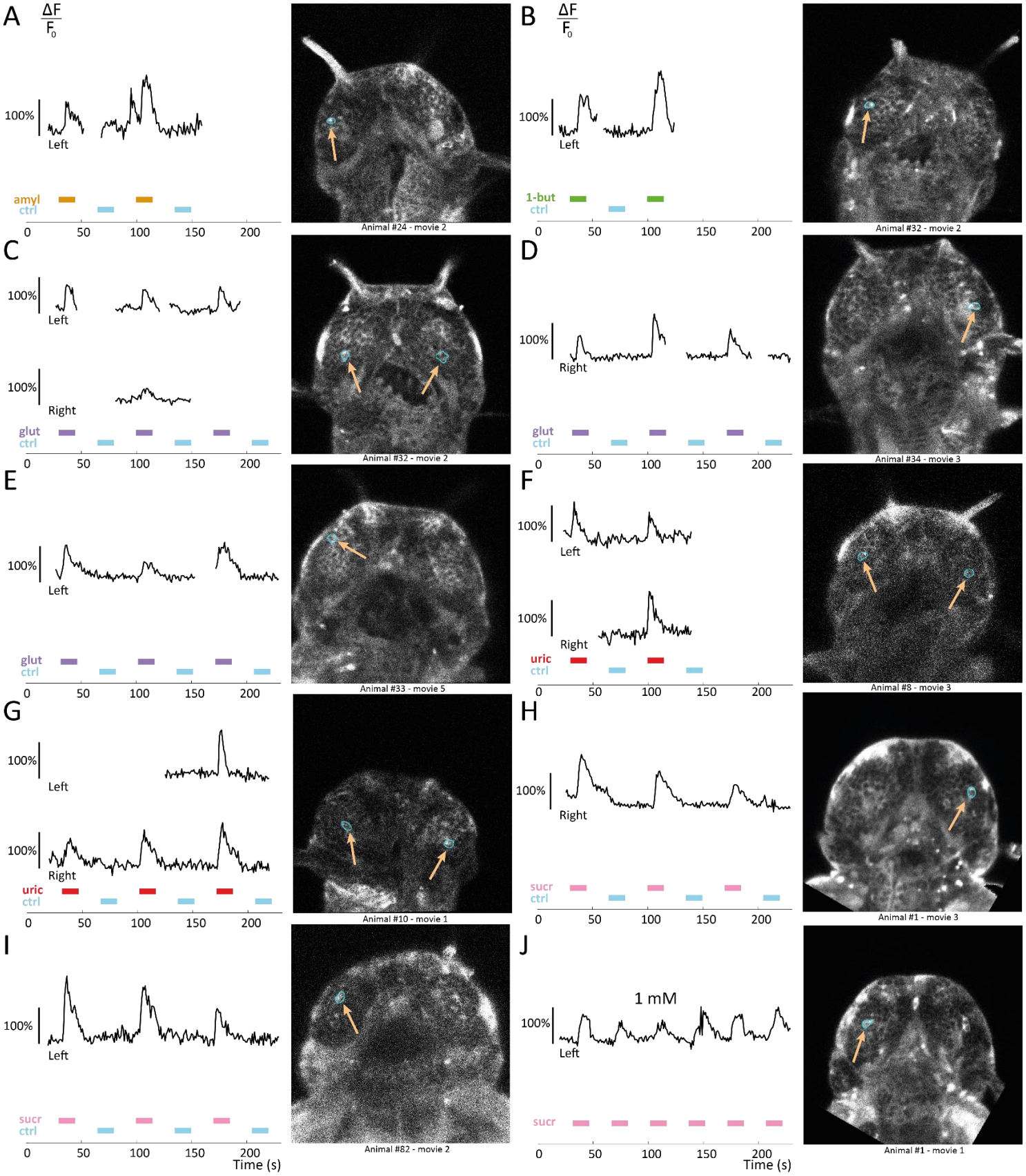

A
ΔF/F0
100%
Left
amyl
ctrl
0 50 100 150 200
Animal #24 - movie 2
B
ΔF/F0
100%
Left
1-but
ctrl
0 50 100 150 200
Animal #32 - movie 2
C
100%
Left
100%
Right
glut
ctrl
0 50 100 150 200
Animal #32 - movie 2
D
100%
Right
glut
ctrl
0 50 100 150 200
Animal #34 - movie 3
E
100%
Left
glut
ctrl
0 50 100 150 200
Animal #33 - movie 5
F
100%
Left
100%
Right
uric
ctrl
0 50 100 150 200
Animal #8 - movie 3
G
100%
Left
100%
Right
uric
ctrl
0 50 100 150 200
Animal #10 - movie 1
H
100%
Right
sucr
ctrl
0 50 100 150 200
Animal #1 - movie 3
I
100%
Left
sucr
ctrl
0 50 100 150 200
Time (s)
Animal #82 - movie 2
J
1 mM
100%
Left
sucr
0 50 100 150 200
Time (s)
Animal #1 - movie 1

Figure IV-20 (previous page) Activity traces of individual cells in the palpal ganglia. Signal plotted as normalised variation of fluorescence $\Delta F/F_0$. Colour bars indicate the durations of chemical stimulations : amyl acetate (amyl), glutamate (glut), uric acid (uric), 1-butanol (1but), sucrose (sucr), all at 10 µM except (J) : 1 mM. Orange arrows on the images point at the cell bodies. The ROIs from which calcium activity was quantified are indicated in blue around the cell bodies. For all images, anterior is up, with animals imaged either from the dorsal or the ventral side.

3.4.4 Tentacular cirri

Prevalence of the responses observed. A few instances of cellular activity upon chemical stimulation were observed in the cirral ganglia, in at least one animal for each of the compounds tested. These responses occured were rarely (see Table IV-7) which indicate that these compounds were generally not detected by the tentacular cirri. Nevertheless, these responses, even if they were rare, were more often observed to the chemical stimuli than to their flow control, suggesting that some events of detection may have been meaningful. The cirral nerves could not by identified with certainty from the calcium recordings, their activation is not quantified here.

Stimulus used		uric acid	1-butanol	amyl acetate	glutamate	sucrose
Number of cirral responses observed	**Cell bodies (stimulus)** Cell bodies (flow control)	**4 / 70** 0 / 35	**7 / 54** 1 / 49	**8 / 86** 0 / 66	**7 / 71** 0 / 66	**3 / 58** 0 / 56
Average percentage of responses	**Stimulus** Flow control *(number of animals)*	**6 %** 0 % *(n = 9)*	**10 %** 1 % *(n = 8)*	**10 %** 0 % *(n = 10)*	**8 %** 1 % *(n = 10)*	**4 %** 0 % *(n = 9)*

Table IV-7 Quantification of response prevalence for the tentacular cirri.

Position and morphology of individual active cells. Figure IV-21 shows examples of activity traces for such cells, as well as the confocal plane in which they were observed (cells are shown in their active state). Cell bodies were rather elongated, with a cell body size (≈ 5-6 µm) comparable to the most cells in the brain. A response could never be observed in both ganglia simultaneously, nor in the cirral nerves. These cirral cells were observed in planes corresponding approximately to planes #7 and #9 of the 6dpf reference immunostaining (see Chapter III).

Calcium activity. The activity traces reveal cells that respond to the onset of chemical stimulation, not to the offset, and not to the flow control. Responses could sometimes be observed repeatedly for a same cell (Figure IV-21B, E, F, H, I), sometimes only once (Figure IV-21A, C, D, G). The amplitude of signal variation observed here is in the order of 60-80%. The calcium level seems to come back to its baseline level after the stimulus offset, i.e. more than 15s after stimulus onset, although this is hard to tell from the small number of traces available. Outside of the stimulation period, no spontaneous firing of these cells was observed. Other cirral cells were sometimes seen to fire, though this always coincided with some movement of the animal.

Overall, these results indicate that chemosensory cells are probably present in the cirral ganglia, but they do not show strong and consistent responses to the compounds tested. Reproducible chemosensory responses could be obtained in 3 animals with glutamate, and 1 animal with uric acid. Tentacular cirri do not appear to be a major chemosensory organ. A few additional cases of response, for which it is unclear whether the cell truly belongs to the cirral ganglia, are shown in Appendix F.

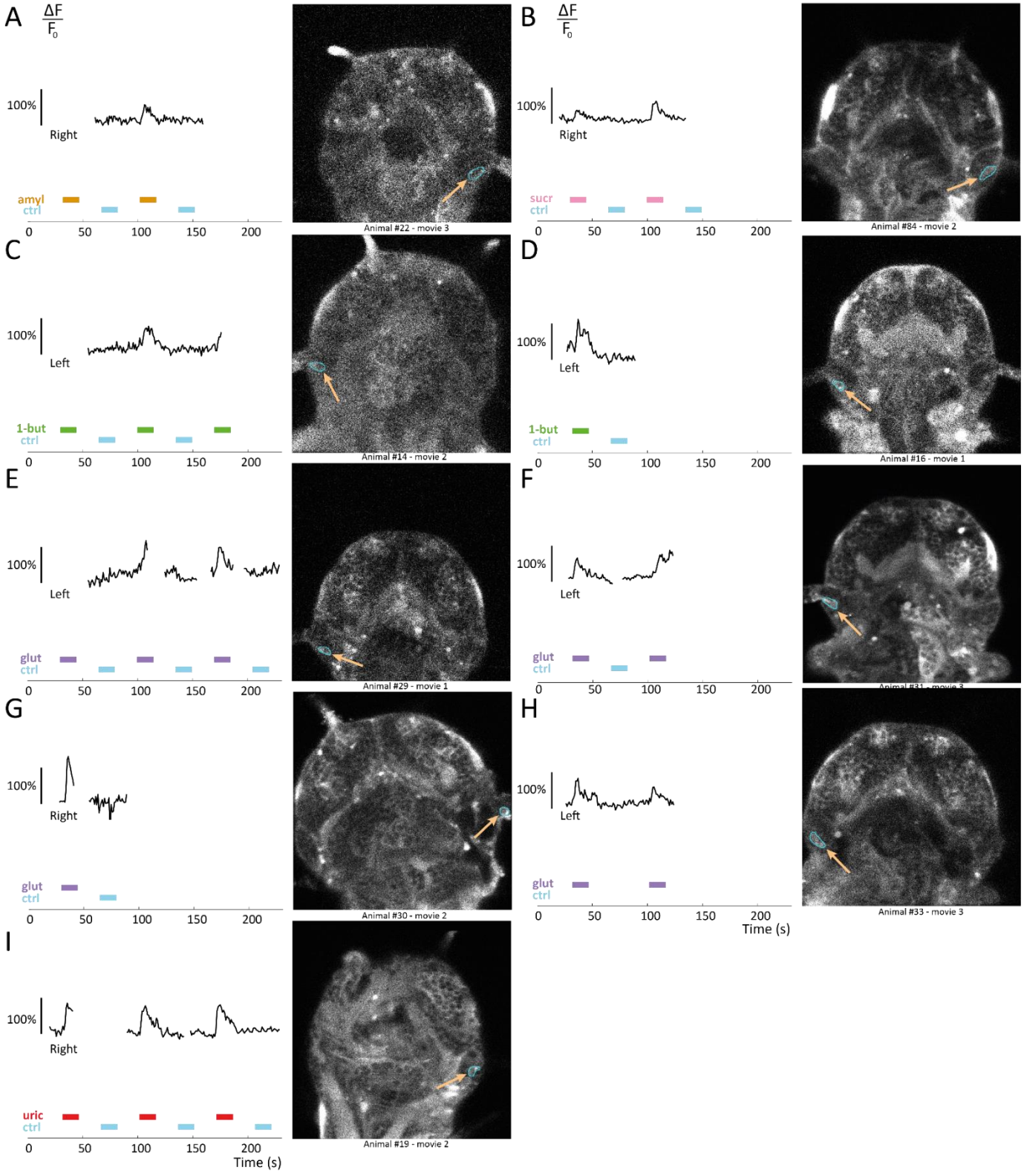


Figure IV-21 Activity traces of individual cells in the cirral ganglia. Signal plotted as normalised variation of fluorescence $\Delta F/F_0$. Colour bars indicate the durations of chemical stimulations : amyl acetate (amyl), glutamate (glut), uric acid (uric), 1-butanol (1but), sucrose (sucr), all at 10 µM. Orange arrows on the images point at the cell bodies. The ROIs from which calcium activity was quantified are indicated in blue around the cell bodies. For all images, anterior is up, with animals imaged either from the dorsal or the ventral side.

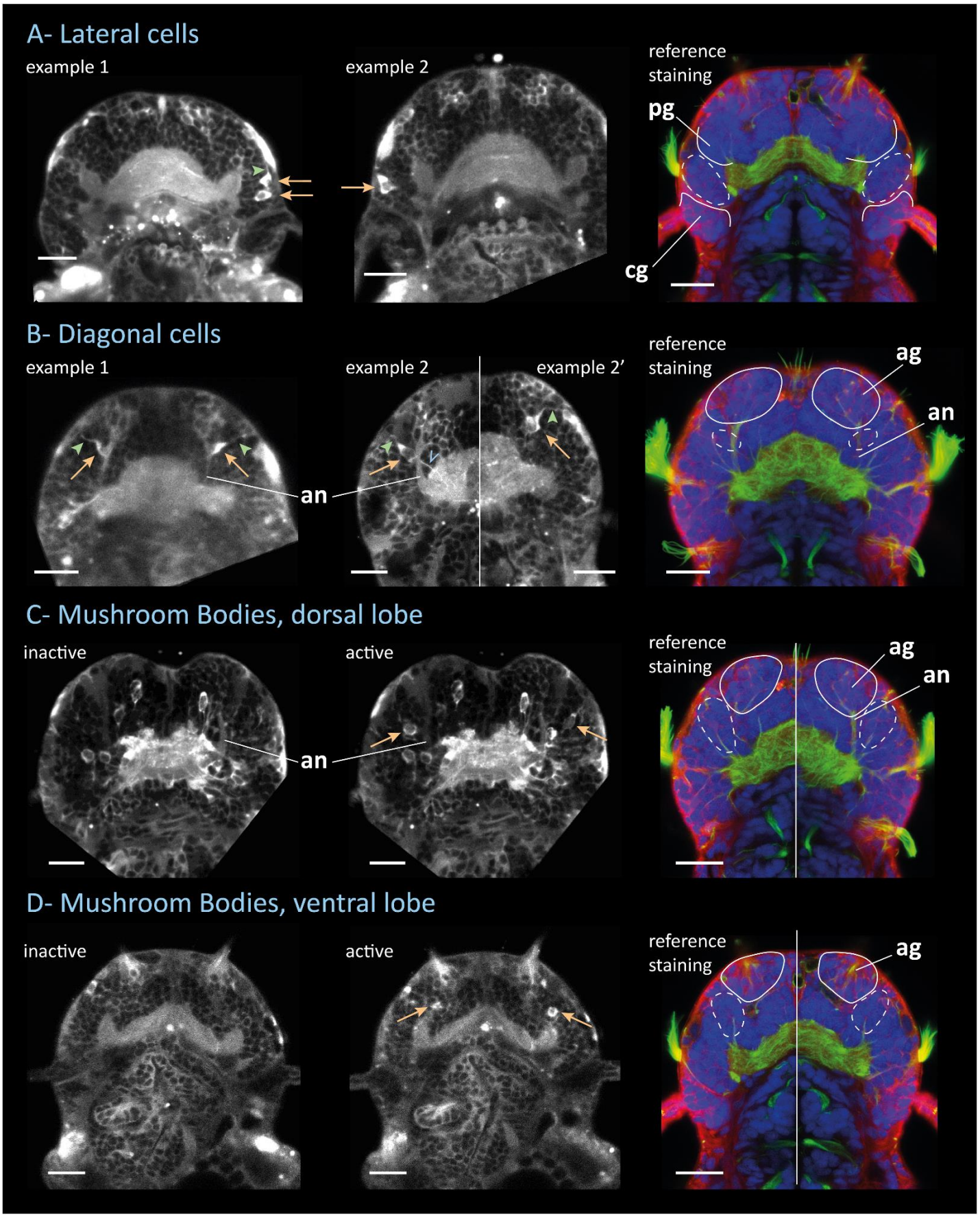

A- Lateral cells
example 1
example 2
reference staining
pg
cg
B- Diagonal cells
example 1
example 2
example 2'
reference staining
ag
an
an
C- Mushroom Bodies, dorsal lobe
inactive
active
reference staining
ag
an
an
D- Mushroom Bodies, ventral lobe
inactive
active
reference staining
ag

Figure IV-22 (previous page) Position of individual cells outside of the candidate chemosensory organs, which respond to chemical stimulations. Examples are given of cells in their active state ; for (C) and (D) the inactive state is also provided. Left and central column : calcium signal ; orange arrows indicate active cell bodies, green arrowheads their dendrites, empty blue arrowheads their axon. Right column : corresponding plane from the reference immunostaining ; dashed lines indicate the areas where these cell bodies have been seen, solid lines indicate known ganglia. Antennal nerve (an), antennal (ag), cirral (cg) and palpal (pg) ganglia. All animals 6dpf except (A) 7dpf, scale bar 20 µm.

3.5 Calcium activity outside of the candidate chemosensory organs, related to the chemical stimulations

Whole-brain recordings have revealed yet uncharacterised cells that show a calcium activity consistently related to the chemical stimuli and not to the control stimuli, but are not located in any of the four candidate chemosensory organs. These cells, whose position and activity are described in more detail hereafter, have been observed in four distinct bilateral regions, as illustrated in Figure IV-22 :

- a lateral region, immediately frontal to the cirral ganglion (Figure IV-22A),
- a region immediately ventral to the antennal nerve (Figure IV-22B),
- a region around the dorsal peduncle of the Mushroom Bodies (Figure IV-22C),
- a region around the ventral peduncle of the Mushroom Bodies (Figure IV-22D).

3.5.1 Lateral cells

Cellular responses upon chemical stimulation were often observed close to the head surface, in the lateral region located between the cirral and the palpal ganglia, as drawn on the reference staining in Figure IV-22A. Across the different experiments, active cells in this region have been observed in coronal planes ranging from plane #6 to #8 of the 6dpf reference immunostaining (see Chapter III). Such responses were seen in experiments involving all chemical compounds except uric acid. Examples of activity traces are shown in Figure IV-23, as well as the confocal plane in which the cells were observed (cells are shown in their active state, interrupted traces reflects the impossibility to follow the cell body during the whole stimulation protocol). In Figure IV-23H, the image was obtained with single-plane imaging settings and thus yielded a better signal quality.

These lateral cells were seen to respond upon exposure to the chemical stimulus, not to the control stimulus. Their cell body had an average size (≈ 5 µm), and often a rather triangular shape ; Figure IV-22A shows how they appear in the calcium signal. They were often seen on both side of a same animal, though not systematically. In some cases where cells were seen on both sides, similarity in position, shape and activity suggest that bilateral pairs were seen (e.g. Figure IV-23I) ; in other cases, differences in position, shape or activity may speak against the existence of pairs (Figure IV-23E, F). In general, no obvious dendritic extension or axonal projection was observed next to these cells.

The activity traces reveal that these cells are consistently activated upon stimulus onset, and not stimulus offset, with an amplitude of calcium response in the order of 100 to 200%. No response was observed upon exposure to the control stimulus (the second peak in Figure IV-23D is an artefact due to another cell responding in a volume close to the cell of interest). Activity peaks are rather short in time, and the cells are typically back to their baseline calcium level before the offset of the chemical stimulus. Outside of the chemical stimulation period, no spontaneous activation was observed for these cells, but some other cells in this area were occasionally seen to fire. Cells of the same side in one animal can show differences in their calcium activity : in Figure IV-23E, cell #1 takes a longer time to come back to its baseline calcium level than cell #2 though their response amplitude is similar ; in Figure IV-23H, the response amplitude decreases upon repeated stimulation in cell #2 whereas it does not in cell #1.

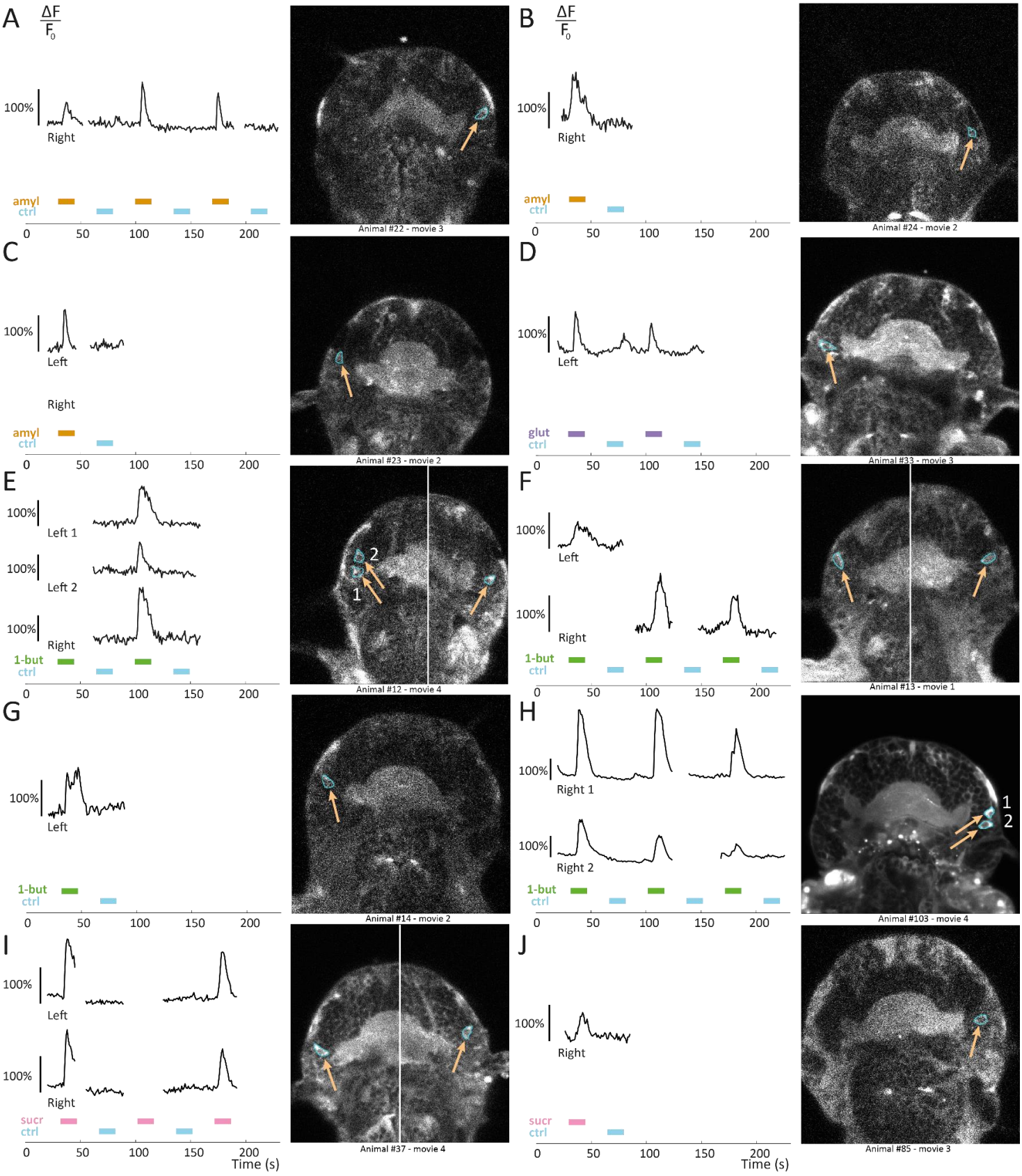

A
ΔF/F0
100%
Right
amyl
ctrl
0 50 100 150 200
Animal #22 - movie 3
B
ΔF/F0
100%
Right
amyl
ctrl
0 50 100 150 200
Animal #24 - movie 2
C
100%
Left
Right
amyl
ctrl
0 50 100 150 200
Animal #23 - movie 2
D
100%
Left
glut
ctrl
0 50 100 150 200
Animal #33 - movie 3
E
100%
Left 1
100%
Left 2
100%
Right
1-but
ctrl
0 50 100 150 200
2
1
Animal #12 - movie 4
F
100%
Left
100%
Right
1-but
ctrl
0 50 100 150 200
Animal #13 - movie 1
G
100%
Left
1-but
ctrl
0 50 100 150 200
Animal #14 - movie 2
H
100%
Right 1
100%
Right 2
1-but
ctrl
0 50 100 150 200
1
2
Animal #103 - movie 4
I
100%
Left
100%
Right
sucr
ctrl
0 50 100 150 200
Time (s)
Animal #37 - movie 4
J
100%
Right
sucr
ctrl
0 50 100 150 200
Time (s)
Animal #85 - movie 3

Figure IV-23 (previous page) Activity traces of individual lateral cells. Signal plotted as normalised variation of fluorescence $\Delta F/F_0$. Colour bars indicate the durations of chemical stimulations : amyl acetate (amyl), glutamate (glut), 1-butanol (1but), sucrose (sucr), all at 10 µM. Orange arrows on the images point at the cell bodies. The ROIs from which calcium activity was quantified are indicated in blue around the cell bodies. For all images, anterior is up, with animals imaged either from the dorsal or the ventral side. Images in (E), (F) and (I) are combined from two different optical planes. The image in (H) is the only one obtained with single-plane imaging settings, its signal quality is thus better.

All lateral responses for which signal quality was sufficient to plot the activity traces have been shown in Figure IV-23Figure IV-20. More instances of responses have been seen in the recordings, for which however, due to movement artefacts, activity traces were too fragmented to be plotted.

3.5.2 Diagonal cells

In a few animals, a peculiar pair of large cells was seen to respond to the chemical stimulation (see in Figure IV-22B their appearance in the calcium channel while activated). These cells, located quite deep in the head, were sitting between the antennal nerve and the ventral lobe of the Mushroom Bodies, as drawn on the reference staining in Figure IV-22B, i.e. in a coronal plane corresponding to plane #6 of the 6dpf reference immunostaining (see Chapter III). In most instances they were seen to fire in synchrony. These cells have been observed in experiments involving all of the five chemical compounds, and never was more than one such cell seen on a single side of the head. Examples of activity traces are shown in Figure IV-24, as well as the confocal plane in which the cells were observed (cells are shown in their active state, interrupted traces reflects the impossibility to follow the cell body during the whole stimulation protocol).

Their cell body was strinkingly large compared to most cells of the head, with an average width of 6 µm and a length of 9 to 14 µm. Their shape was rather triangular, and domed toward a long (typically 10-12 µm) and often curvy dendrite reaching the head surface (see Figure IV-22B, example 1 and 2', Figure IV-24B and C, right side). Sometimes, a clear and straight axonal projection into the main neuropile could be seen (Figure IV-22B, example 2). Despite some variability in the cell's orientation, even sometimes between both sides of an animal (e.g. Figure IV-24A), these cells were overall diagonally oriented direction relative to the antennal nerve. Due to this unique position, size and shape, these cells are named hereafter "diagonal cells".

These cells were seen to respond upon exposure to the chemical stimulus, not to the control stimulus. Contrary to all cells described so far, the response was not immediately following the onset of the chemical stimulus, but instead starting 5 to 10s atfer stimulus onset. What is more, some delay in the response seemed to accumulate upon repeated exposures. In the experiments shown in Figure IV-24B and C, the chemical stimulus was applied with a periodicity of 35s instead of the usual 70s. The cells responded consistently to the stimulation, but the beginning of the response got progressively delayed compared to the stimulus onset ; for example in Figure IV-24C, within three consecutive exposures the response accumulated a delay of 4s reative to the average stimulus onset time. The rise of calcium level in the cell body was also slower, with a maximum reached within approximately 5s, as opposed to 2-3s for other cells. A closer look at the calcium signal time series reveals that the calcium rise spreads from the tip of the dendrite towards the cell body within 2 to 3s, and then progressively fills the whole cytoplasm, indicating that the actual stimulus detection takes place long before calcium activity is seen in the cell body (data not shown).

All diagonal responses for which signal quality was sufficient to plot the activity traces have been shown in Figure IV-24Figure IV-20. More instances of responses have been seen in the recordings, for which however, due to movement artefacts, activity traces were too fragmented to be plotted.

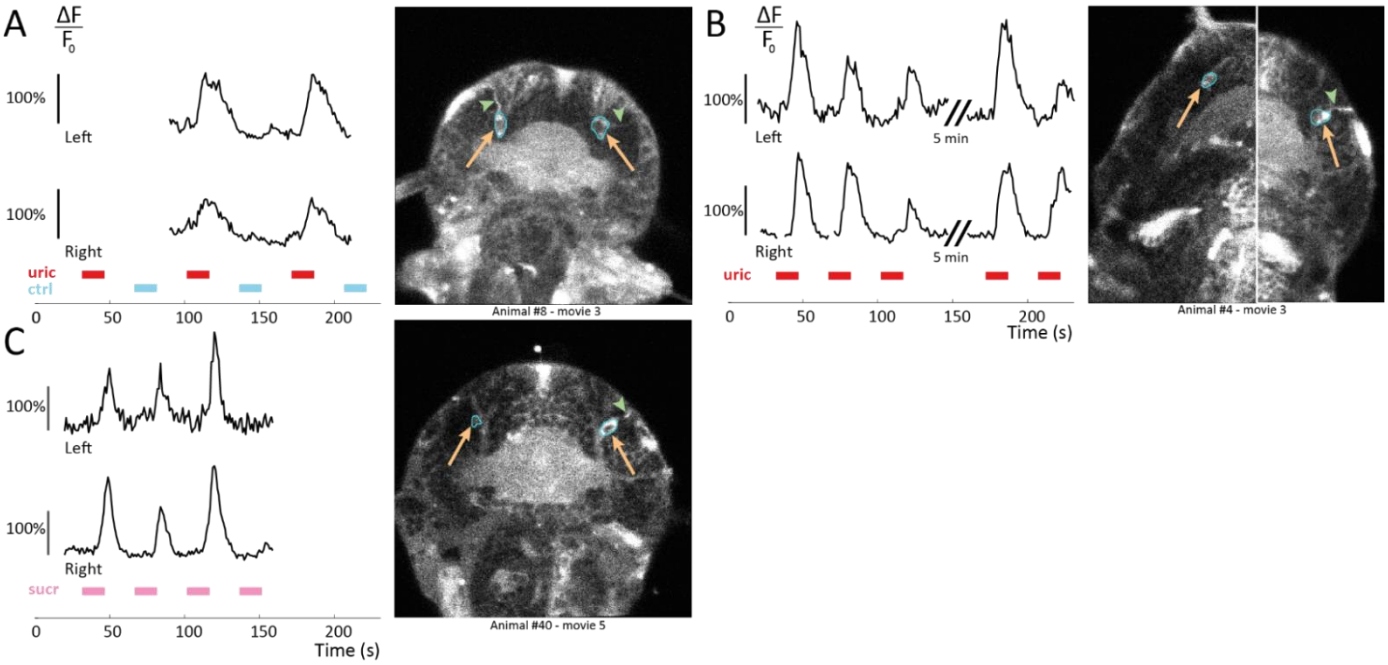


Figure IV-24 Activity traces of diagonal cells. Signal plotted as normalised variation of fluorescence $\Delta F/F_0$. Colour bars indicate the durations of chemical stimulations : uric acid (uric), sucrose (sucr), all at 10 µM. Orange arrows on the images point at the cell bodies, green arrowheads at their dendrite. The ROIs from which calcium activity was quantified are indicated in blue around the cell bodies. For all images, anterior is up, with animals imaged either from the dorsal or the ventral side. The images in (B) is combined from two different optical planes.

Interestingly, these cells are present at 4dpf, and were seen to react to uric acid during preliminary experiments in which the stimulus was delivered manually. A picture of a diagonal cell in calcium signal at 4dpf is shown in Figure IV-25. In this animal, the cell seemed to be even larger than at 6dpf, with a cell body that was 6 µm wide, 15 µm long, and a dendrite of 15 µm.

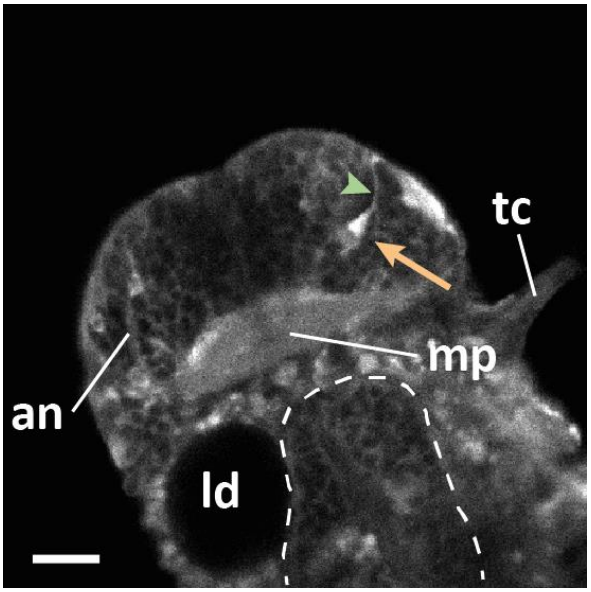


Figure IV-25 A diagonal cell seen in calcium signal in a 4dpf animal. The orange arrow indicates the cell body, the green arrowheads its dendrite. Antennal nerve (an), lipid droplet (ld), main plexus (mp), tentacular cirrus (tc). Anterior up, stomodeum outlines in dashed lines. Scale bar 20 µm.

3.5.3 Cells in the Mushroom Bodies regions

Finally, cells active upon chemical stimulation were often observed in two distinct regions corresponding to the two lobes of the Mushroom Bodies (MB). As described in Chapter III, MB at 6dpf are already developped, comprise a dorsal and a ventral lobe, and can be localised to some extent in a DAPI-tubulin staining. Each lobe's peduncle is formed, however appartenance of a cell to the MB can only be supposed based on proximity to the peduncles, which are rarely seen in the calcium signal. For all presumed MB cells considered here, the following positional criteria were used : for the dorsal lobe, close proximity to the antennal nerve, in a more lateral position, corresponding to planes of the reference immunostaining ranging from #4 to #6 (see Chapter III) ; for the ventral lobe, more ventral than the antennal nerve, posterior to the antennal ganglion, dorsal to the palpal ganglion and immediately dorsal to the antennal appendage, i.e. in a coronal plane in which the main neuropile still consists of a single piece, corresponding to plane #7 of the reference immunostaining (see Chapter III).

Figure IV-22 shows an example of calcium signal of a pair of cells in their unactive and active state, for the dorsal lobe (Figure IV-22C) and for the ventral lobe (Figure IV-22D) ; on the right a local z-projection of the reference 6dpf staining is shown. Such responses were seen in experiments involving all of the five chemical compounds. Examples of activity traces are shown in Figure IV-26, as well as the confocal plane in which the cells were observed (cells are shown in their active state, interrupted traces reflects the impossibility to follow the cell body during the whole stimulation protocol).

In both regions, these cells were seen to respond upon exposure to the chemical stimulus, not to the control stimulus, and whenever they were observed their response always co-occurred with an antennal response ; to visualise this co-occurence, the activity trace of one antennal cell is plotted for each animal in Figure IV-26. In some cases a noticeable response delay of the MB region cell compared to the antennal cell was observed (e.g. Figure IV-26E, third glutamate exposure), in some others not. Cell bodies were rather elongated in the dorsal regions, rather round in the ventral region, both with an average size (≈ 5 µm). Pairs of cells firing in synchrony were often observed in both regions (e.g. Figure IV-26B and C), though sometimes the activity trace could only be plotted for one side. Spontaneous firing of cells from these regions was rarely seen outside of the chemical stimulation period, but did take place occasionally.

There was at least one case for which additional elements made the appartenance to the MB more certain. In the experiment reported in Figure IV-26E, the presumed MB cell was seen to fire at least twice together with a nervous fibre, whose position and orientation fit exactly those of the ventral MB peduncle, as described in the reference immunostaining, plane #7 (see also Figure IV-22D). This nervous fibre and the cell body are shown on Figure IV-26E in their active state (left inset) and inactive state (right inset). This strongly suggests that this cell indeed belonged to the ventral MB lobe, and that its axonal projection running along the ventral peduncle was seen to fire together with the cell body.

All responses for which signal quality was sufficient to plot the activity traces have been shown in Figure IV-26Figure IV-20. More instances of responses have been seen in the recordings, for which however, due to movement artefacts, activity traces were too fragmented to be plotted.

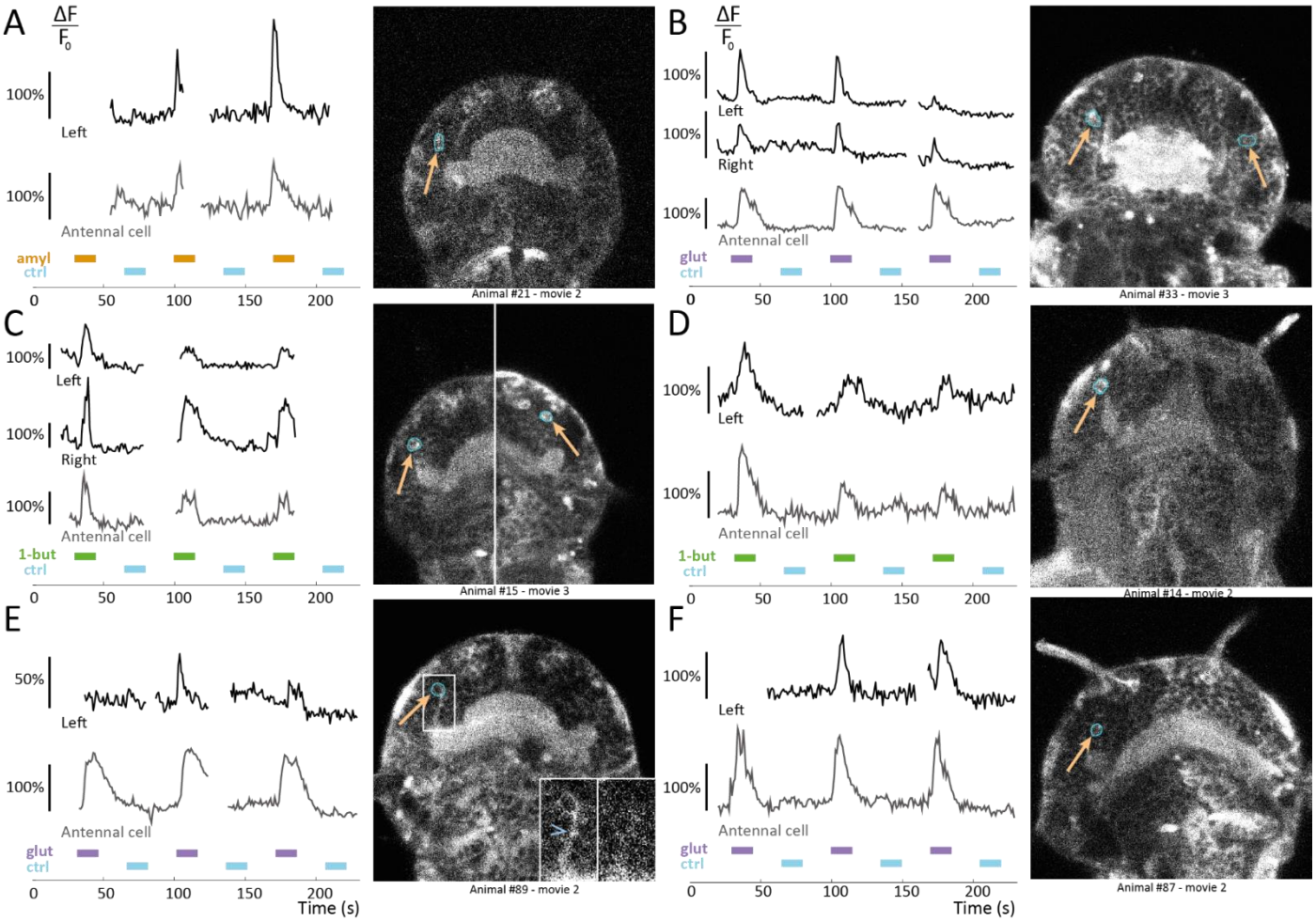


Figure IV-26 Activity traces of individual cells in the regions of the dorsal (A-B) and ventral (C-F) Mushroom Bodies lobes. Signal plotted as normalised variation of fluorescence $\Delta F/F_0$; for each animal the grey trace is recorded from an antennal cell not visible on the calcium image. Colour bars indicate the durations of chemical stimulations : amyl acetate (amyl), glutamate (glut), 1-butanol (1but), all at 10 µM. Orange arrows point at the cell bodies, blue empty arrowheads at Mushroom Bodies peduncles. The ROIs from which calcium activity was quantified are indicated in blue around the cell bodies, except for the antennal cell. For all images, anterior is up, with animals imaged either from the dorsal or the ventral side. The images in (C) is combined from two different optical planes. The insets in (E) show the cell in its active state (left inset) and inactive state (right inset).

3.6 Calcium activity outside of the candidate chemosensory organs, with no direct link to the chemical stimulations

Whole-brain recordings have revealed two additional types of cells, which had an obvious calcium activity, a peculiar shape and position, as well as some synchronisation properties. This in itself was enough to motivate their description hereafter. Moreover, this calcium activity, in most cases unrelated to the chemical stimulation, turned out to have some relation with in a few cases.

The first of these cells were located in the region of the apical organs, close to the neurosecretory plexus. The second ones were frontal cells located more anteriorly, more medially, and slightly more dorsally than the antennal nerves. Examples of these cells in the calcium channel are provided in Figure IV-27A and B respectively, as well as local z-projections of the reference 6dpf staining.

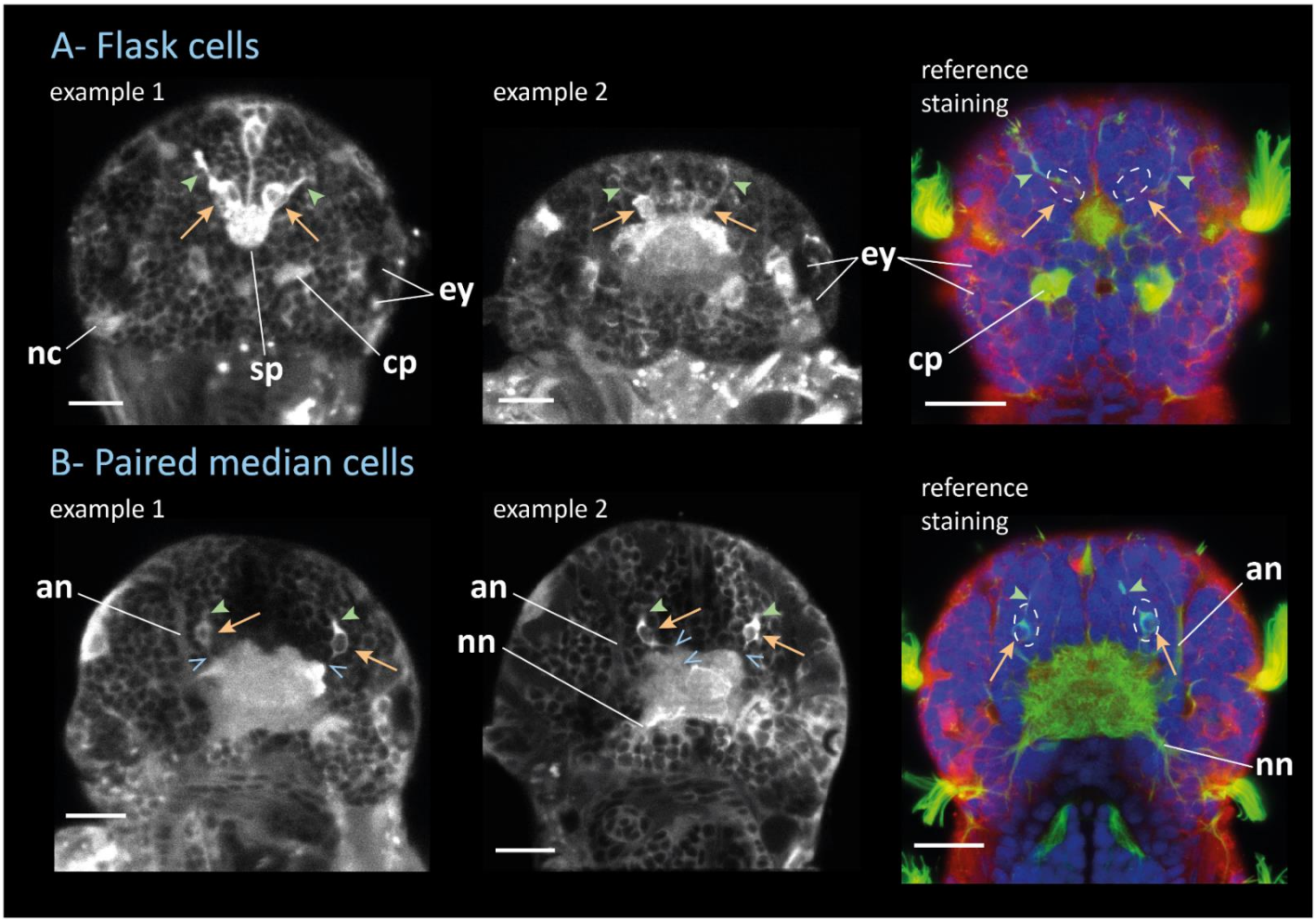


Figure IV-27 Position of individual cells outside of the candidate chemosensory organs, which show obvious calcium activity but no direct link with chemical stimulations : flask cells (A) and paired median cells (B). Left and central column : calcium signal, examples of cells in their active state ; orange arrows indicate active cell bodies, green arrowheads their dendrites, empty blue arrowheads their axonal projection. Right column : corresponding plane from the reference 6dpf immunostaining ; dashed lines indicate the approximative position where the cell bodies have been seen, orange arrows and green arrowheads indicate cells and their cellular extension that are revealed by the tubulin immunostaining and could correspond to the cells observed in the calcium channel. Antennal nerve (an), ciliary photoreceptors (cp), pigmented eyecups (ey), nuchal cavity (nc) and nerve (nn), neurosecretory plexus (sp). All animals 6dpf, scale bar 20 µm

3.6.1 Flask cells

A characteristic population of cells was often seen to be active in the apical organ region, of which most often only one bilateral pair was observed. In every animal in which these cells were active, they displayed permanent calcium fluctuations, that did not have any obvious relation with the chemical stimulation. Such fluctuations were observed in experiments involving all of the five chemical compounds tested. Figure IV-27A shows two examples of such cells as they appear in the calcium channel. In example 1, the cells are a clear bilateral pair and are seen coactivated with the neurosecretory plexus. In example 2, the animal had the front of its head tilted towards the bottom, which gives a different angle of view (with one cirrus visible on the left side), preventing to see the neurosecretory plexus but allowing to see the cellular extension reaching the head surface (right side).

Their general shape is that of a flask, therefore they are hereafter named “flask cells”. Whether or not these cells are the same as the flask cells known to be present in *Platynereis*’ apical organ at 48hpf ([68], [75], [236], see Chapter II) will be dealt with in the discussion part. The position of their cell body corresponds approximately to plane #2 of the reference 6dpf immunostaining (see Chapter III). This staining actually reveals two tubulin-rich structures which seem to reach the head surface (Figure IV-27A, arrowheads), and whose position may be similar to that of the flask cells’ dendrite as seen in the calcium channel.

Figure IV-28 shows examples of activity traces for such cells, as well as the confocal plane in which they were observed (cells are shown in their active state, interrupted traces reflects the impossibility to follow the cell body during the whole stimulation protocol). For each animal, an activity trace of the neurosecretory plexus is also provided. In most cases where flask cells were seen to be active, a bilaterally symmetric pair of cells was observed, that was located anteriorly and laterally to the neurosecretory plexus. These cells had a round and large cell body (≈ 10 µm), a long (> 8 µm) and thick (≈ 1.5 µm) dendrite, oriented towards the front of the animal with an angle of approximately 45° relatively to the midline. In a few instances, more than two active cells were seen in this region of the apical organ, which were all of comparable size. Some of them had the canonical flask shape, while others did not have an obvious dendrite. Figure IV-28D shows such an example upon uric acid stimulation : the cell ‘Right 2’ has the canonical flask shape, but the cells ‘Left’ and ‘Right 1’ do not seem to have an obvious dendrite.

Activity traces reveal that these flask cells had significant variations of their cytoplasmic calcium levels, on the order of 100 to 200 %, and most often fluctuated in synchrony (Figure IV-28C-J), though a few instances of one cell fluctuating without the other were occasionally seen (Figure IV-28A, B, as well as F first peak). The neurosecretory plexus activity was tighly correlated with that of the flask cells (true in all cases, but notably Figure IV-28E, G), as on the one hand any calcium increase observed in at least one of the flask cells coincided with a calcium increase in the plexus, and on the other hand no significant calcium increases in the plexus were seen that did not coincide with a calcium increase of at least one of the cells. In some cases, this synchronous activity of cells and plexus seemed to have some rythmicity (Figure IV-28E, G, J), in other cases this activity appeared totally irregular (Figure IV-28A, D, F, H). When some rythmicity was observed, it did not obviously correlate with the timing of the stimulation protocol, indicating rather an independence of the flask cells’ fluctuations with regards to the chemical stimulations.

Even if the calcium fluctuations themselves do not show any apparent link with the stimulations, these fluctuations could nevertheless be influenced by them. For example, the fluctuations could be taking place only in the presence of chemical stimulation. To test this hypothesis, brain activity was recorded in the whole-brain using the same stimulation protocol but only the control stimulus, and before any chemical stimulus was introduced in the microfluidic chip, to ensure a total absence of stimulation by any of the five chemicals compounds studied. Then, one chemical stimulus was loaded in the chip and the usual experiment was conducted. Activity traces are provided for one animal, upon repeated stimulation with the control stimulus only (Figure IV-28I), and with glutamate alternating with the control stimulus (Figure IV-28J). Prior to any chemical stimulation, the flask cells already displayed a fluctuating activity, synchronised with the neurosecretory plexus, that persisted when glutamate was later applied. Thus, fluctuations in the flask cells’ calcium levels do not require a chemical stimulation to happen. It should be noted that in this example the rhythmicity of the fluctuations seems to have been stronger before the introduction of glutamate.

Only part of all flask cell responses observed have been shown in Figure IV-28 for clarity, more examples of activity traces and their corresponding images are available in Appendix F. Yet more instances of responses have been seen in the recordings, for which however, due to movement artefacts, activity traces were too fragmented to be plotted.

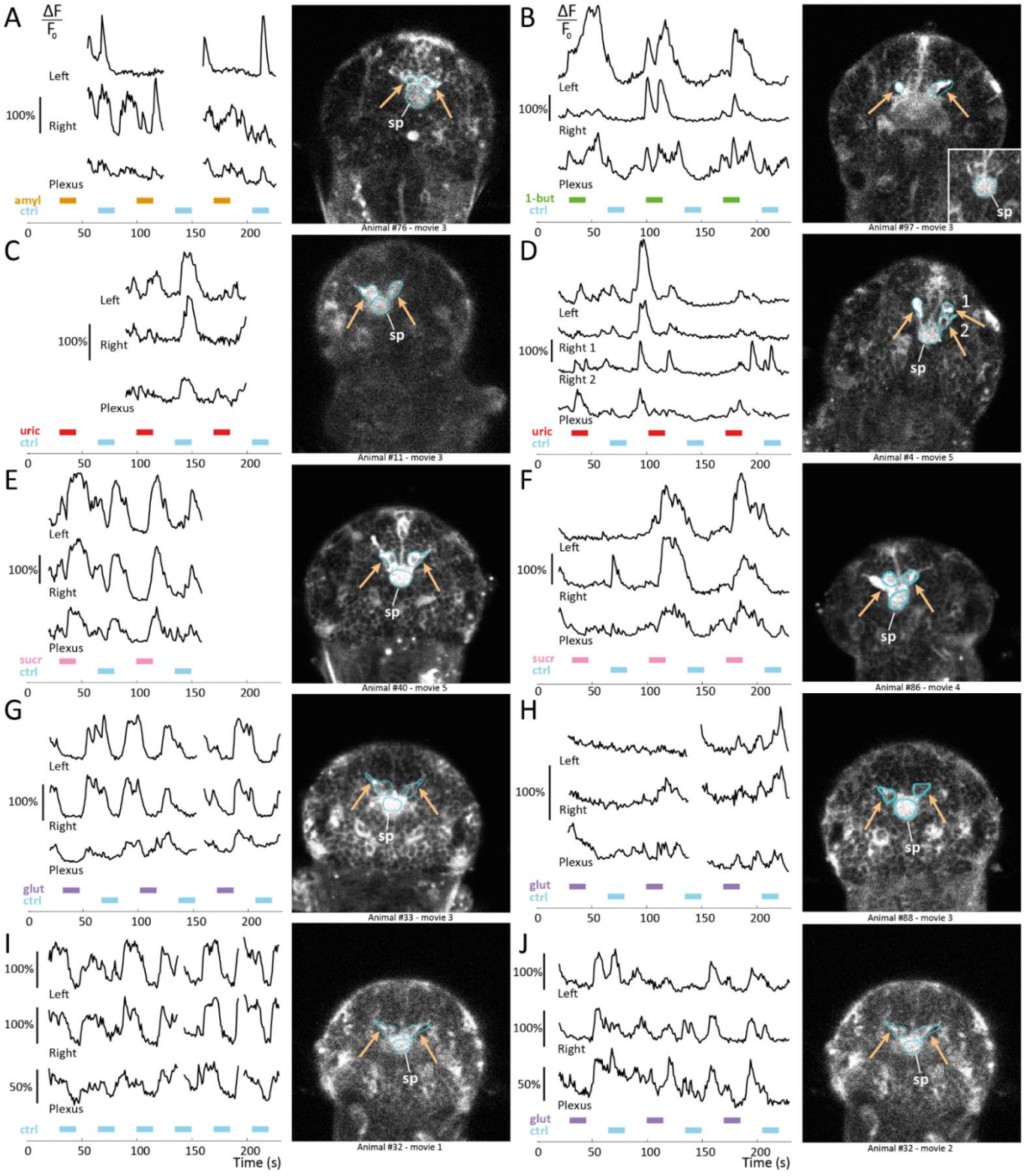


Figure IV-28 Activity traces of individual flask cells and neurosecretory plexus, in the apical organ region. Signal plotted as normalised variation of fluorescence $\Delta F/F_0$. Colour bars indicate the durations of chemical stimulations : amyl acetate (amyl), glutamate (glut), uric acid (uric), 1-butanol (1but), sucrose (sucr), all at 10 µM. Orange arrows point at the cell bodies, the white line at the neurosecretory plexus (sp). The ROIs from which calcium activity was quantified are indicated in blue around the cell bodies and the plexus. For all images, anterior is up. All animals imaged from the dorsal side, except #11 (C) and #32 (I, J), imaged from the ventral side. The inset in (B) shows with the same scale the neurosecretory plexus, located in the next more dorsal imaging plane compared to the cell bodies shown.

Interestingly, in a few animal in which flask cells were rhythmically fluctuating, a pair of unknown cells was sometimes seen that fluctuated in tight synchrony with the flask cells. These cells were located immediately anterior to the eyes, approximately in the same coronal plane as the nuchal organ's revolver cells, i.e. in plane #4 of the 6dpf reference immunostaining (see Chapter III), had a rather average cell body size, and no obvious dendrite or axon. They were named "eyefront cells". Figure IV-29 shows three instances of striking synchrony between flask cells and eyefront cells, that does not appear to be related with the chemical stimulation.

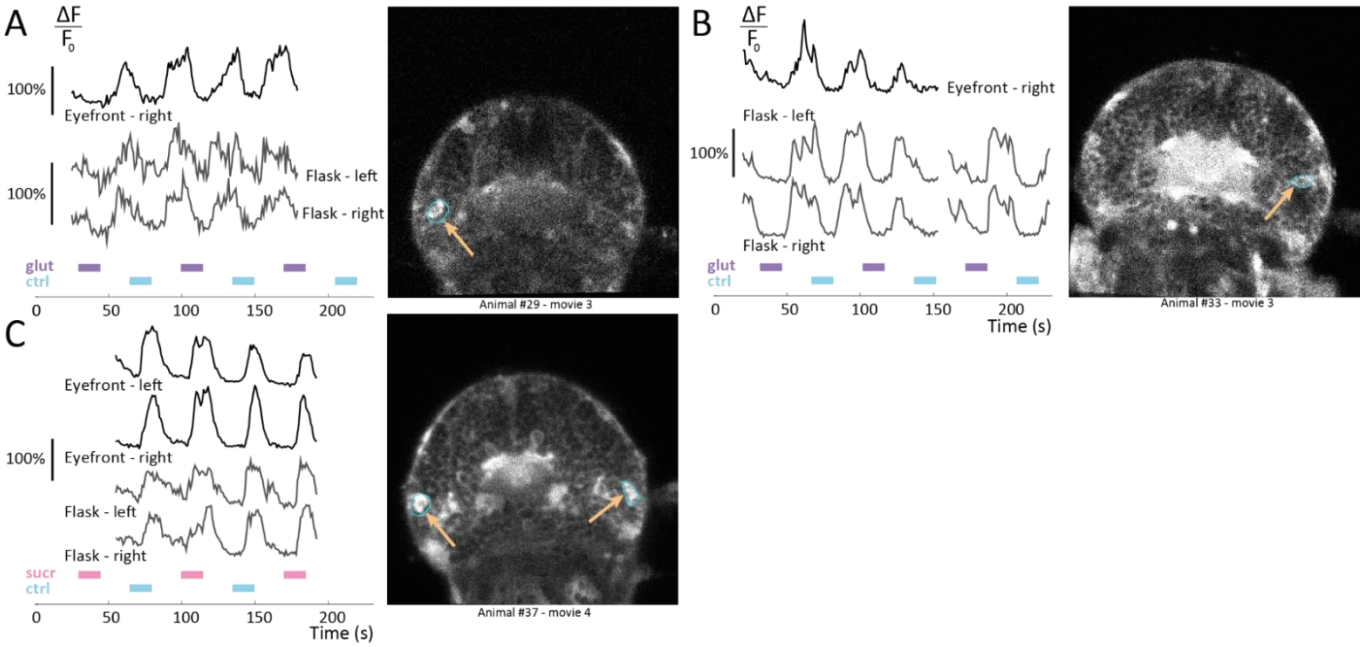


Figure IV-29 Activity traces of eyefront cells and flask cells. Signal plotted as normalised variation of fluorescence $\Delta F/F_0$; for each animal the grey traces are recorded from the flask cells which are not visible on the calcium image. Colour bars indicate the durations of chemical stimulations : glutamate (glut), sucrose (sucr), both at 10 µM. Orange arrows point at the cell bodies. The ROIs from which calcium activity was quantified are indicated in blue around the cell bodies, except for the flask cell. For all images, anterior is up, with animals imaged either from the dorsal or the ventral side.

3.6.2 Paired median cells

Eventually, a frontal pair of cells also showed a striking activity. Figure IV-27B shows two examples of these cells as they appear in the calcium channel, as well as a local z-projection from the 6dpf reference staining. These cells were located anterior to the main neuropile, between the antennal nerves and slightly more dorsal than them, i.e. in a coronal plane corresponding approximately to plane #4 of the reference 6dpf immunostaining (see Chapter III). These cells seemed to have an anterior dendritic extension, and their axonal projection into the main neuropile was often visible in the calcium signal (see arrowheads in Figure IV-27B). The tubulin staining reveals what seems to be two tubulin-rich cell bodies together with tubulin-rich cellular extensions, in a position similar to that of these cells observed in the calcium recordings (Figure IV-27B, right). In almost all instances, these cells were observed as a bilaterally symmetric pair, with no resembling cells at immediate proximity. Due to this, and to their position, they are named hereafter "paired median cells". Figure IV-30 shows examples of activity traces for the paired median cells, as well as the confocal plane in which they were observed (cells are shown in their active state, interrupted traces reflects the impossibility to follow the cell body during the whole stimulation protocol).

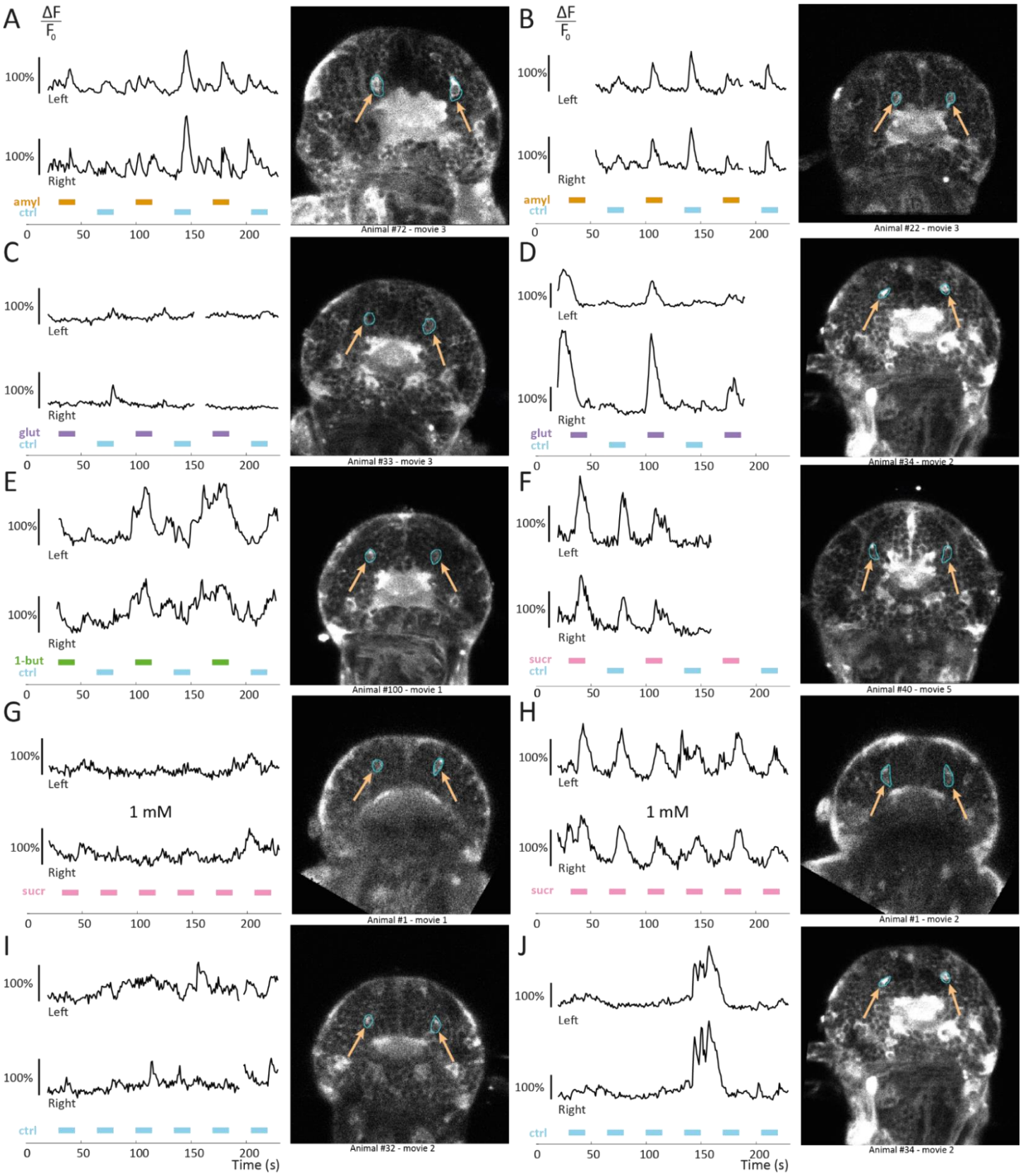


Figure IV-30 Activity traces of the paired median cells. Signal plotted as normalised variation of fluorescence $\Delta F/F_0$. Colour bars indicate the durations of chemical stimulations : amyl acetate (amyl), glutamate (glut), 1-butanol (1but), sucrose (sucr), all at 10 µM. Orange arrows point at the cell bodies. The ROIs from which calcium activity was quantified are indicated in blue around the cell bodies and the plexus. For all images, anterior is up. Animals imaged from dorsal or ventral side.

Activity traces reveal that these cells sometimes had an abundant calcium activity, with amplitudes of variation of typically 100%, and up to 300%. The activity is tightly synchronised between the pair, as can be seen from all recordings available. In a significant number of the cases, the activity peaks of these cells did not co-occur with the chemical stimulations (Figure IV-30A, C, E), while in a number of other cases they did (Figure IV-30B, D, F). However, the activity peaks were sometimes seen to co-occur with the chemical stimulus only (e.g. Figure IV-30D), and sometimes with both chemical and control stimuli (e.g. Figure IV-30B, F). This suggests that the paired median cell are able to respond to both stimulations, though this response does not seem systematic.

To further test whether a repeated chemical stimulation can induce activity in these cells, an animal was stimulated six times with 1 mM sucrose at a 35s-periodicity, and the experiment repeated a second time after 5 minutes. During the first experiments (Figure IV-30G), the paired median cells displayed small and irregular calcium fluctuations on the order of 50%, that had no obvious correlation with the chemical stimulation. In the second experiment, after 5 minutes devoid of chemical stimulation, the cells were seen to fire consistently after each stimulus onset. These observations reinforce the plausibility that the paired median cell are indeed able to respond to chemical stimulations.

As for the flask cells, the existence of calcium responses in the paired median cells could be conditioned to the presence of chemical stimuli. To test this hypothesis, several animals were imaged while exposed repeatedly with the control stimulus only, and before any chemical stimulus was introduced in the microfluidic chip. Two examples of activity traces shown here indicate that both irregular fluctuations (Figure IV-30I) and peaks of large amplitude (Figure IV-30J) can take place in the paired median cells even in the absence of a specifi chemical stimulation. However, no consistent response to the onset of the control stimulus was observed, contrary to the experiments reported in Figure IV-30B and F.

Only some of the paired median cell responses observed have been shown in Figure IV-30Figure IV-16 for clarity, more examples of activity traces and their corresponding images are available in Appendix F. Yet more instances of responses have been seen in the recordings, for which however, due to movement artefacts, activity traces were too fragmented to be plotted.

3.7 Calcium activity at the head surface

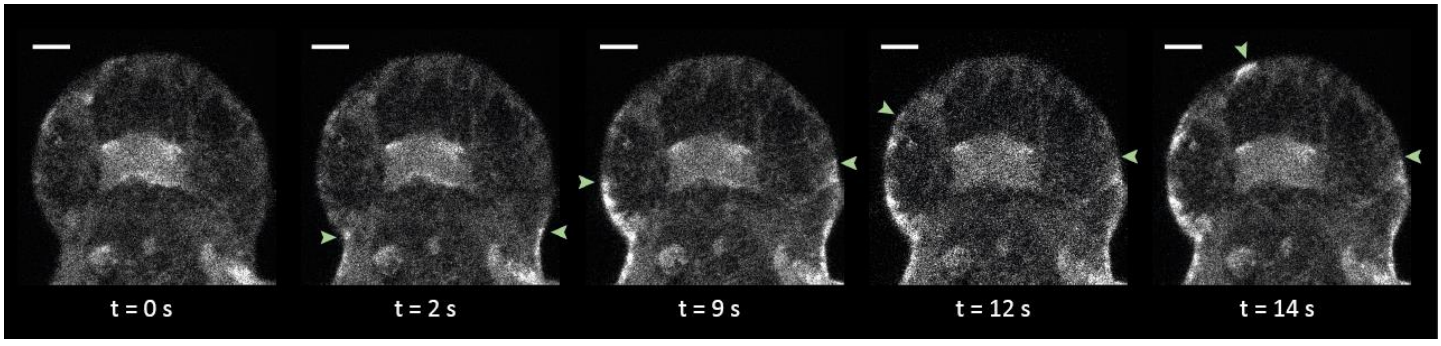


Figure IV-31 Example of calcium propagation in the head of a 6dpf animal. Green arrowheads point at the calcium front travelling from posterior to anterior. Anterior up, scale bar 20 µm.

In the majority of animals observed during these experiments, abundant and permanent calcium fluctuations was observed at the surface of the head. This activity was particularly visible when looking either at the most dorsal or most ventral plane of the animal, and seemed to take place in superficial, thin and wide epithelial cells. Events of calcium propagation were frequently observed at the surface of the animal, that sometimes appeared to be related to its movement, though not always. An example of such propagation in an immobile animal is shown in Figure IV-31. Whether these calcium fluctuations have some importance in the physiology of the animal or are mere passive phenomena is unknown, but could be worth investigating.

IV – 4 Discussion

4.1 Chemosensory systems in the head of 6dpf *Platynereis* larvae

These calcium imaging experiments constitute the first direct and comprehensive physiological study of chemosensory systems in an annelid. They have allowed to test the chemosensory function that had been hypothesised for several head organs, and reveal so far unidentified brain areas involved in chemosensation.

4.1.1 Chemosensory organs and cells

4.1.1.1 Nuchal organs

Nuchal organs are the most conserved sensory organs in polychaetes. Based on morphological descriptions, their chemosensory function had been hypothesised for more than a century and repeatedly proposed since then [93], [116], [122], [173], as detailed in Chapter II. However, no experimental proof was ever provided, and this study provides the first physiological pieces of evidence concerning nuchal organs chemosensitivity.

The present experiments have revealed, the existence in the larval nuchal organs of chemosensory cells that reproducible responses to uric acid and sucrose. For the three other compounds, the few responses observed leave it unclear whether the nuchal organs do really detect them. The possibility that these cells could have responded not to the chemical stimulus, but to the flow disturbance associated with the stimulus delivery, is excluded by the total absence of responses when this flow disturbance alone is provided as a stimulus. In whole-brain imaging settings, activity traces of individual cells showing reproducible responses could be plotted for 5 animals, and activity traces for single instances of response for a total of 12 other animals. In single-plane imaging settings, reproducible responses of the revolver cells to uric acid could be plotted for at least 11 animals.

For nuchal organs in general, no compartmentalisation is visible at 6dpf, and the primary criterion to decide whether a cell body belongs to them or not is proximity with the nuchal cavity, i.e. a weak criterion. However, additional elements of morphology have allowed here to make more certain statements. In many animals, a characteristic bilateral pair of cells, the revolver cells, was seen to respond. These two cells had a clear axonal projection running along the nuchal nerve towards the main neuropile, and possess a curved dendrite that reaches into the nuchal cavity, leaving no doubt about their neuronal nature and their belonging to the nuchal organs. What is more, their morphology is fully consistent with the general sensory cell morphology described in the nuchal organs of various polychaetes [122], [128]. For other cells which did respond in the nuchal organ regions, no dendrite could be observed but the frequent presence of an axon, or at least the coactivation of the nuchal nerve with the cells, make it quite likely that they would indeed be nuchal organ neurons. Nevertheless, only a approach such as serial-section-based tracing of all cells in this region would confirm the outlines of the nuchal organs at 6dpf. Such an approach has been taken already at 3dpf, which has revealed that sensory cells are indeed located in immediate proximity to the nuchal cavity [253]. Two pairs of interneurons have been identified at 3dpf, which are posterior to the main plexus, and rather medial, hence the cells observed here for which no dendrite was seen are nevertheless likely to be sensory cells, due to their lateral position.

The responses of nuchal organ neurons were not systematic, and differences were observed between compounds, with uric acid being the compound that activated the most frequently the nuchal organs. For the other compounds, the responses did not have reduced amplitudes but rather a reduced likelihood of occurrence. These data suggest that nuchal organs possess some ability to discriminate between chemical stimuli, and could indicate that any stimulus coding would be rather based on

frequency of response than on amplitude. This would explain why the responses observed for stimuli other than uric acid were not of smaller amplitude, but rather of rarer occurrence.
Targeted imaging of the revolver cells has revealed that they respond consistently to a 10 µM uric acid stimulation, and that their cell body displays a reproducible calcium activity. The observation of a calcium increase in the axon prior to the increase in the soma suggests that, for this particular pair of cells, the primary signal transduction at the level of the nuchal cavity does not rely on calcium channels but rather on other ion channels.

Uric acid, the compound that was found to most strongly activate the nuchal organs, is known as an adult pheromone triggering sperm release above threshold concentrations on the order of 1 µM. Uric acid as a pheromone is already an unusual molecule, since it is a common animal metabolic product and used at a high concentration, while pheromones are generally specific products and used at much lower concentrations – typically in the nanomolar range [278] and even down to the picomolar range in the example of salmons [279]. While uric acid is more specifically detected by the nuchal organs that an amino acid such as glutamate, it is unclear whether this molecule would be relevant as a pheromone for larvae, for example indicating the presence of conspecifics. If such is the case, behavioural test of attraction or repulsion could inform as to whether for larvae the presence of conspecifics is beneficial (e.g. suitable place for settlement) or detrimental (e.g. resource competition).

Overall, these results show that nuchal organs in *Platynereis* are indeed chemosensory as their cellular morphology suggested. However, the low rate of responses leaves some doubt as to whether their sensory spectrum is as vast as was expected from the broad distribution of these organs in polychaetes. Since 6dpf larvae already show the typical nuchal organ architecture found in adult polychaetes, there is no reason to think that nuchal organs would not be chemosensory too in adults.

4.1.1.2 Palps

These sensory appendages are the second most widespread in polychaetes after the nuchal organs [104], are considered to be homologous [124], and are generally thought to be chemosensory or mechanosensory. In spionid polychaetes, palps are feeding structures, and their chemosensory role has been supported by activity-dependant cell labelling upon chemosensation [154]. In nereids, the effect of palp ablation on chemical avoidance behaviour reported by Gross in *Nereis virens* [170] had suggested that palps are chemosensory, though it is unknown whether the ablations could be conducted without further injury of the animals. So far, there was thus only indirect proof for the chemosensitivity of polychaete palps.

In the present experiments, some cells - rarely more than two per palp - were occasionally observed in the palpal ganglia that showed a calcium response to the chemical stimulus and not to the flow control. These responses could be reproduced in a total of 9 animals, with at least one instance for each of the five chemical compounds tested. These cells often appeared to be bilateral pair, based on position, shape, size and synchrony, and were located at various positions inside the palpal ganglia, with no doubt as to whether they truly belonged to them. No such cell was seen in the protruding tip of the palps, though it does contain cell nuclei (see Chapter III), suggesting that this tip may contain other cell types.

These data show that *Platynereis* palps are endowed with chemosensitivity. However, the number of cells that responded to the stimulations was very low compared to the total number of cells that constitute the palpal ganglia, which raises the question of what all other cells do. Some may not be neurons but rather supporting cells. In case most cells of the palps were indeed chemosensory neurons and not only the small population observed here, this would mean that these late nectochaete larvae are potentially able to detect and discriminate a large number of compounds, and that palps possess a vast chemosensory repertoire. Yet, it is also possible that some cells are neurons supporting a different function, for example mechanosensory. In fact, it would not come as a surprise if palps were mechanosensory, as in nereids they are in permanent contact with the substrate on which the animals

crawl. Moreover, since they are located on each side of the mouth, they are likely to come in contact with food at every feeding event, and could probe food texture by touch. In *Platynereis* adults, palps can in fact be seen to be used in food grasping (personal observations).

While one can assert with some confidence that palps are chemosensory, it seems that the set of stimuli used in the present experiments provoked only minor responses, if one compares with the calcium responses observed in the antennae. This could be the sign of a much larger repertoire as noted above, but could also mean that the stimuli used do not belong to the main class of stimuli detected by the palps. Notably, if palps are indeed involved in food chemoreception as their position and morphology suggests, it is possible that they would detect contact chemical cues, yet such molecules typically have a low water solubility and have thus quite different physico-chemical properties than the molecules tested here. For example, hydrophobic compounds such as terpenes are known to cover the surface of marine animals such as corals, sponges or nudibranch molluscs, and to be used as contact chemical cues by shrimps or fish [280][181]. One can imagine that such cues would be found at the surface of food items eaten by *Platynereis*, and would activate palp chemosensory cells upon contact. They may however not be detected by antennae, which are less likely to come in contact with food. To decide on the validity of this speculation however, a different experimental setup would probably be needed, as this setup was designed to deliver waterborne stimuli, which by definition excludes hydrophobic compounds. It could be tried to coat small inert beads with such hydrophobic compounds, though it is unclear whether they would effectively come in contact with the palps.

4.1.1.3 Antennae

In this set of experiments, antennae were the organs that showed the most systematic calcium responses to chemical stimulations. This finding is rather surprising, since in annelids a major chemosensory role has been hypothesised for nuchal organs, and to a lesser extent for palps, but never for antennae. The only piece of physiological evidence supporting their chemosensory role comes from the experiments conducted by Gross in 1921, who reported a delayed behavioural reaction to aversive chemicals after antennal ablation in *Nereis virens* [170].

Cells responding to the chemical stimulation and not to the flow control have been observed in the antennal regions for each of the five chemical compounds tested, indicating a clear link between these responses and the chemical stimuli. Activity traces of individual cells showing reproducible responses could be plotted for a total of 23 animals, and activity traces for single instances of response could be obtained for yet more animals, leaving no doubt about the reality of these responses. Even though activity traces have been shown only for one, two or three cells per antenna, more cell bodies were frequently seen to respond. In general, no habituation of these response was seen. Since antennal ganglia are already delimited at 6dpf (see Chapter III), there was thus little doubt that these cells were indeed antennal cells. Moreover, the antennal nerves were consistently seen to fire at the same time as the cells, further supporting the idea that these cells are antennal neurons. In a few cases (e.g. Figure IV-16D), a dendrite going into the appendage could be seen that belonged to a responding cell, indicating that the responses observed in the antennae generally involved sensory neurons.

When a chemical stimulus was applied, the number of antennal cells which were seen to respond was on the order of 5, that is, low compared to the total number of antennal cells (more than 50). As for the palps, one can wonder what the function of the remaining cells would be. Some may not be neurons, and rather supporting cells such as glial cells, which are known to exist in larval *Platynereis* [81]. Some may be neurons involved in the detection of other stimuli, chemical or not. Some chemosensory neurons may also have displayed a calcium response that was too small compared to the noise and could not be detected. Another possibility would be that different compounds activate different neurons, and thus even if chemosensory neurons may be numerous in the antennal ganglia

only a subset of them would respond upon a particular chemical stimulation. If this was the case, this would speak in favour of antennae being capable of discriminating between stimuli.

To test this specific point, preliminary experiments were conducted with two different chemical stimuli per animal and the usual stimulus timing, while only the volume of the antennal ganglia was being imaged in multi-plane settings. Such experiments were aimed at visualising individual neurons that would consistently show a different calcium response for the two stimuli. Unfortunately, the first data analysis was so far inconclusive due to data quality (data not shown). These data could be reanalysed in more detail, or the experiments reconducted and extended.

While it seems reasonable to think that all cells that responded to the chemical stimulations were neurons, it cannot be asserted that they were all sensory neurons. In many instances of response, one or two firing cells were seen at the distal end of the antennal nerve, i.e. in the part of the ganglion that is most distant from the appendage. Such cells may well have been interneurons, and one cannot exclude that some signal integration takes place within the antennal ganglion, with a first layer of sensory neurons having their dendrite in the appendage, and a second layer of interneurons receiving input from them and sitting in a more dorsal part of the ganglion. Nothing in the current data allows to decide on that point, and ideally a tracing of antennal neurons based on serial-section electron microscopy should be conducted at 6 dpf to answer the question.

Overall, these results clearly demonstrate the chemosensory function of antennae in *Platynereis* late nectochaete larvae. Based on the small but varied set of compounds tested, these organs appear to be general detectors of chemical stimuli, and nothing speaks against them being capable of stimulus discrimination. Given the similarity of organisation in larval and adult antennae, as well as the developmental continuity documented in Chapter III, it is reasonable to assume that antennae play an important role in chemosensation in adult *Platynereis* too. Even though no indication of flow detection by the antennae was found here, it is still possible that antennae also detect mechanical stimuli, for example contact with objects that the animal would encounter frontally while crawling on the substrate. A mechanosensory function of the antennae has been proposed based on cell morphology for the errant worm *Ophryotrocha puerilis* (Dorvilleidae, [151]), as well as for the sedentary worms *Sabella pavonina* (Sabellidae, [143]) and *Lanice conchilega* (Terebellidae, [144]).

4.1.1.4 Tentacular cirri

For the fourth type of head appendages found on the head of polychaetes, the tentacular cirri, there are a few suggestions of a chemosensory function in *Nereis*, mostly based on the morphology of sensory cells [145]. The present experiments add physiological support to this hypothesis, though a low rate of response was observed upon chemical stimulations, and more observations would be needed to make a definitive claim.

Calcium responses to the onset of a chemical stimulation were indeed seen for 9 animals in cells unambiguously located in the cirral ganglia, though activity traces with more than one instance of response could be plotted in only 5 animals. The cell shape – elongated towards the cirral appendage – and the occasional presence of a dendrite suggest that these cells were indeed neurons, and most likely sensory neurons, but no firing of the cirral nerve could be observed together with a response of such cells. At least one instance of response has been observed for each of the five compounds tested, suggesting that cirri are capable of detecting a large variety of compounds, as do antennae, nuchal organs and palps, though with overall rare or weak responses.

Tentacular cirri can detect touch stimuli, as any simple behavioural experiment on adults reveals. Various elements such as morphology, length and position, speak in favour of cirri being elaborate mechanosensory organs. Their surface is covered with numerous sensory cilia. Their disposition in space provides a good sampling of the free water volume located above the animal's body, with shorter cirri (ventral ones) directed towards the substrate and longer cirri (dorsal ones) directed

upwards. The thus would seem to adequately inform the animal about the presence of objects around its head. For this reason, it is reasonable to assume that a significant part of sensory cells in *Platynereis* tentacular cirri should serve mechanoreception – though it is unknown whether cirri are also mechanosensory in 6dpf larvae. If this is true, then the cirri may have only a small population of cells capable of chemosensation, and may thus be endowed only with a low degree of chemosensitivity. This would be in agreement with Gross's observation in 1921 that ablation of tentacular cirri in *Nereis virens*, in contrast to ablation of palps or antennae, did not cause a difference in behavioural response towards various aversive chemicals [170], and hence their chemosensitivity seemed lower. On the opposite, tentacular cirri could as well be dedicated chemosensory organs in their own rights, and the stimuli used here may not have been the most adequate to reveal their chemosensitivity.

Overall, a dual chemo- and mechanosensory function of tentacular cirri in *Platynereis* is most likely, and would be in agreement with the two populations of surface sensory cells described in Chapter III. More experiments are needed to determine to which extent these head cirri are specialised chemosensory organs.

4.1.1.5 Apical organ

In polychaete larvae as well as in many other marine trochophore larvae, the apical organ is thought to be a sensory structure involved in the modulation of larval settlement and metamorphosis (see Chapter II). In *Platynereis*, there is strong support for an involvement in larval settlement, which is thought be triggered by chemosensation, though only indirect proof of a chemosensory function could be found for the apical organ [75].

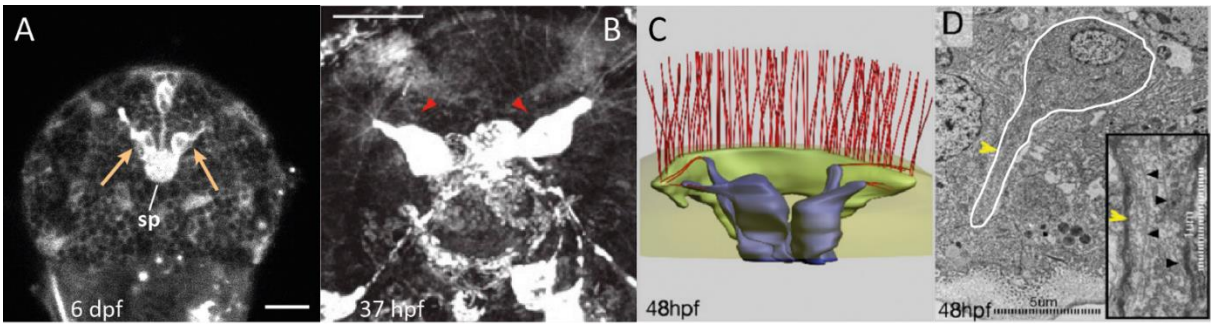


Figure IV-32 Flask cells in the Platynereis apical organ region, observed at 6dpf (A) 1.5 dpf (B) and 2 dpf (C-D). (A) GCaMP6s fluorescence signal in a dorsal confocal plane of the head ; sp = neurosecretory plexus. Dorsal view, anterior is up. (B) MitoTracker fluorescent staining of the apical organ region, with flask cells indicated by arrowheads. Frontal view, ventral is up. Modified from Conzelmann et al., PNAS 2013 [19]. (C) Schematic reconstruction of four flask cells (purple) in the apical organ, showing their thick sensory dendrite with their sensory cilia (red) at their tip. (D) One of the transmission electromicrographs one which (C) in based, showing the thick sensory dendrite (indicated by the yellow arrowhead), and outlines of the cell body in white solid line. Inset : zoom on the dendrite. (C) and (D) : adapted from Tessmar et al., Cell 2007 [20]. Scale bar in (A) and (B) : 20 µm.

The present calcium imaging experiments have revealed in many animals the activity of a bilateral and characteristic pair of cells located in the apical organ region, anterior to the neurosecretory plexus. These cells had a consistent morphology, position and orientation between animals, with a flask shape and a thick dendrite oriented frontwards with an angle of approximately 45° degree compared to the midline. These cells have a striking resemblance with a population of flask-shaped apical organ cells already described at 1.5 and 2 dpf (see Figure IV-32). At 2dpf (48hpf), at least four such cells are known to be present in the apical organ region (Figure IV-32C, D), which express the neuropeptide FMRF-amide, and are thought to be of both sensory and neurosecretory nature [68]. At 1.5 dpf (37hpf), two such flask cells have been described in the apical organ region which are neurosecretory, are revealed

by dye-filling which is a property of chemosensory neurons, and are known to express at 52 hpf the MIP molecule involved in larval settlement. It should be noted that the relative position of the apical organ in the head changes between 2 and 6dpf, progressively transitioning from an apical, i.e. frontal, position at 2 dpf, to a dorsal position at 6dpf. In this way, the frontal pair of dye-filled neurons that are oriented ventrally on Figure IV-32B (image with ventral up) and the dorsal pair of calcium-active cells oriented frontally in Figure IV-32A (image with frontal up) have a similar position relative to the apical organ.

Whether the flask cells active in the calcium experiments at 6dpf are the same as the MIP-expressing flask cells seen at 1.5-2 dpf cannot be asserted based only on this data, but is quite likely. These cells could also express the FMRF-amide neuropeptide, though the fact that the MIP cells were described with one sensory cilium whereas the FMRF cells were described with two would speak against their identity. To decide on this point, laser ablation experiments of the flask cells seen in calcium signal could be performed, and followed by a joint MIP and FMRF immunostaining. This would reveal whether these cells indeed express one or both of these markers.

Though the flask cells are not seen in all animals at 6dpf, whenever they are active the calcium signal reveals permanent fluctuations, that are in some cases rather periodic, in some case rather irregular. Yet, these fluctuations do not depend on the presence of a repeated chemical stimulation, as experiments involving only the flow control have revealed. In all cases for which activity traces could be plotted, a clear synchrony was observed between activity in the flask cells and in the neurosecretory plexus, suggesting that these flask cells are indeed neurosecretory and project to this plexus. This observation reinforces the hypothesis that the 6dpf flask cells are identical to the MIP cells or to some of the FMRF cells.

Nevertheless, the calcium signal did not reveal any obvious relationship between the applied chemical stimulation and the activity of the flask cells at 6dpf, casting some doubt on their presumed chemosensory function. The MIP expressing flask cells are thought to detect some environmental chemical cue, though this could not be demonstrated experimentally. Here as well, no chemical stimulus could be found that obviously activated these cells.

The neurosecretory function, demonstrated in both MIP and FMRF flask cells, seems to be confirmed in the 6dpf flask cells by the fact that the secretory plexus was always coactivated with, and only with, the flask cells. Physiological proof of chemosensation however is still lacking for the population of flask cells in the apical organ, be it at 1.5, 2 or 6dpf, despite a highly suggestive morphology. This question would be particularly important to answer at 6dpf. Indeed, while the apical organ is clearly a larval organ, it is known that it loses its external ciliated morphology in juveniles but not whether it actually disappears. The neuroendocrine brain centres described in adult nereids (e.g. [281]) could be a developmental elaboration on the larval apical organ, with continuity of function, and cell types may be retained. Stainings performed on juveniles could help to decide on this point, for example to visualise the expression of the FMRF neuropeptide, or of marker genes of neurosecretion.

It should be remembered that the flask cells were sometimes seen to fluctuate in tight synchrony with the pair of eyefront cells. This point is discussed below.

4.1.1.6 Diagonal cells

A bilateral pair of large, characteristic and previously unknown sensory cells has been described in the calcium imaging experiments : the diagonal cells. These cells, which are not located close to the head surface and lie immediately ventral to the antennal nerves, possess a long dendrite that reaches the surface, and occasionally respond to chemical stimuli. The low rate of response observed here suggests that these sensory cells are best suited to detect compounds other than those used in the present experiments, or that the concentration used (10 µM) may have been close to their detection threshold.

While all chemosensory appendages described at 6dpf persist in adult animals, it is unknown whether these cells are present only in the larval period, in which case at 6dpf they might be starting to lose their sensory ability, or also persist at later stages. Their large size, as well as the fact that they are already differentiated at 4dpf, suggest some importance in early life. One could hypothesise that they detect specific environmental parameters that are relevant for larvae.

4.1.2 Chemosensory circuits

In addition to the sensory neurons described above, calcium imaging has revealed that cells in other areas are frequently activated upon chemical stimulation, which are not obviously sensory neurons.

4.1.2.1 Lateral cells

In the region located between the palpal and the cirral ganglion, a population of cells frequently responds to the chemical stimuli and not the flow control, showing that this activity is directly linked to the chemical compound. These cells are often of triangular shape, and are located close to the head surface. Though this position would fit with a chemosensory nature, the cells do not show obvious sensory dendrites, and thus no element other than position and activity speaks in favour of them being sensory cells. Since their responses co-occur with some calcium activity in the part of the main plexus that is the closets to them, it is likely however that they are indeed neurons.

Differences in activity patterns, for example in the duration of response or in the rate of habituation, suggest that this population may include several cell identities. Responses are most frequently observed with amyl acetate and 1-butanol than with the other stimuli, which indicate that the response does not correspond to a mere general detection of chemical stimuli, but instead shows some specificity.

No sensory organ is known in this region of the head. A chemosensory function has been suspected for the multiciliated cells of the ciliary bands, based on expression of the transcription factor *prdm1*, the terminal differentiation marker *atonal*, and the sensory effector *trpV1* ([241] p.53, 109), however this expression of genes is known at 48hpf only. These lateral cells at 6df are indeed located close to the prototroch dorsally, and close to the metatroch ventrally. Whether they are sensory neurons or interneurons, they may have some relation with ciliated cells of the prototroch or metatroch, for example they may connect to them and modulate them. In this way, the beating of the ciliary band may be modulated by chemical detection. The lateral cells may also simply happen to be located close to the ciliary bands, with no relation with them, and fulfil another function.

Here again, some cell tracing based on serial-section electron microscopy would be informative on the actual nature of the lateral cells, and would reveal whether or not sensory neurons reside in this region.

Whatever their precise nature, these lateral cells are most likely neurons and their activity is clearly linked with chemical stimulations, which makes them part of the general chemosensory circuits in *Platynereis* 6dpf larvae, either as chemosensory neurons projecting into the main neuropile, or as non-sensory neurons connected to a wider chemosensory circuit.

4.1.2.2 Paired median cells

A bilateral pair of neurons, called paired median cells, is situated in a stereotypic position between the antennal nerves, possesses a clear axonal projection onto the main neuropile and displays a prominent calcium activity. The activity in these cells shows some link with chemical stimulations, but they do not have an obvious chemosensory activity. An experiment demonstrated that repeated exposure of a chemical stimulus can entrain activity in these cells in an animal in which they are initially inactive, however they can also respond to the flow control, which excludes a purely chemosensory function.

Even though they seem to possess a dendrite, their sensory nature is actually doubtful, as they respond sometimes in synchrony with exposure to a chemical stimulus, but sometimes following patterns unrelated to the chemical stimulation.

Instead, these neurons may rather represent a system that signals to the animal how to react to some stimuli. In fact, they are often seen active at the end of an episode of movement – no activity trace can be provided to support this claim since precisely activity traces are impossible to plot when the animal is moving. They were also often observed in preliminary experiments involving quinine (data not shown), when this aversive stimulus would disappear. Consequently, these neurons may be responsible for conveying a "calm down" signal in the brain, in which case they would probably be inhibitory neurons. The hypothesis is that upon exposure to some stimulus, the paired median cells would integrate information from various sources, and compute as their output either an absence of signal if the situation does not require a general inhibition of movement, or a strong inhibitory signal if the situation requires the animal to stop acting. They would not be involved specifically in the processing of chemical sensory information (and they indeed are able to respond to the flow control for example), but constitute a general signalling system that can be recruted as part of the downstream chemosensory circuitry. To test these speculations, these cells and their projection should be first identified in serial-section electron microscopy tracing, which would allow to confirm whether they use an inhibitory neurotransmitter, for example using the siGOLD technique [253]. Then, calcium imaging could be performed on semi-restrained larvae (between slide and coverslip, or in a wide microfluidic chamber) upon various aversive stimulations, to verify whether the end of an escape response for example correlates with an activation of these cells. A molecular profiling of these cells, which are likely to be identifiable as a single pair in gene expression data due to their singular activity, could also inform about their physiology.

Whatever true function of the paired median cells is, it is apparent that their activity patterns are context-dependant or animal-dependant : they can be active upon onset of a chemical stimulation only, upon onset of flow disturbances, in the absence of chemical stimulation, or even not active at all upon repeated chemical stimulations. They thus seem to have variable conditions for activation, which could reflect a dependence on the current physiological state, or an integration of recent behavioural events and stress.

4.1.2.3 Eyefront cells

In a few but nevertheless clear cases, a bilateral pair of cells consistently located immediately frontal to the adult eyes, and called eyefront cells, were seen to fluctuate in tight synchrony with the flask cells. The eyefront cells are located close to the head surface but do not have an obvious sensory morphology. It may not be a coincidence that these cells have been observed only in cases where the flask cells showed rhythmic fluctuations.

The flask cells' rhythmicity is interesting because it can be present in the absence of a fluctuating chemical stimulation, which indicates that it may be intrinsic. Yet it is hard to reconcile with their obvious sensory morphology, since sensory cells would be rather expected to synchronise to a stimulation, if anything. The synchrony between flask and eyefront cells suggests the existence of connections between them. For instance, the eyefront cells may be interneurons receiving some input at the neurosecretory plexus, and the fluctuations of the flask cells in this way would be imposed to them. They could also be interneurons endowed with an intrinsic rhythm, and influence the activity of the flask cells via synaptic contact ; this particular point should be investigated with more care, since eyefront cell rhythmicity was observed in 3 out of the 5 experiments in which flasks cells fluctuated with some periodicity (Animal #29 – movie3, A#33m3, A#37m4, but not A#29m3, A#40m5), and never in cases where the flask cells fluctuated irregularly, which suggests that the rhythm may actually be imposed by the eyefront cells.

Rhythmic oscillations of calcium levels have been observed in motoneurons in 48hpf *Platynereis* larvae, in link with circadian rhythms [70] : the rhythm is absent during day time, present during night time, and can be induced during day time by the application of melatonin. Since the apical organ is thought to be implicated in this process, it needed to be verified whether the rhythmic activity of flask cells observed here had some links with the time at which the larvae had been observed. Interestingly, all but one larvae in which rhythmic flask cell activity has been observed turn out to come from the same batch and to have been imaged on the same day (14/03/2017). On that day, the 12 animals have been imaged at time between 07:45 and 21:45, with individual animals showing rhythmic activity in flask and eyefront cells at 07:45, 11:35 and 17:05, rhythmic activity in flask cells with no eyefront cells visible at 10:50 and 21:10, and no rhythmic activity in flask cells at 08:35, 09:30, 12:40, 15:25, 16:20, 18:45, 19:40. Thus, there does not appear to be a correlation between time of the day and presence of rhythmic activity. Nonetheless, it is striking that almost all these instances of rhythmicity come from the same day of experiments, which suggests that some unknown factor on that particular day may have influenced neuronal activity in all these animals.

Several questions can be raised : what is this rhythm ? where does it come from ? does the rhythmicity itself have a function or is it a fortuitous coincidence of the cells' physiology ? is it linked with the general physiological state of the animal ? Since the apical organ is quite certainly involved in settlement in *Platynereis*, is there a link between these fluctuation and phases of settlement ? For example, the fluctuations could be taking place only in animals that are ready to settle (or the opposite) after having detected the right environmental signals, and communicate this to the brain via rhythmic waves of neurosecretion.

Flask cells are of obvious interest in the 6dpf larva and seem to be part of a long-range circuit involving the apical organ and at least the eyefront cells. Even though their link with chemosensation is still unclear, they are worth further investigation in the context of chemical stimulations.

4.1.2.4 Mushroom Bodies

Finally, cells activated upon chemical stimulations were also observed in the region of the Mushroom Bodies (MB). The paired neuronal structure called Mushroom Bodies is an unmistakable feature of the adult polychaete brain ([111], see also Chapter III), and whose molecular identity in early development in *Platynereis* suggests deep evolutionary connections with nervous centres involved in associative learning in insects and vertebrates. It was thus particularly interesting to observe in *Platynereis* larvae chemically-evoked activity in cells that potentially belong to the MB.

Active cells have been described in the regions corresponding to both lobes of the MB. This activity, when it was observed, was reproducible, and generally coincided with the detection of the chemical stimulus by the antennae.

Cells in the dorsal lobe region are generally elongated along an oblique direction roughly parallel to the dorsal MB peduncle, but never could this peduncle be seen coactivate with one of these presumed MB cells. In a few instances, active cells were seen that seemed to possess a dendrite, which would indicate the presence of sensory cells in this region. Such an observation was made already while working with my Master student Wiebke Dürichen on Chapter III, as tubulin immunostaining reveal in this region a significant number of instances of nervous fibre that seem to reach to the head surface. More details are available in the Master thesis [260]. However, no certainty exists as to whether such apparently sensory cells belong to the MB dorsal lobe or not.

Cells in the ventral lobe region do not show any obvious sensory morphology, and would seem to be rather interneurons. Instances of a delayed response compared to the antennal detection would also speak in favour of a non-sensory nature, but a refined temporal analysis would be needed to settle this question. There was one case of coactivation of a presumed ventral MB cell with the ventral MB peduncle, observed twice consecutively in the same animal, for which the appartenance of this active

cell to the MB was clear. Since all presumed ventral MB cells have similar positions, this further supports the idea that MB cells have indeed been observed in the ventral lobe.

Overall, it would seem that MB consist of interneurons – at least for their ventral lobes – and are already functional at 6dpf. The known role of MB in door associative memory in insects encourages to speculate on a possible involvement of *Platynereis* MB in chemosensory memorisation, though in the present experiment it is unclear what the chemical stimulus would be associated to. Repeated coactivation of one or several MB cells together with antennal neurons could imprint the identity of the stimulus in the MB. If MB cells that are seen to fire upon chemical stimulation could also be seen to fire in the absence of this stimulation, or in response to another stimulation, this would bring some support for a role in memorisation.

Nevertheless, it should be reminded that except in one case, no other criterion than position can be used in this data to infer appartenance to one lobe of the Mushroom Bodies, and thus all preceding comments remain no more than suggestive.

4.1.3 Stimulus integration between organs

Even though antennae appear to be the main chemosensory organs, responses were seen in each of the other organs for almost every compound. The responses were reproducible in palps for all compounds, in nuchal organs for two compounds, and for tentacular cirri only in four instances. These results suggest that all organs are endowed with chemosensitivity, and have varying degrees of specificity and varying scopes of detection. Antennae would be sensitive and broad in scope, palps of intermediate scope and sensitivity, nuchal organs of intermediate scope but rather high sensitivity for some compounds (e.g. uric acid), and tentacular cirri of general scope and low sensitivity. This would mean that whenever a chemical stimulation is applied, the animal can detect it potentially with all head organs, but only antennae, and in some cases palps or nuchal organs, would inform about the nature of the stimulus. Such ability would allow the animal to locate the source of the compound in space, thus potentially to orient itself with regards to it.

4.2 Technical comments on calcium imaging

4.2.1 Animal immobilisation and ecological relevance

As shown in the results section, it is possible to record in a 6-days-old animal calcium activity in individual neuronal somas over several minutes. This constitute a first milestone in the establishment of a mature functional imaging method, and has been enabled by the use of a 4-walls trap in the microfluidic device. Previous calcium imaging experiments had relied either on the embedding of the animal in agar [70], which precludes repeated chemical stimulus delivery, or on a regular slide-coverslip mounting [76], which restricts stimulus delivery to photic and mechanical stimuli and whose low reproducibility makes it difficult to adequately trap a particular larva of interest, e.g. after a laser ablation. These approaches could not be applied at 6dpf due to muscles that are too powerful at that stage, and hence the microfluidic trap offers a first solution for immobilisation.

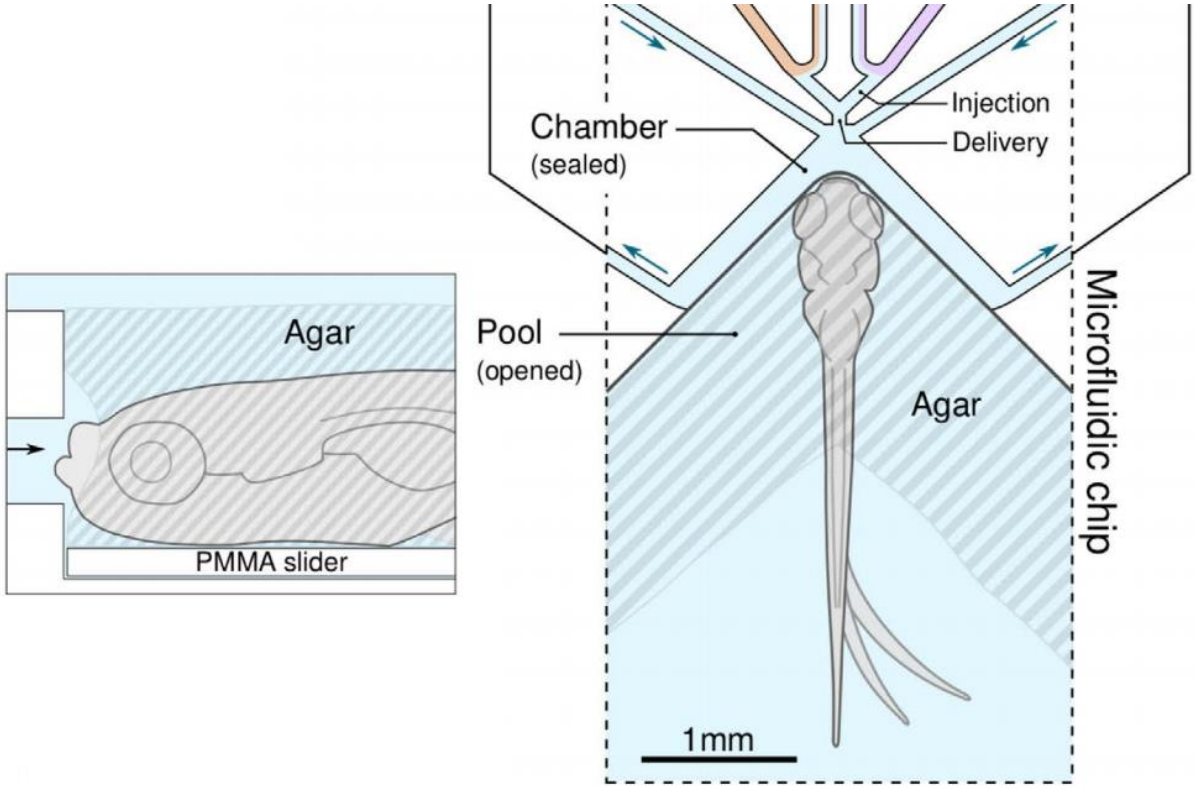


Figure IV-33 Mixed agar and microfluidic trapping for zebrafish larvae, used in a study of chemosensation by Candelier et al, 2015 [265]*. Schematic representation. Note the removed piece of agar around the animal's face.*

The animal, though trapped at the end of the microfluidic channel, still has some freedom of movement. As can be seen form the figures shown, activity traces are sometimes interrupted, which reflects episodes of head strong movement. While these episodes prevent a perfectly continuous observation and restrict the analysis to periods of inactivity, such periods actually constitute the major part of the time when an animal is trapped, hence they constitute a limitation that can be dealt with.

In zebrafish, a mixed agar-embedding and microfluidic trapping approach (see Figure IV-33) has been successfully used to obtain perfectly immobilised animals while still being able to deliver chemical stimuli [265]. Nevertheless, this technique requires manual removal of solidified agar around the animal's heat tip, which would be hard to achieve in *Platynereis* larvae due to their much smaller size (200 µm in length as opposed to 3-4 mm for zebrafish larvae). Moreover, it may be important for the animal to be exposed to stimuli as it would experience them in its natural environment, i.e. with head appendages freely exposed to flowing water rather than surrounded by a gelatinous medium.

For these reasons, the microfluidic trap as it was used here for *Platynereis* seems to offer a good compromise between immobilisation requirements for imaging and ecological relevance, since chemical stimuli are delivered in a way as close as could be to a natural situation.

Importantly, the immobilisation as realised here is purely mechanical and does not require the use of any chemical agent to block muscle activity or ciliary beating. This point was thought to be particularly important to ensure that as little interference as possible with the cellular physiology would take place in the experiments, and thus the calcium activity observed would be less affected by the experimental situation. For example, magnesium chloride at 0.3 M can be used to prevent muscle contractions to some extent in *Platynereis*, but one could fear that the high concentration would interact with ion channels at the level of sensory neurons. Brefeldin A was shown to more effectively prevent muscle activity, even in adult *Platynereis*, however this compound is a general inhibitor of intracellular trafficking, hence it is likely to be harmful for the animal's general physiology.

4.2.2 Image quality

In the experiments as they were performed here, it is crucial to be able to recognise anatomical landmarks from the calcium signal, to determine what cells are being observed. The main obstacle for that is the level of expression of the calcium sensor. Since GCaMP expression is obtained through mRNA microinjection, the mRNA necessarily degrades during the 6 days preceding imaging. The upstream addition of a *Platynereis* ribosomal protein's 5'UTR sequence in the mRNA has improved the expression level left at 6days (see Chapter VI) and yielded a signal high enough to observe cellular activity. Nonetheless, the expression can still show some mosaicism, which in some cases most likely accounts for the inability to observe the bilateral counterpart of some active cells, and in some other cases may have prevent to observe some responses altogether. For these reasons, the frequency of responses observed in the present experiments for a given organ or cell are likely to represent underestimates of the actual response frequencies.

Ideally, a stable transgenic line expressing a calcium sensor such as GCaMP6s should be stablished in *Platynereis*, with either a pan-neuronal or an ubiquitous promoter. This would greatly facilitate the imaging and reduce the time needed to perform the experiments, as notably all injections and screening steps would be suppressed. Alternatively, I could think of using the usual chemical calcium dyes, such as Oregon Green Bapta-1 AM (OGB1), since they do not require injection. I did try to perform calcium imaging with such non-genetic dyes, to find out whether variability in signal intensity between animals and mosaicism effects (as well as the painful microinjection protocol) could be avoided. These attempts were unsuccessful and are described in Chapter VI.

Nevertheless, it is clear that the signal was good enough to observe activity in whole-brain imaging settings. Images of much better quality could be obtained in single-plane recordings (see the example of revolver cells, Figure IV-18) or even local volume imaging (nuchal organs and antennae), which revealed fine structural details of the neurons such as axons and dendrites, and showed that some conclusions about individual cell physiology are possible already from such quality of image.

Finally, it should be reminded that even though high image quality is desirable for conference presentations, it is not a pre-requisite for valid experimental conclusion to be drawn. Only a low number of pixels can be enough to quantify a cellular response, provided that the ROI stays the same and that the signal-to-noise ratio is high enough. Any activity trace enabling to unambiguously demonstrate the existence of a cellular response should be considered of high enough quality, regardless of aesthetic criteria about the image. In fact, some of the clear activity traces shown in this chapter, notably for flask cells in the few cases where the animal was imaged from the opposite side of the body, are obtained from images which at first look could appear unusable.

4.2.3 Spatial sampling and alternative imaging approaches

As exposed in the Materials & Methods section, for whole-brain recordings 12 optical planes with 5 µm-interval were used to sample the head along its doors-ventral axis. Despite a wide confocal pinhole opening (6.4 Airy Units), the effective optical section thickness is less than 5 µm, or at least it is likely that low cellular signals located at equidistance of two consecutive planes will not be captured adequately. Hence, active cells could be missed in the recordings if their calcium response is small, which is probably a second factor after mosaic expression accounting for the absence of bilateral counterpart in a significant number of cellular responses.

A more complete coverage of the head volume could be obtained with different imaging approaches. Light-sheet microscopy allows a fast volume imaging, and has recently undergone rapid technical improvements, driven notably by the field of developmental biology (see for example [282],). It has been applied for whole-brain calcium imaging in agar-embedded zebrafish larvae [283], allowing

analysis of single-cell activity. However, such imaging requires to come in close proximity of the sample with at least two microscope objectives, which is not obviously compatible with the use of a microfluidic device. Light-sheet microscopy has so far mostly relied on agar-embedding, and it is unclear how this could be adapted to the delivery of chemical stimuli. To be feasible, light-sheet microscopy of chemosensation in *Platynereis* will require more technical development. Notably, it should be tested whether imaging with two objectives at a 45° angle, as is being developed for zebrafish larvae (Nils Norlin, unpublished), is a suitable approach with a usual microfluidic device.

Light-field microscopy offers an alternative approach of whole-brain imaging, that was successfully applied to neuronal calcium imaging in the nematode *Caenorhabditis elegans* and in the zebrafish larva [284]. Optically, it is simple to implement as it uses a single objective, and image acquisition would be as easy as for confocal imaging. However, the method requires extensive image deconvolution, which comes with two disadvantages : an substantial computational power is needed, which may not be easily available for every research team, and images cannot be looked at while performing the experiments, which may compromise the relevance of the data collected in the absence of immediate feedback. Hence, both alternative techniques, light-sheet and light-field microscopy, may not be easily implemented in Platynereis for the moment.

Imperfect as the spatial sampling may have been in the current work, the amount of knowledge gained on chemosensory organ physiology in *Platynereis* nevertheless confirms its validity, and much more can still be learned while using the same imaging technique. The last whole-brain experiments conducted, a few of which have been included in the results section, consisted of stacks of 16 confocal planes with a 3.75 µm interval between them. The image resolution was decreased to 256 x 256 pixels to retain a 1 frame per second resolution, but this did not result in a noticeable loss of cellular activity captured. These settings seem well suited for whole-brain recordings. Hence, a technological change does not appear to be yet a priority for *Platynereis*.

4.2.4 Temporal aspects

In the experiments reported in this chapter the temporal resolution for each plane imaged was either 1 frame per second (fps) for the 12- or 16-plane recordings, or 3 fps for single-plane recordings. This is slightly low in comparison with the response speed of GCaMP6s (rise time on the order of 0.4s, [263]), but fast enough so that all significant cellular events should be recorded : in dissociated hippocampal rat neurons for example, the half time of GCaMP6s signal decay after a single action potential is 2 seconds [263].

What this temporal resolution does not allow to observe, in whole-brain settings at 1 fps, are differences in response offset between neurons that are distant of less than 1 second. This means that in the current experiments, it is not possible to tell temporal delays between cells unless they have been observed in single-plane settings. Such delays could be indicative of differences in neuronal natures, for example sensory neurons responding first, rapidly followed by some interneurons. A different imaging approach, such as those mentioned in the previous paragraph, could allow to better answer these questions. Yet, again there is still for the moment enough information that can be gained from experiment with a 1 fps resolution, which does not make such an improvement a priority. If cells of interest are not too distant in the brain, a local volume imaging can be conducted with a couple of planes and/or a smaller image size, that allows already an enhanced time resolution.

One weakness of the current setup is the variability in stimulus onset precision. Even though for a single experiment this variability is less than 1 second, it varies more across experiment, and currently the actual stimulus onset during the experiments can only be estimated from the preliminary calibrations shown. Ideally, some fluorescent dye or material would be mixed in the stimulus solution, that would reveal the arrival of the stimulus when imaged in a different channel than GCaMP, while being inert for the animal. I made several attempts at finding such dyes or materials endowed with red

fluorescence, which were all unsuccessful, since they either stained the animal or induced neuronal responses. These attempts are described in Chapter VI. If such a dye was found, this would solve the problem of stimulus onset variability, since any recording could be calibrated with its own stimulus timing, provided that some volume of water is imaged.

In the current experiments, it is thus hard to make statements based on relative timing of organ responses. At best, a reference such as the antennal response can be used to assess whether the other organs or regions, notably presumed interneurons, tend to respond in synchrony with them, before, or after, and get some sense of how these response are coordinated, though this would still largely be limited by the 1 fps resolution.

This variability does not come from the microfluidic device's design itself, but rather from the quality of the pumps. Indeed, the syringe pumps used are not optimal for solution delivery at such low flow rates. As they apply pulsed rather than continuous mechanical forces, this probably results in flow variability when channels are switched on or off. Trying to replace the basic plastic syringes by glass precision syringes of the type used for gas chromatography, which have extremely low friction artefacts inside the plunger, did not yield any improvement on the variability issue, confirming that this probably comes from the pumps. Pressure-driven pumps instead of mechanical-driven ones could be used, yet such pumps are much more expensive.

4.2.5 Stimulus delivery

One of the main advantages of the present setup is the repeatability of the stimulus exposure, as well as the precision of stimulus concentration. For an agar-embedded animal, it is unclear whether a stimulus solution could be totally washed away, which makes repeated stimulus exposure. At best this can be achieved slowly, which precludes a fast stimulus repetition, and the use of fast stimulus offsets.

The present results have demonstrated the suitability of the microfluidic setup to test the reproducibility of individual neuronal responses, a crucial point to be able to make physiological statements. Indeed, only the repetition of a given stimulus for a certain animal can allow to sort out fortuitous coactivations of neurons.

Moreover, two chemical stimuli can be tested in the device instead of one chemical stimulus and a flow control, which allows to look for differences in response to two compounds in the same animals, hence for stimulus discrimination both inter-organ and intra-organ. Such experiments have been performed, but due to low data quality they were so far inconclusive. Nothing speaks technically against the realisation of such experiments, and obtaining the required data is only a matter of trying again.

The present setup constitutes a clear technical improvement also from a perspective of which stimuli can be used. Indeed, the setup allows the controlled delivery of any waterborne stimulus. This could be :

- further chemical stimuli such as amino acids, nucleotides, salts, small metabolic products, which are known to act as chemical signals in marine animals such as fish or crustaceans [157], and are all water-soluble
- water with different values of physiological parameters such as pH or oxygen concentration
- solid particles of small size (< 10 µm) that would constitute mechanical stimuli
- food particles such as pieces of vegetables, algae

Functional imaging experiments, which had so far mostly been restricted to photic and mechanical stimuli, can now be extended to a whole new repertoire of stimuli.

4.2.6 Cell identification

One of the important aspects to improve in further developments of this method is the identification of individual cells. Indeed, the boundaries of the different regions are not unambiguous in the calcium recordings.

Presently, cells were grossly identified based on their position within the head. This is sufficient to assert that a cell belongs to the antennae, the palps, the cirri, but some uncertainty is unavoidable in less well-delimited regions such as the nuchal organs or the apical organ, if no additional cell features are seen. Activity patterns can help to attribute cells to their respective organs, as was shown here with the antennal or nuchal nerves. It seems justified to identify certain particular cells based only on their appearance in calcium signal and their shape and position, as was mentioned for the revolver neurons, the flask cells and the paired median neurons, though such cases represent only part of the cellular complement.

Nevertheless it could be quite informative to coinject with a general fluorescent marker for cell nuclei or membranes, which would help recognise anatomical landmarks notably when the calcium signal is weak. Such tools, typically a plasmid to be coinjected, have been used already in some experiments and can simply be applied here.

4.3 Conclusion

A chemosensory function could indeed be confirmed for nuchal organs as well as the main head appendages, and additional sensory cells and members of chemosensory cells have been discovered. The most surprising finding is the fact that antennae, and not nuchal organs as had been expected, seem to be the major chemosensory organ. These results indicate that the whole head is able to detect chemicals, with different degrees of specificity between organs.

V –Chemosensory behaviour and associative learning assay

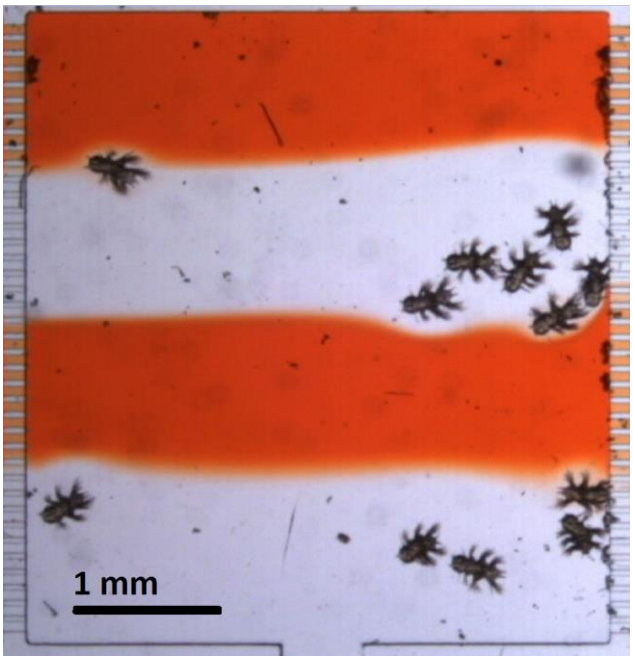
V – 1 Introduction

1.1 Microfluidic devices for behavioural experiments on marine larvae

1.1.1 Laminar flows and stimulus delivery

For behavioural experiments concentrating on the chemosensory modality, an appropriate way to deliver the stimuli is needed, to ensure right concentration and exposure time. Chemical stimuli can be challenging to deliver, as opposed to a physical stimulus such as light. If contact chemosensation is excluded, these stimuli are carried by a material medium which is water or air in most cases, hence the medium movements need to be controlled appropriately. Precise delivery of a volatile compound is best achieved by directing a constant air flow towards an animal or its chemosensory organs, and changing the composition of this flow by adding or removing the stimulus ; such a delivery mode is used for example in standard odour associative learning paradigms in *Drosophila* (see [285]). Precise delivery of a soluble compound can be achieved in two ways. If the animal is in the air, then some water containing the stimulus can be applied to chemosensory organs ; this was the approach adopted in the first experimental demonstration of classical conditioning in insects, made by Nelson in 1971 with the blowfly *Phormia regina* [286]. If the animal is in the water, then the water flow needs to be controlled and its composition changed as for the aerial delivery ; this is commonly used for studies of chemosensation in fish [287] or in crustaceans.

Figure V-1 Example of a spatial chemical pattern obtained in a microfluidic chamber containing Platynereis larvae. Four parallel, permanent water streams flow from left to right, two of which are dyed with Orange G. Chip design : Nirupama Ramanathan and Oleg Simakov.



As explained before, associative phenomena between stimuli can be strongly modulated by differences in exposure timing in the order of a second, which means that the experimental setup needs allow a similar temporal precision. For an animal as small as a 6dpf *Platynereis* larva, water flow cannot be controlled with enough spatial and temporal resolution with a standard, macroscopic setup, as the animals are too small compared to the typical size of fluidic events. Problems such as boundary layer effects and turbulence would introduce massive variability on the stimulus concentration and timing, hence when working at such a scale it is necessary to restrict the space allotted to the animal. Microfluidic devices offer a good opportunity to do so while controlling flow with a high spatial and temporal precision.

Avoiding turbulence means operating in a stable flow regime called **laminar flow**, in which streamlines tend to stay locally parallel. In fluid mechanics, the Reynolds number is a dimensionless quantity that expresses the ratio of inertial forces versus viscous forces. When inertial forces dominated, the flow tends to be turbulent ; when viscous forces dominate, the flow tends to be laminar.

At around 20°C, with a flow speed *u* on the order of one millimetre per second and a characteristic chamber dimension *L* of around 100 µm which is slightly more than a 6dpf larva's height, this number is $Re = \frac{u.L}{\nu} \approx \frac{10^{-3}.10^{-4}}{10^{-6}} = 0.1$, where ν is the kinematic viscosity of water.

For such a value of the Reynolds number, the flow is typically laminar, meaning that it is possible to obtain parallel streams of water that do not mix. A microfluidic environment of such dimensions is thus suited for flow delivery at the scale of *Platynereis* larvae. Such a property can be utilised to obtain precise a stimulus delivery, as well as precise spatial patterns of chemical stimuli. Figure V-1 shows an example of such spatial patterns I generated in a microfluidic chip after having introduced *Platynereis* larvae. Note the sharpness of the stream boundaries compared to the scale. In the absence of animals, the stream boundaries would be horizontal on the picture ; here, since the chamber's height is fitted to the animals' dimensions, the boundaries are slightly affected by the volume of the animals and can be seen to bend around them, however this affects mostly their position, not their sharpness.

1.1.2 Previous experiments with Platynereis larvae

The device whose central chamber is shown in Figure V-1 has been used for experiments on *Platynereis* larvae aimed at quantifying their preference about ecological parameters : water acidity and salinity. They have demonstrated that the larvae are sensitive to these parameters, do have a preferendum, and position themselves in the chamber according to the chemical conditions that suit them [187] (see also section 4.10 in [240], and chapter 2 in [288]). They also showed that such setups are suitable for behavioural studies, since they allow to image and quantify responses of the larvae. Nevertheless this particular device was designed to generate static patterns, and cannot be used for fast flow changes as required by learning experiments.

Besides in the previous experiments, few controls were performed to quantify the influence of the chip and its flow on the larval behaviour, nor to test for possible disturbances of the flow patterns introduced by the animal's movements. Such control experiments thus needed to be performed prior to further investigations of chemically-induced behaviours

1.2 Principle of a classical conditioning protocol

1.2.1 A training and a test phase

A behavioural assay for learning will typically consist of a training phase and a test phase, during which animals are expected to learn and remember the co-occurrence of two stimuli. In Pavlovian assays, or classical conditioning, a reliable behaviour-eliciting stimulus called Unconditioned Stimulus (US) is repeatedly paired with a gentle stimulus that elicits either no response, or at least a response that is distinguishable from the previous one.

During the **training phase**, animals will be exposed repeatedly to the stimuli of interest, in a way that is supposed to affect their behavioural response to these stimuli. These stimuli can represent complex situation, as is the case in spatial learning assays in mice (e.g. the Morris water maze), or simple situations involving two elementary stimuli such as an odour and an aversive stimulus, as is the case for learning assays in most invertebrate species (e.g. odour associative learning in *Drosophila*).

During the **test phase**, the animal's response to these stimuli will be assessed, to determine whether the behaviour has changed compared to before the training phase. The behaviour change can sometimes be evaluated qualitatively, in terms of appearance of disappearance of a response. More often though, the response will not appear or disappear, but persist and only be modulated in its amplitude or frequency. It will then need to be evaluated quantitatively, through the measure of some relevant parameters. In the gastropod mollusc *Aplysia*, conditioning of the siphon withdrawal reflex is quantified as mean withdrawal time, to detect significant increases or decreases in the duration of the

reflex ; this allows to quantify for example how stimulus contingency affects the efficiency of learning [289], or how retention of the learning evolves over time [290].

In the fruit fly *Drosophila*, odour aversive conditioning is often quantified on groups of animals, as a percentage of flies avoiding the previously rather neutral stimulus ; this allows to quantify for example the influence of stimulus intensity, stimulus contingency, and learning performance in several mutants [285]. It should be noted that the conditioned response (CR) resulting from the learned association may be seen to develop during the training phase, if the experimental setup offers the possibility to observe it while training the animals. A plot of the CR across the training, called a **learning curve**, would reveal an increase in the response magnitude, and can be used to determine the minimum number of trials needed to reach a certain level of learning. For a review on the learning curve and its saltatory aspects see [291].

Associative learning can exist at larval stages, as is known from *Drosophila*, but are typically effects of limited amplitude [292]. I was confident that *Platynereis* could learn associations, but managing to reveal it experimentally is another matter, and precise quantifications of behavioural responses were clearly needed. The approach taken has been to quantify both the amplitude of individual responses, and responses probability estimated at the group level.

1.2.2 Stimulus choice and ecological relevance

The choice of stimuli is critical for a successful demonstration of associative learning. Animals endowed with highly elaborate capabilities of stimulus perception and memorisation, such as mammals and cephalopods, are probably able to learn associations between any stimuli, but this is certainly not true for animals with a more simple nervous system, such as nudibranch molluscs, nematodes, insects or annelids. Indeed, the ecological relevance of the stimuli seems to be of high importance, especially for the conditioned stimulus (CS).

The ecological likelihood of the US (unconditioned stimulus) is not crucial, provided that it does triggers a response or physiological effect. As a matter of fact, some standard associative learning protocols have been established with stimuli that for sure do not exist in the animal's natural environment, such as electrical shocks for the fly *Drosophila* [285] or the terrestrial plant extract quinine for the cuttlefish Sepia [293], nevertheless they can be used effectively as USs. The CSs are the stimuli that typically elicit no behavioural response when presented alone – or at least not the same response as the US – but will be encountered by the animal in its environment together with the US that produces a strong response. Whether or not the animal can learn that a CS co-occurs with the US, i.e. learn to produce the response in presence of the CS only, depends on how relevant such an association would be in the nature. It should be remembered that in the classical example of eyelid conditioning used in mammals, the animals do learn what seems to be a pure arbitrary, non-ecologically relevant stimulus association – a sound (CS) and a puff of air on the eye (US) – however this learning takes no less than several hundreds of trials to develop [294] ! In stark contrast, an adequate choice of stimuli and animal physiological state can lead to a strong associative learning after one trial only, as demonstrated on hungry freshwater snails using food as a US and a chemical cue as a CS [295]. Seligman has brought forward in 1970 the notion of *preparedness*, rebutting the idea that stimuli would be equally associable [296]. In this paper he reviewed numerous pieces of evidence illustrating that animals cannot learn anything, at least not equally, for example rats are *prepared* to associate tastes with illness, but not tastes with footshock.

I reasoned that this would be all the more true if one is dealing with a simple nervous system with limited sensory capabilities, as is the case for 6dpf *Platynereis* larvae. My choice has thus been for chemical stimuli, which I though the larvae could best discriminate at 6dpf among all possible sensory modalities.

1.2.3 Stimulus parameters

Disposing of relevant stimuli is no guarantee of success for a demonstration of associative learning. Indeed, several parameters of stimulus presentation, and notably temporal parameters, have been shown to be important in the learning process, and associative effects could easily be missed in an experiment if they are not well adjusted to the animal. These are :
- intensity and duration of CS and US
- time between CS onset and US onset, or Inter-Stimulus Interval (ISI)
- time between two consecutive CS onsets, or Inter-Trial Interval (ITI)
- number of CS-US pairings, or trials
- time between last trial and test

Some of them are represented in Figure V-2.

Stimulus intensity and duration are two parameters to adjust in the first place. The US should trigger a response that does not decrease in amplitude. A decrease would mean either that the animals stop taking the stimulus into consideration, i.e. are habituating to it, which will eventually perturb its possible association with the CS, or that they stop being able to respond due to damage or to exhaustion, which will eventually prevent a possible conditioned response (CR) to develop. The US intensity should be just high enough to produce the unconditioned response (UR), but not higher. Its duration should be long enough to enable the observation of the UR, but not longer to avoid unnecessary exposure. Regarding the CS, the intensity likewise should be just high enough to be sure that the animal detects it, and the duration just long enough to enable the observation of the developing CR.

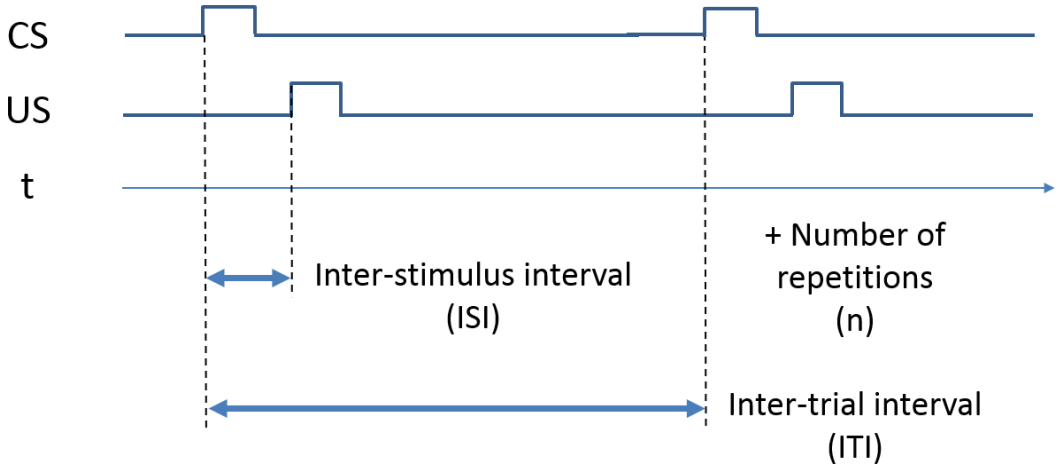


Figure V-2 Repeated stimulus exposure and temporal parameters in associative learning. The time between CS onset and US onset is called "Inter-stimulus interval" (ISI), the time between two successive CS presentations "Inter-trial interval" (ITI).

In most paradigms of classical conditioning, the CS is presented before the US, which is called *forward conditioning*, as opposed to the reverse kind of presentation or *backward conditioning*. The CS can be presented with or without overlap with the US. A forward pairing confers to the CS a predictive value : if the animal can associate the stimuli, it can learn to anticipate its response and produce it even before the US is presented, since the US is so to speak always announced by the CS. This interval between CS onset and US onset, or ISI, can have dramatic effects on the learning phenomenon, and a few seconds can cause an experimenter to miss evidence of learning, as illustrated on Figure V-3 in a paradigm of discriminative conditioning between a paired (CS+) and an unpaired (CS-) conditioned stimulus.

The time interval between trials or ITI is known to influence the type and strength of the memory that is formed. Typically, a spaced training that leaves more time between trials allows the formation of a long-term type of memory lasting sometimes for days, that is dependent on protein synthesis and involves synaptic rearrangements (see [297] for the fly *Drosophila*, [298] for the nematode

Caenorhabditis), whereas a massed training with little time between trials allows the formation of a short-term type of memory only.

The number of trials also plays a role in establishing a learned association. Repeated exposure strengthen the learning, but only up to a certain point (see an example in [298]).

Finally, the time given to the animal between the last trial and the test can affect the performances, as animals can be unable to produce the learned response shortly after a trial, but able to do so later.

The importance of all these parameters for the development of an associative learning protocol requires patient endeavour, and identifying the first signs of associative learning in an animal for which it is undocumented will be the most difficult point to reach, allowing then a progressive to refine the protocol from this entry point.

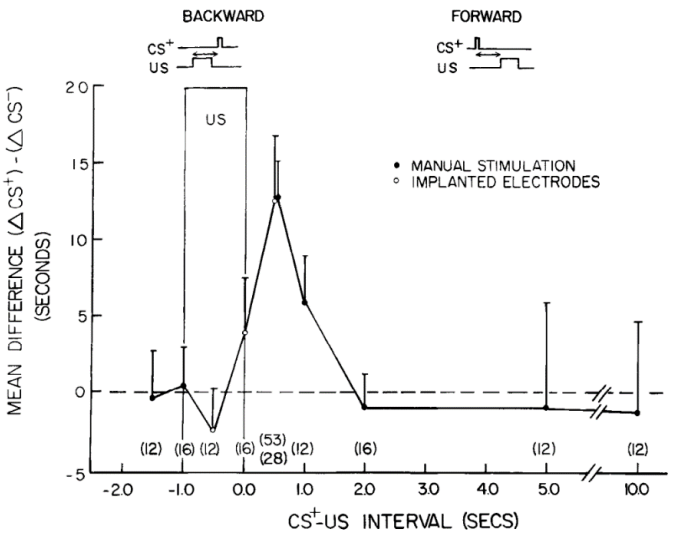


Figure V-3 One of the parameters influencing associative learning : the temporal CS-US contingency, exemplified in the mollusc Aplysia californica. CS+ designates a conditioned stimulus that is paired with the US, CS- one that is specifically unpaired. The strength of associative learning is quantified as a difference (ΔCS+ – ΔCS-) between the increase in responding to the CS+ after training (ΔCS+) and the increase in responding to the CS- after training (ΔCS-). Learning is assessed for different intervals between CS and US, for negative (backward conditioning) and positive (forward conditioning) interval values. The experiment reveal an optimum of learning when the CS is presented 0.5s before the US. Reproduced from Hawkins et al., 1986 [289].

1.2.4 Required controls

In a paradigm of excitatory classical conditioning as is envisaged here, the occurrence of associative learning will be revealed experimentally by the appearance of a response or an increase in its amplitude. However, other factors than a stimulus pairing, notably sensitisation to a single stimulus, can also produce such an effect. In order to exclude that non-associative factors would account for this change, a certain number of standard controls should be performed on other animals :

1- training with the CS alone, i.e. a control for familiarity with the CS
2- training with the US alone, i.e. a control for sensitisation by or habituation to the US
3- training with CS and US explicitly unpaired, i.e. an unpaired control, or a random control if the stimuli are presented in a(n almost) random manner
4- training with one paired (CS+) and one unpaired (CS-) stimulus, i.e. a discriminative conditioning
5- test with a novel CS, i.e. a control for the unconditioned effects of the CS

Rescorla in 1967 has shown that all these control procedures have flaws, as they either introduce non-associative factors not present for the experimental subjects, or switch from an excitatory to an inhibitory contingency [299]. As a solution, he suggested what he calls a truly random control procedure, in which CS and US are totally independent of each other, and as a result will be most often unpaired, but sometimes will. Such a procedure is in agreement with his different vision of associative phenomena, based on the contingency and not the pairing of the stimuli, in other terms based on the degree of temporal existing between the stimuli. Whether or not one agrees with Rescorla's view, such a control is indeed a useful one to perform and, if it does not replace the others, should at least be

included with other controls, to avoid that the CS predicts the absence of US in all controls, which represents rather an inhibitory conditioning.

1.3 Learning in annelids

Annelids have long been recognised as valuable animals for understanding the constitution and function of nervous systems, including behavioural modifications. Here is Bullock and Quarton's opinion in 1966 in a bulletin of the Neurosciences Research Program : "*Annelids offer some of the most promising material for study of learning mechanisms in simple systems […] their availability, simplicity, phylogenetic position, learning capacity, and tolerance of mutilation suggests that they are well worth new attention*" ([300] p. 116). It is unfortunate that research on annelid learning has slowed down since the late 1970s, especially given today's flourishment of molecular and neurobiological techniques and their rapid adaptation to non-standard animal models. Nevertheless, a number of studies before that date have reported learning phenomena in annelids, regarding non-associative as well as associative forms, with the withdrawal reflex as a commonly investigated behavioural response. In earthworms, most behavioural studies have been performed on the species *Lumbricus terrestris*, while in leeches investigations have eventually focused on *Hirudino medicinalis*, the medicinal leech. In polychaetes, as for anatomical studies, research was mainly carried out with nereidid worms, notably the genus *Nereis*, with most results due to Clark and Evans. It is notable that various surgical manipulations can be conducted on nereidids in combination with behavioural experiments : sensory deprivation, brain extirpation, regeneration [123], [301]–[303]. Here is a brief review of evidence for three types or learning in annelids : habituation and sensitisation (non-associative), and classical conditioning (associative).

Habituation. Convincing demonstrations have been given in earthworms for habituation of the rapid withdrawal response to thermal, mechanical and electrical stimuli [304], and to photic stimuli [305]. In leeches, habituation of undulatory movements to shadows was demonstrated in *Dina microstoma* [306] and in *Haemopis* [307], as well as habituation to mechanical stimulation in *Dina* [306]. Habituation of the shortening reflex to light flashes was also demonstrated in *Hirudo medicinalis* [308]. In polychaetes, habituation of the withdrawal response is known both in errant and sedentary worms. It is particularly well documented in errant polychaetes, "*primarily due to the research effort of Clark and his students at the University of Bristo*l" as commented by Dyal ([309] p. 240). Nereidids habituate rapidly to touch or to changes in illumination (after about 20 stimulations in *Nereis pelagica* [310],[311], *Nereis diversicolor* and *Platynereis dumerilii* [312],[313]), and habituation was described in straight alley runs in the polynoid *Hesperonoë adventor* [314]. Studies on sedentary polychaetes such as the sabellid *Branchiomma vesiculosum* have revealed habituation to tactile [315] and photic [316] stimuli.

Sensitisation. Sensitisation in earthworms does not seem to have been the focus of any study reported in the literature, even though indications for it are found as side observations in studies of classical conditioning (see [309], p. 250). In leeches, the phenomenon was demonstrated in *Hirudo medicinalis*, in which electric shocks sensitise the shortening reflex to touch [317]. Sensitisation in nereidid polychaetes was extensively studied by Evans, notably in attempts to demonstrate classical conditioning, using food, touch or electric shocks as sensitising stimulus, and light-elicited withdrawal or tube entering as a sensitised response [318]–[320].

Classical conditioning. The first rigorous demonstration of classical conditioning in earthworms was given by Ratner and Miller in 1959, using a gentle vibration as conditioned stimulus (CS) and a bright light as an unconditioned stimulus (US) eliciting rearing and withdrawal [321]. The set of experiments included controls for sensitisation by the vibration or by the light, and for the base rate of spontaneous responses. The existence of conditioning in leeches was not proved until Henderson and Strong's experiments in 1972, using light this time not as a US but as a CS, and electric shocks as a US eliciting a shortening response [322], in a device similar to that of Ratner and Miller (see Figure V-4). They included convincing controls for random and unpaired CS-US presentations, and for Cs or US alone.

Another study by Sahley & Ready in 1988 showed that a tactile stimulus can also be used as a CS to condition the shortening response, as well as the so-called stepping response which is a locomotor pattern typical for leeches [323]. These experiments included the following controls : CS alone, US alone, and CS-US unpaired, thus providing reliable evidence for the effect.

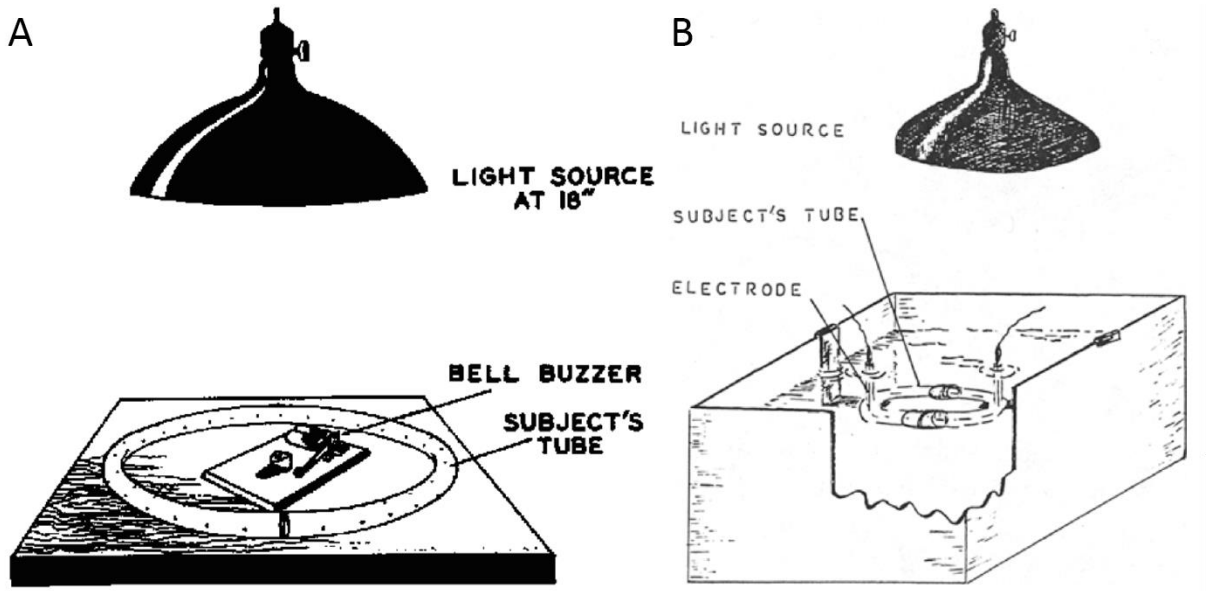


Figure V-4 Experimental setup for conditioning in earthworms (A) and in leeches (B). The animal is introduced in a tube to control stimulus delivery. Reproduced from (A) Ratner & Miller, 1959 [321] *and (B) Henderson & Strong, 1972* [322].

In polychaetes, two early studies reported by Copeland in 1930 and Copeland & Brown in 1934 indicated that *Nereis virens* could learn to associate changes in illumination [324] or touch stimuli [325] with the presence of food, but the number of subjects was low and important controls lacking, and later authors regard these experiments as inconclusive [326],[327]. Few other attempts at demonstrating the existence of associative learning in polychaetes are reported in the literature, none for *Platynereis dumerilii*. Evans, who worked with nereidids, is probably the one who went the furthest in that direction [318]–[320], but he failed to find behavioural effects that could not be accounted for by sensitisation mechanisms. He concluded that nereidids are probably not able to learn associations, and even argued that associative learning may be detrimental for these animals due to a low discriminative ability between stimuli, which would result in learning irrelevant associations [319]. He adds : "*Even if the necessary mechanisms existed, conditioning […] would be of doubtful value to the animal*". ([319] p. 948). As of today, associative learning remains undemonstrated in polychaetes.

It is clear that annelid worms in general offer an interesting opportunity to study learning phenomena with experimental access to neuronal mechanisms. The medicinal leech *Hirudino* has proved to be a valuable preparation for electrophysiology, and learning forms such as sensitisation and classical conditioning were shown to take place in semi-intact animals. Such behavioural paradigms have opened the door to detailed cellular investigations and led to important insights in the neuronal circuits involved, notably the identification of neuronal components of the CS and US pathway (a review of learning studies in leeches is given by Sahley, 1995 [328]). Research on leeches behaviour has since focused rather on locomotor activities (for a review, see Friesen & Kristan, 2007 [329]).

As reviewed extensively in Chapter II, polychaetes as opposed to their terrestrial relatives have elaborate sensory appendages, and thus offer a better experimental access to sensory detection and integration. Evans' unsuccessful attempts at demonstrating classical conditioning in nereidids may have been due to inappropriate experimental approaches. Indeed in most experiments he tried to

make the worms learn to avoid one side of a T-maze or to avoid entering a tube [303],[318],[319],[320]. Although being in a tube probably represents a comfortable and natural situation for a polychaete worm, such actions may be of limited ecological relevance as it is unclear for example when a worm would have to remember to turn left or right. It is surprising that he did not focus on food searching or grasping behaviours, notably proboscis extension. Besides, methods such as handling the worms with a paintbrush could have introduced confounding factors. What is more, chemical cues were never used as conditioned stimuli, despite their highly probable importance based on the worms' neuroanatomy known at that time, and based on Case's experiments on chemosensation in *Nereis* reported in 1962 [185]. In all likelihood polychaetes are able to learn associations in the same way as leeches and earthworms do, and it is probably time to resume learning experiments, this time focussing on different behaviours, and maybe including chemical cues as potential CSs.

1.4 Strategy for establishing a chemosensory associative learning protocol

In the distant perspective of combining functional imaging with behavioural experiments, efforts were put into developing a protocol for classical conditioning adapted for *Platynereis* at the 6dpf larval stage, and which would rely on chemical cues, at least as CSs. Expecting that behavioural effects would be more obvious at later stages, experiments were conducted between 6dpf and the 5-segmented stage. The requirements for stimulus delivery at such a small scale prompted to develop a new microfluidic device for learning experiments, that would allow adequate stimulus switching together with the generation of spatial chemical patterns. This was encouraged by the preliminary experiments described above, conducted on *Platynereis* larvae in microfluidic environments. The global approach was to run experiments with several animals in the same chamber, to be able to average behavioural effects over large numbers of animals, and be faster in revealing possible conditioned responses that could be of low amplitude.

V – 2 Materials and Methods

2.1 *Platynereis* culture

See Chapter III.

2.2 Chip designs

3-chambers design : A microfluidic chip organised around three chambers and possessing five inlet channels was used, as shown in Figure V-5. The central chamber is where the animals are introduced and confined. It has a size of 2.5mm x 2mm (width x length) and a height of 100 µm which is uniform in the whole chip. This height allows the larvae to freely move, but not to overlap when imaged from the top, which is important to monitor their behaviour. The two lateral chambers are located on each side of the main chamber. They have a size of 1.5mm x 2mm (width x length), thus the same length as the central chamber. Their height is 100 µm as for the whole chip. The three chambers are delimited upstream and downstream by small restriction channels which have a height of 30 µm.

The central inlet channels numbered 0 to 2 are the main inlets, used for stimulus delivery and switching. Channel 0 is filled with Natural Sea Water (NSW), channel 1 and 2 are filled with stimulus solutions. The lateral inlet channels numbered 3 and 4 are optional inlets, that can be filled with a dye solution to monitor the flow during the experiment if wanted, or left closed otherwise. The chip is used in such a way that the control dyes never reach the animals and are confined to the side chambers. The small channel 5 is used to introduce animals in the central chamber. Channel 6 is the general outlet channel for the whole chip.

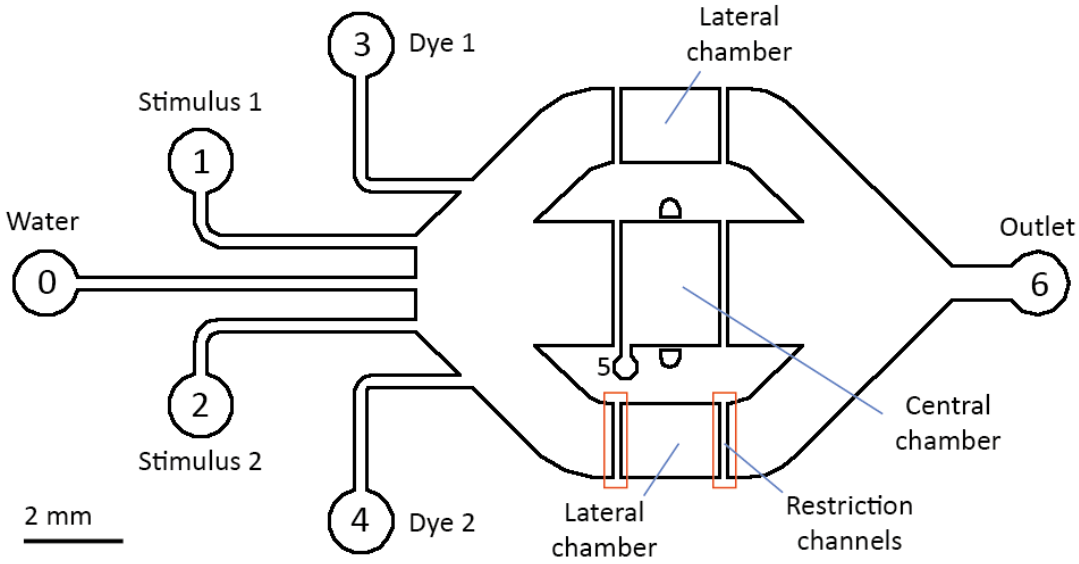


Figure V-5 Design of the 3-chambers chip for behaviour experiments. Animals are confined to the central chamber. Red rectangles indicate the location of restriction channels for one lateral chamber.

1-chamber design : An additional, more simple chip design was used in some experiments, which contains only one chamber and 2 inlet channels, one used for water and the other for a stimulus. The design is shown in Figure V-6. Animals are introduced in the chamber by either of two introduction channels ; it has a size of 2.5mm x 4mm (width x length) and a height of 100 µm which is uniform in the whole chip. Likewise animals can freely move inside the chamber but not overlap when imaged

from the top. The chamber is delimited upstream and downstream by small restriction channels with a height of 30 µm. Channel 4 is the general outlet channel for the whole chip.

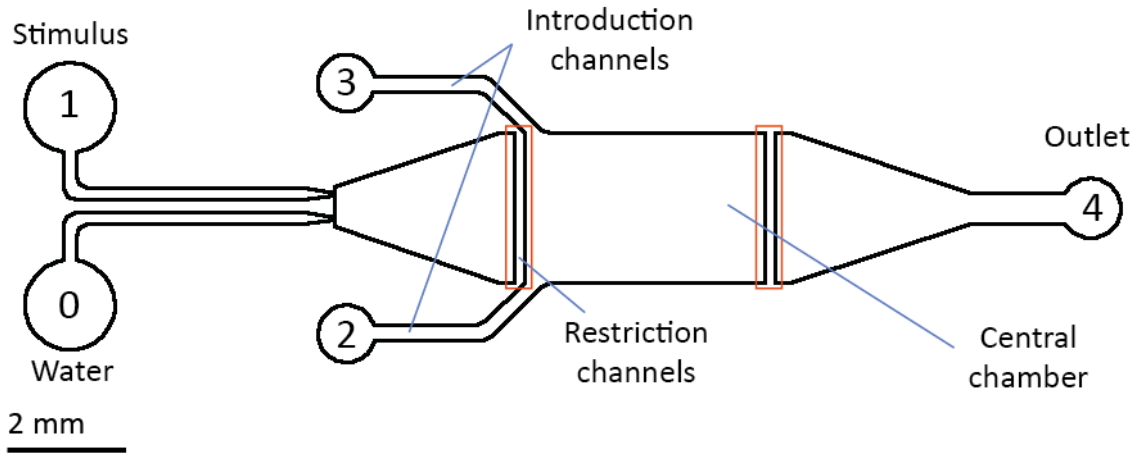


Figure V-6 Design of the 1-chamber chip for behaviour experiments. Animals are confined to the central chamber. Red rectangles indicate the location of restriction channels for the chamber.

For both designs, each inlet channel was supplied by a dedicated 5 mL syringe (Luer Plastipak 302817, BD, USA, with an inner diameter of 11.99 mm), except for the dye channels 3 and 4 of the 3-chambers design when they were used, in which case the solution was loaded in a 1 mL syringe (Luer Plastipak 300013, BD, USA, with an inner diameter of 4.70 mm) to ensure a lower flow rate. Polytetrafluotoethylene (PTFE) tubing (inner diameter 0.59 mm, outer diameter 1.06 mm, wall thickness 0.25 mm, TW24, Adtech Polymer Engineering Ltd, UK) was used to connect chip and syringes in all experiments. Since the outer diameter (1.06 mm) is slightly larger than the hole size (1 mm), tubings can be connected to the chip by simply forcing them into the PDMS holes, which ensures sufficient sealing at the ranges of pressure used here. Connection of the tubings to the syringes was done thanks to metallic needles (Microlance #20, 302200, BD, USA). The outflow was collected in a disposal beaker.

2.3 Stimulus delivery

1- chamber design : The sum of flow rates for channel 0 and 1 is kept constant during the experiments. When one rate is decreased or increased the other are adjusted accordingly, which allows to keep a roughly constant flow speed in the central chamber containing the animals, in order to minimise mechanical disturbance. A total flow rate of 2000 µL/h = 33.33 µL/min was used in the experiments, which corresponds to a flow speed of $\frac{33.33}{60} \times \frac{1}{0.1 \times 2.5} = \frac{0.555}{0.25} \approx 2.2\ mm/s$ in the central chamber. For a half-half condition inside the chamber, a flow rate of 1000 µL/h is used for each pump. This simple design is limited by a problem of pressure release while switching stimuli, as described in Chapter VI, hence it was used for preliminary experiments only.

3-chambers design : The sum of flow rates for channel 0, 1 and 2 is kept constant during the experiments, and likewise when one rate is decreased or increased the two others are adjusted accordingly. A total flow rate of 4000 µL/h = 66.66 µL/min was used in the experiments, which corresponds to a flow speed of $\frac{66.66}{60} \times \frac{1}{0.1 \times (1.5+2.5+1.5)} = \frac{1.111}{0.55} \approx 2\ mm/s$ in the central chamber. Three different flow rates are used : rActive = 60 µL/min, rStimulus = 63.33 µL/min and rPassive = 3.333 µL/min. Figure V-7 shows how switching between these flow rates enables stimulus delivery. The respective flow rates for channels 0, 1 and 2 are called r0, r1 and r2. When a flow rate is strongly decreased, e.g. from rActive to 0, some pressure release takes place in the corresponding channel, since pressure is stored in the tubing and in the PDMS walls of the chip itself. The lateral chambers are

the places where pressure release takes place (see top lateral chamber in Figure V-7C for example), and in this way the 3-chambers design solves the problems of stimulus switching inherent to the 1-chamber design : if there was only one chamber, this would prevent an effective wash and affect the stimulus switch (see Chapter VI). This experimental setup thus allows a fast stimulus switch inside the main chamber, even in the absence of valves to operate the channels switches.

For both designs, the total flow speed corresponds to a Reynolds number of about 0.2, which satisfies the conditions for laminar flow explained above. Moreover, such a speed ensures that the animals will not disturb spatial patterns of chemicals (for examples of such disturbance, see animal-flow interaction in the present chapter), while still being able to freely move.

The syringes were operated each by a separate pump (see Chapter IV), except for the additional dye syringes 3 and 4 in the 3-chambers design, which were operated by the same pump as syringes 1 and 2 respectively, to indicate when these channels were active. The pumps were controlled via Micro Manager as described in Chapter IV. A detailed description of the hardware-software configuration is given in Appendix D, the scripts used in the present conditioning experiments can be found at : https://github.com/ThomasChartier/Experimental_scripts

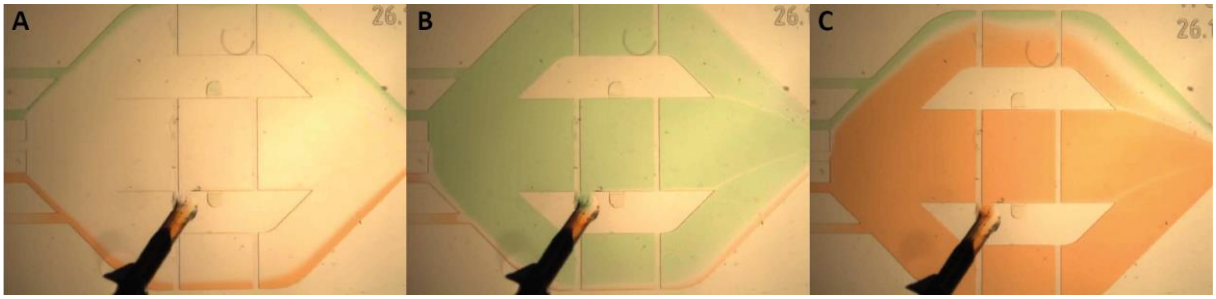


Figure V-7 Principle of stimulus delivery in the 3-chambers design. (A) Resting state, animals exposed to water, r0 = rActive, r1 = r2 = rPassive. (B) Animals exposed to stimulus 1, r0 = 0, r1 = rStimulus, r2 = rPassive. (C) Animals exposed to stimulus 2, r0 = 0, r1 = rPassive, r2 = rStimulus. Flow from left to right

2.4 Conditioning protocol

The protocol used in the present conditioning experiments and their controls is described in Figure V-8. The first stimulus S1 is presented for 15 s, immediately followed by the second stimulus S2 for another 15s without overlap ; this corresponds to an Inter-Stimulus Interval (ISI) of 15s. The Inter-Trial Interval (ITI) was set at 5min in all experiments, i.e. there was an interval of 4min 30s between one S2 offset and the next S1 onset. Each cycle was repeated for 5 times in most experiments and 4 in a few of them. Before the first stimulus onset, a resting period of 5 minutes was given to the animals in order for them to habituate to the chamber.

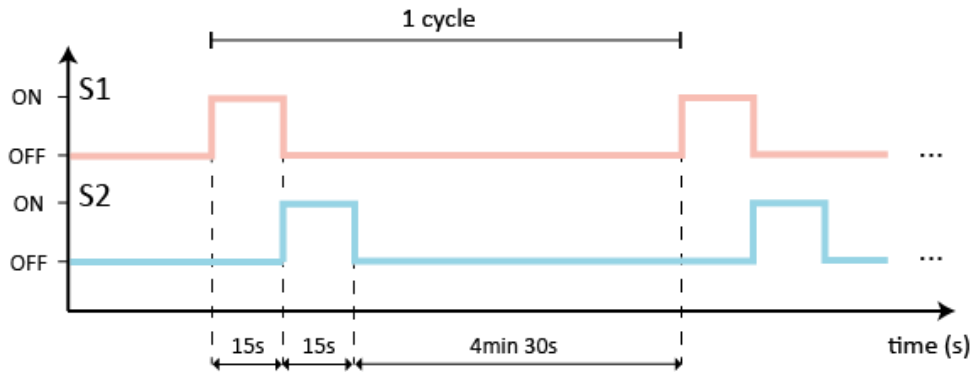


Figure V-8 Stimulus protocol used for conditioning experiments.

2.5 Stimulus preparation

See Chapter IV.

2.6 Experimental setup

An overview of a behavioural chip is given in Figure V-9 (note that this is an older chip design but the principle is identical). The chip, closed by a microscope glass slide, is placed under a stereomicroscope and imaged from above. It is taped to the stage. A pin closing the introduction channel allows to open and close it for animal introduction and removal. Care should be taken that no air enters the chip while manipulating it, it may be very difficult to remove. Pumps and their syringes are located on the left side and are handled in a manner identical to that described in Chapter IV.

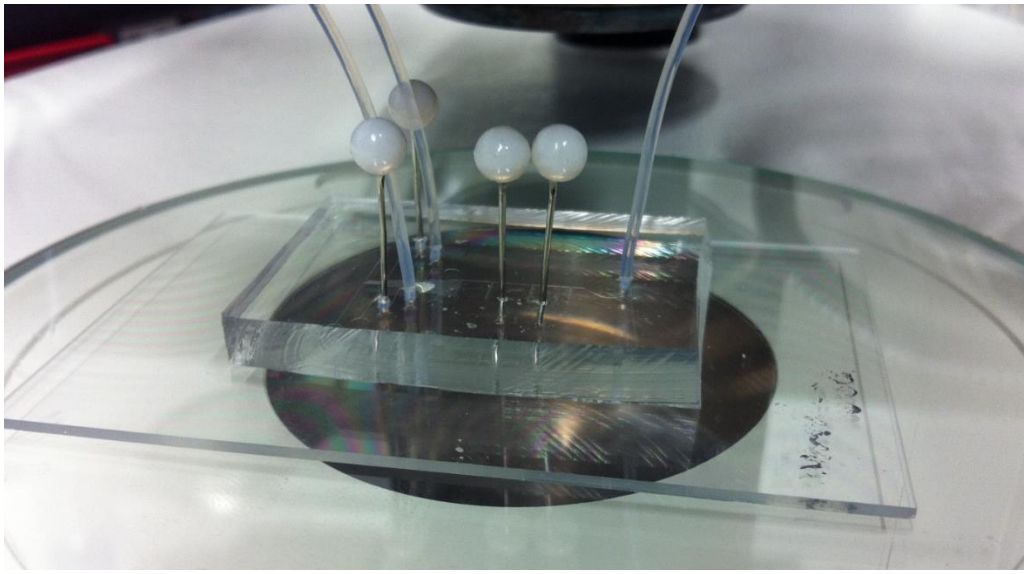


Figure V-9 Overview of a microfluidic device used for behavioural experiments, placed under a stereomicroscope. Inlet (left) and outlet (right) tubings are visible, unused channels are closed by pins. Brightfield illumination comes from below, and the animal chamber is imaged from above, through the PDMS.

2.7 Imaging

The central chamber was imaged with a colour camera (DFK23UM021, The Imaging Source Europe GmbH, Germany) acquiring at 3 frames per second, and mounted on a Leica MZ16 stereomicroscope. Images in a microfluidic chamber are best acquired through the glass or PDMS layer that closes the design – in the present case a glass slide for microscopy – however here it was enough for the required image quality to observe from the other side, i.e. through the PDMS. This had the advantage of positioning the chip directly on the stereomicroscope stage without the need of a specific chip holder, and being able to manipulate conveniently the chip notably during animal introduction or removal (see Figure V-9). In most experiments the image size was 528 x 636 pixels with no binning. Videos were saved in a .avi format and compressed using MJPEG with a compression rate of 65%.

2.8 Preference index

A preference index (PI) reflecting a positional bias toward the left or the right side of the chamber is calculated as follows :

$$PI = \frac{(\#L - \#R)}{(\#L + \#R)}$$

with #L and #R referring to the number of animals located in the left or right half of the chamber respectively. This index will be 0 if animals are equally distributed in the chip, +1 or -1 if they are all located in one or the other half of the chip, and have intermediate values in other case. The PI is calculated from images taken every 15 seconds, and its evolution plotted over time to reflect global movements of the group of animals.

2.9 Behavioural analysis

Each experiment was filmed and the video subsequently analysed. Behavioural responses at each stimulus onset were quantified manually and a score of avoidance response representing responses of increasing intensity was assigned to each animal, according to the following unambiguous criteria :

- 0 = no backward movement
- 0.25 = only parapodial pointing towards the front
- 0.50 = parapodial pointing towards the front, plus backward movement inferior to one body length
- 0.75 = backward movement superior to one body length
- 1 = backward movement superior to one body length, plus body squirming

In each experiment, to average individual differences these scores are plotted in a cumulative manner for the whole group of animals, with a maximum score of 5 (when all 5 animals show the strongest avoidance reaction) and a minimum of 0 (when none of the 5 animals shows any avoidance reaction).

2.10 Master mould and PDMS chips fabrication

All master mould fabrication was performed as described in Chapter IV except for the layers' height. The moulds for these behavioural chips have two layers : layer 1 for the general height of the chip (30 µm), layer 2 for the height of restriction channels (100 µm). Layer 1 of the mould was made using SU-8 2025, a spinning speed of 500 rpm for 10s then 2500 rpm for 40s, and baking times of 2+6 and 1+6 minutes for soft and post-bake at 65°C/95°C respectively. Layer 2 of the mould was made using SU-8 2150, a spinning speed of 500 rpm for 10s then 2300 rpm for 40s, and baking times of 7+50 and 5+16 minutes for soft and post-bake at 65°C/95°C respectively. Information on temperatures and duration were adapted from the manufacturer's manual. An operational protocol for master mould fabrication is available in Appendix E

Chip fabrication was performed as described in Chapter IV, except that a standard glass slide for microscopy was used instead of a coverslip, and hole diameters were 1 mm for inlet and outlet channels and 0.75 mm for the animal introduction hole.

Before usage, the chips were immersed in distilled water and kept for 20 minutes in a standard laboratory vacuum desiccator, to help water wet and fill the channels and remove all air from inside the chip.

V – 3 Results

3.1 A constant flow in a microfluidic chamber influences larval behaviour

Using a microfluidic device for the delivery of chemical stimuli introduces a factor that may not be often present in the natural environment, and for sure not in petri dish where the animals' behaviour could also be observed : a constant, monodirectional, and potentially strong flow. Indeed, sea water is never totally still in the nature, nor are usual flows ever monodirectional. What is more, although a flow speed such as 2 mm/s may appear quite low for us, it needs to be put in relation with the animals' size, as it indeed represents a water displacement of no less than 10 body lengths per second. For humans this would be equivalent to a constant strong wind of 20 m/s ≈ 70 km/h, not to mention the fact that water is 1.000 times more dense than air. Such a flow is therefore a strong mechanical stimulus for the larvae, and prior to conducting any further experiment it needs to be tested to which extent their spontaneous behaviour is affected by the presence of such a flow.

To that aim, simple experiments were devised, in which animals between the 5 and 7dpf stage were introduced in a chip (design shown in Figure V-11, 4 x 4 mm chamber) and their behaviour monitored in the presence and absence of flow. A simple quantification of their spatial left-right distribution was monitored over time, starting immediately after their introduction (see the definition of the preference index in 2.8). Groups of 20 or 30 larvae were introduced, and tested with three replicates per condition in randomised order. For the animals who started without flow, the same current as for the others was established after 10 minutes, to observe its influence on animals used to a still condition. The results of these experiments are presented in Figure V-10.

A comparison of the groups without current (Figure V-10A and C) and with current (Figure V-10B and D) reveals that the position of the animals is more variable in the absence of current, and that this variability is maintained over 10 minutes. This shows that mechanically undisturbed animals adopt – at least during 10 minutes – an attitude of rather permanent movement instead of stopping at a certain place. A close look at individual behaviours in videorecordings shows that this movement actually consists of periods of immobility interrupted by (mostly) forward spontaneous movement and forward/backward movements provoked by the interaction with other individuals (data not shown here). On the contrary, in the presence of current the animals tend to reduce their activity and settle somewhere in the chip where they will be the least disturbed by others, as can be seen from the individual curves in Figure V-10B and D where the preference index tends to be stabilised over time. If a current is introduced for animals which were previously undisturbed (Figure V-10E and F), the activity is reduced and animals tend to settle at a certain place, whereas they would permanently move before.

These results clearly establish that the flow speeds used in subsequent experiments do influence the animals' locomotion, in making them more or less mobile. Thus, it should be remembered that any exploratory activity will be reduced under a flow condition, which can become important if a spatial pattern of chemicals is introduced in the chip : it should be verified whether or not the animals will spontaneously move enough to experience differences in their chemical environment. An absence of behavioural response may thus be attributed simply to an absence of exposure to more than one condition.

The flow chosen in behavioural experiments should not be too strong, otherwise animals may stay immobile and any reaction due to a chemical stimulation would be masked. On the other hand, if the flow speed is reduced too drastically, it is possible that the animals' movement starts to affect this flow, and hence the desired spatial patterns. This point was the next to be tested.

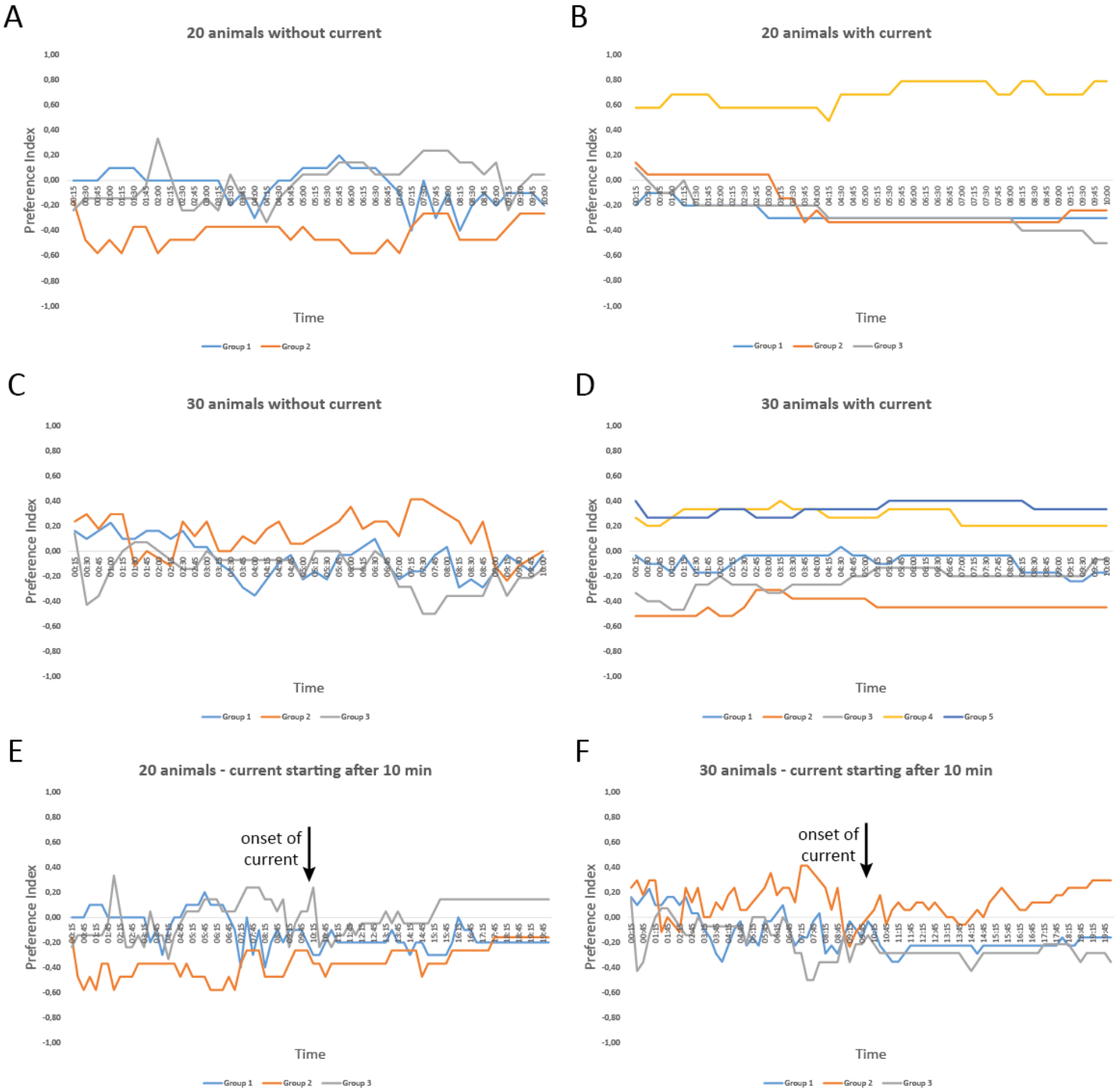


Figure V-10 Influence of flow on the position of larvae inside a microfluidic chamber. The Preference Index (see Methods) is plotted against time. The first ten minutes of graphs (E) and (F) are identical as graphs (A) and (C) respectively. In graph (E) and (F), onset of current takes place after 10 minutes of experiment.

3.2 Larvae can interact with the chemical patterns

For behavioural experiments, it should be kept in mind that the animals inside the chip are relatively big, both in comparison with the scale of fluidic events, and in comparison with the total volume of the chamber. In these conditions, the animals will necessarily interact with the flow, and an appropriate flow speed needs to be identified so that such effects stay neglectible.

In the real experiments, no dye can be used to visualise the boundaries between stimulus streams, because the animals would detect the dye as a chemical stimulus itself and this would affect the perception of the relevant stimuli. Without dyes, the animal-fluid interaction can become problematic if it affects the effective duration of stimulus exposure or the position of stream boundaries in a static configuration.

A striking example of animal-flow interaction at a too low flow speed in shown in Figure V-11 (flow from left to right). In that case, alternate water streams with and without orange dye are supposed to generate a pattern of four horizontal and parallel bands in the central chamber ; however the flow speed is too low and the pattern formation is totally impeded by the animals' movements. Without dyes to reveal such a problem (as was actually the case in experiments conducted previously in the lab), the experimenter would think that the pattern is established, and would draw wrong conclusions from the animals positions. Indeed here, some animals are exposed to the dye that are not supposed to, and conversely some animals supposedly in the dye areas experience rather an absence of dye, which invalidates any conclusion based on the supposed spatial pattern.

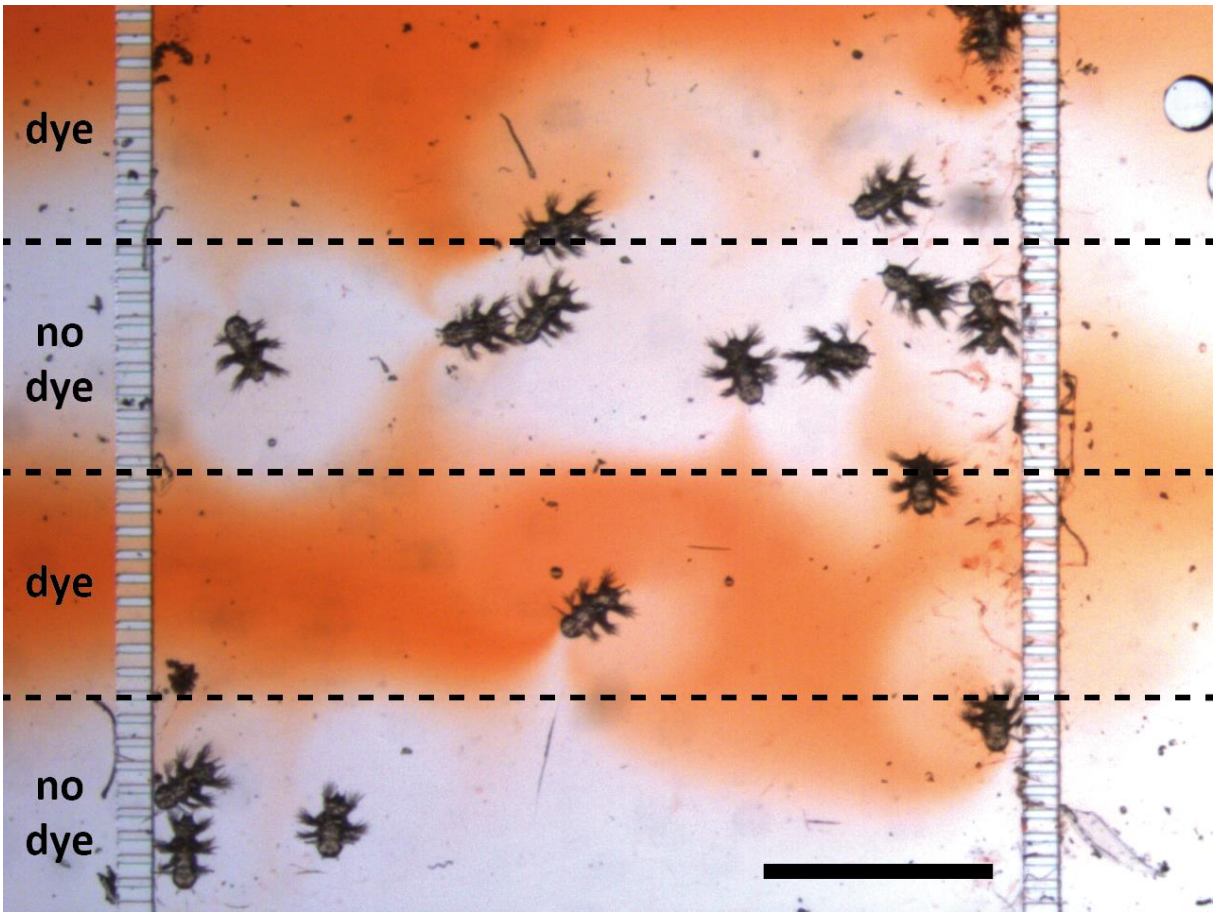


Figure V-11 Example of a spatial chemical pattern disturbed by the animals' movement and ciliary beating. Flow is from left to right. Dashed lines indicate the theoretical boundaries of dyed and non-dyed water streams if the animals were absent. Scale bar 1 mm.

As can be seen on Figure V-13, the flow perturbations introduced by the larvae seem to extend to a distance larger than would intuitively be expected from crawling body movements only. The rather circular halos observed around the animals suggest the existence of a local flow, and an obvious phenomenon that could account for this effect is the beating of the larval ciliary bands. Larvae are indeed equipped with 5 well-developed ciliary bands [82], [138] that are spontaneously active in immobile animals [136].

To further investigate the origin of such flow perturbations, and test specifically whether ciliary beating is responsible for the halos observed, the following experiments were conducted. A dye front at low speed was introduced in the chamber in separate experiments involving two groups of animals : one group was kept untreated, while the other was simply euthanised with an ethanol treatment to make sure ciliary beating would not take place. It is actually unknown how to stop the ciliary beating in living animals and ciliated cells will keep their spontaneous beating activity even in a dying animal or when dissociated – magnesium chloride treatment blocks muscle contraction but not ciliary beating. The animals were imaged when reached by the dye front, and the perturbations could be characterised simply by looking at the halo shape around the animals. One snapshot for each condition is presented in Figure V-12 (flow from top to bottom). On the left in the absence of animal movement and ciliary beating, the dye reveals a simple passive hydrodynamic effect around the bodies which is of limited range, comparable to the body width. On the right, in the presence of ciliary beating, an active flow disturbance in the form of large halos around the animals is observed, even though most of them were immobile when the snapshot was taken. This shows that the halos are indeed due to the ciliary beating (a complementary experiment with $MgCl_2$-treated animals not shown here revealed the presence of halos of comparable size). These effects can extend to a radius of almost twice the body length (400 µm), which is large compared to the width of the microfluidic chambers used here (around 2 mm). The ciliary beating creates a local water current of the dipolar type, responsible for the roughly circular halo observed around the animals, and particularly apparent for the downstream-facing animal on the right side of Figure V-12B.

These results establish that ciliary beating can induce dramatic interactions with the flow when its speed is too low, and totally disrupt a desired spatial pattern. Hence, for each chip design, it needs to be verified in which flow regime this interaction will be small enough to be neglected. Preliminary experiments allowed me to identify 1 mm/s as a relevant order of magnitude to avoid such effects without flushing away the animals to the downstream side of the chamber, and such flow speeds were subsequently used in the experiments.

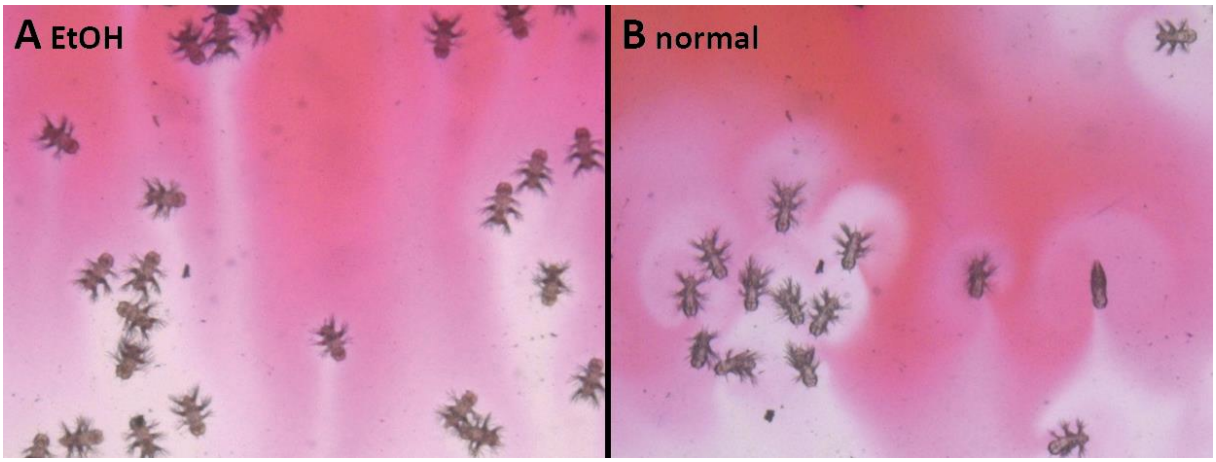


Figure V-12 Example of passive (A) and active (B) flow perturbation created by Platynereis larvae inside a microfluidic chamber when the flow speed is too low. (A) EtOH-treated animals (euthanised) and (B) normal animals. General flow is from top to bottom, the dye used is xylenol orange.

3.3 Towards a pavlovian assay for learning

3.3.1 The chip design allows a rapid change of stimulus

As a first validation of the 3-chambers design, I needed to verify if stimuli could be switched fast enough in its central chamber, to provide the temporal pace of stimulus change that may be required for associative phenomena to take place (see Introduction). I thus filled the two stimulus channels with dye solutions and ran the conditioning protocol. The changes in dye concentration in a particular spot inside the chip are estimated from the measured light intensity plotted it against time.

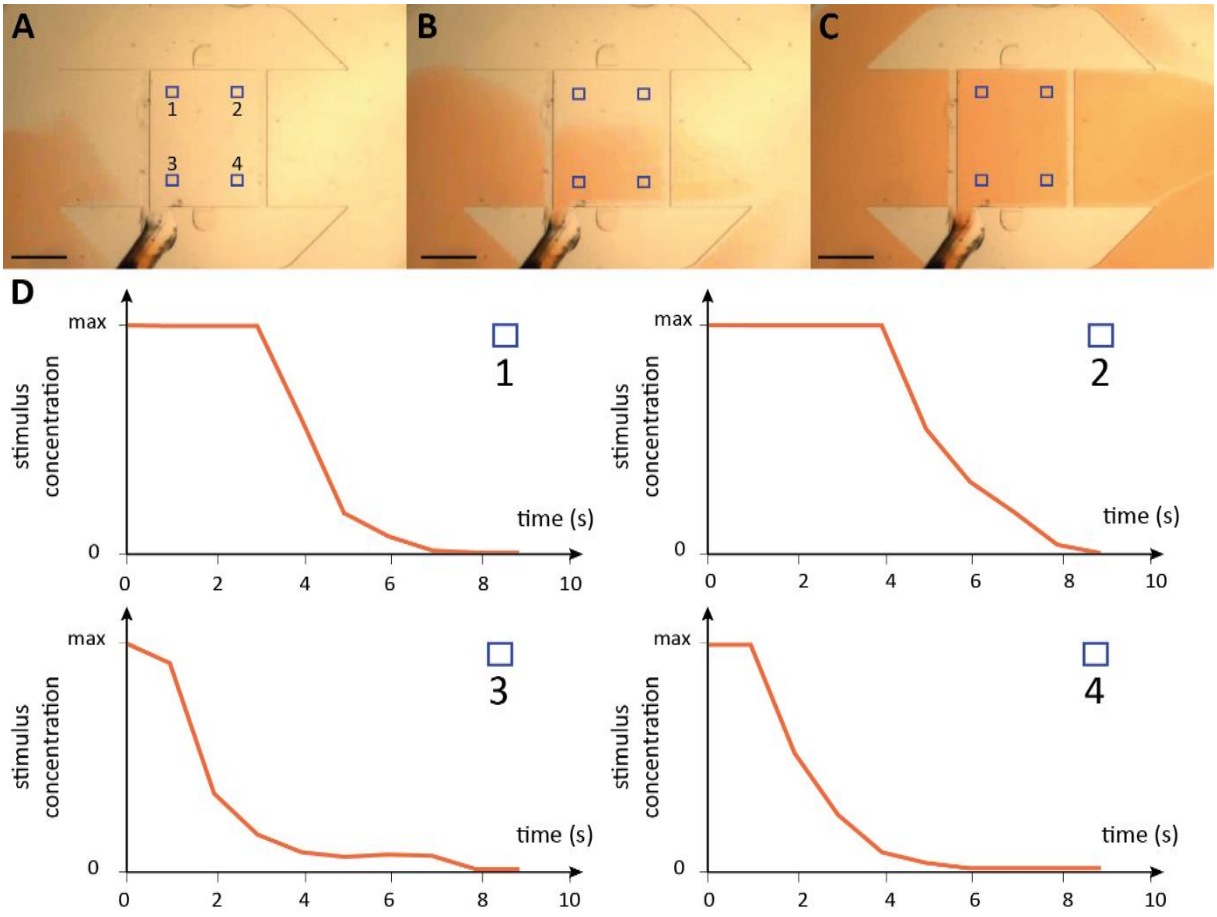


Figure V-13 Kinetics of stimulus change inside the central chamber. Pictures (A) to (C) give an overview at three different time points of how the stimulus is being exchanged, flow is from left to right. (D) Stimulus concentration, as estimated by light intensity due to the dye, is plotted against time for the four regions of interest indicated as blue squares in (A). Pictures (A), (B) and (C) correspond to time points 0, 3 and 9s respectively. Scale bar 1 mm.

As can be seen from the graphs in Figure V-13D, it takes on the order of 3 seconds to transition from absence of stimulus to stimulus at full concentration at a fixed point, which is what an immobile animal would experience. The most extreme transition times experienced by a mobile animal could be at least 2 seconds for an animal moving from point 2 at time 4s to point 3 at time 6s (a larva does not move faster), and at most 7 seconds for an animal moving from point 3 at time 1s to point 2 at time 8s. Movement of an animal before the stimulus arrives is independent on stimulus change, hence statistically these variations would gradually cancel out across trials, so that on average any animal would indeed experience a transition time of 3 seconds. Similar calibrations conducted on the stimulus offset gave similar results despite a somehow higher speed, and are not shown here. Since the chip design is symmetric, both side behave the same way, thus the S1 and S2 deliveries are similar. The 3-chambers design is thus suited for behavioural experiments with rapid stimulus changes.

3.3.2 *Quinine as a US triggers stereotyped avoidance responses*

In the study of taste and chemosensory behaviours in insects and in mammals, the alkaloid quinine is a substance known for its bitter taste and aversive effects [270],[269]. It has been used as an aversive US for classical conditioning in honey bees [330] and ants [331]. In preliminary experiments on adult *Platynereis*, I had observed strong reactions to quinine, which prompted its use in larvae.

Using the 1-chambre microfluidic device I could show that larvae do avoid quinine, as shown in Figure V-14, and I was able to identify a concentration of around 30 µM as the threshold for aversion. In these experiments, after 30s of imaging a quinine solution in Natural Sea Water (NSW) is introduced (orange arrows in Figure V-14) in the top half of the chamber while the other half contains NSW, and animals are given 2 minutes to react. A snapshot is taken after 2 minutes, and the Preference Index (PI) is plotted over time. Three examples of such experiments are shown here, conducted with quinine at 10, 30 and 100 µM with 22, 21 and 23 animals in the chamber respectively. At 30 and 100 µM, most animals accumulated in the bottom half of the chamber that is free of quinine, while the ones located in the quinine half are actively moving (indicated by pink stars). The evolution of the PI over time is consistent with this position, and indicates that animals preferentially stay in the quinine-free area. At 10 µM, animals are not preferentially located on one side or the other, and active animals can be seen equally on both sides after two minutes (Figure V-14A). The PI reveals a stable balanced distribution of animals inside the chip. These quantifications illustrate the aversive effect of quinine above 30 µM, and demonstrate that animals do find a suitable position in the chip with regards to this stimulus.

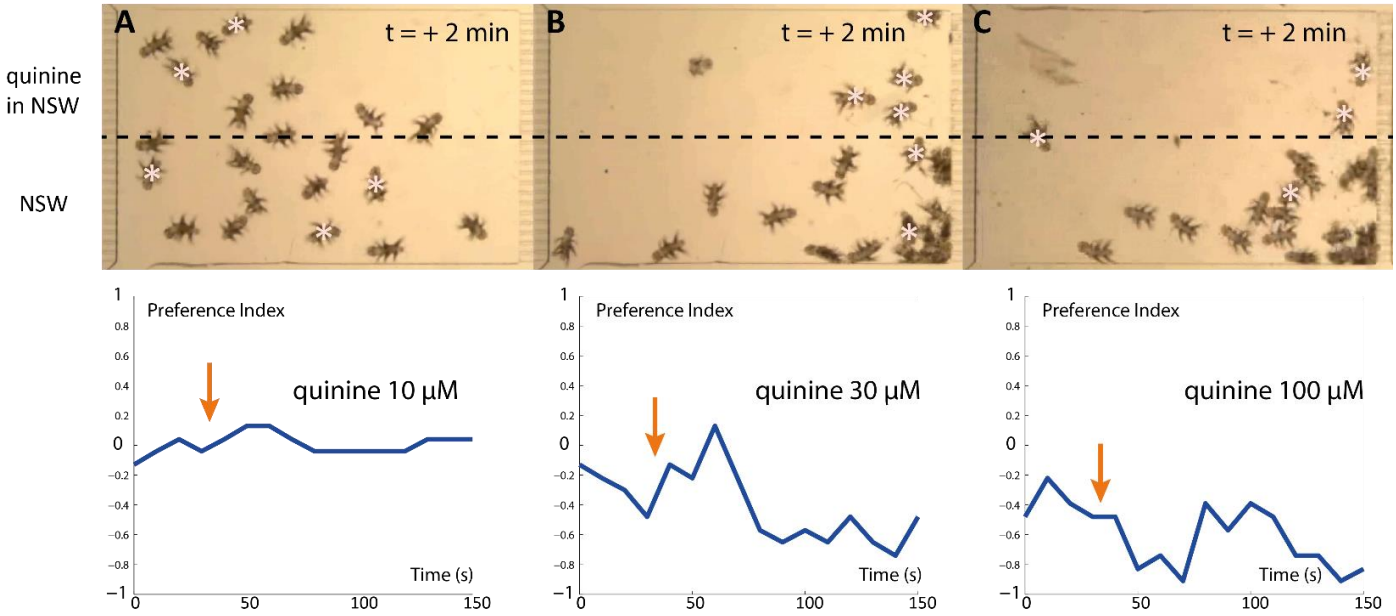


Figure V-14 Avoidance for quinine at different concentrations, assayed in an old chip design. Platynereis larvae at 10dpf. Pink stars indicate the animals that are moving when the snapshot is taken, 2 minutes after the start of quinine exposure in the top half of the chamber. Orange arrows on the temporal graphs indicate the onset of quinine. Chamber dimensions are 2.5 x 4 mm, flow is from left to right.

In order to further characterise this avoidance reaction, I decided to take a closer look at the animals' behaviour at the particular moment when they detect quinine. I performed experiments in the three-chamber chip, in which the timing of stimulus delivery is well-known (see Figure V-13 above). Upon exposure to 100 µM quinine, *Platynereis* larvae show a backward crawling reaction, as can be seen by comparing their position at t = 0s when quinine reaches the chamber (Figure V-15A) and at later time points (Figure V-15B to D). This first reaction is then followed by a turn and by a rather fast forward crawling movement (not shown here). Repeated experiments revealed that the backward crawling

reaction is rather stereotypic. The reaction to quinine above the aversion threshold of 30 µM thus clearly appears to be an escape response.

These experiments establish that quinine can be used as a US for conditioning experiments of aversive learning, in that it produces a clear behavioural response that is easy to recognise. The stimulus intensity should be chosen slightly above the aversion threshold, i.e. between 30 and 100 µM : intense enough to reproducibly trigger the response, but not too intense to avoid undesired fatigue effects. It was thus set at 50 µM for subsequent experiments.

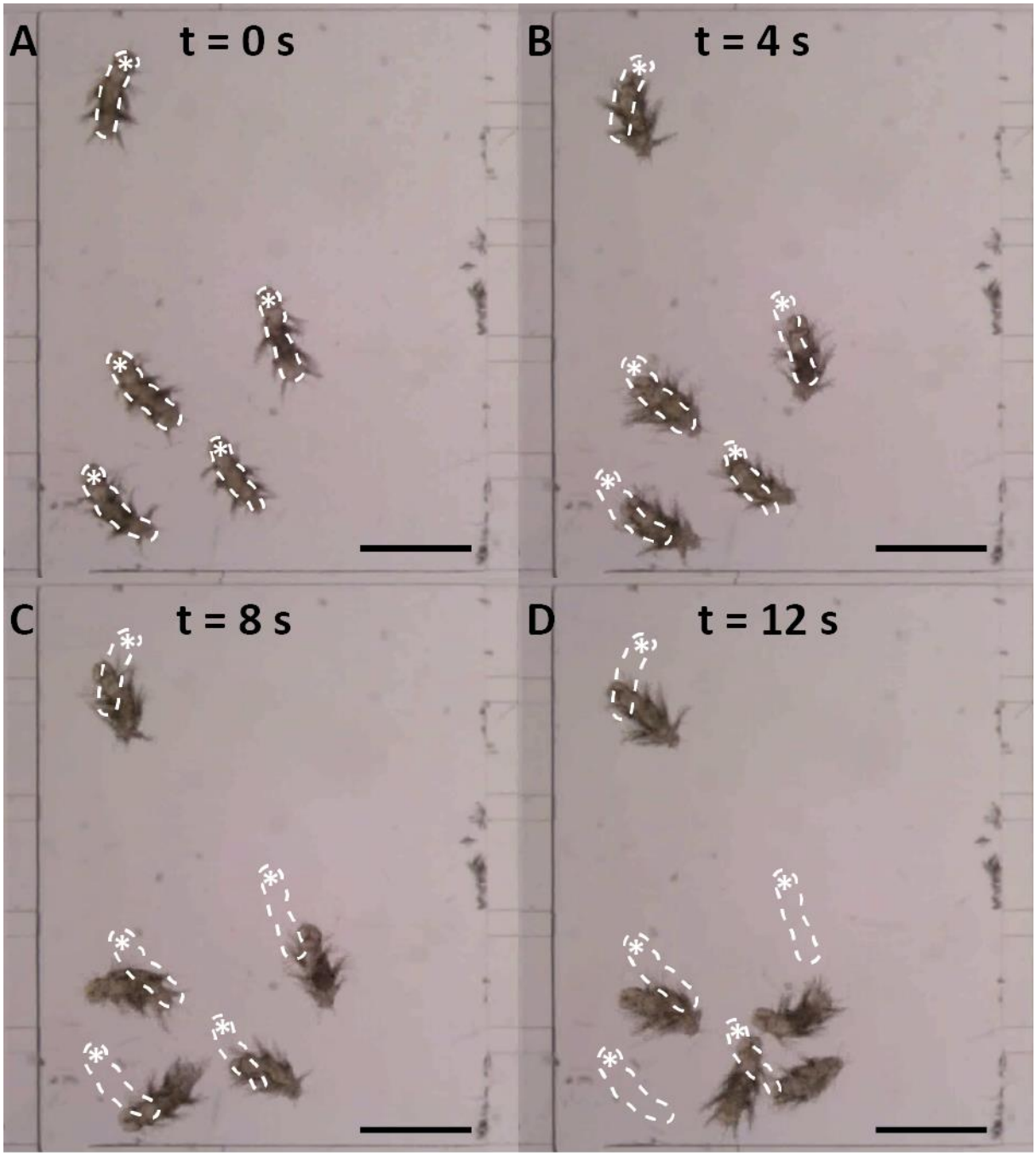


Figure V-15 Escape response to 100 µM quinine in 4-segmented Platynereis larvae, imaged in the chip's central chamber at four different time points, t = 0s corresponds to the moment when the quinine reaches the left (upstream) side of the chamber. Dashed lines indicated the position of the animals and white stars the position of their head at t = 0s. Flow is from left to right. Scale bar 0.5 mm.

3.3.3 1-butanol as a neutral, non-behaviour-eliciting stimulus

Functional imaging has revealed that 1-butanol at 10 µM is detected by 6dpf *Platynereis* larvae, and does not provoke strong behavioural responses (see Chapter IV). I asked whether this stimulus could be used as a CS for associative learning.

In an assay similar to that described in Figure V-14 and with the same chip design, I investigated how larvae (here at 7dpf) would react to 10 µM 1-butanol. The stimulus was first presented in the whole chamber during 30 seconds, then switched only in the bottom half of the chamber for several minutes, and the animals were observed while freely moving. The evolution of the PI over time reveals a fluctuating position (see three snapshots) around a balanced top-bottom distribution of the animals in the chamber (Figure V-16). Movement still observed in a few animals on the butanol side after 1 min is mostly due to packing. Repetitions of the experiment confirmed that the PI was typically around 0, indicating an absence of attractive or aversive effect of 1-butanol at 10 µM.

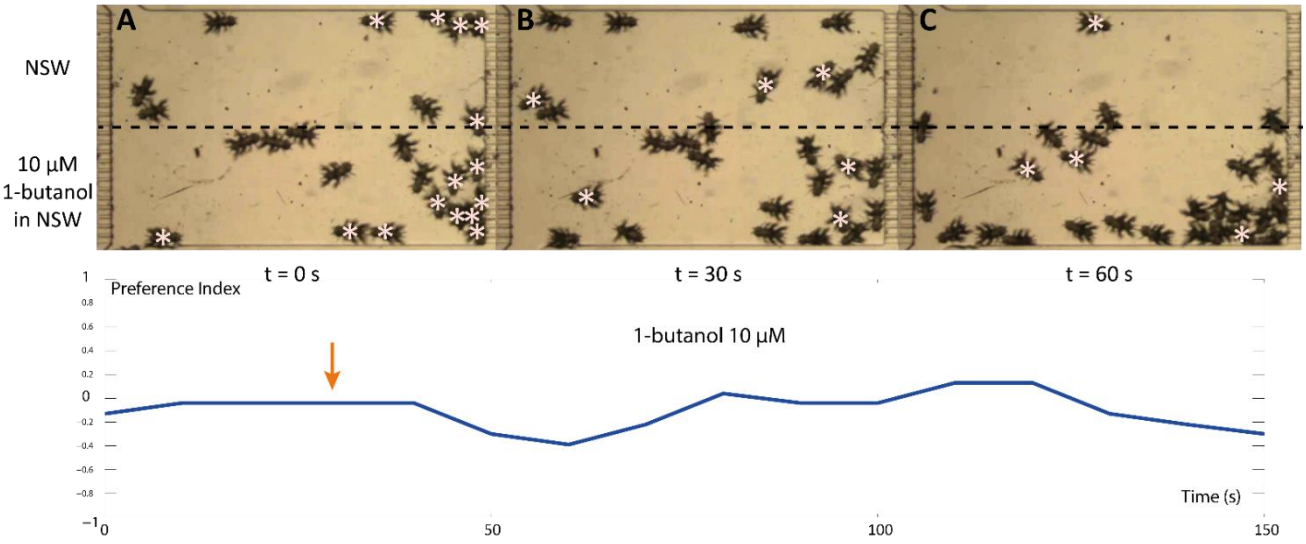


Figure V-16 Attraction for 1-butanol over the course of 1 minute, Platynereis larvae at 7dpf. Three time points are presented (A) to (C). t = 0s corresponds to the moment when 1-butanol stop to be present in the whole chamber and is switched to the bottom half only. Pink stars indicate the animals that are moving when the snapshot is taken. Chamber dimensions are 2.5 x 4 mm, flow is from left to right.

During these experiments, no clear reaction to butanol was seen at the precise moment when the animals received the stimulus for the first time. If any, then the effect was rather a slow, forward movement that was interpreted as a searching response. An escape response similar to the one described for quinine was never observed.

It appears that a chemical cue such as 1-butanol is a good candidate to be used as a CS in a conditioning experiment. Indeed, it does not spontaneously induce the response triggered by the US ; what is more, if any effect at all, it produces a slightly exploratory response that is distinct from the avoidance (forward versus backward). Thus, if the slight attraction or absence of attraction to 1-butanol could be turned into an aversion upon repeated co-exposure with quinine, this would make it even more convincing that the effects would be associative.

3.3.4 Testing interaction effects between quinine (US) and 1-butanol (CS)

In an attempt to observe associative effects, I then submitted early *Platynereis* juveniles (between 12dpf and 5 segments) to repeated conditioning cycles, using quinine at 50 µM as a US, and 1-butanol at 10 µM as a CS. I had conducted several such experiments before developing the 3-chambers chip

design ; even though a few of them showed encouraging results, including avoidance responses to the CS after CS-US pairing but not after exposure to US alone, these experiments are too disparate to be reported here, and I am presenting only the latest ones.

In this set of experiments, the design included the following groups :
- S1 = water / S2 = water, as a control for the base rate of avoidance responses in presence of the low yet unavoidable flow perturbation introduced by the stimulus switching
- S1 = CS / S2 = US, i.e. paired presentation of CS and US in a forward manner, as the conditioning group
- S1 = CS / S2 = water, i.e. CS alone as a control for sensitisation of the avoidance response by the CS
- S1 = water / S2 = US, i.e. US alone as a control for sensitisation of the avoidance response by the US

Results for experiments conducted each on 5 individuals in the same chamber with 5 consecutive S1-S2 presentations are shown in Figure V-17. Each individual graph correspond to a separate experiment, and shows cumulated responses of the 5 animals as bar plots, each animal being coded by a colour.

As can be seen, in most cases of US presentation all 5 animals display the strongest avoidance response with backward movement and body squirming, corresponding to an individual score of 1/1, which results in a cumulated score of 5 (Figure V-17B and D). Occasionally, one animal would be less responsive, for example animal #5 in graph B-4, but overall these scores reflect the stereotyped nature of the avoidance response to quinine. Moreover, it is apparent that this response does not habituate across 5 consecutive trials, which validates the range of US intensity, and shows that an ITI of 5 minutes is sufficient for the animals to recover from the stress induced by the US. However the responses to flow appear to be weaker in the US alone control than in the base rate control, which is unexpected and could still indicate a certain fatigue or decreased responsiveness of the animals due to the US.

Upon repeated paired presentation of CS and US (Figure V-17B), avoidance responses to the CS can be observed in some, but not all, of the animals. From a comparison with the US alone control (Figure V-17D), it is apparent that these responses are not sensitised responses triggered by the flow, otherwise they would also be seen in the US alone case. In addition, these responses are overall stronger than in the base rate control (Figure V-17A), indicating that they are indeed triggered by the CS itself, not by the flow. Thus, avoidance responses to the CS are observed when it is paired with the US.

To determine whether these avoidance responses would represent conditioned responses attributable to the CS-US pairing, it first needs to be verified whether they are present in the CS alone controls. Actually, this is the case, as can be seen in Figure V-17C : animals do sometimes show avoidance reactions to the CS in the absence of US. If ones adds the scores of these responses for each experiment, it gives total CS avoidance scores of 2, 3.25, 3, 3.5 for the conditioning groups and 0.5, 3.25, 2.25 for the CS alone group, which may indicate that these responses are overall weaker in the absence of CS and thus enhanced by the pairing with the US, nevertheless more data would be needed to conduct satisfactory statistical analysis.

A look at individual responses reveals consistent patterns across trials. For example, animal #3 in experiment B-4 repeatedly shows an avoidance response to the CS, more so than the other animals. A higher responsiveness to stimulation is also apparent for animal #3 in experiment C-3.

The results reported here show that occasional avoidance responses are observed to the CS in the conditioning group, which may indicate the development in these animals of an associatively learnt response. Nevertheless, the control groups CS alone have revealed that such avoidance responses to the CS do occur in the absence of US exposure, contrary to what was though before these experiments. This shows that behavioural effects may be subtle, that responses need to be quantified at a more precise level than only presence or absence, and that the approach taken here seems adequate. Though there is no obvious difference in the amplitude of CS responses in the present set of experiments, more statistical power, i.e. more replicates, could allow to test this hypothesis satisfactorily, and may reveal small but statistically significant differences.

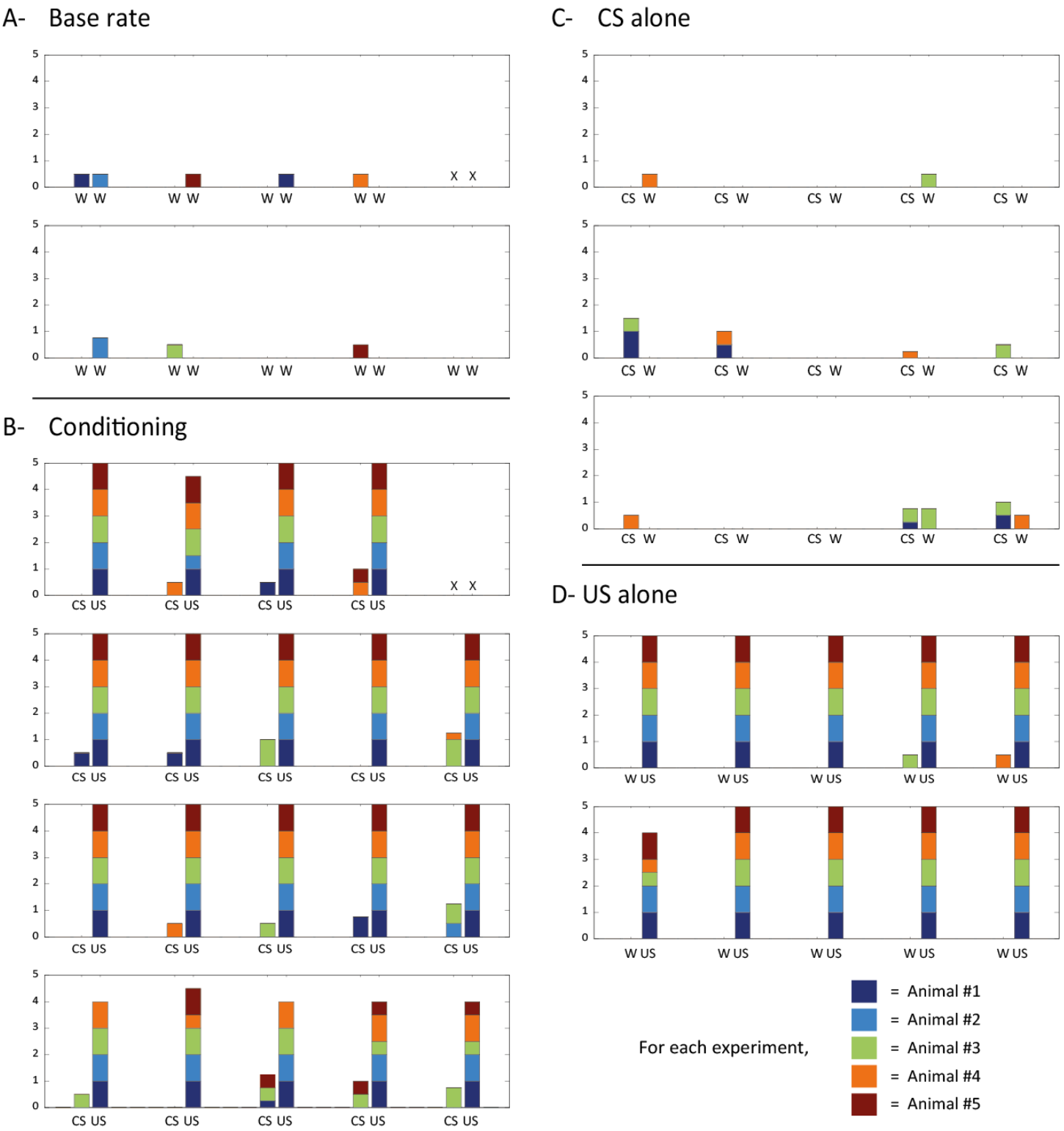


Figure V-17 Quantification of avoidance responses in conditioning and control experiments. Letters refer to what is used as Stimulus 1 and 2 (see stimulus protocol in the method section) : Natural Sea Water (NSW), Conditioned Stimulus = 1-butanol (CS), Unconditioned Stimulus = quinine (US). An X indicated missing data points. Avoidance responses are shown for the following situations : (A) responses to water stimulations only, (B) responses to CS and US successively (conditioning), (C) responses to the CS only, (D) responses to the US only.

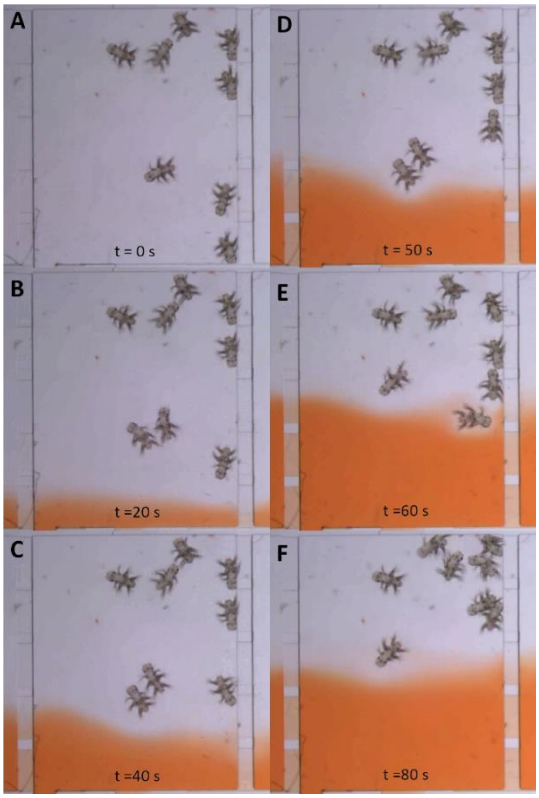
Yet, even such a result would not be sufficient to determine whether these effects are associative or not, since they could still be due to a pure sensitisation of the CS response by the US. To settle this question, an additional control with unpaired CS-US presentation would be needed : if the effect is present in the paired case but not the unpaired one, then it will most likely be associative. I unfortunately did not have enough time to conduct more experiments.

3.3.5 Test for avoidance responses after training

In the experiments reported in Figure V-17, the approach taken to reveal the development of a response was to plot a learning curve, but a dedicated test would be complementary and more convincing. To test the animals for their "performance" after training, i.e. to test whether they have learnt to produce the response when presented with the CS only, one needs to observe a difference between response to the CS before and after training.

In the first place, I had envisaged to test the animals by simply filling half of the chamber with the CS, and looking for an escape towards the CS-free, other half of the chamber to reveal a conditioned response. In the first experiments however, I could observe that, after conditioning, the animals tested in such a way would show some reactions to the CS onset, but these reactions would stop after a few seconds, without the animals moving to a different place at all. Any quantification of behaviour that relied on movement of the animals to the CS-free side of the chip was thus failing to reveal a reaction at all, even though it was clear that the animals were reacting. Worse, when I conducted such a test with two strongly aversive stimuli as a verification – quinine and xylenol orange – I could see that some animals would fail to escape the highly aversive area. This shows that the exposure to the stimulus is too brutal, and does not give sufficient spatial information for the animals to escape. As a result, some of them eventually stop moving and stay in the aversive area.

To improve this, I took two parallel approaches. One was to quantify the immediate reactions, in the manner illustrated in Figure V-17, which is independent of whether the animals are able to move to a different location. The other was still to try to have the animals moving towards one side of the chip as a result of a conditioned aversion to the CS, but with a different, softer CS exposition.



This second approach is illustrated in Figure V-18, with an orange dye to visualise where the CS would be if this assay was used after a conditioning experiment. For an aversive stimulus such as the one used here (Ponceau 4R at high concentration), the animals are effectively pushed to the top, stimulus-free half of the chamber where they all are at the end of the test (Figure V-18F). This would correspond to a Preference Index of -1, i.e. maximum aversion. Note that the flow condition is now established over one and a half minute, which gives the animals more time to orient themselves and avoid the stimulus. Moreover, they are all exposed to the stimulus boundary and are thus in a choice situation, as opposed to the previous situation where they were finding themselves brutally in the stimulus solution, with no other information about where to escape. This test thus looks quite promising, unfortunately I did not have time to exploit it.

Figure V-18 Test for avoidance. Six different time points (from A to F) are shown, and an aversive orange dye shows here where the CS would be in the real test.

V – 4 Discussion

4.1 Experimental setup

The first requirement of a setup for learning experiments, ensuring a fast stimulus change, has been met as demonstrated by the temporal calibration experiments (Figure V-13). It is reasonable to assume that a stimulus onset or offset time on the order of three seconds is comparable to what a *Platynereis* larva would experience in a natural environment with stimuli transported primarily by flow turbulence. Medium exchange at the level of surface receptors is anyway limited by pure effects of fluid mechanics such as diffusion through the fluid's boundary layer, as illustrated in Chapter V, and chemical stimuli cannot appear or disappear as fast as physical stimuli such as light.

Ideally, two inert dyes undetectable to the animals would be mixed with the two stimulus solutions, that would enable to visualise the precise flow dynamics of stimulus exchange, to quantify the exact exposure time of individual animals despite their movement in the chamber, and to relate this time to the behavioural effects observed. This was already achieved to some extent in the present experiments, and individual reactions of the animals could be shown to match the predicted stimulus on- and offset rather well (Figure V-20), though the calibration was always carried out in the same chip at the end of the session after the animals had been removed from the chamber, and progressive channel clogging by dirt during the experiments could result in slightly different flow patterns. Since the chip can be imaged through the PDMS without compromising image quality and behavioural analysis, as was done here in all experiments, one could also imagine to stick two chips back to back, one containing the animals and the stimuli, the other containing dye solutions that could be seen through the first chip while filming in the animal's plane and would be operated by the same pumps as the stimuli, so that the dyes would precisely match the stimulus delivery and all information would be captured in a single image. However, a stimulus monitoring with inert dyes mixed to the stimulus solutions would always be superior, since any calibration in which the dye does not come in contact with the animals cannot capture animal-flow interactions that can delay the stimulus on- or offset (see examples in Chapter V).

From an imaging point of view, the setup has proved its suitability for precise quantifications of behaviour, including actions such as startling, biting or parapodial pointing. It thus appears that no further improvements of the setup are currently needed.

4.2 Stimuli

It was shown in Chapter IV that the CS used here, 1-butanol, is detected by the larvae. These behavioural experiments have proved that this stimulus can also trigger behavioural responses (Figure V-17). The stimulus is behaviourally rather neutral at 10 µM, in that spontaneous locomotor reactions are infrequent (Figure V-17C). Overall, 1-butanol probably constitutes a good CS.

To test whether the unconditioned response would be a meaningful one in a more natural environment, such avoidances were looked for in the boxes in which the animals are raised. These boxes contain algae, nutrients, and allow the worms to freely crawl on the substrate or swim. *Platynereis* juveniles after the 20-segmented stage are active feeders and will readily eat smaller *Platynereis*, they represent a danger for younger juveniles or larvae. When introducing small worms next to a much bigger one, I could observe escape responses, one example of which is depicted in Figure V-19. In this case, after the 5-segmented worm has touched the bigger ones with its head, it displays a backward crawling response very similar to the one observed as a reaction to quinine and described in Figure V-15. This backward movement likewise is followed by a turn and a fast forward crawling movement (not shown here). The response here is probably triggered by a mechanical stimulus rather than a chemical one. The escape response to quinine thus seems to be a general,

stereotyped, and natural escape response that *Platynereis* larvae and juveniles are able to produce, and which can be displayed among others upon encounter with aversive chemicals.

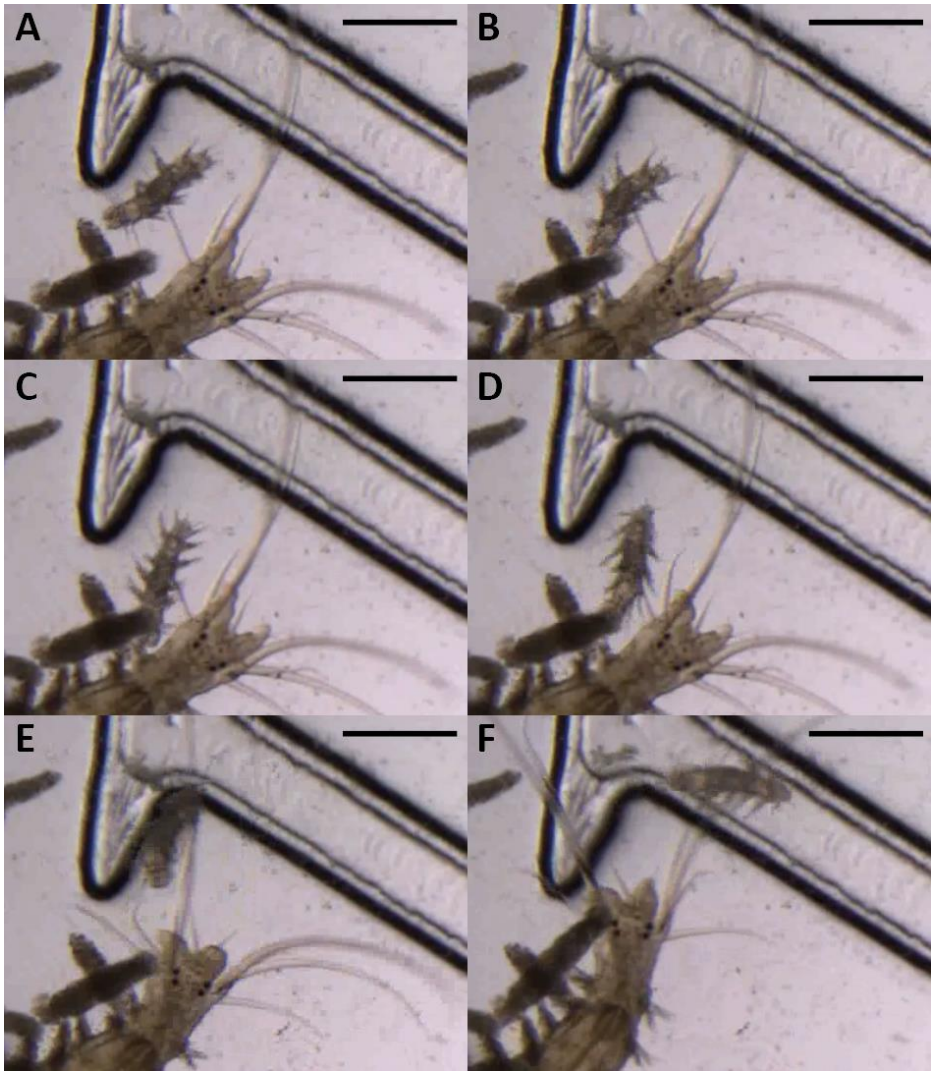


Figure V-19 Escape response in a more natural context, at six different time points ((A) to (F)) spanning a total of about three seconds. A 5-segmented worm approaches an older juvenile, makes contact with it at frame (C) and starts escaping at frame (D). The bigger worm detects the contact but does not seem to identify it as a prey, or at least makes no attempt to catch. Scale bar 0.5 mm.

Quinine at 50 µM has been found to trigger a marked (Figure V-14), stereotyped (Figure V-15) escape response, that is probably the animal's natural escape response to a danger (Figure V-19). This response does not habituate across trials (Figure V-17B and D), though possible fatigue effects were pointed at. Even if quinine, a terrestrial plant extract, is unlikely to be present in marine environments, the unconditioned response it induces has characteristics that make it a suitable US. Nevertheless, there may be reasons to look for an alternative US. At a late moment during my PhD, I became aware that quinine is known to inhibit calcium-dependent potassium channels, at least as demonstrated in cell cultures of rat pancreatic cells [332] and guinea-pig liver cells [333]. Its effects as a potential neuromuscular blocker are thus documented, which fits with paralysis effects I had observed early in my project (and then forgotten about) : *Platynereis* larvae become paralysed when exposed to 1mM quinine for too long – cilia however keep beating. Recovery upon washing is total but takes several hours. If quinine interacts with potassium or other channels in *Platynereis*, as appears to be the case, one may as well fear that the chemosensory transduction itself could be affected, and impede a correct CS detection. Besides, it may be better to work with a CS and a US of different sensory modalities, which permits their independent delivery with no restriction regarding stimulus overlap. Indeed in a

conditioning paradigm, the CS can be presented with or without overlap with the US. I had chosen to avoid overlap, since I was concerned that two chemical stimuli could interact at the level of receptor proteins. Moreover, it is known for example in insect olfaction that binary mixtures of odorants are detected in a non-linear fashion, either as independent of each other, or with agonistic or antagonistic effects [334],[335]. A non-chemical US would eliminate this concern. If other stimuli are looked for, obvious CS candidates are given by the results of calcium imaging reported in Chapter IV, and US candidates could be searched among light or mechanical stimuli.

4.3 Response and quantification

As demonstrated in the results of Figure V-17, precise quantifications of behavioural responses are needed to reveal subtle effect. To further improve this precision, in particular to be able to precisely relate the responses to the temporal variations of the chemical stimuli, a few preliminary experiments were conducted, which included a calibration with dyes instead of stimuli after each experiment : the conditioning programme was simply run again after animals had been removed. These images reveal the kinetics of water streams, and since they can be synchronised to the behavioural videos, they allow to visualise virtually the stream boundaries around the animals, which helps interpreting behaviours. Figure V-20 shows an example of montage where a calibration image (right for each panel) is placed next to the image of the corresponding time frame in the conditioning experiment (left for each panel) ; the purple dye represents the CS, the orange one the US. It becomes obvious why at a certain time point some animals react while others do not, for example in Figure V-20B' : both animals at the bottom are already exposed to quinine and show an avoidance response, while the three others are not and do not react yet (the animal below the front, head downstream, delays the stimulus onset with its body – see Chapter V). This calibration approach appears suitable to the precise temporal quantification of responses ; to avoid a doubled experimental time it could simply run in a parallel chip.

Another important point should be discussed, namely the possibility to look for an appetitive paradigm instead of an aversive one, which means using a US that induces feeding, food-searching responses, or at least approach responses, rather than an escape. In the present experiments, as for the functional imaging experiments, I have preferred not to use food-related solutions or filtrates, on the basis that it would be hard to know or even reproduce their chemical composition, yet this issue is less crucial here, where one is not looking for responses of individual neurons but for global behavioural responses. Provided that one finds food-related stimuli that produce a non-habituating response, associative learning would probably take place independently of small compositional variations. It is thus an interesting direction to investigate. Noxious stimuli are always relevant for an animal, and are therefore easier to identify. Electric shocks regardless of their ecological relevance, strong touch stimuli or noxious chemicals as US can elicit strong associative effects, and even one-trial learning (for example in the mollusc *Aplysia* [336]). On the contrary, what will attract an animal is more dependent on its ecology, and therefore more challenging to identify in the first place, notably for animals such as polychaetes in which behaviour has received little attention. Nevertheless, it is known that physiological parameters can dramatically affect learning abilities, negatively in the example of sleep-deprivation in *Drosophila* [337], positively in the example of food-deprivation in the freshwater snail *Lymnea* [266]. In these animals, when sufficiently food-deprived, a single trial with a food-related US can even create an associative memory that last for at least 19 days [295]. Food can thus be seen as an advantage when used as a US. On the other hand, authors working on the nematode *Caenorhabditis* have argued that food stimuli should be avoided in learning experiments, as food dramatically affects the worm's behaviour [298]. It is clear that *Platynereis* larvae at around 6dpf start searching for food [138], even though they are equipped with yolk and can survive for at least two weeks in the absence of food and resume a normal development afterwards (personal observations). In any case, whether or not appetitive learning is relevant in *Platynereis* larvae should better be tested than debated.

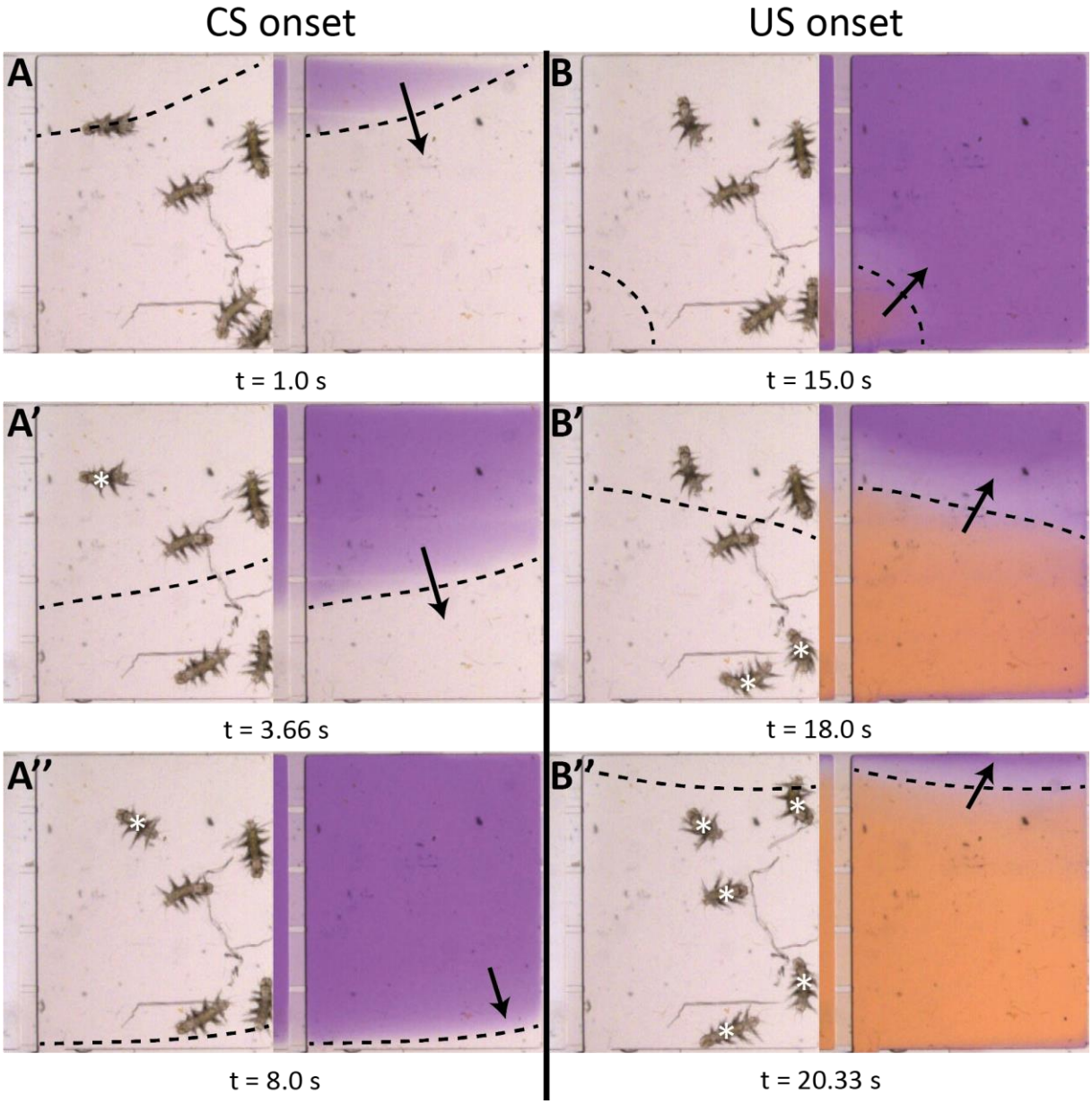


Figure V-20 Principle of stimulus visualisation to help the behavioural analysis, shown for CS onset (A to A'') and for US onset (B to B''). Arrows indicate the lateral displacement of the chemical front , white stars indicate the animals that are displaying an avoidance reaction. Here, 5 animals react to the US (B''), and one only to the CS (A'').

Regarding the conditioned response and its quantification, my personal impression after conducting all these experiments is that is not always unambiguous. Instead, in some instances of response to the CS, animals can be seen to first move forward before displaying the more stereotyped avoidance response. It may therefore be useful to develop a more elaborate, or more adapted, behavioural quantification. Tobias Rasse from the microscopy core facility at EMBL has developed for me a computer programme of automated image analysis and feature detection running as a Fiji plugin, which allows to detect and quantify both forward and backward movements, and which I would be happy to use in future experiments.

Independently of the paradigm and of the behavioural analysis, more replicates than in the experiments presented here are obviously needed, if any statistical significance is to be attained. I am aware of this flaw, and that has been nothing more than a lack of time to conduct further experiments once the 3-chamber chip design had finally been established.

4.4 Protocol parameters

The stimulus intensity and duration is acceptable for both CS and US, since they do trigger a response without overly long exposure. If anything, the durations could be slightly reduced, maybe down to 10 seconds. An ISI of 10-15s also seems appropriate, since the animals have time to react to both stimuli successively and these responses can be distinguished in time, while there is no unnecessary waiting time in between. The ITI may be a more important parameter to adjust, and indeed in preliminary experiments not reported here I had seen probable sensitisation effects by the US quinine with shorter ITIs such as 90 seconds. The relevant range of this parameter is probably highly dependent on the species, since for example robust, long-term associative learning can be obtained with ITIs as short as 10 minutes in *Caenorhabditis* [298], or as long as 90 minutes in *Lymnea* (with 15 trials distributed over 3 days [338]). It seems that the speed at which associative behavioural modifications take place may globally correlate with an animal's baseline locomotor speed and activity. I would expect rather fast phenomena in *Platynereis* larvae, which are active animals, though the immaturity of their nervous system may require more time for associations to be established. Here again, only further experiments will tell us what it is are relevant.

4.5 Perspectives

Overall, I regard as encouraging the results presented here, especially since a long time needed to be spent in developing the experimental setup, and only a handful of rigorous experiments could be conducted so far. A less elaborate setup may have left more time for the learning experiments themselves, nevertheless I am convinced that the setup provides a solid basis for systematic investigations of all kinds of chemosensory behaviours and behavioural modifications, as was demonstrated notably in Figure V-13, Figure V-15, Figure V-17 and Figure V-20, and was thus worth the time spent on it. Moreover, it is now automated, easy to use, and can generate dynamic spatial patterns of chemical stimuli, as opposed to the setup used previously in experiments on responsiveness to pH and salinity.

I am convinced that further efforts can lead to the successful establishment of a classical conditioning protocol. I did not bring convincing evidence for it, and it remains as yet unproven whether polychaetes and in particular *Platynereis* are capable of associative learning, nevertheless I hold the view that they most likely can. As reviewed extensively in Chapter II, polychaetes as opposed to their terrestrial relatives have elaborate sensory appendages, which is likely to represent the ancestral state for annelid worms [104], [339]. It would be most surprising that marine annelids cannot learn associations whereas terrestrial ones can [321],[322], as it would mean that the obvious decreases in morphological complexity that have accompanied the transition from marine to terrestrial life in annelids, notably sensory organ reductions, would have correlated with an increased ability to integrate sensory information and modify behaviour accordingly. The objection that *Platynereis* could learn associations but not as young as at the 6dpf stage is a valid one, and this is why I also included older animals up to the 5-segmented stage (3-4 weeks) in my experiments. However, calcium activity in what is most likely Mushroom Bodies cells has been observed at 6dpf during protocols of chemical stimulations, as reported in Chapter IV, and these cells as well as the paired median cells are not obviously sensory, which would suggest that some experience-dependent neuronal activity might already be taking place at this late nectochaete stage.

Polychaetes overall offer both a better experimental access to sensory detection and integration than oligochaetes and leeches, and a more interesting phylogenetic position for deep evolutionary relationships between nervous systems. They are thus most promising as an annelid model for learning, one can only wish more research had been conducted on their behavioural modifications.

VI – Other behavioural and physiological results

VI – 1 Behavioural experiments

1.1 A one-chamber design cannot provide a fast stimulus switching

As a first attempt for a behavioural chip enabling repeated changes of chemical environment, I tried a simple design containing a single chamber in which the animals are introduced. This chamber has two inlet channels, containing natural sea water (NSW) with and without the stimulus. Technically, it is a 2-layer design, with a main height of 100 µm for the chamber to allow the larvae to freely move, and a secondary height of 30 µm for the upstream and downstream restriction channels (black dashed lines in Figure VI-1) that let water flow through but not the animals.

Visualisation of the stream boundaries with a dye reveals that the stimulus onset is far too slow for such a design to be used in learning experiments (Figure VI-1). At a flow speed suited to the animals, it takes over 30 seconds for the stimulus to have reached the entire chamber, as can be seen with the animals that are still in a transparent area at t = 30s. This may already be longer than a CS or US would need to be. What is more, large variations on the actual exposure time to the stimulus are introduced, since some animals could theoretically be exposed at least 30 seconds longer than others. Such temporal characteristics are not acceptable, and prompt a refinement of the microfluidic chip design.

The problem in this design is the time needed for pressure release in the water channel, after its pump has been turned off. The stimulus change is rather rapid in central parts of the chamber – in this case it is completed in less than 10 seconds – but slow in lateral parts of the chamber. My next idea was thus to get rid of this pressure release, by restricting this lateral, slowly-changing zone in other chambers where the animals would not be.

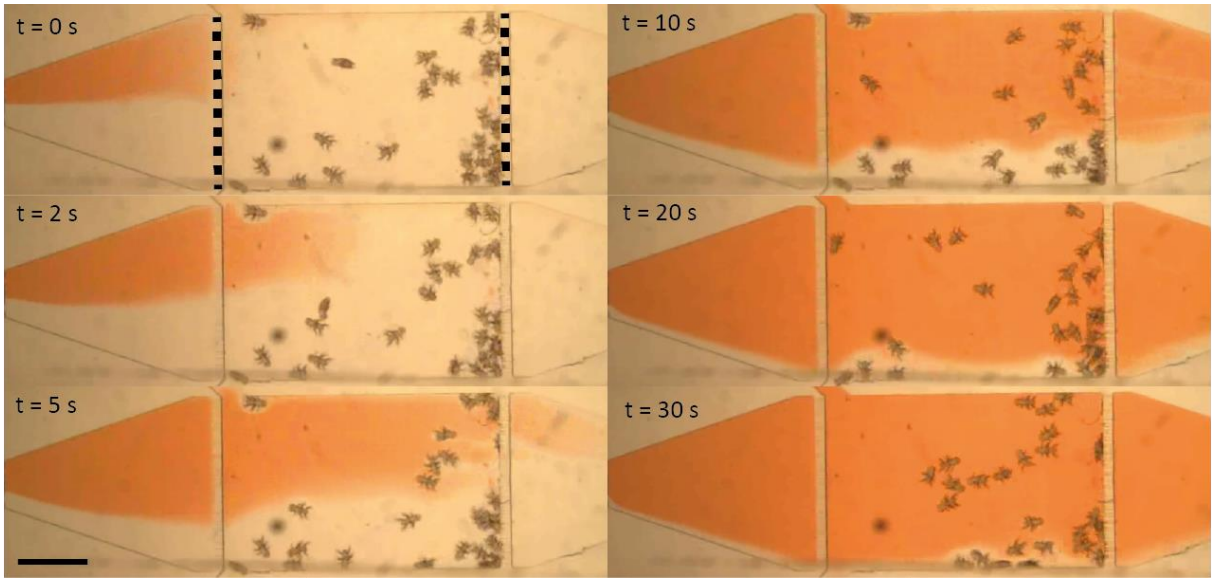


Figure VI-1 Dynamics of stimulus onset in a simple 1-chamber design, visualised with an orange dye. Platynereis late nectochaete larvae. Flow is from left to right. Scale bar 1 mm.

1.2 Identifying an optimal animal density in a microfluidic chamber

While performing experiments on groups rather than on individuals has the advantage of allowing a faster acquisition of data, this approach carries with it a potentially critical drawback : animals have the possibility to interact with each other. Therefore, behavioural responses can also be caused by inter-individual contact, instead of only by external signals and spontaneous individual actions. In experiments during which a highly aversive xylenol orange solution was introduced in half of the chamber, I could observe that many animals, while actively trying to escape this repellent condition,

were still staying on the xylenol side due to the water side being overcrowded. In that case, a measure such as the Preference Index introduced above does not reflect the attraction or repulsion towards a stimulus, because this effect is overwhelmed by interactions between animals. This issue is crucial if one wishes to reveal attraction/repulsion based on the movement of the animals towards a certain area of the chamber, as it may prevent them from showing their true preference.

Several calibrations experiments (not shown here) have allowed to evaluate that a density of 3 animals per square millimetre for stages younger than 2 weeks was a good compromise between behavioural responses being masked by overcrowding effects, and too few animals being tested at the same time. Such a density should be considered as the maximal possible density during an experiment : for example, an experiment in which animals are expected to accumulate in one half of the chamber should be started at half this optimal density, otherwise the expected situation requires a density of 6 animals/mm^2, meaning that responses will be largely masked by the animals' interactions.

VI – 2 Functional imaging

2.1 Identifying relevant dimensions for a microfluidic trap

As a preamble to the creation of a microfluidic chip for functional imaging, I designed a simple chip consisting mainly of a channel with a constant height of 60 or 75 µm, whose width decreases linearly along its main axis from 150 µm (more than the head width) to 30 µm (less than the head width). I introduced animals in this channel, and observed their position when they were efficiently trapped. In 6dpf larvae, the head is the widest part of the body and thus constitutes the limiting size.

Calling 0 the channel's beginning (wide part), 1 the channel's end (narrow part), and x between 0 and 1 the abscissa of the head position along the axis, the width w at the level of the head is equal to w = 150 – 120x. Figure VI-2 illustrates the principle of width determination. After measurements on about 40 animals, I concluded that a width between 70 and 90 µm, and a height between 60 and 75 µm would be relevant for trapping 6dpf larvae.

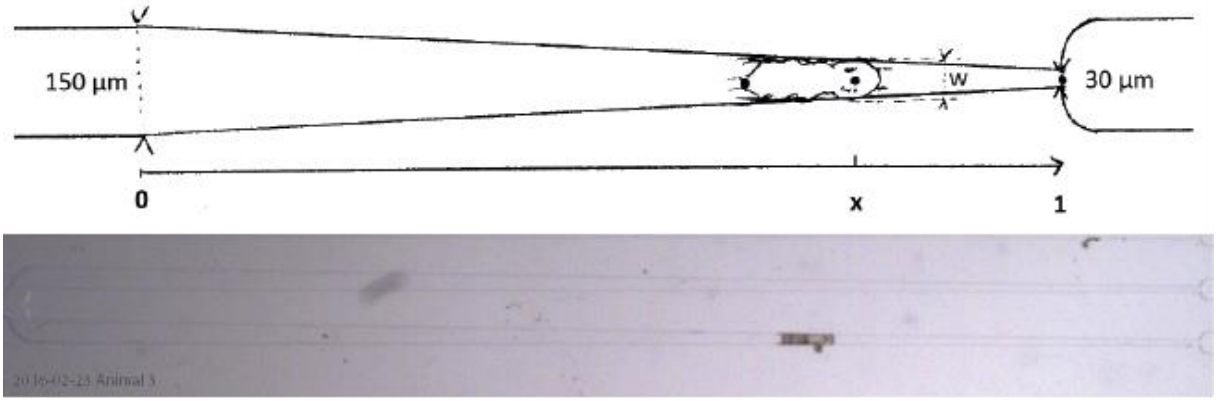


Figure VI-2 Determination of the relevant trap width. Top : schematic drawing, proportions not respected. Bottom : picture of the real chip with a 6dpf larva trapped inside.

To test for potential body damage introduced by the trapping, I released all trapped larvae and let them rest in their usual natural sea water. After some minutes they were crawling or swimming as they would normally do, though some of them were slower than usual. After a couple hours all larvae would feed on algae and after a few days all would have followed their regular development, indicating that introducing them in the device did not caused more than a limited and temporary stress, and impaired neither their health nor their ability to move, feed or develop.

I also tested 3dpf larvae, which turned out to be much more fragile than 6dpf ones. Their head is wider – about 120 µm – and damage in the form of leakage appears as soon as they are introduced in a channel narrower than that. Microfluidic trapping of 3dpf larvae is possible and I was indeed able to perform a few calcium imaging experiments in chips with them, but requires much more care. 6dpf larvae on the contrary proved to be impressively robust, as for example they still recovered after I accidentally trapped a few of them in a much too narrow channel.

2.2 Adding a 5'UTR sequence to the GCaMP mRNA improves expression of the calcium sensor

A determining factor for signal quality is the type of mRNA used for microinjections. A modified version of the GCaMP6s mRNA, called **GCaMP6s-miR**, had been generated previously in the lab by Maria Tosches and Paola Bertucci with the aim of reducing GCaMP expression in muscles, by adding in the 3' untranslated regions (3'UTR) of the mRNA a known target of a microRNA specific for trunk muscles and called miR-1 (see figure 4i in [242]). Another modified version, called **P2-GCaMP6s**, had been generated by the Jékely lab, which includes upstream of the GCaMP open reading frame a 5' UTR from a *Platynereis* ribosomal protein called P2, with the aim of making the mRNAs more stable and more highly translated. This mRNA was used in the calcium imaging experiments in [81],[76],[82]. I could verify that GCaMP6s-miR has a low expression in trunk muscles, notably in the stomodeum (compare Figure VI-3 left with Figure VI-3 right, taking the main neuropile as a reference). I also observed that P2-GCaMP6s yields a significantly better signal quality, as illustrated in Figure VI-3.

It is possible to observe activity traces of individual neurons with the miR version, and indeed some of the calcium imaging experiments reported in Chapter IV were performed with it, notably on the nuchal organs. However, in a whole-brain imaging settings, the signal becomes too low due to the high imaging speed (8 kHz), and thus it was necessary to use the P2 version. The fact that GCaMP expression was not reduced in muscles was not a major problem since few muscles are present in the head at 6dpf – except in the palps. I did not compare signal brightness between GCaMP6s-miR or P2-GCaMP6s and the regular GCaMP6s mRNA. The P2-GCaMP6s version of the mRNA was thus used for most experiments. Maps and full sequences of the different GCaMP6s plasmids used during or generated as part of this work can be found in Appendix C.

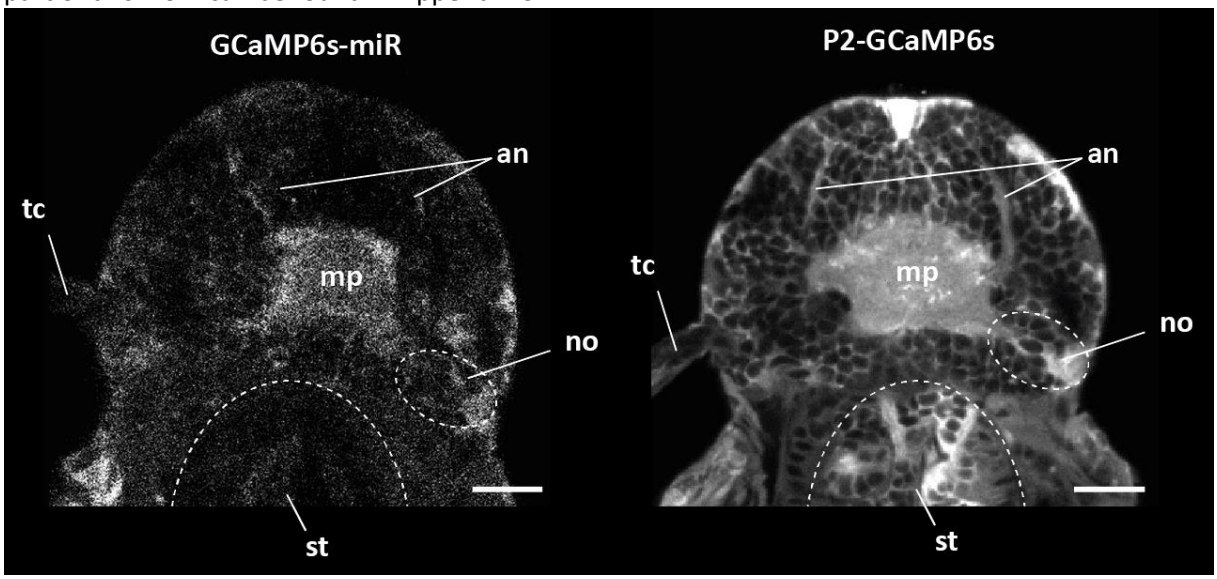


Figure VI-3 Comparison of calcium signal brightness in a 6dpf head for two versions of the mRNA : (left) GCaMP6s-miR and (right) P2- GCaMP6s, both injected at around 800 ng/µL. Landmarks : antennal nerve (an), main plexus or main neuropile (mp), nuchal organ (no), stomodeum (st), tentacular cirri (tc). Note that the imaging plane is not horizontal with respect to the animal : the nuchal organ is better visible on the right side, the cirrus visible on the left side only. Scale bar 20 µm.

2.3 Looking for an inert dye to visualise stimulus changes

To go beyond the limitation introduced by the variability of stimulus onset, I looked for a way to visualise the stimulus changes in fluorescence. This would allow to make more precise statements concerning the timing of neuronal responses relative to the stimulus.

Fluorescent beads can allow to visualise the flow but tend to stick to the animal, notably to its appendages and cilia, which may affect stimulus detection. Figure VI-4 shows an example of a bead-containing solution imaged in three channels : the beads are easily detected in the red channel (central image), are invisible in the green calcium channel as they should be (left image), but rapidly aggregate at the head surface, as can be seen in the red and in the transmitted light channel (right image).

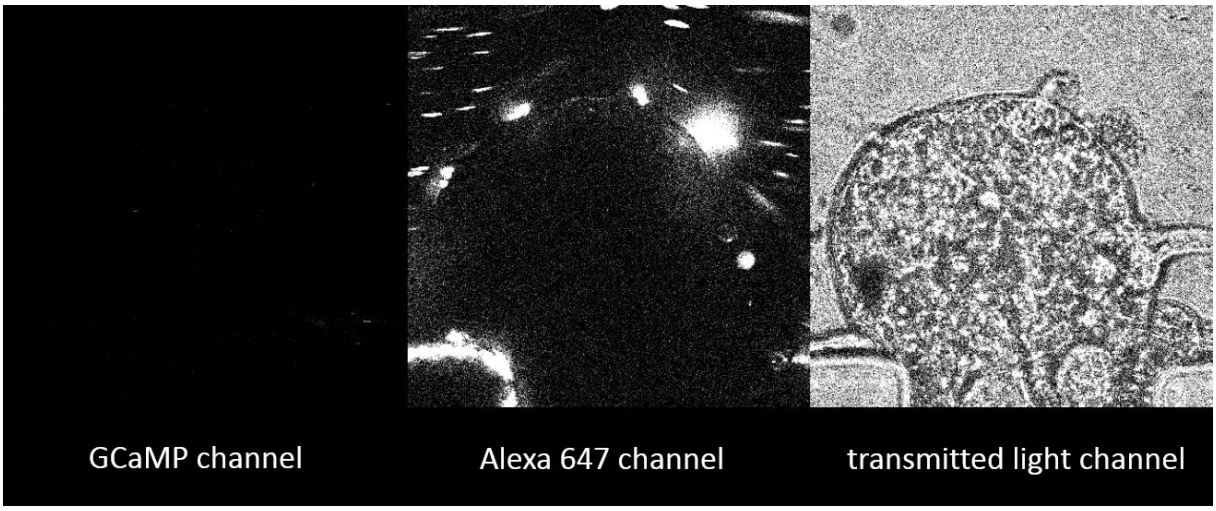


Figure VI-4 Stimulus onset around a 6dpf animal's head visualised by fluorescent beads. Note the accumulation of beads at the head surface, notably on the right side.

The red fluorescent dye Rhodamine 6B enters the cytoplasm of all animal's cells within a few minutes and may as well interfere with physiology. Figure VI-5 illustrates how pervasive the rhodamine staining is only after three 15s-exposures.

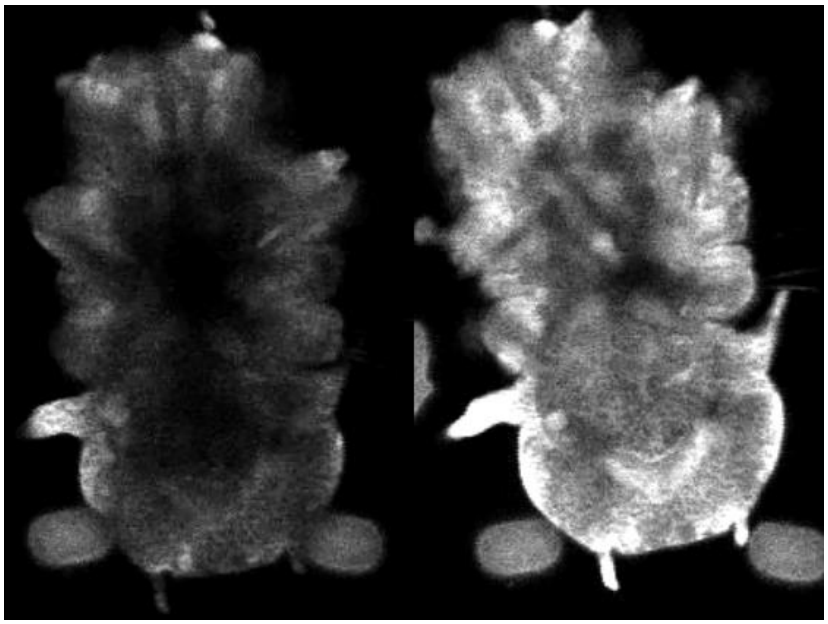


Figure VI-5 A 6dpf animal before (left) and after (right) a 4 min protocol with 3 exposures of 15s to Rhodamine 6B.

A fluorescent dextran was tried, which did not penetrate or stick to the animal, but induced clear neuronal responses notably in the antennae. To exclude that dextran was detected by the animal, the corresponding fluorescent dye alone was tried, Alexa 647, but this also induced neuronal activity. Figure VI-6 shows an example of antennal response upon exposure to Alexa 647 at a low concentration. Even though such a synthetic chemical compound is totally irrelevant for the animal in its natural context, such experiments can actually yield useful information on the kinetics of responses. In this case, it is evident that the antennal response, at least on the right side of the animal, starts within less than one second after stimulus onset, since the stimulus arrives later than t = 0s and one antennal nerve is already activated at t = 1s.

If such an inert fluorescent dye could be found, this would greatly improve the calcium imaging experiments and inform better about the temporal modalities of chemical stimulus detection.

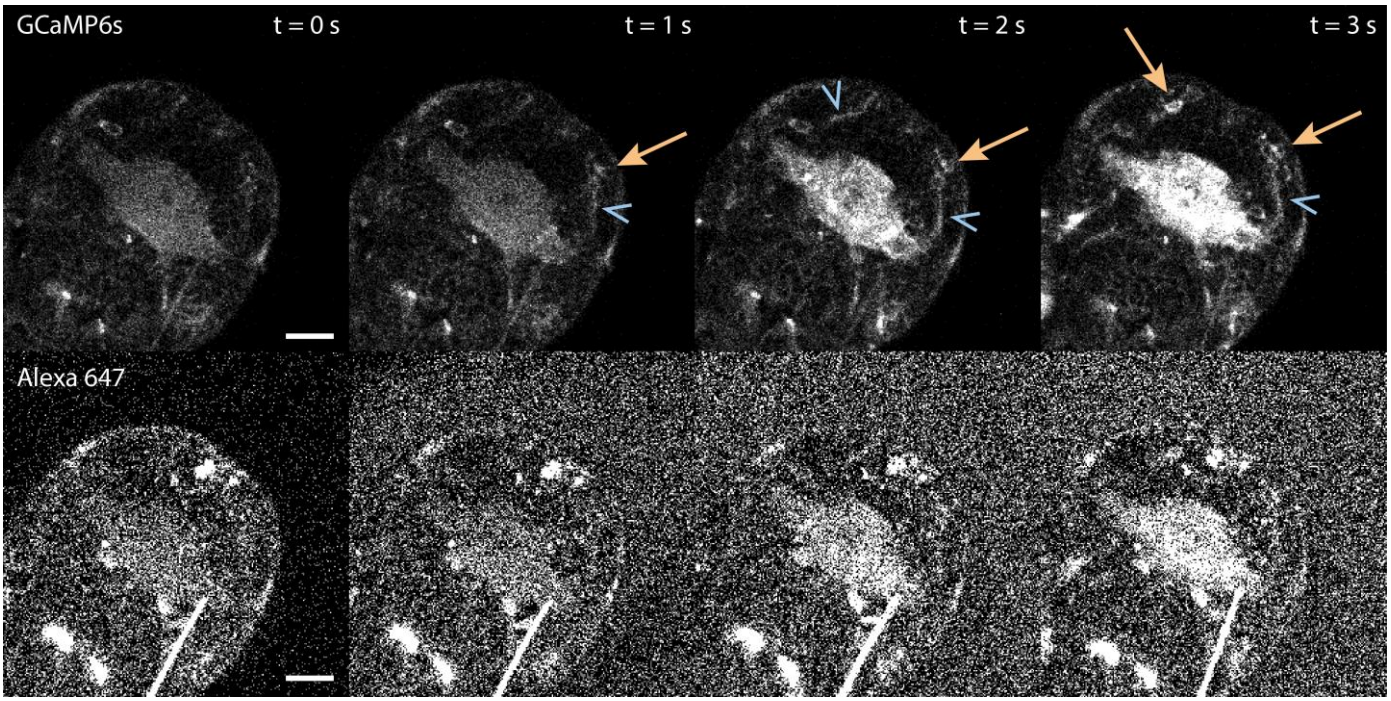


Figure VI-6 Neuronal response in a 6dpf animal upon exposure to the Alexa 647 dye. Top row : GCaMP6s fluorescence signal, showing cellular calcium activity. Bottom row : red fluorescence channel showing the dye in solution arriving around the animal's head at t = 1s. Orange arrows indicate active neuronal cell bodies, blue arrowheads indicate the activated antennal nerve. Scale bar 20 µm.

2.4 Calcium imaging with non-genetic dyes

Since expression of the calcium sensor is not specific and present in the whole body, I asked whether a non-genetic dye instead of GCaMP could be used to monitor cellular calcium levels. Such dyes are easy to use as they only require immersion of the sample in a solution. They have been developed for cells in culture on solid substrates or in suspension, but also used in brain tissues and delivered by local injection [340]. I tried whether simple immersion of *Platynereis* larvae in such a solution would be enough to perform calcium imaging in the brain, encouraged by the fact that many molecules such as neurotransmitters easily diffuse in their bodies. Aliquots of Fluo-4 AM and Rhod-3 AM kindly provided by Sebastian Hauke from the Schultz Lab at EMBL allowed to perform test experiments. As can be seen on Figure VI-7, Fluo-4 does not stain the main plexus but instead is rather confined to the surface. This indicates that the dye may not have penetrated easily the cuticle. When animals were imaged at the head surface, no calcium activity could be seen in the subcuticular layers (Figure VI-8, Left column), while in a GCaMP6s-injected animal these tissues always show abundant calcium fluctuations (Figure VI-8, Right column). This further supports that dye penetration was hindered by the cuticular layers.

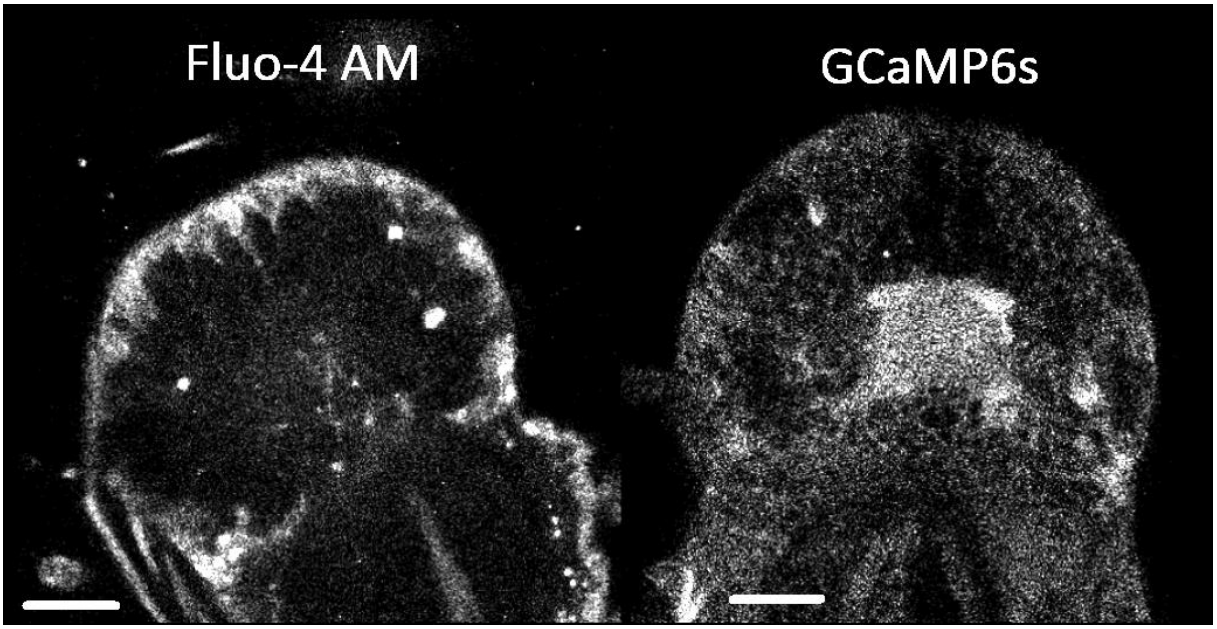


Figure VI-7 Comparison of fluorescent signal between (Left) a Fluo-4 stained animal (immersed for 180 min at 10 µM) and (Right) a GCaMP6s-injected animal, imaged in the plane of the nuchal organ's revolver cells. Scale bar 20µm.

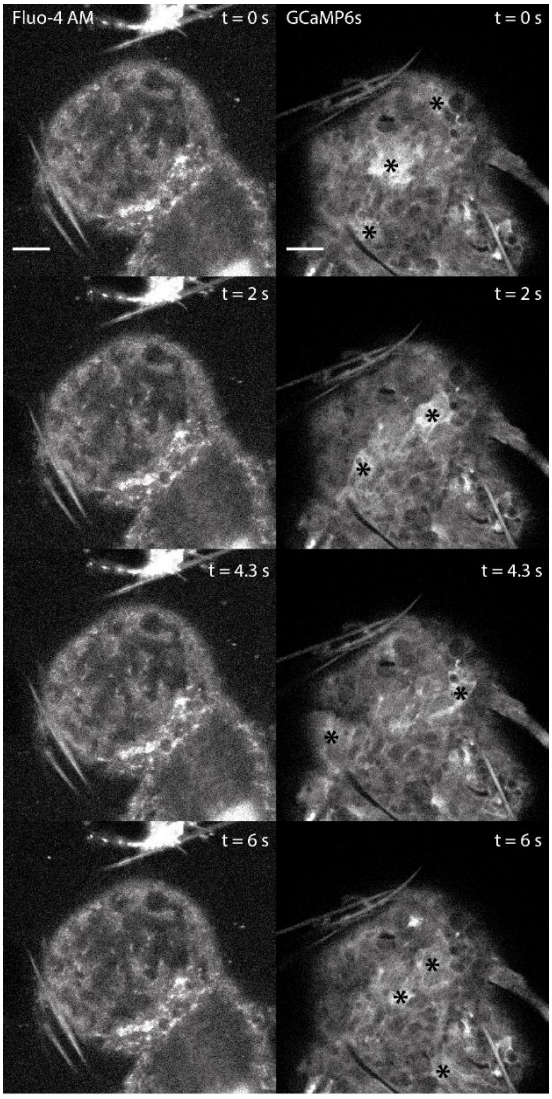


Figure VI-8 Comparison of fluorescent signal between (Left column) a Fluo-4 stained animal (immersed for 180 min at 10 µM) and (Right column) a GCaMP6s-injected animal, both imaged in the dorsal-most plane of the head. Black asterisks indicate areas of increased calcium levels. Scale bar 20µm.

Following the observation that Rhodamine 6B easily stains cytoplasmic contents, I asked whether a Rhodamine-based calcium dye such as Rhod-3 AM would better penetrate the tissues and stain the whole brain. Besides, in a cell preparation, an adjuvant such as Pluronic is sometimes used to improve penetration of the dye into the cell. I conducted new experiments using Fluo-4 AM as well as Rhod-3 AM, both with the addition of the adjuvant Pluronic at 1 µM final concentration. Fluo-4 AM still did not stain the main plexus (Figure VI-9 Left). Rhod-3 AM showed a good staining of major brain structures (Figure VI-9 Right), and actually revealed more details than a usual GCaMP6s signal does. However, no calcium variation was observed at all, indicating that such staining is still not suitable for calcium imaging experiments.

Probably for both dyes, or at least for Rhod-3, it appears that some saturation phenomenon takes place, which prevents the fluorescent probes to modulate their activity following calcium variations. The Rhod-3 may be interesting for future attempts, but I stopped there my tests.

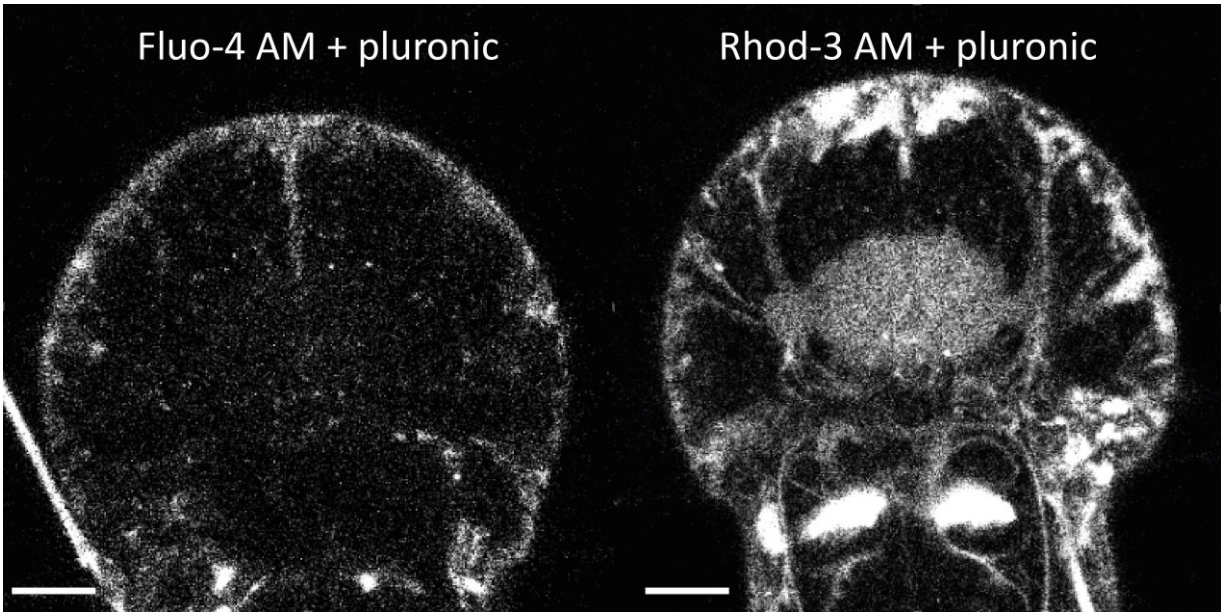


Figure VI-9 Comparison of fluorescent signal between (Left) a Fluo-4 stained 6dpf animal (immersed for 60 min at 5 µM, with addition of 1 µM Pluronic) and (Right) a Rhod-3 stained 6dpf animal (immersed for 60 min at 5 µM, with addition of 1 µM Pluronic), both imaged in the plane of the antennal nerves. Scale bar 20 µm.

VII – General discussion

VII – 1 Polychaete chemical senses and the evolution of chemosensation

1.1 The function of polychaete sensory appendages

1.1.1 Attributing a function to candidate organs

The calcium imaging experiments presented in this work constitute the first direct and comprehensive physiological study of chemosensory systems in an annelid. They have allowed to physiologically test hypotheses that had so far mostly relied on organ and cell morphology. While additional systematic experiments as well as experiments targeted at certain organs would be needed to precise the repertoire and sensitivity of the different organs, a first picture has emerged concerning the function of sensory appendages in *Platynereis*, which sheds light on chemosensation in polychaetes in general.

As was reviewed in Chapter II, among presumed chemosensory cells in polychaetes the most common type consists of mono- or multi-ciliated cells equipped with cilia that protrude out of the cuticle, and are thus directly exposed to the outside environment. These cells can be found on all body appendages as well as generally on the body surface. Another common type is that usually found in nuchal organs, which are the most conserved sensory organ in polychaetes : sensory cells with a dendrite bearing usually one cilium and microvilli. Overall, as noted by Purschke [116], the immense morphological variety observed in polychaetes at the level of sensory organs contrasts with the relative homogeneity of the sensory cells they harbour. This is maybe most obvious in nuchal organs, which drastically vary in size, shape, position, can be rather concave or convex, and yet comprise morphologically similar sensory cells. Since stimulus detection is carried out by the cells, it is likely that the functions of polychaete sense organs are much more comparable between species than their external appearances would suggest. Hence, physiological proofs obtained in one species are informative about other families.

The present findings confirm that nuchal organs, palps, antennae and tentacular cirri can be regarded as chemosensory organs in polychaetes. While this is so far proved in *Platynereis* only, it seems reasonable to extend the statement to other species as follows.

Nuchal organs are so conserved and their cellular architecture so similar across species that one can propose without too much risk that nuchal organs are chemosensory in polychaetes in general. Most morphological and histological investigations reported in the literature had come to that conclusion, and the observation of nuchal organ activity in response to chemical stimuli as reported here for the first time comes as no surprise.

The conservation of presumed chemosensory cell types is less well known for **palps**, but as reviewed in Chapter II, penetrative mono- or multi-ciliated sensory cells have been found on palps in clades as distant as the orders Phyllodocida (nereidids), Eunicida (the dorvilleid *Ophryotrocha*) and Canalipalpata (spionids). Moreover, palps are feeding appendages in spionids and activity-dependent labelling has revealed candidate chemosensory cells in the palps of *Dipolydora* [154], which gives additional support for palps being chemosensory in polychaetes in general. It is possible that palps are also endowed with mechanosensitivity, yet this point has not been investigated much so far. The different cells types observed in *Platynereis* palps (see Chapter III) would be in agreement with such a statement.

Regarding **antennae**, a chemosensory function was suggested in *Nereis* and *Ophryotrocha* only, based on cellular morphology. Ultrastructural investigations in the antennae of *Sabella* led to the hypothesis that the highly ciliated sensory cells found there are rather mechanoreceptive than chemoreceptive, based on the stiffness of their cilia, on the mechanosensory function in other phyla of cells equipped with such stiff cilia, and on "*preliminary physiological investigations*" ([143] p. 169). Although these preliminary experiments are not exposed, the authors report observing these cilia "*flicking*

spontaneously as well as a result of being struck by water-borne particles". However, the similar cell type found in the antennae of another sedentary worm, *Lanice*, was not considered as mechanoreceptive [144] but indeed chemoreceptive, though a collar-type and hence presumably mechanoreceptive type was also found. Both chemoreceptive and mechanoreceptive cells are reported in the dorvilleid *Ophryotrocha*, and authors have found them all over the body especially on appendages, though they do not indicate whether both are present on antennae. It is apparent that no clear statement can be made currently regarding a general function of antennae in polychaetes, and it is likely that antennae generally can at least serve one or two of the mechanoreceptive and chemoreceptive functions, though this may vary largely between clades. In *Platynereis*, it is clear from the present study that antennae are chemosensory, and might even be the main chemosensory organ – at least in larval stages. No experiments were conducted however to test for mechanosensitivity. Since nereidids show an overall similar appendage morphology, antennae are likely to be chemosensory in the whole clade of nereidids, and based on morphology the statement may also be valid for closely-related clades such as hesionids and syllids. For sabellids or terebellids such as *Sabella* and *Lanice*, as well as most of the other polychaete families, physiological evidence or at least a closer comparison of sensory cell types will be needed before any assertion can be made.

Descriptions of sensory cells on **tentacular cirri** in polychaetes have concerned only the genus *Nereis*, and a chemosensory function has been suggested, which is strongly supported by the observation here of chemosensory responses in *Platynereis*' tentacular cirri. Physiological and/or morphological evidence supports a chemosensory function for parapodial cirri in several nereidids (*Nereis, Platynereis, Perinereis)* as well as in the polynoid *Harmothoë* (also from the order Phyllodocida) and in the dorvilleid *Ophryotrocha* (order Eunicida). Based on the close evolutionary relationship of tentacular cirri with parapodial ones, and even though tentacular cirri are less common in polychaetes than the other appendages mentioned above, a general chemosensory function seems likely for tentacular cirri.

1.1.2 Organ specialisation

While all these organs have been hypothesised to be chemosensory in several polychaete families, there were until yet few elements to argue whether one or the other would be specialised or rather generalist in its sensory repertoire. In fact, nuchal organs and not antennae were thought to be a general chemical detector, which seems questionable at least for nereidids, given the present results. In any case, the consistent differences in morphology between appendages make it obvious that they would serve different sensory functions, even if these may overlap. Overall, if one integrates organ and cell morphology, together with these first physiological results, here are general hypotheses that can be made concerning the role of the respective polychaete sensory organs.

All body appendages (antennae, palps and all types of cirri) as well as nuchal organs are chemosensory, and have the ability to detect a wide variety of compounds.

Parapodial, tentacular and anal cirri have a low degree of chemosensitivity, with few cells broadly detecting chemical compounds, and these appendages primarily inform about the localisation of the cues with regard to the body, not about their identity. Additionally, some specialisation can be observed between the different types of cirri, with anal and peristomial ones being generally used for mechanosensation as well, and parapodial ones sometimes used for specific chemosensory roles, such as the detection of sexual pheromones in mature adult nereidids.

Antennae, when present, are specialised in the detection and discrimination of soluble compounds. Temporal and spatial information coming from the different antennae is used to localise sources of chemicals relative to the head, and orient the animal towards or away from these sources. An additional general function as frontal or dorsal mechanosensory detectors in complement to peristomial cirri is likely.

Palps are specialised in the detection and probably discrimination of food-related cues. They may detect soluble compounds, but also hydrophobic ones that may lie at the surface of potential food items, with which their tip come in contact. In some species such as spionids, chemosensitivity ma be directly coupled to the feeding role of these appendages.

Nuchal organs, whose sensory processes are shielded from the outside by cuticular and extracellular layers, probably have a different mode of chemical detection than the appendages, hence a different purpose. Their high degree of conservation indicates a general biological importance for polychaetes. Contact chemoreception is excluded. Their structure and position would speak in favour of them detecting ambient chemicals, rather than fluctuating ones as the antennae seem to be best suited for. Such chemicals could be notably messengers for intra- or inter-species communication, i.e. pheromones or kairomones. In this case, nuchal organs would detect rather their presence than their localisation, and may be specialised in the detection of such compounds at very low concentrations, as they indeed tend to be. The strong responses elicited in *Platynereis* larvae by the adult pheromone uric acid in the nuchal organs support such a view, though this remains a single observation. Moreover, molecular data for *Platynereis* nuchal organs suggest that they would develop from a placodal-like region homologous to the vertebrate adenohypophyseal placode (Maria A. Tosches, unpublished), further supporting a role in the detection of hormones or pheromones. Alternatively, nuchal organs could detect ambient environmental cues, such as general metabolites indicative of food availability.

The study of candidate chemosensory receptor proteins in *Platynereis*' genomic resource can potentially inform about the specialisation of the different organs. Indeed, such candidates can be identified by constructing phylogenetic trees of DNA sequences of receptors, and their spatial distribution in the body visualised by *in situ* mRNA hybridisation, now a routine technique in *Platynereis*. If some candidates are expressed in chemosensory organs, this will suggest that they may be indeed chemoreceptor proteins. Moreover, finding spatial segregation across organs between receptor proteins of different families would indicate different specialisations for the different organs and, if there are known ligands for the homolog genes in other species, this could even indicate which types of molecules are detected by these organs. Such an effort has been undertaken already, some genes have been cloned and their patterns of expression imaged. Preliminary results would suggest that some candidate chemoreceptors are indeed expressed in chemosensory organs, but this work is ongoing (Tomas Larsson, Paola Bertucci, Wiebke Dürichen, unpublished).

1.2 Chemosensory systems in *Platynereis* compared to other phyla

1.2.1 Receptor proteins

In *Platynereis*, nothing is currently known regarding receptor proteins for chemical compounds. Nevertheless, three studies concerned with the molecular evolution of insect chemoreceptor proteins have included genomic information from annelids. This has revealed that at least two families of insect chemoreceptors are present in annelids : the ancient gustatory receptor like receptors (Grls), present in the polychaete *Capitella teleta* and the leech *Helobdella robusta* [341][342], and a subset of ionotropic receptors called IRs, present in *Capitella* [343]. This two families are also found in molluscs : Grls and IRs for *Lottia gigantea*, *Aplysia californica*, and Grls for *Crassostrea gigas* [341][342][343]. This indicates that annelids may in general possess candidate chemoreceptor proteins which appear to be present in Lophotrochozoa. IRs have been found so far in all clades of Protostomia investigated, namely gastropods, annelids, chelicerates, crustaceans, nematodes, but not in Deuterostomia, and are thought to have evolved from non-NMDA ionotropic glutamate receptors in stem protostomes [343]. Grls have been described in protostomes, in non-chordate deuterostomes, as well as in cnidarians and placozoans [341], indicating a pre-bilaterian origin. However, in the cnidarian *Nematostella vectensis* two such genes are expressed in early development but not after the gastrula stage [341], i.e. before

any putative chemosensory organ is formed, hence even if they may detect a chemical signal, they are not chemoreceptor proteins in the sense of a being part of a differentiated chemosensory organ.

It should be tested whether these candidate chemoreceptor proteins are present in the genome of *Platynereis* as in *Capitella* and *Helobdella*, by blasting their sequences against the available transcriptomic resource, and if yes, where they are expressed in *Platynereis* larvae, by performing simple mRNA *in situ* hybridisation. The fact that they are related to functional chemoreceptors in insects does not mean that they would be used as such in *Platynereis*, as the example of *Nematostella* demonstrates, but any expression in the now identified chemosensory organs of *Platynereis* would be a clear indication that they are indeed chemoreceptors in annelids.

1.2.2 Chemosensory cells

Chemosensory neurons in many phyla follow this overall morphology : bipolar neurons with a dendrite reaching into a fluid medium, and often bearing ciliary and/or microvillar extensions, as is the case for example in crustaceans, insect and vertebrates [50][36][47]. Presumed chemosensory neurons in polychaetes also follow this global organisation, as detailed in the review chapter. However, there are some differences at the level of the sensory endings. Ciliated cells with penetrative cilia are widespread in polychaetes and generally considered to be chemosensory [116]. In these cells, the cilia are directly exposed to the water environment. In this regard, they are different from the chemosensory neurons found in olfactory and bimodal chemo-/mechanosensory sensilla of insects and crustaceans [47] , for which the fluid is covered by a permeable of porous cuticle. They appear to be also different from chemosensory neurons of the vertebrate olfactory epithelium (see Introduction, Fig. 3), in which cilia are immersed in a mucus which is itself in contact with the environment, however it cannot be excluded that sensory cilia of some polychaete chemosensory cells would be immersed in a mucus as well, and thus in indirect contact with the water environment, since electron microscopy investigations have often reported secretory cells in immediate proximity of presumed chemosensory cells.

The presence of these secretory cells raises an additional question, namely whether odorant binding proteins (OBPs) would be exist in polychaetes, and potentially be present in a mucus covering chemosensory cilia. OBPs help solubilise volatile and hydrophobic odorants in the mucus of chemosensory organs, to facilitate binding to the olfactory receptors [344][345]. Such proteins have been found so far only in hexapods and vertebrates, not in crustaceans or in myriapods, and seem to have appeared independently as an adaptation to terrestrial life [47]. However, hydrophobic compounds are known to be used as chemical cues in aquatic environments [280], therefore OBPs could also be present in aquatic organisms and used to facilitate the detection or relevant non-soluble cues.

In the present work, a global morphology could be observed only in a few number of sensory neurons of *Platynereis*, and they were consistent with the general chemosensory cell morphology mentioned above. In the case of antennae and tentacular cirri, a few instances of sensory cells located at the base of the appendage with a long dendrite extending into the appendage have been observed in calcium imaging. As revealed by the immunostainings, at least two types of sensory endings are present in the tentacular cirri and palps of juveniles with at least one type consisting of cilia – the ultrastructural study in *Nereis* mentioned in the review chapter [145] would speak in favour of them being monociliated sensory cells. At the surface of antennae, cilia that most likely belong to sensory cells are also present. Overall for *Platynereis'* appendages, no relationship could be established between the calcium response of a chemosensory neuron and its sensory endings, but it appears likely that chemosensory neurons would be ciliated with penetrative cilia.

Regarding nuchal organs, chemosensory neurons with non-penetrative sensory cilia is the general rule in polychaetes [122][130][128], and applies for *Platynereis* as well [233]. The sensory cilia of these cells are thus in indirect contact with the outside environment and sheltered by a permeable cuticle, as is the case for chemosensory neurons of insects and crustaceans. In the experiments reported here, the

revolver cells are the only sensory neurons of the nuchal organs for which a dendrite was observed. No sensory cilium could be seen, but since these cells possess the typical morphology of nuchal organ sensory cells, and since only sensory cells with non-penetrative cilia are present in adults, there is little doubt that the revolver cells indeed carry non-penetrative cilia.

In *Platynereis*, two distinct types of chemosensory neurons could be present :
- one found on palps, antennae or cirri, with sensory cilia directly exposed to the outside, even though no physiological data is yet available to prove that such cells are indeed chemosensory,
- one found at least in nuchal organs, with sensory cilia indirectly exposed to the outside and lying under the cuticle. Sensory endings which are not obviously cilia have been reported here in the immunostainings of palps and tentacular cirri ; it is not excluded that they could be of this type as well but this is so far unclear what they are.

Finally, it should be noted that no evidence for non-ciliated chemosensory cells exists so far in polychaetes, contrary to other aquatic animals such as teleost fish in which both ciliated and microvillar chemosensory cells are described [7].

1.2.3 Glomerular neuropils

Given the widespread occurrence of glomeruli in animal chemosensory systems, it is an obvious question whether such neuronal architectures are present in at least some of the chemosensory organs of polychaetes such as *Platynereis*.

Glomeruli may be present in the brain of the polynoid *Harmothoë areolata,* as reported in a study of neuroanatomy in which “clusters of small spherical structures that are reminiscent of arthropod olfactory glomeruli” have been observed [346]. These clusters are supposedly associated with the Mushroom Bodies and innervated by fibres originating from the palpal nerve, though these points are difficult to judge based on the images provided in the publication. The authors further indicate that such structures are not visible in the brain of the nereidid *Nereis diversicolor*, and comment that the brain of polynoids has been argued to be the most complex of all annelids [98], which may account for this absence. If this latter point is true, then the study would support the view that glomeruli, in polychaetes as in many other taxa, would have evolved independently in chemosensory systems.

For *Platynereis*, there is currently no data to support the absence of presence of glomeruli in chemosensory organs, yet their absence in adult *Nereis* suggests that they could be absent in *Platynereis* as well.

1.2.4 Distributed chemical sensitivity

The physiological data provided in this work point at polychaetes probably possessing a distributed sense of chemoreception. Evidence now exists for *Platynereis* being able to detect chemical compounds with all head appendages, nuchal organs, and based on the anatomical similarity between parapodial, anal and tentacular cirri, with all body appendages. In addition, a general, unspecific chemosensitivity may be present all over the body surface of polychaetes, as suggested by ultrastructural studies in *Arenicola* [153], and behavioural experiments in *Arenicola*, *Nepthys* and *Nereis* [161]. An additional level of chemosensitivity would come on top, provided by the palps, nuchal organs and antennae. While the first level may inform the animals about where the stimulus is, the second level may tell them what it is and possess high discriminative abilities as has been suggested above for antennae and palps. Alternatively, a distributed chemosensitivity on the body surface and segmental appendages may inform about compounds specifically related to substrate quality and help the animals find suitable habitats.

Distributed chemoreception is well documented in arthropods, with for example the decapod crustacean *Panulirus argus* being endowed with chemosensitivity on its antennules, second antennae,

mouthpart appendages, legs, tail, and the fruit fly *Drosophila melanogaster* possessing chemosensory cells on its antennae, maxillary palps, proboscis, legs, abdominal tip and wing edges [47]. Different roles could be assigned to these organs ; for example the antennules, which are the most frontal appendages in decapod crustaceans, are known to be involved in courtship and food-searching behaviours in the lobster *Panulirus* or the blue crab *Callinectes*, while mouthpart appendages are involved in food quality assessment [347]. Laser-mediated ablations are easy to perfom on appendages of larval *Platynereis* and, in combination with behavioural experiments, would be a straightforward way to test both for different roles of the appendages, as was done by Gross in adult *Nereis* in 1921 [170], and for the existence of a general tegumentary chemosensitivity.

1.3 Towards a study of chemical senses in other marine invertebrates ?

The results of the calcium imaging experiments presented in this thesis have demonstrated the feasibility of a systematic functional imaging study of chemosensation in a non-standard animal model, and there are good reasons to believe that such experiments could be conducted in various other marine species.

The only genomic information used here was the 5'UTR sequence of the P2 ribosomal protein, used to improve the levels of GCaMP expression, but this sequence was not even required since valid experiments could be conducted without it, for example the ones on the revolver cells reported in 3.4.2. In fact, to successfully conduct such experiments, the only technical requirements specifically dependant on 6dpf *Platynereis* larvae have been the following :

- an established technique to express mRNAs, such as a microinjection protocol, needs to be available, and the animals have to develop correctly until the desired stage
- the animals need to be immobilisable in a microfluidic trap without harm
- the animals need to be transparent

This means that any transparent, aquatic animal small enough to be introduced in a microfluidic device is potentially suitable to conducting such physiological experiments of neurobiology, provided that efforts are put in reliably expressing mRNAs – or that chemical calcium dyes can operate. Since a majority of small aquatic animals are indeed transparent, at least in their early stages, one can hope to establish such a technique to a wide variety of species.

Obviously, one needs a relevant motive to justify developing functional imaging in a non-standard model, and the species should be useful to address biological questions that standard models are not informative about, since the experimental power of models such as the mouse, the nematode and the fruit fly will remain unmatched. Two straightforward types of such questions concern evolution and lifestyle, and the fact that *Platynereis* is a good example for both of them will be commented below. Indeed, the three major models mentioned represent three phyla only out of more than twenty, and tell us nothing about chemosensation in marine environments.

A variety of new animal models have recently emerged for which molecular tools are available, thanks notably to the decreasing costs of sequencing technologies. Several such models have been established in the field of evo-devo, and have demonstrated the necessity of a more complete phylum sampling in evolutionary studies [348][349][350]. The nervous system has proved to be highly conserved compared to other features of animal bodies [351], but many aspects of its evolution such as centralisation or the diversification of sensory organs remain poorly explained. In order to better understand crucial steps of this evolution, since most of animal diversity originated in the sea, more marine models are needed for comparative studies of nervous systems and their functions.

Preliminary experiments conducted during this PhD work suggest that marine bilaterian animals such as flatworm larvae or acoels are compatible with experiments in microfluidic devices, and well as planula larvae of sea anemones. The possibility of testing the physiology of the nervous system in such animals is particularly appealing, due both to the distant phyla they represent and to the small size of

their neuronal complement, and may open the door to the inclusion of new, understudied phyla in comparative neurobiology.

Regarding purely material aspects, the present experiments have shown that a setup such as the one used here can reasonably be fully operated by a single person, and so does the production of PDMS microfluidic devices. The setup is simple in its composition and thus inexpensive. A bench for the routine production and use of standard PDMS microfluidic devices can be fully equipped for around 5.000€ including a plasma oven, and the cost of the pumps as well as the rest of the material needed is such that buying equipment for these experiments would represent an investment of less than 10.000€. Provided that a master mould is provided or developed by a collaborator, and that a confocal microscope is available in-house, potentially any laboratory can afford investing in such experiments.

1.4 Evolution of chemical senses and the adaptation to terrestrial life

As was alluded to in the general introduction, in a comparative and evolutionary perspective it may be better to regard chemosensation as the general ability to detect molecules, without too much importance placed on the spatial range of the cues, or on the anatomy of the systems that perceive them. There are indeed several reasons for that.

One reason is that importance placed on spatial range has led to the anthropomorphic dichotomy between smell and taste. When applied to different species and notably aquatic species, this concept often leads to confusion. For example, should the detection of amino acids by fish be considered as olfaction, since these cues can act at long range, or considered as gustation, since distant cues in water are necessarily soluble and are thus the same kinds of molecules detected by the mammalian sense of taste ? Another reason is that relying on anatomy leads to equally confusing view. For example, olfaction if vertebrates is defined as chemosensory information mediated by the cranial nerve I, yet what is called olfactory organ in teleost fish or terrestrial mammals detects totally different set of chemical compounds (soluble versus volatile).

Mollo et al. have argued that chemosensation should be studied and classified according to the physico-chemical properties of the compounds, not on their association with distance or on the organs that detect them [352]. They propose to reconsider aquatic 'noses' such as the olfactory pits of teleost fish as actual aquatic 'tongues', based on their detecting water-soluble compounds. Countering the idea of defining olfaction as the detection of distance cues, they mention the examples of aerosols as non-volatile compounds able to travel long-distances in the air, and hydrophobic micelles as their equivalent in water [352].

Such a view is interesting in several regards : not only does I solve the contradictions mentioned above, but it also allows to reconcile the apparent need of a massive apparition of receptor proteins suited for the detection of volatile compounds during the adaptations to terrestrial life, with the rapidity at which such evolutionary processes seem to have taken place. Indeed, transitioning from aquatic to terrestrial environments animals would have needed suddenly to detect compounds with different physico-chemical properties, and for which they would not have had adequate proteinic receptors. Mollo et al. provide examples of hydrophobic, volatile compounds that are used as meaningful chemical cues in the sea since they are found to at the surface of cnidarians, sponges, and nudibranch molluscs [352]. A further publication from the same group of collaborators illustrates how such compounds are detected as contact signals by shrimps and fish [280]. They generally point at how underestimated the importance and prevalence of such non-soluble cues is for chemosensation in aquatic environments, and suggest that their detection may be a widespread ability in animals. In this regard, animals adapting to life in contact with the air may already have been equipped with suitable types of receptors proteins, that may just have needed to be recruited to different organs, as would probably have been the case e.g. in the vertebrate organ associated with cranial nerve I. Such a point

of view appears sufficiently supported and meaningful, to prompt a reconsideration of chemosensory systems classification.

The evolution of chemoreception and its puzzling variety of receptor proteins remains enigmatic. Photoreception used to be believed to have evolved at least fifty times independently [353], yet its evolutionary history has been clarified now, and a more unified picture has emerged from molecular studies [56]. It is hard to know whether chemoreception is still awaiting for more studies that will lead to such a unification, or whether its history definitely has been less straightforward. There are fundamental reasons to believe that the latter case may rather be true.

One reason is that molecules are discrete entities, and can be at the same time well defined and extremely specific. With the combinatorial possibilities of organic chemistry, the number of molecules that can be produced is potentially infinite. Since most chemical cues are organic particles released by living organisms themselves, be it as by-products of metabolism, as external secretions or as products of decaying organisms, the chemical landscape experienced by an organism is highly dependent on the state of its ecosystem, and subject to enormous variations depending on weather, season, climate, appearance or disappearance of species, soil nutrient content and other parameters. Thus this landscape can be highly variable, prompting organisms to constantly adapt and match their detection abilities to the relevant chemical cues available. Bargmann has expressed this opinion, stating that chemical cues are much less stable than physical cues : "*The visual system and auditory system are stable because light and sound are immutable physical entities. By contrast, the olfactory system, like the immune system, tracks a moving world of cues generated by other organisms, and must constantly generate, test and discard receptor genes and coding strategies over evolutionary time*" ([48] p. 300). This statement needs to be qualified, these since physical entities are not "immutable". Certainly, sunlight is a stable source of physical stimuli, however it is subjected to significant variations due to atmospheric content, clouds, water turbidity as in sediment and biomass content, and these parameters can change over evolutionary times ; depth in the water dramatically affects not only light intensity, but also its colour spectrum and this influences photoreception notably below ten meters where blue-green light dominates [354]. Mechanical stimuli are also subjected to significant variations, depending on the substrate quality : again, hour of the day, weather, climate, biomass and species content, atmospheric content influence the propagation of water-borne, air-borne and substrate-borne signals, which affects for example animal communication [355], and can lead to changing mechanical environments. However, it is true that physical signals are overall more stable over evolutionary times, and not as dependent on the previous evolutionary history as chemical signals are, therefore they require less adaptation of the relevant receptors in sensory systems.

The taxon of polychaetes is appealing as an object of research to better understand the evolutionary study of chemoreception, notably thanks to the well-developed and widespread appendages that these possess. The morphology of these appendages shows a great deal a variation, and so do polychaete lifestyles. It is possible that the establishment of more genomic resources in polychaetes will reveal yet more diversity of chemoreceptor proteins than are currently known. Moreover, annelids seem to represent a suitable phylum in which to study the molecular evolution of chemosensory systems, as they comprise representatives of all intermediate lifestyles : terrestrial and freshwater leeches, as well as marine, freshwater and terrestrial polychaetes. As an example, the nervous system of the freshwater *Potamodrilus fluviatilis* has been described by Purschke & Hessling in the context of annelid phylogeny [109], which may serve as a starting point for such studies.

VII – 2 *Platynereis* as a model for neurobiology

2.1 Is an annelid model relevant in neurobiology ?

Fundamental biological features are conserved between distant animals, such as the use of neurons or the mechanisms of cell death, hence the invertebrate models *Drosophila melanogaster* and *Caenorhabditis elegans* have been particularly powerful in informing us about the genetic and molecular mechanisms of such processes in humans, even though these species differ from us in so many regards.

Yet, vertebrates, despite their evolutionary success, remain only one out of many branches in the animal tree, and therefore one should not attribute to this branch more significance than others in reconstructing the evolution of animal features. Nor should one consider that non-vertebrate animals are adequately represented by the two main invertebrate models, *Drosophila melanogaster* and *Caenorhabditis elegans.* Evolutionary studies that compare vertebrates with these two species represent only three phyla out of more than twenty, hence constitute a poor sampling of animal diversity. And indeed erroneous statements can been made if one considers only these three such phyla. For example, smooth muscles are absent in the nematode and the fly but present in vertebrates, hence they had been hypothesised to be a vertebrate novelty [356], [357], while it is now established that in fact they are present in other phyla including annelids and their origin probably predates bilaterians [358]. Other examples such as some opsins, neurosecreted hormones, and proteins involved in innate immunity are absent in *Drosophila* and *Caenorhabditis* but present in other non-vertebrate phyla [67][68][359][360], further exemplifying the insufficiency, and sometimes even the inadequacy of these two models for inferences over long evolutionary distances.

Therefore, in the study of nervous system evolution, it is crucial to make general statements rely on more phyla, and specially to include species representative of the major clade of Lophotrochozoa, to which the fly and the nematode do not belong. *Platynereis dumerilii*, thanks to its position as a lophotrochozoan and to its slow-evolving genome, has proved to be a relevant such species [66][358]. It is thus *a priori* justified to claim that *Platynereis* is an informative species in complement to the fly and the nematode regarding the evolution of the nervous system.

Other lophotrochozoan models are already used for comparative neurobiology, such as the gastropod mollusc *Aplysia*, but the annelid *Platynereis* offers some advantages compared to them. The transparency and small size of its larvae notably allow powerful whole-body reconstructions of nervous circuits [81], [82] as well as single-cell characterisations of gene expression [59], [73], to an extent that is not conceivable in the other lophotrochozoan models. These points will be detailed below. Hence, *Platynereis* has a clear value in comparative neurobiology, all the more that studies are rather limited by the techniques available than by some intrinsic characteristic of the species, as is partially the case in the two major invertebrate models. Indeed, *Platynereis* has lost less ancestral features than the fast-evolving genera *Drosophila* and *Caenorhabditis*, and has retained the marine biphasic lifestyle representative of ancient bilaterian conditions. It may thus yield numerous discoveries such as the recent ones on the ancestral role of melatonin [70], and as a model is well worth further technical developments.

In terms of nervous system, *Platynereis* 6dpf larvae and their estimated 2.500 head cells are of intermediate size between adult *Caenorhabditis elegans* (nematode, 302 neurons in total) or larval *Ciona intestinalis* (urochordate, 177 brain neurons), and the larvae of the zebrafish *Danio rerio* (vertebrate). They are far more simple than adult *Drosophila melanogaster* (insect, around 100.000 brain neurons).

2.2 Functional imaging in *Platynereis*

Functional imaging in *Platynereis* using the genetic calcium sensor GCaMP6s has been pioneered by Maria A. Tosches [70] and has been used since a few years to visualise muscle activity [81],[361] in larvae until 6.5 dpf, and activity of individual sensory neurons [76] and motoneurons [82] in larvae up to 4 dpf. The strong muscles present in late nectochaete had prevented reliable calcium imaging of individual cells so far but this difficulty has started to be overcome in the present study, yielding insights into *Platynereis*' adult chemosensory systems physiology from experiments conducted in larvae. Moreover, the present study provides a proof-of-principle for the feasibility of whole-brain imaging approaches, which reinforces the attractiveness of *Platynereis* larvae as models for system-wide understanding of nervous circuits. Only the head was imaged here, but the body is not significantly larger and the limitation for imaging the entire animal is only the time needed for technical refinements, nothing intrinsic to the animal – all the more that whole-brain imaging has been achieved in the larger larvae of zebrafish [283]. Thus, mounting and imaging approaches will keep up with the experimenter's will to achieve this goal. More elaborate microfluidic traps than the simple one used here can be devised to improve the fine tune the immobilisation, and one can reasonably hope that whole-body calcium imaging could be performed within a few years, notably in the experimentally challenging context of chemosensation. This will pave the way to a physiological mapping of sensory cells in the entire body, as well as their downstream circuits.

The example of GCaMP6s, reported in 2013 [263] and applied in *Platynereis* for a publication in 2014 [70], has proved that new molecular tools can be rapidly translated from conventional models to models such as *Platynereis*. Hence, fast developing tools such as fluorescent voltage sensors which allow to monitor action potentials in neurons [362][363], or photoconvertible probes such as CaMPARI [364] which allow to integrate neuronal activity in a chosen period of time, could well be applied in *Platynereis* in the coming years and broaden the scope of functional imaging.

Platynereis larvae are ideal for light microscopy and for staining techniques, their main limitation as experimental models still relies in the paucity of genetic tools, hence of cellular targetability, but some current research efforts are going in that direction (see section 2.5). Experimentally, these larvae are equally promising as those of the ascidian *Ciona intestinalis*, for which connectomic data is also available [365], yet functional imaging results in *Ciona* are scarce so far.

2.3 Connectomic data and behaviour

Neuronal circuits are interesting before all if one can relate them to behaviour, that is, to sensory detection, integration, decision making, spontaneous activity, reflexes, orientation, locomotor patterns, etc. This has proved to be the case in *Platynereis*, for which direct links could already be established between circuit and behaviour in the cases of visual phototaxis [120][81], ciliary swimming coordination [82] and startle response (Luis Bezares, unpublished). As was shown here, several chemosensory organs are functional at 6dpf, and at least a few of them at 3dpf (nuchal organ) and 4dpf (diagonal cells) already. The connectome of the whole cell complement of the nuchal organ at 3dpf has been reconstructed already [253], which can serve as a useful basis for linking this chemosensory organ with behaviour.

The number of cells involved in the circuits reconstructed so far is rather limited – e.g. 71 for the visual circuit [81] and 39 for the nuchal organ [253] – which may give hope that a detailed physiological understanding with behavioural predictions could emerge from further studies, notably thanks to the use of calcium imaging. However, the potential physiological complexity of a nervous circuit even with such a low number of elements should not be underestimated. As an example, the stomatogastric nervous system of lobsters and crabs has been an object of research for about 50 years [366], and despite the reduced number of neurons in key components such as the stomatogastric ganglion – a small rhythmic motor circuit with around 30 neurons – many dynamic aspects of the system remain

non understood, which may be due among others to significant inter-individual variability in neuronal morphology [367].

Long ago, Hamaker warned us against the difficulty of a system-wide understanding of a nervous system : "*Although so much has been written on the nervous system […], we are as yet far from thoroughly understanding the action of the myo-neural mechanism of any animal. It is true, much light has been thrown upon the subject during the last decade through the use of the newer methods of investigation; but the many valuable facts that have been established are as yet so disconnected, that they can scarcely be said to be more than suggestive. In no case has the myo-neural system of an animal been at all completely worked out*." ([94], p.89-90) It is as interesting as humbling to compare this warning, formulated as early as in 1898, with our inability still in 2017 to fully understand the physiology of any nervous system, even in the small nematode *Caenorhabditis elegans* despite its complete neuronal connectome being available for more than 30 years now [368].

The development of a connectomic resource (at 3dpf) and of an atlas of gene expression (at 6dpf) in *Platynereis* larvae have uncovered a puzzling diversity of cell types already present at such early stages of development. The physiological evidence reported here for numerous chemosensory organs being differentiated at 6dpf further supports these observations. The recent discovery of intrinsic rhythms and their modulation at larval stages as early as 48 or 36 hpf [70][82] is in line with such findings, and suggests that these apparently simple larvae may be capable of behaviours more complex than previously appreciated.

With modulation comes the question of behavioural modifications, that is to say possibly the question of learning. The likelihood of learning abilities being present at trochophore stages is very low due to its questionable relevance and to the small number of differentiated neurons. At stages when the animals are still swimming in the water column, i.e. 3 to 5 dpf, non-associative behavioural modifications may be present, and in this regard the clear startle response triggered by mechanical stimuli may represent an interesting behaviour for the study of habituation.

Starting from stages when larvae are settling on the sea floor, i.e. around 6dpf, it becomes plausible that these animals may be endowed with more complex behavioural modifications and notably associative ones. Indeed, newly settled larvae explore unknown environments and have to identify suitable places as shelters and food sources. Given the unpredictability of environments to which planktonic larvae can be transported by marine currents over several days after fertilisation, a place selection upon settlement that would rely exclusively on reflex behaviours would appear of low adaptive value, therefore one may expect that these small, active animals are able to learn to avoid certain sets of stimuli. The partial evidence reported here for some Mushroom Bodies cells being already differentiated at 6dpf can make one speculate that interneurons specialised in the memorisation of stimuli and possibly their co-occurrence may exist at such stages, yet this is pure speculation and may be biased by the expectation that annelid and insect Mushroom Bodies would perform similar roles. Alternatively, it remains possible that all behavioural modifications in newly settled *Platynereis* larvae are non-associative, and that the survival of the species does not rely on the larvae's adaptability but solely on their abundance, i.e. a pure *r strategy* for reproduction [369].

In any case, the behavioural repertoire of *Platynereis* larvae is rich, and further behaviours such as orientation in spatial patterns of chemicals suggested by a previous study [187] and by the present work are likely to exist that ought to be further characterised. The behaviour of *Platynereis* larvae appears to be a comparable complexity as that of the nematode *Caenorhabditis elegans*, or of *Drosophila melanogaster* larvae, which encourages the comparative study of behaviours between these species.

2.4 Single-cell gene expression data

A key strength of *Platynereis* as a model organism is its available whole-body atlas of gene expression (PrImR and ProSPr resources, [59][370][73]). The fact that this atlas concerns an entire body make it unmatched by comparison with other organisms, as such atlases exist but are restricted to the brain in the mouse (Allen brain atlas [371]) or in zebrafish [372], to the wing embryonic bud in the chicken [373] or to the blastodermal embryo in the fruit fly [374]. This atlas has allowed to reveal striking resemblances in gene expression patterns between anatomical structures in distant species, such as the annelid Mushroom Bodies and the developing vertebrate cortex [59] or interneurons and motoneurons types in the annelid ventral nerve cord and the vertebrate neural tube [73], and demonstrated its usefulness as a tool for testing evolutionary scenarios of cell types across distant phyla.

Single-cell transcriptomic data obtained from *Platynereis* early larvae can be mapped to such resources, which allows in some cases to identify the original localisation of dissociated cells based only on their gene expression profile [78], and such approaches may be used for example in sponges (Arendt Lab, unpublished) in a comparative perspective to test evolutionary hypotheses on cell type diversification.

The possibility of mapping connectomic data onto such resources would open the door to yet more powerful investigations of cell types, and represents another level in the system-wide understanding of organs and cell types in *Platynereis*. Such an approach has already been taken in the study of neurosecretion in the apical nervous system of 3dpf larvae, which has stressed the importance of peptidergic signalling in these small animals and extended the known diversity of neurosecretory cell types. The addition of physiological data of single cells as obtained in the present work would greatly complement the body-wide characterisation of cell types, and further extend the usefulness of *Platynereis* as a model organism. For this a suitable experimental approach for reliably registering calcium recordings onto an atlas such as ProSPr still needs to be established.

2.5 Molecular and functional tools

Despite the relatively recent establishment of *Platynereis* as a model organism, a number of standard molecular tools have been successfully applied, such as chromosomal FISH mapping [375], gene knock-down with morpholino-oligomers in the example of receptors for the Myo-Inhibitory Peptide [75], or the now routinely used whole-mount mRNA *in situ* hybridisation [119][69][236], cornerstone of the whole-body atlas of gene expression.

The set of genetic and genomic tools available for *Platynereis* has been recently reviewed [376]. Stable transgenesis was achieved with the Tc1/mariner-type element Mos1 in the example of the r-opsin locus [77], and another transposable element called hAT/Tol2, though probably silenced during germline transmission after its integration, as proved to be a valuable tool for visualising in first-generation animals the full expression pattern regulated by a given enhancer. Using the recent CRISPR/Cas9 technology, stable gene knock-outs have been achieved, for example for a photosensitive protein (Go-opsin1, [76]) and for a mechanosensory channel (Luis Bezares, unpublished) ; gene knock-ins have been more challenging so far but are being tried.

Even though the reproductive cycle of *Platynereis* is long compared to the two main invertebrate models *Caenorhabditis* and *Drosophila* (3 to 6 months to reach sexual maturity, compared to some days) and limits the pace at which such tools are being developed, this cycle duration is comparable with that of the mouse which has been established as a powerful genetic model, therefore there is no biological objection to establishing a wide complement of genetic tools in *Platynereis* and such developments will depend mostly on the size of the *Platynereis* research community and its different research interests.

2.6 Conclusions

Platynereis, thanks to its phylogenetic position, experimental suitability and nervous system architecture, is a model organism potentially of high value in the study of comparative and evolutionary neurobiology. It represents a relevant complement to the two main invertebrate models, *Caenorhabditis elegans* and *Drosophila melanogaster*, and possesses some advantages that these models do not have, notably in the higher conservation of ancestral features of its body plan and general complement of cell types. The present work has demonstrated its suitability for whole-brain investigations of neuronal physiology, and in this regard *Platynereis* has a similar experimental potential as the larva of the fruit fly *Drosophila* or the zebrafish *Danio*. Thanks to its ancestral, biphasic marine lifestyle, *Platynereis* can inform about chemosensation in marine environments in complement to fish and crustacean models, as well as about general nervous system physiology in marine ciliated larvae and its evolution in the context of the diversification of bilaterian animals.

Appendix

A. Species and synonyms in the comparative review

People in a field of research change over time, so do sometimes the words they use. I provide here a list of anatomical synonyms employed in the numerous available papers, which may save the interested reader some days of confuse cross-reading as I have experienced while delving into the rich polychaete literature.

Anal cirri = pygidial cirri = urites (Schlawny et al. for *Ophryotrocha puerilis* [152])

Antennae = tentacles = prostomial tentacles

Brain = cerebral ganglia = cephalic ganglion = supra-pharyngeal ganglion = supra-oesophageal ganglion
(not to be confused with the sub-oesophageal ganglion, located ventrally under the mouth)

Head cirri = tentacular cirri = peristomial cirri = cephalic cirri = prostomial cirri

Heteronereis = epitoke = post-sexual-metamorphosis adult nereidid = sexually mature nereidid

Main plexus = main neuropile = zentrale Nervenfaser-Masse des Gehirns

Mushroom Bodies = corpora pedunculata = corps pédonculés = Pilzkörper = vordere Haufen grober Körner (Retzius 1895 [90])

Nuchal organs = ciliated grooves

Peri-oesophageal ring or collar = peri-pharyngeal ring = circum-oesophageal connectives = circum-oral nerve ring

Capitella teleta = *Capitella* sp. 1

Janua brasiliensis = Dexiospira brasiliensis

Nereis acuminata = Nereis arenaceodentata = Nereis caudata = Neanthes caudata

Nereis diversicolor = Hediste diversicolor

Nereis japonica = Neanthes japonica

Nereis longissima = Eunereis longissima = Heteronereis paradoxa

Nereis pelagica = Nereis zonata = Heteronereis grandifolia

Nereis succinea = Nereis limbata = Alitta succinea

Nereis virens = Alitta virens = Neanthes virens

Platynereis dumerilii = Heteronereis fucicola

Additionally, to get a better sense of how strongly represented different families of polychaetes are in the literature reviewed, I provide here a list of species investigated in all articles cited. It is apparent that among all, nereidids were the most often examined.

Table 1 Summary of polychaete species in the literature cited, in chronological order of publication.

Reference / Families	Nereididae	Eunicidae	Aphroditidae	Hesionidae	Spionidae	Opheliidae	Other families
Spengel 1882 [125]							Oenonidae *(Oligognathus bonneliae)*
Retzius 1892 [89], 1895 [90], 1900 [91], 1902 [92]	*Nereis diversicolor*						
Racowitza 1896 [93]	*Platynereis dumerilii*						Amphinomidae, Euphrosinidae, Spintheridae, Maldanidae, Chrysopetalidae
Hamaker 1898 [94], Langdon 1900 [95]	*Nereis virens*						
Hempelmann 1911 [96]	*Platynereis dumerilii*						
Holmgren 1916 [97]	*Nereis diversicolor*						
Gross 1921 [170], Copeland & Wieman 1924 [202]	*Nereis virens*						
Schmidt 1922 [161]	*Nereis pelagica*						Arenicolidae, Nephtyidae
Heider 1925 [112]		*Eunice fasciata, Eunice punctata*					
Hanström 1927 [134]	*Nereis virens, Nereis pelagica*	*Leodice norveg. Leodice Gunn. Hyalinoecia tub. Diopatra cupr. Lumbrinereis fr.*	*Laetmonice filicornis*	*Podarke obscura*		*Ammotrypane aulogaster*	Sigalionidae, Polynoidae Cirratulidae, Maldanidae, Sabellidae & others
Hanström 1928 [98]	*Nereis diversicolor, Nereis pelagica, Nereis virens*	*Hyalinoecia tubicola, Eunice punctata*	*Laetmonice filicornis, Hermione hystrix*	*Podarke obscura, Leocrates*			Glyceridae, Nephtydidae
Hanström 1928 [377]					*Scolecolepis sq., Nerine fuliginosa*		Polygordiidae, Tomopteridae
Wells 1939 [231]	*Nereis irrorata, Perinereis cultrifera*						
Dales 1950 [107]	*Nereis diversicolor*						
Defretin 1955 [99]	*Nereis irrorata, Nereis pelagica, Perinereis cultrifera, Nereis longissima*						
Smith 1957 [110]	*Nereis diversicolor, Nereis virens, Platynereis dumerilii*						
Gilpin-Brown 1958 [121]	*Nereis diversicolor, Nereis virens*						
Case 1962 [185]	*Nereis virens*						

Haffner 1962 [113]		*Hyalinoecia tubicola, Lumbriconereis fragilis, Eunice harassii, Lysidice ninetta, Nematonereis unicornis*					
Horridge 1963 [156]							Polynoidae *(Harmothoë)*
Dorsett 1964 [137]	*Nereis diversicolor*						
Flint 1965 [123]	*Nereis diversicolor*						
Boilly-Marer 1966 [147] [148]	*Nereis pelagica*						
Lawry 1967 [150]							Polynoidae *(Harmothoë)*
Boilly-Marer 1967 [174] 1968 [188]	*Platynereis dumerilii*						
Dorsett & Hyde 1969 [145]	*Nereis virens*						
Hauenschild & Fischer 1969 [65]	*Platynereis dumerilii*						
Mangum & Cox 1971 [208]							Onuphidae (*Diopatra cuprea*)
Santer & Laverack 1971 [143]							Sabellidae (*Sabella pavonina*)
Boilly-Marer 1972 [149]	*Nereis pelagica, Perinereis cultrifera, Platynereis dumerilii*						
Whittle & Zahid 1974 [128]	*Nereis diversicolor*						Glyceridae *(Glycera rouxi),* Nephtyidae *(Nephtys caeca)* Phyllodocidae *(Eulalia viridis)*
Schulte & Riehl 1976 [144]							Terebellidae (*Lanice conchil.*)
Boilly-Marer 1978 [168]	*Nereis succinea*						
Rice 1978 [199]					*Polydora*		
West 1978 [126]						*Ophelia bicornis*	
Boilly-Marer 1980 [167]	*Nereis irrorata, Nereis longissima, Nereis pelagica, Nereis succinea, Perinereis cultrifera, Platynereis dumerilii*						
Kirchman et al. 1982 [217]							Serpulidae *(Janua brasil.)*
Dauer 1984 [162]					*Streblospio benedicti*		
Dhainaut-Courtois et al. 1985 [100]	*Nereis diversicolor*						
Toulmond et al. 1984 [232] Jouin et al. 1985 [153]							Arenicolidae (*Arenicola marina*)
Miller & Jumars 1986 [204]					*Pseudopolydora kempi*		

Purschke 1986 [103]							Parergodrilidae (*Stygocapitella subterranea*)
Schlötzer-Schrehardt 1986 [130], 1987 [131]					*Pygospio elegans*		
Windoffer & Westheide 1988 [155]							Dorvilleidae *(Dinophilus gyrociliatus)*
Zeeck et al. 1988 [189], Zeeck et al. 1998 [192]	*Platynereis dumerilii*						
Bentley et al. 1990 [198], Pacey & Bentley 1992 [194], Hardege et al. 1996 [196] Hardege & Bentley 1997 [195] Watson & Bentley 1998 [197]							Arenicolidae (*Arenicola marina*)
Weinberg et al. 1990 [229] Sutton et al. 2005 [230]	*Nereis acuminata*						
Dauer 1991 [164]					*Polydora commens.*		
Schlawny et al. 1991 [152] [151]							Dorvilleidae *(Ophryotrocha)*
Biggers & Laufer 1992 [176]							Capitellidae (*Capitella capitata*)
Orrhage 1993 [133]	*Nereis virens, Nereis pelagica*		Aphroditidae	Hesionidae	*Laonice*		Amphinomidae, Aphroditacea, Chaetopteridae, Cirratulidae & others
Woodin et al. 1993 [221]							Terebellidae (Thelepus crispus)
Orrhage 1995 [124]		*Eunice norvegica & pennata*					Onuphidae
Fewou & Dhainaut-Courtois 1995 [158]	*Nereis diversicolor*						
Bartels-Hardege et al. 1996 [191]	*Nereis japonica*						
Fischer et al. 1996 [234]	*Nereis virens, Platynereis dumerilii*						
Dauer 1997 [165]					*Marenzelleria viridis*		
Hardege et al. 1997 [193], Ram et al. 1999 [169]	*Nereis succinea*						
Levin et al. 1997 [205]							Maldanidae
Purschke 1997 [122]	*Nereis diversicolor*			*Hesionides arenaria, Microphtalmus similis*	*Scolelepis sp.*	*Ophelia rathkei & others*	Pisionidae, Hesionidae, Syllidae, Dinophilidae, Glyceridae & others

Holm et al. 1998 [178], Pechenik &Qian 1998 [216], Harder & Qian 1999 [215], Unabia & Hadfield 1999 [219], Lau & Qian 2001 [218], Harder et al. 2002 [220]							Serpulidae (*Hydroides elegans*)
Zeeck et al. 1998 [33],[190]	*Nereis succinea*						
Biggers & Laufer 1999 [177] Snelgrove et al. 2001 [225] Marinelli & Woodin 2004 [224]							Capitellidae (*Capitella teleta*)
Ferner & Jumars 1999 [209]					*Boccardia proboscid,. Polydora cornuta, Pseudopoly dora kempi*		
Kihslinger & Woodin 2000 [207] Mahon & Dauer 2005 [210] Esser et al. 2008 [223]					*Streblospio benedicti*		
Watson et al. 2000 [200] Gaudron et al. 2007 [201]							Polynoidae (*Harmothoe imbricata*)
Worsaae 2001 [166]					*Dipolydora coeca, Dipolydora quadrilob., Polydora ciliata, Polydora cornuta, Pseudopoly dora pulch.*		
Purschke & Hessling 2002 [109]							Potamodrilidae (*Potamodrilus fluviatilis*)
Riordan & Lindsay 2002 [186] Lindsay et al. 2004 [154]					*Dipolydora quadrilob.*		
Arendt et al. 2002 [119], 2004 [67], Denes et al. 2007 [69], Tessmar et al. 2007 [68], Christodoulou et al. 2010 [242], Marlow et al. 2014 [236]	*Platynereis dumerilii* (larvae)						
Fischer & Dorresteijn 2004 [235]	*Platynereis dumerilii*						

Orrhage & Müller 2005 [108]	*Nereis*	*Eunicia*		*Leocrates*	*Laonice*		Polynoidae, Amphinomidae, Syllidae, Glyceridae & others
Schleicherova et al. 2005 [228]							Dorvilleidae (Ophryotrocha diadema)
Watson et al. 2005 [203]	*Nereis virens*						
Jékely et al. 2008 [120], Conzelmann et al. 2011 [239], 2013 [75], Randel et al. 2014 [81], Bauknecht & Jékely 2015 [180]	*Platynereis dumerilii* (larvae)						
Heuer & Lösel 2008 [101]	*Nereis diversicolor*						
Voronezhskaya et al. 2008 [378]	*Platynereis dumerilii*						
Fischer et al. 2010 [138]	*Platynereis dumerilii*						
Heuer et al. 2010 [111]	*Nereis diversicolor*	*Eunice torquata*	*Aphrodita aculeata*	*Hesione panther.*		*Ophelia limacina*	Arenicolidae, Lumbrinereid., Nephtyidae, Polynoidae, Phyllodocidae, Sabellidae, Scalibregmatid., Sigalionidae, Syllidae, Terebellidae, Tomopteridae
Winchell et al. 2010 [246]	*Neanthes arenaceodentata*						
Schmidtberg & Dorresteijn 2010 [233]	*Platynereis dumerilii*						
Backfish et al. 2013 [77]	*Platynereis dumerilii*						
Wäge et al. 2015 [245]	*Platynereis dumerilii*						
Starunov et al. 2017 [102]	*Platynereis dumerilii*						

B. Microinjections in fertilised *Platynereis* eggs

Micro-injections were performed according to a protocol initially developed in the Arendt Lab by Nicola Kegel and Benjamin Backfisch, and progressively optimized by several lab members. It mainly consists in adequately preparing the fertilized eggs and placing them on an agar stage, to facilitate both penetration and extraction of the injection needle. In all steps, the sea water used is natural, and has been sterile-filtered with 0.22 µm filters (Millipore). This water is designated hereafter as FNSW for Filtered Natural Sea Water.

1. operational injection protocol

- separate crosses of sexually mature wild-type *Platynereis* are set up, with one male and one female in each Zentis cup, filled with FNSW. At least three good batches are recommended, to keep high chances of having good eggs. In case too much sperm has been released (milky appearance), the water is diluted with additional FNSW to prevent polyspermy. Batches are put in a 18°C incubator. After 5-10 minutes, eggs observed under a stereomicroscope will be arranged in a very regular hexagonal pattern if they have been fertilized. Indeed, fertilization triggers the release of the cortical granules, which are composed of mucopolysaccharides and will form a gelatinous mass (a 'jelly') around the zygotes (Fischer et al., 1996 [234]). This jelly will be removed before injecting, as it would prevent the needle from easily entering in the eggs.

- while the eggs are developing, several agar stages are prepared with 2% agar in FNSW, by using a microscopy slide and a custom-made mould (similar dimensions as the microscopy slide but with a 0.3 mm x 0.5 mm step on one side). The low wall has the same height as the zygote diameter. A fine syringe needle is used to prepare scratches in the low wall, perpendicular to the main groove, which will help extracting the needle from the eggs. Each stage is placed in a Nunclon plate, filled with FNSW.

- to prepare a fresh injection solution, a 1µL-aliquot of GCaMP6s mRNA is taken from the -80°C freezer, diluted with RNAse-free water to the final concentration of 1.000 ng/µL, and centrifuged for 5 min to prevent the pipetting of any precipitates that could later clog the needle tip. This solution will be loaded in the injection needle right before starting the injection.

- at around 45 minutes post-fertilization, the best batch is selected among those set up. Alternatively, two batches can be mixed to increase the chances of survival and correct development among the injected zygotes. The quality of the zygotes is evaluated according to the following criteria : 1) the shape should be spherical, 2) the surface should be smooth, 3) the colour should be rather light, and 4) the yolk granules should accumulate at the periphery. Wrinkled, oval or darker zygotes should be avoided, as they are unlikely to survive. Unfertilized eggs will be bigger and sit at the bottom.

- a fresh solution of 46.7 µg/mL proteinase K in FNSW is prepared, by diluting a 70µL-aliquot of 20 mg/mL proteinase K stock solution in 30 mL FNSW.

- at 50 minutes post-fertilization, zygotes are dejellied by a thorough and repeated rinse with FNSW through a custom-made sieve (made from 50 mL Falcon tubes and a nylon mesh with 100 µm mesh size, NITEX, Gebr. Stallmann). While rinsing, it is important to never expose the eggs to the air, to avoid any dehydration damage. This step will require approximately 600 mL of FNSW.

- the periphery of the eggs is then digested by immersing them for 50 seconds in the proteinase K solution, and immediately rinsed with about 200mL FSNW to avoid over-digestion. The eggs can be taken out of the sieve and place in a dish filled with FNSW ; they are now ready for injection. Eggs not touching the bottom of their dish will be a sign for an insufficient dejellying.

- while eggs are sinking in their dish, the needle is loaded with at least 0.5µL of the injection solution. This step needs to be anticipated, as it will take some minutes until the solution, running by capillarity along the filament, reaches the tip of the needle.

- about 50 eggs are kept in a 6-wells plate as a control for the batch quality. It is not uncommon that most eggs would misdevelop or die. Especially while learning how to inject, it is important to know what is due to the injections and what is not. A portion of the zygotes can be stored at 4 °C up to 90 min to be injected.

- eggs are placed in the groove of an agar stage, and the stage placed on the injection setup, composed of an Axiovert 40C inverted microscope (Zeiss) equipped with a micromanipulator and a FemtoJet microinjector (Eppendorf). Injections will be performed under a 10x magnification. The needle is brought in position.

- for injection, the zygotes are pushed with the tip of the needle against the high wall. After delivery of the injection solution, the needle is released by passing through one of the scratches of the low wall. This prevents the zygote from sticking to the

needle. The injecting pressure will be regularly adapted (typically between 100 and 400 hPa) to maintain the injected volume constant. This volume should visually appear as a disk whose diameter represents 15-20% of the zygote's diameter, and be delivered in its centre.

- after injection, the embryos are transferred to the 6-wells plate. An additional 50 non-injected zygotes can be taken from the agar stage as a control for stage conditions.

- one day later, misdeveloped or dead embryos are removed from the well, to avoid any contamination of the healthy ones. This is particularly important if many eggs have been introduced in the same well. This sorting has to be repeated in the following days. It happens that embryos look good until 4 or 5 days post-fertilization, when they start to reveal some misdevelopment.

2. preparation of injection needles

Needles used were pooled from glass capillaries (1mm diameter, with filament, Harvard apparatus) using a Sutter needle pooler. The following parameters were used :

PULL 548
HEAT 040
VELOCITY 130
TIME 125

After pulling, needles are kept in a large, round plastic Petri dish, in which they are held by a bar of plasticine.

3. preparation of GCaMP6s mRNA injection solution

A stock solution of GCaMP6s mRNA in RNAse-free water is stored at -80°C in 1µL aliquots, and diluted freshly to the final concentration of 1.000 ng/µL before each injection.

These capped and polyadenylated mRNAs are produced by *in vitro* transcription, performed from linear DNA templates in the form of a purified PCR product. The PCR product was generated from a plasmid construct (courtesy of Jékely lab, see plasmid #984 in Appendix C), in which two sequences have been cloned between the BamHI and the NsiI restriction sites of the pUC57 plasmid backbone : the full GCaMP6s coding region, downstream of a 169-base-pair 5' UTR from the *Platynereis* 60S acidic ribosomal protein P2 (as described in Randel et al. 2014, [81]). This 'P2' element has been found to enhance expression levels of the GCaMP6s protein in *Platynereis* larvae (see Chapter VI for an illustration).

Customized PCR primers used (courtesy of Luis Bezares, Jékely lab) :

pUC-Forward (5' to 3') :
GATCCCCCTCGGATCCTAATACGACTCACTATAGGGAGATTTGATGTTTACAGGGC
(T7 promoter site underlined)

pUC-Reverse (5' to 3') :
GAATTCGAGCTCGGTACCTCGCGAATGCATCTAGATCCAATTTTCTCTTAAACAACTCC

PCR reaction used, following the Phusion PCR kit from New England Biolabs, and cycling program :

dH_2O	to 50 µL	
Green HF buffer	10 µL	*5x*
dNTPs	1 µL	*10mM, final concentration 200 µM each*
Forward primer	2.5 µL	*10 µM, final concentration 0.5 µM*
Reverse primer	2.5 µL	*10 µM, final concentration 0.5 µM*
Plasmid template	5 µL	*2ng/µL max, < 10ng for 50µL*
Phusion polymerase	0.5 µL	

1x	98 °C	1 min 30s
35x	98 °C	10s
	72 °C	45s
1x	72 °C	10 min

From these templates, mRNAs were synthesised using the T7 mMessage mMachine Ultra Kit (Life Technologies). Capping and polyadenylation strongly reduces degradation of the mRNAs after they are injected in the zygotes, which is necessary to ensure that the protein will be expressed after up to 7 days of development.

Transcription reaction : T7 mMessage mMachine Ultra Kit

Thaw reagents.
Keep the NTPs on ice, but assemble the reaction at room temperature, with the following amounts :

Nuclease-free water	to 20 µL
2x NTP/ARCA	10 µL
10x T7 buffer	2 µL
PCR product/linear plasmid	200 / 1000 ng
Perlimpinpin powder	200 ng
T7 enzyme mix	2 µL

Mix well but gently.
Incubate at 37 °C for 2-4 h, or even overnight. Option : for a higher yield, add 1 µL of fresh enzyme for the last hour of synthesis.
Add 1 µL of Turbo DNase, mix well but gently.
Incubate at 37 °C for 15 min.
Put poly(A) reagents (E-PAP buffer, $MnCl_2$ solution and ATP solution) at room temperature, they will thaw during this incubation.

Poly(A) tailing reaction :

Previous reaction	20 µL
Nuclease-free water	36 µL
5x E-PAP buffer	20 µL
20 mM $MnCl_2$	10 µL
ATP solution	10 µL
E-PAP enzyme	4 µL
Total	100 µL

Incubate at 37 °C for 30-45 min. Then, place on ice.

Prepare electrophoresis gel (before purification)

Mix 20 mL of 2% agar/TAE with 4 µL of SYBR or EtBr.
Add 40 mL of TAE buffer.
Pour the gel in its mould, remove bubbles.
Place the comb.

Purification. Option 1 : with Qiagen Kit

In a 1.5 mL Eppendorf containing 100 µL of the previous reaction, add 350 µL of RTL buffer and mix.
Add 250 µL of 100% ethanol and mix.
Transfer to a column and centrifuge for 15 s at maximum speed.
Dispose of the liquid.
Add 500 µL of RPE buffer.
Centrifuge for 15 s at maximum speed and dispose of the liquid.
Add 500 µL of RPE buffer.
Centrifuge for 2 min at maximum speed and dispose of the liquid.
Again, centrifuge for 1 min at maximum speed to remove the residual buffer. Dispose of the liquid.
Place the column in a 1.5 mL tube and label it.
Put 30 µL of Nuclease-free water on the centre of the filter.
Let the column stand for 1 min.
Centrifuge for 1 min at maximum speed. Option : 2x (15 µL and centrifuge)

Or

Purification. Option 2 : with Lithium Chloride (LiCl) precipitation

In a 1.5 mL tube containing 100 µL of the previous reaction, add 50 µL of LiCl (7.5 M, 100 mM of EDTA), or 30 µL of LiCl and 30 µL of Nuclease-free water.
Mix well and leave the tube for 30 min or more at -20 °C.
Centrifuge for 15 min at 4 °C at maximum speed.
Remove the supernatant and keep it.
Wash the pellet with 200 µL of 70% ethanol.
Centrifuge for 15 min at 4 °C at maximum speed.

Carefully remove the ethanol with a P200 pipette, then with a P10 pipette until there is no more liquid. The pellet will sit on the side of the tube.
Let the open tube dry for 5 to 10 min at room temperature.
Re-suspend the pellet in 30 µL of Nuclease-free water.

Gel loading

Immerse the gel in 250 mL of TAE buffer.
In each well, add a mixture of :
2.5 µL of RNA sample (denatured beforehand for 10 min at 70°C)
2.5 µL of 2x RNA loading dye
For the RNA ladder, 1 µL is enough
Run the gel for 30 to 40 min with 7 V/cm (about 90 V) and 400 mA.

Nanodrop

In RNA mode, make 3 measures from 1:10 dilutions for each sample, to improve precision. Indeed, the measure becomes imprecise if the concentration is above 1000 ng/µL as is the objective here. This can be done while the gel is running.

Aliquots

Prepare 1 or 2µL-aliquots of the purified RNA solution in PCR tubes. This can be done while the gel is running. As aliquoting takes a long time, all work has to be done on ice. A multi-pipette is too imprecise for such small volumes and should not be used. Each aliquoted tube should be labelled, to avoid confusion between different aliquots, typically if falling one day from a freezer box.

Once ready, the aliquots are placed all at once in a -80°C freezer. They can be kept for many months. More than high temperatures, repeated changes in temperature affect the RNA's stability and structure, and should be avoided. An aliquot that has been thawed can be placed at -20°C to be re-used in the following days, but not longer.

4. preparation of an agar stage

In order to adequately hold the eggs while they are being injected, a customised agar stage (see Figure B-1) is used, using approximately 2% agar in sea water. The liquefied agar solution is poured onto a custom mould that produces a 1 mm groove between a high wall and a low wall of agarose ; the latter wall has the same height as the egg diameter. Scratches are made by hand in this low wall with a fine syringe needle, to allow withdrawing the needle without taking the egg with is, since eggs tends to stick to it.

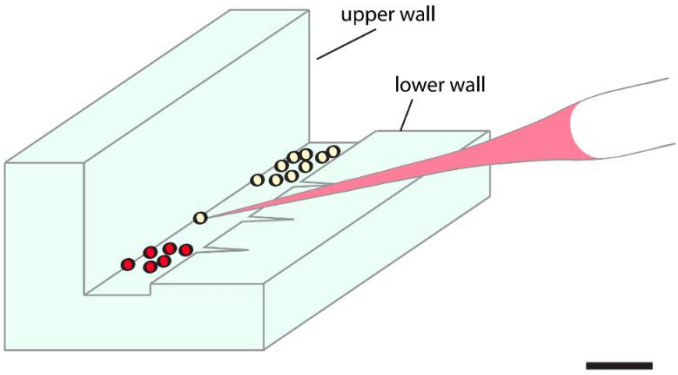


Figure B-1 Schematic overview of the agar stage used for microinjections. Scale bar 1 mm. Image reproduced from Maria Tosches, [237].

C. Plasmids used for GCaMP mRNA synthesis

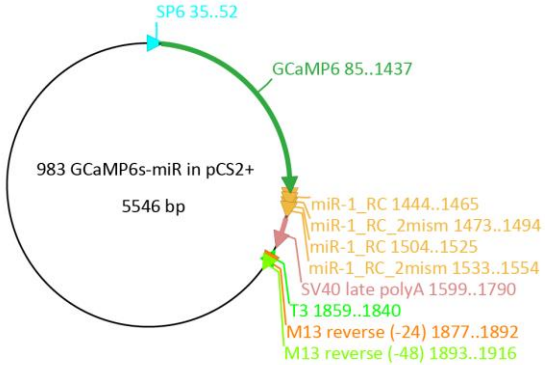
Plasmid #982 was provided by Maria A. Tosches ; Plasmid #983 was assembled by Maria A. Tosches and Paola Bertucci ; Plasmid #984 was provided by Gáspár Jékely (MPI Tübingen) ; Plasmid #985 was assembled by Thomas Chartier and Mairi Clarke. Numbers refer to the Arendt Lab internal plasmid database.



Plasmid #982 full sequence (SP6 promoter underlined) :

CGCCATTCTGCCTGGGGACGTCGGAGCAAGCTTGATTTAGGTGACACTATAGAATACAAGCTACTTGTTCTTTTTGCAGGATCCATGGGT
TCTCATCATCATCATCATCATGGTATGGCTAGCATGACTGGTGGACAGCAAATGGGTCGGGATCTGTACGACGATGACGATAAGGATCTC
GCCACCATGGTCGACTCATCACGTCGTAAGTGGAATAAGACAGGTCACGCAGTCAGAGCTATAGGTCGGCTGAGCTCACTCGAGAACGT
CTATATCAAGGCCGACAAGCAGAAGAACGGCATCAAGGCGAACTTCCACATCCGCCACAACATCGAGGACGGCGGCGTGCAGCTCGCCT
ACCACTACCAGCAGAACACCCCCATCGGCGACGGCCCCGTGCTGCTGCCCGACAACCACTACCTGAGCGTGCAGTCCAAACTTTCGAAAG
ACCCCAACGAGAAGCGCGATCACATGGTCCTGCTGGAGTTCGTGACCGCCGCCGGGATCACTCTCGGCATGGACGAGCTGTACAAGGG
CGGTACCGGAGGGAGCATGGTGAGCAAGGGCGAGGAGCTGTTCACCGGGGTGGTGCCCATCCTGGTCGAGCTGGACGGCGACGTAAA
CGGCCACAAGTTCAGCGTGTCCGGCGAGGGTGAGGGCGATGCCACCTACGGCAAGCTGACCCTGAAGTTCATCTGCACCACCGGCAAG
CTGCCCGTGCCCTGGCCCACCCTCGTGACCACCCTGACCTACGGCGTGCAGTGCTTCAGCCGCTACCCCGACCACATGAAGCAGCACGAC
TTCTTCAAGTCCGCCATGCCCGAAGGCTACATCCAGGAGCGCACCATCTTCTTCAAGGACGACGGCAACTACAAGACCCGCGCCGAGGT
GAAGTTCGAGGGCGACACCCTGGTGAACCGCATCGAGCTGAAGGGCATCGACTTCAAGGAGGACGGCAACATCCTGGGGCACAAGCTG
GAGTACAACCTGCCGGACCAACTGACTGAAGAGCAGATCGCAGAATTTAAAGAGGCTTTCTCCCTATTTGACAAGGACGGGGATGGGAC
AATAACAACCAAGGAGCTGGGGACGGTGATGCGGTCTCTGGGGCAGAACCCCACAGAAGCAGAGCTGCAGGACATGATCAATGAAGT
AGATGCCGACGGTGACGGCACAATCGACTTCCCTGAGTTCCTGACAATGATGGCAAGAAAAATGAAATACAGGGACACGGAAGAAGAA
ATTAGAGAAGCGTTCGGTGTGTTTGATAAGGATGGCAATGGCTACATCAGTGCAGCAGAGCTTCGCCACGTGATGACAAACCTTGGAGA
GAAGTTAACAGATGAAGAGGTTGATGAAATGATCAGGGAAGCAGACATCGATGGGGATGGTCAGGTAAACTACGAAGAGTTTGTACAA
ATGATGACAGCGAAGTGAGAATTCAAGGCCTCTCGAGCCTCTAGAACTATAGTGAGTCGTATTACGTAGATCCAGACATGATAAGATAC
ATTGATGAGTTTGGACAAACCACAACTAGAATGCAGTGAAAAAAATGCTTTATTTGTGAAATTTGTGATGCTATTGCTTTATTTGTAACCA
TTATAAGCTGCAATAAACAAGTTAACAACAACAATTGCATTCATTTTATGTTTCAGGTTCAGGGGGAGGTGTGGGAGGTTTTTTAATTCGC
GGCCGCGGCGCCAATGCATTGGGCCCGGTACCCAGCTTTTGTTCCCTTTAGTGAGGGTTAATTGCGCGCTTGGCGTAATCATGGTCATAG
CTGTTTCCTGTGTGAAATTGTTATCCGCTCACAATTCCACACAACATACGAGCCGGAAGCATAAAGTGTAAAGCCTGGGGTGCCTAATGA
GTGAGCTAACTCACATTAATTGCGTTGCGCTCACTGCCCGCTTTCCAGTCGGGAAACCTGTCGTGCCAGCTGCATTAATGAATCGGCCAA
CGCGCGGGGAGAGGCGGTTTGCGTATTGGGCGCTCTTCCGCTTCCTCGCTCACTGACTCGCTGCGCTCGGTCGTTCGGCTGCGGCGAGC
GGTATCAGCTCACTCAAAGGCGGTAATACGGTTATCCACAGAATCAGGGGATAACGCAGGAAAGAACATGTGAGCAAAAGGCCAGCAA
AAGGCCAGGAACCGTAAAAAGGCCGCGTTGCTGGCGTTTTTCCATAGGCTCCGCCCCCCTGACGAGCATCACAAAAATCGACGCTCAAG
TCAGAGGTGGCGAAACCCGACAGGACTATAAAGATACCAGGCGTTTCCCCCTGGAAGCTCCCTCGTGCGCTCTCCTGTTCCGACCCTGCC
GCTTACCGGATACCTGTCCGCCTTTCTCCCTTCGGGAAGCGTGGCGCTTTCTCATAGCTCACGCTGTAGGTATCTCAGTTCGGTGTAGGTC
GTTCGCTCCAAGCTGGGCTGTGTGCACGAACCCCCCGTTCAGCCCGACCGCTGCGCCTTATCCGGTAACTATCGTCTTGAGTCCAACCCG
GTAAGACACGACTTATCGCCACTGGCAGCAGCCACTGGTAACAGGATTAGCAGAGCGAGGTATGTAGGCGGTGCTACAGAGTTCTTGA
AGTGGTGGCCTAACTACGGCTACACTAGAAGGACAGTATTTGGTATCTGCGCTCTGCTGAAGCCAGTTACCTTCGGAAAAAGAGTTGGT
AGCTCTTGATCCGGCAAACAAACCACCGCTGGTAGCGGTGGTTTTTTTGTTTGCAAGCAGCAGATTACGCGCAGAAAAAAAGGATCTCAA
GAAGATCCTTTGATCTTTTCTACGGGGTCTGACGCTCAGTGGAACGAAAACTCACGTTAAGGGATTTTGGTCATGAGATTATCAAAAAGG
ATCTTCACCTAGATCCTTTTAAATTAAAAATGAAGTTTTAAATCAATCTAAAGTATATATGAGTAAACTTGGTCTGACAGTTACCAATGCTT
AATCAGTGAGGCACCTATCTCAGCGATCTGTCTATTTCGTTCATCCATAGTTGCCTGACTCCCCGTCGTGTAGATAACTACGATACGGGAG
GGCTTACCATCTGGCCCCAGTGCTGCAATGATACCGCGAGACCCACGCTCACCGGCTCCAGATTTATCAGCAATAAACCAGCCAGCCGGA
AGGGCCGAGCGCAGAAGTGGTCCTGCAACTTTATCCGCCTCCATCCAGTCTATTAATTGTTGCCGGGAAGCTAGAGTAAGTAGTTCGCCA
GTTAATAGTTTGCGCAACGTTGTTGCCATTGCTACAGGCATCGTGGTGTCACGCTCGTCGTTTGGTATGGCTTCATTCAGCTCCGGTTCCC
AACGATCAAGGCGAGTTACATGATCCCCCATGTTGTGCAAAAAAGCGGTTAGCTCCTTCGGTCCTCCGATCGTTGTCAGAAGTAAGTTGG

CCGCAGTGTTATCACTCATGGTTATGGCAGCACTGCATAATTCTCTTACTGTCATGCCATCCGTAAGATGCTTTTCTGTGACTGGTGAGTA
CTCAACCAAGTCATTCTGAGAATAGTGTATGCGGCGACCGAGTTGCTCTTGCCCGGCGTCAATACGGGATAATACCGCGCCACATAGCA
GAACTTTAAAAGTGCTCATCATTGGAAAACGTTCTTCGGGGCGAAAACTCTCAAGGATCTTACCGCTGTTGAGATCCAGTTCGATGTAAC
CCACTCGTGCACCCAACTGATCTTCAGCATCTTTTACTTTCACCAGCGTTTCTGGGTGAGCAAAAACAGGAAGGCAAAATGCCGCAAAAA
AGGGAATAAGGGCGACACGGAAATGTTGAATACTCATACTCTTCCTTTTTCAATATTATTGAAGCATTTATCAGGGTTATTGTCTCATGAG
CGGATACATATTTGAATGTATTTAGAAAAATAAACAAATAGGGGTTCCGCGCACATTTCCCCGAAAAGTGCCACCTAAATTGTAAGCGTT
AATATTTTGTTAAAATTCGCGTTAAATTTTTGTTAAATCAGCTCATTTTTTAACCAATAGGCCGAAATCGGCAAAATCCCTTATAAATCAAA
AGAATAGACCGAGATAGGGTTGAGTGTTGTTCCAGTTTGGAACAAGAGTCCACTATTAAAGAACGTGGACTCCAACGTCAAAGGGCGAA
AAACCGTCTATCAGGGCGATGGCCCACTACGTGAACCATCACCCTAATCAAGTTTTTTGGGGTCGAGGTGCCGTAAAGCACTAAATCGGA
ACCCTAAAGGGAGCCCCCGATTTAGAGCTTGACGGGGAAAGCCGGCGAACGTGGCGAGAAAGGAAGGGAAGAAAGCGAAAGGAGCG
GGCGCTAGGGCGCTGGCAAGTGTAGCGGTCACGCTGCGCGTAACCACCACACCCGCCGCGCTTAATGCGCCGCTACAGGGCGCGTCCC
ATTCGCCATTCAGGCTGCGCAACTGTTGGGAAGGGCGATCGGTGCGGGCCTCTTCGCTATTACGCCAGTCGACCATAGCCAATTCAATAT
GGCGTATATGGACTCATGCCAATTCAATATGGTGGATCTGGACCTGTGCCAATTCAATATGGCGTATATGGACTCGTGCCAATTCAATAT
GGTGGATCTGGACCCCAGCCAATTCAATATGGCGGACTTGGCACCATGCCAATTCAATATGGCGGACTTGGCACTGTGCCAACTGGGGA
GGGGTCTACTTGGCACGGTGCCAAGTTTGAGGAGGGGTCTTGGCCCTGTGCCAAGTCCGCCATATTGAATTGGCATGGTGCCAATAATG
GCGGCCATATTGGCTATATGCCAGGATCAATATATAGGCAATATCCAATATGGCCCTATGCCAATATGGCTATTGGCCAGGTTCAATACT
ATGTATTGGCCCTATGCCATATAGTATTCCATATATGGGTTTTCCTATTGACGTAGATAGCCCCTCCCAATGGGCGGTCCCATATACCATAT
ATGGGGCTTCCTAATACCGCCCATAGCCACTCCCCCATTGACGTCAATGGTCTCTATATATGGTCTTTCCTATTGACGTCATATGGGCGGT
CCTATTGACGTATATGGCGCCTCCCCCATTGACGTCAATTACGGTAAATGGCCCGCCTGGCTCAATGCCCATTGACGTCAATAGGACCACC
CACCATTGACGTCAATGGGATGGCTCATTGCCCATTCATATCCGTTCTCACGCCCCCTATTGACGTCAATGACGGTAAATGGCCCACTTGG
CAGTACATCAATATCTATTAATAGTAACTTGGCAAGTACATTACTATTGGAAGGACGCCAGGGTACATTGGCAGTACTCCCATTGACGTC
AATGGCGGTAAATGGCCCGCGATGGCTGCCAAGTACATCCCCATTGACGTCAATGGGGAGGGGCAATGACGCAAATGGGCGTTCCATT
GACGTAAATGGGCGGTAGGCGTGCCTAATGGGAGGTCTATATAAGCAATGCTCGTTTAGGGAAC

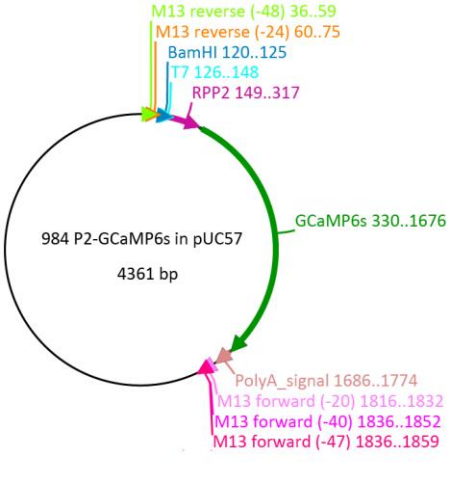


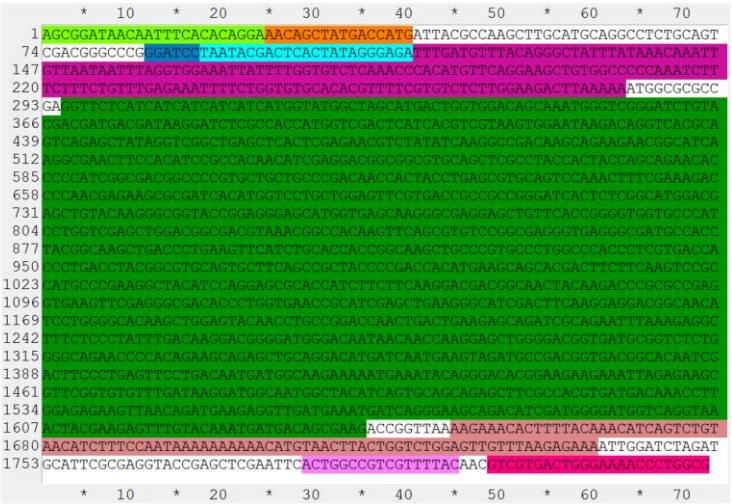


Plasmid #983 full sequence (SP6 promoter underlined) :

CGCCATTCTGCCTGGGGACGTCGGAGCAAGCTTG<u>ATTTAGGTGACACTATAG</u>AATACAAGCTACTTGTTCTTTTTGCAGGATCCATGGGT
TCTCATCATCATCATCATCATGGTATGGCTAGCATGACTGGTGGACAGCAAATGGGTCGGGATCTGTACGACGATGACGATAAGGATCTC
GCCACCATGGTCGACTCATCACGTCGTAAGTGGAATAAGACAGGTCACGCAGTCAGAGCTATAGGTCGGCTGAGCTCACTCGAGAACGT
CTATATCAAGGCCGACAAGCAGAAGAACGGCATCAAGGCGAACTTCCACATCCGCCACAACATCGAGGACGGCGGCGTGCAGCTCGCCT
ACCACTACCAGCAGAACACCCCCATCGGCGACGGCCCCGTGCTGCTGCCCGACAACCACTACCTGAGCGTGCAGTCCAAACTTTCGAAAG
ACCCCAACGAGAAGCGCGATCACATGGTCCTGCTGGAGTTCGTGACCGCCGCCGGGATCACTCTCGGCATGGACGAGCTGTACAAGGG
CGGTACCGGAGGGAGCATGGTGAGCAAGGGCGAGGAGCTGTTCACCGGGGTGGTGCCCATCCTGGTCGAGCTGGACGGCGACGTAAA
CGGCCACAAGTTCAGCGTGTCCGGCGAGGGTGAGGGCGATGCCACCTACGGCAAGCTGACCCTGAAGTTCATCTGCACCACCGGCAAG
CTGCCCGTGCCCTGGCCCACCCTCGTGACCACCCTGACCTACGGCGTGCAGTGCTTCAGCCGCTACCCCGACCACATGAAGCAGCACGAC
TTCTTCAAGTCCGCCATGCCCGAAGGCTACATCCAGGAGCGCACCATCTTCTTCAAGGACGACGGCAACTACAAGACCCGCGCCGAGGT
GAAGTTCGAGGGCGACACCCTGGTGAACCGCATCGAGCTGAAGGGCATCGACTTCAAGGAGGACGGCAACATCCTGGGGCACAAGCTG
GAGTACAACCTGCCGGACCAACTGACTGAAGAGCAGATCGCAGAATTTAAAGAGGCTTTCTCCCTATTTGACAAGGACGGGGATGGGAC
AATAACAACCAAGGAGCTGGGGACGGTGATGCGGTCTCTGGGGCAGAACCCCACAGAAGCAGAGCTGCAGGACATGATCAATGAAGT
AGATGCCGACGGTGACGGCACAATCGACTTCCCTGAGTTCCTGACAATGATGGCAAGAAAAATGAAATACAGGGACACGGAAGAAGAA
ATTAGAGAAGCGTTCGGTGTGTTTGATAAGGATGGCAATGGCTACATCAGTGCAGCAGAGCTTCGCCACGTGATGACAAACCTTGGAGA
GAAGTTAACAGATGAAGAGGTTGATGAAATGATCAGGGAAGCAGACATCGATGGGGATGGTCAGGTAAACTACGAAGAGTTTGTACAA
ATGATGACAGCGAAGTGAGAATTGCTACATACTTCTTTACATTCCAGACTATTCTACATACTTCACTACATTCCAATGGAATTGCTACATAC
TTCTTTACATTCCAGACTATTCTACATACTTCACTACATTCCAATGGAATTCTATCTAGAACTATAGTGAGTCGTATTACGTAGATCCAGAC
ATGATAAGATACATTGATGAGTTTGGACAAACCACAACTAGAATGCAGTGAAAAAAATGCTTTATTTGTGAAATTTGTGATGCTATTGCT
TTATTTGTAACCATTATAAGCTGCAATAAACAAGTTAACAACAACAATTGCATTCATTTTATGTTTCAGGTTCAGGGGGAGGTGTGGGAG
GTTTTTTAATTCGCGGCCGCGGCGCCAATGCATTGGGCCCGGTACCCAGCTTTTGTTCCCTTTAGTGAGGGTTAATTGCGCGCTTGGCGTA
ATCATGGTCATAGCTGTTTCCTGTGTGAAATTGTTATCCGCTCACAATTCCACACAACATACGAGCCGGAAGCATAAAGTGTAAAGCCTG
GGGTGCCTAATGAGTGAGCTAACTCACATTAATTGCGTTGCGCTCACTGCCCGCTTTCCAGTCGGGAAACCTGTCGTGCCAGCTGCATTA

ATGAATCGGCCAACGCGCGGGGAGAGGCGGTTTGCGTATTGGGCGCTCTTCCGCTTCCTCGCTCACTGACTCGCTGCGCTCGGTCGTTCG
GCTGCGGCGAGCGGTATCAGCTCACTCAAAGGCGGTAATACGGTTATCCACAGAATCAGGGGATAACGCAGGAAAGAACATGTGAGCA
AAAGGCCAGCAAAAGGCCAGGAACCGTAAAAAGGCCGCGTTGCTGGCGTTTTTCCATAGGCTCCGCCCCCCTGACGAGCATCACAAAAA
TCGACGCTCAAGTCAGAGGTGGCGAAACCCGACAGGACTATAAAGATACCAGGCGTTTCCCCCTGGAAGCTCCCTCGTGCGCTCTCCTGT
TCCGACCCTGCCGCTTACCGGATACCTGTCCGCCTTTCTCCCTTCGGGAAGCGTGGCGCTTTCTCATAGCTCACGCTGTAGGTATCTCAGT
TCGGTGTAGGTCGTTCGCTCCAAGCTGGGCTGTGTGCACGAACCCCCCGTTCAGCCCGACCGCTGCGCCTTATCCGGTAACTATCGTCTT
GAGTCCAACCCGGTAAGACACGACTTATCGCCACTGGCAGCAGCCACTGGTAACAGGATTAGCAGAGCGAGGTATGTAGGCGGTGCTA
CAGAGTTCTTGAAGTGGTGGCCTAACTACGGCTACACTAGAAGGACAGTATTTGGTATCTGCGCTCTGCTGAAGCCAGTTACCTTCGGAA
AAAGAGTTGGTAGCTCTTGATCCGGCAAACAAACCACCGCTGGTAGCGGTGGTTTTTTTGTTTGCAAGCAGCAGATTACGCGCAGAAAA
AAAGGATCTCAAGAAGATCCTTTGATCTTTTCTACGGGGTCTGACGCTCAGTGGAACGAAAACTCACGTTAAGGGATTTTGGTCATGAGA
TTATCAAAAAGGATCTTCACCTAGATCCTTTTAAATTAAAAATGAAGTTTTAAATCAATCTAAAGTATATATGAGTAAACTTGGTCTGACA
GTTACCAATGCTTAATCAGTGAGGCACCTATCTCAGCGATCTGTCTATTTCGTTCATCCATAGTTGCCTGACTCCCCGTCGTGTAGATAACT
ACGATACGGGAGGGCTTACCATCTGGCCCCAGTGCTGCAATGATACCGCGAGACCCACGCTCACCGGCTCCAGATTTATCAGCAATAAAC
CAGCCAGCCGGAAGGGCCGAGCGCAGAAGTGGTCCTGCAACTTTATCCGCCTCCATCCAGTCTATTAATTGTTGCCGGGAAGCTAGAGT
AAGTAGTTCGCCAGTTAATAGTTTGCGCAACGTTGTTGCCATTGCTACAGGCATCGTGGTGTCACGCTCGTCGTTTGGTATGGCTTCATTC
AGCTCCGGTTCCCAACGATCAAGGCGAGTTACATGATCCCCCATGTTGTGCAAAAAAGCGGTTAGCTCCTTCGGTCCTCCGATCGTTGTC
AGAAGTAAGTTGGCCGCAGTGTTATCACTCATGGTTATGGCAGCACTGCATAATTCTCTTACTGTCATGCCATCCGTAAGATGCTTTTCTG
TGACTGGTGAGTACTCAACCAAGTCATTCTGAGAATAGTGTATGCGGCGACCGAGTTGCTCTTGCCCGGCGTCAATACGGGATAATACC
GCGCCACATAGCAGAACTTTAAAAGTGCTCATCATTGGAAAACGTTCTTCGGGGCGAAAACTCTCAAGGATCTTACCGCTGTTGAGATCC
AGTTCGATGTAACCCACTCGTGCACCCAACTGATCTTCAGCATCTTTTACTTTCACCAGCGTTTCTGGGTGAGCAAAAACAGGAAGGCAA
AATGCCGCAAAAAAGGGAATAAGGGCGACACGGAAATGTTGAATACTCATACTCTTCCTTTTTCAATATTATTGAAGCATTTATCAGGGT
TATTGTCTCATGAGCGGATACATATTTGAATGTATTTAGAAAAATAAACAAATAGGGGTTCCGCGCACATTTCCCCGAAAAGTGCCACCT
AAATTGTAAGCGTTAATATTTTGTTAAAATTCGCGTTAAATTTTTGTTAAATCAGCTCATTTTTTAACCAATAGGCCGAAATCGGCAAAATC
CCTTATAAATCAAAAGAATAGACCGAGATAGGGTTGAGTGTTGTTCCAGTTTGGAACAAGAGTCCACTATTAAAGAACGTGGACTCCAAC
GTCAAAGGGCGAAAAACCGTCTATCAGGGCGATGGCCCACTACGTGAACCATCACCCTAATCAAGTTTTTTGGGGTCGAGGTGCCGTAA
AGCACTAAATCGGAACCCTAAAGGGAGCCCCCGATTTAGAGCTTGACGGGGAAAGCCGGCGAACGTGGCGAGAAAGGAAGGGAAGAA
AGCGAAAGGAGCGGGCGCTAGGGCGCTGGCAAGTGTAGCGGTCACGCTGCGCGTAACCACCACACCCGCCGCGCTTAATGCGCCGCTA
CAGGGCGCGTCCCATTCGCCATTCAGGCTGCGCAACTGTTGGGAAGGGCGATCGGTGCGGGCCTCTTCGCTATTACGCCAGTCGACCAT
AGCCAATTCAATATGGCGTATATGGACTCATGCCAATTCAATATGGTGGATCTGGACCTGTGCCAATTCAATATGGCGTATATGGACTCG
TGCCAATTCAATATGGTGGATCTGGACCCCAGCCAATTCAATATGGCGGACTTGGCACCATGCCAATTCAATATGGCGGACTTGGCACTG
TGCCAACTGGGGAGGGGTCTACTTGGCACGGTGCCAAGTTTGAGGAGGGGTCTTGGCCCTGTGCCAAGTCCGCCATATTGAATTGGCAT
GGTGCCAATAATGGCGGCCATATTGGCTATATGCCAGGATCAATATATAGGCAATATCCAATATGGCCCTATGCCAATATGGCTATTGGC
CAGGTTCAATACTATGTATTGGCCCTATGCCATATAGTATTCCATATATGGGTTTTCCTATTGACGTAGATAGCCCCTCCCAATGGGCGGT
CCCATATACCATATATGGGGCTTCCTAATACCGCCCATAGCCACTCCCCCATTGACGTCAATGGTCTCTATATATGGTCTTTCCTATTGACG
TCATATGGGCGGTCCTATTGACGTATATGGCGCCTCCCCCATTGACGTCAATTACGGTAAATGGCCCGCCTGGCTCAATGCCCATTGACGT
CAATAGGACCACCCACCATTGACGTCAATGGGATGGCTCATTGCCCATTCATATCCGTTCTCACGCCCCCTATTGACGTCAATGACGGTAA
ATGGCCCACTTGGCAGTACATCAATATCTATTAATAGTAACTTGGCAAGTACATTACTATTGGAAGGACGCCAGGGTACATTGGCAGTAC
TCCCATTGACGTCAATGGCGGTAAATGGCCCGCGATGGCTGCCAAGTACATCCCCATTGACGTCAATGGGGAGGGGCAATGACGCAAAT
GGGCGTTCCATTGACGTAAATGGGCGGTAGGCGTGCCTAATGGGAGGTCTATATAAGCAATGCTCGTTTAGGGAAC

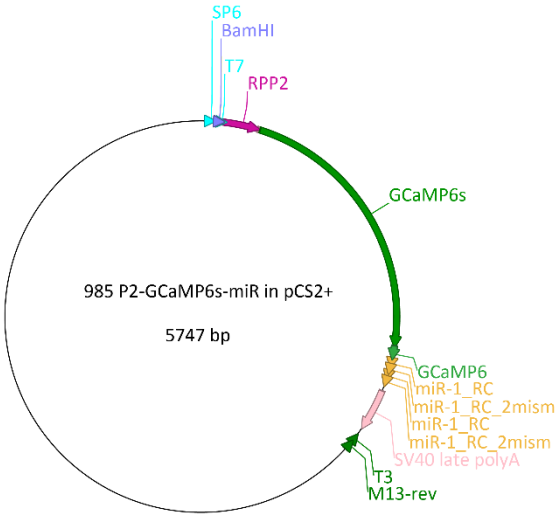


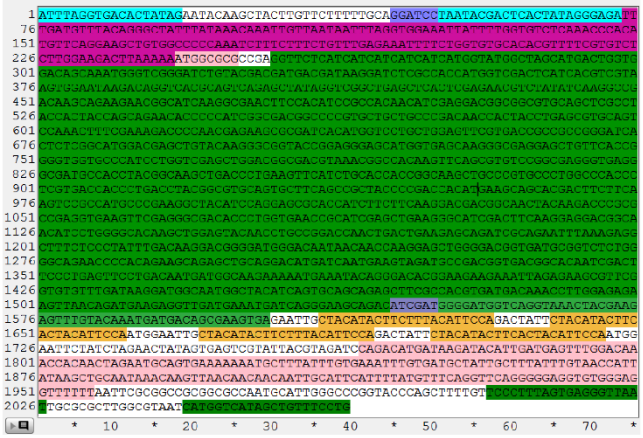


Plasmid #984 full sequence (T7 promoter underlined) :

AGCGGATAACAATTTCACACAGGAAACAGCTATGACCATGATTACGCCAAGCTTGCATGCAGGCCTCTGCAGTCGACGGGCCCGGGATC
CTAATACGACTCACTATAGGGAGATTTGATGTTTACAGGGCTATTTATAAACAAATTGTTAATAATTTAGGTGGAAATTATTTTGGTGTCT
CAAACCCACATGTTCAGGAAGCTGTGGCCCCCAAATCTTTCTTTCTGTTTGAGAAATTTTCTGGTGTGCACACGTTTTCGTGTCTCTTGGAA
GACTTAAAAAATGGCGCGCCGAGGTTCTCATCATCATCATCATCATGGTATGGCTAGCATGACTGGTGGACAGCAAATGGGTCGGGATC
TGTACGACGATGACGATAAGGATCTCGCCACCATGGTCGACTCATCACGTCGTAAGTGGAATAAGACAGGTCACGCAGTCAGAGCTATA
GGTCGGCTGAGCTCACTCGAGAACGTCTATATCAAGGCCGACAAGCAGAAGAACGGCATCAAGGCGAACTTCCACATCCGCCACAACAT

CGAGGACGGCGGCGTGCAGCTCGCCTACCACTACCAGCAGAACACCCCCATCGGCGACGGCCCCGTGCTGCTGCCCGACAACCACTACC
TGAGCGTGCAGTCCAAACTTTCGAAAGACCCCAACGAGAAGCGCGATCACATGGTCCTGCTGGAGTTCGTGACCGCCGCCGGGATCACT
CTCGGCATGGACGAGCTGTACAAGGGCGGTACCGGAGGGAGCATGGTGAGCAAGGGCGAGGAGCTGTTCACCGGGGTGGTGCCCATC
CTGGTCGAGCTGGACGGCGACGTAAACGGCCACAAGTTCAGCGTGTCCGGCGAGGGTGAGGGCGATGCCACCTACGGCAAGCTGACCC
TGAAGTTCATCTGCACCACCGGCAAGCTGCCCGTGCCCTGGCCCACCCTCGTGACCACCCTGACCTACGGCGTGCAGTGCTTCAGCCGCT
ACCCCGACCACATGAAGCAGCACGACTTCTTCAAGTCCGCCATGCCCGAAGGCTACATCCAGGAGCGCACCATCTTCTTCAAGGACGACG
GCAACTACAAGACCCGCGCCGAGGTGAAGTTCGAGGGCGACACCCTGGTGAACCGCATCGAGCTGAAGGGCATCGACTTCAAGGAGGA
CGGCAACATCCTGGGGCACAAGCTGGAGTACAACCTGCCGGACCAACTGACTGAAGAGCAGATCGCAGAATTTAAAGAGGCTTTCTCCC
TATTTGACAAGGACGGGGATGGGACAATAACAACCAAGGAGCTGGGGACGGTGATGCGGTCTCTGGGGCAGAACCCCACAGAAGCAG
AGCTGCAGGACATGATCAATGAAGTAGATGCCGACGGTGACGGCACAATCGACTTCCCTGAGTTCCTGACAATGATGGCAAGAAAAATG
AAATACAGGGACACGGAAGAAGAAATTAGAGAAGCGTTCGGTGTGTTTGATAAGGATGGCAATGGCTACATCAGTGCAGCAGAGCTTC
GCCACGTGATGACAAACCTTGGAGAGAAGTTAACAGATGAAGAGGTTGATGAAATGATCAGGGAAGCAGACATCGATGGGGATGGTC
AGGTAAACTACGAAGAGTTTGTACAAATGATGACAGCGAAGACCGGTTAAAAGAAACACTTTTACAAACATCAGTCTGTAACATCTTTCC
AATAAAAAAAAAACATGTAACTTACTGGTCTGGAGTTGTTTAAGAGAAAATTGGATCTAGATGCATTCGCGAGGTACCGAGCTCGAATTC
ACTGGCCGTCGTTTTACAACGTCGTGACTGGGAAAACCCTGGCGTTACCCAACTTAATCGCCTTGCAGCACATCCCCCTTTCGCCAGCTGG
CGTAATAGCGAAGAGGCCCGCACCGATCGCCCTTCCCAACAGTTGCGCAGCCTGAATGGCGAATGGCGCCTGATGCGGTATTTTCTCCTT
ACGCATCTGTGCGGTATTTCACACCGCATATGGTGCACTCTCAGTACAATCTGCTCTGATGCCGCATAGTTAAGCCAGCCCCGACACCCGC
CAACACCCGCTGACGCGCCCTGACGGGCTTGTCTGCTCCCGGCATCCGCTTACAGACAAGCTGTGACCGTCTCCGGGAGCTGCATGTGTC
AGAGGTTTTCACCGTCATCACCGAAACGCGCGAGACGAAAGGGCCTCGTGATACGCCTATTTTTATAGGTTAATGTCATGATAATAATGG
TTTCTTAGACGTCAGGTGGCACTTTTCGGGGAAATGTGCGCGGAACCCCTATTTGTTTATTTTTCTAAATACATTCAAATATGTATCCGCTC
ATGAGACAATAACCCTGATAAATGCTTCAATAATATTGAAAAAGGAAGAGTATGAGTATTCAACATTTCCGTGTCGCCCTTATTCCCTTTT
TTGCGGCATTTTGCCTTCCTGTTTTTGCTCACCCAGAAACGCTGGTGAAAGTAAAAGATGCTGAAGATCAGTTGGGTGCACGAGTGGGTT
ACATCGAACTGGATCTCAACAGCGGTAAGATCCTTGAGAGTTTTCGCCCCGAAGAACGTTTTCCAATGATGAGCACTTTTAAAGTTCTGCT
ATGTGGCGCGGTATTATCCCGTATTGACGCCGGGCAAGAGCAACTCGGTCGCCGCATACACTATTCTCAGAATGACTTGGTTGAGTACTC
ACCAGTCACAGAAAAGCATCTTACGGATGGCATGACAGTAAGAGAATTATGCAGTGCTGCCATAACCATGAGTGATAACACTGCGGCCA
ACTTACTTCTGACAACGATCGGAGGACCGAAGGAGCTAACCGCTTTTTTGCACAACATGGGGGATCATGTAACTCGCCTTGATCGTTGGG
AACCGGAGCTGAATGAAGCCATACCAAACGACGAGCGTGACACCACGATGCCTGTAGCAATGGCAACAACGTTGCGCAAACTATTAACT
GGCGAACTACTTACTCTAGCTTCCCGGCAACAATTAATAGACTGGATGGAGGCGGATAAAGTTGCAGGACCACTTCTGCGCTCGGCCCTT
CCGGCTGGCTGGTTTATTGCTGATAAATCTGGAGCCGGTGAGCGTGGGTCTCGCGGTATCATTGCAGCACTGGGGCCAGATGGTAAGCC
CTCCCGTATCGTAGTTATCTACACGACGGGGAGTCAGGCAACTATGGATGAACGAAATAGACAGATCGCTGAGATAGGTGCCTCACTGA
TTAAGCATTGGTAACTGTCAGACCAAGTTTACTCATATATACTTTAGATTGATTTAAAACTTCATTTTTAATTTAAAAGGATCTAGGTGAAG
ATCCTTTTTGATAATCTCATGACCAAAATCCCTTAACGTGAGTTTTCGTTCCACTGAGCGTCAGACCCCGTAGAAAAGATCAAAGGATCTT
CTTGAGATCCTTTTTTTCTGCGCGTAATCTGCTGCTTGCAAACAAAAAAACCACCGCTACCAGCGGTGGTTTGTTTGCCGGATCAAGAGCT
ACCAACTCTTTTTCCGAAGGTAACTGGCTTCAGCAGAGCGCAGATACCAAATACTGTTCTTCTAGTGTAGCCGTAGTTAGGCCACCACTTC
AAGAACTCTGTAGCACCGCCTACATACCTCGCTCTGCTAATCCTGTTACCAGTGGCTGCTGCCAGTGGCGATAAGTCGTGTCTTACCGGGT
TGGACTCAAGACGATAGTTACCGGATAAGGCGCAGCGGTCGGGCTGAACGGGGGGTTCGTGCACACAGCCCAGCTTGGAGCGAACGA
CCTACACCGAACTGAGATACCTACAGCGTGAGCTATGAGAAAGCGCCACGCTTCCCGAAGGGAGAAAGGCGGACAGGTATCCGGTAAG
CGGCAGGGTCGGAACAGGAGAGCGCACGAGGGAGCTTCCAGGGGGAAACGCCTGGTATCTTTATAGTCCTGTCGGGTTTCGCCACCTC
TGACTTGAGCGTCGATTTTTGTGATGCTCGTCAGGGGGGCGGAGCCTATGGAAAAACGCCAGCAACGCGGCCTTTTTACGGTTCCTGGC
CTTTTGCTGGCCTTTTGCTCACATGTTCTTTCCTGCGTTATCCCCTGATTCTGTGGATAACCGTATTACCGCCTTTGAGTGAGCTGATACCG
CTCGCCGCAGCCGAACGACCGAGCGCAGCGAGTCAGTGAGCGAGGAAGCGGAAGAGCGCCCAATACGCAAACCGCCTCTCCCCGCGCG
TTGGCCGATTCATTAATGCAGCTGGCACGACAGGTTTCCCGACTGGAAAGCGGGCAGTGAGCGCAACGCAATTAATGTGAGTTAGCTCA
CTCATTAGGCACCCCAGGCTTTACACTTTATGCTTCCGGCTCGTATGTTGTGTGGAATTGTG





Plasmid #985 full sequence (SP6 promoter underlined) :

CGCCATTCTGCCTGGGGACGTCGGAGCAAGCTTGATTTAGGTGACACTATAGAATACAAGCTACTTGTTCTTTTTGCAGGATCCTAATACGACTCACTATAG
GGAGATTTGATGTTTACAGGGCTATTTATAAACAAATTGTTAATAATTTAGGTGGAAATTATTTTGGTGTCTCAAACCCACATGTTCAGGAAGCTGTGGCCC
CCAAATCTTTCTTTCTGTTTGAGAAATTTTCTGGTGTGCACACGTTTTCGTGTCTCTTGGAAGACTTAAAAAATGGCGCGCCGAGGTTCTCATCATCATCATC
ATCATGGTATGGCTAGCATGACTGGTGGACAGCAAATGGGTCGGGATCTGTACGACGATGACGATAAGGATCTCGCCACCATGGTCGACTCATCACGTCG
TAAGTGGAATAAGACAGGTCACGCAGTCAGAGCTATAGGTCGGCTGAGCTCACTCGAGAACGTCTATATCAAGGCCGACAAGCAGAAGAACGGCATCAA
GGCGAACTTCCACATCCGCCACAACATCGAGGACGGCGGCGTGCAGCTCGCCTACCACTACCAGCAGAACACCCCCATCGGCGACGGCCCCGTGCTGCTG
CCCGACAACCACTACCTGAGCGTGCAGTCCAAACTTTCGAAAGACCCCAACGAGAAGCGCGATCACATGGTCCTGCTGGAGTTCGTGACCGCCGCCGGGA
TCACTCTCGGCATGGACGAGCTGTACAAGGGCGGTACCGGAGGGAGCATGGTGAGCAAGGGCGAGGAGCTGTTCACCGGGGTGGTGCCCATCCTGGTC
GAGCTGGACGGCGACGTAAACGGCCACAAGTTCAGCGTGTCCGGCGAGGGTGAGGGCGATGCCACCTACGGCAAGCTGACCCTGAAGTTCATCTGCACC
ACCGGCAAGCTGCCCGTGCCCTGGCCCACCCTCGTGACCACCCTGACCTACGGCGTGCAGTGCTTCAGCCGCTACCCCGACCACATGAAGCAGCACGACTT
CTTCAAGTCCGCCATGCCCGAAGGCTACATCCAGGAGCGCACCATCTTCTTCAAGGACGACGGCAACTACAAGACCCGCGCCGAGGTGAAGTTCGAGGGC
GACACCCTGGTGAACCGCATCGAGCTGAAGGGCATCGACTTCAAGGAGGACGGCAACATCCTGGGGCACAAGCTGGAGTACAACCTGCCGGACCAACTG
ACTGAAGAGCAGATCGCAGAATTTAAAGAGGCTTTCTCCCTATTTGACAAGGACGGGGATGGGACAATAACAACCAAGGAGCTGGGGACGGTGATGCGG
TCTCTGGGGCAGAACCCCACAGAAGCAGAGCTGCAGGACATGATCAATGAAGTAGATGCCGACGGTGACGGCACAATCGACTTCCCTGAGTTCCTGACAA
TGATGGCAAGAAAAATGAAATACAGGGACACGGAAGAAGAAATTAGAGAAGCGTTCGGTGTGTTTGATAAGGATGGCAATGGCTACATCAGTGCAGCAG
AGCTTCGCCACGTGATGACAAACCTTGGAGAGAAGTTAACAGATGAAGAGGTTGATGAAATGATCAGGGAAGCAGACATCGATGGGGATGGTCAGGTAA
ACTACGAAGAGTTTGTACAAATGATGACAGCGAAGTGAGAATTGCTACATACTTCTTTACATTCCAGACTATTCTACATACTTCACTACATTCCAATGGAATT
GCTACATACTTCTTTACATTCCAGACTATTCTACATACTTCACTACATTCCAATGGAATTCTATCTAGAACTATAGTGAGTCGTATTACGTAGATCCAGACATG
ATAAGATACATTGATGAGTTTGGACAAACCACAACTAGAATGCAGTGAAAAAAATGCTTTATTTGTGAAATTTGTGATGCTATTGCTTTATTTGTAACCATT
ATAAGCTGCAATAAACAAGTTAACAACAACAATTGCATTCATTTTATGTTTCAGGTTCAGGGGGAGGTGTGGGAGGTTTTTTAATTCGCGGCCGCGGCGCC
AATGCATTGGGCCCGGTACCCAGCTTTTGTTCCCTTTAGTGAGGGTTAATTGCGCGCTTGGCGTAATCATGGTCATAGCTGTTTCCTGTGTGAAATTGTTATC
CGCTCACAATTCCACACAACATACGAGCCGGAAGCATAAAGTGTAAAGCCTGGGGTGCCTAATGAGTGAGCTAACTCACATTAATTGCGTTGCGCTCACTG
CCCGCTTTCCAGTCGGGAAACCTGTCGTGCCAGCTGCATTAATGAATCGGCCAACGCGCGGGGAGAGGCGGTTTGCGTATTGGGCGCTCTTCCGCTTCCTC
GCTCACTGACTCGCTGCGCTCGGTCGTTCGGCTGCGGCGAGCGGTATCAGCTCACTCAAAGGCGGTAATACGGTTATCCACAGAATCAGGGGATAACGCA
GGAAAGAACATGTGAGCAAAAGGCCAGCAAAAGGCCAGGAACCGTAAAAAGGCCGCGTTGCTGGCGTTTTTCCATAGGCTCCGCCCCCCTGACGAGCATC
ACAAAAATCGACGCTCAAGTCAGAGGTGGCGAAACCCGACAGGACTATAAAGATACCAGGCGTTTCCCCCTGGAAGCTCCCTCGTGCGCTCTCCTGTTCCG
ACCCTGCCGCTTACCGGATACCTGTCCGCCTTTCTCCCTTCGGGAAGCGTGGCGCTTTCTCATAGCTCACGCTGTAGGTATCTCAGTTCGGTGTAGGTCGTTC
GCTCCAAGCTGGGCTGTGTGCACGAACCCCCCGTTCAGCCCGACCGCTGCGCCTTATCCGGTAACTATCGTCTTGAGTCCAACCCGGTAAGACACGACTTAT
CGCCACTGGCAGCAGCCACTGGTAACAGGATTAGCAGAGCGAGGTATGTAGGCGGTGCTACAGAGTTCTTGAAGTGGTGGCCTAACTACGGCTACACTAG
AAGGACAGTATTTGGTATCTGCGCTCTGCTGAAGCCAGTTACCTTCGGAAAAAGAGTTGGTAGCTCTTGATCCGGCAAACAAACCACCGCTGGTAGCGGTG
GTTTTTTTGTTTGCAAGCAGCAGATTACGCGCAGAAAAAAAGGATCTCAAGAAGATCCTTTGATCTTTTCTACGGGGTCTGACGCTCAGTGGAACGAAAAC
TCACGTTAAGGGATTTTGGTCATGAGATTATCAAAAAGGATCTTCACCTAGATCCTTTTAAATTAAAAATGAAGTTTTAAATCAATCTAAAGTATATATGAGT
AAACTTGGTCTGACAGTTACCAATGCTTAATCAGTGAGGCACCTATCTCAGCGATCTGTCTATTTCGTTCATCCATAGTTGCCTGACTCCCCGTCGTGTAGAT
AACTACGATACGGGAGGGCTTACCATCTGGCCCCAGTGCTGCAATGATACCGCGAGACCCACGCTCACCGGCTCCAGATTTATCAGCAATAAACCAGCCAG
CCGGAAGGGCCGAGCGCAGAAGTGGTCCTGCAACTTTATCCGCCTCCATCCAGTCTATTAATTGTTGCCGGGAAGCTAGAGTAAGTAGTTCGCCAGTTAAT
AGTTTGCGCAACGTTGTTGCCATTGCTACAGGCATCGTGGTGTCACGCTCGTCGTTTGGTATGGCTTCATTCAGCTCCGGTTCCCAACGATCAAGGCGAGTT
ACATGATCCCCCATGTTGTGCAAAAAAGCGGTTAGCTCCTTCGGTCCTCCGATCGTTGTCAGAAGTAAGTTGGCCGCAGTGTTATCACTCATGGTTATGGCA
GCACTGCATAATTCTCTTACTGTCATGCCATCCGTAAGATGCTTTTCTGTGACTGGTGAGTACTCAACCAAGTCATTCTGAGAATAGTGTATGCGGCGACCG
AGTTGCTCTTGCCCGGCGTCAATACGGGATAATACCGCGCCACATAGCAGAACTTTAAAAGTGCTCATCATTGGAAAACGTTCTTCGGGGCGAAAACTCTC
AAGGATCTTACCGCTGTTGAGATCCAGTTCGATGTAACCCACTCGTGCACCCAACTGATCTTCAGCATCTTTTACTTTCACCAGCGTTTCTGGGTGAGCAAAA
ACAGGAAGGCAAAATGCCGCAAAAAAGGGAATAAGGGCGACACGGAAATGTTGAATACTCATACTCTTCCTTTTTCAATATTATTGAAGCATTTATCAGGG
TTATTGTCTCATGAGCGGATACATATTTGAATGTATTTAGAAAAATAAACAAATAGGGGTTCCGCGCACATTTCCCCGAAAAGTGCCACCTAAATTGTAAGC
GTTAATATTTTGTTAAAATTCGCGTTAAATTTTTGTTAAATCAGCTCATTTTTTAACCAATAGGCCGAAATCGGCAAAATCCCTTATAAATCAAAAGAATAGA
CCGAGATAGGGTTGAGTGTTGTTCCAGTTTGGAACAAGAGTCCACTATTAAAGAACGTGGACTCCAACGTCAAAGGGCGAAAAACCGTCTATCAGGGCGA
TGGCCCACTACGTGAACCATCACCCTAATCAAGTTTTTTGGGGTCGAGGTGCCGTAAAGCACTAAATCGGAACCCTAAAGGGAGCCCCCGATTTAGAGCTT
GACGGGGAAAGCCGGCGAACGTGGCGAGAAAGGAAGGGAAGAAAGCGAAAGGAGCGGGCGCTAGGGCGCTGGCAAGTGTAGCGGTCACGCTGCGCG
TAACCACCACACCCGCCGCGCTTAATGCGCCGCTACAGGGCGCGTCCCATTCGCCATTCAGGCTGCGCAACTGTTGGGAAGGGCGATCGGTGCGGGCCTC
TTCGCTATTACGCCAGTCGACCATAGCCAATTCAATATGGCGTATATGGACTCATGCCAATTCAATATGGTGGATCTGGACCTGTGCCAATTCAATATGGCG
TATATGGACTCGTGCCAATTCAATATGGTGGATCTGGACCCCAGCCAATTCAATATGGCGGACTTGGCACCATGCCAATTCAATATGGCGGACTTGGCACT
GTGCCAACTGGGGAGGGGTCTACTTGGCACGGTGCCAAGTTTGAGGAGGGGTCTTGGCCCTGTGCCAAGTCCGCCATATTGAATTGGCATGGTGCCAATA
ATGGCGGCCATATTGGCTATATGCCAGGATCAATATATAGGCAATATCCAATATGGCCCTATGCCAATATGGCTATTGGCCAGGTTCAATACTATGTATTGG
CCCTATGCCATATAGTATTCCATATATGGGTTTTCCTATTGACGTAGATAGCCCCTCCCAATGGGCGGTCCCATATACCATATATGGGGCTTCCTAATACCGC
CCATAGCCACTCCCCCATTGACGTCAATGGTCTCTATATATGGTCTTTCCTATTGACGTCATATGGGCGGTCCTATTGACGTATATGGCGCCTCCCCCATTGA
CGTCAATTACGGTAAATGGCCCGCCTGGCTCAATGCCCATTGACGTCAATAGGACCACCCACCATTGACGTCAATGGGATGGCTCATTGCCCATTCATATCC
GTTCTCACGCCCCCTATTGACGTCAATGACGGTAAATGGCCCACTTGGCAGTACATCAATATCTATTAATAGTAACTTGGCAAGTACATTACTATTGGAAGG
ACGCCAGGGTACATTGGCAGTACTCCCATTGACGTCAATGGCGGTAAATGGCCCGCGATGGCTGCCAAGTACATCCCCATTGACGTCAATGGGGAGGGGC
AATGACGCAAATGGGCGTTCCATTGACGTAAATGGGCGGTAGGCGTGCCTAATGGGAGGTCTATATAAGCAATGCTCGTTTAGGGAAC

D. Aladdin pumps hardware-software configuration

Computer-Pumps communication with Windows.

- Download and install Micro Manager 1.4.21
- Copy the *mmgr_dal_Aladdin.dll* driver file in the folder *C:\Program Files\Micro-Manager-1.4*
- Install the pumps as follows :

- Attribute unique network addresses from #0 to #(n-1) to the n pumps. This is done manually in the Setup menu of the pumps, which can be accessed by pressing for 3 seconds on the Diameter/Setup button. Pressing more times browses the menu and eventually displays the pump's address which has to be set (e.g. 'Ad:02' for pump #2). The next property, the baud rate, should be set to 19200 (caution : it is displayed as '1920').
- Connect the following cables :

Between a USB port of the computer and the 'RS-232 To Computer' port of pump #0, a Serial-to-USB converter connected to a GN-PC7 cable (supplied by WPI). It is important to verify if a COM port is correctly created when connecting the converter, and under which number. This can be seen in Control Panel > Device manager, where a new identifier should appear under 'Ports (COM & LPT)', for example 'USB Serial Port (COM3)'. If this is not the case, the computer will not then be able to communicate with the hardware, consequently either another USB port should be used or another Serial-to-USB converter, until a COM port is effectively added. USB 3.0 ports can occasionally create problems.
Between the 'RS-232 To Network' port of pump #0 and the 'RS-232 To Computer' port of pump #1, a GN-NET7 cable (supplied by WPI), and so on for pump #1 and #2, #2 and #3, etc. All n pumps, from #0 to #(n-1), are then connected in series to the computer. Be aware that GN-NET7 cable look exactly like standard 4-pin cables, but of course the company swaps the connections inside to make sure you buy the cables from them.

- Start Micro Manager 1.4.21 and set the hardware configuration.

- Once all pumps are connected, start the software, choose 'none' for Startup configuration, and open the Configuration Wizard (Menu Tool > Hardware Configuration Wizard).
- Select 'Create new configuration', then 'Next'
- In 'Available devices', select 'Aladdin', then 'Aladdin | Aladdin syringe pump' and 'Add…'
- Set 'Port' to the appropriate COM port number (e.g. 'COM3'), and the value of 'PumpNr' to n the number of pumps. Set the COM Port Properties to the following values then click 'OK' :

AnswerTimeOut	:	500.0000
BaudRate	:	19200 (has to match the pumps baud rate)
DelayBetweenCharsMs	:	0.0000
Handshaking	:	Off
Parity	:	None
StopBits	:	1
Verbose	:	1

At this point, the software closing may indicate one of the following improper situations : mismatch between computer baud rate and pump baud rate, pumps not connected, wrong number of pumps connected, incorrect network addresses.

- Click 'Next' for the 4 coming steps while keeping all default values.
- Name the configuration file and click on 'Finish'. The computer is now ready to send instructions to the pumps. The next time Micro Manager is started, simply select this .cfg configuration file as Startup configuration, or load it from Menu Tool > Load Hardware Configuration.

It should be remembered that for each number of pumps used, a new configuration file needs to be created, and the appropriate configuration file needs to be loaded before using controlling the pumps with the computer. Trying to load a configuration with an incorrect number of pumps will simply close the software.

- Design your pumping programs to automatize the experiment.

A pumping program is a set of maximum 41 phases (pump memory limit), each phase being an action like 'Pump 60 µL at 10 µL/min' or 'Pause for 35 seconds' or 'Start a new loop'. For repeated sets of phases, loops can be used. These phases can be entered manually in the pumps, by pressing buttons, but for elaborate programs this is time-consuming and lacks flexibility. It is important to note that programs are always entered phase by phase, thus phases that are unchanged when entering a new program are still active. For example, if a new program consisting of 15 phases is entered while the previous one consisted of 20 phases, the phase 16 of the old program will be executed after phase 15 of the new program is finished. To avoid such undesired events, it is a good practice to end all programs by a stop phase, displayed as 'STOP' on the pump screen :

```
mmc.setProperty("Aladdin","Phase Pump0",15);
mmc.setProperty("Aladdin","Function Pump0","STP");
```

The program content of a pump can be cleared at any time by turning the pump off and keeping the rightmost arrow button pressed while turning the pump back on ; however parameters such as network address and baud rate will also be reset by doing so.

Details on how to use and enter programs are available in the pump documentation.

- Create scripts to send instructions to the pumps.

Micro Manager scripts allow to easily load programs into the pump memory load. It is equivalent to, but much faster than, manually entering the programs.
Typically, a script will be a list of program phases, each of which has a number and a function instructed as follows :

```
mmc.setProperty("Aladdin","Phase Pump0",11);
mmc.setProperty("Aladdin","Function Pump0","LPS");
```

In this example, the 11th program phase of pump #0 is set to "LPS", i.e. a loop start, displayed as 'LP:ST' on the pump screen.
A pumping phase requires additional instructions, for example

```
mmc.setProperty("Aladdin","Phase Pump"+pumpNb,21);
mmc.setProperty("Aladdin","Function Pump"+pumpNb,"RAT");
mmc.setProperty("Aladdin","Rate (uL/min) Pump"+pumpNb,rActive);
mmc.setProperty("Aladdin","Volume (uL) Pump"+pumpNb,1);
mmc.setProperty("Aladdin","Direction Pump"+pumpNb,"Infuse");
```

In this case, the 21st program phase of pump *#pumpNb* is set to "RAT", i.e. a pumping rate, displayed as 'RATE' on the pump screen ; the rate is set to *rActive*, the volume to be dispensed to 1 µL, and the pumping direction to 'Infuse'.
As seen here, parameters such as pump number, phase number, pumping rate, volume, can be set as variables. This facilitates their adjustment at every new program loading.
Additionally, other instructions than program phases can be sent to the pumps. For examples, the syringe diameter can be set using this command :

```
mmc.setProperty("Aladdin","Diameter (mm) Pump0",12);
```

Finally, the pump program can be started by changing the *Run* property from 0 to 1 :

```
mmc.setProperty("Aladdin","Run Pump0",1);
```

Scripts can be created in the Script Panel (Menu Tools > Script Panel). They are written in the Bean Shell language (.bsh files), which is similar to the ImageJ macro language.

Most errors in sending instructions to the pumps will come from sending parameters in a wrong format number ; the instruction is then ignored by the pump.

- a pumping rate or volume has to be a double with maximum 4 digits, possibly with a comma, e.g. '7' or '4000' or '0.25' or '20.53'
- a number of loops has to be a 2-digits integer, e.g. 'LOP25' or 'LOP07'
- a pause duration has to be either an integer smaller than 100, or a 2-digits double with a comma, e.g. 'PAS20' or 'PAS3' or 'PAS0.7'

Any operation on variables may result in numbers with a wrong format, hence to a miscommunication. To avoid this, a formatting function can be applied every time a parameter is calculated from variables :

```
//function to ensure the volumes are sent to the pumps in the right number format.
truncature(number) {
	index = -1;
	if (number >= 10000) {
		index=-3;
	} else if (number >= 1000 && number < 10000) {
		index=1;
	} else if (number >= 100 && number < 1000) {
		index=10;
	} else if (number >= 10 && number < 100) {
		index=100;
	} else if (number >= 0 && number < 10) {
		index=1000;
	} else if (number < 0) {
		index=-2;
	}
	if (index==-1) {
		print("Number not found");
		result = index;
```

```
        } else if (index==-2) {
                print("Negative number");
                result = index;
        } else if (index==-3) {
                print("Number out of range");
                result = index;
        } else {
                result = Math.floor(index*number)/index;
        }
        return (result);
}
```

- Synchronize pumps with each other

By default, the pumps will not receive any external input other than the initial 'Run' instruction from the computer. As pumps will receive this instruction successively, they will start one after the other and accumulate some delay ; this can be easily overcome by entering an appropriate pause as the first phase of each program (all pumps are waiting to start together with the last one). If the programs are simple, this trick may be enough to keep the synchronization of all pumps until the program ends. With more complex programs however, it is likely that regular switches between phases, and pumping rate imprecision over long times, will progressively introduce delays between pumps, which is detrimental in experiments requiring a good temporal precision.

A good solution is to define a 'master' pump (typically pump #0), that will send a synchronization signal to all other 'slave' pumps whenever a new sequence of the program is started. This can be achieved using the TTL ports in the back of the pump. For this, the TTL output pin (#5) of the master pump needs to be connected to the TTL input pin (#4) of each slave pump, as well as all ground pins (#9) with each other. A TTL output from the master pump, unlike instructions from the computer via RS-232 cables, is received at the same time by all slave pumps, and enables synchronization.
The following instruction in the master pump program :

```
mmc.setProperty("Aladdin","Phase Pump0",k);
mmc.setProperty("Aladdin","Function Pump0","OUT0");
```

combined for example with the following instructions in a slave pump program :

```
mmc.setProperty("Aladdin","Phase Pump1",5);
mmc.setProperty("Aladdin","Function Pump1","EVN7");
mmc.setProperty("Aladdin","Phase Pump1",6);
mmc.setProperty("Aladdin","Function Pump1","RAT");
```

will switch the master pump output from 1 to 0 (i.e. a 'falling edge') while the slave pump is performing its pumping phase 6, causing the slave pump to jump to the specified phase, in this case phase 7. The phase 5 is there to specify that phase 6 will be stopped if a TTL input (an 'event trigger') is received before its end, or otherwise executed until its end. In this way, the phase 7 of the slave pump and the phase (k+1) of the master pump will start at the same time.
Before the master pump can send another signal, its output needs to be set back to 1 :

```
mmc.setProperty("Aladdin","Function Pump0","OUT1");
```

which has to take place at least 0.2s after the previous 'OUT0' instruction.
To achieve a perfect initial synchronization between all pumps, the following instructions can be used at the beginning of the programs :
for the master pump,

```
mmc.setProperty("Aladdin","Phase Pump0",1);
mmc.setProperty("Aladdin","Function Pump0","OUT1");
mmc.setProperty("Aladdin","Phase Pump0",2);
mmc.setProperty("Aladdin","Function Pump0","PAS"+tIni);
mmc.setProperty("Aladdin","Phase Pump0",3);
mmc.setProperty("Aladdin","Function Pump0","OUT0");
```

where *tIni* is a number of seconds sufficient for all other pumps to have received their start signal from the computer,
and for all slave pumps,

```
mmc.setProperty("Aladdin","Phase Pump"+pumpNb,1);
mmc.setProperty("Aladdin","Function Pump"+pumpNb,"EVN3");
mmc.setProperty("Aladdin","Phase Pump"+pumpNb,2);
mmc.setProperty("Aladdin","Function Pump"+pumpNb,"PAS"+tIni2);
```

where *+tIni2* is greater than *tIni*. In this way, the slave pumps are waiting for an event trigger, and all pumps jump synchronously to their real first phase : #4 for the master pump, #3 for the slave pumps.

More information about TTL logic can be found in the pump documentation.

E. Operational protocol for master mould fabrication

The following protocol described the steps to be followed to create a two-layers PDMS master mould on silicon wafers, in the clean room available at EMBL Heidelberg, Genome Biology Unit. With some experience, several moulds can be fabricated in parallel. For a one-layer design thinner than 70 µm, two copies of the mould can be fully prepared within 2h15 ; for a multi-layer design with thicker layers, this may take a whole working day.

Turn on hoods, and the four valves for pressurised air and nitrogen. Turn on heating plates, set one at 150°C and the other at 65°C. Turn on the mask aligner (Karl Süss MA45) by pressing 'Power', 'Start'. Turn on the vacuum pumps for the mask aligner and for the spin coater. Turn on the UV lamp by pressing 'Power', and then once 'rdy' (= ready) is displayed by pressing 'Start'. If 'fire' is displayed on the lamp, do not panic, simply nod and smile and wait, this lamp is an old person and therefore not everything it says should be taken seriously. The lamp needs to be turned on in advance to ensure it will be at sufficiently high power for the subsequent UV cross-linking.

Take one or two new silicon wafers, put them on the hot plate at 150°C for 5 minutes to evaporate residual solvents, and turn off the plate right after, so that it cools down to 95°C. Warm wafers can simply be laid on a horizontal lint-free cloth, they cool down rapidly ; never place them directly on a cold surface, this would make them crack.

Spin coating. Turn on the spin coater, protect the inside with aluminium foil to gather residual photoresist during coating. Press 'Programme' to choose the number of steps, press 'F1' to make modifications, use the arrows to choose the values and press 'F1' again to validate the modifications. Press 'Enter'. A coating programme typically comprises :
- 10 s at 500 rpm to grossly spread the resin,
- 40s at the calculated speed (acceleration 408 rpm/s) to obtain the desired coating height.

Position a wafer centred on the spin coater, press 'Vacuum' to hold the wafer. After having verified that the two hot plates are respectively at 65°C and 95°C, slowly pour a few millilitres of the adequate photoresist (I was told the size of a 2-euros coin, but given the price of a bottle it is rather a 20-euros coin) on the centre of the wafer without creating bubbles, and wipe the bottleneck with acetone – especially important for thick photoresists if one wishes to open this expensive bottle again one day. Not centring the resin may result in non-uniform coating. At this step, be aware that despite scientific calculation of the optimal spinning speed from the calibration curves available in the manufacturer's instructions, this old, cheap and often non-horizontal machine is mostly a random generator of coating heights, which will cause you to redo this coating step multiple times, maybe even with decreasing success over time. Close the spin coater's lid, pray and then press 'Run'. After the programme is finished, open the lid and press 'Vacuum' to release the wafer, hold it from its periphery to avoid altering the coating. Without waiting, place the coated wafer (with coating facing up…) on the 65°C plate to start the soft bake, then on the 95°C plate for the required time. The 95°C soft bake is long for thick layers and can be a good opportunity for a lunch break. After the soft bake, place the wafer on a cloth to let it cool down.

UV exposure for cross-linking. The photoresist will now be cross-linked according to the mask design.
Press 'Start' to place the mask aligner in starting position. Take the glass plate out of its case, wipe it with ethanol and a lint-free cloth, fix it on the metallic holder by applying vacuum. Introduce the mask holder in its slot, press the button 'Maskholder' to air-push it inside the slot towards the top. Be careful with the machine, be aware that it is second-hand and dates from soviet times and is no longer maintained by the company who produced it. Place the wafer on its metallic support, and place the mask on the wafer always so that text can be read from above. It is recommended to tape the mask to avoid that it moves while the wafer is introduced in the machine. Set the exposure time with the screwdriver (x 10s or x 1s) and the time knob. Twice the theoretical exposure time is recommended because the UV lamp is old and someone too stingy to replace it, otherwise the photoresist is insufficiently cross-linked and peels off from the wafer later on. Verify that the knob for the maskholder's height is not too high (below 2) otherwise you will break it for the hundredth time and irritate Thomas Heinzman from the workshops who will not organise Oktoberfest, then press on the pedal to introduce the wafer in the machine. Then press exposure and look away, since the UV radiation is strong and harfmul for the eyes. Also warn other people in the room and ask them to look away, not because of you but because of the UV light. At the end of the exposure time, the wafer is released and can be placed on the 65°C plate to start the post-exposure bake, then on the 95°C plate for the required time. The post-exposure bake is shorter than the soft bake, but rather annoying because neither is there enough time to leave the cleanroom and do something, nor is there much to do in this dull and noisy orange room. Feel free to listen to some music, or chat with your colleagues and be friendly with them. If you are alone in the room, make physical exercise, call your colleagues with the room's phone, write nice text messages to your boy/girlfriend, or practice meditation. The post-exposure bake stiffens the cross-linked resin so that it adopts the desired patterns and does not come off during subsequent developing steps. After the post-exposure bake, place the wafer on a cloth to let it cool down.

Development. In a large beaker under the fume hood, immerse the wafer in one centimetre of the adequate developer (mr-Dev600 for SU8 photoresists) and put it to stir. After a few minutes, change the solution and let it stir for 10-20 min depending on the layers height. This operation removes the non-cross-linked photoresist and reveals the mask pattern – this pattern is already visible after the post-exposure bake. Work carefully under the hood to avoid breathing more toxic vapours than needed. Although this will save you a trip to Amsterdam it may as well cause you neurologic lesions and prevent you from achieving one's basic life goals such as buying bread or setting your alarm clock for the next morning. Do not stop the development until all black regions of the mask are mirror-like again. After that, place the wafer on the spin coater and let the machine run at 2500 rpm for 40s to dry it ; this should be stored in a dedicated programme for convenience. If only one layer is needed, turn off the hot plates and the mask aligner (see below) and go to Height measurements.

Additional cycles of coating (optional). For a multiple-layers design, a new cycle of coating, post-exposure bake and development is performed, which requires to align the mask of the next layer to the layer(s) already created. This is the most tricky part of the process and may cause you to prematurely lose your capillary endowment if you do not follow my wise recommendations. Hence, start by taping under the glass plate the mask of the next layer (remove the maskholder by pressing 'maskholder', tape, reintroduce the maskholder and press

'maskholder' again), in a way that it will align as well as possible with the wafer's pattern. Hence, also tape the wafer on its metallic disc support so that it does not move when entering the machine. Once the wafer is in and positioned under the mask and the glass plate (in this order), you will need to align both. For that, look into the two objectives illuminated with dim red light that you set to its maximum intensity. You will see nothing and it is normal because I told you that the machine is old and cheap. Nevertheless, make sure you do see something, which allows you to visualise the alignment marks. At this point, if you do not know what alignment marks are, or if you forgot to include them in your mask design, go home and meet some friends to avoid wasting the rest of your day. However, if you are lucky and your design includes long linear channels you can still manage to align. Regarding alignment marks, crosses in the corner as is sometimes done is useless, draw rather a rectangular shape around your chip designs, that is not too big to still fit at least partly on the wafer. These perpendicular lines will save your life and are the easiest way to achieve rapid alignment of two layers ; they should be identical on all masks for a given design. You will use alternately one line and a line perpendicular to it, to achieve the best alignment. So, look through the mask's transparent areas with the mediocre red lights to bring one of these lines of the wafer close to its corresponding line on the mask. To do this, release the wafer by pressing 'Maskholder' and use the three grey alignment knobs located close to the mask holder : two are for translation in x and y directions and one is for rotation in a limited range. Always set the rotation first then the translation, never the opposite. If you are not sure why, review your geometry class from high school. Alternatively, try the second method first and struggle for hours, then try the first one and succeed rapidly, and you will remember. So, use the rotation knob to bring two long lines of the mask and the wafer as parallel from each other as possible. The longer the easier, that is why small fancy crosses in the corners are useless. After each movement, you need to put the wafer up again by pressing 'Maskholder' to look at it, then down again to adjust it. Once this is done, it will be easy to set the translations, maybe you need to refine the rotation once or twice not more, that's it you are done and you can sigh in satisfaction ; also feel free to spread this alignment technique around you because I saw so many people struggling for nothing and swearing against this poor soviet-old unmaintained mask aligner. You can then proceed with exposure, remember to look away, and with post-exposure, development and drying. You may be reckless and enthusiastic and carry on with more layers in your design, in which case you will repeat this whole cycle for every new layer, but you will probably stop at two layers. After your last exposure, remove the metallic maskholder, release the vacuum to remove the glass plate, wipe it with ethanol and a lint-free cloth and put it back in its case. Turn off the mask aligner by pressing 'Power' to prolong its lifetime, turn off the UV lamp but do not close the nitrogen valve : the lamp needs it to cool down in the same way as some elderly people need their oxygen mask to sleep, and you will close it at the very end when you leave the room. If you release the vacuum before removing the mask holder from the machine, the plate will fall inside the machine in a frighteningly alarming noise that should cause you to never do that again, and you may struggle to remove it – I tried already. If the evil eye is on you on that day, you might even break the plate and have to replace it ; in that case, Saint Leo, patron of the mechanical workshops, will be your ally. Once you are done with the last post-exposure bake turn off the hot plates, as it is warm enough in this damn cleanroom. During final development, check on the little microscope that your finest mould structures are effectively developed, repeat immersion in the developer as long as needed.

Hard bake (optional). This steps prolongs the lifetime of your master mould but you can also omit it if you had a hard enough day already ; if you're not in a hurry to leave work and have a social life, do it, or maybe better do it overnight and finish the next day. Place the wafer on a plate at room temperature – do not place it on a plate that is still hot otherwise the coating might crack and you would have lost one day of work, that's why I told you to turn off the plates as soon as you were done with them. Set the plate for 5-10 min at 50°C, then 5-10 min at 100°C, then 5-10 min at 150°C, then turn it off and let everything cool down to room temperature, which takes like 45-60 min. After that are still more steps to perform.

Layer's height measurement. On the computer, turn on the Surface Profiler (Profilometer, Faulhaber) and launch the software Dektak 32. Wait. Place your wafer under the measuring device, click on 'Tower Down to null position' and let the stylus slowly come down and touch the wafer. Be very careful to never touch the device's stylus with any object otherwise you will break it or bend it and the device will have to be repaired. Never move the wafer while the stylus is in contact with it. Then, click on 'Window' > 'Sample positioning' (or press Ctrl + 3), and 'Run currently active scan routine' (or press F4). The device measures a height inferior to 110 µm along a line of fixed length. Once you are used to it, it will take you one minute per measurement. At this point you may appreciate how admirably the spin coater has produced a non-uniform coating. If knowing the precise height (not achieving a precise height – forget that) is important for your experiments, you may measure your heights of interest for every chip design replicate and write these down behind the wafer at the corresponding positions.

PDMS embedding. After all measurements are done, the wafer needs to be embedded in PDMS. Note that measurements are much harder to perform once your micrometric channel patterns lie under one centimetre of polymerised silicone. It is possible to cut and rip off all the polymerised PDMS to free the master mould and measure it again but you may easily break it while doing so as it is as fragile as your grandmother's femoral head, so check before you embed and write the measurements on the back of the wafer, not on some flying piece of paper that you will lose. 72g of PDMS mixed with 8g of curing agent are enough to fill a large square Petri dish. After degasing in a vacuum dessicator, pour a bit of this mixture in a square Petri dish (to avoid trapping air below the wafer), place the wafer on top, and pour gently the rest of the mixture on top to avoid air bubbles at the wafer surface. Then, degas the fluid PDMS until no more air bubbles are seen and put the dish horizontally and overnight in a 65°C incubator. The process of master mould fabrication is over, congratulations if ever you have reached that point on your first day of trying, that's it and you have now benefited from my main tricks and avoided many of my mistakes. Remember to turn off the nitrogen valve when you leave the room, and to thoroughly clean the spin coater with acetone except on its central black seal.

First PDMS preparation. On the next day, you can produce your first PDMS devices from the mould, this is when you will verify whether your design was meaningful and sometimes you will cry while remembering the useless hours of your life spent in this orange noisy toxic room, but it was not useless you have been practicing and improving. After cutting off a full block of PDMS, a 27g+3g mixture should be enough to re-fill it in preparation for the next chips. When establishing a new design, I recommend including several versions of it on the same mask instead of making one mask thus one mould per version – notably to fine tune a given channel width. Remember : any variation on height can be done while fabricating the mould by spinning at different speeds (and praying), any variation that does not concern height depends on the mask thus it may take until the next round of masks are ordered by the Merten lab to try it, i.e. several weeks. Keep good track of what your different mould versions are to avoid having to re-do them – especially if by chance you had eventually reached the desired height with the spin coating.

F. Additional calcium activity traces

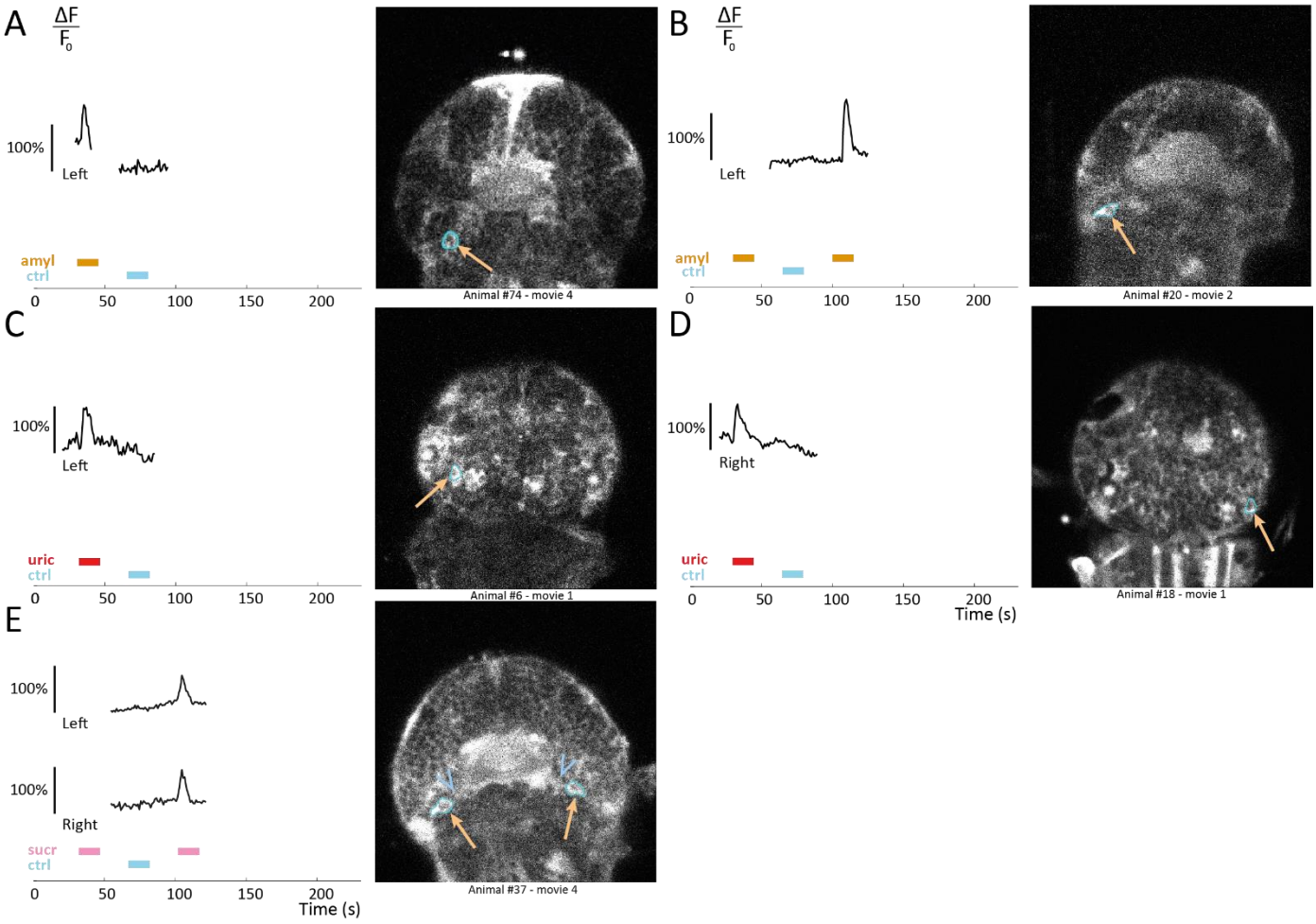


Figure VII-2 Additional activity traces of individual cells around the nuchal cavities.

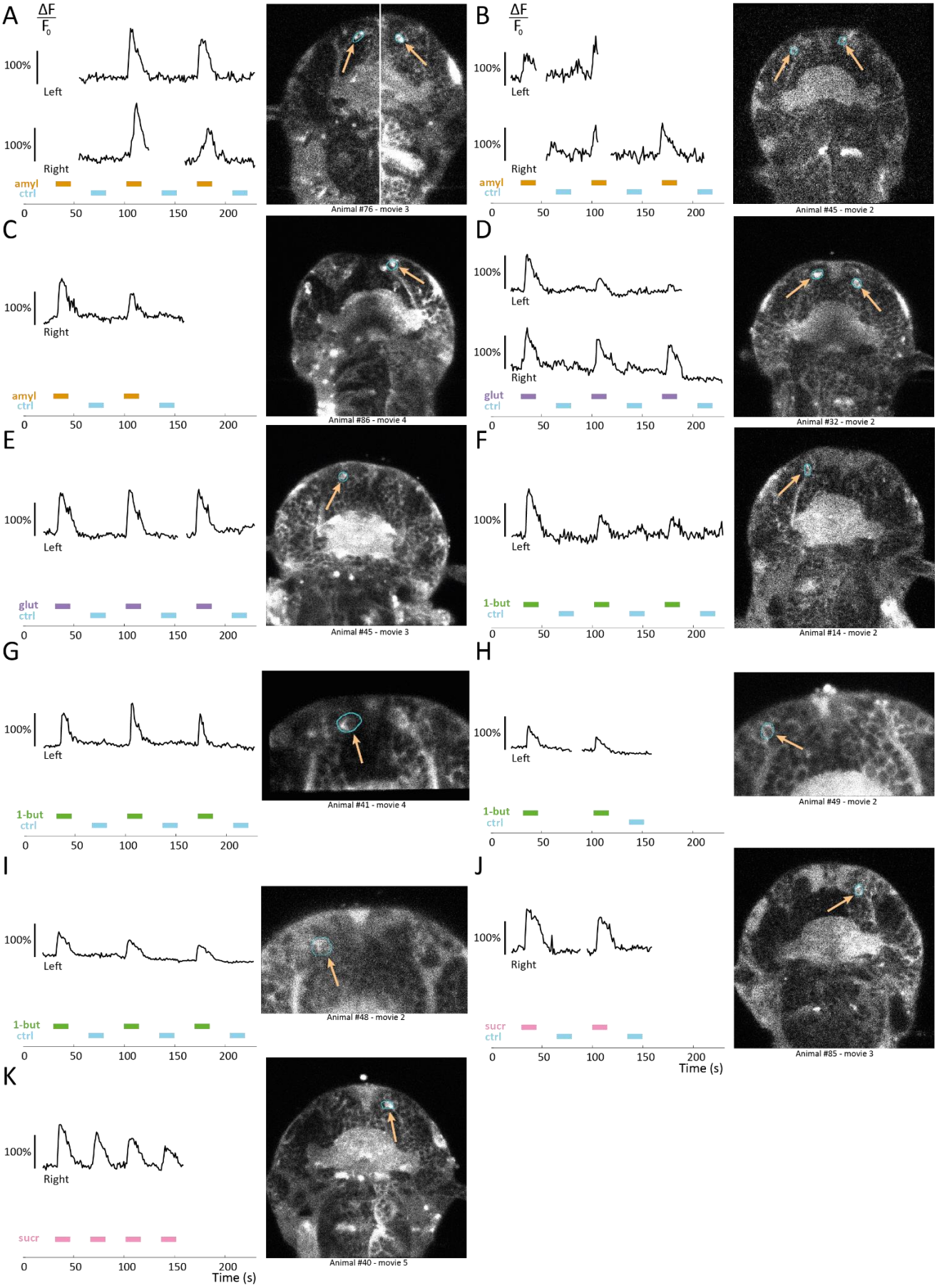


Figure VII-3 Additional activity traces of individual cells in the antennal ganglia.

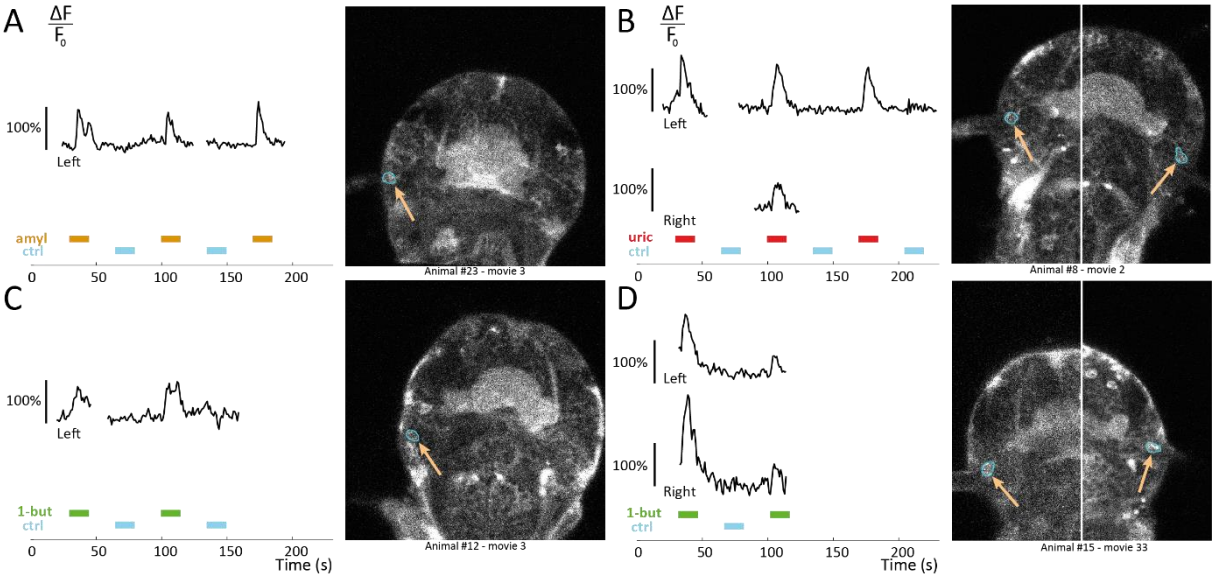


Figure VII-4 Activity traces of potential individual cells in the cirral ganglia.

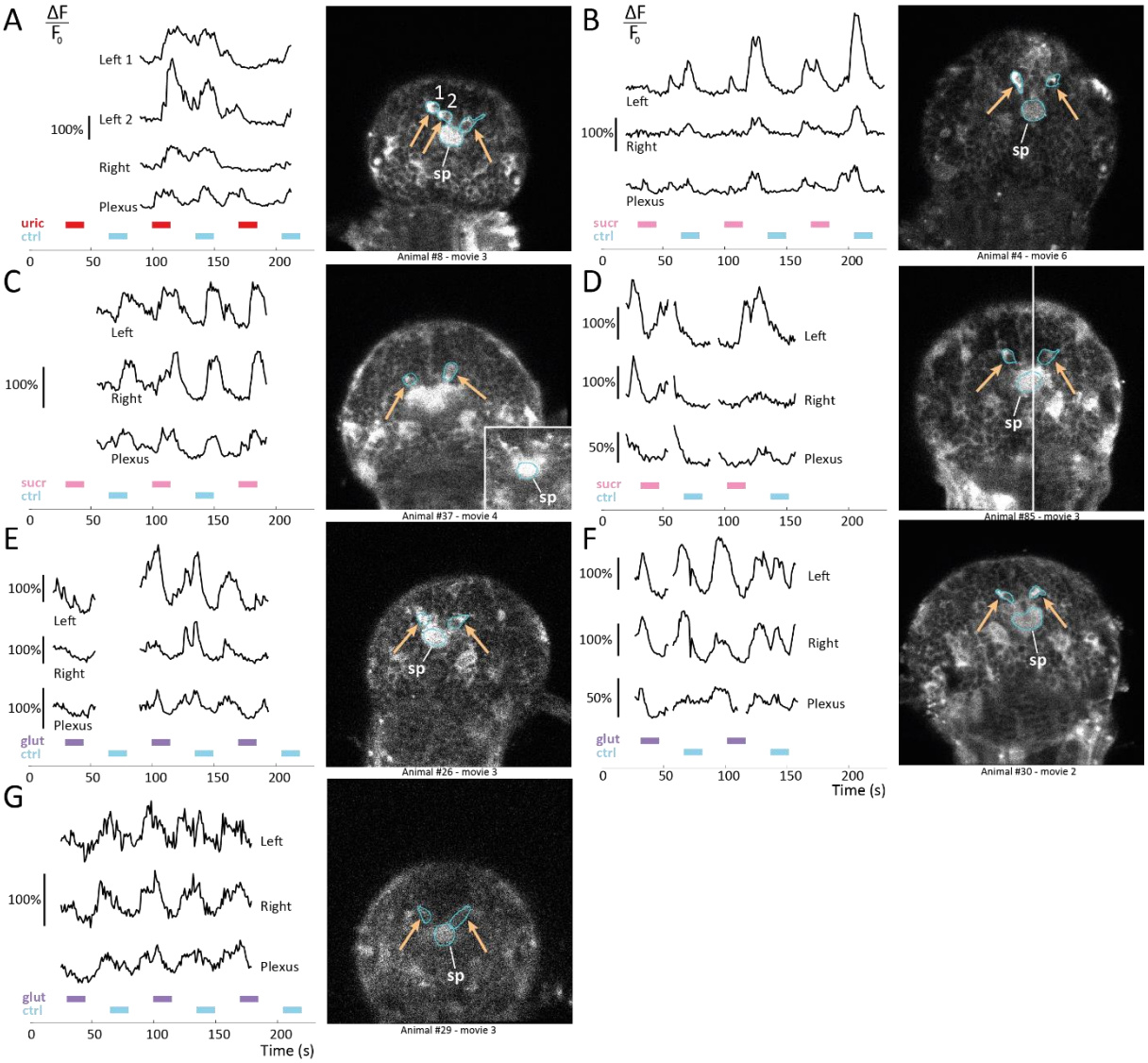


Figure VII-5 Additional activity traces of individual flask cells and neurosecretory plexus, in the apical organ region.

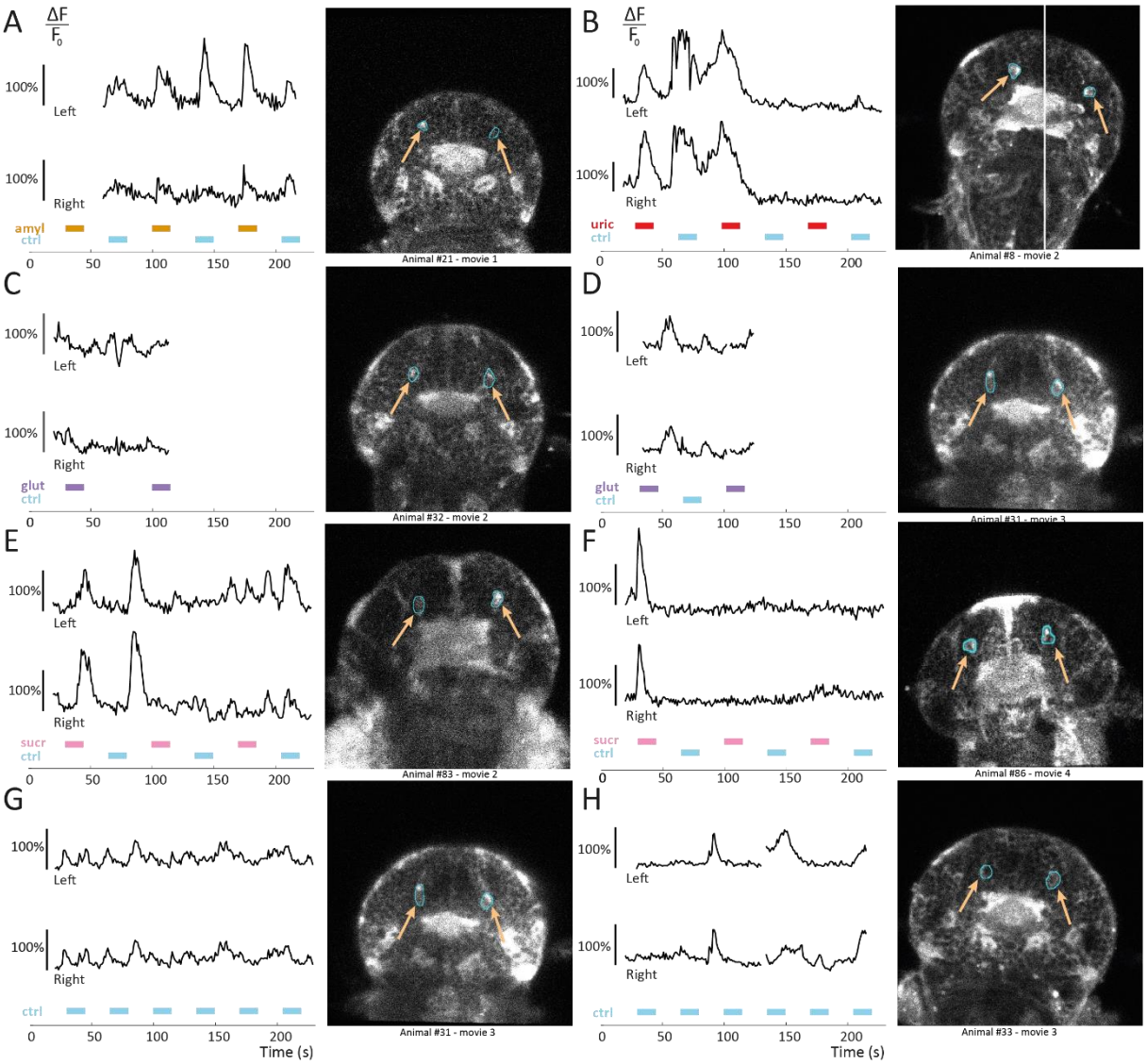


Figure VII-6 Additional activity traces of the paired median cells.

References

[1] M. I. Simon, A. Krikos, N. Mutoh, and A. Boyd, "Sensory Transduction in Bacteria," *Current Topics in Membranes and Transport*, vol. 23. pp. 3–16, 1985.

[2] J. T. Bonner and L. J. Savage, "Evidence for the formation of cell aggregates by chemotaxis in the development of the slime mold Dictyostelium discoideum," *Journal of Experimental Zoology Part A: Ecological Genetics and Physiology*, vol. 106, no. 1. pp. 1–26, Oct-1947.

[3] C. Zipfel, "Plant pattern-recognition receptors," *Trends in Immunology*, vol. 35, no. 7. pp. 345–351, Jul-2014.

[4] A. O. D. Willows, "Physiology of feeding in Tritonia I. behavior and mechanics," *Marine Behaviour and Physiology*, vol. 5, no. 2. pp. 115–135, 1978.

[5] K.-E. Kaissling, "Insect Olfaction," in *Handbook of Sensory physiology pp. 351-431*, vol. 4 / 1, Springer, Berlin Heidelberg, 1971.

[6] S. Hayden, M. Bekaert, T. A. Crider, S. Mariani, W. J. Murphy, and E. C. Teeling, "Ecological adaptation determines functional mammalian olfactory subgenomes," *Genome research*, vol. 20. pp. 1–9, 2010.

[7] T. J. Hara, "Olfaction and gustation in fish: an overview," *Acta Physiologica*, vol. 152, no. 2. pp. 207–217, Oct-1994.

[8] B. S. Hansson and M. C. Stensmyr, "Evolution of Insect Olfaction," *Neuron*, vol. 72, pp. 698–711, Dec. 2011.

[9] R. Benton, "Chemical sensing in Drosophila," *Curr. Opin. Neurobiol.*, vol. 18, pp. 357–363, Aug. 2008.

[10] T. E. Audesirk, "Chemoreception in Aplysia californica. I. behavioral localization of distance chemoreceptors used in food-finding," *Behavioral Biology*, vol. 15, no. 1. Sep-1975.

[11] C. D. Derby and P. W. Sorensen, "Neural Processing, Perception, and Behavioral Responses to Natural Chemical Stimuli by Fish and Crustaceans," *J. Chem. Ecol.*, vol. 34, pp. 898–914, Jun. 2008.

[12] J.-P. Rospars, P. Lansky, M. Chaput, and P. Duchamp-Viret, "Competitive and Noncompetitive Odorant Interactions in the Early Neural Coding of Odorant Mixtures," *J. Neurosci.*, vol. 28, pp. 2659–2666, Mar. 2008.

[13] N. Deisig, M. Giurfa, H. Lachnit, and J.-C. Sandoz, "Neural representation of olfactory mixtures in the honeybee antennal lobe," *Eur. J. Neurosci.*, vol. 24, pp. 1161–1174, Aug. 2006.

[14] M. S. Savoca and G. A. Nevitt, "Evidence that dimethyl sulfide facilitates a tritrophic mutualism between marine primary producers and top predators," *Proc. Natl. Acad. Sci.*, vol. 111, pp. 4157–4161, Mar. 2014.

[15] M. A. Willis, J. Murlis, and R. T. Cardé, "Pheromone-mediated upwind flight of male gypsy moths, Lymantria dispar, in a forest," *Physiological Entomology*, vol. 16, no. 4. pp. 507–215, Dec-1991.

[16] M. J. Weissburg and R. K. Zimmer-Faust, "Odor plumes and how blue crabs use them in finding prey," *Journal of Experimental Biology*, vol. 197. pp. 349–375, 1994.

[17] M. J. Weissburg, "Waterborne Chemical Communication: Stimulus Dispersal Dynamics and Orientation Strategies in Crustaceans," in *Breithaupt T., Thiel M. (eds) Chemical Communication in Crustaceans, pp. 63-83*, Springer, New York, NY, 2010.

[18] G. Laurent, "Olfactory network dynamics and the coding of multidimensional signals," *Nat. Rev. Neurosci.*, vol. 3, pp. 884–895, Nov. 2002.

[19] J. M. Gray *et al.*, "Oxygen sensation and social feeding mediated by a C. elegans guanylate cyclase homologue," *Nature*, vol. 430. pp. 317–322, 15-Jul-2004.

[20] J. W. Petranka, L. B. Kats, and A. Sih, "Predator-prey interactions among fish and larval amphibians: use of chemical cues to detect predatory fish," *Animal Behaviour*, vol. 35, no. 2. pp. 420–425, 02-Apr-1987.

[21] C. Melcher, R. Bader, and M. J. Pankratz, "Amino acids, taste circuits, and feeding behavior in Drosophila: towards understanding the psychology of feeding in flies and man," *Journal of Endocrinology*, vol. 192. pp. 467–472, 01-Mar-2007.

[22] R. K. Zimmer and C. A. Butman, "Chemical signaling processes in the marine environment," *The Biological Bulletin*, vol. 198. pp. 168–187, Apr-2000.

[23] L. Kornreich and A. L. Kleinhaus, "Postingestive Chemosensation and Feeding by Leeches," *Physiology & Behavior*, vol. 67, no. 5. pp. 635–341, 00-Nov-1999.

[24] E. E. Little, "Conditioned Aversion to Amino Acid Flavors in the Catfish, Ictalurus Punctatus," *Physiology & Behavior*, vol. 19. pp. 743–747, 1977.

[25] R. H. Porter and J. M. Cernoch, "Maternal recognition of neonates through olfactory cues," *Physiology & Behavior*, vol. 30, no. 1. pp. 151–154, Jan-1983.

[26] E. E. Little, "Chemical communication in maternal behaviour of crayfish," *Nature*, vol. 255. pp. 400–401, 29-May-1975.

[27] S. Shabani, M. Kamio, and C. D. Derby, "Spiny lobsters use urine-borne olfactory signaling and physical aggressive behaviors to influence social status of conspecifics," *J. Exp. Biol.*, vol. 212, pp. 2464–2474, Jul. 2009.

[28] J. H. Borden, L. Chong, J. A. McLean, K. N. Slessor, and K. Mori, "Gnathotrichus sulcatus: synergistic response to enantiomers of the aggregation pheromone sulcatol," *Science*, vol. 192, no. 4242. pp. 894–896, 28-May-1976.

[29] K. Jaffe and H. Puche, "Colony-specific territorial marking with the metapleural gland secretion in the ant Solenopsis geminata (Fabr)," *Journal of Insect Physiology*, vol. 30, no. 4. pp. 265–270, 1984.

[30] F. Rosell and L. J. Sundsdal, "Odorant source used in Eurasian beaver territory marking," *Journal of Chemical Ecology*, vol. 27, no. 12. pp. 2471–2491, Dec-2001.

[31] R. J. Beynon and J. L. Hurst, "Urinary proteins and the modulation of chemical scents in mice and rats," *Peptides*, vol. 25, no. 9. pp. 1553–1563, Sep-2004.

[32] R. T. Cardé and A. K. Minks, "Control of moth pests by mating disruption: Successes and Constraints," *Annual Review of Entomology*, vol. 40. pp. 559–585, 1995.

[33] E. Zeeck *et al.*, "Cysteine-glutathione disulfide, the sperm-release pheromone of the marine polychaete Nereis succinea (Annelida: Polychaeta).," *Chemoecology*, vol. 8, no. 1. pp. 33–38, Apr-1998.

[34] "Kin recognition pheromones in social wasps: combining chemical and behavioural evidence," *Animal Behaviour*, vol. 51, no. 3. pp. 625–629, Mar-1996.

[35] T. P. Quinn and C. A. Busack, "Chemosensory recognition of siblings in juvenile coho salmon (Oncorhynchus kisutch)," *Animal Behaviour*, vol. 33, no. 1. pp. 51–56, Feb-1985.

[36] U. B. Kaupp, "Olfactory signalling in vertebrates and insects: differences and commonalities," *Nat. Rev. Neurosci.*, Feb. 2010.

[37] H. Yamasaki, Y. Kubota, H. Takagi, and M. Tohyama, "Immunoelectron-microscopic study on the fine structure of substance-P-containing fibers in the taste buds of the rat," *Journal of Comparative Neurology*, vol. 227, no. 3. pp. 380–392, 10-Aug-1984.

[38] J. Adler, "Chemotaxis in Bacteria," *Science*, vol. 153, no. 3737. pp. 708–716, 12-Aug-1966.

[39] T. P. Henkel and J. R. Pawlik, "Host specialization of an obligate sponge-dwelling brittlestar," *Aquat. Biol.*, vol. 12, pp. 37–46, Mar. 2011.

[40] Y.-J. Huang *et al.*, "Mouse Taste Buds Use Serotonin as a Neurotransmitter," *Journal of Neuroscience*, vol. 25, no. 4. pp. 843–847, 26-Jan-2005.

[41] L. Buck and R. A. Axel, "A novel multigene family may encode odorant receptors: a molecular basis for odor recognition," *Cell*, vol. 65. pp. 175–187, 05-Apr-1991.

[42] R. Benton, S. Sachse, S. W. Michnick, and L. B. Vosshall, "Atypical Membrane Topology and Heteromeric Function of Drosophila Odorant Receptors In Vivo," *PLoS Biology*. 17-Jan-2006.

[43] R. Benton, K. S. Vannice, C. Gomez-Diaz, and L. B. Vosshall, "Variant Ionotropic Glutamate Receptors as Chemosensory Receptors in Drosophila," *Cell*, vol. 136, pp. 149–162, Jan. 2009.

[44] A. F. Silbering and R. Benton, "Ionotropic and metabotropic mechanisms in chemoreception: 'chance or design'?," *EMBO reports*, vol. 11, pp. 173–179, Jan. 2010.

[45] E. M. Neuhaus, G. Gisselmann, W. Zhang, R. Dooley, K. Störtkuhl, and H. Hatt, "Odorant receptor heterodimerization in the olfactory system of Drosophila melanogaster," *Nat. Neurosci.*, vol. 8, pp. 15–17, Dec. 2004.

[46] J. Vidic *et al.*, "On a chip demonstration of a functional role for odorant binding protein in the preservation of olfactory receptor activity at high odorant concentration," *Lab Chip*, vol. 8, p. 678, 2008.

[47] C. D. Derby, M. T. Kozma, A. Senatore, and M. Schmidt, "Molecular Mechanisms of Reception and Perireception in Crustacean Chemoreception: A Comparative Review," *Chem. Senses*, vol. 41, pp. 381–398, Apr. 2016.

[48] C. I. Bargmann, "Comparative chemosensation from receptors to ecology," *Nature*, vol. 444, pp. 295–301, Nov. 2006.

[49] S. M. Helluy, M. L. Ruchhoeft, and B. S. Beltz, "Development of the olfactory and accessory lobes in the American lobster: an allometric analysis and its implications for the deutocerebral structure of decapods," *Journal of Comparative Neurology*, vol. 357, no. 3. pp. 433–445, 1995.

[50] H. L. Eishten, "Why are olfactory systems of different animals so similar ?," *Brain, Behavior and Evolution*, vol. 59. pp. 273–293, 2002.

[51] K. J. Ressler, S. L. Sullivan, and L. B. Buck, "Information coding in the olfactory system: evidence for a stereotyped and highly organized epitope map in the olfactory bulb," *Cell*, vol. 79, no. 7. pp. 1245–1255, 1994.

[52] L. B. Vosshall, A. M. Wong, and R. Axel, "An olfactory sensory map in the fly brain," *Cell*, vol. 102, no. 2. pp. 147–159, 2000.

[53] M. N. Vorontsova, L. P. Nezlin, and I. A. Meinertzhagen, "Nervous system of the larva of the ascidian Molgula citrina (Alder and Hancock, 1848)," *Acta Zoologica*, vol. 78, no. 3. pp. 177–185, 1997.

[54] Q. Bone, "The central nervous system in amphioxus," *Journal of Comparative Neurology*, vol. 115, no. 1. pp. 27–64, 1960.

[55] N. J. Strausfeld and J. G. Hildebrand, "Olfactory systems: common design, uncommon origins?. Current opinion in neurobiology," *Cell*, vol. 9, no. 5. pp. 634–639, 1999.

[56] D. Arendt, "The evolution of cell types in animals: emerging principles from molecular studies," *Nat. Rev. Genet.*, vol. 9, pp. 868–882, Nov. 2008.

[57] M. Nei, Y. Niimura, and M. Nozawa, "The evolution of animal chemosensory receptor gene repertoires: roles of chance and necessity," *Nat. Rev. Genet.*, vol. 9, pp. 951–963, Dec. 2008.

[58] X. Zhang and S. Firestein, "The olfactory receptor gene superfamily of the mouse," *Nature Neuroscience*, vol. 5. pp. 124–133, 22-Jan-2002.

[59] R. Tomer, A. S. Denes, K. Tessmar-Raible, and D. Arendt, "Profiling by Image Registration Reveals Common Origin of Annelid Mushroom Bodies and Vertebrate Pallium," *Cell*, vol. 142, pp. 800–809, Sep. 2010.

[60] S. M. Farris and N. S. Roberts, "Coevolution of generalist feeding ecologies and gyrencephalic mushroom bodies in insects," *Proceedings of the National Academy of Sciences*, vol. 102. pp. 17394–17399, 2005.

[61] C. Nielsen, "Animal Evolution, interrelationships of the Living Phyla." Oxford University Press Inc., New York, 2012.

[62] H. M. Robertson and K. W. Wanner, "The chemoreceptor superfamily in the honey bee, Apis mellifera: Expansion of the odorant, but not gustatory, receptor family," *Genome Research*, vol. 16. pp. 1395–1403, 2006.

[63] D. C. Peñalva-Arana, M. Lynch, and H. M. Robertson, "The chemoreceptor genes of the waterflea Daphnia pulex: many Grs but no Ors," *BMC Evol. Biol.*, vol. 9, p. 79, 2009.

[64] M. Spehr and S. D. Munger, “Olfactory receptors: G protein-coupled receptors and beyond,” *J. Neurochem.*, vol. 109, pp. 1570–1583, Jun. 2009.
[65] C. Hauenschild and A. Fischer, *Mikroskopische Anatomie, Fortpflanzung, Entwicklung von Platynereis dumerilii.*, vol. Großes Zoologisches Praktikum, Heft 10b. Gustav Fischer, Stuttgart, 1969.
[66] F. Raible *et al.*, “Vertebrate-type intron-rich genes in the marine annelid Platynereis dumerilii.,” *Science*, vol. 310, no. 5752. pp. 1325–1326, 2005.
[67] D. Arendt, K. Tessmar-Raible, H. Snyman, A. W. Dorresteijn, and J. Wittbrodt, “Ciliary Photoreceptors with aVertebrate-Type Opsin inan Invertebrate Brain,” *Science*, vol. 306, no. 5697. pp. 869–871, 29-Oct-2004.
[68] K. Tessmar-Raible *et al.*, “Conserved Sensory-Neurosecretory Cell Types in Annelid and Fish Forebrain: Insights into Hypothalamus Evolution,” *Cell*, vol. 129, pp. 1389–1400, Jun. 2007.
[69] A. S. Denes *et al.*, “Molecular Architecture of Annelid Nerve Cord Supports Common Origin of Nervous System Centralization in Bilateria,” *Cell*, vol. 129, pp. 277–288, Apr. 2007.
[70] M. A. Tosches, D. Bucher, P. Vopalensky, and D. Arendt, “Melatonin Signaling Controls Circadian Swimming Behavior in Marine Zooplankton,” *Cell*, vol. 159, pp. 46–57, Sep. 2014.
[71] P. R. H. Steinmetz, R. P. Kostyuchenko, A. Fischer, and D. Arendt, “The segmental pattern of otx, gbx, and Hox genes in the annelid Platynereis dumerilii,” *Evol. & Dev.*, vol. 13, pp. 72–79, Jan. 2011.
[72] A. Lauri *et al.*, “Development of the annelid axochord: insights into notochord evolution,” *Science*, vol. 345, no. 6202. pp. 1365–1368, 2014.
[73] H. M. Vergara *et al.*, “Whole-organism cellular gene-expression atlas reveals conserved cell types in the ventral nerve cord of Platynereis dumerilii,” *Proc. Natl. Acad. Sci.*, vol. 114, pp. 5878–5885, Jun. 2017.
[74] N. Randel, R. Shahidi, C. Verasztó, L. A. Bezares-Calderón, S. Schmidt, and G. Jékely, “Inter-individual stereotypy of thePlatynereislarval visual connectome,” *eLife*, vol. 4, Jun. 2015.
[75] M. Conzelmann *et al.*, “Conserved MIP receptor-ligand pair regulates Platynereis larval settlement,” *Proc. Natl. Acad. Sci.*, vol. 110, pp. 8224–8229, Apr. 2013.
[76] M. Gühmann *et al.*, “Spectral Tuning of Phototaxis by a Go-Opsin in the Rhabdomeric Eyes of Platynereis,” *Curr. Biol.*, vol. 25, pp. 2265–2271, Aug. 2015.
[77] B. Backfisch *et al.*, “Stable transgenesis in the marine annelid Platynereis dumerilii sheds new light on photoreceptor evolution,” *Proc. Natl. Acad. Sci.*, vol. 110, pp. 193–198, Jan. 2013.
[78] K. Achim *et al.*, “High-throughput spatial mapping of single-cell RNA-seq data to tissue of origin,” *Nature biotechnology*, vol. 33, no. 6. pp. 503–509, 13-Apr-2015.
[79] M. Conzelmann and G. Jékely, “Antibodies against conserved amidatedneuropeptide epitopes enrich the comparative neurobiology toolbox,” *EvoDevo*, vol. 3, no. 23. 01-Oct-2012.
[80] H. Martinez Vergara *et al.*, “A whole-organism cellular gene expression atlas reveals conserved cell type clusters in the ventral nerve cord of Platynereis dumerilii.” 2017.
[81] N. Randel *et al.*, “Neuronal connectome of a sensory-motorcircuit for visual navigation,” *eLife*, vol. 3. eLife Sciences Organisation, Ltd., 27-May-2014.
[82] C. Verasztó *et al.*, “Ciliomotor circuitry underlying whole-body coordination of ciliary activity in the Platynereis larva,” *eLife*, vol. 6, no. e26000. 2017.
[83] A. de Quatrefages, “Etudes sur les types inférieurs de l’embranchement des Annelés,” *Annales de Sciences Naturelles, Série 3, Zoologie*, vol. 14. pp. 281–289.
[84] E. Ehlers, *Die Borstenwürmer (Annelida chaetopoda) nach systematischen und anatomischen Untersuchungen dargestellt.*, vol. XX + 748. Engelmann, Leipzig.
[85] P. Langerhans, “Die Wurmfauna Madeiras. II.,” *Zeitschrift für wissenschaftliche Zoologie*, vol. 33. pp. 271–316, 1880.
[86] B. Friedländer, “Beiträge zur Kenntnis des Centralnervensystems von Lumbricus,” *Zeitschrift für wissenschafliche Zoologie*, vol. 47. pp. 47–84, 1888.
[87] M. von Lenhossék, “Ursprung, Verlauf unf Endigung der sensiblen Nervenfasern bei Lumbricus,” *Archive für mikroskopische Anatomie*, vol. 39. pp. 102–136, 1892.
[88] P. Cerfontaine, “Contribution à l’étude du système nerveux central du Lombric terrestre,” *Bulletin de l’Académie Royal de Belgique*, vol. 3. pp. 742–752, 1892.
[89] G. Retzius, “Das sensible Nervensystem der Polychäten,” *Biologische Untersuchungen Neue Folge IV (1)*. 1892.
[90] G. Retzius, “Zur Kenntnis des Gehirnganglions und des sensiblen Nervensystems der Polychäten,” *Biologische Untersuchungen Neue Folge VII*. 1895.
[91] G. Retzius, “Zur Kenntnis des sensiblen und des sensorischen Nervensystems der Würmer und Mollusken,” *Biologische Untersuchungen Neue Folge IX*. 1900.
[92] G. Retzius, “Weiteres zur Kenntnis des Sinneszellen des Evertebraten,” *Biologische Untersuchungen Neue Folge X*. 1902.
[93] E. G. Racovitza, “Le lobe céphalique et l’encéphale des annélides polychètes. (Anatomie, morphologie, histologie.),” *Archives de Zoologie Expérimentale, Série S, Tome 4, No. 1,2*. pp. 133, 143, 1896.
[94] J. I. Hamaker, “The Nervous System of Nereis virens Sars. A study of comparative neurology,” *Bulletin of the Museum of Comparative Zoology at Harvard*, vol. 32. pp. 89–124, 1898.
[95] F. Langdon, “The sense-organs of nereis virens, sars,” *Journal of Comparative Neurology*, vol. 10. 1900.
[96] F. Hempelmann, “Zur Naturgeschichte von Nereis dumerilii Aud. et Edw.,” *Zoologica*, vol. 62. 1911.
[97] N. Holmgren, “Zur vergleichenden Anatomie des Gehirns Polychaeten, Onychophoren, Xiphosuren, Arachniden, Crustaceen, Myriapoden, und Insekten,” *Kungliga Svenska Vetenskapsakademiens Handlingar*, vol. 56. pp. 1–103, 1916.
[98] B. Hanström, *Vergleichende Anatomie des Nervensystems der wirbellosen Tiere unter Berücksichtigung seiner Funktion*. Springer, Berlin, 1928.
[99] R. Defretin, “Recherches cytologiques et histochimiques sur le système nerveux des Néréidiens. La neurosécrétion des polyosides et ses rapports avec l’épitoquie.,” *Archives de Zoologie Expérimentale et Générale*, vol. 92. pp. 73–140, 10-Jun-1955.
[100] N. Dhainaut-Courtois, M. Dubois, G. Tramu, and M. Masson, “Occurrence and coexistence in Nereis diversicolor O.F. Müller (Annelida Polychaeta) of substances immunologically related to vertebrate neuropeptides.,” *Cell and Tissue Research*, vol. 242. pp. 97–108, 1985.
[101] C. M. Heuer and R. Loesel, “Immunofluorescence analysis of the internal brain anatomy of Nereis diversicolor (Polychaeta, Annelida),” *Cell Tissue Res.*, vol. 331, pp. 713–724, 2008.
[102] V. V. Starunov, E. E. Voronezhskaya, and L. P. Nezlin, “Development of the nervous system in Platynereis dumerilii (Nereididae, Annelida),” *Front. Zool.*, vol. 14, May 2017.
[103] G. Purschke, “Ultrastructure of the nuchal organ in the interstitial polychaete Stygocapitella subterranea (Parergodrilidae),” *Zoologica Scripta*, vol. 15. pp. 13–20, 1986.
[104] G. Purschke, “On the ground pattern of Annelida,” *Organisms, Diversity and Evolution*, vol. 2. pp. 181–196, 2002.
[105] L. A. Parry, G. D. Edgecombe, D. Eibye-Jacobsen, and J. Vinther, “The impact of fossil data on annelidphylogeny inferred from discretemorphological characters,” *Proceedings of the Royal Society B*, vol. 283. 2016.
[106] T. H. Bullock and G. A. Horridge, *Structure and Function of the Nervous System in Invertebrates*. Freeman, San Francisco, 1965.
[107] R. P. Dales, “The reproduction and larval development of Nereis diversicolor O. F. Müller,” *Journal of the Marine Biological Association of the United Kingdom*, vol. 29. 1950.
[108] L. Orrhage and M. Müller, “Morphology of the nervous system of Polychaeta (Annelida),” *Hydrobiologia*, vol. 535/536. pp. 79–111, 2005.
[109] G. Purschke and R. Hessling, “Analysis of the central nervous system and sense organs in Potamodrilus fluviatilis (Annelida: Potamodrilidae),” *Zoologischer Anzeiger-A Journal of Comparative Zoology*, vol. 241, no. 1. pp. 19–35, 2002.
[110] J. E. Smith, “The Nervous Anatomy of the Body Segments of Nereid Polychaetes,” *Philosophical Ttransactions of the Royal Society B*, vol. 240, no. 661. 03-Jan-1957.
[111] C. M. Heuer, C. H. Müller, C. Todt, and R. Loesel, “Comparative neuroanatomy suggests repeated reduction of neuroarchitectural complexity in Annelida,” *Frontiers in Zoology*, vol. 7, no. 13. 04-May-2010.
[112] K. Heider, “Über Eunice. Systematisches, Kiefersack, Nervesystem,” *Zeitschrift für wissenschafliche Zoologie*, vol. 125. pp. 55–90, 1925.
[113] K. v. Haffner, “Über die Abhängigkeit des Gehirnbaues von den Sinnesorganen. Vergleichende Untersuchungen an Euniciden (Polychaeta),” *Zoologische Jahrbücher, Anatomie*, vol. 80. pp. 159–212, 1962.
[114] C. R. Gardner, “The neuronal control of locomotion in the earthworm,” *Biological Reviews*, vol. 51, no. 1. pp. 25–52, Feb-1976.
[115] W. B. J. Kristan, R. L. Calabrese, and W. O. Friesen, “Neuronal control of leech behavior,” *Progress in Neurobiology*, vol. 76, no. 5. pp. 279–327, Aug-2005.
[116] G. Purschke, “Sense organs in polychaetes (Annelida),” *Hydrobiologia*, vol. 535/536. pp. 53–78, 2005.
[117] D. Arendt and J. Wittbrodt, “Reconstructing the eyes of Urbilateria,” *Philos. Trans. R. Soc. B: Biol. Sci.*, vol. 356, pp. 1545–1563, Oct. 2001.
[118] G. Purschke, D. Arendt, H. Hausen, and M. C. M. Müller, “Photoreceptor cells and eyes in Annelida,” *Arthropod Structure & Development*, vol. 35, no. 4. pp. 211–230, Dec-2006.
[119] D. Arendt, K. Tessmar, M.-I. Medeiros de Campos-Baptista, A. Dorresteijn, and J. Wittbrodt, “Development of pigment-cup eyes in the polychaete Platynereis dumerilii and evolutionary conservation of larval eyes in Bilateria,” *Development*, vol. 129. pp. 1143–1154, 2002.
[120] G. Jékely *et al.*, “Mechanism of phototaxis in marine zooplankton,” *Nature*, vol. 456, pp. 395–399, Nov. 2008.
[121] J. B. Gilpin-Brown, “The development and structure of the cephalic nerve in Nereis,” *Journal of Comparative Neurology*, vol. 109. Jun-1958.
[122] G. Purschke, “Ultrastructure of nuchal organs in polychaetes (Annelida) - new results and review,” *Acta Zoologica (Stockholm)*, vol. 78. pp. 123–143, 1997.
[123] P. Flint, “The effect of sensory deprivation on the behaviour of the polychaete Nereis in t-mazes,” *Animal Behaviour*, vol. 13, no. 1. pp. 187–193, Jan-1965.
[124] L. Orrhage, “On the Innervation and Homologues of the Anterior End Appendages of the Eunicea (Polychaeta), with a Tentative Outline of the Fundamental Constitution of the Cephalic Nervous System of the Polychaetes,” *Acta Zoologica (Stockholm)*, vol. 76, no. 3. pp. 229–248, Jul-1995.
[125] J. W. Spengel, “Oligognathus bonneliae eine schmarotzende Eunice,” *Mittheilung der Zoologischen Station von Neapel*, vol. 3. pp. 15–52, 1882.
[126] D. L. West, “Comparative ultrastructure of juvenile and adult nuchal organs of an annelid (Polychaeta : Opheliidae),” *Tissue & Cell*, vol. 10. pp. 243–257, 1978.
[127] R. B. Clark, “The gross morphology of the anterior nervous system of Nephtys,” *Journal of Cell Science*, vol. 3, no. 46. pp. 205–220, 1958.
[128] A. C. Whittle and Z. R. Zahid, “Fine structure of nuchal organs in some errant polychaetous annelids.,” *Journal of Morphology*, vol. 144. pp. 167–184, 1974.
[129] G. Purschke, “Comparative electron microscopic investigation of the nuchal organs in Protodriloides, Protodrilus, and Saccocirrus (Annelida, Polychaeta),” *Canadian journal of zoology*, vol. 68, no. 2. pp. 325–338, 1990.
[130] U. Schlötzer-Schrehardt, “Ultrastructural investigation of the nuchal organs of Pygospio elegans (Polychaeta). I. Larval nuchal organs,” *Helgoländer Meeresuntersuchungen*, vol. 40, no. 4. pp. 397–417, 1986.
[131] U. Schlötzer-Schrehardt, “Ultrastructural investigation of the nuchal organs of Pygospio elegans (Polychaeta). II. Adult nuchal and dorsal organs,” *Zoomorphology*,

vol. 107, no. 3. pp. 169–179, 1987.
[132] G. W. Rouse and K. Fauchald, “Cladistics and polychaetes,” *Zoologica Scripta*, vol. 26, no. 2. pp. 139–204, Apr-1997.
[133] L. Orrhage, “On the Microanatomy of the Cephalic Nervous System of Nereidae (Polychaeta), with a Preliminary Discussion of Some Earlier Theories on the Segmentation of the Polychaete Brain,” *Acta Zoologica (Stockholm)*, vol. 74. pp. 145–172, 1993.
[134] B. Hanström, “Das zentrale und periphere Nervensystem des Kopflappens einiger Polychäten,” *Zeitschrift für Morphologie und Ökologie*, vol. 7. 00-1927.
[135] G. Purschke, “Sense organs in polychaetes (Annelida),” *Hydrobiologia*, vol. 535/536. pp. 53–78, 2005.
[136] M. Imajima, “Review of the annelid worms of the family Nereidae of Japan, with descriptions of five new species or subspecies,” *Bulletin of the National Science Museum Tokyo*, vol. 15. pp. 37–153, 1972.
[137] D. A. Dorsett, “The sensory and motor innervation of Nereis,” *Proceedings of the Royal Society of London. Series B, Biological Sciences*, vol. 159. pp. 652–667, 17-Mar-1964.
[138] A. H. Fischer, T. Henrich, and D. Arendt, “The normal development of Platynereis dumerilii (Nereididae, Annelida),” *Frontiers in Zoology*, vol. 7, no. 31. 30-Dec-2010.
[139] G. Purschke and A. Tzetlin, “Dorsolateral Ciliary Folds in the Polychaete Foregut : Structure, Prevalence and Phylogenetic Significance,” *Acta Zoologica (Stockholm)*, vol. 77. pp. 33–49, 1996.
[140] G. Purschke and A. Tzetlin, “Pharynx and intestine,” *Hydrobiologia*, vol. 535/536. pp. 199–225, 2005.
[141] G. Purschke and M. C. Müller, “Structure of prostomial photoreceptor-like sense organs in Protodriloides species (Polychaeta, Protodrilida),” *Cahiers de Biologie Marine*, vol. 37. pp. 205–219, 1996.
[142] G. Purschke, “Structure of the prostomial appendages and the central nervous system in the Protodrilida (Polychaeta),” *Zoomorphology*, vol. 113, no. 1. pp. 1–20, 1993.
[143] R. M. Santer and M. S. Laverack, “Sensory innervation of the tentacles of the polychaete, Sabella pavonina,” *Zeitschrift füt Zellforschunng*, vol. 122. pp. 160–171, 1971.
[144] E. Schulte and R. Riehl, “Elektronenmikroskopische Untersuchungen an den Tentakeln von Lanice conchilega (Polychaeta, Sedentaria),” *Helgoländer wissenschaftliche Meeresuntersuchungen*, vol. 28, no. 2. pp. 191–205, 1976.
[145] D. A. Dorsett and R. Hyde, “The fine structure of the compound sense organs on the cirri of Nereis diversicolor,” *Zeitschrift für Zellforschung und Mikroskopische Anatomie*, vol. 97, no. 4. pp. 512–527, Dec-1969.
[146] J. D. Hardege, “Nereidid polychaetes as model organisms for marine chemical ecology,” *Hydrobiologia*, vol. 402. pp. 145–161, 1999.
[147] Y. Boilly-Marer, “Contribution à l’étude des cirres parapodiaux dorsaux des formes épitoques chez Nereis pelagica L. (Annélide Polychète),” *Comptes rendus hebdomadaires des séances de l’Académie des sciences. Série D, Sciences naturelles*, vol. 262. pp. 2052–2054, 1966.
[148] Y. Boilly-Marer, “Etude ultrastructurale des modifications hétéronéréidiennes des cirresparapodiaux chez Nereis pelagica L. (Annélide Polychète),” *Comptes rendus hebdomadaires des séances de l’Académie des sciences. Série D, Sciences naturelles*, vol. 263. pp. 142–144, Jul-1966.
[149] Y. Boilly-Marer, “Etude ultrastructurale des cirres parapodiaux de Néréidiens atoques (Annélides Polychètes),” *Zeitschrift für Zellforschung*, vol. 131. pp. 309–327, 1972.
[150] J. V. J. Lawry, “Structure and function of the parapodial cirri of the polynoid polychaete, Harmothoë,” *Zeitschrift für Zellforschung*, vol. 82. pp. 345–361, 1967.
[151] A. Schlawny, C. Griinig, and H.-D. Pfannenstiel, “Sensory and secretory cells of Ophryotrocha puerilis (Polychaeta),” *Zoomorphology*, vol. 110, no. 4. pp. 209–215, Jul-1991.
[152] A. Schlawny, T. Hamann, M. A. Miiller, and H.-D. Pfannenstiel, “The catecholaminergic system of an annelid (Ophryotrocha puerilis, Polychaeta),” *Cell and Tissue Research*, vol. 265, no. 1. pp. 175–184, 1991.
[153] C. Jouin, C. Tchernigovtzeff, M. F. Baucher, and A. Toulmond, “Fine structure of probable mechano- and chemoreceptors in the caudal epidermis of the lugworm Arenicola marina (Annelida, Polychaeta),” *Zoomorphology*, vol. 105, no. 2. pp. 76–82, Apr-1985.
[154] S. M. Lindsay, T. J. Riordan, and D. Forest, “Identification and activity-dependent labeling of peripheral sensory structures on a spionid polychaete,” *Biological Bulletin*, vol. 206. pp. 65–77, Apr-2004.
[155] R. Windoffer and W. Westheide, “The Nervous System of the Male Dinophilus gyrociliatus (Annelida: Polychaeta). I. Number, Types and Distribution Pattern of Sensory Cells,” *Acta Zoologica*, vol. 69, no. 1. pp. 55–64, Mar-1988.
[156] G. A. Horridge, “Proprioceptors, Bristle Receptors, Efferent Sensory Impulses, Neurofibrils and Number of Axons in the Parapodial Nerve of the Polychaete Harmothoe,” *Proceedings of the Royal Society B*, vol. 157, no. 967. 26-Feb-1963.
[157] M. Kamoi and C. D. Derby, “Finding food: how marine invertebrates use chemical cues to track and select food,” *Natural Product Reports*, vol. 34. pp. 514–528, 2017.
[158] J. Fewou and N. Dhainaut-Courtois, “Research on polychaete annelid osmoregulatory peptide(s) byimmunocytochemical and physiological approaches. Computer reconstruction of the brain and evidence for arole of angiotensin-like molecules in Nereis (Hediste) diversicolor OF Muller,” *Biology of the Cell (Paris)*, vol. 85. pp. 21–33, 1995.
[159] K. Moritz and V. Storch, “Elektronenmikroskopische untersuchung eines mechanorezeptors von evertebraten (Priapuliden, Oligochaeten),” *Cell and Tissue Research*, vol. 117, no. 2. pp. 226–234, Jun-1971.
[160] A. I. Farbman, *Cell Biology of Olfaction*. Cambridge University Press, Cambridge, U.K., 1992.
[161] H. Schmidt, “Untersuchungen über den chemischen Sinn einiger Polychaeten,” *Biologisches Zentralblatt*, vol. 42. pp. 193–200, May-1922.
[162] D. M. Dauer, *Functional morphology and feeding behaviour of Streblospio benedicti (Polychaeta: Spionidae)*. The Linnean Society of New South Wales, Sydney, 1984.
[163] D. M. Dauer, “Systematic significance of the morphology of spionid polychaete palps,” *Bulletin of the Biological Society of Washington*, vol. 7. pp. 41–45, 1987.
[164] D. M. Dauer, “Functional morphology and feeding behavior of Polydora commensalis (Polychaeta: Spionidae),” *In: Petersen, M.E. & Kirkegaard, J.B. (Eds.) Systematics, Biology and Morphology of World Polychaeta. Proceedings of the 2nd International Polychaete Conference, Copenhagen 1986. Ophelia Supplement*, vol. 5. pp. 607–614, 1991.
[165] D. M. Dauer, “Functional morphology and feeding behavior of Marenzelleria viridis (Polychaeta: Spionidae),” *In: Reish, D. & Qian, P.-Y. (Eds.) Fifth International Polychaete Conference, held at Qingdao, People’s Republic of China, July 1-6, 1995. Bulletin of Marine Science*, vol. 60. pp. 512–516, 1997.
[166] K. Worsaae, “The systematic significance of palp morphology in the Polydora complex (Polychaeta: Spionidae),” *Zoologischer Anzeiger*, vol. 240. pp. 47–59, 2001.
[167] Y. Boilly-Marer and B. Lassalle, “Electrophysiological responses of the central nervous system in the presence of homospecific and heterospecific sex pheromones in nereids (Annelida polychaeta),” *Journal of Experimental Zoology*, vol. 213. pp. 33–39, 1980.
[168] Y. Boilly-Marer and B. Lassalle, “Electrophysiological responses of Heteronereis stimulated with sex pheromones (Annelida Polychaeta),” *Journal of Experimental Zoology*, vol. 205. pp. 119–124, 1978.
[169] J. L. Ram, C. T. Müller, M. Beckmann, and J. D. Hardege, “The spawning pheromone cysteine-glutathione disulfide (‘nereithione’) arouses a multicomponent nuptialbehavior and electrophysiological activity in Nereis succinea males,” *The FASEB Journal*, vol. 13. pp. 945–952, 1999.
[170] A. O. Gross, “The feeding habits and chemical sense of Nereis virens, Sars,” *Journal of Experimental Zoology*, vol. 32. pp. 427–442, 1921.
[171] W. A. Nagel, “Vergleichend-physiologische und anatomische Untersuchungen über den Geruchs- und Geschmackssinn und ihre Organe, mit einleitenden Betrachtungen aus der allgemeinen vergleichenden Sinnesphysiologie.,” *Bibliotheca Zoologica, Stuttgart*, vol. 7. 1894.
[172] S. M. Lindsay, “Ecology and biology of chemoreception in polychaetes,” *Zoosymposia*, vol. 2. pp. 339–367, 31-Aug-2009.
[173] F. Rullier, “Rôle de l’organe nucal des annélides polychètes,” *Bulletin de la Société Zoologique de France*, vol. 75. pp. 18–24, 1950.
[174] Y. Boilly-Marer, “Contribution à l’étude du déterminisme de l’émission des produits génitauxchez un Néréidien (Platynereis dumerilii Aud. et M. Edw., Annélide Polychète).,” *Comptes rendus hebdomadaires des séances de l’Académie des sciences. Série D, Sciences naturelles*, vol. 264. pp. 2200–2202, May-1967.
[175] W. C. Michel, P. Steullet, H. S. Cate, Burns C.J., A. B. Zhainazarov, and C. Derby, “High-resolution functional labeling of vertebrate and invertebrate olfactory receptor neurons using agmatine, a channelpermeant cation,” *Journal of Neuroscience Methods*, vol. 90, no. 2. pp. 143–156, 15-Aug-1999.
[176] W. J. Biggers and H. Laufer, “Chemical induction of settlement and metamorphosis of Capitella capitata sp. I(Polychaeta) larvae by juvenile hormone-active compounds,” *Invertebrate Reproduction and Development*, vol. 22. pp. 39–46, 1992.
[177] W. J. Biggers and H. Laufer, “Settlement and metamorphosis of Capitella larvae induced by juvenile hormoneactive compounds is mediated by protein kinase C and ion channels.,” *Biological Bulletin*, vol. 196. pp. 187–198, 1999.
[178] E. R. Holm, B. T. Nedved, E. Carpizo-Ituarte, and M. G. Hadfield, “Metamorphic-signal transduction in Hydroides elegans (Polychaeta: Serpulidae) is not mediated by a G protein.,” *Biological Bulletin*, vol. 195. pp. 21–29, Aug-1998.
[179] J. Krieger and H. Breer, “Olfactory Reception in Invertebrates,” *Science*, vol. 286, no. 5440. pp. 720–723, 22-Oct-1999.
[180] P. Bauknecht and G. Jékely, “Large-Scale Combinatorial Deorphanization of Platynereis Neuropeptide GPCRs,” *Cell Reports*, vol. 12, pp. 684–693, Jul. 2015.
[181] E. Mollo, M. J. Garson, G. Polese, P. Amodeo, and M. T. Ghiselin, “Taste and smell in aquatic and terrestrial environments,” *Natural Product Reports*, vol. 34. 2017.
[182] C. A. Edwards and P. J. Bohlen, *Biology and ecology of earthworms (third edition)*. Chapman & Hall, London, 1996.
[183] F. E. Mc Manus and E. J. Wyers, “Olfaction and selective association in the earthworm, Lumbricus terrestris,” *Behavioral and Neural Biology*, vol. 25. pp. 39–57, 1979.
[184] E. J. Elliott, “Chemosensory stimuli in feeding behavior of the leech Hirudo medicinalis,” *Journal of Comparative Physiology A*, vol. 159, no. 3. pp. 391–401, May-1986.
[185] J. Case, “Responses of Nereis virens to alcohols,” *Comparative Biochemistry and Physiology*, vol. 6. pp. 47–56, 1962.
[186] J. Riordan and S. M. Lindsay, “Feeding responses to particle-bound cues by a deposit-feeding spionidpolychaete, Dipolydora quadrilobata (Jacobi 1883),” *Journal of Experimental Marine Biology & Ecology*, vol. 277. pp. 79–95, 2002.
[187] N. Ramanathan, O. Simakov, C. A. Merten, and D. Arendt, “Quantifying Preferences and Responsiveness of Marine Zooplankton to Changing Environmental Conditions using Microfluidics,” *PLoS One*. 30-Oct-2015.
[188] Y. Boilly-Marer, “Sur le rôle chimiorécepteur des cirres parapodiaux hétéronéréidiens dePlatynereis dumerilii Aud. et M. Edw. (Annélide Polychète).,” *Comptes rendus hebdomadaires des séances de l’Académie des sciences. Série D, Sciences naturelles*, vol. 266. pp. 1583–1585, 1968.
[189] E. Zeeck, J. Hardege, H. Bartels-Hardege, and G. Wesselmann, “Sex pheromone in a marine polychaete:determination of the chemical structure.,” *Journal of Experimental Zoology*, vol. 246. pp. 285–292, 1988.
[190] E. Zeeck, T. Harder, and M. Beckmann, “Inosine, L-glutamic acid and L-

glutamine as components of a sex pheromone complex of the marine polychaete Nereis succinea (Annelida: Polychaeta)," *Chemoecology*, vol. 8. pp. 77–84, 1998.
[191] H. D. Bartels-Hardege, J. D. Hardege, M. Beckmann, and C. Muller, "Sex pheromones in marine polychaetesV: Biologically active compound from the coelomic fluid of female Nereis japonica (Annelida Polychaeta).," vol. 201. pp. 275–284, 1996.
[192] E. Zeeck, T. Harder, and M. Beckmann, "Uric Acid: The Sperm-Release Pheromone of the Marine Polychaete Platynereis dumerilii," *Journal of Chemical Ecolog*, vol. 24. pp. 13–23, 1998.
[193] J. D. Hardege, M. Beckmann, and C. Müller, "A waterborne female sex pheromone in the ragworm, Nereis succinea (Annelida,Polychaeta)," *Polychaete Research*, vol. 17. pp. 18–21, 1997.
[194] A. A. Pacey and M. . Bentley, "The fatty acid 8,11,14-eicosatrienoic acid induces spawning in the male lugworm Arenicola marina," *Journal of Experimental Biology*, vol. 173. pp. 165–179, 00-1992.
[195] J. D. Hardege and M. G. Bentley, "Spawning synchrony in Arenicola marina: evidence for sex pheromonal control," *Proceedings of the Royal lSociety B*, vol. 264, no. 1384. 22-Jul-1997.
[196] J. D. Hardege, M. G. Bentley, M. Beckmann, and C. Müller, "Sex pheromones in marine polychaetes: volatile organic substances (VOS) isolated from Arenicola marina," *Marine Ecology Progress Series*, vol. 139. pp. 157–166, 29-Aug-1996.
[197] G. Watson and M. Bentley, "Action of CMF (Coelomic Maturation Factor) on oocytes of the polychaete Arenicola marina (L.)," *The Journal of Experimental Zoology*, vol. 281. pp. 65–71, 1998.
[198] M. G. Bentley, S. Clark, and A. A. Pacey, "The Role of Arachidonic Acid and Eicosatrienoic Acids in the Activation of Spermatozoa in Arenicola marina L. (Annelida: Polychaeta)," *The Biological Bulletin*, vol. 178. pp. 1–9, Feb-1990.
[199] S. A. Rice, "Spermatophores and Sperm Transfer in Spionid Polychaetes," *Transactions of the American Microscopical Society*, vol. 97. pp. 160–170, Apr-1978.
[200] G. J. Watson, F. M. Langford, S. M. Gaudron, and M. G. Bentley, "Factors influencing spawning and pairing in the scale worm Harmothoe imbricata (Annelida: Polychaeta)," *The Biological Bulletin*, vol. 199. pp. 50–58, Aug-2000.
[201] S. M. Gaudron, G. J. Watson, and M. G. Bentley, "Induction of pairing in male scale worm Harmothoe imbricata (Polychaeta: Polynoidae) by chemical signals," *Journal of the Marine Biological Association of the United Kingdom*, vol. 87, no. 5. pp. 1115–1116, 18-Oct-2007.
[202] M. Copeland and H. L. Wieman, "The chemical sense and feeding behavior of Nereis Virens, Sars," *Biological Bulletin, Woods Hole*, vol. 47. pp. 231–238, 1924.
[203] G. J. Watson, K. M. Hamilton, and W. E. Tuffnail, "Chemical alarm signalling in the polychaete Nereis (Neanthes) virens (Sars) (Annelida: Polychaeta)," *Animal Behaviour*, vol. 70, no. 5. pp. 1125–1132, Nov-2005.
[204] D. C. Miller and P. A. Jumars, "Pellet accumulation, sediment supply, and crowding as determinants of surfacedeposit-feeding rate in Pseudopolydora kempi japonica Imajima and Hartman (Polychaeta: Spionidae).," *Journal of Experimental Marine Biology & Ecology*, vol. 99. pp. 1–17, 1986.
[205] L. Levin *et al.*, "Rapid subduction oforganic matter by maldanid polychaetes on the North Carolina slope," *Journal of Marine Research*, vol. 55. pp. 595–611, 1997.
[206] U. Witte *et al.*, "In situ experimental evidence of the fate of a phytodetritus pulse at the abyssal sea floor," *Nature*, vol. 424. pp. 763–766, 2003.
[207] R. L. Kihslinger and S. A. Woodin, "Food patches and a surface deposit feeding spionid polychaete," *Marine Ecology Progress Series*, vol. 201. pp. 233–239, 2000.
[208] C. P. Mangum and C. D. Cox, "Analysis of the feeding response in the onuphid polychaete Diopatra cuprea(Bosc)," *Biological Bulletin*, vol. 140. pp. 215–229, 1971.
[209] M. C. Ferner and P. A. Jumars, "Responses of deposit-feeding spionid polychaetes to dissolved chemical cues.," *Journal of Experimental Marine Biology & Ecology*, vol. 236. pp. 89–106, 1999.
[210] H. K. Mahon and D. M. Dauer, "Organic coatings and ontogenetic particle selection in Streblospio benedictiWebster (Spionidae: Polychaeta)," *Journal of Experimental Marine Biology & Ecology*, vol. 323, no. 1. pp. 84–92, 28-Sep-2005.
[211] R. M. Rieger, "The Biphasic Life Cycle—A Central Theme of Metazoan Evolution," *Integrative and Comparative Biology*, vol. 34, no. 4. pp. 484–491, 00-1994.
[212] M. G. Hadfield, "Why and how marine-invertebrate larvae metamorphose so fast," *Seminars in Cell & Developmental Biology*, vol. 11, no. 6. pp. 437–443, Dec-2000.
[213] J. R. Pawlik, "Chemical ecology of the settlement of benthic marine invertebrates," *Oceanography and Marine Biology Annual Review*, vol. 30. pp. 273–335, 1992.
[214] M. G. Hadfield, E. A. Meleshkevitch, and D. Y. Boudko, "The apical sensory organ of a gastropod veliger is a receptor for settlement cues," *The Biological Bulletin*, vol. 198. pp. 67–76, Feb-2000.
[215] T. Harder and P.-Y. Qian, "Induction of larval settlement and metamorphosis in the serpulid polychaete Hydroides elegans by dissolved free amino acids: isolation and identification," *Marine Ecology Progress Series*, vol. 179. pp. 259–271, 1999.
[216] J. A. Pechenik and P.-Y. Qian, "Onset and maintenance of metamorphic competence in the marine polychaeteHydroides elegans Haswell in response to three chemical cues.," *Journal of Experimental Marine Biology and Ecology*, vol. 226, no. 1. pp. 51–74, 1998.
[217] D. Kirchman, S. Graham, D. Reish, and R. Mitchell, "Bacteria induce settlement and metamorphosis ofJanua (Dexiospira) brasiliensis Grube (Polychaeta: Spirorbidae)," *Journal of Experimental Marine Biology and Ecology*, vol. 56. pp. 153–163, 1982.
[218] S. C. K. Lau and P.-Y. Qian, "Larval settlement in the serpulid polychaete Hydroides elegans in response tobacterial films: an investigation of the nature of putative larval settlement cue.," *Marine Biology*, vol. 138. pp. 321–328, 2001.
[219] C. R. C. Unabia and M. G. Hadfield, "Role of bacteria in larval settlement and metamorphosis of the polychaete Hydroides elegans.," *Marine Biology*, vol. 133. pp. 55–64, 1999.
[220] T. Harder, S. C. K. Lau, H.-U. Dahms, and P.-Y. Qian, "Isolation of bacterial metabolites as natural inducers for larval settlement in the marine polychaete Hydroides elegans (Haswell).," *Journal of Chemical Ecology*, vol. 28. pp. 2029–2043, 2002.
[221] S. A. Woodin, R. L. Marinelli, and D. E. Lincoln, "Allelochemical inhibition of recruitment in a sedimentary assemblage.," *Journal of Chemical Ecology*, vol. 19. pp. 517–530, 1993.
[222] S. A. Woodin, S. M. Lindsay, and D. E. Lincoln, "Biogenic bromophenols as negative recruitment cues," *Marine Ecology Progress Series*, vol. 157. pp. 303–306, 1997.
[223] F. Esser, M. Winterberg, Z. Sebesvari, and T. Harder, "Effects of halogenated metabolites from infaunalpolychaetes on larval settlement of the spionid polychaete Streblospio benedicti," *Marine Ecology Progress Series*, vol. 355. pp. 161–172, 2008.
[224] R. L. Marinelli and S. A. Woodin, "Disturbance and recruitment: a test of solute and substrate specificity usingMercenaria mercenaria and Capitella sp.," *Marine Ecology Progress Series*, vol. 269. pp. 209–221, 2004.
[225] P. V. R. Snelgrove, J. P. Grassle, and C. A. Zimmer, "Adult macrofauna effects on Capitella sp. I larval settlement: a laboratory flume study," *Journal of Marine Research*, vol. 59. pp. 657–674, 2001.
[226] S. J. Engstrom and R. L. Marinelli, "Recruitment response of benthic infauna to manipulated sedimentgeochemical properties in natural flows," *Journal of Marine Research*, vol. 63. pp. 407–436, 2005.
[227] E. E. Voronezhskaya, K. I. Glebov, M. Y. Khabarova, E. G. Ponimaskin, and L. P. Nezlin, "Adult-to-embryo chemical signaling in the regulation of larval development in trochophore animals: Cellular and molecular mechanisms," *Acta Biologica Hungarica*, vol. 59. pp. 117–122, 2008.
[228] D. Schleicherova, M. C. Lorenzi, and G. Sella, "How outcrossing hermaphrodites sense the presence of conspecifics and suppress female allocation," *Behavioral Ecology*, vol. 17. pp. 1–5, 2005.
[229] J. R. Weinberg, V. R. Starczak, C. Mueller, G. C. Pesch, and S. M. Lindsay, "Divergence between populationsof a monogamous polychaete with male parental care: premating isolation and chromosome variation," *Marine Biology*, vol. 107. pp. 205–213, 1990.
[230] R. Sutton, E. Bolton, H. D. Bartels-Hardege, M. Eswards, D. J. Reish, and J. D. Hardege, "Chemical signal mediated premating reproductive isolation in a marine polychaete, Neanthes acuminata (arenaceodentata)," *Journal of Chemical Ecology*, vol. 31. pp. 1865–1876, 2005.
[231] G. P. Wells, "Intermittent activity in polychaete worms," *Nature*, vol. 144. pp. 940–941, 02-Dec-1939.
[232] A. Toulmond and C. Tchernigovtzeff, "Ventilation and respiratory gas exchanges of the lugworm Arenicola marina (L.) as functions of ambient PO2 (20–700 torr)," *Respiration Physiology*, vol. 57, no. 3. pp. 349–363, Jul-1984.
[233] Schmidtberg and A. Dorresteijn, "Ultrastructure of the nuchal organs in the polychaete Platynereis dumerilii (Annelida, Nereididae)," *Invertebrate Biology*, vol. 129. pp. 252–265, 2010.
[234] A. Fischer, A. W. C. Dorresteijn, and U. Höger, "Metabolism of oocyte construction and the generation of histospecificity in the cleaving egg. Lessons from nereid annelids," *International Journal of Developmental Biology*, vol. 40. pp. 421–430, 1996.
[235] A. Fischer and A. Dorresteijn, "The polychaete Platynereis dumerilii (Annelida): a laboratory animal with spiralian cleavage, lifelong segment proliferation and a mixed benthic/pelagic life cycle," *BioEssays*, vol. 26, pp. 314–325, 2004.
[236] H. Marlow *et al.*, "Larval body patterning and apical organs are conserved in animal evolution," *BMC Biology*, vol. 12, no. 7. 2014.
[237] M. A. Tosches, "Development and function of brain photoreceptors in the annelid Platynereis dumerilii," 2013.
[238] E. R. Troemel, J. H. Chou, N. D. Dwyer, H. A. Colbert, and C. I. Bargmann, "Divergent seven transmembrane receptors are candidate chemosensory receptors in C. elegans.," *Cell*, vol. 83. pp. 207–218, 1995.
[239] M. Conzelmann, S.-L. Offenburger, A. Asadulina, T. Keller, T. A. Munch, and G. Jekely, "Neuropeptides regulate swimming depth of Platynereis larvae," *Proc. Natl. Acad. Sci.*, vol. 108, p. 1174, Oct. 2011.
[240] O. Simakov, "Linking micro- and macro-evolution at the cell type level," 2013.
[241] A. Lauri, "The evolution of the neural crest from an annelid perspective : conserved cell types and signaling pathways in Platynereis dumerilii," 2013.
[242] F. Christodoulou *et al.*, "Ancient animal microRNAs and the evolution of tissue identity," *Nature*, vol. 463, pp. 1084–1088, Jan. 2010.
[243] F. Christodoulou, "Animal microRNAs and the evolution oftissue identity," 2009.
[244] I. Röhl, B. Schneider, B. Schmidt, and E. Zeeck, "L-Ovothiol A: The Egg Release Pheromone of the Marine Polychaete Platynereis Dumerilii: Annelida: Polychaeta," *Zeitschrift für Naturforschung C*, vol. 54, no. 12. pp. 1145–1174, 1999.
[245] J. Wäge *et al.*, "Effects of low seawater pH on the marine polychaete Platynereis dumerilii," *Marine Pollution Bulletin*, vol. 95, no. 1. pp. 166–172, 15-Jun-2015.
[246] C. Winchell, J. E. Valencia, and D. K. Jacobs, "Confocal analysis of nervous system architecture in direct-developing juveniles of Neanthes arenaceodentata (Annelida, Nereididae)," *Frontiers in Zoology*, vol. 7, no. 17. 16-Jun-2010.
[247] L. Orrhage, "On the Microanatomy of the Cephalic nervous System of Nereidae (Polychaeta), with a Preliminary Discussion of Some Earlier Theories on the Segmentation of the Polychaete Brain," *Acta Zoologica (Stockholm)*, vol. 74. pp. 145–172, 00-1993.
[248] C. M. Heuer and R. Loesel, "Immunofluorescence analysis of the internal brain anatomy of Nereis diversicolor (Polychaeta, Annelida)," *Cell Tissue Res.*, vol.

331, pp. 713–724, Dec. 2007.
[249] N. Rebscher, A. K. Lidke, and C. F. Ackermann, “Hidden in the crowd: primordial germ cells and somatic stem cells in the mesodermal posterior growth zone of the polychaete Platynereis dumerillii are two distinct cell populations,” *EvoDevo*, vol. 3, no. 1. 2012.
[250] K. Pfeifer, A. W. C. Dorresteijn, and A. C. Fröbius, “Activation of Hox genes during caudal regeneration of the polychaete annelid Platynereis dumerilii,” *Dev. Genes Evol.*, vol. 222, pp. 165–179, May 2012.
[251] V. V. Starunov, N. Dray, E. V. Belikova, P. Kerner, M. Vervoort, and G. Balavoine, “A metameric origin for the annelid pygidium?,” *BMC Evol. Biol.*, vol. 15, no. 25, 2015.
[252] V. V. Kozin, N. A. Filippova, and R. P. Kostyuchenko, “Regeneration of the nervous and muscular system after caudal amputation in the polychaete Alitta virens (Annelida: Nereididae),” *Russ. J. Dev. Biol.*, vol. 48, pp. 198–210, May 2017.
[253] R. Shahidi *et al.*, “A serial multiplex immunogold labeling method for identifying peptidergic neurons in connectomes,” *eLife*, vol. 4, Dec. 2015.
[254] J. S. De Belle and M. Heisenberg, “Associative odor learning in Drosophila abolished by chemical ablation of mushroom bodies.,” *Science*, vol. 263, no. 5147. pp. 692–694, 1994.
[255] R. Tomer, “The evolution of mushroom body andtelencephalic cell types, studied by single cell expression profiling of Platynereis dumerilii larvae,” 2009.
[256] J. Schindelin *et al.*, “Fiji: an open-source platform for biological-image analysis,” *Nat. Methods*, vol. 9, pp. 676–682, Jun. 2012.
[257] C. Ackermann, A. Dorresteijn, and A. Fischer, “Clonal domains in postlarvalPlatynereis dumerilii (Annelida: Polychaeta),” *J. Morphol.*, vol. 266, pp. 258–280, 2005.
[258] N. Dhainaut-Courtois, “Étude histologique et ultrastructurale des cellules nerveuses du ganglion cérébral de Nereis pelagica L.(Annélid-Polychète). Comparaison entre les types cellulaires I–VI et ceux décrits anterieurement chez les nereidae,” *General and Comparative Endocrinology*, vol. 11, no. 2. pp. 414–443, 1968.
[259] E. A. Williams *et al.*, “Synaptic and peptidergic connectome of a neurosecretory centre in the annelid brain,” *bioRxiv*, vol. 115204. 2017.
[260] W. Dürichen, “Neuroanatomy and Function of Mushroom Bodies in 6 and 12 days old Platynereis dumerilii larvae,” 2016.
[261] J. Nakai, M. Ohkura, and K. Imoto, “A high signal-to-noise Ca2+ probecomposed of a single green fluorescent protein,” *Nature Biotechnology*, vol. 19. pp. 137–141, Feb-2001.
[262] R. M. Paredes, J. C. Etzler, L. T. Watts, W. Zheng, and J. D. Lechleiter, “Chemical calcium indicators,” *Methods*, vol. 46, pp. 143–151, Nov. 2008.
[263] T.-W. Chen *et al.*, “Ultrasensitive fluorescent proteins for imaging neuronal activity,” *Nature*, vol. 499, pp. 295–300, Jul. 2013.
[264] S. H. Chalasani *et al.*, “Dissecting a circuit for olfactory behaviour in Caenorhabditis elegans,” *Nature*, vol. 450, pp. 63–70, Nov. 2007.
[265] R. Candelier, M. S. Murmu, S. A. Romano, A. Jouary, G. Debrégeas, and G. Sumbre, “A microfluidic device to study neuronal and motor responses to acute chemical stimuli in zebrafish,” *Sci. Reports*, vol. 5, Jul. 2015.
[266] T. E. Audesirk, J. E. Alexander, G. J. Audesirk, and C. M. Moyer, “Rapid, Nonaversive Conditioning in a Freshwater Gastropod: I. Effects of age and motivation,” *Behavioral and Neural Biology*, vol. 36. pp. 379–390, 1982.
[267] H. K. Taukulis, “Odor Aversions Produced over Long CS-US Delays,” *Behavioral Biology*, vol. 10. pp. 505–510, 1974.
[268] K. Takeda, “Classical conditioned response in the honey bee,” *Journal of Insect Physiology*, vol. 6. pp. 168–179, 1961.
[269] D. Blades and B. K. Mitchell, “Effect of alkaloids on feeding by Phormia regina,” *Entomologia Experimentalis et Applicata*, vol. 41, no. 3. pp. 299–304, Aug-1986.
[270] J. C. Boudreau, L. T. Do, L. Sivakumar, J. Oravec, and C. A. Rodriguez, “Taste systems of the petrosal ganglion of the rat glossopharyngeal nerve,” *Chemical Senses*, vol. 12, no. 3. 01-Jul-1987.
[271] A. Edelstein, N. Amodaj, K. Hoover, R. Vale, and N. Stuurman, “Computer control of microscopes using μManager,” *Current protocols in molecular biology*, vol. 92, no. 14.20. pp. 1–17, Oct-2010.
[272] C. A. Schneider, W. S. Rasband, and K. W. Eliceiri, “NIH Image to ImageJ: 25 years of image analysis.,” *Nature methods*, vol. 9, no. 7. pp. 671–675, Jul-2012.
[273] P. Thevenaz, U. E. Ruttimann, and M. Unser, “A pyramid approach to subpixel registration based on intensity.,” *IEEE transactions on image processing*, vol. 7, no. 1. pp. 27–41, Jan-1998.
[274] S. Brittain, K. Paul, X.-M. Zhao, and G. Whitesides, “Soft lithography and microfabrication.,” *Physics World*, vol. 11. pp. 31–36, 1998.
[275] D. Qin, Y. Xia, J. A. Rogers, R. J. Jackman, X.-M. Zhao, and G. M. Whitesides, “Microfabrication, microstructures and microsystems.,” in *Microsystem technology in chemistry and life science*, Springer, 1998.
[276] J. D. Wang, N. J. Douville, S. Takayama, and M. ElSayed, “Quantitative analysis of molecular absorption into PDMS microfluidic channels,” *Annals of biomedical engineering*, vol. 40. pp. 1862–1873, 2012.
[277] H. Martínez Vergara, “Descriptive and functional approaches for a system-level understanding ofPlatynereis dumerilii and the evolution oflocomotor circuits in Bilateria. PhD thesis.,” 2016.
[278] T. D. Wyatt, *Pheromones and Animal Behaviour : Communication by Smelland Taste, p 408*. Cambridge University Press, Cambridge, UK, 2003.
[279] H. Yambe *et al.*, “L-Kynurenine, an amino acid identified as a sex pheromone in the urine of ovulated female masu salmon,” *Proceedings of the National Academy of Sciences*, vol. 103, no. 42. pp. 15370–15374, 2006.
[280] G. Giordano *et al.*, “Volatile secondary metabolites as aposematic olfactory signals and defensive weapons in aquatic environments,” *Proc. Natl. Acad. Sci.*, vol. 114, pp. 3451–3456, Mar. 2017.
[281] D. K. Hofmann, “Regeneration and endocrinology in the polychaete Platynereis dumerilii. An experimental and structural study,” *Development Genes and Evolution*, vol. 180. pp. 47–71, 1976.
[282] G. de Medeiros, B. Balázs, and L. Hufnagel, “Light-sheet imaging of mammalian development,” *Semin. Cell & Dev. Biol.*, vol. 55, pp. 148–155, Jul. 2016.
[283] M. B. Ahrens, M. B. Orger, D. N. Robson, J. M. Li, and P. J. Keller, “Whole-brain functional imaging at cellular resolution using light-sheet microscopy,” *Nat. Methods*, vol. 10, pp. 413–420, Mar. 2013.
[284] R. Prevedel *et al.*, “Simultaneous whole-animal 3D imaging of neuronal activity using light-field microscopy,” *Nature methods*, vol. 11, no. 7. pp. 727–730, 2014.
[285] T. Tully and W. G. Quinn, “Classical conditioning and retention in normal and mutant Drosophila melanogaster,” *Journal of Comparative Physiology A*, vol. 157. pp. 263–277, 1985.
[286] M. C. Nelson, “Classical conditioning in the blowfly (Phormia regina): associative and excitatory factors.,” *Journal of comparative and physiological psychology*, vol. 77, no. 3. pp. 353–368, 1971.
[287] T. Valentincic, J. Kralj, M. Stenovec, A. Koce, and J. Caprio, “The behavioral detection of binary mixtures of amino acids and their individual components by catfish.,” vol. 203, no. 21. pp. 3307–3317, 2000.
[288] N. Ramanathan, “Monitoring the response of cells andorganisms to different chemical cues using microfluidics,” 2015.
[289] R. D. Hawkins, T. J. Carew, and E. R. Kandel, “Effects of interstimulus interval and contingency on classical conditioning of the Aplysia siphon withdrawal reflex.,” *Journal of Neuroscience*, vol. 6, no. 6. pp. 1695–1701, Jun-1986.
[290] T. J. Carew, E. T. Walters, and E. R. Kandel, “Classical conditioning in a simple withdrawal reflex in Aplysia californica,” *Journal of Neuroscience*, vol. 1, no. 12. pp. 1426–1437, Dec-1981.
[291] C. R. Gallistel, S. Fairhurst, and P. Balsam, “The learning curve: implications of a quantitative analysis,” *Proceedings of the national academy of Sciences of the united States of america*, vol. 101, no. 36. pp. 13124–13131, 2004.
[292] T. Hendel *et al.*, “The carrot, not the stick: appetitive rather than aversive gustatory stimuli support associative olfactory learning in individually assayed Drosophila larvae,” *Journal of Comparative Physiology A*, vol. 191. Mar-2005.
[293] A. S. Darmaillacq, L. Dickel, M. P. Chichery, V. Agin, and R. Chichery, “Rapid taste aversion learning in adult cuttlefish, Sepia officinalis,” *Animal Behaviour*, vol. 68, no. 6. p. 1291–1298., Dec-2004.
[294] N. Schneiderman, I. Fuentes, and I. Gormezano, “Acquisition and extinction of the classically conditioned eyelid response in the albino rabbit,” *Science*, vol. 136, no. 3516. pp. 650–652, 1962.
[295] J. Alexander, T. E. Audesirk, and G. J. Audesirk, “One-trial reward learning in the snail Lymnea stagnalis,” *Journal of Neurobiology*, vol. 15, no. 1. pp. 67–72, 1984.
[296] M. E. Seligman, “On the generality of the laws of learning,” *Psychological review*, vol. 77, no. 5. pp. 406–418, 1970.
[297] T. Tully, T. Preat, S. C. Boynton, and M. Del Vecchio, “Genetic dissection of consolidated memory in Drosophila,” *Cell*, vol. 79, no. 1. pp. 35–47, 1994.
[298] H. Amano and I. N. Maruyama, “Aversive olfactory learning and associative long-termmemory in Caenorhabditis elegans,” *Learning & Memory*, vol. 18. pp. 654–665, 2011.
[299] R. A. Rescorla, “Pavlovian conditioning and its proper control procedures,” *Psychological review*, vol. 74, no. 1. pp. 71–80, 1967.
[300] T. H. Bullock and G. C. Quarton, “Simple Systems for the Study of Learning Mechanisms,” *Neurosciences Research Program Bulletin, Work session held June 2-3, 1965.*, vol. 4. pp. 105–233, 1966.
[301] R. B. Clark and S. M. Evans, “The effect of delayed brain extirpation and replacement on caudal regeneration in Nereis diversicolor,” *Development*, vol. 9, no. 1. pp. 97–105, 1961.
[302] S. M. Evans, “The effect of brain extirpation on learning and retention in nereid polychaetes.,” *Animal Behaviour*, vol. 11, no. 1. pp. 172–178, 1963.
[303] S. M. Evans, “Behaviour of the polychaete Nereis in T-mazes,” *Animal Behaviour*, vol. 11, no. 2. pp. 379–392, 1963.
[304] P. Künzer, “Verhaltensphysiologische untersuchungen über das zucken des regenwurms,” *Zeitschrift für Tierpsychologie*, vol. 15, no. 1. pp. 31–49, 12-Jan-1958.
[305] S. C. Ratner and D. G. Stein, “Responses of worms to light as a function of intertrial interval and ganglion removal.,” *Journal of comparative and physiological psychology*, vol. 59, no. 2. p. 301, 1965.
[306] W. Gee, “The behavior of leeches with especial reference to its modifiability,” *University of California Publications in Zoology*, vol. 2. p. 197, 1912.
[307] F. Kaiser, “Beiträge zur bewegungsphysiologie der Hirudineen.,” *Zoologisches Jahrbuch (Allgemeine Zoologie)*, vol. 65. p. 59, 1954.
[308] S. R. Lockery, J. N. Rawlins, and J. A. Gray, “Habituation of the shortening reflex in the medicinal leech,” *Behavioral neuroscience*, vol. 99, no. 2. pp. 333–341, 1985.
[309] J. A. Dyal, “Behavior modification in annelids,” in *Invertebrate learning (pp. 225-290)*, Springer US, 1973.
[310] R. B. Clark, “Habituation of the polychaete Nereis to sudden stimuli. 1. General properties of the habituation process,” *Animal Behaviour*, vol. 8, no. 1. pp. 82–91, 1960.
[311] R. B. Clark, “Habituation of the polychaete Nereis to sudden stimuli. 2. Biological significance of habituation,” *Animal Behaviour*, vol. 8, no. 1. pp. 92–103, 1960.
[312] S. M. Evans, “Habituation of the withdrawal response in nereid polychaetes: 2. Rates of habituation in intact and decerebrate worms,” *The Biological Bulletin*, vol. 137, no. 1. pp. 105–117, 1969.
[313] S. M. Evans, “Habituation of the withdrawal response in nereid polychaetes: 1. The habituation process in Nereis diversicolor,” *The Biological Bulletin*, vol. 137, no. 1. pp. 95–104, 1969.
[314] J. A. Dyal and K. Hetherington, “Habituation in the polychaete Hesperonoë adventor.,” *Psychonomic Science*, vol. 13, no. 5. pp. 263–264, 1958.

[315] F. B. Krasne, “Escape from recurring tactile stimulation in Branchiomma vesiculosum,” *Journal of Experimental Biology*, vol. 42, no. 2. pp. 307–322, 1965.
[316] J. A. C. Nicol, “Responses of Branchiomma vesiculosum (Montagu) to photic stimulation,” *Journal of the Marine Biological Association of the United Kingdom*, vol. 29, no. 2. pp. 303–320, 1950.
[317] D. Stoller and C. Sahley, “Habituation and sensitization of the shortening reflex in the leech, Hirudo medicinalis,” *Society of Neuroscience Abstracts*, vol. 367. 1985.
[318] S. M. Evans, “Non-associative behavioural modifications in the polychaete Nereis diversicolor,” *Animal behaviour*, vol. 14, no. 1. pp. 107–119, 1966.
[319] S. M. Evans, “Non-associative behavioural modifications in nereid polychaetes,” *Nature*, vol. 211, no. 5052. pp. 945–948, 1966.
[320] S. M. Evans, “Non-associative avoidance learning in nereid polychaetes,” *Animal behaviour*, vol. 14, no. 1. pp. 102–106, 1966.
[321] S. C. Ratner and K. R. Miller, “Classical conditioning in earthworms, Lumbricus terrestris,” *Journal of Comparative and Physiological Psychology*, vol. 52, no. 1. pp. 102–105, 1959.
[322] T. B. Henderson and P. N. Strong, “Classical conditioning in the leech Macrobdella Ditetra as a function of CS and UCS intensity,” *Conditional reflex: a Pavlovian journal of research & therapy*, vol. 7, no. 4. pp. 210–215, 1972.
[323] C. L. Sahley and D. F. Ready, “Associative learning modifies two behaviors in the leech, Hirudo medicinalis,” *Journal of Neuroscience*, vol. 8, no. 12. pp. 4612–4620, 1988.
[324] M. Copeland, “An apparent conditioned response in Nereis virens.,” *Journal of Comparative Psychology*, vol. 10, no. 4. pp. 339–354, 1930.
[325] M. Copeland and F. A. Brown Jr, “Modification of behavior in Nereis virens.,” *The Biological Bulletin*, vol. 67, no. 3. pp. 356–364, 1934.
[326] S. C. Ratner, “Annelids and learning: A critical review,” in *Chemistry of Learning (pp. 391-406)*, Springer US, 1967.
[327] S. M. Evans, “Behavior in polychaetes,” *The Quarterly Review of Biology*, vol. 46, no. 4. pp. 379–405, 1971.
[328] C. L. Sahley, “What we have learned from the study of learning in the leech,” *Developmental Neurobiology*, vol. 27, no. 3. pp. 434–445, 1995.
[329] W. O. Friesen and W. B. Kristan, “Leech locomotion: swimming, crawling, and decisions,” *Current opinion in neurobiology*, vol. 17, no. 6. pp. 704–711, 2007.
[330] G. A. Wright *et al.*, “Parallel Reinforcement Pathways for Conditioned Food Aversions in the Honeybee,” *Curr. Biol.*, vol. 20, pp. 2234–2240, Dec. 2010.
[331] F. J. Guerrieri and P. d’Ettorre, “Associative learning in ants: Conditioning of the maxilla-labium extension response in Camponotus aethiops,” *Journal of Insect Physiology*, vol. 56, no. 1. pp. 88–92, Feb-2010.
[332] I. Findlay, M. J. Dunne, S. Ullrich, C. B. Wollheim, and O. H. Petersen, “Quinine inhibits Ca2+-independent K+ channels whereas tetraethylammonium inhibits Ca2+-activated K+ channels in insulin-secreting cells,” *FEBS letters*, vol. 185, no. 1. pp. 4–8, 1985.
[333] N. Cook and D. Haylett, “Effects of apamin, quinine and neuromuscular blockers on calcium-activated potassium channels in guinea-pig hepatocytes.,” *Journal of Physiology*. pp. 373–394, 01-Jan-1985.
[334] R. De Jong and J. H. Visser, “Specificity-related suppression of responses to binary mixtures in olfactory receptors of the Colorado potato beetle,” *Brain research*, vol. 447, no. 1. pp. 18–24, 26-Apr-1988.
[335] J. Joerges, A. Küttner, C. G. Galizia, and R. Menzel, “Representations of odours and odour mixtures visualized in the honeybee brain,” *Nature*, vol. 387, no. 6630. pp. 285–288, 1997.
[336] R. D. Hawkins, T. W. Abrams, T. J. Carew, and E. R. Kandel, “A cellular mechanism of classical conditioning in Aplysia: activity-dependent amplification of presynaptic facilitation,” *Science*, vol. 219, no. 4583. pp. 400–405, 28-Jan-1983.
[337] L. Seugnet, Y. Suzuki, J. M. Donlea, L. Gottschalk, and P. J. Shaw, “Sleep deprivation during early-adult development results in long-lasting learning deficits in adult Drosophila,” *Sleep*, vol. 34, no. 2. pp. 137–146, 2011.
[338] G. Kemenes and P. R. Benjamin, “Appetitive learning in snails shows characteristics of conditioning in vertebrates,” *Brain research*, vol. 489, no. 1. pp. 163–166, 1989.
[339] T. H. Struck *et al.*, “Phylogenomic analyses unravel annelid evolution,” *Nature*, vol. 471, pp. 95–98, Mar. 2011.
[340] O. Garaschuk, R. I. Milos, and A. Konnerth, “Targeted bulk-loading of fluorescent indicators for two-photon brain imaging in vivo,” *Nature protocols*, vol. 1, no. 1. p. 380, 2006.
[341] M. Saina *et al.*, “A cnidarian homologue of an insect gustatory receptor functions in developmental body patterning.,” *Nature communications*, vol. 6. Jan-2015.
[342] H. M. Robertson, “The Insect Chemoreceptor Superfamily Is Ancient in Animals,” *Chem. Senses*, vol. 40, pp. 609–614, Sep. 2015.
[343] V. Croset *et al.*, “Ancient protostome origin of chemosensory ionotropic glutamate receptors and the evolution of insect taste and olfaction,” *PLoS genetics*, vol. 6, no. 8. 2010.
[344] K. Tsuchihara, “An Odorant-binding Protein Facilitates Odorant Transfer from Air to Hydrophilic Surroundings in the Blowfly,” *Chem. Senses*, vol. 30, pp. 559–564, Jul. 2005.
[345] C. Gomez-Diaz, J. H. Reina, C. Cambillau, and R. Benton, “Ligands for pheromone-sensing neurons are not conformationally activated odorant binding proteins,” *PLoS biology*, vol. 11, no. 4. 2013.
[346] C. M. Heuer and R. Loesel, “Three-dimensional reconstruction of mushroom body neuropils in the polychaete species Nereis diversicolor and Harmothoe areolata (Phyllodocida, Annelida),” *Zoomorphology*, vol. 128, pp. 219–226, Jun. 2008.
[347] C. D. Derby, “Learning from spiny lobsters about chemosensory coding of mixtures,” *Physiology & behavior*, vol. 69, no. 1. pp. 203–209, 2000.
[348] F. Lapraz *et al.*, “Put a tiger in your tank: the polyclad flatworm Maritigrella crozieri as a proposed model for evo-devo.,” *EvoDevo*, vol. 4, no. 1. p. 29, 2013.
[349] N. Konstantinides and M. Averof, “A common cellular basis for muscle regeneration in arthropods and vertebrates,” *Science*, vol. 343, no. 6172. pp. 788–791, 2014.
[350] J. M. Martín-Durán, G. H. Wolff, N. J. Strausfeld, and A. Hejnol, “The larval nervous system of the penis worm Priapulus caudatus (Ecdysozoa).,” *Phil. Trans. R. Soc. B*, vol. 371, no. 1685. 2016.
[351] D. Arendt, A. S. Denes, G. Jekely, and K. Tessmar-Raible, “The evolution of nervous system centralization,” *Philos. Trans. R. Soc. B: Biol. Sci.*, vol. 363, pp. 1523–1528, Apr. 2008.
[352] E. Mollo, A. Fontana, V. Roussis, G. Polese, P. Amodeo, and M. T. Ghiselin, “Sensing marine biomolecules: smell, taste, and the evolutionary transition from aquatic to terrestrial life,” *Front. Chem.*, vol. 2, Oct. 2014.
[353] L. Salvini-Plawen and E. Mayr, “On the evolution of photoreceptors and eyes,” in *Hecht MK, Steere WC, Wallace B (eds) Evolutionary Biology, pp. 207-263*, vol. 10, Plenum Publ Co, New York, 1977.
[354] N. K. Michiels *et al.*, “Red fluorescence in reef fish: A novel signalling mechanism?,” *BMC Ecol.*, vol. 8, p. 16, 2008.
[355] P. M. Narins, “Seismic Communication in Anuran Amphibians,” *Bioscience*, vol. 40. pp. 268–274, Apr-1990.
[356] H. V. Goodson and J. A. Spudich, “Molecular evolution of the myosin family: relationships derived from comparisons of amino acid sequences,” *Proceedings of the National Academy of Sciences*, vol. 90, no. 2. pp. 659–663, 1993.
[357] S. Oota and N. Saitou, “Phylogenetic relationship of muscle tissues deduced from superimposition of gene trees,” *Molecular Biology and Evolution*, vol. 16, no. 6. pp. 856–867, 1999.
[358] T. Brunet, A. H. Fischer, P. R. Steinmetz, A. Lauri, P. Bertucci, and D. Arendt, “The evolutionary origin of bilaterian smooth and striated myocytes,” *eLife*, vol. 5, Dec. 2016.
[359] B. Altincicek and A. Vilcinskas, “Analysis of the immune-related transcriptome of a lophotrochozoan model, the marine annelid Platynereis dumerilii,” *Frontiers in zoology*, vol. 4, no. 1. p. 18, 2007.
[360] M. Koyanagi, A. Terakita, K. Kubokawa, and Y. Shichida, “Amphioxus homologs of Go-coupled rhodopsin and peropsin having 11-cis-and all-trans-retinals as their chromophores,” *FEBS letters*, vol. 531, no. 3. pp. 525–528, 2002.
[361] E. A. Williams, M. Conzelmann, and G. Jékely, “Myoinhibitory peptide regulates feeding in the marine annelid Platynereis,” *Front. Zool.*, vol. 12, p. 1, 2015.
[362] L. Jin, Z. Han, J. Platisa, J. R. A. Wooltorton, L. B. Cohen, and V. A. Pieribone, “Single Action Potentials and Subthreshold Electrical Events Imaged in Neurons with a Fluorescent Protein Voltage Probe,” *Neuron*, vol. 75, pp. 779–785, Sep. 2012.
[363] F. St-Pierre, J. D. Marshall, Y. Yang, Y. Gong, M. J. Schnitzer, and M. Z. Lin, “High-fidelity optical reporting of neuronal electrical activity with an ultrafast fluorescent voltage sensor.,” *Nature neuroscience*, vol. 17, no. 6. pp. 884–889, 22-Apr-2014.
[364] B. F. Fosque, Y. Sun, C. T. Yang, T. Ohyama, M. R. Tadross, and V. Jayaraman, “Labeling of active neural circuits in vivo with designed calcium integrators,” *Science*, vol. 347, no. 6223. pp. 755–760, 2015.
[365] K. Ryan, Z. Lu, and I. A. Meinertzhagen, “The CNS connectome of a tadpole larva ofCiona intestinalis(L.) highlights sidedness in the brain of a chordate sibling,” *eLife*, vol. 5, Dec. 2016.
[366] E. Marder and D. Bucher, “Understanding Circuit Dynamics Using the Stomatogastric Nervous System of Lobsters and Crabs,” *Annu. Rev. Physiol.*, vol. 69, pp. 291–316, Mar. 2007.
[367] A. G. Otopalik, “Mapping neuronal morphology to physiology in a rhythmic motor circuit,” 2017.
[368] J. G. White, E. Southgate, J. N. Thomson, and S. Brenner, “The Structure of the Nervous System of the Nematode Caenorhabditis elegans,” *Philosophical Transactions of the Royal Society B*, vol. 314. pp. 1–340, 12-Nov-1986.
[369] R. H. MacArthur and E. O. Wilson, *The theory of island biogeography. p.203*. Princeton Univ. Press, Princeton, N.J., 1967.
[370] A. Asadulina, A. Panzera, C. Verasztó, C. Liebig, and G. Jékely, “Whole-body gene expression pattern registration in Platynereis larvae.,” *EvoDevo*, vol. 3, no. 1. 2012.
[371] E. S. Lein *et al.*, “Genome-wide atlas of gene expression in the adult mouse brain.,” *Nature*, vol. 445, no. 7124. p. 168, 2007.
[372] O. Ronneberger *et al.*, “ViBE-Z: a framework for 3D virtual colocalization analysis in zebrafish larval brains,” *Nature Methods*, vol. 9, no. 7. pp. 735–742, 2012.
[373] M. E. Fisher *et al.*, “Integrating technologies for comparing 3D gene expression domains in the developing chick limb,” *Developmental biology*, vol. 317, no. 1. pp. 13–23, 2008.
[374] C. C. Fowlkes *et al.*, “A quantitative spatiotemporal atlas of gene expression in the Drosophila blastoderm.,” *Cell*, vol. 133, no. 2. pp. 364–374, 2008.
[375] J. H. Hui, N. Kortchagina, D. Arendt, G. Balavoine, and D. E. Ferrier, “Duplication of the ribosomal gene cluster in the marine polychaete Platynereis dumerilii correlates with ITS polymorphism,” *Journal of The Marine Biological Association of The United Kingdom*, vol. 87, no. 2. pp. 443–449, 2007.
[376] J. Zantke, S. Bannister, V. B. V. Rajan, F. Raible, and K. Tessmar-Raible, “Genetic and Genomic Tools for the Marine Annelid Platynereis dumerilii,” *Genetics*, vol. 197, pp. 19–31, May 2014.
[377] B. Hanström, “Weitere Beiträge zur Kenntnis des Gehirns und der Sinnesorgane der Polychäten (Polygordius, Tomopteris, Scolecolepsis),” *Zeitschrift für Morphologie und Ökologie der Tiere*, vol. 13. 1928.
[378] E. Voronezhskaya, K. Glebov, M. Khabarova, E. Ponimaskin, and L. Nezlin, “Adult-to-embryo chemical signaling in the regulation of larval development in trochophore animals: Cellular and molecular mechanisms,” *Acta Biol. Hung.*, vol. 59, pp. 117–122, Jun. 2008.